Caledonian magmatism and major tectonic structures in the SW highlands of Scotland: implications for ascent, siting and emplacement

John Mark Jacques

CALEDONIAN MAGMATISM AND MAJOR TECTONIC STRUCTURES IN THE SW HIGHLANDS OF SCOTLAND: IMPLICATIONS FOR ASCENT, SITING AND EMPLACEMENT.

John Mark Jacques

PH.D. Thesis

VOLUME 2

A thesis submitted in partial fulfillment of the degree of Doctor of Philosophy at the Department of Geological Sciences, University of Durham.

1995

CONTENTS

VOLUME 2

FIELD DATA OF ASSOCIATED EMPLACEMENT PHENOMENA AND INTERPRETATIONS AND MODELS

PART I: FIELD DATA OF ASSOCIATED EMPLACEMENT PHENOMENA

CHAPTER 7: HIGH LEVEL EMPLACEMENT PHENOMENA:
The Glencoe Fault Intrusion and Etive Quarry Intrusion

The Glencoe Fault Intrusion

The Etive Quarry Intrusion

CHAPTER 8: THE ETIVE DYKE SWARM

PART II: INTERPRETATIONS AND MODELS

CHAPTER 9: CALEDONIAN MAGMATISM AND MAJOR LINEAMENTS

Major lineaments within the SW Highlands

CHAPTER 10: THE CONTROL ON GRANITE EMPLACEMENT STYLES BY THE INTERACTION OF SHEAR ZONES AND DEEP CRUSTAL LINEAMENTS: the influence of crustal depth and rheology

CHAPTER 11: MECHANISMS OF SPACE CREATION DURING PLUTON CONSTRUCTION

APPENDICES

APPENDIX 1: CALEDONIAN MAGMATISM AND MAJOR LINEAMENTS (Continued from Chapter 9)

Major lineaments within the NE Highlands

Major lineaments within the NW Highlands

A major tectonic boundary: the northern margin of a major deep crustal terrane ?

APPENDIX 2: MAIFIC ENCLAVE STRAIN DATA: SHAPE RATIOS AND LOG MEANS

CHAPTER 7

HIGH LEVEL EMPLACEMENT PHENOMENA: the Glencoe Fault Intrusion and Etive Quarry Intrusion

Purpose of study

The purpose of this investigation was to study the internal and external deformational features associated with the emplacement of the Glencoe Fault Intrusion and Etive Quarry Intrusion, in order to 'shed light' on the actual mechanism(s) operating during their construction. However, a detailed comprehensive study of the internal deformational characteristics of the cauldron block still remains to be achieved.

The Fault Intrusion will receive particular attention because of its exposure, its extent around the circumference of the cauldron block, and its well collated data base concerning associated deformational features within the down-faulted mass and the surrounding country rocks. Since the classic work of Clough *et al.* (1909) within Glencoe, relating the development of the ring-dyke intrusions with the formation of surface calderas, the Glencoe Cauldron Subsidence has received considerable attention. The Fault Intrusion was referred to in Anderson's structural interpretation of ring dyke formation (*in the* Mull Memoir: Bailey *et al.* 1924, p. 12), and subsequently became the type example of ring dyke development along outwardly dipping ring faults or 'annular fractures' (Richey 1932, p.121; Buddington 1959, p. 680). The Glencoe Cauldron Subsidence has since been regarded as an example of coherent piston-like collapse (*en bloc* models of Clough *et al.* 1909; Smith & Bailey 1968; Lipman 1984).

Both the Fault Intrusion of Glencoe, and the Quarry Intrusion of the Etive complex have been regarded by many workers (see Ch.'s 3 & 4, and in this Chapter) as representing "partial ring dykes" intruded along ring fault structures developed around the outer margin of the complexes during episodes of cauldron subsidence. Although these intrusive bodies are intimately associated with the development of their respective deeper level 'plutonic bodies', mechanisms operating during the emplacement of the two types were clearly different. For this reason, the deformational features associated with the emplacement of these relatively higher level intrusives are discussed separately in this Chapter. The initial

development of the ring fault system bounding the coherent down-faulted block may have extremely important implications for how space was created during the construction of the plutonic complex sited directly below (see Ch. 11).

THE GLENCOE FAULT INTRUSION

7.1 INTRODUCTION: THE GLENCOE CAULDRON SUBSIDENCE AND ASSOCIATED FAULT INTRUSION

As described in Chapter 4, the Glencoe Fault Intrusion takes the form of a "partial ring dyke", encircling the Glencoe cauldron block (Fig. 7.1). It forms several intrusive bodies associated with a major ring fault system. The Glencoe Fault Intrusion, and associated fault-rocks and structures (see Section 7.2), have received considerable attention, from the earlier works of Clough *et al.* (1909), and Bailey and Maufe (1916), through to recent investigations (Garnham 1988). It is generally regarded that the Early and Main Fault Intrusions represent two major distinct episodes, emplaced during cauldron subsidence along the Early and Main Ring Fault systems respectively (Fig. 7.1). The recognition of two ignimbrite horizons within the lava sequence forming part of the down-faulted cauldron (Roberts 1966a), resulted in much discussion during the 1960's to 1970's about how such 'volcanic cycles' could be related to caldera-collapse (Roberts 1966a, 1966b; Taubeneck 1967). It was suggested that the eruption of the lower and upper ignimbrite horizons were related to the emplacement of the Early and Main Ring Fault Intrusions respectively (Roberts 1966a, 1974; Taubeneck 1967).

Although these studies have covered in some detail the petrographical variation throughout the intrusion, and described the types of fault-rocks and structures developed within both the down-faulted block and surrounding country rocks, they have not addressed: (i) the actual mechanism(s) operating during the construction of both "ring-dyke units"; (ii) their distribution and form; and (iii) the actual 'structural' processes operating to create space for the intrusion of this high level emplacement phenomena.

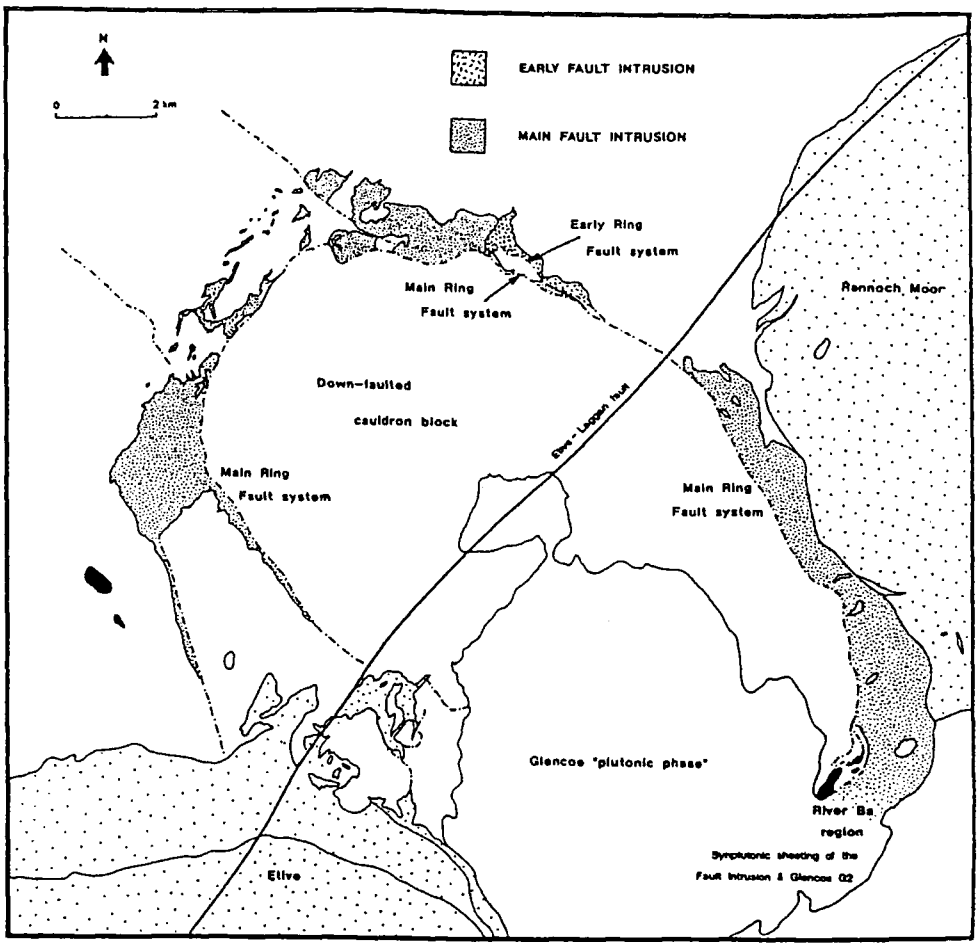

Fig. 7.1. Sketch map showing the form of the Glencoe Fault Intrusion. The Early and Main Fault Intrusion are shown, together with their respective ring fault systems.

There are two major assumptions with the generally accepted "Glencoe Cauldron Subsidence model":

(i) It assumes that there was a significantly large enough volume of magma already below the cauldron block for it to subside into. No attempt is made to explain how space was created for the 'pre-existing magma chamber' which has to be large enough to accommodate part of the cauldron block.

(ii) It assumes a general outward-dip of the main boundary fault surrounding the Glencoe cauldron block, suggesting that the necessary space needed for the contemporaneous emplacement of the Fault Intrusion was created "dilationally" along the ring faults as the cauldron block descended, thus complying with the 'bell-shape' required by Anderson's classic "dynamical theory of the formation of ring-dykes" (Anderson 1951), providing a solution to the space problem.

However, several observational features question a 'bell-shaped' geometry for the down-faulted block. These have been addressed by Reynolds (1956), Roberts (1966a, 1966b) and Taubeneck (1967), and verified within this study (see Section 7.3). These features include:

① The general inward-dip of the Ring Fault system surrounding the Glencoe cauldron subsidence suggests that the down-faulted block has an overall form of an upward-opening cone, not the classic 'bell-shape' required for the formation of ring-dykes. This would imply that the ring faults converged at depth, essentially forming 'cone fracture-type' geometries, in which it has been shown by theoretical modelling by Anderson (1951) that such structures would steepen upwards towards the free surface, possibly accounting for many of the ring-faults being sub-vertical in many places (Reynolds 1956).

② Presumably, if the Ring Fault system originally formed arcuate fractures which dipped outwards, an annular space would have been created and exploited by the Fault Intrusion as the cauldron block subsided. This would have resulted in a fairly continuous ring-dyke body encircling the down-faulted mass. However, "this is not the case. The fault intrusions are discontinuous masses, presenting smooth inner contacts against the ring faults, but with highly irregular outer contacts with the country rocks. Further, the fault intrusions often riddle the country rocks as isolated diatreme-like intrusions" (Roberts 1966a; see Fig. 7.1). This led Roberts (1966a) to conclude that the "ring faults originally dipped inwards, the fault intrusions forcibly penetrating the country rocks either as magma or as fluidised systems". The ring faults would therefore possess 'cone-fracture-type' geometries, which have been interpreted by Anderson (1951) as resulting from an upward directed uniaxial pressure acting at depth. It is therefore quite feasible that such structures were initially developed during the *in situ* expansion of the Glencoe plutonic complex. These volcanotectonic faults were therefore produced to accommodate expansion-related strains associated with the construction of the Clach Leathad facies (G2) (see Ch. 11).

③ Other evidence for an upward pressure of an underlying magma during the initial stages of caldera development is the presence of a small, but significant number of radial, red felsite dykes (Taubeneck 1967). Clough *et al.* (1909, p. 655) concluded that the dykes "are probably older than even the early fault intrusion: for they do not cut the latter, although it crosses the zone of their maximum development".

This suggests that this phase of dyke emplacement relates to an episode of doming that preceded the formation of the Ring Fault system.

④ The down-faulting and subsequent deformation associated with the subsidence of a cauldron block with an overall form of an 'upward opening cone' is substantiated by the pronounced marginal upturn of the volcanic pile against the encircling ring fault.

These features therefore suggest that the Glencoe cauldron block does not have the classic 'bell-shape' required to overcome the space problem by simply creating space "dilationally" along the ring faults as the block descended. This Chapter will address this problem, and provide an alternative model for the emplacement of the Glencoe Fault Intrusion.

7.2 THE GLENCOE FAULT INTRUSION

The Glencoe Fault Intrusion takes the form of a "partial ring dyke", encircling a down-faulted block (13 x 10 km) of metasedimentary rocks (Fig. 7.2), which are overlain unconformably by Lower Devonian volcanics. The NW-SE elongation of the cauldron block is probably due to the subsequent emplacement of the NE-SW-trending Etive Dyke Swarm (Fig. 7.2); removal of the dykes gives an original circular form to the down-faulted mass.

The Glencoe Fault Intrusion was first described by Clough *et al.* (1909), and subsequently by Bailey and Maufe (1916) and Bailey (1960). During the 1960's and 1970's the intrusion and its relationships to the Glencoe cauldron and surrounding country rocks was described by Roberts (1963, 1966b, 1974), Taubeneck (1967) and Bussel (1979). These relationships have been described more recently by Garnham (1988) using modern geochemical and microscope techniques. The early studies (see Clough *et al.* 1908; Bailey & Maufe 1916) recognised that the Fault Intrusion could be essentially sub-divided into two distinct facies: (i) an earlier intrusive phase, ranging from diorite to porphyrite compositions, known as the "Early Glencoe Fault Intrusion" (Fig. 7.1). Within this compositionally diverse facies are hornblendic varieties which, as noted by Bailey (1960), "are extremely similar to the basic phase of the Beinn a' Bhuiridh Diorite at the south-east

corner of the Etive complex"; and (ii) a later phase, known as the "Main Glencoe Fault Intrusion" (Fig. 7.1), which compositionally varies from granitoid to porphyroid varieties, and which may be pink or grey. The Early and Main Glencoe Fault Intrusions are therefore thought to represent two major distinct intrusive episodes, emplaced during cauldron subsidence along the Early and Main Ring Fault systems respectively (Fig. 7.1).

In the NW of the intrusion, in and around the An t-Sron mass, pink varieties of variable composition are dominant, containing large amounts of country rock xenoliths. This phase often sheets and veins the surrounding Dalradian rocks, and parts of this mass may represent a slightly later intrusive phase of the Main Glencoe Fault Intrusion (see below).

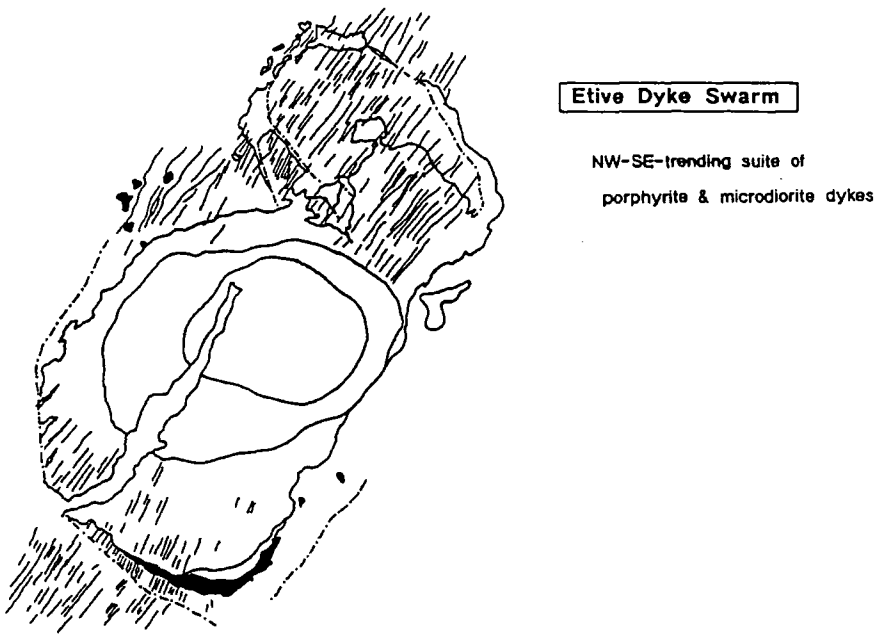

Fig. 7.2. Map of the high level Glencoe Fault Intrusion and associated plutonic complex. Distribution of the Etive Dyke Swarm is shown.

7.2.1. The Early Glencoe Fault Intrusion

A large mass of this phase occurs along the outer ring fault at Stob Mhic Mhartuin (Fig. 7.1). It is essentially a fine- to medium-grained porphyry, of tonalitic composition. It tends to contain quite a large number of country xenoliths and is generally highly altered by hydrothermal veining and pervasive fracturing. A large number of these brittle fractures have been infilled by "flinty crush-rock" (FCR), a term first used by Clough *et al.* (1909) to describe a thin band of material developed along the ring fault surfaces. The origin and

nature of this FCR has received much attention and remains controversial (see below; sub-section 7.2.3). Garnham (1988) suggested that the FCR within the Early Glencoe Fault Intrusion was generated simultaneously with the production of FCR along the main ring fault during the emplacement of the Main Glencoe Fault Intrusion; concluding that the outer intrusion had in fact intruded and crystallised prior to movements along the Main Ring Fault system. Due to the sheared and altered nature of these rocks, Clough *et al.* (1909) regarded them as being a distinct earlier intrusive phase, and hence, referred to them as the "Early Glencoe Fault Intrusion", although petrologically and geochemically they are very similar to varieties within the later "Main Glencoe Fault Intrusion" (see Garnham 1988). Compositionally this phase ranges from monzonitic - monzodioritic through to monzogranitic varieties.

General petrographical description

Early Glencoe Fault Intrusion: an extremely variable intrusive phase, ranging from monzonitic through to monzogranitic compositions. The bulk of the phase is a fine- to medium-grained, extremely porphyritic monzodiorite. Phenocryst phases include plagioclase, amphibole, and biotite, set within a finer-grained groundmass (< 0.5 mm) of plagioclase, quartz, alkali feldspar and biotite. Plagioclase phenocrysts are subhedral (up to 1 cm in length), are generally normally zoned (andesine to oligoclase) and are often broken. Plagioclase crystals within the matrix are compositionally similar to that of the phenocryst phase. Both amphibole and biotite form well developed crystals, up to 4.0 mm in length. Biotite laths are often bent and kinked. Accessory minerals include iron ores, apatite, zircon and sphene.

7.2.2. The Main Glencoe Fault Intrusion

In the NW of the intrusion, in and around the An t-Sron mass (Fig. 7.1), pink varieties of variable composition are dominant, containing large amounts of country rock xenoliths. This phase often sheets and veins the surrounding Dalradian rocks, and parts of this mass may represent a slightly later intrusive phase of the Main Glencoe Fault Intrusion (see below).

The centre of the mass (An t-Sron) is essentially composed of tonalite, whereas within the eastern part of the intrusion, along the faulted contact, the rock is monzogranitic. Contact relationships seen between the two facies are extremely rare, but where they do occur, they suggest that the pink, monzogranitic material represents a slightly later intrusive phase. Isolated, small bodies of diorite occur within the 'monzogranite'. Within the

western part of the intrusion, granitic rocks are also present and often sheet (generally < 10 m in width) into the adjacent country rock. In the NW of the An t-Sron intrusion, medium- to coarse-grained granophyric monzogranitic rocks are common. They are essentially composed of alkali feldspar, quartz and plagioclase (oligoclase). Graphic intergrowths with quartz occur within both types of feldspar. Muscovite is common, whereas biotite is subsidiary, or completely absent. Zircon occurs as an accessory mineral.

The bulk of the Main Glencoe Fault Intrusion can be described as a medium- to coarse-grained, porphyritic tonalite. As mentioned above, the centre, and majority of the An t-Sron intrusive mass (Fig. 7.1), is composed of this intrusive phase. Other major masses occur along the inner ring fault of Stob Mhic Mhartuin and form the 1-2 km wide, main dyke-like arcuate body which extends round the East and SE of the complex. Further south in the Allt Coire an Easain-River Bà region (Fig. 7.2) it appears to synplutonically 'merge' with the plutonic intrusive phase G2 (Clach Leathad facies).

General petrographical description

The Main Fault Intrusion; the tonalite phase: a medium- to coarse-grained, porphyritic tonalite, containing phenocrysts of plagioclase (35-40 %; interstitial plagioclase 10-20 %), biotite (up to 18 %), and amphibole (5-11 %). The plagioclase phenocrysts (labradorite-bytownite) are generally euhedral to subhedral, often zoned and range from 3-8 mm in length. Plagioclase crystals within the fine-grained groundmass are somewhat different, often possessing anhedral forms and discontinuous zoning. Truncation of the zoning by non-crystallographic grain boundaries may indicate that the crystals represent broken fragments of larger phenocrysts (see Roberts 1966b). Amphibole phenocrysts generally have elongate, euhedral forms (2.0-3.5 mm in length), whereas the biotite phenocrysts are much less well developed, often forming much smaller crystals (< 1.0 mm). Pyroxene (augite) may occur, forming euhedral to subhedral crystals, generally < 1.0 mm in length. The groundmass is essentially composed of plagioclase, small amounts of quartz (up to 10 %) and minor amounts of amphibole and biotite. Accessory minerals include iron ores. Chlorite may occur as an alteration product.

7.2.3 The "Flinty Crush-rock" and associated fault-rocks

As mentioned above, the term "Flinty Crush-rock" (FCR) was first employed by Clough *et al.* (1909) to describe a thin band of material generated along the ring fault surfaces of the down-faulted cauldron block; separating the Fault Intrusion from the Dalradian metasedimentary rocks (pelites and quartzites), within the subsided block. The

FCR also occurs along parts of the Fault Intrusion outer contact, against the surrounding metasedimentary country rocks (Roberts 1966b).

Along the inner contact the FCR is associated with a zone of fault-rocks, ranging from approximately 0.5-1 m wide. The general distribution of the different types and their characteristics have been addressed by Roberts (1966b) for the fault zone occurring along the Main Fault Intrusion at Stob Mhic Mhartuin (see below; Fig. 7.3) (Plate 7.1). In general, the fault zone can be sub-divided into four main zones (this change is gradational and the progressive decrease in grain-size occurs towards the Fault Intrusion): (i) a zone of brecciated and shattered country rock; (ii) through to a zone of fine-grained "white crush-rock"; (iii) into a zone of "grey crush-rock", which may form a banded breccia; and (iv) into the black "flinty crush-rock" (FCR) (Plates 7.2 & 7.3). This change is gradational and the progressive decrease in grain-size occurs towards the Fault Intrusion.

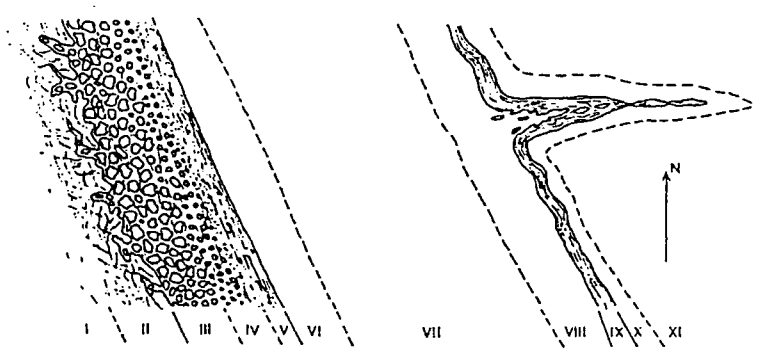

Fig. 7.3. Schematic diagram (not to scale) showing the contact relations of the Main Fault Intrusion at Stob Mhic Mhartuin. Non-transitional contacts are shown by solid lines.

I. Bedded quartzites within the Glencoe Cauldron.
II. Quatzites cut by veinlets of granulitic quartz.
III. "White crush-rock".
IV. "Banded breccia with matrix of flinty crush-rock."
V. "Flinty crush-rock".
VI. South-western marginal facies of the Fault Intrusion.
VII. Fault Intrusion porphyrite
VIII. North-eastern marginal facies of the Fault Intrusion.
IX. "Flinty crush-rock".
X. Sheared quatzose microbreccia.
XI. Micaceous quartzites and semi-pelitic granulites outside the Glencoe Cauldron.
(After Roberts 1966b.)

Plate 7.1. The Main Ring Fault at Stob Mhic Mhartuin (looking NW). Geological hammer marks the 0.5-1.0 m wide zone of 'fault-rocks' (see Plates 7.2 & 7.3); right of these is the Main Glencoe Fault Intrusion.

As mentioned previously, the origin and nature of the FCR has received much attention and remains controversial. Due to the ultra fine-grain size of the FCR and the fine-grained nature of its associated fault-rocks, their relationship with the emplacement of the Fault Intrusion has remained a problem as their grain-size limits the usefulness of normal microscopic techniques. However, more recent work by Garnham (1988), using scanning electron microscopy (SEM) together with conventional microscopy, has enabled a more useful mineralogical and texturalogical evaluation. In the past, the term "Flinty Crush-rock" has been used as a field term to incorporate all fine-grained fault rocks associated with the ring faults and outer contacts of the Fault Intrusion. Garnham (1988) has proposed that the term should be used solely for the 3-8 cm wide band, of black, ultra fine FCR which occurs immediately adjacent to the Fault Intrusion (Fig. 7.4). Garnham (1988) has identified a number of mineralogically and texturally distinct zones within the (approximately) 1 m wide fault rocks. These are described briefly below, together with observations made during the current study.

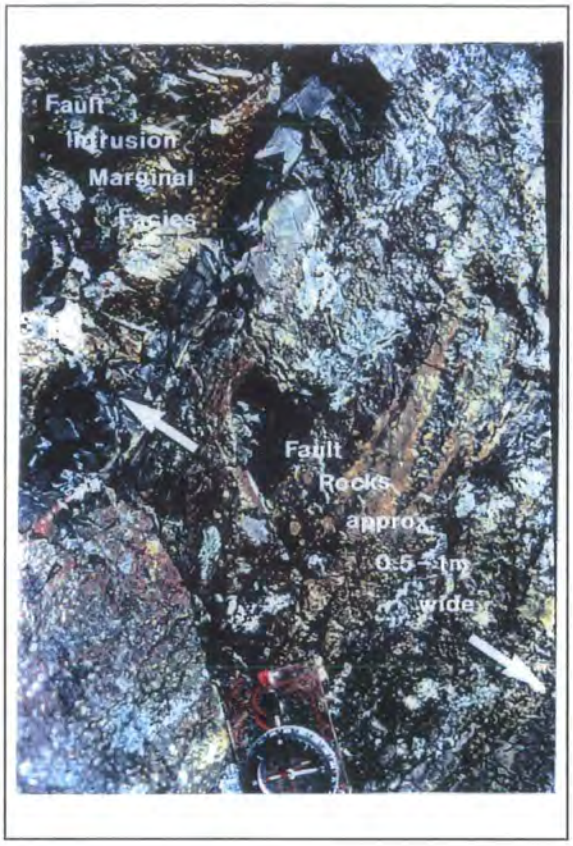

Plate 7.2. Main Ring Fault at Stob Mhic Mhartuin (looking SE). Shows a section through the 'zone of fault-rocks'. Note the inclination of the fault zone, which infers an outward-dip of approximately 65-70°.

Plate 7.3. A closer view of the 'zone of fault-rocks' shown in Plate 7.2. (For the true inclination of the fault zone see Plate 7.2). The "zones" described by Roberts (1966b) can be easily identified. Note that the changes are gradational and the progressive decrease in grain-size occurs towards the Fault Intrusion, culminating in the development of the FCR.

***(i) Ring Fault / Marginal breccias*:** these occur within the quartzites, pelitic-quartzites and schists of the Glencoe Cauldron and surrounding country rocks. The majority of these breccias occur within the quartzites close to the ring faults. Shattered and brecciated quartzites also occur within narrow shear zones (generally between 4-7 cm wide, but may reach up to 25 cm wide) within the down-faulted cauldron block (as described by Clough *et al.* 1909). They generally run sub-parallel to the Main Ring Fault and may represent subsidiary shears to that structure. They are essentially composed of fragments of country rock, generally < 10 cm in length, which have been fractured and sheared to form a breccia/microbreccia.

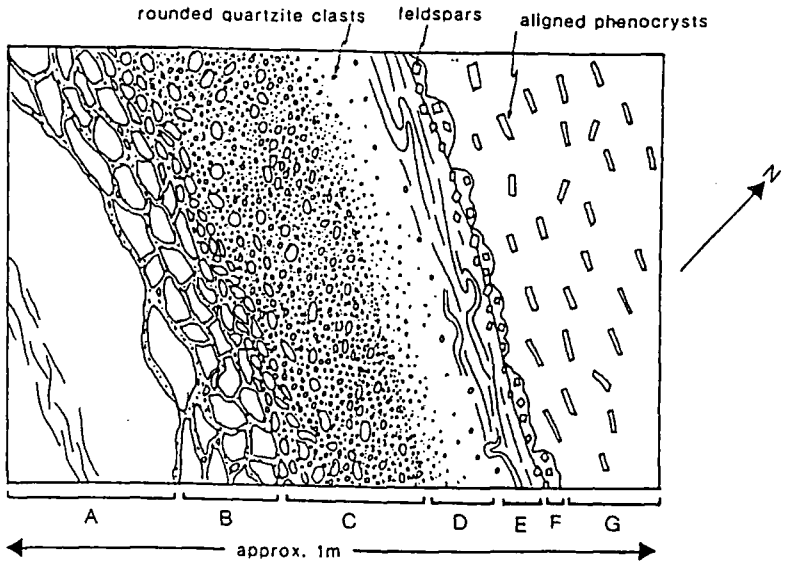

Fig. 7.4. A schematic map showing the gradation from quartzitic country rock to flinty crush-rock as seen on the inner ring fault at Stob Mhic Mhartuin (partly after Roberts 1966b). A is flaggy quartzite, B is brecciated and shattered quartzite, C is 'white' crush-rock, D is grey crush-rock, E is black, flinty crush-rock with flow banding, F is red felsite with phenocrysts, and G is inner ring-intrusion. (After Garnham 1988).

The marginal breccias are predominantly developed in the micaceously laminated psammitic rocks of the Eilde Flags and to a much lesser extent in the quartzitic rocks of the Eilde Quartzite, which have been down-faulted during the development of the caldera. Breccias developed within the quartzitic rocks are characterised by sub-angular to rounded quartzite clasts (approximately 5-10 cm in diameter) which are supported in a much finer-grained quartz matrix derived from the host rock. The quartz crystals within the clasts exhibit undulose extinction and are strained. These microstructural features are also present within the undeformed quartzitic rocks outside the fault zones, and therefore indicates that they are related to an earlier, probably regional, deformational event. However, in the more pelitic-rich quartzites, biotite is undeformed in both the country rocks outside these zones and in the undeformed clasts of the breccia, but within the matrix it is bent, kinked, altered and often sheared out to form highly elongate swathes; thus indicating that the deformation of the biotite occurred during the development of the breccia. Where these marginal breccias occur within the pelitic-rich horizons, the biotite may wrap around lenticular aggregates or lenses of recrystallised quartz in a sigmoidal fashion, indicating a sinistral sense of shear during their development. Even within the down-faulted schistose country rocks up to 300-350 m away from the Main Ring Fault [e.g. 236 534], quartz ribbons (approx. 1-3 cm wide) are unusually common and record a component of sinistral shear parallel to the ring fault. This suggests that a deformation associated with the emplacement of the Fault Intrusion may have penetrated into the surrounding wall rocks.

(ii) Ring Fault / marginal cataclastites: these fault rocks are compositionally similar to the breccias, representing a gradational decrease in grain-size and lower clast to matrix ratio. It is composed of angular to sub-rounded host rock clasts set in an ultra fine-grained groundmass of host material. Large quartz clasts, up to 2-3 mm in diameter, and smaller quartz fragments (< 1 mm in diameter) are set in a much finer-grained quartz matrix. The rock has been brittly deformed, predominantly by frictional sliding, resulting in grain rotation and a reduction in grain-size.

(iii) Ring Fault / marginal and splays of flinty crush rock (FCR): FCR not only occurs as a thin band at the ring faults and outer contacts of the Fault Intrusion, but may also occur as veins and synthetic splays, up to 5-8 cm wide, intruding both the country rocks and the Fault Intrusion. The form of these splays have been used to determine the sense of motion along the ring fault structures, in relation to the emplacement of the Main Fault Intrusion (see sub-section 7.3.2).

Moving from the "white crush-rocks" (up to 60 cm wide) (i.e. the breccias and cataclasites), towards the Fault Intrusion, the gradual decrease in grain-size is maintained fairly constantly throughout this part of the fault zone and into the zone of "grey crush-rocks". This latter zone (approx. 30 cm wide) is composed of sub-rounded to rounded clasts of quartzite, which is often in a banded matrix, compositionally similar to the FCR. The matrix banding is contorted and may represent "flow". From this "grey crush-rock" there is a transitional zone into brown, through to black FCR (Plate 7.4). Garnham (1988) attributed this change in colour to a progressive change in grain-size, indicating that the darker FCR is finer in grain-size. The intensely black, semi-vitreous FCR, generally forms a thin band approximately 3-8 cm wide and characteristically contains a strong banding which is often sub-parallel to the contact with the Fault Intrusion. Banding is also present within the lighter coloured, browner FCR and often diverges around quartz fragments (generally < 1 mm in diameter) and euhedral feldspar megacrysts (which may reach up to 5 mm in length) forming pressure shadow structures, swirls and eddies. The feldspar megacrysts are internally undeformed and are generally not fractured. They often form graphic intergrowths with quartz and are generally surrounded by overgrowths and/or a thin film of rhyolitic material. These features together with mixing relationships between the FCR and the cataclasites, and the FCR with a marginal facies of red felsite (see below), which occurs along the contact of the Fault Intrusion, led Garnham (1988) to conclude that the FCR essentially represents a hybrid zone, where there was a progressive increase in mixing between the cataclasite and the rhyolitic magma (red felsite). During the mixing process, feldspar megacrysts were incorporated into the resultant FCR from the red felsite. Gradational and sometimes sharp contacts between the FCR and the adjacent cataclasite and red felsites suggests that this mixing process occurred under varying physical

conditions, such as changes in pressure, temperature and viscosity. Garnham (1988), thus concluded that this black, ultra fine-grained material, commonly referred to as "flinty crush-rock", should be genetically termed a tuffsite, agreeing with Reynolds (1954).

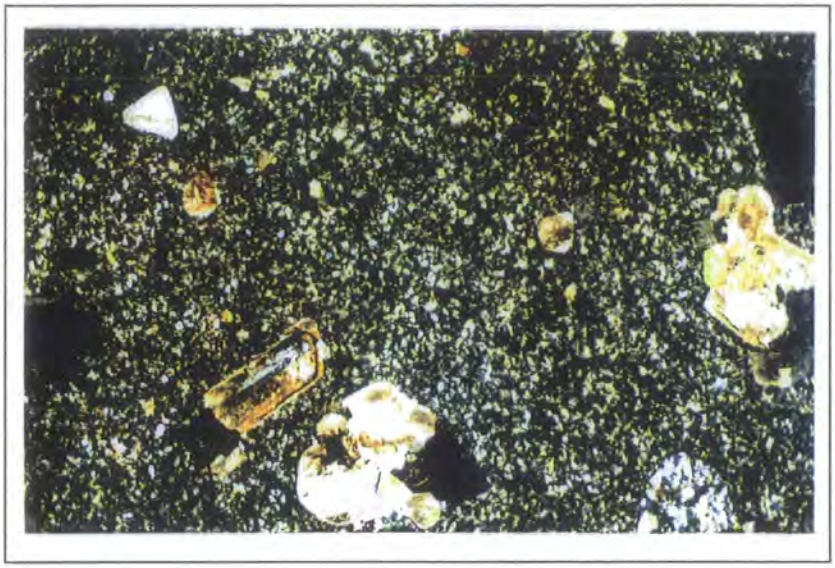

Plate 7.4. Photomicrograph of "grey crush rock"/FCR. Taken from the Main Ring Fault at Stob Mhic Mhartuin. (Field of view approximately 18 mm).

(iv) Marginal facies of the Fault Intrusion: this fine-grained marginal facies (approximately 1-2 m wide) occurs along both the inner and outer contacts of the Early and Main Fault Intrusions, and may occur as irregular masses (up to approximately 5 m^2) or small lenses within both the surrounding country rock and the main body of the Fault Intrusion. Previous studies (e.g. Bailey 1960) have regarded this material as being a chilled margin to the ring-intrusion, but petrographically (Garnham 1988) and structurally (this study) this facies may represent a distinct intrusive phase to that of the tonalitic material of the Main Fault Intrusion; forming chilled contacts against the Early Fault Intrusion, but possessing synplutonic relationships with the later, Main Fault Intrusion.

The facies is essentially a fine-grained, reddish pink porphyrite. Compositionally the rock is rhyolitic and less basic than the majority of the Fault Intrusion, and could be best described as a slightly porphyritic red felsite. The phenocrysts are plagioclase and alkali feldspar, with both types reaching up to 5-6 mm in length. The groundmass crystals are < 0.1 mm and comprise of plagioclase, alkali feldspar, quartz, biotite and hornblende. Small phenocryst phases of biotite and hornblende may occur; the latter phase only forming at the

inner contact of the Main Fault Intrusion. Many of the plagioclase and alkali feldspar phenocrysts may be broken, and biotite is often heavily altered. The reddish appearance of this facies may suggest that the rock was subjected to late stage oxidation and/or hydrothermal alteration by fluids exploiting the ring fault system.

The fault-rocks separating the Fault Intrusion from the country rocks outside the Cauldron

The outer contact of the Fault Intrusion with the surrounding Dalradian country rocks is somewhat different from the inner ring fault contacts discussed above. Again, a marginal facies (approx. 1-2 m wide) of pink porphyrite (red felsite material) occurs in contact with the FCR, and cataclasite through to microbreccias into breccias are observed moving away from the Fault Intrusion into the country rocks. However, unlike the inner contact, a transitional zone is generally not observed between the FCR and the cataclasites/microbreccias (but is more commonly abrupt), and the zone of brittle deformation is generally less than half the width seen at the inner ring fault contact. The major difference between the breccias and the cataclasite rocks ("flinty crush-rocks") at the two contacts, is the presence in the quartzite clasts, at the outer contact, of extremely strained quartz, with marked undulose extinction, together with a high degree of recrystallisation. The highly strained quartz fragments are generally sub-angular compared to the well-rounded clasts developed at the inner contact. These features led Roberts (1966b) to propose that the country rocks adjacent to the outer contact have been strongly sheared, and the sharp and non-transitional contact between the FCR and the "microbreccia" (cataclasite) was as a result of shearing. As stated by Roberts (1966b p.313), "It is ironic that shearing has only affected the country rocks at the outer contact where it cannot be due to movement on either the Main or the Early Ring faults (cf. Clough *et al.* 1909). It is clear, from the development of the sheared microbreccia everywhere along the highly irregular outer contact of the Fault-Intrusion, that this shearing resulted from shear stresses acting along the wall-rocks during its emplacement.". Roberts (1966b) attributed this development of shearing along the outer contact (and not along the inner contact), to a difference in the temperature of the country rocks on either side of the Main Ring fault system. At the outer contact, the country rocks have been thermally metamorphosed by the Fault Intrusion, whereas rocks within the cauldron block have remained relatively unaffected (Clough *et al.* 1909), indicating that the country rocks at the inner contact remained relatively cold. Roberts (1966b) concluded that the shear stresses imposed by the contemporaneous down-faulting of the cauldron block and emplacement of the Main Fault Intrusion, "brecciated the relatively cold country rocks at the inner contact,

whereas at the outer contact the country rocks were sufficiently hot for plastic deformation to form the sheared microbreccia"; with increasing amounts of tonalitic material, ascending by a process of multiple sheeting/dyking along the outer parts of the "Ring fault System", would lead to a progressive rise in temperature and in the relative amount of ductile deformation in the surrounding country rocks. This could create a situation, where at the initial stage of emplacement of the Main Fault Intrusion, brittle-type processes were dominant, such as stoping, incorporating large amounts of Dalradian metasedimentary xenoliths and blocks of Rannoch Moor G2 (see sub-section 7.3.1), whereas with increasing input of hot magma at the outer contact there was a progressive increase in ductile flow type processes as a mechanism of space creation (Section 7.4).

The formation of the "Flinty Crush-rock": a number of alternative models have been put forward to explain the nature and formation of the FCR and its association with the emplacement of the Fault Intrusion. It was originally thought that the rock was derived from a melt produced by frictional heating during fault movement as the cauldron block subsided (Clough *et al.* 1909; Bailey 1960), (essentially producing a pseudotachylite). The resultant "flinty crush-rocks" were then partially removed as magma penetrated upwards via the ring faults, resulting only in a thin veneer of FCR along the fault surfaces. The problem with this model is that it does not account for the intrusive nature of the FCR; which clearly cross cuts the Fault Intrusion (both "Early" and "Main") as veins and splays. This objection was subsequently challenged by Reynolds (1956) who attributed the formation of the FCR to a process known from industrial practices as gas-fluidisation (Reynolds 1954). This suggested that the FCR was an ultra fine-grained intrusive breccia or tuffisite formed by magmatic gases brecciating the country rock. Such a process was also envisaged by Hardie (1963),Taubeneck (1967) and Roberts (1966b, 1974), coming to the general opinion that the intrusive breccia was carried up the ring fault to form the ultra fine-grained material. Roberts (1966b), thus concluded that the FCR represents an "advanced guard" to the Main Fault Intrusion, indicating that the ring intrusion was emplaced as an entrained fluidised system of gas, solid phenocrysts and, probably, liquid droplets.

More recent studies by Garnham (1988), using SEM, has suggested that the generation of the "flinty crush-rocks" was by a multiple mechanism of cataclasis, explosive volcanism and rhyolitic intrusion. She envisaged a basic three-stage process: (i) explosive activity resulting in the development of volcano-tectonic faults. Movement along the resultant ring-fractures led to brittle deformation and the formation of marginal breccias and cataclasites. This was further enhanced by thermal spalling, a process of thermal expansion during seismic faulting (Moore and Sibson 1978), leading to stress enhancement and subsequent rock fragmentation; (ii) an entrained fluidised system of gas blasting up the

ring-fracture to be erupted as tuffs. Magma droplets which did not reach the surface were able to mix with the rock fragments formed by cataclasis to produce the FCR. This is very similar to the gas-fluidisation theory proposed by Reynolds (1954, 1956); and finally (iii) viscous rhyolite intruding up the ring fault and mixing turbulently with the partially solidified FCR, to produce the flow banded structures and the incorporation of large plagioclase and K-feldspar megacrysts. This was subsequently followed by the emplacement of the Main Fault Intrusion. An important aspect of this model is that these stages are not believed to have acted independently of each other, but are interactive, with overlap of the different processes, occurring along different parts of the ring fault and at different times relative to each other (Garnham 1988). Such processes may account for the formation and nature of the "flinty crush-rocks" which border the Fault Intrusion, but do not by any means account for the space needed to accommodate the main phase of the Fault Intrusion as a large "ring dyke body".

7.2.4 Geochemical analysis of the Glencoe Fault Intrusion

The Glencoe Fault Intrusion is composed of a diverse range of rock types, ranging from gabbros, diorites, monzodiorites, through to monzogranites. This mineralogical variation has been attributed by Garnham (1988) to fractional crystallisation within a zoned magma chamber; the source magma being basaltic in composition and becoming contaminated by partial-melt derived from the upper crust, prior to the fractionation process. The rhyolitic magma, which generally preceded the emplacement of the Main Fault Intrusion and was so influential in the development of the FCR along the ring-fault surfaces (see sub-section 7.2.3), was not derived by fractional crystallisation of the magma which produced the ring-intrusives, but possibly derived from an independent source (Garnham 1988).

7.3 FABRIC DEVELOPMENT: EVOLUTION OF MICROSTRUCTURES

The purpose of this Section is to present the type of fabrics and microstructures which are common within the Early and Main Glencoe Fault Intrusions. It is not intended as a detailed discussion on the textural development and mechanisms operating during fabric evolution.

Based on the orientation of fabrics, strain distribution, local emplacement phenomena, and the distribution and form of the Fault Intrusion, the "partial ring dyke" has been sub-divided into three main 'units' (Fig. 7.5): (i) the 1-2 km wide, "main" dyke-like arcuate body which extends round the east and SE of the complex (Plate 7.5). This will be referred to as the "Coupall-Creag Dhubh-Bà unit"; (ii) the bodies of both the Early and Main Glencoe Fault Intrusion which occur along the Early and Main Fault systems respectively, within the north and NE of the complex. This will be referred to as the "Aonach Eagach-Stob Mhic Mhartuin unit".; and (iii) the An t-Sron mass, in the NW of the intrusion.

Plate 7.5. View from Stob Mhic Mhartuin looking south-eastwards, showing the "topographical expression" of the "Coupall-Creag Dhubh-Bà unit" (Fint). Note its arcuate form.

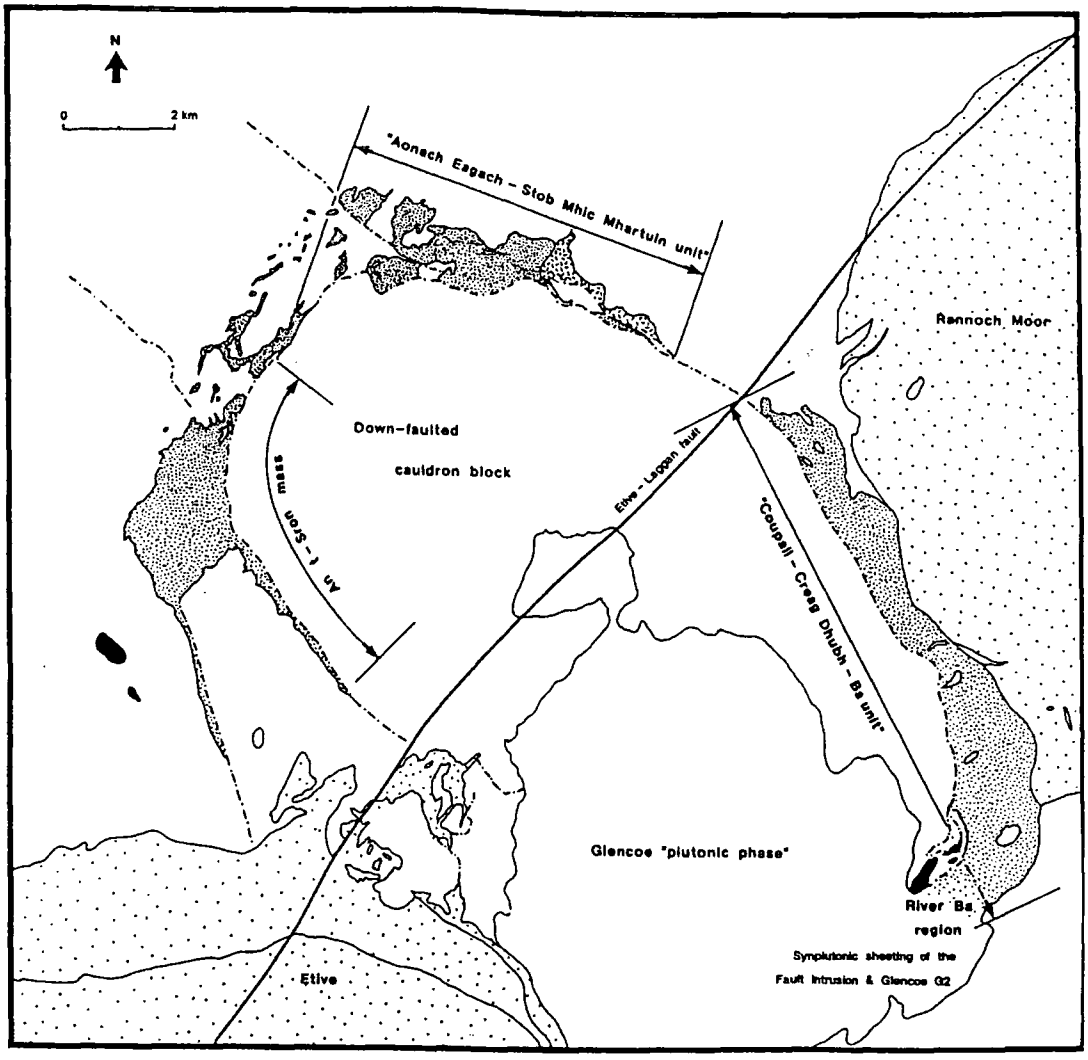

Fig. 7.5. Sketch map showing the sub-division of the Fault Intrusion into three main 'units', based on fabric development, strain distribution, local emplacement phenomena, and the distribution and form of the intrusion: (i) the "Coupall-Creag Dhubh-Bà unit" in the east and SE; (ii) the "Aonach Eagach-Stob Mhic Mhartuin unit" in the north and NE; and (iii) the An t-Sron mass.

7.3.1 Fabric development and strain distribution within the "Coupall-Creag Dhubh-Bà unit"

This dyke-like body is predominantly composed of a grey, medium- to coarse-grained porphyritic tonalite (see sub-section 7.2.2). Throughout this 'unit', a weak to moderately developed bimodal PFC fabric is developed (Fig. 7.6). Both sets of fabric are generally defined in hand-specimen by the preferred dimensional orientation of euhedral to subhedral plagioclase (35-40 %; 3-8 mm in length) and euhedral amphibole (5-11 %; 2.0-

3.5 mm in length) phenocrysts. In thin-section, biotite (approximately 18 %; generally < 1.0 mm) laths may form a crude alignment. These phenocryst phases are set in a relatively undeformed groundmass of interstitial plagioclase (10-20 %), quartz (up to 10 %), and minor amounts of amphibole and biotite.

Both sets of fabrics appear to be defined by plagioclase and amphibole in approximately the same proportions suggesting that these sub-fabrics have not been produced primarily by a 'process of angular sorting', unlike the bimodal fabrics developed throughout the 'Chaorainn pulse' of the Glencoe plutonic phase (see Ch. 4, sub-section 4.4.2.1). One set generally trends 140-160°, sub-parallel to the elongation of this dyke-like body, and the other set trends between 015-064°, orientated oblique to the Main Ring Fault and to its outer contact with the Dalradian metasediments (Fig. 7.6a). This oblique set may represent a 'tiling-type fabric' or 'imbricate' texture, formed due to the interaction of crystals slowing down their rotation and causing them to pile up and 'lock' during non-coaxial deformation (see Ch. 1, sub-section 1.7.3). This 'locking' effect accounts for the high angle of obliquity between the two sub-fabrics, as phenocrysts outside these 'lock-up zones' are allowed to rotate more freely towards the shear plane (Fig. 7.7; see below). Strain may have been focussed into this 'lock-up' zone at an early stage in the crystallisation of the magma. This may explain why microdioritic enclaves which often form two populations, each aligned sub-parallel to one set of PFC fabrics, generally show an apparent greater magnitude of strain from X/Z ratios (horizontal surfaces) of enclaves orientated sub-parallel to this 'tiling fabric' (Fig. 7.7; see below). Whereas, the phenocrysts outside these 'lock-up zones' are allowed to rotate more freely towards the shear plane, allowing the strain imposed to be accommodated by the liquid matrix. As the deformation continues, and crystallisation increases, it is envisaged that these phenocrysts form a sub-fabric orientated close or sub-parallel to the shear plane, eventually forming discrete PFC 'lock-up shears' (Fig. 7.7). This implies that during PFC fabric development strain was partitioned, leading to the formation of two sets of PFC fabric (Plates 7.6 & 7.7). The angular relationship of these sub-fabrics suggests a sinistral shear component during their development, with the shear direction (shear plane) orientated sub-parallel to the overall elongation of this dyke-like body, and to the Main Ring Fault system (Fig. 7.6).

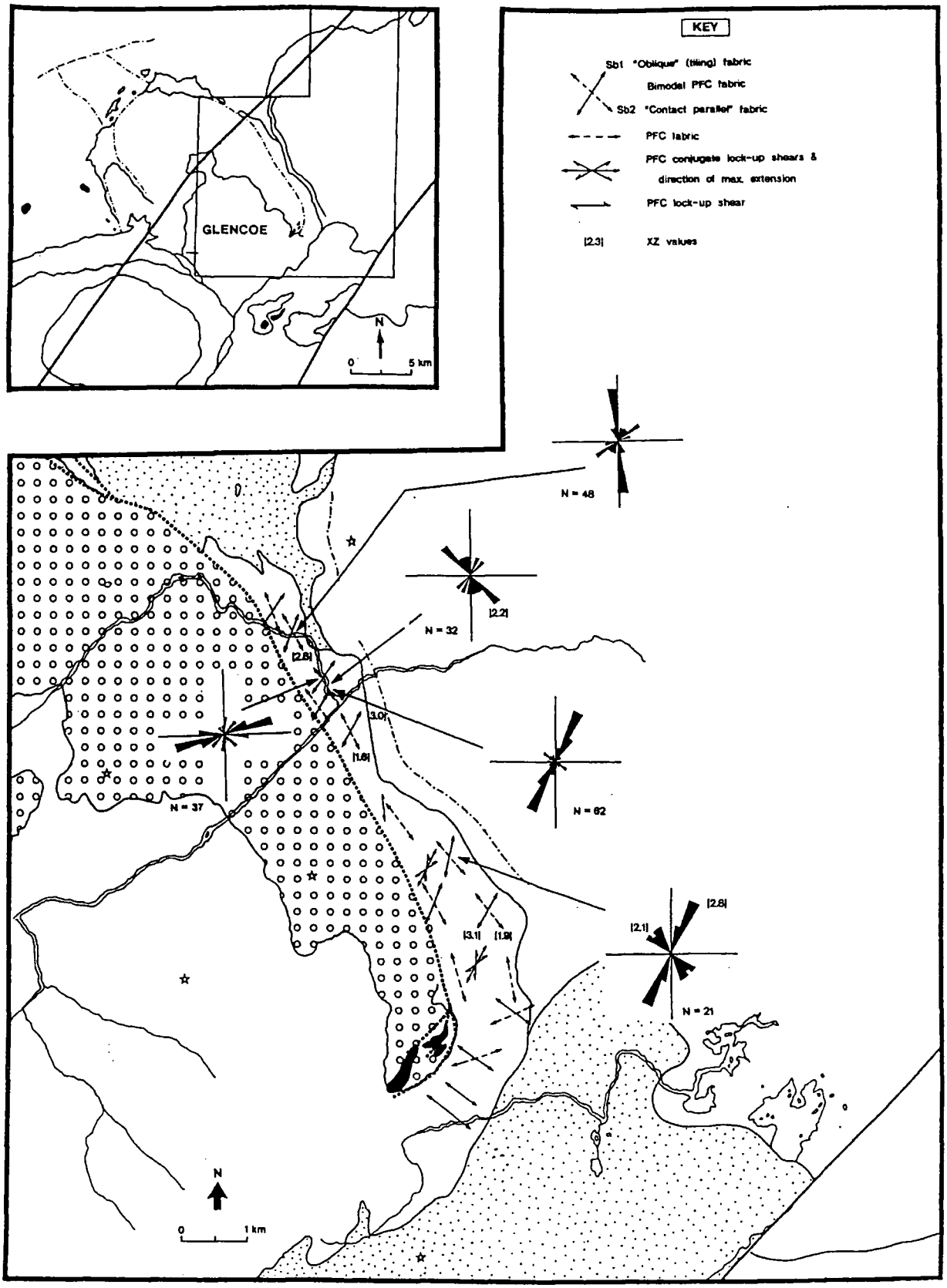

Fig. 7.6. Sketch map of PFC bimodal fabrics and "contact-parallel" fabrics within the "Coupall-Creag Dhubh-Bà unit". X/Z values of microdioritic enclaves aligned parallel to each fabric direction are shown, together with 'rose' diagrams showing the distribution of the long-axes of microdioritic enclaves and lenticular country rock xenoliths.

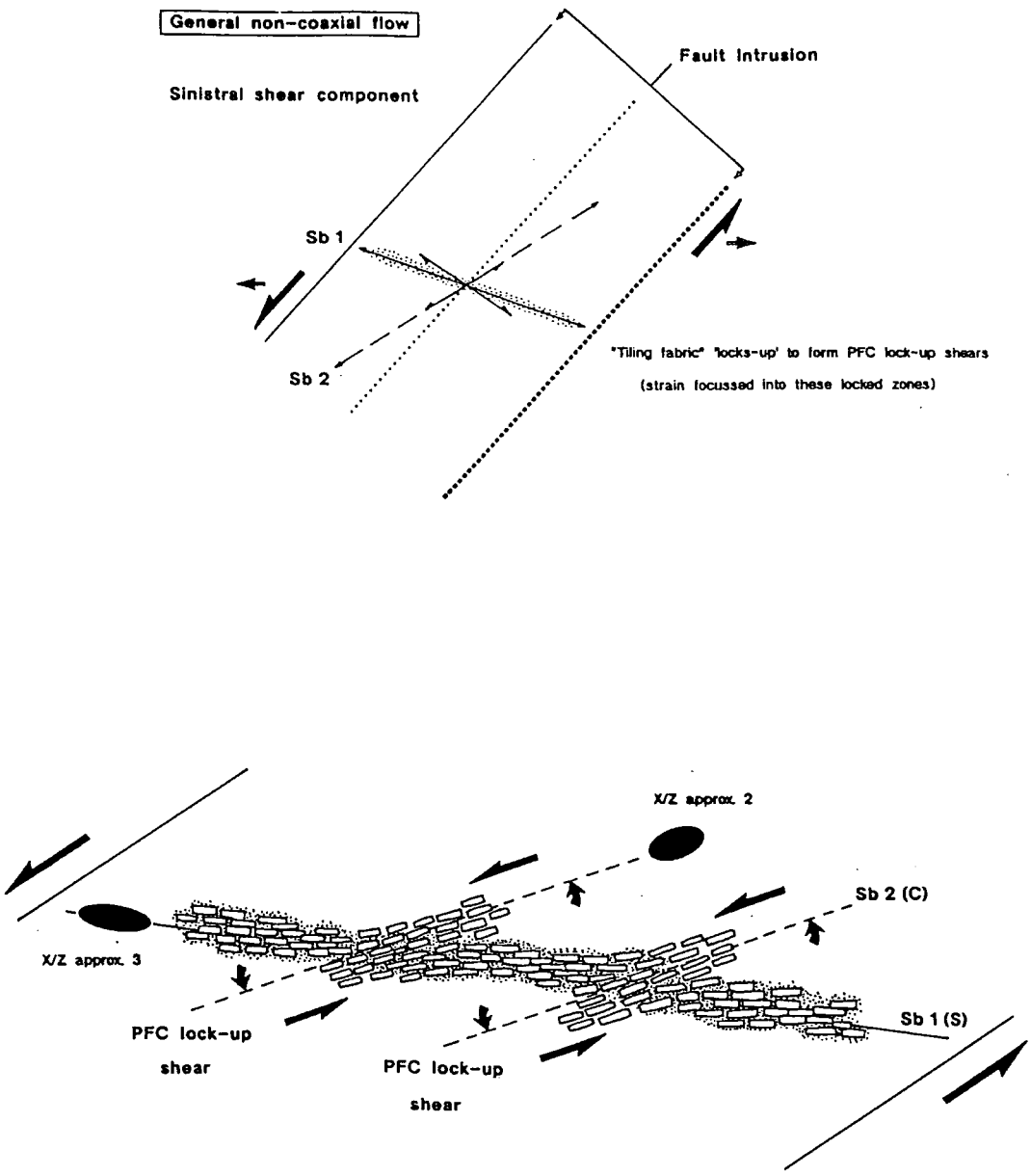

Fig. 7.7. A generalised model showing the possible development of the bimodal PFC fabric.

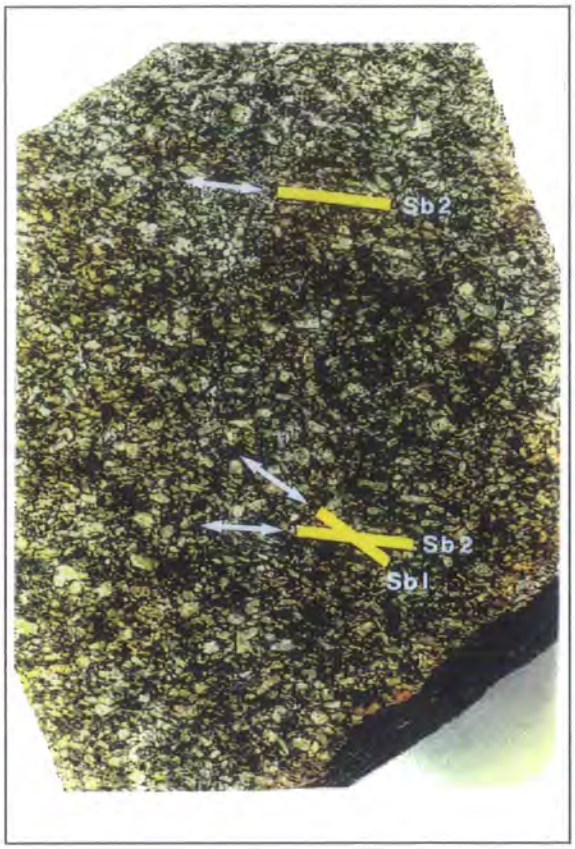

Plate 7.6. Hand-specimen of the Main Fault Intrusion (tonalitic material) from the "Coupall-Creag Dhubh-Bà unit" [NN 254 526]. It possesses a PFC bimodal fabric: Sb1, oblique 'tiling-type fabric'; Sb2, 'shear parallel' sub-fabric (see text for explanation). (Yellow 'bar' is approximately 2 cm long).

As mentioned above, the orientation of the X axis of microdioritic enclaves and lenticular country rock xenoliths may form two populations (Fig. 7.6b), one aligned sub-parallel to the "oblique tiling fabric" (generally 015-064°), and the other sub-parallel to the "shear parallel PFC lock-up microshears" (generally 140-160°). An estimate of strain from X/Z ratios of microdioritic enclaves orientated sub-parallel to the 'tiling fabric' indicate values between 2.2 and 3.1, generally higher than values recorded for enclaves aligned sub-parallel to the 'PFC lock-up microshear fabric' which give values ranging from 1.6 to 2.1 (see Fig. 7.6a). Vertical joint surfaces are extremely rare, preventing feasibly large enough populations of Y/Z ratios to be obtained for the three-dimensional analysis of these enclaves (K value determinations). However, where observed, enclaves possess elongate disc shapes ($0 < K < 1$) to plane strain shapes ($K \approx 1$).

Plate 7.7. Photomicrograph of hand-specimen shown in Plate 7.6. (Field of view approximately 18 mm).

Along both contacts of this 'body', i.e. along the inner, faulted contact, and the outer, irregular margin, a vertical, weak to moderately developed, contact parallel (or sub-parallel) PFC fabric is generally observed within a 20-30 m wide zone. A sub-horizontal stretching lineation is generally defined by amphibole laths, and to a lesser extent by biotite crystals. Moving towards the centre of the body, there does not appear to be a progressive increase in the dominance of the "oblique, tiling fabric" (see above), to produce the bimodal arrangement common throughout the central parts of the intrusion. Instead, the change is intermittent, leading to a sporadic distribution of zones possessing both sets of fabrics, with zones containing contact-parallel fabrics only (see Fig. 7.6a). The width of these zones is extremely variable, from 5-20 m across, occasionally reaching widths of 30-40 m. It is generally most commonly developed within the outer margin of the 'body'. The reason why strain should be heterogeneously distributed throughout this part of the intrusion is unclear. However, two possible reasons could be: (i) the outer contact is irregular, forming a somewhat 'en-echelon' form (see Fig. 7.7); (ii) the large number of country rock xenoliths/rafts, metres across (see below), dispersed throughout this region may have led to 'localised strain partitioning'.

Throughout this 'unit', the tonalite contains an extremely large number of both small, rectilinear country rock xenoliths (cm's across) (Plate 7.8), and large angular/sub-angular blocks of country rock and Rannoch Moor G2 (m's across) (Plate 7.9). Within the well exposed White Corries region (Fig. 7.6), an extremely high concentration of xenolithic material occurs (Plate 7.8). The smaller, rectilinear xenoliths may form two distributions

(see Fig. 7.6b), each population aligned approximately sub-parallel to one of the sets of PFC fabric which constitute the bimodal arrangement. The larger, angular blocks are more randomly orientated. The majority of the country rock xenoliths are psammitic or schist. Many of the smaller inclusions show a high degree of ductile deformation, giving them a "sheared" appearance, in which their foliation/schistosity has been modified and deflected, and occasionally exploited by granitic melt. Around a large number of the xenolithic blocks, the PFC fabric within the tonalite has been deflected to form a contact-parallel, intense PFC fabric. This may suggest that during pre-full crystallisation deformation, the shear component was locally focussed along these petrologically and rheologically defined contacts. This strain localisation is best seen within many of the blocks of Rannoch Moor G2, in which at the edges of the block the low temperature, intensely developed CPS fabric within G2 (see Ch. 5, sub-section 5.4.2.3) has been modified and rotated (Plate 7.10).

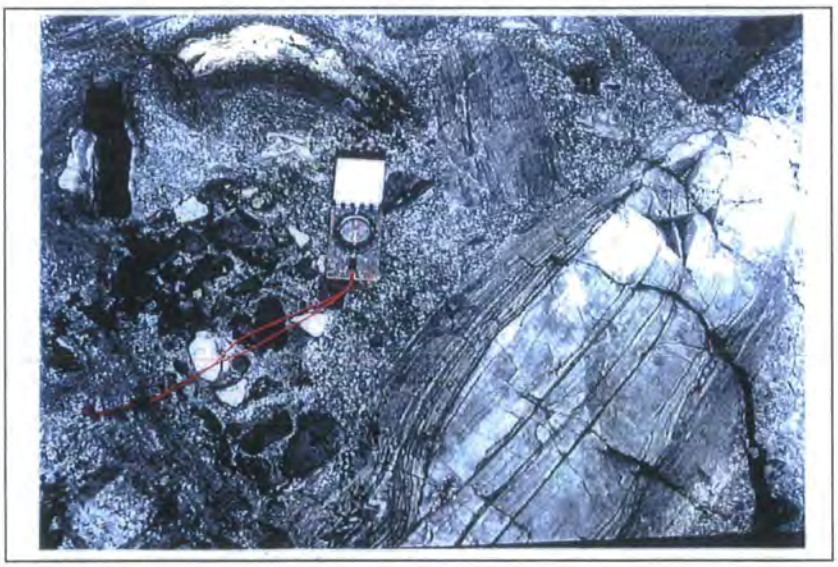

Plate 7.8. Country rock xenoliths encorporated within the "Coupall-Creag Dhubh-Bà unit" at White Corries [NN 262 522].

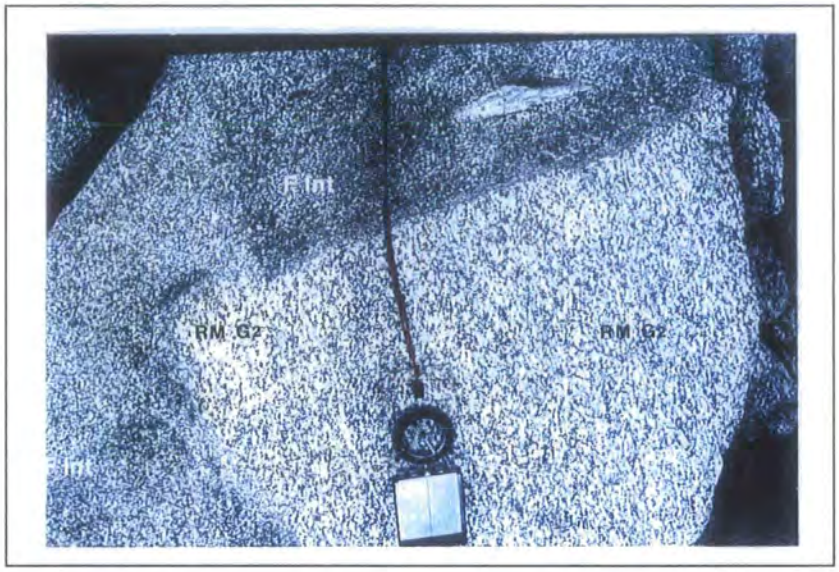

Plate 7.9. Blocks of Rannoch Moor G2 encorporated within the "Coupall-Creag Dhubh-Bà unit" [NN 257 518]. G2 possesses the 'typical' low temperature CPS fabric as seen within the Kinghouse region of the Rannoch Moor pluton (see Ch. 5, sub-section 5.4.2.3).

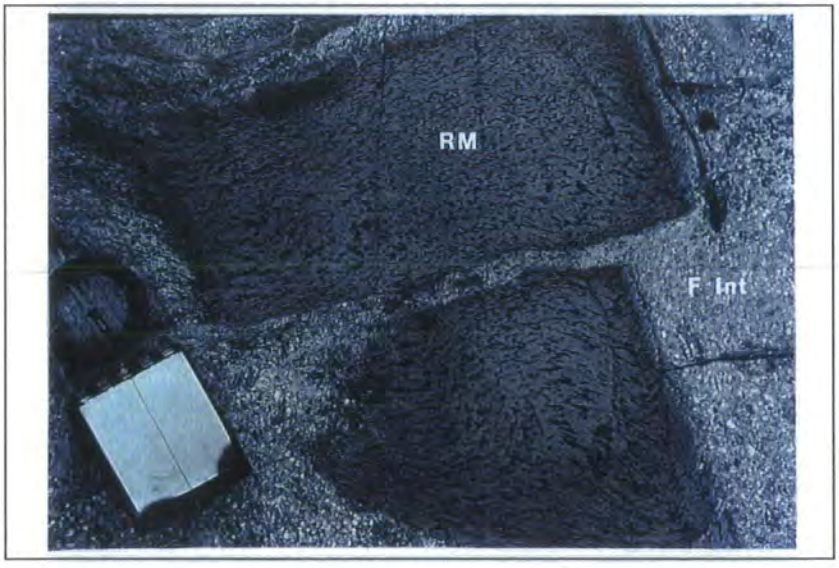

Plate 7.10. Blocks of Rannoch Moor G2 encorporated within the "Coupall-Creag Dhubh-Bà unit" [NN 262 522]. Note how the intense low temperature CPS fabric developed within G2 has been modified and rotated.

The Main Ring Fault can be observed within the several stream sections which pass down the north-eastern slope of Stob a' Ghlais Choire [NN 240 516] (Fig. 7.6). Within Càrn Ghlinne the ring fault is exposed several times, (Fig. 7.6) separating unaltered, undisturbed lavas (Lower Devonian volcanics) of the down-faulted cauldron block, and a zone of fault-rocks developed along the ring fault, from the Fault Intrusion. Moving from the unaltered lavas towards the ring fault, the fault zone can be sub-divided into two main "units" which run sub-parallel to the Main Ring Fault: (i) a 15-20 cm wide zone composed of bands (approximately 2.0-2.5 cm wide) of black "flinty crush rock" (FCR), which alternate with bands of brecciated/microbrecciated lava which are set in a matrix of FCR (Plate 7.11); and (ii) an approximately 1 m wide zone of "grey/black ultra fine-grained crush-rock", which may form a banded cataclasite. Separating the ring fault from the main phase of the Fault Intrusion is a 1.75-2.0 m wide zone of fine-grained, reddish-pink porphyrite material. This may represent a distinct intrusive phase to that of the tonalite material of the Main Fault Intrusion. This 'marginal facies' could be best described as a slightly porphyritic red felsite. No chilled margins were observed between this 'marginal phase' and the main tonalite phase of the Fault Intrusion, possibly suggesting a penecontemperaneous relationship.

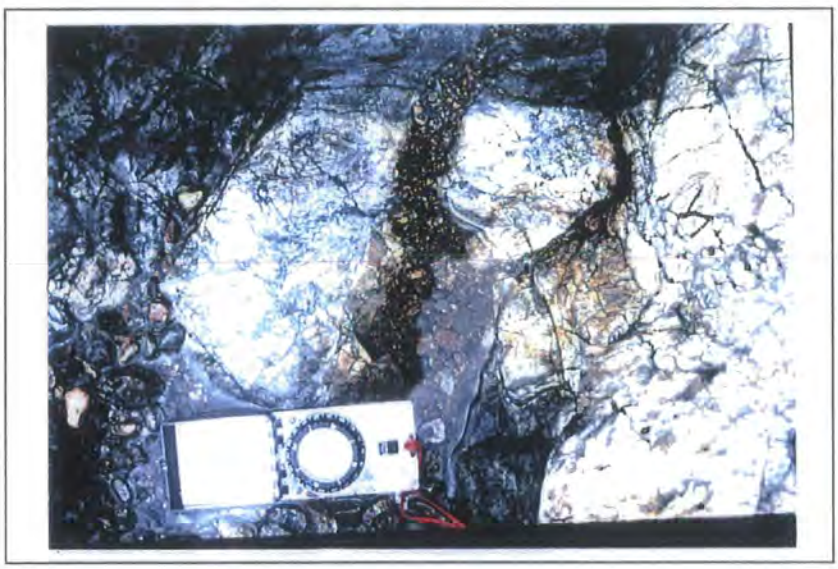

Plate 7.11. Bands of brecciated/microbrecciated lava, set in a matrix of FCR. These tend to run sub-parallel to the Main Ring Fault in the Stob a' Glais Choire area (Càrn Ghleann [NN 249 525]. (Horizontal surface).

Also exposed within the Allt Càrn Ghlinne stream section [NN 250 524] is an unusual arcuate multiple intrusion, approximately 1 m wide (Plate 7.12). This small intrusive body occurs on the down-faulted side of the ring fault, however, separated from the country rocks within the cauldron block by a band (approximately 0.5 cm, up to 1.0 cm wide) of black FCR. Petrologically this intrusion has been described by Garnham (1988), recognising four distinct intrusive phases: (i) gabbro; (ii) tonalite; (iii) porphyritic felsite (rhyolite); and (iv) aphyric felsite (rhyolite). Chilling relationships may suggest that the aphyric felsite is the oldest and the gabbro the youngest. The gabbro possesses a weak to moderately developed sub-horizontal PFC fabric, defined by plagioclase phenocrysts. The porphyritic reddish-pink felsite may be petrographically similar to the 'marginal facies' which occurs along the Main Ring Fault within this area (see above).

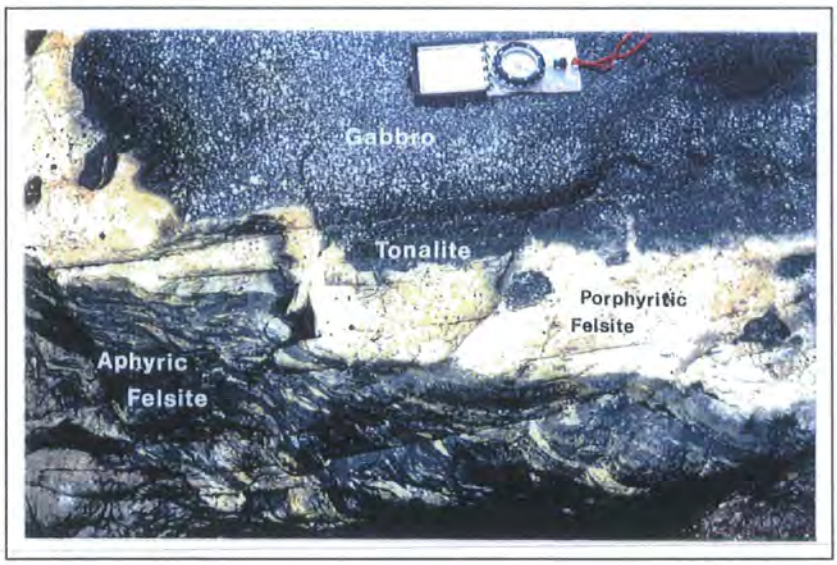

Plate 7.12. Small multiple intrusion exposed within the Allt Càrn Ghlinne stream section [NN 250 524]. See text for explanation. (Horizontal surface).

Allt Coire an Easain-River Bà region:

Further south in the Allt Coire an Easain-River Bà region (Fig. 7.6) this partial ring dyke body appears to synplutonically 'merge' with the Glencoe plutonic intrusive phase G2 (Clach Leathad facies; see Ch. 4, sub-section 4.2.2). Contact relationships are best observed within the Allt Coire an Easain river section, where a number of sheet-like bodies (approximately 0.5-1.5 m wide) of both grey porphyritic tonalite of the Fault Intrusion, and

pink/red monzogranitic material, presumably the Clach Leathad facies G2, occur (Plates 7.13 & 7.14). The sheets generally trend approximately 020°, sub-parallel to the walls of the "Coupall-Creag Dhubh-Bà unit" (Fig. 7.6). Most contacts between "G2" and the tonalitic phase of the Fault Intrusion are irregular, often exhibiting cuspate/lobate geometries. However, in certain areas it is not uncommon for sharp and planar contacts to be developed, with either phase chilling against each other. G2 may intrude the tonalite as discrete veins, and incorporate small inclusions of tonalite which sometimes show evidence of partial digestion, indicative of magma 'mingling' processes.

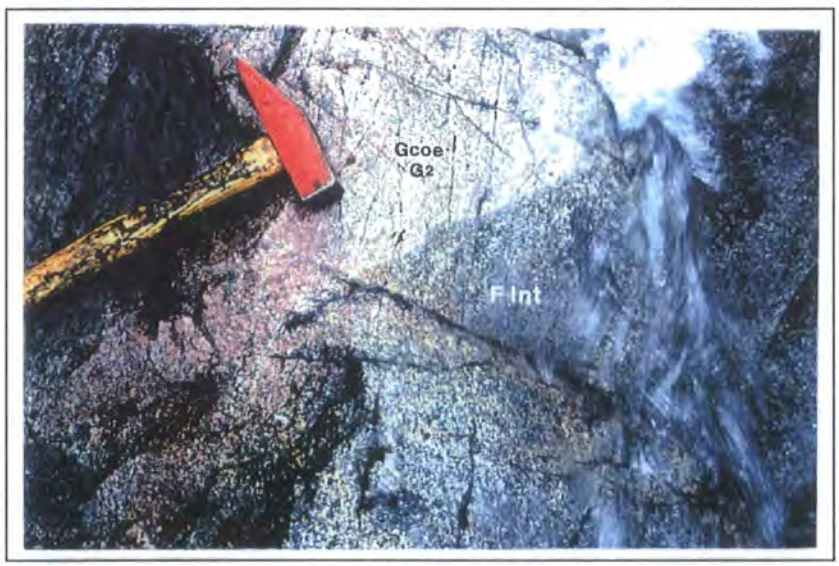

Plate 7.13. Synplutonic contact between the Main Fault Intrusion (Fint) and Glencoe G2 (Gcoe G2). No chilled contact exists in either facies. Contact relationship observed in the Allt Coire an Easain-River Bà region. (Horizontal surface).

PFC fabrics within both phases may form a bimodal arrangement. The generally weaker of the two sub-fabrics trends 020-030°, possibly contact-parallel to the 'synplutonic sheets', whereas the dominant sub-fabric is orientated around 120-135° (Fig. 7.6). The angular relationship between these two fabrics is unclear. However, moving south-westwards into the main phase of the plutonic body (G2), the 'oblique' fabric trending 120-135° intensifies, and is generally overprinted by a weak to moderately developed, high temperature, coplanar CPS fabric. This NW-SE-trending solid state overprint becomes more extensively developed moving into the Clach Leathad facies (G2). Fabric

development within this region may have been influenced by the same deformational affects as those experienced by the 'Chaorainne pulse', G2 (see Ch. 4, sub-section 4.4.2.1).

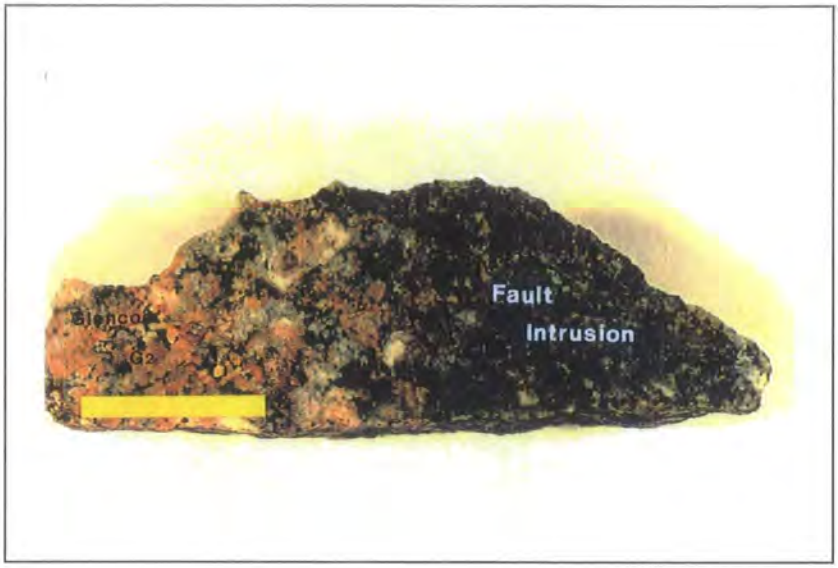

Plate 7.14. Hand-specimen showing synplutonic contact between the Glencoe Fault Intrusion and Glencoe G2 (Clach Leathad facies). (Yellow 'bar' is approximately 2 cm long).

Dip of the Main Ring Fault System bounding the "Coupall-Creag Dhubh-Bà unit"

The Main Ring Fault is exposed on the west side of Stob Beinn a' Chrùlaiste [NN 225 563] (Fig. 7.8), dipping outwards at an angle of approximately 85°. Moving south-eastwards the fault steepens and is exposed within the numerable stream sections within the Càrn Ghleann region (Fig. 7.8) where it is essentially vertical. It is again exposed for some distance in the Allt Coire an Easain section (9-10 m), possessing an inward-dip of around 69-77°.

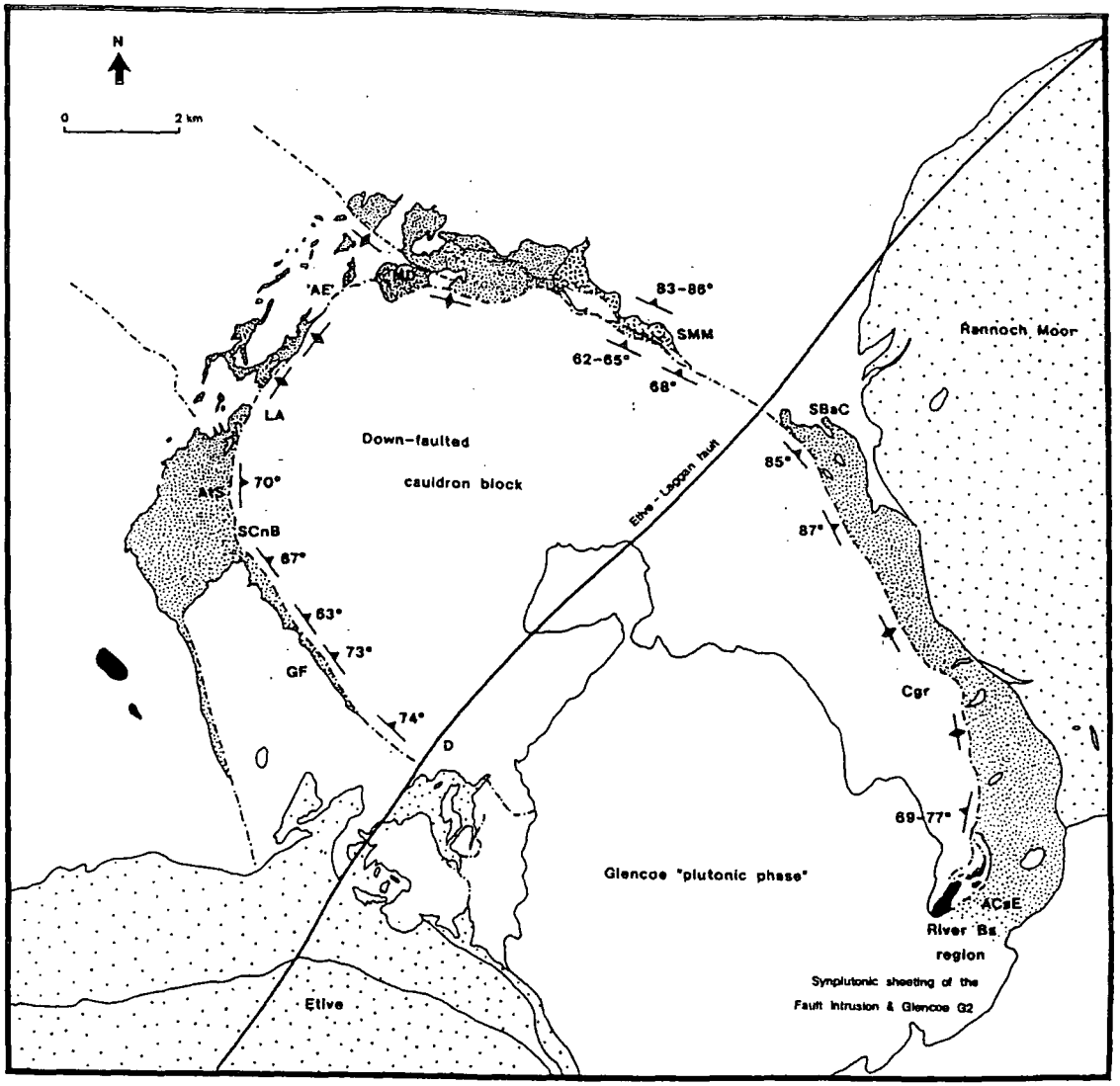

Fig. 7.8. Sketch map showing the dip of the Main Ring Fault system around the Glencoe Cauldron block. Places referred to in the text: SBaC Stob Beinn a'Chrùlaiste; Cgr Cam Ghleann region; ACaE Allt Coire an Easain; SMM Stob Mhic Mhartuin; MD Meall Dearg; 'AE' "Aonach Eagach ridge system'; LA Loch Achtnochtan; AtS An t-Sron; SCnB Stob Coire nam Beith; BnB Bidean nam Bian; GF Gleann Fhaolain; D Dalness.

7.3.2 Fabric development and strain distribution within the "Aonach Eagach-Stob Mhic Mhartuin unit"

Stob Mhic Mhartuin [NN 208 575] is the type locality for the Main Fault Intrusion and provides one of the best exposures of the Ring Fault system and associated fault-rocks (see sub-section 7.2.3; Roberts 1966b). Within this locality, both the Early and Main Fault Intrusions occur as dyke-like bodies along the outer, Early and inner, Main Ring Faults respectively (Fig. 7.9), separated by an intervening belt of quartzite. Quartzite also occurs adjacent to the inner ring fault within the Glencoe cauldron, and at the outer, irregular

margin of the Early Fault Intrusion forming the surrounding Dalradian country rocks (Fig. 7.9).

The Main Fault Intrusion

This occurs as a 30-40 m wide NW-SE-trending dyke-like body, intruded along the inner, Main Ring Fault (Fig. 7.9). This medium- to coarse-grained porphyritic tonalite (see sub-section 7.2.2) possesses a moderately developed contact-parallel PFC fabric, which generally trends 120°. This phenocryst alignment was noted by Garnham (1988) where the tonalite of the Main Intrusion is in contact with the fault-rocks of the Main Ring Fault (see Fig. 7.4). The fabric is defined by plagioclase (35-40 %), amphibole (5-11 %), and to a lesser extent by biotite (up to 18 %) phenocrysts. This preferred dimensional orientation is probably a reflection of the form of the phenocrysts, as the plagioclase crystals are generally euhedral to subhedral (3-8 mm in length), and amphibole has often a euhedral, elongate form (2.0-3.5 mm in length), whereas biotite is much less well developed, forming much smaller crystals (< 1.0 mm). They are set in an undeformed groundmass of plagioclase, quartz, and minor amounts of amphibole and biotite.

At the contact with the inner, Main Ring Fault, the contact-parallel PFC fabric, dips outwards, generally between 70-85° sub-parallel to the Ring Fault system. A sub-horizontal stretching lineation is generally defined by amphibole crystals.

This contact-parallel PFC fabric appears to be most intensely developed along the inner ring fault, within a zone which varies from a few metres, up to 5-6 m or so. However, even within this zone , a weak secondary PFC fabric trending approximately N-S (000-010°) can be identified. This bimodal PFC fabric arrangement is very similar in terms of its geometrical relationship to the ring fault, to that observed throughout the "Coupall-Creag Dhubh-Bà unit" (see sub-section 7.3.1). However, one fundamental difference is that the sub-fabric trending sub-parallel to the elongation of the intrusive body (approximately 120°), is clearly much more dominant than the set of fabrics which trend between 000-010°, oblique to the inner, Main Ring Fault and to its outer contact with the Dalradian quartzites. One possible reason, is that the Main Fault Intrusion along this part of the ring fault is only 30-40 m wide, compared to the 1-2 km wide dyke-like arcuate body which extends around the E and SE of the complex ("Coupall-Creag Dhubh-Bà unit") (Fig. 7.5). As with the latter "unit", their relationship suggests that the 'oblique' sub-fabric represents a 'tiling-type fabric' or 'imbricate' texture, whereas the contact-parallel set of fabrics (approximately 120°) form 'discrete' PFC lock-up microshears, orientated close or sub-parallel to the shear direction (see sub-section 7.3.1). This implies that the environment was one of non-coaxial deformation during full crystallisation; leading to

strain partitioning and the development of two sets of PFC fabric (Plates 7.15, 7.16, 7.17 & 7.18). The angular relationship of these sub-fabrics suggests a sinistral shear component during their development, with the shear direction (shear plane) orientated sub-parallel to the Main Ring Fault system, as seen throughout the 'Coupall-Creag Dhubh-Bà unit' to the south. A sinistral component of shear is also inferred from some of the subsidiary shears within the down-faulted cauldron block, which run sub-parallel to the Main Ring Fault (Fig. 7.9), and as mentioned by Garnham (1988) "in proximity of both ring faults at Stob Mhic Mhartuin and the ring fault at An t-Sron the strike of the within-cauldron country-rock bedding changes, such that it becomes sub-parallel. Also the dip of the bedding steepens to near-vertical, indicating cauldron subsidence". At Stob Mhic Mhartuin, country rock foliation in the quartzites within the down-faulted block changes from an orientation around 160°/75° W, to an orientation sub-parallel to the inner, Main Ring Fault (approximately 110-120°), combined with a progressive steepening (Fig. 7.9). The sense of rotation, again implies a sinistral sense of shear along the Main Ring Fault system. A similar situation may occur in the quartzites bounding the outer, Early Ring Fault. However, this is less certain due to lack of exposure. The form and internal deformational features of synthetic splays of 'flinty crush-rock' (FCR) may also suggest a sinistral sense of motion along the ring fault, in relation to the emplacement of the Main Fault Intrusion. Such a phenomenon was recognised by Garnham from a splay at Stob Mhic Mhartuin, stating that its shear structure "indicates a sinistral sense of movement, and leads to the speculation that, in addition to the down-faulting of the cauldron, strike-slip processes may have been operating".

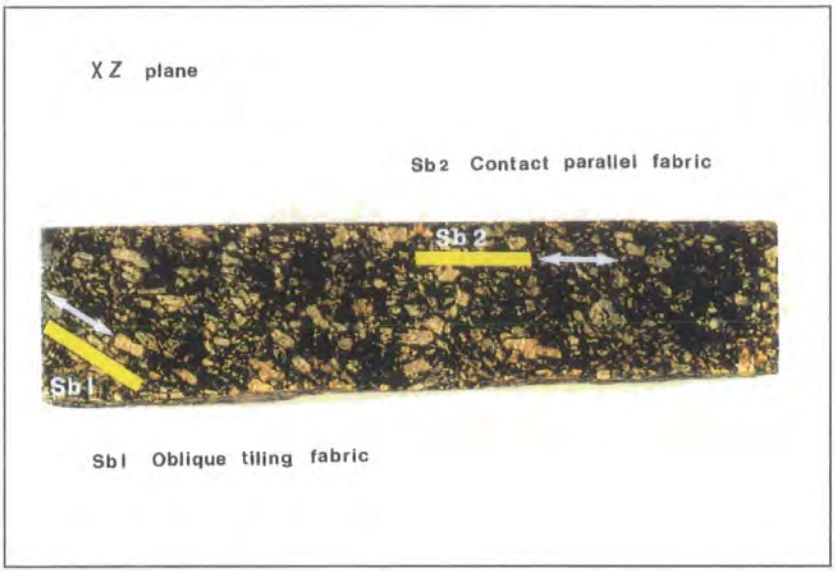

Plate 7.15. Hand-specimen of the Main Fault Intrusion from Stob Mhic Mhartuin. It possesses a PFC bimodal fabric: Sb 1, oblique 'tiling-type fabric'; Sb 2, 'shear parallel' sub-fabric (see text for explanation). (Yellow 'bars' are approximately 2 cm long).

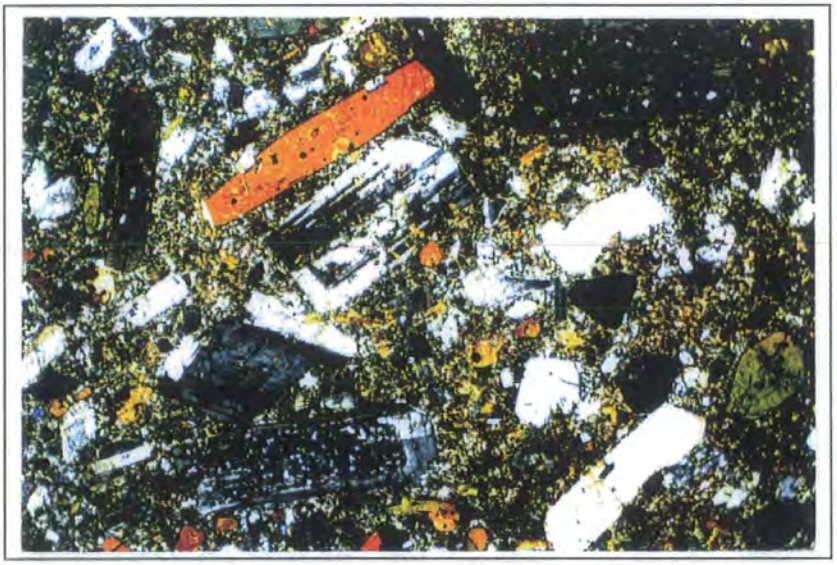

Plate 7.16. Photomicrograph of hand-specimen shown in Plate 7.15. (Field of view approximately 18 mm).

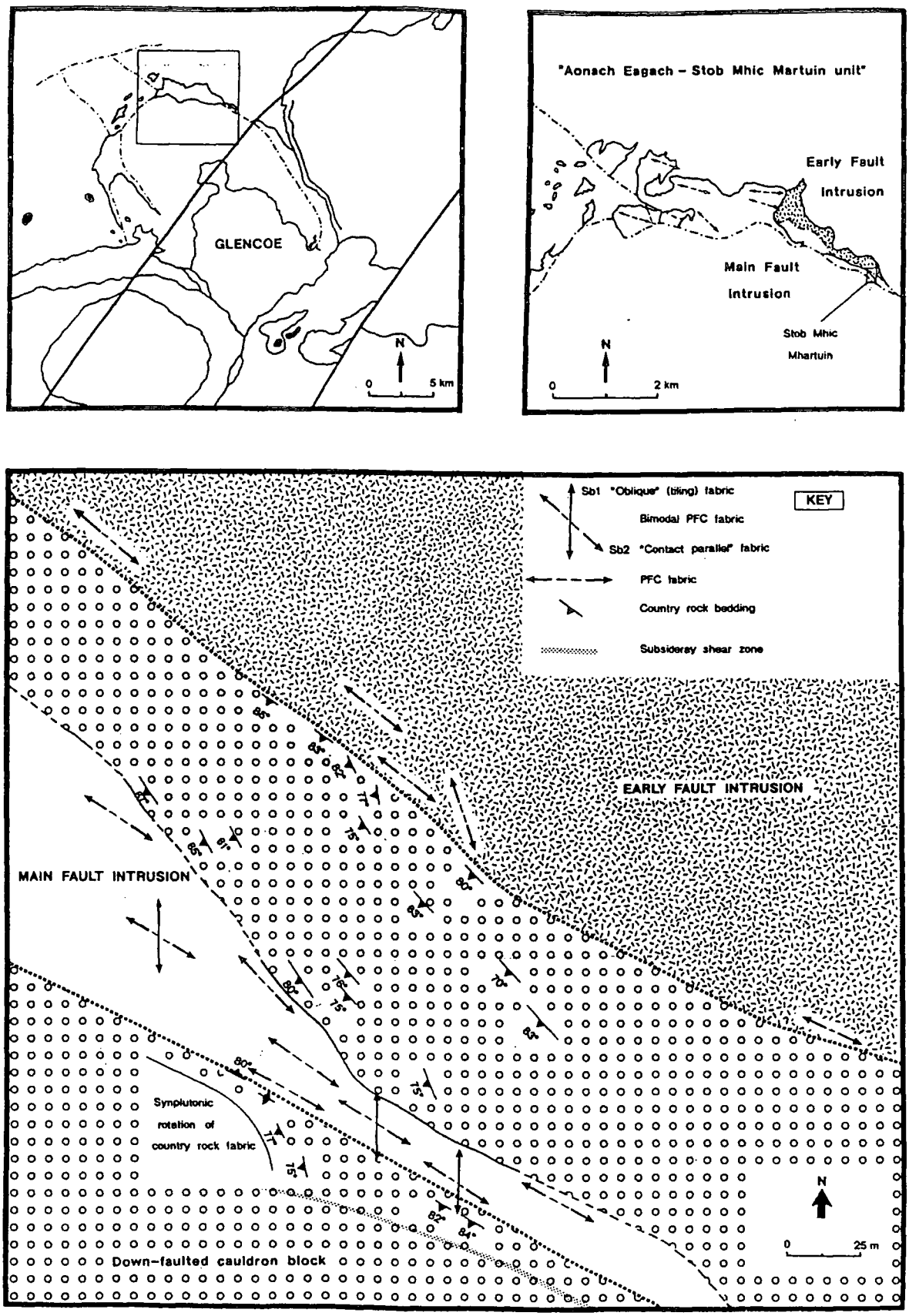

Fig. 7.9. Sketch map of Stob Mhic Mhartuin showing the distribution of fabrics within both the Early and Main Fault Intrusions, the orientation of regional fabrics, and structures associated with the Ring Fault System. Insets show location of Stob Mhic Mhartuin.

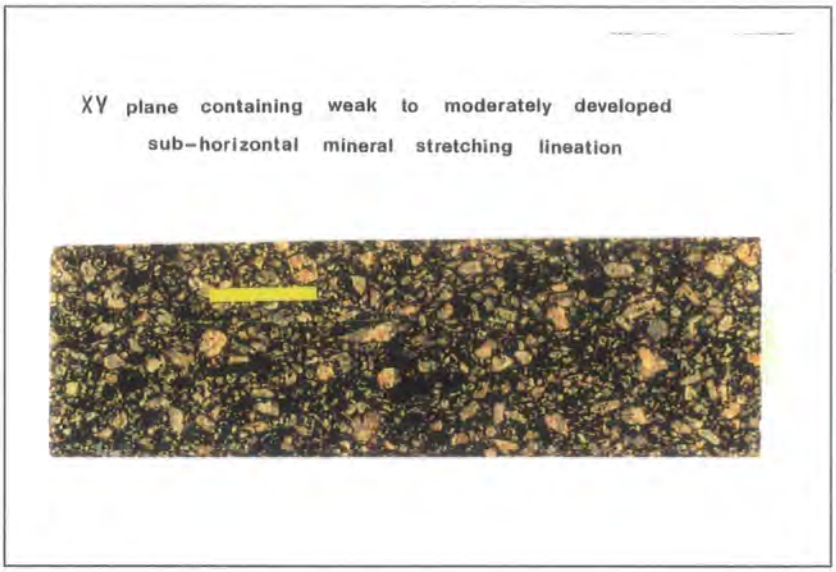

Plate 7.17. Hand-specimen of the Main Fault Intrusion from Stob Mhic Mhartuin. "XY plane" of hand-specimen shown in Plate 7.15. It contains a weakly developed sub-horizontal mineral stretching lineation. (Yellow 'bar' approximately 2 cm long).

The Early Fault Intrusion

This phase is generally 40-50 m wide, occurring as an irregular dyke-like mass along the outer, Early Ring Fault (Fig. 7.9). This fine- to medium-grained porphyry is compositionally very similar to the tonalitic phase of the Main Fault Intrusion. However, the striking difference between the two phases, is that this phase (i.e. the "Early" Fault Intrusion) is generally highly altered by hydrothermal veining and pervasive fracturing, with many of these brittle fractures infilled by "flinty crush rock" (FCR; see sub-section 4.2.1.1). This has led many workers (e.g. Clough *et al.* 1909; Garnham 1988) to conclude that this outer intrusion has intruded and crystallised prior to movements along the Main Ring Fault system. Two main observations made during this study to substantiate that this outer body represents a distinct earlier intrusive phase, are: (i) it has been cross cut by dyke-like and irregular masses of red felsite (Fig. 7.9) which possess chilled contacts against the Early Fault Intrusion, but synplutonic relationships with the later, Main Fault Intrusion; and (ii) it possibly possesses a weak PFC fabric which is contact-parallel to the outer, Early Ring Fault (Plate 7.18). However, this has been modified by a solid state deformation which is represented by bent and kinked biotite laths, with many plagioclase phenocrysts broken, indicating low temperature (< 450°C; Simpson 1985) CPS

deformation (Plate 7.19). This may suggest that this intrusive phase had crystallised and cooled significantly, prior to the emplacement of the Main Fault Intrusion.

Within the north of the complex, along the "Aonach Eagach ridge system" a number of irregular, isolated bodies of the Main Fault Intrusion occur (Fig. 7.9). They are extremely variable in composition, ranging from porphyroid to granitoid varieties. Most contain a weak to moderately developed, steep PFC fabric, which generally trends sub-parallel to the Main Ring Fault system.

Dip of the Early and Main Faults bounding the "Aonach Eagach-Stob Mhic Mhartuin unit"

As shown in Figure 7.9, at Stob Mhic Mhartuin [NN 208 575] the outer, Early Ring Fault has an outward-dip of between 83-86°, whereas the inner, Main Ring Fault has a slightly less steep outward-dip of generally 62-65° (up to 85° in places). Moving northwards to Meall Dearg [NN 162 583], both faults are generally vertical. However, the outer, Early Ring Fault is generally obscured by the subsequent intrusion of isolated bodies of the Main Fault Intrusion, and in several places many have been steepened by this event. From Meall Dearg (see Fig. 7.8), the Main Ring Fault passes down from the "Aonach Eagach ridge system" towards Loch Achtnochtan [NN 141 568]. It is exposed several times, and is essentially vertical.

Plate 7.18. Hand-specimen of the Early Fault Intrusion from Stob Mhic Mhartuin, showing a weakly developed fabric. (Yellow 'bar' is approximately 2 cm long).

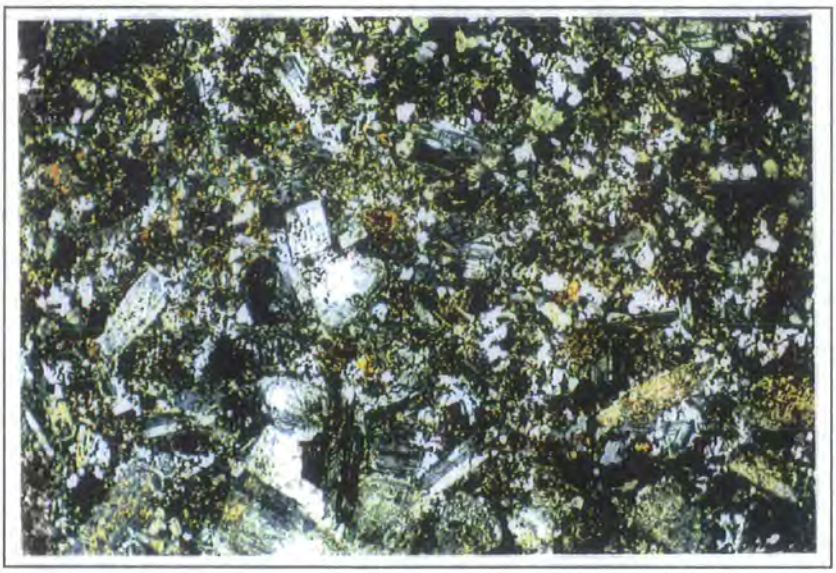

Plate 7.19. Photomicrograph of hand-specimen shown in Plate 7.18. Shows extensive modification by a low temperature solid state overprint. Compare with Main Fault Intrusion (Plate 7.16). (Field of view approximately 18 mm).

7.3.3 Fabric development and strain distribution within the An t-Sron mass

The An t-Sron mass is much wider than the rest of the Fault Intrusion (Fig. 7.10), and appears to be much more compositionally diverse (see sub-section 7.2.2). Fabric determination and strain distribution within this body was mainly achieved along the Fionn Ghleann stream section and its associated tributaries. These sections provided information regarding the tonalitic phase within the centre of the mass.

The tonalite possesses weak to moderately developed bimodal PFC fabrics (Plate 7.20) very similar to those observed within the 'Coupall-Creag Dhubh Bà' (sub-section 7.3.1) and 'Stob Mhic Mhartuin' (sub-section 7.3.2) bodies. However, within the An t-Sron mass, there is a greater diversity in the orientation of the fabrics throughout the body (see Fig. 7.10). Even with this complexity, two predominant fabric sets may occur: one set of fabrics generally trend 030-060°, and the other sub-
fabric is generally orientated 120-142° (Fig. 7.10a). As in the 'Coupall-Creag Dubh Bà unit', country rock xenoliths of generally pelite and quartzite may form two populations aligned sub-parallel to each sub-fabric direction (Fig. 7.10b). However, field observations of the dominance of the two sub-fabrics relative to each other, and microstructural analysis suggests that in general there may be a difference in distribution of fabric types within the north and south of the body. In the north (e.g. [NN 123 552]), the fabric set which trends approximately NW-SE (120-142°) dominates, generally forming a 'tiling-type fabric' or

'imbricate' texture, whereas the secondary, weaker fabric orientated NE-SW (030-060°), is often seen forming discrete, PFC 'lock-up microshears'. In the south (e.g.[NN 126 542]), this relationship is reversed, with the 'tiling-type fabric now orientated NE-SW, and the PFC 'lock-up microshear fabric' trending NW-SE (Fig. 7.10a). In both cases, the apparently more dominant sub-fabric in hand-specimen is the 'tiling-type fabric'.

The angular relationship of these two sub-fabrics suggests a sinistral shear component during pre-full crystallisation. This is consistent with the relationships observed within the 'Coupall-Creag Dhubh Bà unit' in particular (see sub-section 7.3.1). However, the difference in the orientation of the two 'types' of fabric in the north and south of this body may reflect the orientation of the Main Ring Fault system in relation to these two zones. In the northern part of An t-Sron mass the orientation of the Main Ring Fault moving northwards progressively changes from a NW-SE direction to a NE-SW trend. The orientation of the PFC 'lock-up microshear fabric' within this region may indicate that the shear direction was orientated approximately NE-SW, aligned sub-parallel to the Main Ring Fault in the northern part of the mass (Fig. 7.10a). Whereas, in the 'southern zone' the PFC 'lock-up microshear fabric' suggests that the shear direction was orientated NW-SE, which would be orientated sub-parallel to the Main Ring Fault system with this part of the region (Fig. 7.10a). In the central part of the intrusion, between these two 'zones', the relative dominance of a set of sub-fabrics, and the type of fabric they may represent, changes quite considerably, generally over distances of 25-35 m. This may indicate that this area represents a zone where there was interference between the two respective strain fields established within the north and south of the complex. This hypothetical solution accounting for the heterogeneous strain distribution throughout this part of the body. Another possible reason is the large amount of country rock xenoliths within this part of the mass. Some of the blocks are metres across, possibly leading to localised strain partitioning.

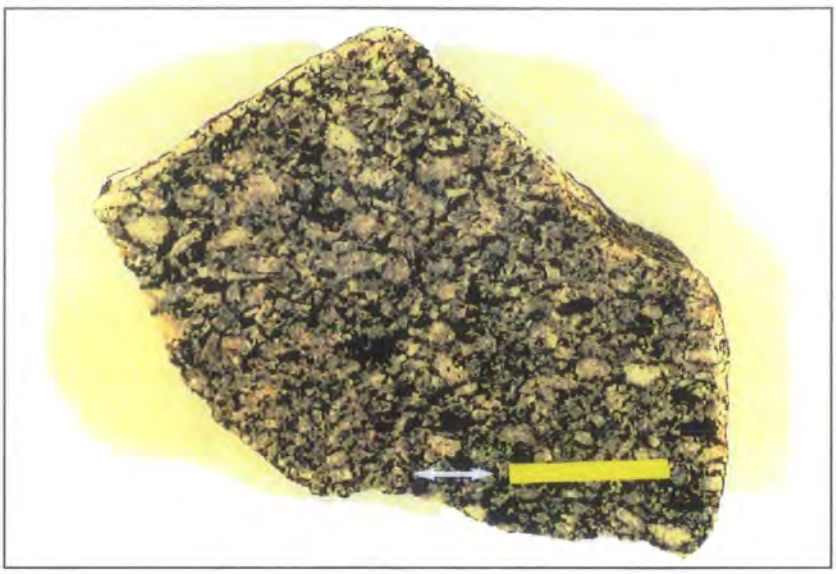

Plate 7.20. Hand-specimen of the Main Fault Intrusion from the An t-Sron mass. It possesses a moderately developed PFC fabric. An extremely weak 'secondary' PFC sub-fabric occurs, but can only be identified in thin-section. (Yellow 'bar' is approximately 2 cm long).

Towards the western margin of the body there is a gradual increase in the concentration of country rock xenoliths. The outer contact marked on the British Geological Survey Sheet 53 is conjectural, as no 'defined' contacts occur between the Fault Intrusion and the surrounding country rock as seen along the majority of the Main Fault Intrusion, i.e. along the 'Coupall-Creag Dhubh Bà unit' and at Stob Mhic Mhartuin. Instead, an "intricate intrusion complex" occurs involving transtensional sheeting.

A number of NE-SW-trending Etive dykes cross cut the An t-Sron mass. Contact relationships such as cuspate/lobate geometries, and the way some porphyrite dykes have synplutonically deflected the PFC fabric within their host, suggests that an early phase of porphyrite dykes were intruded into this region before the tonalitic phase of the Main Fault Intrusion had fully crystallised. This time relationship may be similar to that observed within the Glencoe plutonic phase, G2 (Clach Leathad facies; see Ch.'s 4 & 8).

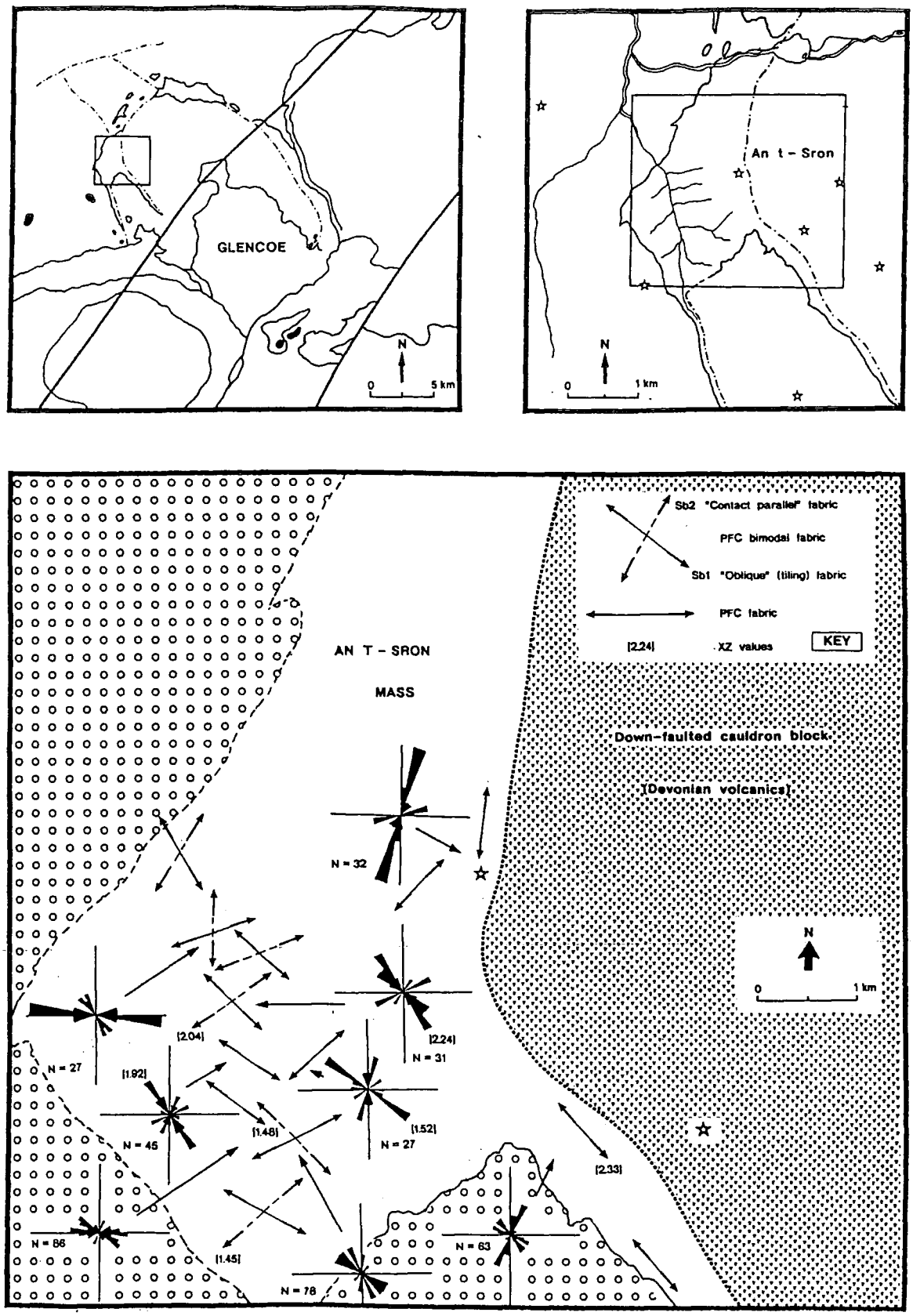

Fig. 7.10. Sketch map shows the distribution of PFC bimodal fabrics within the An t-Sron mass, together with strain values and 'rose' diagrams which show the distribution of the long-axes of lenticular country rock xenoliths and the occasional microgranitoid enclave.

Throughout the western margin, and to a lesser extent within the central parts of the An t-Sron mass, evidence for a process of multiple sheeting as a mechanism of construction is clearly evident. Particularly within the western parts of the body, a number of strike-parallel bands of pelitic country rock xenoliths ("raft trains") can be traced back into the surrounding country rocks, showing that they are in structural continuity. To the north of the main An t-Sron mass, an easily accessible section showing such features is seen within the River Coe [NN 135 567]. At this locality, the strike-parallel zones of pelitic xenoliths trend approximately 168°, sub-parallel to the country rock schistocity (around 172°) within the surrounding country rock (Plates 7.21 & 7.22). The width between the pelitic bands is on average approximately 0.75-1.0 metres. Whether this is the width of an individual sheet is unclear, because chilled margins are not observed, with many of the sheets appearing to coalesce. Such features may suggest that the multiple intrusion of petrographically similar sheets possessing high melt contents, may result in physical and chemical mixing across their boundaries (Pitcher & Berger 1972). Such a process causing multiple sheets to coalesce, resulting in the appearance of a relatively homogeneous body (see Hutton 1992).

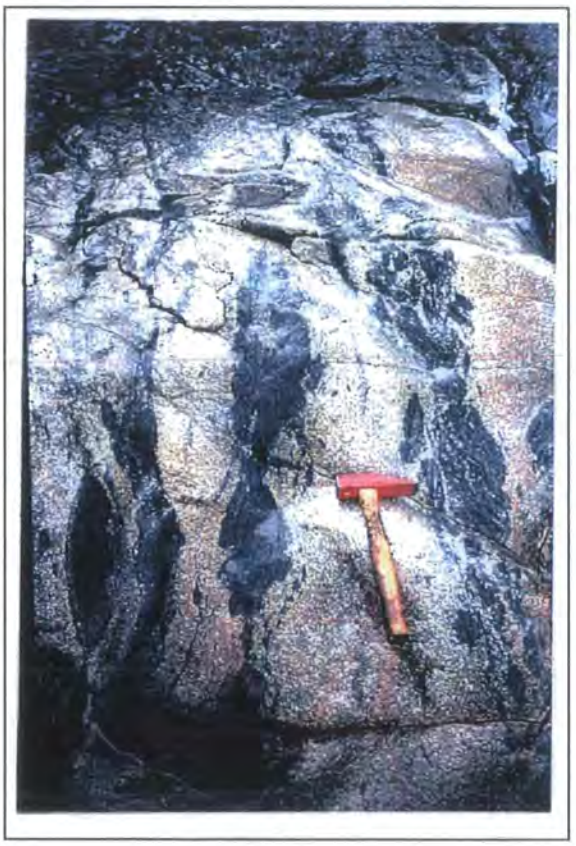

Plate 7.21. Strike-parallel zones of pelitic country rock xenoliths exposed within the River Coe section. (Horizontal surface).

Along the River Coe section, two 'sets' of PFC fabric can be identified: one set trending approximately N-S (165-176°), and the other set orientated roughly E-W (around 094°). They do not occur as a bimodal arrangement, but appear to occur separately, changing from one direction to the other, what appears to be 'instantaneously'. Both fabric sets are weak to moderately developed, and defined by the general alignment of small, lenticular country rock xenoliths. At one particular locality [NN 134 566], where the PFC fabric and bands of pelitic xenolith trend approximately 172°, a psammite xenolith appears to have been fragmented, and the resultant 'units' (about 5 cm x 4 cm) synplutonically rotated. The 'units' appear to show antithetic slip on fracture planes orientated approximately 040°, which were melt-filled as they were being transtensionally pulled-apart. These features may suggest a sinistral transcurrent component.

Plate 7.22. Closer view of Plate 7.21. Note, the pelitic bands have "pinch" and "swell" type geometries.

Dip of the Main Ring Fault System bounding the An t-Sron mass

From An t-Sron, through Stob Coire nam Beith, to Bidean nam Bian, the Main Ring Fault is easily recognisable due to the presence of a 30-40 cm wide 'marginal facies' of red felsite (see sub-section 7.2.3). The inclination of the fault varies from 60-87°, and is always inwardly-dipping. The fault can be traced from Bidean nam Bian south-eastwards along the northern slopes of Gleann Fhaolain towards Dalness [NN 167 512] (see Fig. 7.8), and continues to inwardly-dip at angles between 60-82°. Near Dalness, the Main Ring Fault does not continue south-eastwards, but appears to have been cross cut by the Etive Cruachan facies (G2; see Ch. 3), as noted by Anderson (1937). The Cruachan facies also intrudes and metamorphoses the Main Fault Intrusion within this region (Bailey 1960). However, in the SE of the Glencoe complex, the Main Fault Intrusion possesses a synplutonic relationship with the Glencoe plutonic phase, G2 (Clach Leathad facies; see Ch. 4). Bailey (1960) reported a gradational contact between these two intrusive phases, several hundred metres wide. These relationships led Perkins (1986) to suggest that the Glencoe plutonic phase (G2) is contemporary with the Glencoe Fault Intrusion, while at least a part of the Etive Cruachan facies (G2) is later. This view is endorsed by this present study.

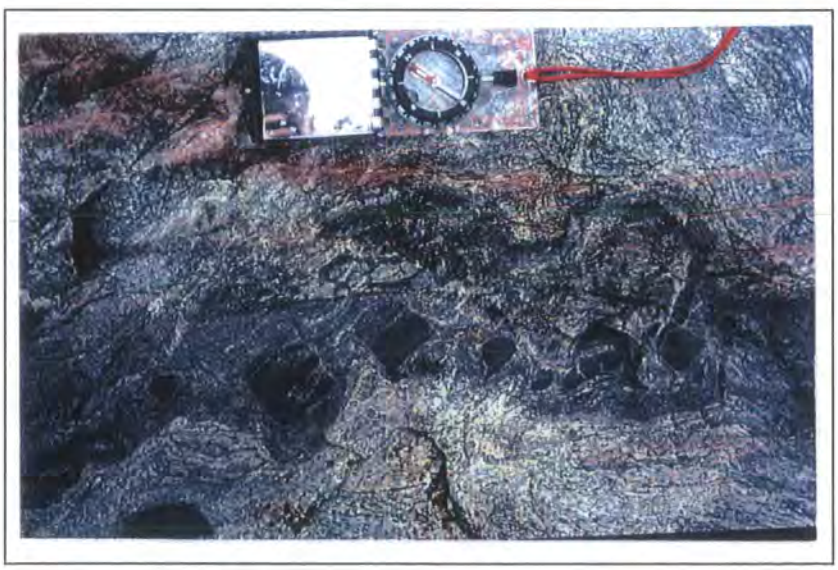

Plate 7.23. Country rock xenolith(s) which appear to have been fractured, and the resultant 'units' synplutonically rotated (see text) within the River Coe section. (Horizontal surface).

7.4 EMPLACEMENT MODEL PROPOSED FOR THE CONSTRUCTION OF THE GLENCOE FAULT INTRUSION

Summary of the main internal and associated external deformational features of the Glencoe Fault Intrusion: implications for its emplacement.

❶ Several features indicate that the outer, "Early" Fault Intrusion is in fact a distinct, earlier intrusive phase, compared to the intrusive bodies which constitute the Main Fault Intrusion (Clough *et al.* 1909): (i) the Early Fault Intrusion has been extensively altered by hydrothermal veining and pervasive fracturing, with many brittle fractures being infilled by "flinty crush rock" (FCR). Such features are likely to have been formed due to movements along the Main Ring Fault system during contemporaneous emplacement of the Main Fault Intrusion, as this later intrusive phase shows little sign of such brittle deformation; (ii) the Early Fault Intrusion appears to have been modified by a low temperature CPS deformation, probably associated with the emplacement of the Main Fault Intrusion; and (iii) cross cutting dyke-like and irregular bodies of red felsite possess chilled contacts against the Early Fault Intrusion, but synplutonic relationships with the later, Main Fault Intrusion.

It is therefore concluded that the Early and Main Fault Intrusions do indeed represent two major, distinct intrusive episodes, emplaced during cauldron subsidence along the Early and Main Ring Fault systems respectively.

❷ The FCR and associated fault-rocks developed along the Main Ring Fault system are likely to have been generated simultaneously with the emplacement of the Main Fault Intrusion. Garnham (1988) concluded that the FCR essentially represents a hybrid zone, where there was a progressive mixing between cataclasite and the marginal facies of red felsite (see sub-section 7.2.3), and it was observed within this study that the red felsite possesses syn-plutonic relationships with the Main Fault Intrusion, indicating that processes, i.e. movements along the Ring Fault system, generation of fault-rocks, and emplacement of both the marginal facies and main phase of the Main Fault Intrusion, must have been closely related in time and space.

❸ A number of kinematic indicators suggest that in addition to down-faulting, a significant sinistral strike-slip component occurred along the Main Ring Fault system during the cauldron subsidence process. A number of independent shear

sense criteria have been identified: (i) Within the down-faulted cauldron block, narrow shear zones (generally between 4-7 cm wide) of shattered and brecciated quartzite run sub-parallel to the Main Ring Fault. Some of these subsidiary shears exhibit internal deformational characteristics indicative of sinistral shear; (ii) The form and internal deformational features of synthetic splays of FCR may suggest a sinistral sense of motion along the Main Ring Fault system; (iii) In the surrounding country rocks, within the matrix of marginal breccias developed in the more pelitic-rich quartzites, biotite is bent, kinked and often forms highly elongate swathes. The biotite may wrap around lenses of recrystallised quartz in a sigmoidal fashion, indicating a sinistral sense of shear; (iv) Quartz ribbons within the down-faulted country rocks, indicate a component of sinistral shear parallel to the Main Ring Fault; (v) In several places, within-cauldron country rock bedding appears to have been syn-plutonically rotated in a sinistral fashion to become sub-parallel to the Main Ring Fault. A similar situation may have occurred along the Early Ring Fault system; (vi) The Main Fault Intrusion generally possesses a moderately developed, bimodal PFC fabric. One set is usually orientated oblique to the Main Ring Fault and to its outer contact with the Dalradian metasediments, forming a 'tiling-type fabric' or 'imbricate' texture. The other set is sub-parallel to the elongation of the intrusion and the Main Ring Fault, and may form discrete PFC 'lock-up microshears' orientated close or sub-parallel to the shear direction. This implies that the environment was one of non-coaxial deformation during pre-full crystallisation; leading to strain partitioning and the development of two sets of PFC fabric. The angular relationship of these sub-fabrics suggests a sinistral shear component during their development, with the shear direction orientated sub-parallel to the Main Ring Fault system; (vii) Even the overall 'crude en-echelon form' of the "Coupall-Creag Dhubh Bà dyke-like body" (Fig. 7.11) suggests that it was emplaced within a sinistral shear regime. Such 'en-echelon geometries' are common on a much smaller scale, with the emplacement of the Etive Dyke Swarm (see Ch. 8).

❹ Strike-parallel zones of pelitic xenoliths may suggest that the Main Fault Intrusion was constructed by a process of multiple sheeting.

❺ It is concluded from this study that the country rocks adjacent to the outer contact of the Fault Intrusion have been strongly sheared, resulting in the sharp and non-transitional contact between the FCR and the "microbreccia" (cataclasite). This is in contrast to the inner ring fault contact, in which the FCR and cataclasites/microbreccias form a transitional zone of fault-rocks. The zone of

brittle deformation along the outer contact is also generally less than half the width seen at the inner ring fault contact, leading to the same conclusions made by Clough *et al.* (1909) and Roberts (1966b), that such features indicate that there was a difference in temperature of the country rocks on either side of the Main Ring Fault system, with country rocks at the outer contact being thermally metamorphosed by the Fault Intrusion, whereas rocks within the down-faulted mass remained cold and relatively unaffected. These features may suggest that the Fault Intrusion was constructed by a process of multiple sheeting/dyking along the outer parts of the Ring fault system. With increasing amounts of tonalitic material, the temperature of the outer, country wall rocks would have progressively risen, consequently leading to an increase in the relative amount of ductile deformation the outer wall rocks could accommodate. This may explain the large amount of Dalradian metasedimentary xenoliths and blocks of Rannoch Moor G2, as in the initial stages of emplacement the outer wall rocks would have been relatively cold, leading to brittle-type processes dominating, such as stoping. However, with increasing input of hot magma at the outer contact there was a progressive increase in ductile flow type processes as a mechanism of creating space. Although such ductile bulk wall rock shortening was probably an extremely important mechanism in creating space, the spatial distribution of the largest igneous bodies of the Main Fault Intrusion occur within the NW (An t-Sron mass) and SE ("Coupall-Creag Dhubh Bà unit") of the complex, corresponding to the theoretical 'extensional quadrants' which could be produced in an overall, regional, sinistral transtensional environment (Fig. 7.11). It is interesting to note that the outer contact of An t-Sron mass forms an "intricate intrusion complex", involving transtensional sheeting. It is proposed that such an extensional regime prevailed around this time, as shown by the emplacement of Rannoch Moor G4 (see Ch. 5, sub-section 5.4.4) and the subsequent emplacement of the NE-SW-trending Etive Dyke Swarm (Morris & Hutton 1993; see Ch. 8). An early, porphyrite phase of the Etive Dyke Swarm has clear synplutonic relationships with the main phase of the Main Fault Intrusion. Rannoch Moor G4 forms a sheet-like body intruded between the "Coupall-Creag Dhubh-Bà unit" of the Main Fault Intrusion and Rannoch Moor G2, and possess synplutonic relationships such as slight lobate/cuspate geometries with dykes of the Etive Swarm.

Model Proposed

The mechanisms operating during the construction of the Early Fault Intrusion remain unclear due to: (i) its limited occurrence; and (ii) internal deformation features related to its emplacement were probably overprinted and/or obliterated by movements along the Main Ring Fault System and the subsequent emplacement of the Main Fault Intrusion. However, its spatial distribution along the Early Ring Fault, form and the preservation in certain areas of a weakly developed, generally contact-parallel PFC fabric, may suggest that the mechanisms operating to create space for its emplacement were very similar to those operating during the construction of the Main Fault Intrusion (see below).

It is envisaged that expansion-related strains related to the construction of the Glencoe plutonic complex (Clach Leathad facies, G2; see Ch. 4) were accommodated within the overlying cover rocks by the development of volcanotectonic faults and a small, but significant amount of roof updoming (see Ch. 11). These expansion-related strains causing an upward directed uniaxial pressure, leading to the formation of ring faults with 'cone fracture-type' geometries, thus, resulting in the crustal block having an overall form of an upward-opening cone. During a regional transtensional phase, and/or the result of a period of reduced magmatic pressure beneath the block, the block subsided, leading to the emplacement of the Main Fault Intrusion along parts of the peripheral ring fault structure. The Glencoe complex, as a whole, is bisected by the NE-SW-trending Etive-Laggan shear zone (see Ch. 4) and is essentially bounded to the north and south by major NE-SW-trending structures, which have been shown in previous chapters to have been operating as major sinistral shear zones during this period of magmatism. It is proposed that sinistral transcurrent motion along these NE-SW-trending structures resulted in a small, but "gross sinistral rotational component" along the Main Ring Fault System during the cauldron subsidence process (see Fig. 7.11).

Within the SE of the complex (along the River Bà), synplutonic sheeting of the main phase of the pluton (G2) and tonalitic material of the Main Fault Intrusion is clearly visible. This indicates that the development of this high level emplacement phenomena must have occurred simultaneously with the main phase of pluton construction. As the cauldron block subsided into the plutonic body below, magma was 'forcibly' intruded by a process of multiple sheeting along parts of the Main Ring Fault, initially creating space for itself by encorporating xenolithic blocks of country rock, probably produced prior to this event by explosive volcanic activity (see "The formation of the Flinty Crush Rock", sub-section 7.2.3). With increasing input of hot magma against the outer contact of the intrusion, ductile flow type processes within the adjacent country rocks as a mechanism of space creation became progressively more dominant. The overall, regional, sinistral transtensional regime established during this event may explain the spatial distribution of

the Main Fault Intrusion (see Fig. 7.11). The largest intrusive bodies, i.e. the An t-Sron mass and the "Coupall-Creag Dhubh-Bà unit", may have been constructed in two corresponding zones undergoing a large component of extension created by sinistral transcurrent motion along the bounding shear zones (Fig. 7.11). Outside these zones, the bounding shear zones may have imposed a somewhat 'contractional' component to the ring fault system, explaining why along this part of the peripheral ring fault system, tonalite occurs as small, isolated discontinuous sheet-like bodies.

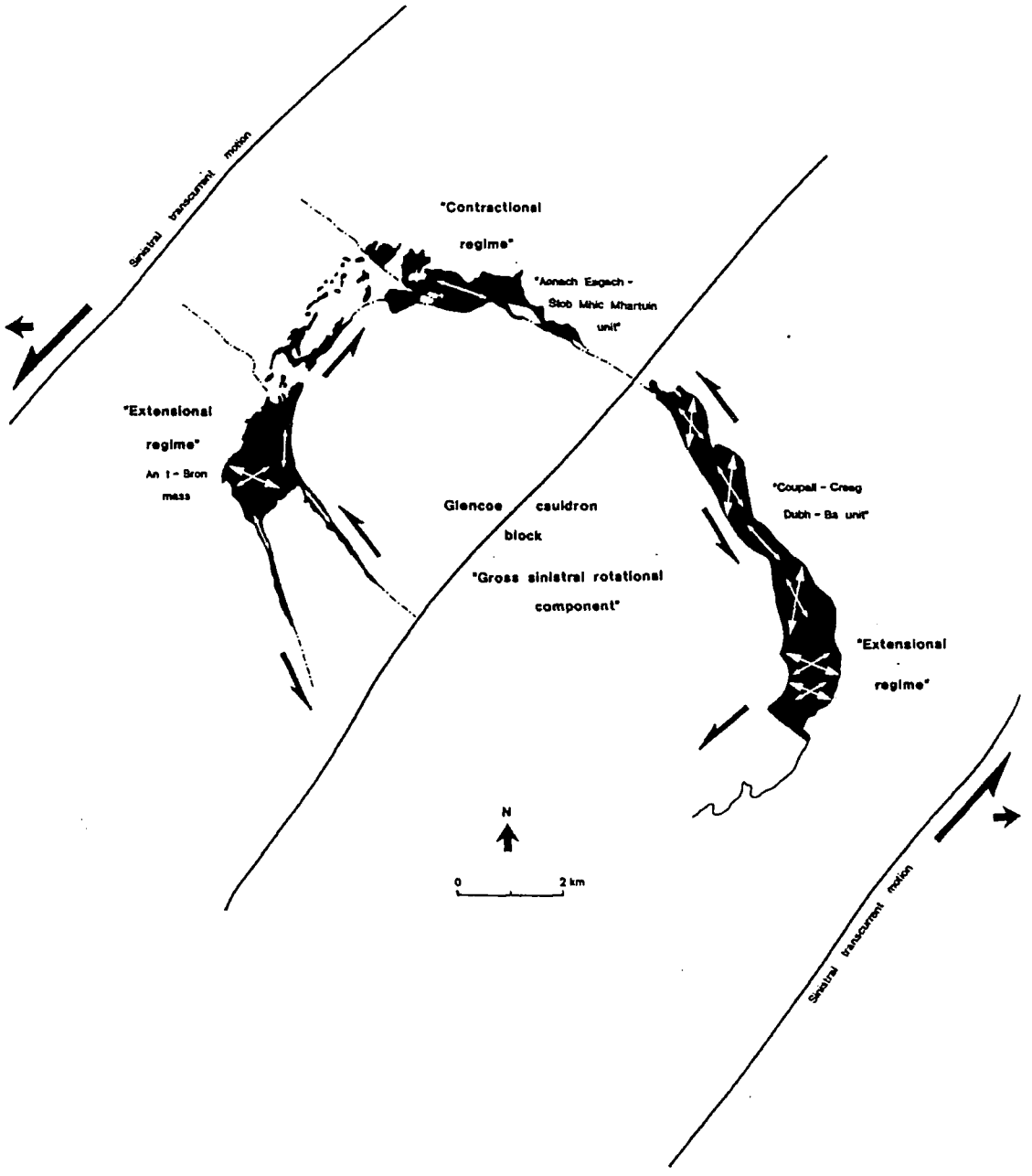

Fig. 7.11. Generalised model for the emplacement of the Glencoe Fault Intrusion.

THE ETIVE QUARRY INTRUSION

7.5 THE ETIVE QUARRY INTRUSION

7.5.1 The Quarry Intrusion, isolated intrusive bodies and the Beinn a' Bhuiridh screen

The Quarry Intrusion has generally been regarded as the earliest intrusive component of the Etive complex (however, see below). As described in Chapter 3 (sub-section 3.2.1), this quartz-diorite/diorite intrusion takes the form of a "partial ring dyke" (Anderson 1937) along the south-eastern margin of the complex between the Dalradian metasediments and the down-faulted Beinn a' Bhuiridh country rock andesite screen (Fig. 7.12). It forms an arcuate outcrop for approximately 10 km, with a maximum width of 1 km.

This intrusive phase was first referred to by Kynaston and Hill (1908, p. 84) as a "more basic type" within the Cruachan facies (G2). It was later recognised as a distinct petrological unit by Anderson (1937), sub-dividing it into an outer quartz-dioritic facies and an inner dioritic unit (Fig. 7.12). No chilled margins occur between these two phases, being described by Anderson (1937, p. 492) as two facies "which everywhere merge into one another", i.e. a synplutonic relationship.

The outer contact of the Quarry Intrusion is unchilled and extensively veins the surrounding Dalradian metasediments. At the inner contact, Anderson (1937) has described the dioritic facies as either being separated from the Beinn a' Bhuiridh screen by: (i) in the northern parts of the intrusion, a fine-grained porphyritic acid rock, which can either have a sharp or gradational contact with the dioritic facies; or (ii) in the southern part as merging into a basic porphyrite against the andesitic screen.

General petrographical description

Outer, quartz-dioritic facies: a fine- to medium-grained (1-3 mm) quartz-diorite. Somewhat porphyritic, containing zoned plagioclase (oligoclase-andesine, 40-45 %) phenocrysts approx. 2 mm in length, set in a groundmass of quartz (8-12 %), feldspar (40-50 %), biotite (10-15 %) and hornblende (20 %). Pyroxene is generally absent, but can occur as small euhedral crystals fringed by hornblende (up to 10 %). Hornblende may also overgrow early biotite. Accessories include apatite, zircon and opaque minerals.

Inner, dioritic facies: a moderate- to coarse-grained diorite, containing phenocrysts of plagioclase (andesine, 45-50 %) which occur as broad laths up to 3-4 mm in length, producing a fairly well developed porphyritic texture. Relatively large amounts of hornblende (25 %) and biotite (15 %) occur, together with a much smaller percentage of augite. Quartz (5 %) and orthoclase are subordinate and occur as interstitial crystals within the matrix. Accessories include magnetite and apatite.

7.5.1.1. Petrological variation within the Quarry Intrusion and contact relationships

Within the vicinity of Allt Mhoille [NN 297 130] and towards the NE (Fig. 7.12), the outer quartz-dioritic facies extensively veins the country wall rocks (Glencoe Quartzite), but is not chilled against them. Moving from this southern contact towards the Beinn a' Bhuiridh screen, the facies becomes progressively finer-grained and darker in appearance, forming a basic porphyritic rock at the contact with the andesitic screen. However, a different situation is observed along the contact between the more basic dioritic facies and the Beinn a' Bhuiridh andesite. Within the Beinn a' Bhuiridh [NN 094 282] and Monadh Driseig [NN 113 282] regions, an intense "crush" zone, approximately 2-3 cm wide, occurs along the contact and the moderately coarse-grained dioritic facies appears to gradually pass into a fine-grained porphyritic felsite, within approximately 1.5 m of the contact.

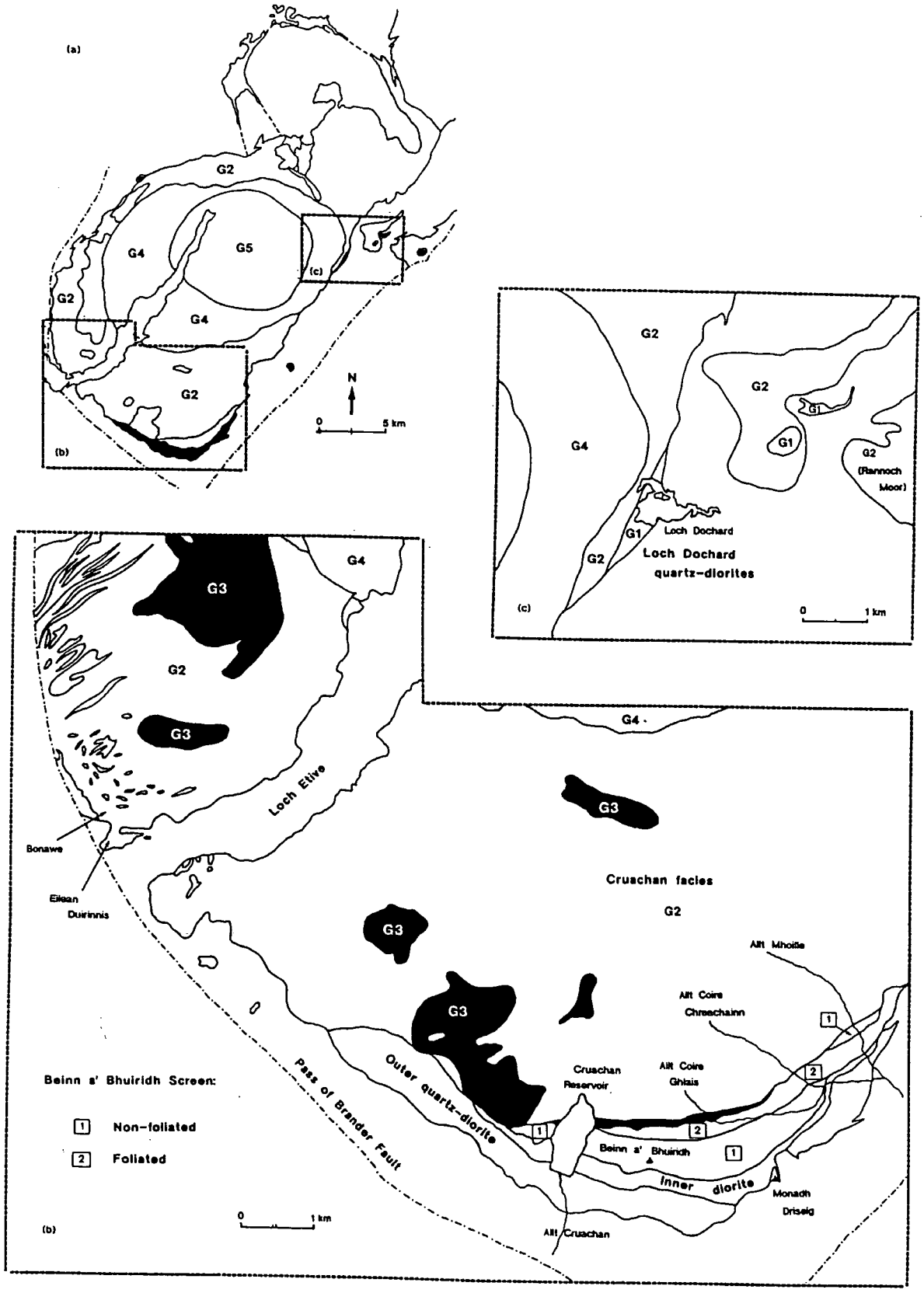

Fig. 7.12. Inset showing the position of (b) an enlarged map of the Quarry, Bonawe and Eilean Duirinnis intrusions (G1), and (c) an enlarged map of the Loch Dochard quartz-diorites (G1).

7.5.1.2. The Beinn a' Bhuiridh screen

This country rock screen contains important information relating to the emplacement of the Quarry Intrusion and is described separately. As shown by Figure 7.12 (Anderson 1937) the screen can be sub-divided into: (i) an outer non-foliated andesite, of both non-porphyritic and porphyritic varieties; and, (ii) a strongly foliated biotite-rich schistose andesite (Plates 7.24 & 7.25). A perfect transition occurs from the non-foliated into the foliated andesite. In Allt Coire Ghlais (Fig. 7.12) the foliation is vertical and generally trends WSW as far as the contact with G2 (Cruachan facies) [NN 115 292]. Towards the NE, in the Allt Mhoille region, a small lens of non-foliated andesite occurs in contact with G2 [NN 126 301]. It appears to have been extensively veined by aplite and G2, but otherwise shows no signs of disturbance. A similar situation can be observed in Allt Coire Chreachainn, where highly foliated schistose andesites are extensively veined at the contact with G2 [NN 120 297]; again showing no signs of movement after their emplacement into the down-faulted andesitic screen.

At Lairig Torrain [NN 095 287] and westwards towards Allt Cruachan (Fig. 7.12), the screen possesses a more intense schistosity and the foliation trend changes from a WSW orientation in the Allt Coire Ghlais region to an E-W strike. East of Allt Cruachan, this intense schistosity may disappear rather rapidly, forming alternating zones of weak or non-foliated rock with zones which clearly possess a fabric.

General petrographical description

Non-foliated/non-brecciated andesite: as already mentioned, both porphyritic and non-porphyritic varieties occur throughout the screen. The majority are vesicular in nature, containing granular quartz within the cavities. Compositionally the andesite varies in the relative amount of plagioclase, pyroxene and amphibole. Plagioclase (andesine) is abundant within the fine-grained matrix, generally forming well developed crystals (0.5-2.5 mm in length). The ferromagnesian minerals, of which augite constitutes a large percentage, have equidimensional forms approximately 1-2 mm in diameter. Accessory minerals include apatite and magnetite. Contact alteration is pervasive throughout the non-foliated screen, leading to the development of secondary hornblende and biotite, and the clouding of plagioclase.

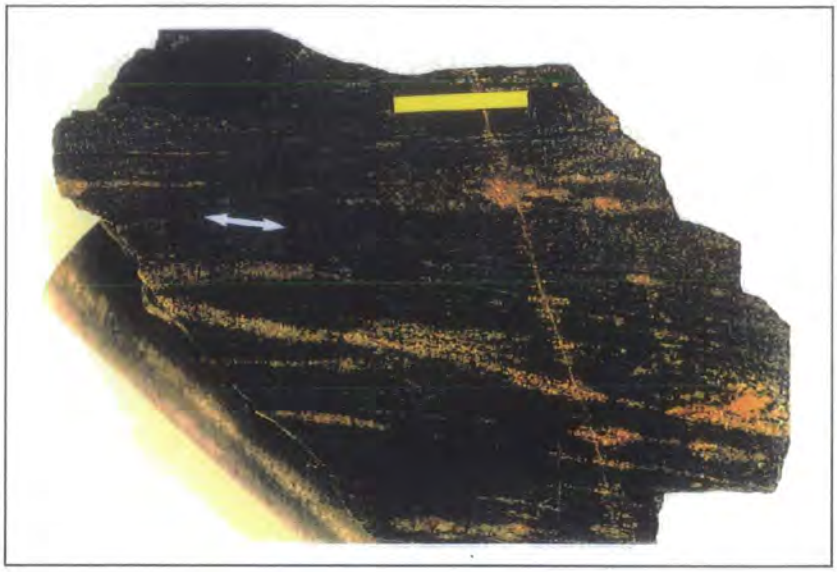

Plate 7.24. Hand-specimen of foliated Beinn a' Bhuiridh screen. (Yellow 'bar' is approximately 2 cm long).

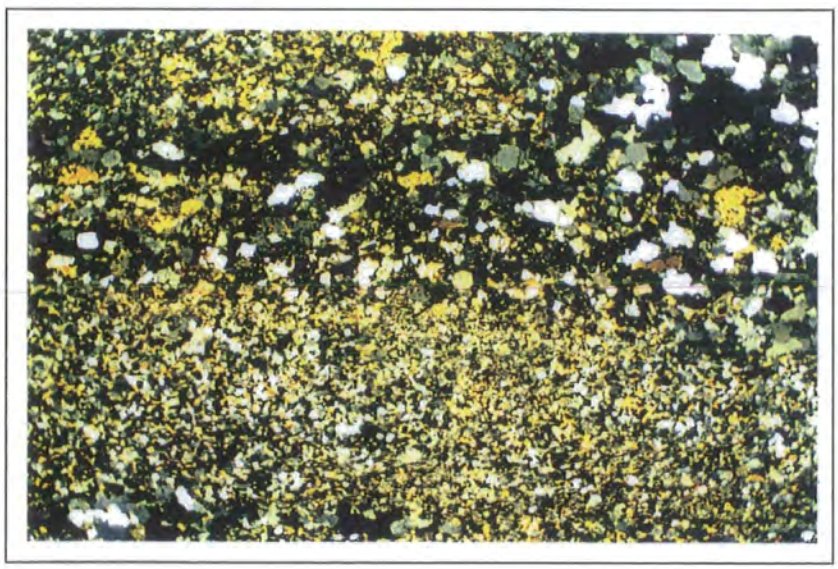

Plate 7.25. Photomicrograph of hand-specimen shown in Plate 7.24. (Field of view approximately 18 mm).

Highly foliated biotite-schist/andesite: this unit is essentially composed of quartz, biotite, plagioclase and quite a large percentage of pyrite and other iron ores. Two types of plagioclase can be recognised: (i) relicts of the phenocrysts (andesine) of the original andesite, forming large (up to 2.5 mm in length), broken crystals, which are often quite heavily sericitised (producing sericite, a fine-grained white mica formed by the alteration of feldspar, usually occurs in the form of aggregates at the centre of the crystals); and (ii) much smaller interstitial crystals within the matrix of labradorite composition. The schistosity is essentially attributable to the alignment of biotite crystals, which range from 1.0-1.5 mm in length.

7.5.1.3. The Loch Dochard region

Isolated representatives of the Quarry Intrusion occur in a small area along the eastern periphery of the complex (Kynaston & Hill 1908; Anderson 1937; Fig. 7.12). Within a region SW of Stob Ghabhar, G2 (Cruachan facies) rapidly thins out towards Loch Dochard. In the stream sections SW of Loch Dochard, darker more basic quartz-dioritic rocks are exposed, which show evidence of decreasing grain-size towards G2, rather than towards the country wall rocks. Petrologically its very similar to the outer quartz-dioritic facies of the Quarry Intrusion, leading to the possibility that it may represent an isolated part of the continuation of that "ring dyke body".

General petrographical description

Loch Dochard quartz-diorites: these are essentially fine-grained quartz-dioritic facies. Plagioclase (oligoclase-andesine, 40-45 %) crystals tend to be approx. 0.75 mm in length, but may be up to 1.5 mm, producing a porphyritic texture. Biotite (12-15 %) and hornblende (20 %) occur in quite large amounts. Quartz and orthoclase are subordinate, occurring interstitially within the groundmass. The rock shows strong contact-alteration, in the replacement of biotite and hornblende, and in the clouding of plagioclase crystals.

A simple explanation for the features observed could be: (i) the quartz-diorite represents part of a ring fault intrusion which chilled against the cooler down-faulted cauldron block. A similar situation has been observed by Clough *et al.* (1909) for the Glencoe Fault Intrusion (see sub-section 7.2.3); (ii) construction of G2 caused the block to be removed, probably back towards the free surface (see Ch.'s. 4 & 11), allowing G2 to be emplaced against the quartz-diorites, resulting in the strong contact-alteration of G1. This will be addressed further in Chapter 11.

7.5.1.4 Satellite intrusions

Small, fairly circular intrusive bodies and sheets of appinite, kentallenite and diorites occur around the periphery of the complex (Fig. 7.13). A number of these bodies, particularly the larger ones, are distributed along the NW-SE-trending Cruachan lineament (see Chapter 9). Such concentration of small intrusions within the adjacent Dalradian country rocks was noted by Anderson (1937) to the south-east of the complex, and to the E and NE of Beinn Eunaich [NN 135 328]. Many of these bodies consist of a coarse, grey granodiorite facies similar to the main phase of G2 of the Etive complex. Large masses of more basic composition also occur, the largest in the Beinn Lurachan intrusion [NN 171 340] (Kynaston & Hill 1908), which is predominantly composed of porphyritic augite-diorite. Smaller dioritic bodies also occur near Meall Copagach [NN 153 341]. In the north of the complex are also a number of satellite intrusions along the line of the Cruachan lineament. These occur within the Glen Ure area and are essentially fine- to medium-grained quartz-diorites.

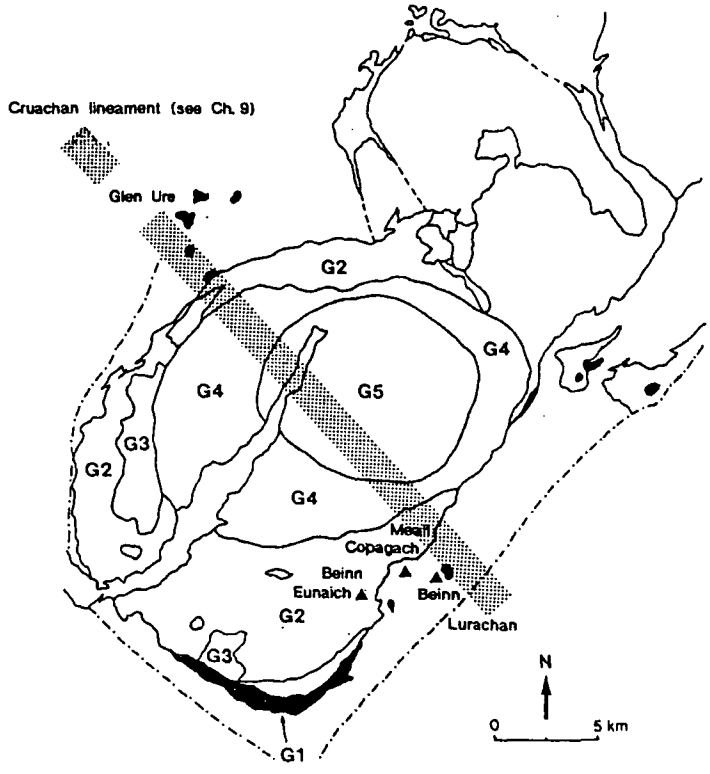

Fig. 7.13. Distribution of satellite intrusions (G1) around the periphery of the Etive complex.

7.5.1.5 The Bonawe and Eilean Duirinnis Intrusions

The Bonawe Intrusion is an isolated body in the SW of the complex [NN 014 335] (Fig. 7.12b). It is separated from G2 (Cruachan facies) by a screen of schists, which Anderson (1937) suggested may represent country rock down-faulted during the emplacement of this intrusive phase by a process of ring-faulting and cauldron subsidence. Geochemical analysis by Batchelor (1987) shows that it plots close to the field of the outer, felsic Cruachan monzogranite (G2). Also within this area, to the SW, occurs the Eilean Duirinnis Intrusion [NN 011 331] (Fig. 7.12b; Anderson 1937). Petrologically it is very similar to the quartz diorite facies of Loch Dochard (Fig. 7.12c), an exception being that it is somewhat coarser-grained. This may also represent an isolated part of the "ring dyke", which initially may have extended around the periphery of the complex. Subsequent emplacement of G2 may have disrupted and removed large parts of this ring intrusion, leaving the main mass, the Quarry Intrusion, and smaller more isolated parts as "relict structures". As with the quartz-diorites at Loch Dochard, it also shows evidence of contact-alteration.

General petrographical description

Bonawe Intrusion: a fine- to medium-grained monzogranite. As mentioned above, geochemically it is very similar to the outer, felsic Cruachan monzogranite (Batchelor 1987) and therefore could have been placed in the G2 (Cruachan facies) section. Zoned plagioclase crystals (30-45 %), which are approx. 0.75-1.0 mm in length, are abundant, together with alkali-feldspar (orthoclase and microcline, 25-35 %) and quartz (15-30 %), which both tend to form irregular crystals ranging from 0.5-0.75 mm in diameter. The plagioclase is heavily sericitised. Significant amounts of biotite (5-10 %) occur, which tends to be altered to chlorite. Hornblende (2-3 %) is present, but only in small amounts.

Eilean Duirinnis Intrusion: a fine- to medium-grained (1-3 mm) quartz-dioritic facies. Slightly porphyritic, containing plagioclase (oligoclase-andesine, 40-45 %) crystals approximately 1.0 mm to 2.0 mm in length, set in a groundmass of biotite (10-15 %), hornblende (15-20 %), quartz and orthoclase. Contact-alteration is clearly visible; biotite and hornblende replacement, and clouding of plagioclase crystals.

7.6 FABRIC DEVELOPMENT: EVOLUTION OF MICROSTRUCTURES

The purpose of this Section is to present the type of fabrics and microstructures which are common within the major occurrences of G2, the Etive Quarry Intrusion and the Loch Dochard quartz-diorites. It is not intended as a detailed discussion on the textural development and mechanisms operating during fabric evolution.

7.6.1 The Etive Quarry Intrusion

Throughout both the outer quartz-diorite facies and the inner dioritic unit, weak to moderately developed PFC fabrics are intermittently developed (Fig. 7.14). The fabric in both is defined by the alignment of plagioclase phenocrysts and particularly within the inner, dioritic phase, by hornblende and biotite.

The fabric is generally vertical or steeply dipping, but its orientation can be highly irregular throughout both phases. However, in general the most well developed fabrics are orientated sub-parallel to the elongation of the body. Bimodal PFC fabrics are not uncommon, particularly within the centre of the widest parts of the Etive Quarry Intrusion, e.g. Allt Cruachan [NN 081 277]. However, their distribution is often extremely sporadic, separated by 'zones' containing fabrics which do not appear to have any consistent orientation, or no fabrics at all. Where the bimodal PFC fabrics are developed, it is common for elongate country rock xenoliths to be aligned sub-parallel to either fabric direction. The general angular relationship of these sub-fabrics show very similar characteristics to those observed within the Main Glencoe Fault Intrusion (see Section 7.3). One set generally trends sub-parallel to the elongation of the Etive Quarry dyke-like body (around 098° in the Cruachan region; Fig. 7.14), and the other set is generally orientated oblique to the inner contact with the Beinn a' Bhuiridh country rock screen and its outer contact with the Dalradian metasediments (in the Cruachan region for example, this is generally around 140°; Fig. 7.14). Microstructural analysis during this study suggests that the oblique set may represent a 'tiling-type fabric' or 'imbricate' texture, whereas the other set may form discrete PFC 'lock-up microshears' orientated close or sub-parallel to the shear direction. As with such fabric development within the Main Glencoe Fault Intrusion, this may suggest that the environment was one of non-coaxial deformation during pre-full crystallisation; leading to a process of strain partitioning and the development of two sets of PFC fabric. Their angular relationship suggests a sinistral component of shear during their

development, with the shear direction orientated sub-parallel to the inner contact with the Beinn a' Bhuiridh screen and the overall elongation of the intrusive body. These relationships are remarkably similar to those observed throughout the larger intrusive bodies of the Main Fault Intrusion of Glencoe. The reason why such fabrics are not so well preserved within the Quarry Intrusion might be because the Etive complex as a whole underwent a large amount of 'modification' by the subsequent intrusion of G3, G4 and G5 (see below), and strains related to their emplacement may have modified, and in certain areas, removed 'primary' structures related to the construction of this higher level emplacement phenomenon. Whereas, within the Glencoe complex, the plutonic phase, G2 (Clach Leathad facies) may have been largely constructed prior to the emplacement of the Fault intrusion, and was not modified by the subsequent emplacement of large intrusive phases (there is no evidence for a G4 or G5 phase).

Within parts of the foliated Beinn a' Bhuiridh screen, quartzo-feldspathic layers may have sinuous forms indicative of sinistral shear (see below). A sinistral component of shear is also inferred from the geometry of quartz ribbons developed within the Glencoe Quartzites, adjacent to the outer contact of the Quarry Intrusion, e.g. Allt Cruachan [NN 082 274]. Whether these features are related to the emplacement of the Quarry Intrusion is unclear, but it does suggest that the region as a whole was subjected to significant component of sinistral shear. These shear sense indicators, developed within the adjacent wall rocks, also infer that the shear direction was approximately sub-parallel to the elongation of the Quarry intrusion; the same as the PFC bimodal fabrics developed in the quartz-dioritic body (see above).

Within the Allt Coire Ghlais-Allt Mhoille region (Fig. 7.12) the inner dioritic facies becomes an extremely narrow dyke-like body, approximately 50-100 m wide. Throughout this area the contact-parallel PFC fabric has been generally overprinted by a coplanar moderately developed high temperature solid state deformation. The resultant CPS fabric is characterised by the ductile deformation of quartz (forming lenticular, elongate crystals) and biotite (which is often bent and kinked). Within this region, the Allt Mhoille river section (Fig. 7.12) provides an invaluable transect across the outer Dalradian metasediments, both phases of the Quarry Intrusion, the Beinn a' Bhuiridh screen, and into the 'plutonic body' of the complex, the Cruachan facies (G2). Several observations along this section may have extremely important implications on the emplacement of the Quarry Intrusion:

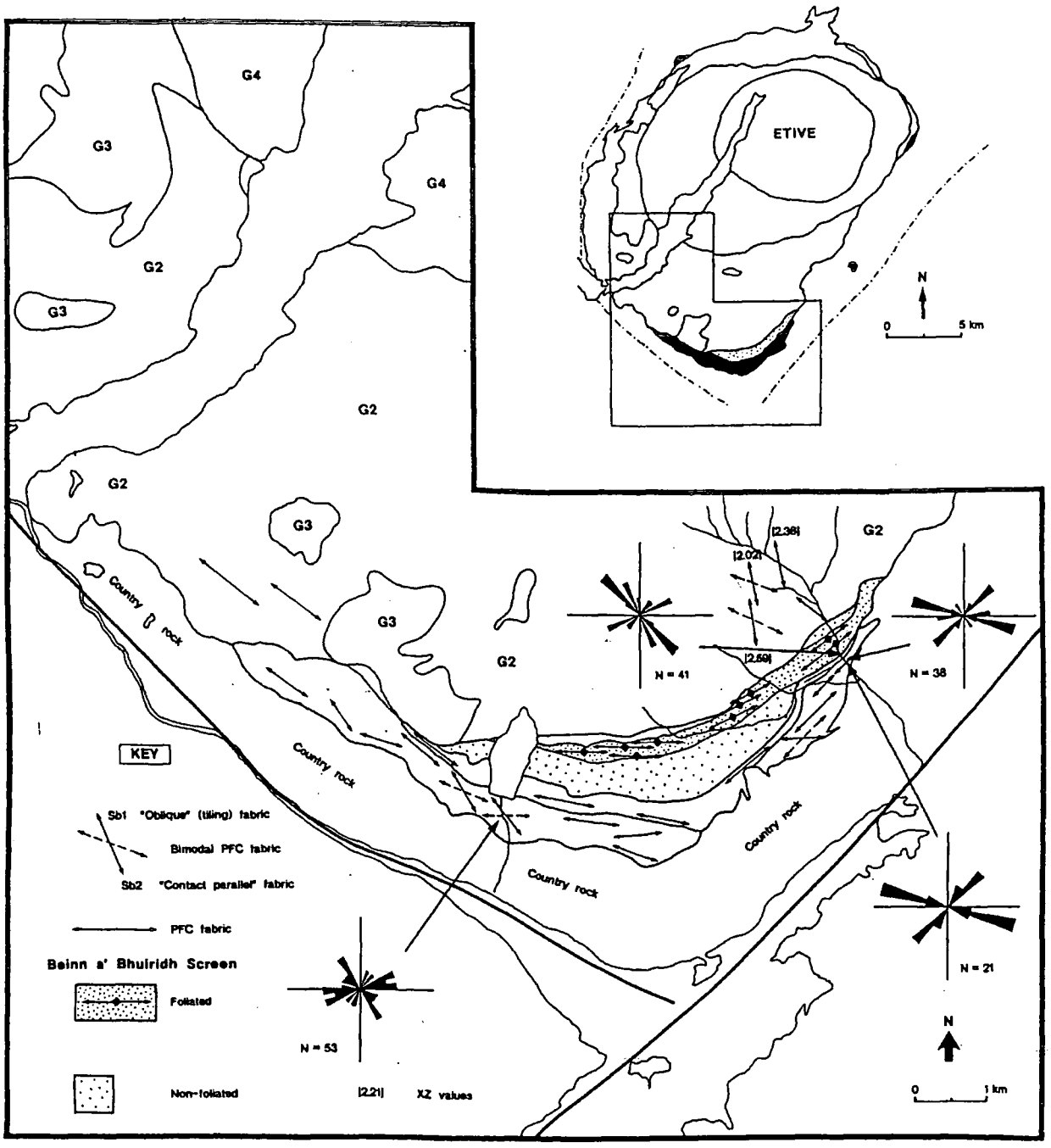

Fig. 7.14. The distribution of PFC fabrics, strain values and 'rose' diagrams which show the distribution of the long axes of lenticular country rock xenoliths and enclaves within the Etive Quarry Intrusion, and fabrics developed within the immediate G2.

① At the outer contact of the Quarry Intrusion, the quartz-dioritic facies extensively veins the Glencoe Quartzite, but is not chilled against it. This relationship is seen right around the external contact of the Quarry Intrusion (G1). However, moving from this southern contact towards the Beinn a' Bhuiridh country rock screen, G1 becomes progressively finer-grained and darker in appearance. This is coeval with

an increase in the development of a high temperature CPS overprint seen within the inner dioritic phase, as mentioned above.

② Within the adjacent Glencoe Quartzites, a number of melt-filled brittle-ductile shears (generally < 1 cm wide) form conjugate arrangements. The resultant 'veins' are extremely pink in appearance, composed essentially of quartz and K-feldspar. The shears form two dominant trends: NE-SW (around 032-036°) and E-W (approximately 086-090°). Along these shears, the adjacent quartzite forms a "pink crush-rock" composed of angular to sub-rounded pink clasts of quartz (generally 1-4 mm in diameter) set in an ultra fine-grained (< 1 mm in diameter) groundmass of host material. In certain areas the matrix is grey to black and resembles the "flinty crush-rock" (FCR) (Plate 7.26) so commonly associated with such fault-rocks within the Glencoe region (Fault Intrusion; see sub-section 7.2.3). These microbreccias/cataclasites may have a banded appearance. Moving away from these zones there is generally a progressive increase in the size of the clasts and the matrix, forming a zone of brecciated and shattered quartzites. This transition generally ranges from 0.5-1 m wide, from the brittle-ductile shears into undisturbed country rock.

It is not uncommon for these 'fault-rock zones' to be intimately associated with quartz-dioritic material. The igneous component often encloses clasts of brecciated quartzite.

Plate 7.26. Breccia/microbreccia (Glencoe Quartzite) set in FCR. Exposed within the Allt Mhoille river section. (Horizontal surface).

③ The majority of the Beinn a' Bhuiridh screen throughout this transect possesses an intense schistosity. The foliation is vertical and generally contact parallel (056-060°). This relationship is seen throughout the foliated parts of the andesitic screen (see below).

As mentioned above, the sinuous form of the quartzo-feldspathic layers, particularly within the porphyritic, foliated andesite varieties, may suggest a sinistral shear component.

④ An intense zone of sheeting occurs along the inner contact of the Beinn a' Bhuiridh screen, with the Cruachan facies (G2) encorporating large angular blocks of andesite schist. The width of the zone is extremely variable, from approximately 75-150 m wide. The G2 sheets range from cm's across, often up to several m's wide, and generally trend sub-parallel to the contact with the metasedimentary screen. Moving from this zone, northwards into G2, there appears to be a progressive reduction in size of the country rock xenoliths. The majority of the smaller, elongate inclusions are generally aligned sub-parallel to the weak to moderately developed PFC fabric formed in G2. However, within this region, G2 does not possess the 'typical' pseudoconcentric PFC fabric which is pervasively developed throughout the majority of the southern part of the complex (see Ch. 3, sub-section 3.4.2.1), but a PFC fabric which generally trends around 170° (approximately N-S) (Fig. 7.14). Microdioritic enclaves are also orientated in this direction, and give X/Z values (horizontal surfaces) which range from 2.02-2.59.

Both pink monzogranitic and grey monzodioritic varieties of G2 occur throughout this region. Where observed, the 'contacts' between these two petrographically distinct units show synplutonic relationships. This part of the complex may be roughly coincident with the area designated by Batchelor (1987; see Ch. 3, sub-section 3.2.2) for the 'mergence' of the northern monzogranitic facies, with the monzodiorites of the south. Both phases of G2 have synplutonic relationships with dyke-like bodies and irregular masses of dioritic material. The diorite is fine- to medium-grained (1-3 mm), possesses lobate/cuspate geometries with G2, and may contain feldspar phenocrysts obtained from G2 suggesting magma 'mingling' processes. At several localities the diorite is associated with N-S-trending (approximately 170°) PFC ductile shears, often forming a melt-filled component. Mineralogically this diorite is very similar to the inner dioritic facies of the Quarry Intrusion, leading to the possibility that at least part of G1 and G2 in terms of emplacement and crystallisation were penecontemporaneous.

7.6.2 The Loch Dochard region

The Loch Dochard intrusion (Fig. 7.12) appears to have been modified by strains related to the *in situ* expansion of the Etive plutonic complex (see Ch. 3). To the west these quartz-diorites form a contact with the Cruachan facies (G2) which represents part of the "Allt Doireann/Kingsglass High Strain Zone" (see Ch. 3; sub-section 3.4.2.2) formed as a consequence of the *in situ* expansion of the Central Starav facies (G4/G5). This deformational episode has led to the formation of relatively moderately developed, high to moderate temperature crystal plastic strain fabrics both within the Loch Dochard quartz-diorites (G1; Plate 7.27) and the Cruachan facies (G2; Plate 7.28). The fabric orientation in both phases is generally contact-parallel, roughly trending NE-SW (Fig. 7.15).

Within the adjacent country rocks, particularly within the Allt Coire Beithe stream section, a number of melt-filled (granitic) shears occur. These shears are orientated approximately 145° and possess a sinistral shear component, displacing the veins of G2 from around 2 cm up to 8 cm. These may represent extensional shears related to G4/G5 expansion.

Plate 7.27. Hand-specimen of G1 from the Loch Dochard intrusion. It possesses a relatively high to moderate temperature CPS fabric. (Yellow 'bar' is approximately 2 cm long).

Plate 7.28. Hand-specimen of G2 from near the contact with the Loch Dochard intrusion (G1). It possesses a high to moderate temperature CPS fabric. (Yellow 'bar' is approximately 2 cm long).

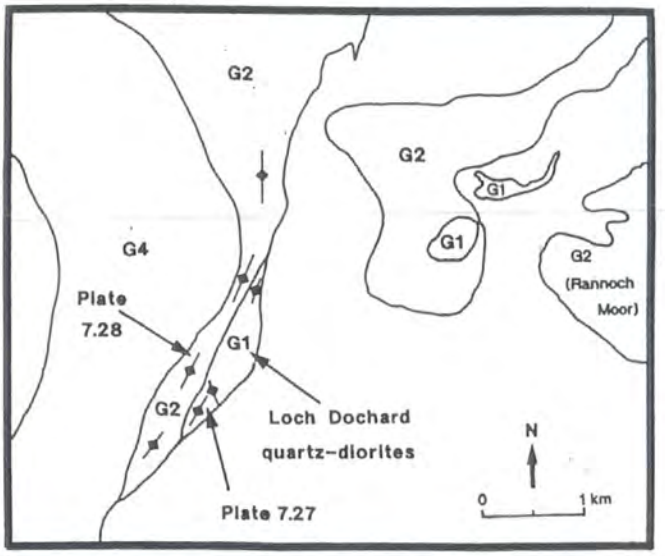

Fig. 7.15. The distribution of fabrics in G1 and G2 within the Loch Dochard region.

7.7 EMPLACEMENT MODEL PROPOSED FOR THE CONSTRUCTION OF THE ETIVE QUARRY INTRUSION

Summary of the main internal and associated external deformational features of the Etive Quarry Intrusion: implications for its emplacement.

❶ As with the Glencoe Fault Intrusion, a number of kinematic indicators both within the main intrusive body and its external contacts suggest that in addition to down-faulting, a significant component of sinistral shear may have occurred during the cauldron subsidence process. A number of independent shear sense criteria have been identified: (i) Quartzo-feldspathic layers within parts of the Beinn a' Bhiuridh screen may have sinuous forms indicative of sinistral shear; (ii) A sinistral shear component has also been deduced from quartz ribbons developed in the surrounding country rocks; (iii) The angular relationship of PFC bimodal fabrics developed within the Quarry Intrusion generally suggest a sinistral component during their development, with the inferred shear direction often aligned sub-parallel to the elongation of the Etive Quarry "dyke-like body". The lack of development of this bimodal fabric throughout the intrusion may suggest that 'primary' deformational features have been modified by strains related to the subsequent emplacement of G3, G4 and G5 of the Etive plutonic complex.

❷ Right around the external contact of the Quarry Intrusion, the quartz-dioritic facies extensively veins the surrounding country rocks, but it is not chilled against them. However, at the inner contact against the Beinn a' Bhuiridh country rock screen, G1 appears to have chilled and a high temperature solid state overprint may occur. Again this shows similarities with the Glencoe Fault Intrusion, suggesting that there was a difference in the temperature of the country rocks either side of the intrusion during its development . Many features throughout the Etive Quarry Intrusion show similarities to the Glencoe Fault Intrusion. It is therefore proposed that the Etive Quarry Intrusion was also constructed by a process of multiple sheeting/dyking along the outer parts of the Beinn a' Bhuiridh screen, which probably represents a relict part of a much larger cauldron block (see below). It is envisaged that during the early construction of the Etive plutonic complex, strains related to its *in situ* expansion were accommodated by the development of volcanotectonic faults within the overlying cover rocks. This probably produced a peripheral ring fault system very similar to that seen in the nearby Glencoe Fault Intrusion. As with the Glencoe

Fault Intrusion, it is likely that during a regional transtensional phase, and/or the result of a period of reduced magmatic pressure beneath the resultant crustal block, the block descended leading to 'classic' cauldron subsidence and the emplacement of the Quarry Intrusion. As shown in Chapter 3, the Etive complex was bounded and bisected by major NE-SW-trending structures, which have been shown to have been operating as major sinistral shear zones during this period of magmatism. It is possible that sinistral transcurrent motion along these NE-SW-trending structures resulted in a small, but significant "gross sinistral rotational component" along the fault bounded contact of the descending block (Fig. 7.16) The distribution of quartz-dioritic bodies along the NW-SE-trending Cruachan lineament (see Ch. 9) may suggest that movements along this structure were facilitating their ascent and emplacement. Similarly, movements along the fault may have been influential during the construction of the Quarry Intrusion. Assuming that a component of sinistral shear was occurring along the Pass of Brander fault, related to the "overall gross sinistral rotational component" established 'around' the complex, it would explain the spatial development of the Quarry Intrusion in an "extensional quadrant" established within the SE of the complex (Fig. 7.16). This again may show simularities to the Fault Intrusion, where in Glencoe the largest intrusive bodies are spatially coincident with the theoretical 'extensional quadrants' which would be produced by an overall, regional, sinistral transtensional environment. The difference being that in Glencoe the NE-SW-trending structures were the dominant control, whereas during the emplacment of the Etive Quarry Intrusion, sinistral transcurrent motion along NW-SE-trending structures may have dominanted, thus explaining the siting of quartz-dioritic and appinitic bodies along the NW-SE-trending Cruachan lineament (Fig. 7.16) (see Ch. 9).

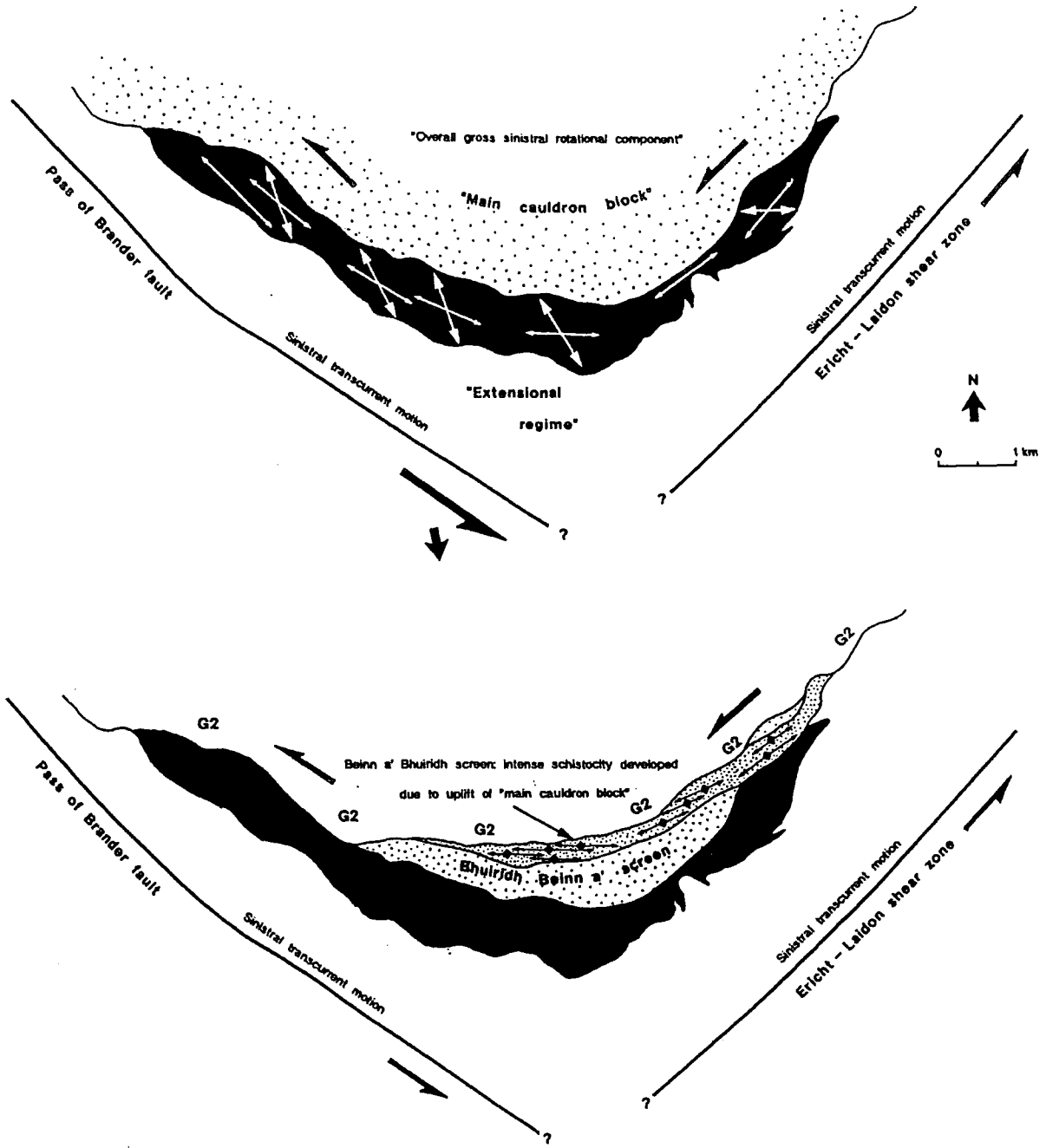

Fig. 7.16. Generalised model for the emplacement of (a) the Etive Quarry Intrusion, and (b) the development of the Beinn a' Bhuiridh screen.

It is possible that the actual emplacement mechanism operating during the construction of the Quarry Intrusion was the same as that proposed for the Glencoe Fault Intrusion. Both show evidence that there was a difference in temperature on either side of the intrusive bodies, with colder and relatively unaffected rocks occurring within the down-faulted mass; possibly suggesting that they were

constructed by a process of multiple sheeting/dyking. With continued input of hot magma along the outer part of the ring fault system, the temperature of the outer, country wall rocks would have progressively risen, consequently leading to an increase in the amount of ductile 'flow type' deformation the outer wall rocks could accommodate. This model would explain why in both Etive and Glencoe the country wall rocks surrounding the ring intrusions show evidence of a significant amount of deformation, whereas the immediate country rocks within the down-faulted cauldron block have remained relatively unaffected. It is therefore assumed that the sheets in general were intruded along the outer most parts of the 'body', hence the surrounding rocks were continually heated and deformed. In the case of the Etive Quarry Intrusion, this explains why most of the outer parts of the Beinn a'Bhuiridh country rock screen, which is in contact with the Quarry Intrusion, has remained unaffected forming a zone of non-foliated, non-brecciated andesites. However, the reverse is true within the inner part of the screen, where it forms a zone of strongly foliated 'biotite schist'. This may be explained by how the Beinn a' Bhuiridh screen was left as a 'relict' part of the down-faulted cauldron block. It is envisaged that after the emplacement of the Quarry Intrusion, strains related to the *in situ* expansion of the 'main' plutonic complex (possibly during the 'main' construction of G2) were accommodated by the development of a "new" volcanotectonic fault, along what is now, the inner contact of the Beinn a' Bhuiridh screen. The main part of the cauldron block was uplifted towards the Earth's surface ('cauldron upheaval'), whereas part remained to form the screen presently exposed. This 'upheaval' process leading to the development of high shear stresses along the walls of the Beinn a' Bhuiridh screen and the uplifted block, thus causing brecciation and the formation of an intense zone of schistosity. It is also possible that this schistosity was 'enhanced' by the emplacement of subsequent phases into the 'main' plutonic complex. Along the inner contact of the Beinn a' Bhuiridh screen it was noted by Anderson (1937), and during this present study, that the screen has been extensively veined by aplite and G2, which show no signs of disturbance. This together with synplutonic relationships observed between quartz-diorites (possibly G1) and G2 (see sub-section 7.6.1) suggest that the screen was left during this stage and not down-faulted during some later episode.

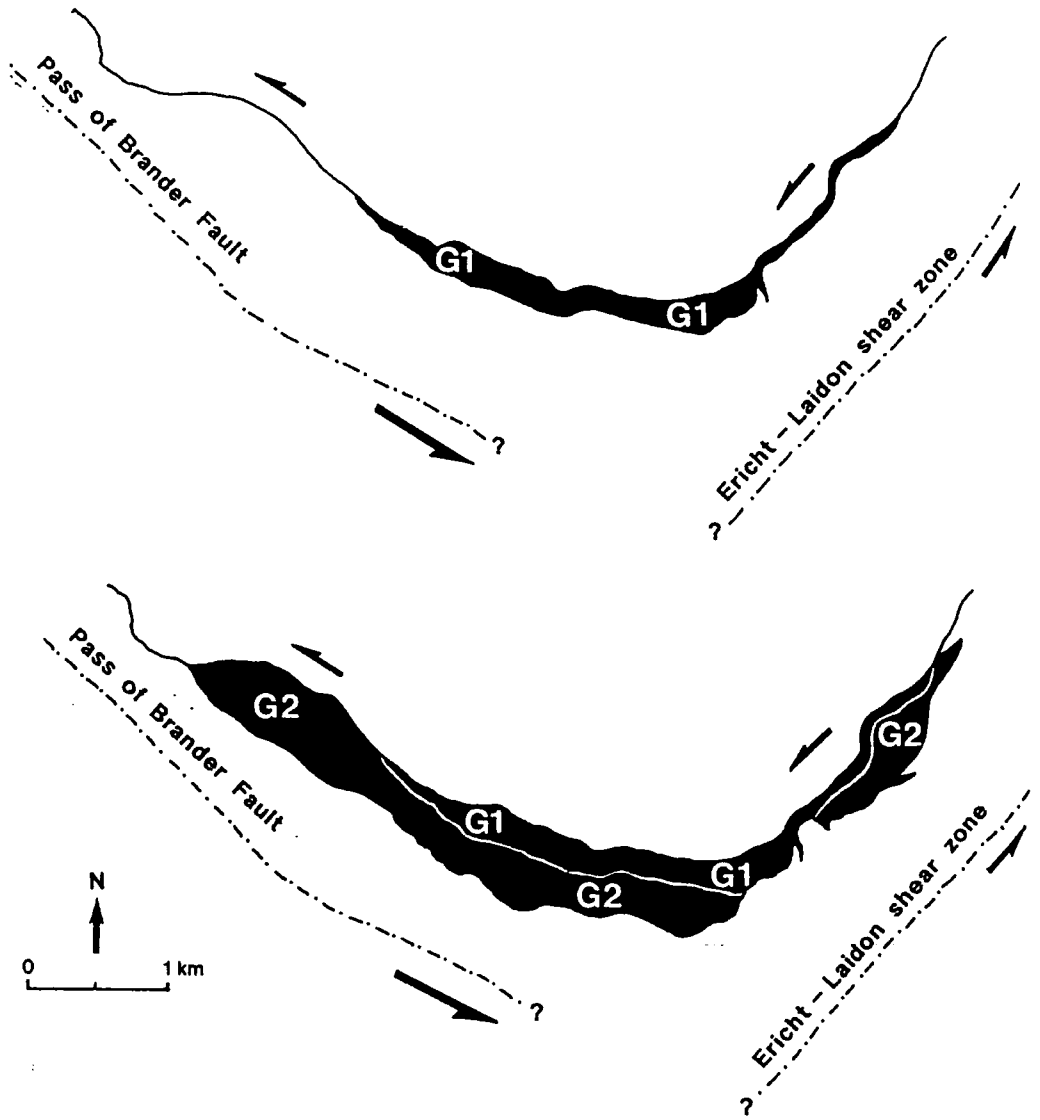

Fig. 7.17. Generalised model explaining the form and distribution of the (a) inner diorite and (b) outer quartz-diorite phases.

CHAPTER 8

EMPLACEMENT OF THE ETIVE DYKE SWARM

8.1 INTRODUCTION

This suite of NE-SW-trending dykes is concentrated on the centre of the Etive plutonic complex (Fig. 8.1), and forms one of the largest dyke swarms in the British Caledonides, extending some 80-120 km in length. The Etive dykes are concentrated in a zone approximately 15-18 km wide essentially bounded by the NE-SW-trending Allt Buidhe/Laggan Dam Fault in the north and the Ericht-Laidon shear zone in the south (Fig. 8.1). Running through the centre of the swarm is the major NE-SW-trending Etive-Laggan shear zone.

This Chapter deals with the internal microstructural characteristics of the dykes and their influence on fabric development, strain distribution and associated structures developed within their surrounding plutonic host rocks. Most of this work has been carried out in the main plutonic phase (G2) of the Glencoe complex for two principal reasons: (i) it provides an excellent section through part of the dyke swarm, particularly within the Glen Etive region; and (ii) the Clach Leathad facies (G2) was incompletely crystallised during part of the dyke emplacement phase (see sub-section 8.3.1.1), resulting in the host (G2) developing fabrics and structures which are related to the emplacement of the dykes.

Recently, Morris and Hutton (1993) have shown from matching contact re-entrants, asymmetric dyke terminations, oblique dyke offshoots, and oblique bridges that sinistral shear was associated with dyke emplacement. This together with larger scale en echelon and stepping patterns led them to conclude that sinistral shear was an important component during the intrusion of the Etive Dyke Swarm as a whole, a conclusion which is consistent with the data presented in this thesis for the sense of shear imposed by a number of major Caledonian NE-SW-trending regional shear zones during the general period of Caledonian magmatism. Morris and Hutton (1993) also make the point that although much of the

sinistral deformation was associated with oblique convergence during this time (Hutton 1987), sinistral transtension associated with the emplacement of this dyke swarm was a significant tectonic event. This combined with the emplacement dynamics of Rannoch Moor G4, which occurs as a 'marginal facies' (see Ch. 5), and the construction of the Glencoe Fault Intrusion (see Ch. 7) suggests that this transtensional phase was an extremely important regional event.

The purpose of this Chapter is to present both field data and microstructural observations which may help to explain:

❶ The actual mechanism operating to create space during dyke emplacement.

❷ The overall parallelism of the NE-SW-trending dykes.

❸ Why does the concentration of dykes clearly diminish towards the contact of the "cross-cutting" Porphyritic Starav facies, as noted by Bailey and Maufe (1916).

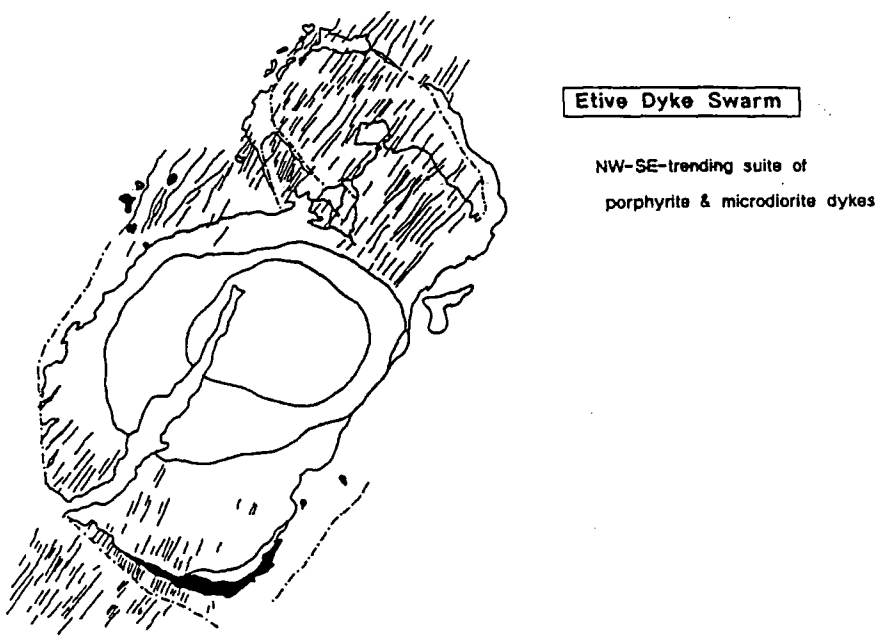

Fig. 8.1. Sketch map showing the location and distribution of the Etive Dyke Swarm.

❹ Why, as the Porphyritic Starav facies is approached, does the orientation of the dykes change from the general NE-SW-trend to a radial disposition; "keeping at right angles to the curving margin of the Starav granite" (Anderson 1937).

8.2 CHARACTERISTICS OF THE ETIVE DYKE SWARM

8.2.1 Age relationships with the major intrusive phases of the Etive complex.

The Etive dykes cut the earliest intrusive phases, G1 and G2 of the Etive complex, and the majority cross-cut the Meall Odhar facies (G3). A few dykes are cut by G3 (Bailey & Maufe 1916) and may represent a distinct earlier intrusive phase. Almost all are earlier than the emplacement of the Porphyritic Starav facies (G4) (Fig. 8.1).

8.2.2 Petrological variation

Petrological analysis of the dyke suite has been carried by Kynaston and Hill (1908), Bailey and Maufe (1916), Anderson (1937), and Bailey (1960). Anderson (1937) sub-divided the suite into four groups: (i) felsite and porphyry; (ii) porphyrite; (iii) microdiorite; and (iv) lamprophyre dykes.

The largest portion of the dyke swarm is acid to intermediate porphyrites. They are fine- to medium-grained phaneritic rocks, containing hornblende or biotite and phenocrysts of plagioclase. Quartz and feldspar occur as interstitial crystals. Microdiorites and quartz-porphyries are not uncommon and often occur together in multiple dykes.

In general, field observations and microstructural analysis (see Section 8.1) suggest that the dyke swarm can be sub-divided into: (i) an earlier phase of pink and grey porphyrite dykes, which have intruded into the Glencoe Clach Leathad facies (G2) whilst its host was still incompletely crystallised; and (ii) a later somewhat more minor phase of microdiorite dykes which intruded into Glencoe G2 when the host was near or fully crystallised. The microdiorite dykes often intrude into the earlier phase forming a composite arrangement.

8.2.3 Size and form of the dykes

The dykes trend NE-SW to NNE-SSW and the majority are vertical, with some dipping steeply towards the SE (generally > 75°). As mentioned above, the dyke swarm is approximately 15-18 km wide, and is some 80-100 km long. A qualitative estimate of the concentration of the dykes within this zone, is shown by the NW-SE elongation of the Glencoe Cauldron block (see Fig. 8.1). It is assumed that the cauldron block was originally circular in plan, approximately 11.5 km in diametre, and was subsequently elongated NW-SE by the emplacement of the Etive Dykes to its present form (long axis approximately 16.5 km). This would suggest an overall crustal dilation of around 30 %. This however, may be somewhat of an overestimate as the Glencoe complex as a whole may have been elongated further by the deformation imposed by the *in situ* expansion of the adjacent Etive complex; these effects are clearly seen in fabric development within the Glencoe "plutonic phase" (see Ch. 4). Actual measurements to determine the percentage dilation associated with the dykes were carried out mainly in the Glen Etive River section. For example, within this section the width of sixteen dykes were recorded over a distance of approximately 515 m, suggesting an increase in width of approximately 24.6 % by the emplacement of the Etive dykes within this area. Other estimates include the percentage of dilation for the Lairig Gartain area; 22.4 %.

Dyke widths are variable generally averaging 2-4 m. Occasionally dykes may reach up to 10 m wide, but in most cases these have been constructed by multiple emplacement of different intrusive phases, e.g. porphyrite phase intruded somewhat later by a microdioritic phase.

Particularly within the Glen Etive region, where the dykes intruded into the monzogranites of the 'Chaorainn pulse' (G2) of the Glencoe complex (see Ch. 4; sub-section 4.4.2.1), the two distinct phases of dyke emplacement relative to the crystallisation state of G2 often show slightly different forms: (i) the earlier porphyrite dykes are generally more en echelon in form, and contacts often show synplutonic relationships with its host G2. Such features include lobate/cuspate margins and non-truncated crystals which appear to lie across the contact (see sub-section 8.3.1.1); (ii) the later, microdiorite dykes generally possess much more planar contacts and the en echelon behaviour is generally less frequent (see sub-section 8.3.1.2).

Due to these differences, combined with the fact that each dyke phase has deformed Glencoe G2 by different processes (governed by the relative crystallisation state of G2 during their emplacement), the external deformational characteristics of each phase will be discussed separately.

8.3 FABRIC DEVELOPMENT AND ASSOCIATED STRUCTURES

8.3.1 Internal fabrics

Internal, pre-full crystallisation (PFC) fabrics are generally characterised, both within the grey/pink porphyrite dykes and microdiorite dykes, by the preferred dimensional orientation of the plagioclase phenocrysts (Plates 8.1 & 8.2). To a lesser extent the fabric is defined by hornblende and/or biotite laths. These 'phenocryst' phases are set in an undeformed matrix of interstitial quartz and feldspar. PFC fabrics are most easily recognisable in the field within the wider porphyrite dykes due to their slightly coarse grain-size. However, with the microdioritic dyke phase PFC fabrics are generally infrequent due to their lack of phenocryst phases.

Internal, crystal plastic strain (CPS) fabrics may occur, especially along the dyke contact where there has been a localisation of strain which continued into the solid state. These areas are often associated with discrete syn-magmatic shears (generally < 1.5 cm wide). These discrete shears are not always confined to the walls of the dyke, as they may obliquely cut across the width of the body, generally overprinting pre-existing PFC 'lock-up' shears (see below). This high temperature CPS deformation is often characterised by the following microstructural features: (i) Plagioclase phenocrysts have often undergone marginal sub-graining, leading to an annealed texture, and exhibits evidence of internal ductile deformation (most commonly in the form of deformation lamellae and undulose extinction. Magmatic features such as zoning have often been removed by recrystallisation processes and twinning is occasionally lost due to dissolution; (ii) Hornblende and biotite laths show evidence of internal ductile deformation in the form of bent and kinked crystals, very often wrapped around the much larger feldspar phenocrysts; (iii) Interstitial quartz forms lenticular crystals which have undergone sub-graining and recrystallisation.

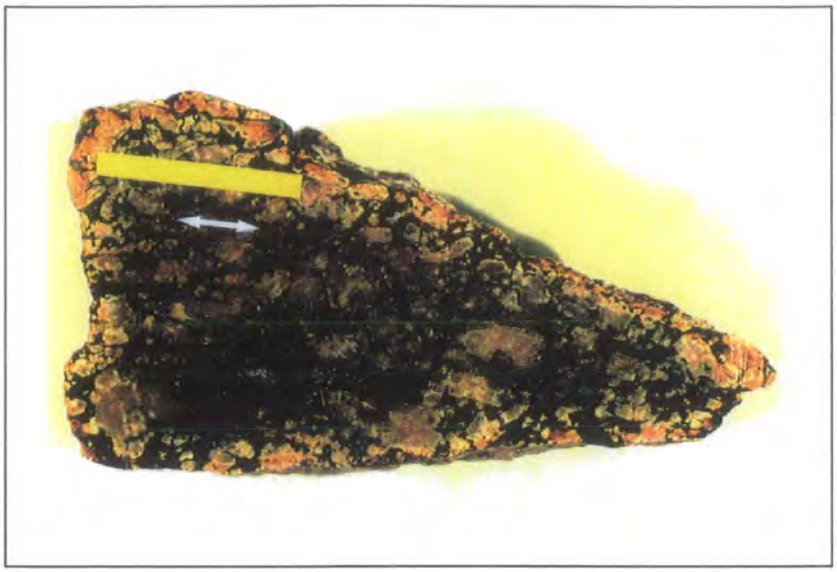

Plate 8.1. Hand-specimen of Etive porphyrite dyke from the River Etive section [NN 210 514]. It possesses a weak to moderately developed PFC fabric, which is defined by plagioclase phenocrysts. (Yellow 'bar' is approximately 2 cm long).

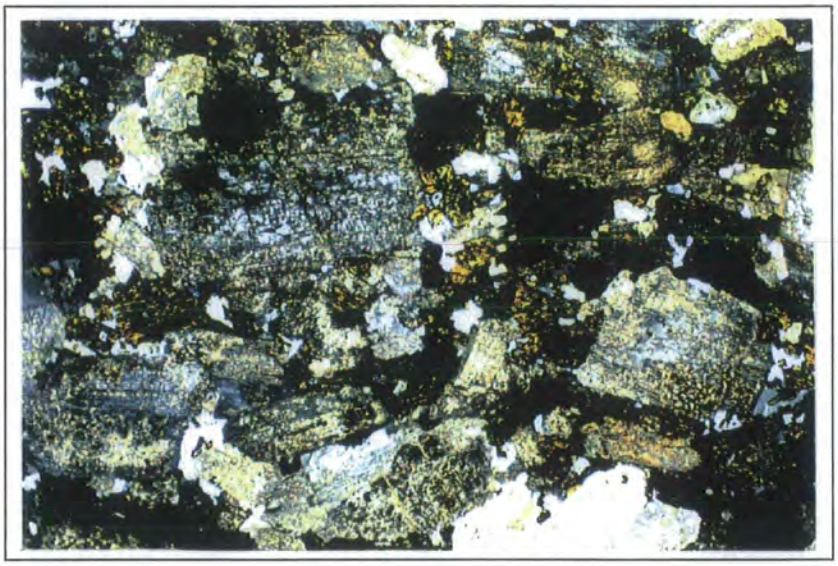

Plate 8.2. Photomicrograph of hand-specimen shown in Plate 8.1. (Field of view approximately 18 mm).

Internal fabric trajectories

If preserved, pre-full crystallisation (PFC) fabrics are generally only weak to moderately developed, and are most apparent within the outer parts of the dyke body. The most intense PFC fabrics are usually confined to the margins of the dyke and are most often contact parallel. However, moving into the centre of the dyke the fabric intensity generally diminishes quite gradually until the fabric is lost completely (Fig. 8.2a). This decrease in fabric intensity is sometimes coeval with a change in fabric orientation, with the fabric becoming progressively more oblique to the walls of the dyke as the centre of the body is approached. In several places the PFC fabric has been traced right across the width of the dyke, showing a sigmoidal fabric swing which is indicative of sinistral shear during its emplacement and crystallisation (Fig. 8.2b). This sense of shear is consistent with kinematic observations within the surrounding host (see sub-section 8.3.2.1).

Occasionally more complex situations are recognised, where instead of the PFC fabric trace being approximately symmetrical on either side of the centre of the dyke (as shown in Fig. 8.2b) an asymmetric pattern may occur (Fig. 8.2c). In this situation the fabric type and intensity changes across the width of the dyke. Where the fabric forms a large, open, concentric trace it is defined by a weak to moderately developed PFC fabric. This is in contrast to the situation where when the fabric dramatically changes in orientation along one side of the dyke, it is generally characterised by a high temperature solid state overprint which intensifies towards the dyke margin where the fabric becomes contact-parallel. This localised zone of CPS deformation often occurs along a sinistral syn-magmatic shear which has developed along the internal contact of the dyke wall. As shown in Figure 8.2c this has resulted in the localisation of higher strains along one side of the dyke due to the establishment of a differential shear component. This component has possibly been produced by the localisation of shear along the walls of the dyke during magma flow. Assuming the direction of magma flow is the same as the direction of fracture propagation (which is likely to be the case), these geometrical features in nearly all cases suggest that the dyke propagated away from the centre of the Etive complex, and sinistral shear was associated with the dyke emplacement mechanism. This direction of magma flow is also substantiated by the development of "imbricate/tiling fabrics" (Den Tex 1969; Blanchard *et al.* 1979; and see Knight & Walker 1988).

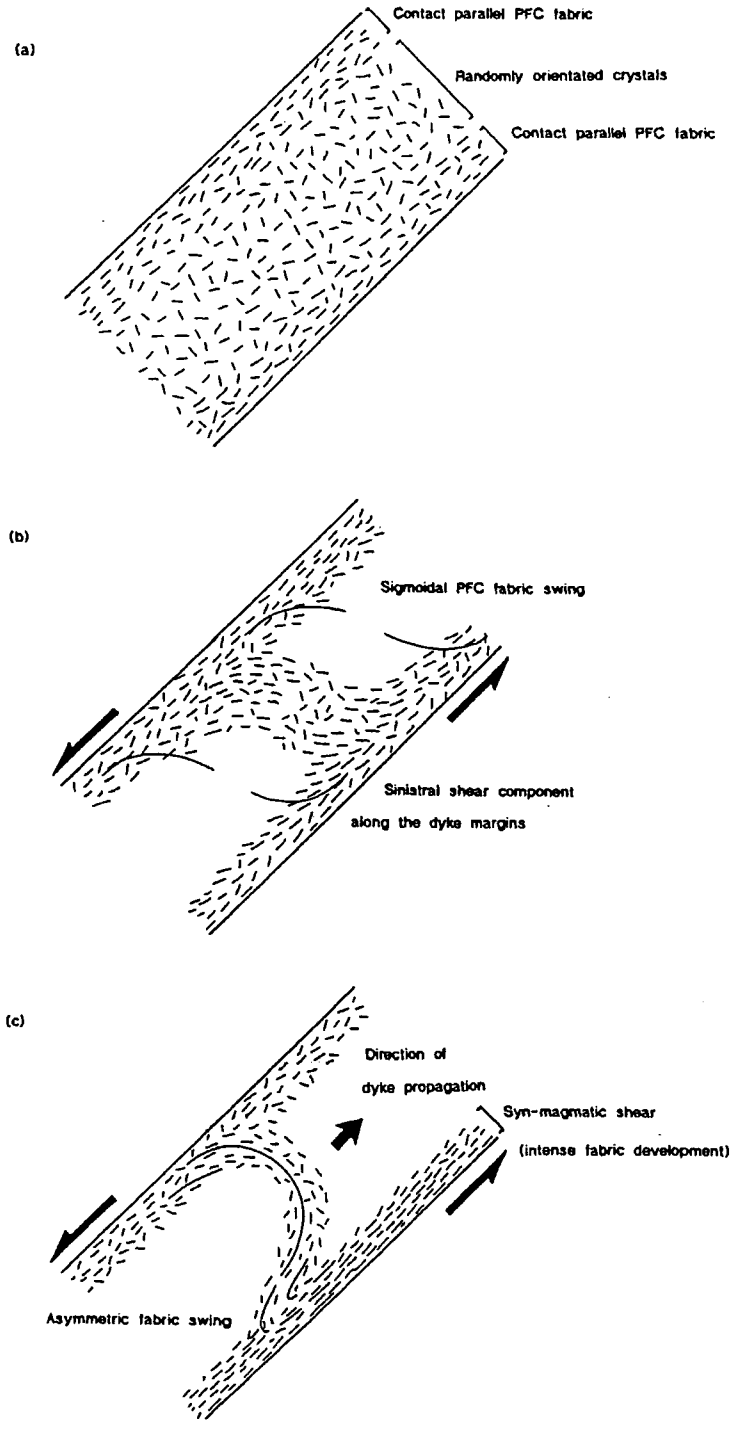

Fig. 8.2. Internal PFC fabric trajectories: (a) contact parallel PFC fabrics only (most common situation); (b) symmetrical sigmoidal fabric swing indicative of sinistral shear; and (c) asymmetric fabric swing and associated syn-magmatic shear. The latter geometrical relationships can be used to determine the direction of dyke propagation.

8.3.2 External fabric development within the plutonic host

The following field and microstructural observations are mainly concerned with the deformational features developed within the Glencoe Clach Leathad facies (G2) associated with the emplacement of the Etive Dyke Swarm. As mentioned in Section 8.1 this is because of two reasons: (i) Glen Etive provides an excellent section through the dyke swarm; and (ii) the crystallisation state of G2 (i.e. incompletely crystallised during part of the dyke emplacement phase) means that the deformational features produced within the plutonic host provide important information regarding the mechanisms operating during the construction of the dykes and their relative time of emplacement. Many of the features described below can be applied to some extent to the dyke-related fabrics produced within the Etive Cruachan facies (G2).

8.3.2.1 The Early phase of pink and grey porphyrite dykes: emplacement into an incompletely crystallised host

Contact relationships and external deformational characteristics within the plutonic host, Glencoe G2, suggest that a large proportion of the grey to pink porphyrite dykes represent a distinct earlier intrusive phase, compared to the majority of microdioritic dykes (see sub-section 8.2.1.2).

The contacts between the porphyrite dykes and the plutonic host G2, often exhibit synplutonic relationships including lobate/cuspate geometries, and the incorporation of undeformed feldspar phenocrysts from the host (G2) into the dyke (Plate 8.3). Both features can be observed within the field. Microscopically, the contact between the host and dyke is often 'defined' by interlocking, non-truncated crystals; indicative of "fracturing and diking in incompletely crystallized granitic plutons" (see Hibbard & Watters 1985). Even where the contact between dyke and host appears to be sharp and planar in the field, microscope analysis may show that the contact is in fact interlocking, with these crystals showing no evidence of fracturing. However, along certain parts of the dyke wall, the localisation of strain and shear movement appears to have continued for a short period across the "rheological critical melt fraction" (Arzi 1978; Van der Molen & Patterson 1979; see Ch. 1) resulting in the fracturing and truncation of crystals along the contact and imposition of crystal plastic strain (see below).

At the confluence between the River Etive and Allt Fionn Ghleann, several porphyrite dykes show evidence that this earlier phase has locally induced ductile strains up to 2-3 m from the dyke margin, expressed as changes in host pre-existing PFC fabric orientation and the development of strain gradients. At one locality [NN 225 523], a

porphyrite dyke possesses a composite arrangement, in which the earlier, pink porphyrite has been intruded by a slightly later, more basic, grey porphyrite phase. A synplutonic contact is observed between the two. The contact between the pink porphyrite and the host G2 also exhibits synplutonic relationships and shows clear evidence of sinistral shear along the dyke walls by the syntectonic rotation of the PFC/CPS fabric within G2. This fabric reorientation within G2 generally occurs over a distance of approximately 0.5 m, but appears to depend greatly on the width of the associated dyke body; with some extremely wide dykes (> 5 m) causing a syntectonic rotation of the host fabric up to 3-4 m from its margin. In several places, the long axis of microdioritic enclaves define this fabric swing and show no evidence of recrystallisation. Their X/Z ratios indicate an apparent slight increase in strain towards the dyke margin.

As mentioned in sub-section 8.2.3., many of the porphyrite dykes viewed on horizontal surfaces have en echelon forms (see Plate 8.4). Such behaviour is occasionally seen on vertical surfaces, as shown by Plate 8.5 (see Fig. 8.3). Both field and microstructural observations suggest that during dyke emplacement strain was focussed along certain parts of the dyke wall. In general, corresponding zones of higher strain occur along the stepping or "en echelon" parts of the dyke margin, i.e. where the dyke contact changes in strike from a general NE-SW orientation (around 030-045°; which will be referred to as the "strike-parallel contact") to a NW-SE-trend (approximately 110-130°; which will be referred to as the "en echelon contact") (Plate 8.5). Within these 'high strain zones' (see Plate 8.6) localised syn-magmatic shears occur along the contact within G2 (Clach Leathad facies). Microstructural features suggest that in most cases the deformation along these zones continued into the solid state, resulting in a localised zone of moderate to well developed high temperature CPS deformation. As shown by Plates 8.7 and 8.8, these features can be observed "megascopically". In many cases the sense of shear can be deduced along these zones by the way the pre-existing fabric within G2 has been deflected along the contact, and by the way plagioclase phenocrysts have been rotated and deformed, often wrapped by biotite crystals, to produce a high temperature CPS, "annealed-type" fabric (Plates 8.7 & 8.8). Microstructural analysis along the "strike-parallel contacts" often indicates a sinistral shear component during the construction of the dykes. This is verified by larger scale features such as matching re-entrants of dyke contacts on opposite sides of the body, and the en echelon form of oblique dyke offshoots. Thus implies a sinistral sense of opening of the dykes during their emplacement. In general, the "strike-parallel contacts" are irregular and often exhibit features which are indicative of a synplutonic relationship with its host (G2). However, along the "en echelon contacts" (see Plate 8.6) such features do not generally occur and the contacts are somewhat more planar. Also microstructural features often suggest that along these 'higher strain (en-echelon) contacts' an apparent dextral shear component may occur (see Plate 8.8); with these margins operating as dextral

syn-magmatic shears. One simple solution to account for their development is that they formed a conjugate arrangement, interacting with the overall sinistral shear component established along the "strike-parallel contacts" of the dyke producing a bulk extensional component, which allowed the dyke to open obliquely in an overall sinistral shear regime (see Fig. 8.3).

Plate 8.3. Hand-specimen showing a synplutonic contact between Etive grey porphyrite dyke material and Glencoe G2. (Yellow 'bar' is approximately 2 cm long).

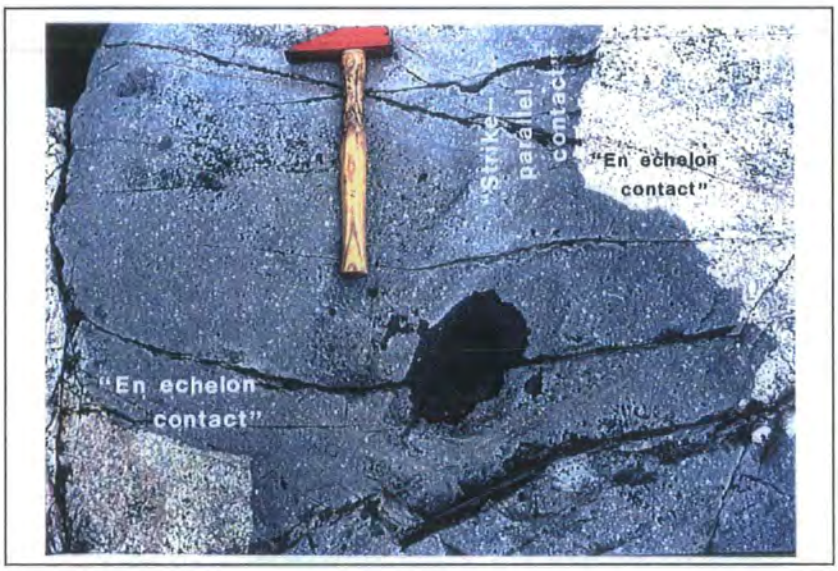

Plate 8.4. En echelon form of porphyrite dyke viewed on horizontal surface, showing "strike-parallel contact" and stepping or "en echelon" parts of the dyke margin. River Etive section.

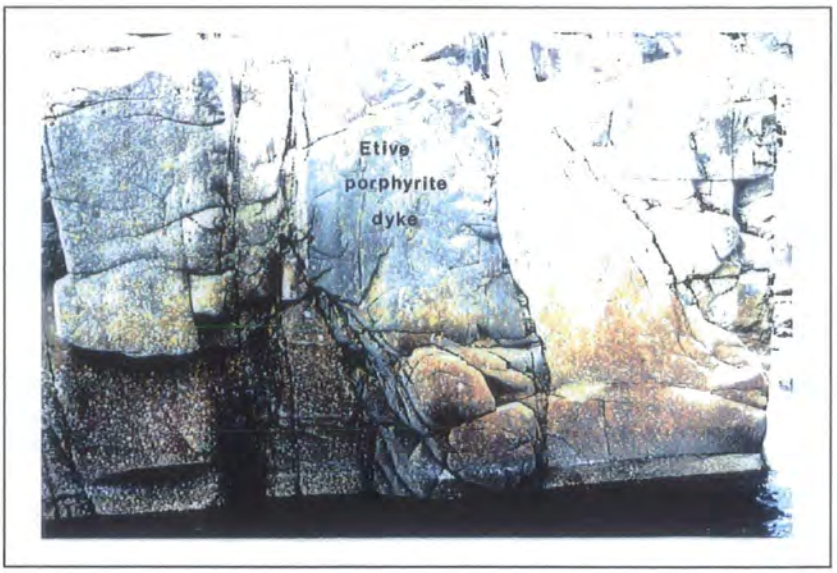

Plate 8.5. En echelon form of porphyrite dyke viewed on vertical surface. This is a vertical view of the dyke seen in Plate 8.4.

Plate 8.6. En echelon form of porphyrite dykes showing approximate positions of high strain ("strike parallel contacts") and low strain ("en echelon contact") zones. Strain intensity progressively changes between the two zones. (Horizontal surface).

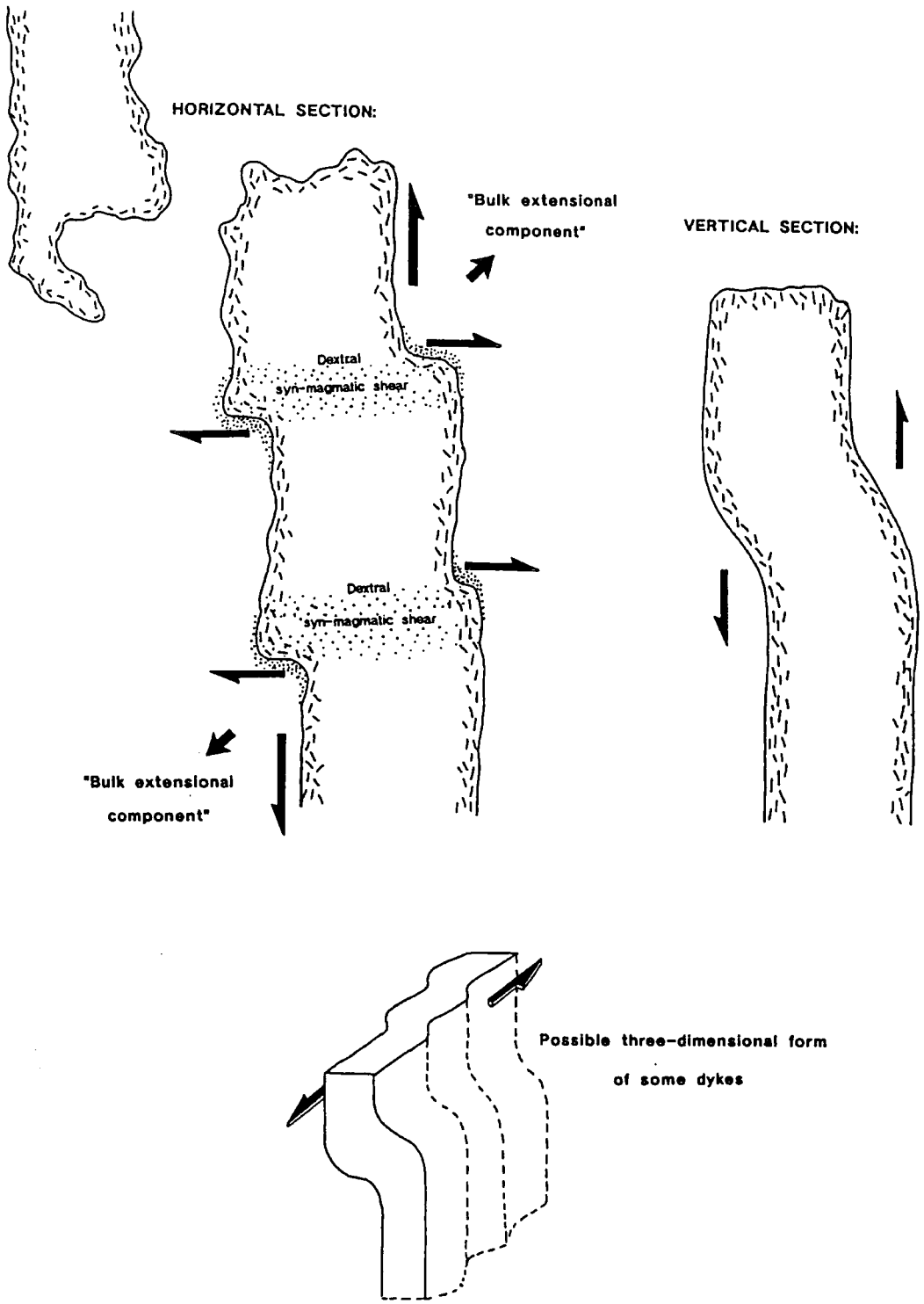

Fig. 8.3. An idealised model of the possible three-dimensional form of a porphyrite dyke and its mechanism of emplacement.

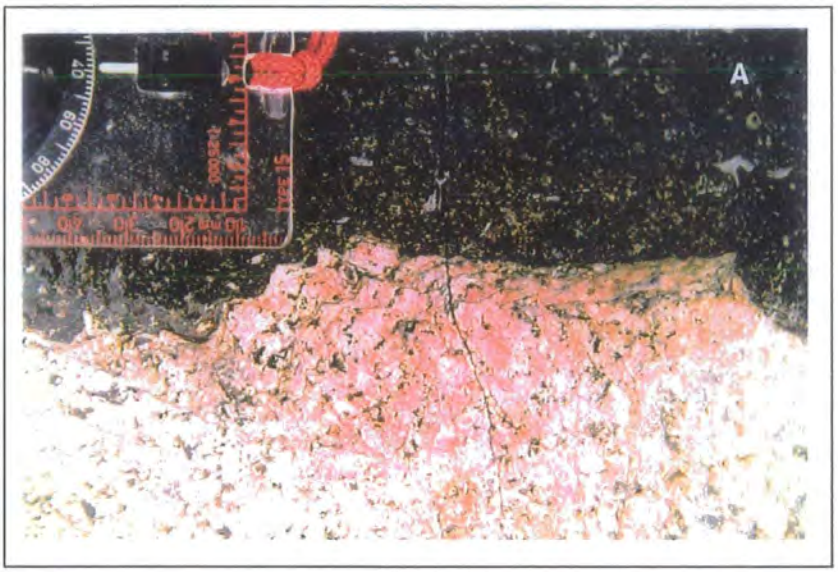

Plate 8.7. Closer view of part of "en echelon contact" as shown in Plate 8.6, marked A. High temperature CPS deformation localised along the contact within host Glencoe G2. Note its annealed texture and the rotation of the feldspar crystals implying a sinistral sense of shear.

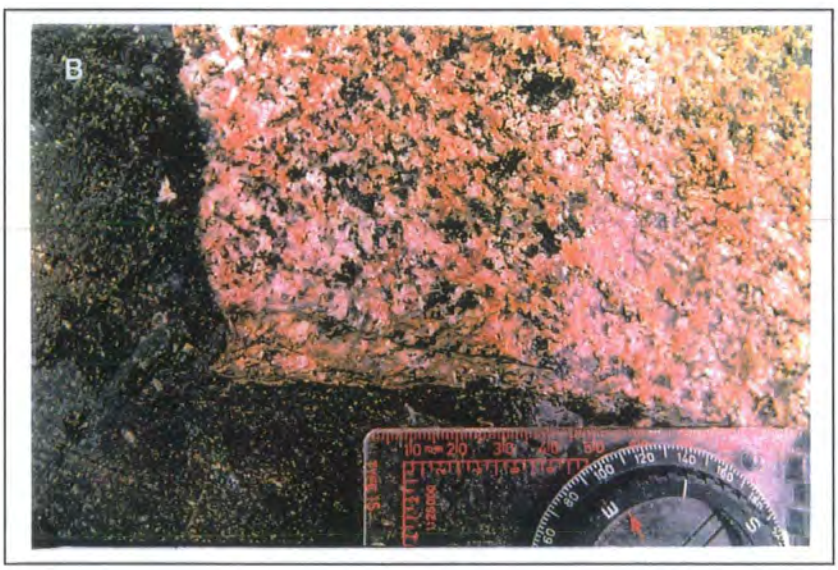

Plate 8.8. Closer view of part of "en echelon contact" as shown in Plate 8.6, marked B. High temperature CPS deformation localised along the contact within host Glencoe G2. A dextral sense of shear is implied by the way mafics have been deflected.

8.3.2.2 The later phase of microdioritic dykes: emplacement into a mainly crystallised host

Microstructural features presented below suggest that the majority of this more minor dyke phase intruded into Glencoe G2 when the host was near to full crystallisation. These features together with megascopic observations of structures developed within G2 which are associated with dyke emplacement are listed below:

① A great majority of the microdioritic dykes have sharp, planar contacts, in contrast with the earlier, porphyritic phase (see sub-section 8.3.1.1). Host crystals have been fractured and truncated along the contacts.

② Localised, high to moderate temperature CPS fabrics occur along the dyke margin within G2 (Plates 8.9 & 8.10). This is in contrast to the majority of the adjacent microdioritic dyke material which exhibits generally weak to moderately developed pre-full crystallisation deformation, often contact parallel.

③ Discrete, brittle-ductile shears are common, often seen diverging from the dyke contact, generally up to 0.5 m from the dyke wall. The majority possess a component of sinistral shear, exhibited by several criteria: (i) geometrical relationships (Plates 8.11 & 8.12); (ii) the displacement of pre-existing inclusions such as microdioritic enclaves (Plate 8.13); (iii) the syntectonic rotation of phenocrysts. Along these zones, down-temperature deformation has often led to the development of a thin veneer of mylonite (generally < 2 mm wide) showing considerable grain size reduction. This mylonisation is often localised along the walls of the dyke (see Plate 8.10).

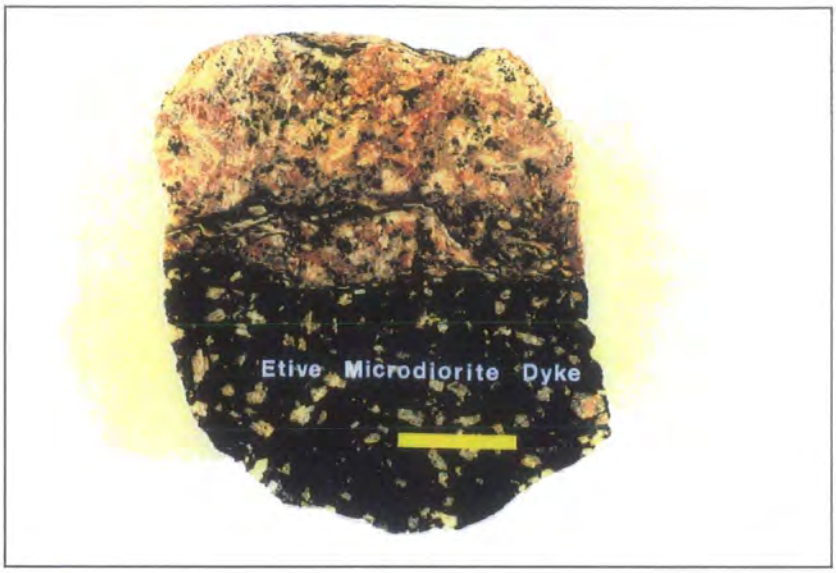

Plate 8.9. Hand-specimen showing a "sheared" contact between Etive microdiorite dyke and Glencoe G2. Note the CPS deformation occurs within the host G2. (Yellow 'bar' is approximately 2 cm long).

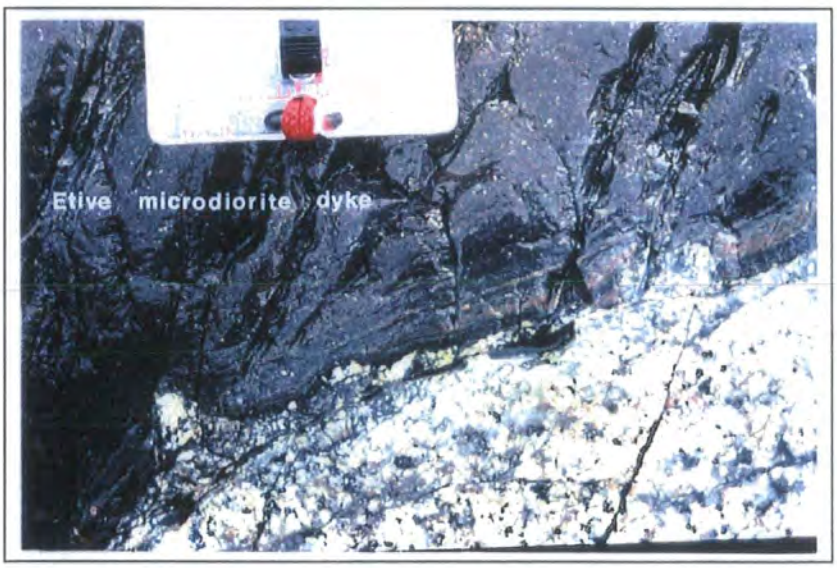

Plate 8.10. Contact between microdiorite dyke and Glencoe G2. Both have experienced localised, high to moderate temperature CPS deformation. Continued down-temperature deformation has resulted in mylonisation along contact. (Horizontal surface).

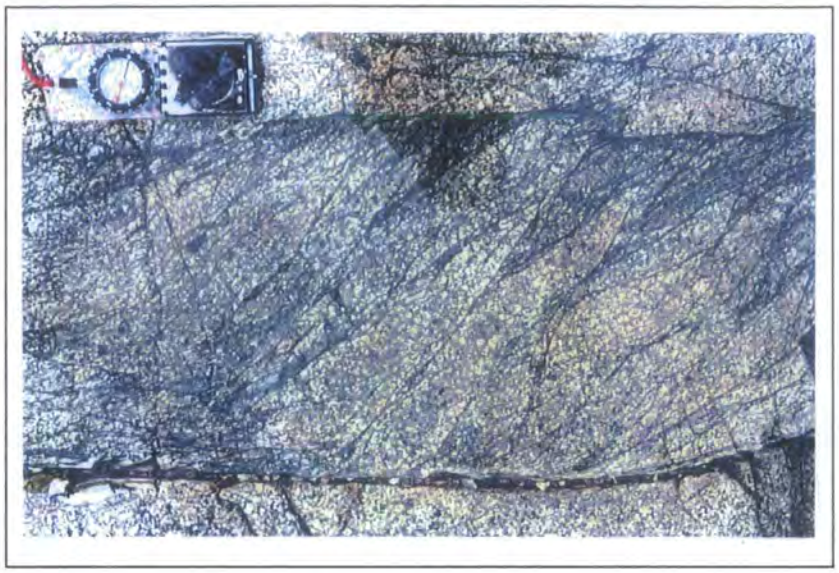

Plate 8.11. Network of brittle-ductile shears. (Horizontal surface).

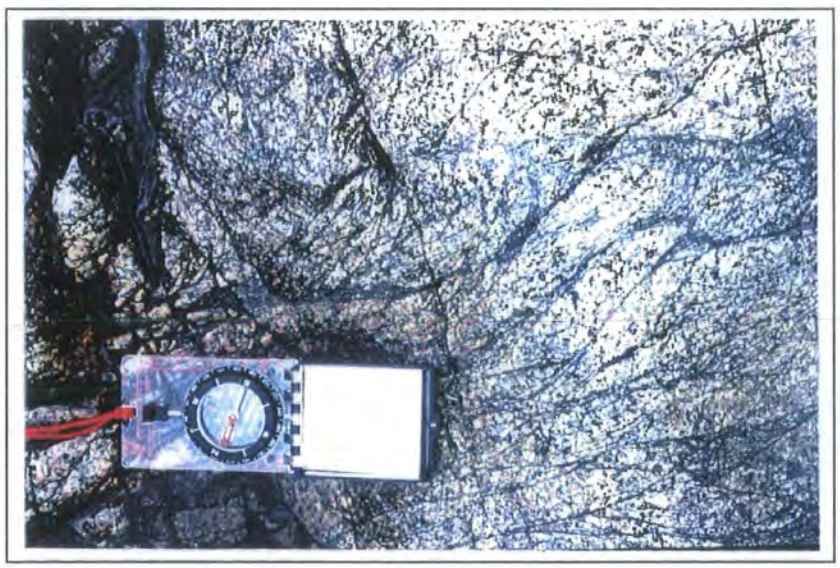

Plate 8.12. Closer view of part of Plate 8.11: 'typical' kinematic indicators within Glencoe G2.

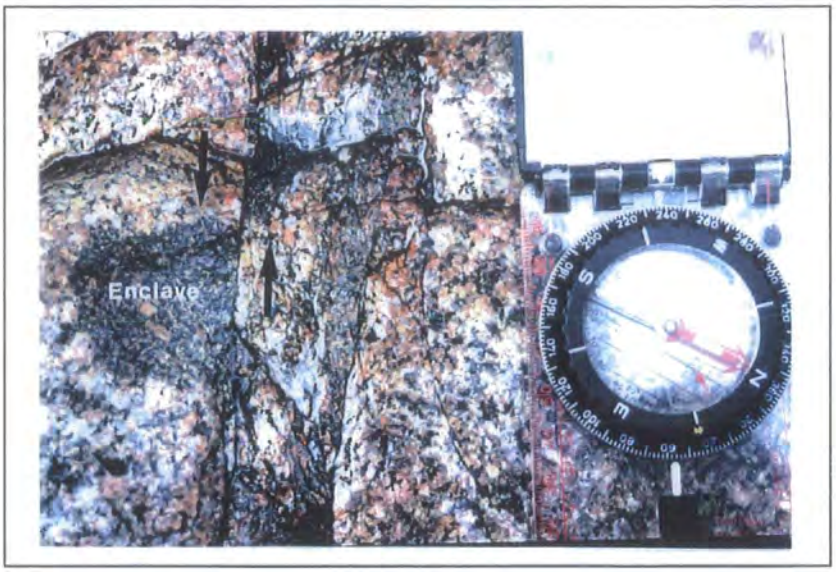

Plate 8.13. Brittle-ductile shear has sinistrally displaced enclave. (Horizontal surface).

8.4 DISCUSSION

The observed internal and external deformational features related to the emplacement of the Etive Dyke Swarm implies a regional sinistral sense of deformation during their development. Fabric development both within the dyke and the wall rocks of the host, together with associated structures, imply that each dyke could be regarded as representing a "minor, sinistral transcurrent shear zone" related to an overall regional transtensional phase (see Fig. 8.3). The dyke swarm is essentially localised along the NW-SE-trending Etive-Laggan shear zone and bounded to the north by the Allt Buidhe/Laggan Dam Fault and to the south by the Etive shear zone. These major structures have been shown to have possessed a sinistral transtensional component during this period of magmatism; as shown by the emplacement of Rannoch G4 (Ch. 5, sub-section) and the construction of the Glencoe Fault Intrusion (Ch. 7) (both these intrusive phases have synplutonic relationships with the Etive Dyke Swarm). This therefore suggests that the dykes are orientated at an acute angle to the maximum principal strain imposed throughout the region (see Fig. 8.4). This implies that the dykes have intruded into a 'shear failure

zone/fracture' developed within the host G2 and the surrounding country rocks, explaining their NE-SW-trend. *In some sections this has produced up to 25 % dilation of the crust.*

However, at the centre of the Etive complex where the 'regional strain field' has been overprinted by the local development of expansion-related strains associated with the emplacement of the Etive Starav facies (G4/G5), this has led to a change in the orientation of the dykes from the general NE-SW-trend to a radial disposition. They occur at right angles to the curving margin of the Starav facies suggesting that the dykes within this localised zone are aligned parallel to the maximum principal strain direction imposed by the *in situ* expansion of G4/G5 (Fig. 8.4). This is consistent with the model presented by Anderson (1936, 1951) in which the dyke intrudes in a plane perpendicular to the least principal strain, parallel to the maximum principal strain. This is also consistent with laboratory testing (Knapp & Knight 1977), which shows that hydraulic fracturing will occur parallel to the maximum principal strain direction when the rock fluid pressure exceeds the tensile strength of the rock mass and regional strain field.

The last question to answer, is why does the concentration of dykes diminish towards the contact of the "cross-cutting" Porphyritic Starav facies (G4) (Fig. 8.4). This might be because the percentage of melt remaining within G2 (the host) was greater than 30 %, therefore above its "critical melt fraction" (see Ch. 1, sub-section 1.5.2) and so preventing it from transmitting shear stresses.

8.5 CONCLUSIONS

Two main phases of dyke emplacement have been recognised: (i) an earlier phase, the majority of which are pink and grey porphyrites which have been intruded into Glencoe G2 whilst its host was still incompletely crystallised; and (ii) a later, somewhat more minor phase of microdiorite dykes which intruded Glencoe G2 when the host was near to or fully crystallised. Sinistral shear was an extremely important component during dyke construction, which is consistent with observations made by Morris and Hutton (1993). This implies that during their emplacement a regional sinistral shear regime prevailed, which is consistent with data presented within this thesis for the sense of shear imposed by a number of major Caledonian NE-SW-trending regional shear zones during this period of Caledonian magmatism.

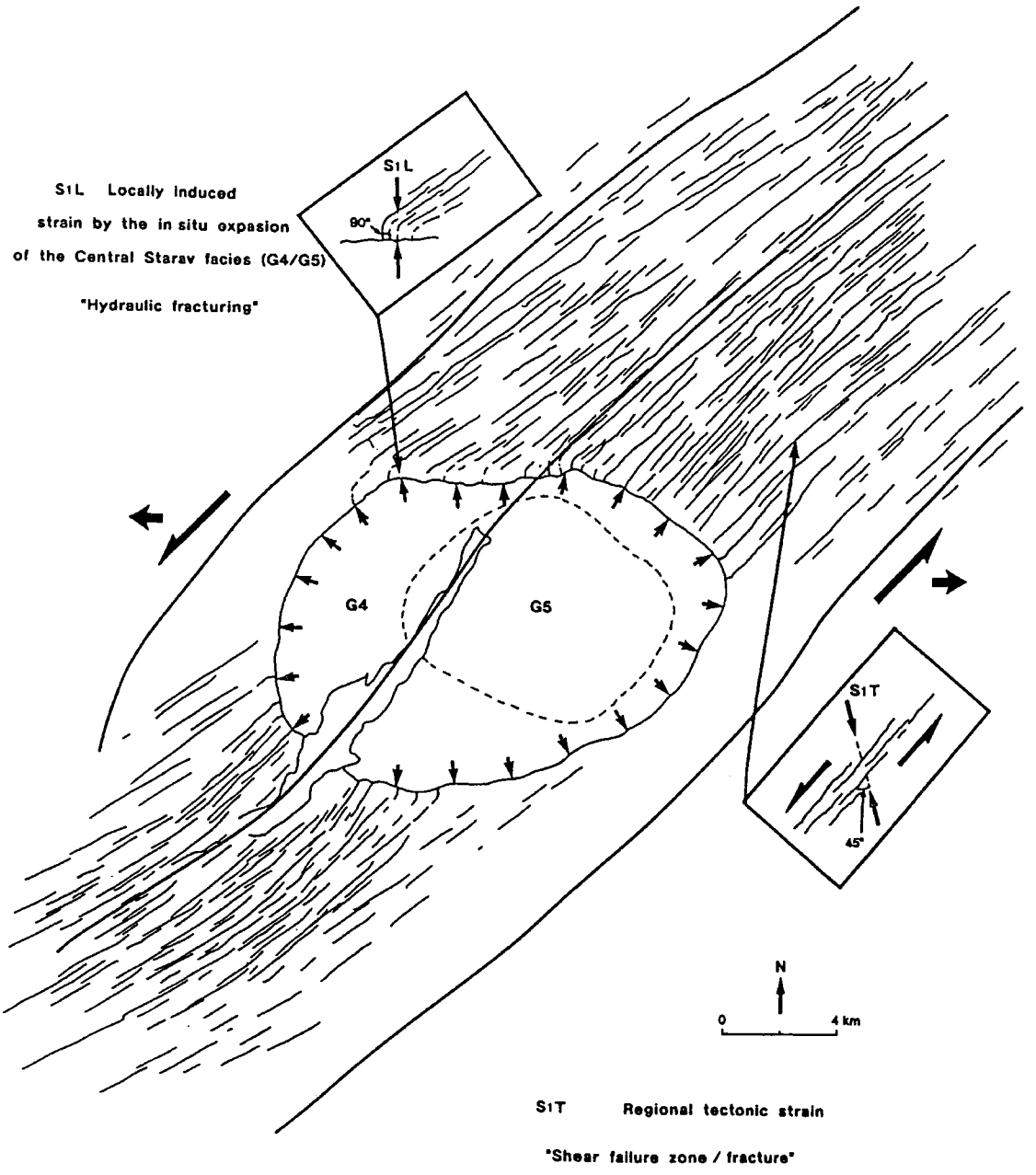

Fig. 8.4. Generalised model explaining the orientation and distribution of the Etive Dyke Swarm.

CHAPTER 9

CALEDONIAN MAGMATISM AND MAJOR LINEAMENTS

9.1 INTRODUCTION

The close spatial and temporal relationships between the late Caledonian granites in Scotland and Ireland and sinistral strike-slip faults and shear zones have been addressed by several workers (Fig. 9.1). Watson (1984) suggested that the post-collisional tectonic regime dominated by strike-slip movement was the "crucial factor responsible for the onset of magmatism", and that the relationship between tectonics and magmatism was therefore genetic.

The tectonic environment at the time of plutonism (425-400 Ma) has been related (Soper & Hutton 1984; Hutton 1987) to the final oblique closure of Iapetus (see Ch. 2). Hutton & Reavy (1992) have argued that the Caledonides during this period were therefore subjected to a gross sinistral transpressional deformation, and that NE-SW-trending transpressional faults and shear zones, such as those described by Watson (1984), are the typical expression of this event. Hutton & Reavy (1992) have further argued that such structures not only controlled the siting and ascent of magma and the emplacement of plutons, but may have been ultimately responsible for granite genesis due to anatexis of thickened crust at the lower limits of transpressional crustal scale shear zones detaching into the Moho (see Ch. 2, Section 2.3).

Watson (1984) also pointed out the importance of a NW-SE set of lineaments in controlling early Caledonian magmatism (Fig. 9.2a). In Scotland, the Loch Shin line and the Cruachan line may represent older pre-Caledonian structures in the lower crust which played a crucial part in determining the sites of Caledonian magmatism. It is of significance that these structures seem to define the distribution of zones of appinitic pipes in Scotland (Fig. 9.2b) and in Ireland, the appinites associated with the Ardara pluton lie along a similar NNW-SSE-trending "Donegal line" (Murphy 1981) (Fig. 9.2a). It therefore

appears that the distribution of sites of magmatic activity may be controlled by the combined influences of Caledonian transpressional and reactivated pre-Caledonian transverse lineaments, faults and shear zones.

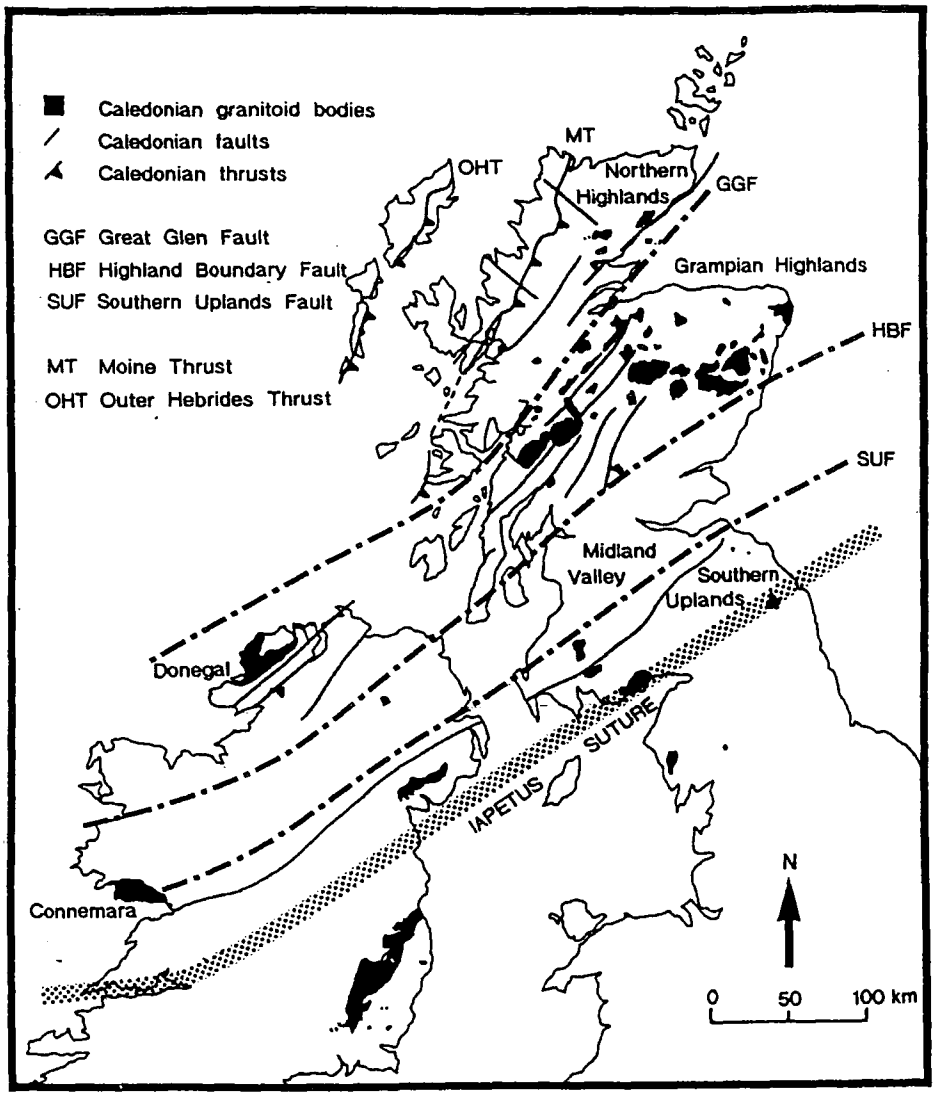

Fig. 9.1. Locality map showing major Caledonian fault systems and associated plutonic bodies.

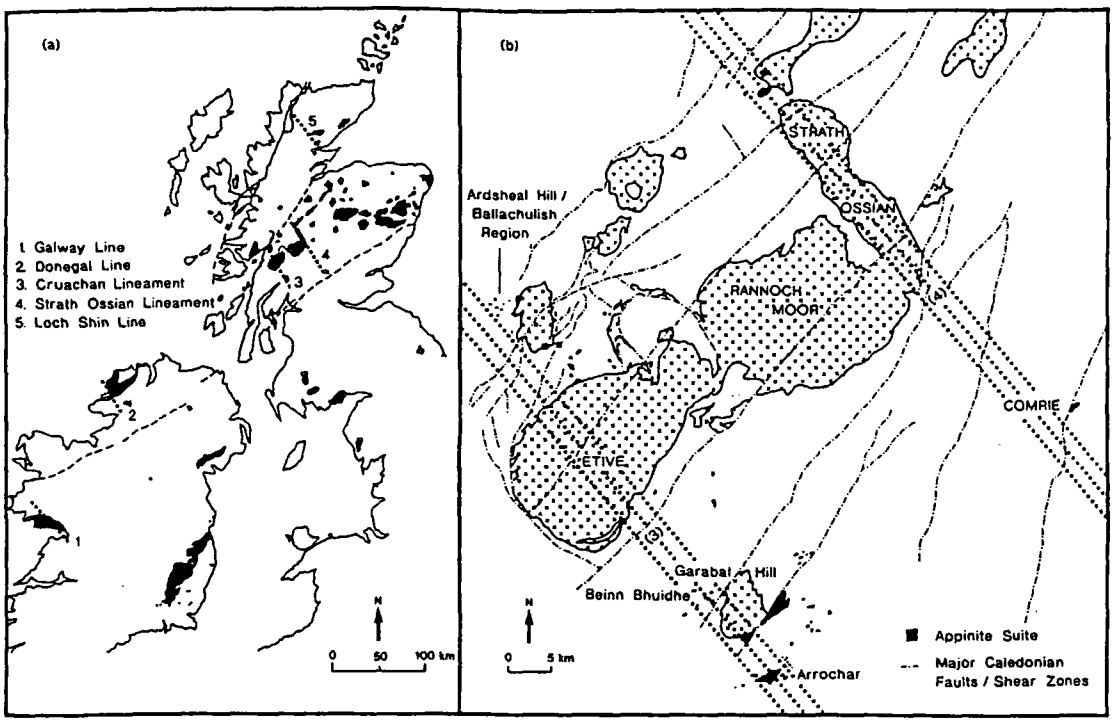

Fig. 9.2. **(a)** Distribution of late Caledonian granites and associated NW-SE trending lineaments in Scotland and Ireland. **(b)** Distribution of appinitic bodies along the Cruachan lineament (3) and the Strath Ossian lineament (4).

MAJOR LINEAMENTS WITHIN THE SW HIGHLANDS

The following sections on Caledonian magmatism, and major lineaments and shear zones within the SW Highlands are based on the new geological data acquired during this study (summarising the emplacement mechanisms, distribution of intrusive facies and tectonic controls), work presented by Jacques and Reavy (1994), titled "Caledonian plutonism and major lineaments in the SW Scottish Highlands", and where referenced, pre-existing data.

9.2 THE ARGYLL SUITE

The plutons which have been studied in the SW Highlands are the Ballachulish (1), Ben Nevis (6), Etive (2), Glencoe (3), Rannoch Moor (7) and Strath Ossian (8) (Fig. 9.3). On a variety of petrographic, geochemical and isotopic criteria, these plutons fall within the "Argyll Suite" of Stephens & Halliday (1984). The plutons of the Argyll Suite typically show a range of rock types ranging from appinite, through hornblende diorite, to granodiorite and granite. Chemically they have calc-alkalic, high Na_2O compositions with marked enrichments in Sr and Ba and low values of Nb, Th and Rb. The southern boundary of the suite is the isotopically-defined "Mid-Grampian Line" (Halliday & Stephens 1984) (Fig. 9.3), north of which ε_{Nd} in the granitoids are always < -6, compared to higher values to the south. Stephens and Halliday (1984) proposed that the Sr and Ba enrichments could be due to transfer of enriched mantle-derived fluids into the lower crust which then became associated with (and possibly initiated) melting. Certainly the strongly negative ε_{Nd} values, which correlate with those granitoids with inherited zircons, dictate a crustal source for this suite of granitoids. Stephens & Halliday (1984) believe that the Argyll Suite is sourced from old crust probably underlain by old mantle metasomatically enriched in K, Ba and Sr.

Although there are many possible causes for differences in petrological and geochemical character between adjacent suites, it is apparent from Fig. 9.3 that the Argyll Suite coincides closely with the region where transpressional strike-slip faults are demonstrably present. Such faults are less obviously present in the NE Highlands, the area designated as the Cairngorm Suite (Stephens & Halliday (1984). This raises the possibility that differences in tectonic environment during anatexis and magma emplacement could have been a strong influencing factor in determining petrological characteristics (see Section 9.9).

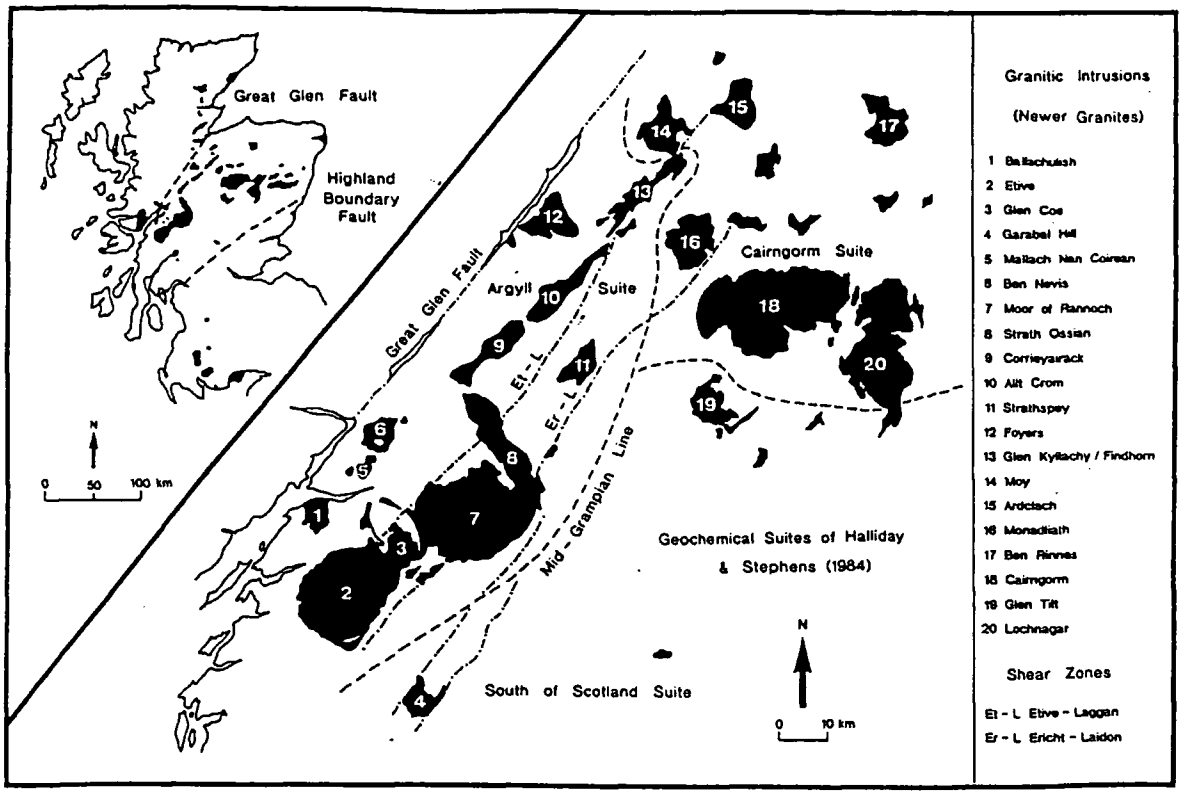

Fig. 9.3. Distribution of granitoids in the Grampian Highlands, showing boundaries of geochemical suites of Halliday and Stephens (1984).

9.3 STRUCTURAL CONTROLS ON PLUTONISM

The site and shape of a particular pluton and the internal distribution of its constituent component facies may reflect (i) orientations of deep basement shear zones which controlled melting sites, (ii) ascent mechanisms (e.g. sheeting within a shear zone) and (iii) higher level emplacement geometries; obviously a combination of such controls is possible. It is therefore important to try to distinguish between ascent (transport) and emplacement (arrival) configurations. Alignment of plutons in gross linear arrays such as within the Argyll Suite could reflect a linear thickened crustal source region as proposed by Hutton and Reavy (1992). Within such an array, if melting and ascent are controlled by the same structure, transport within shear zones is likely to be a major mechanism of ascent by

a process of dyke-like sheeting, proposed by Reavy (1989), McCaffrey (1992) and Hutton (1992) as models for granite ascent in the Portuguese Hercynian and the Irish Caledonian. Crystallisation of magma during such transport will produce sheeted plutons with the sheets parallel to the strike of the shear zones, as reported by these workers. Although shear zones provide an obvious ascent pathway for magma ascent, it is possible that where two crustal structures intersect at depth, relative movements between them will create extensional zones which could be utilized during ascent. This would tend to site plutons above intersections of two structural features. Emplacement (arrival) behaviour such as "ballooning" (expansion) or cauldron subsidence is clearly distinct from the ascent process and features seen are more likely to reflect magma buoyancy or interaction with local structures and / or the free surface, and may therefore give no clue to the precise ascent mechanism. Magma rising in sheets within shear zones could feed into some ballooning structure, as could ascending pulses (see Ch. 3, Section 3.7) in an extensional zone. Any assessment of structural controls on magmatism must therefore attempt to distinguish where possible between those responsible for (i) siting of melting, (ii) ascent (transport), and (iii) emplacement (arrival) where these are different.

It has been established above that the granites which comprise the Argyll Suite are spatially associated with major pre-Caledonian and Caledonian structures. The data presented below shows how the relative movements on these structures could have, (i) controlled the siting of magmatism, (ii) allowed magma to be channelled into ascent conduits and (iii) controlled ascent via such conduits of individual facies to form plutons at higher levels.

9.4 REGIONAL GEOLOGY

The calc-alkaline intrusive complexes under discussion are the Etive (Ch. 3), Glencoe (Ch. 4), Rannoch Moor (Ch. 5), Strath Ossian (Ch. 6), Ballachulish and Ben Nevis plutons. Previous research on these bodies is summarised in Table 9.1. They are late-Caledonian complexes emplaced at 425-400 Ma into Dalradian metasediments of the SW Highlands. These Siluro-Devonian granitoid plutons, known as the Newer Granites (Read 1961) form part of the Argyll Suite (Stephens & Halliday 1984) (Fig. 9.3).

Several workers (Francis 1978, Watson 1984, Hutton & Reavy 1992) have drawn

attention to the linear arrays of plutons in the SW Grampians and their strong spatial correlation with NE-SW strike-slip faults and shear zones parallel or sub-parallel with the Caledonian trend (Fig. 9.4).

Three such NE-SW-trending structures have long been recognised in this area; moving from the NW they are the Laggan Dam fault (Anderson 1956), the Etive-Laggan fault (Hinxman *et al.* 1923), and the Ericht-Laidon fault (Hinxman *et al.* 1923). Data presented within this thesis, based on the recognition of "pre-full crystallisation" (PFC) and "crystal plastic strain" (CPS) fabrics (Hutton 1988) in granites, show that where these structures are spatially associated with plutons, they were acting as shear zones during magmatism; this work has led to the recognition of a fourth major structure in the NW, named the Ballachulish-Corrieyairack shear zone (Jacques & Reavy 1994).

A number of major trans-Caledonoid lineaments have also been recognised throughout Scotland and Ireland (Fig. 9.2a), namely the Galway (Watson 1984); Donegal (Murphy 1981); Cruachan (Hall 1985, 1986; Graham 1986); Strath Ossian (Forrest & Key 1989); and Loch Shin (Bott *et al.* 1972) lineaments. It has been proposed, principally on petrological, geochemical, stratigraphical and geophysical evidence (see Fettes *et al.* 1986), that such structures may be pre-Caledonian basement structures. The role of the Cruachan line in the evolution of the Dalradian cover sequence has been addressed by e.g. Graham 1976, Ashcroft *et al.* 1984, Harte *et al.* 1984, and Fettes *et al.* 1986. Watson (1984) suggested that these lineaments actively controlled the siting and channeling of the early appinite suite of intrusions.

The influence of trans-Caledonoid structures in controlling Dalradian sedimentation is becoming increasingly more apparent. Anderton (1985) has argued that attenuation of the continental crust and basin development during late Proterozoic times (see Ch. 2) was achieved by the development of a series of Caledonoid-trending listric normal faults with several km's of downthrow, interacting with a set of transverse non-Caledonoid transfer faults. The latter structures are defined by sharp lateral facies changes. Such a situation has been described by Anderton (1976; 1977) in Jura, defining two NW-SE-trending transfer faults which can be traced through Scarba and Islay (Fig. 9.5; Anderton 1985).

Probably the most obvious along-strike variation in Dalradian lithostratigraphy, is that across a NW-SE-trending lineament in the SW Highlands, the 'Cruachan Line' (Graham 1986). Combined information from the LISPB and WINCH seismic reflection profiles (Hall *et al.* 1984; Hall 985), from magnetic anomaly data (Westbrook & Borradaile 1978), and from Bouger gravity anomalies (Hipkin & Hussain 1983) suggests that the Cruachan Line, which itself is marked by a strong gravity gradient, may separate two different basement types (see Graham 1986).

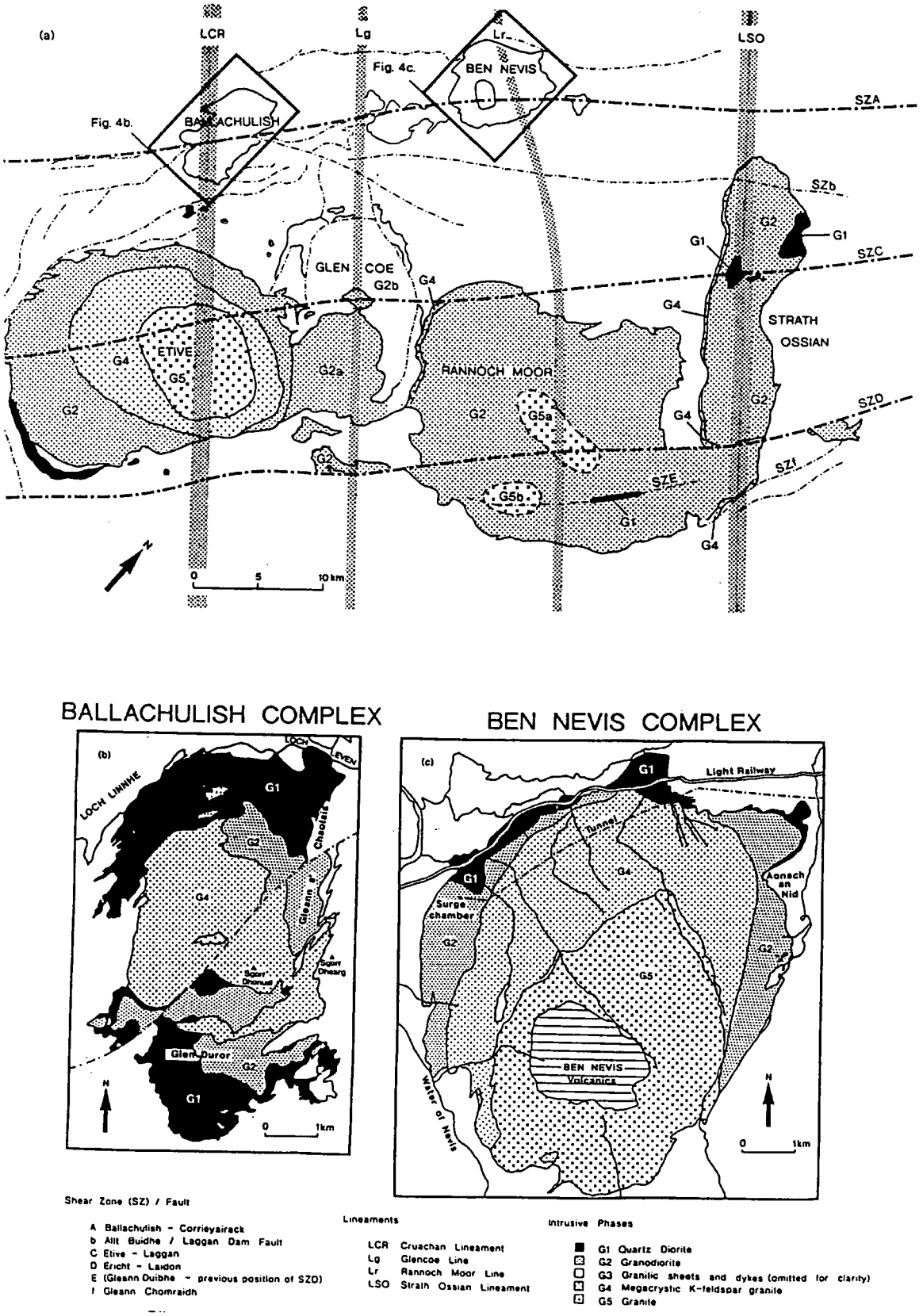

Fig. 9.4. Sketch map of the SW Grampians showing major structural features and the Caledonian plutons under study. All intrusive phases (G1 to G5) within the plutons are shown.

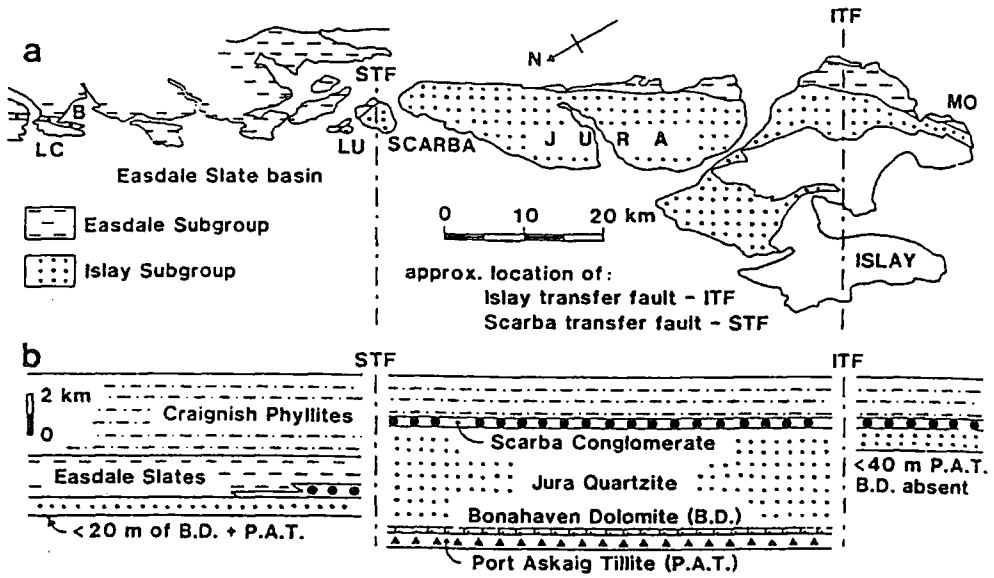

Fig. 9.5. **(a)** Outcrop of the Islay and Easdale Subgroups in the Argyll seaboard area showing approximate position of transfer faults. Locality abbreviations: B, Benderloch; LC, Loch Creran; LU, Lunga; MO, Mull of Oa. **(b)** NE-SW longitudinal section of the Islay and Easdale Subgroups in the area of map. After Anderton (1985).

To the SW of the Cruachan Line, the Tayvallich Subgroup comprises of a thick sequence of Tayvallich Volcanics and associated dykes and sills (Knill 1963; Gower 1977; Graham 1976), comprising approximately 30 % of the Dalradian Succession in that area (Fig. 9.6). However, in the region to the NE of the Cruachan Line, such basaltic rocks are rare. The Tayvallich Lavas, and associated intrusives have tholeiitic chemistry typical of basalts formed at accreting plate margins (Graham 1976; Graham & Bradbury 1981).

The recognition of these NW-SE, traverse structures has challenged the 'traditional view' that Dalradian depositional basins are elongated parallel to the regional Caledonian trend (Graham 1986; see Fettes *et al.* 1986). Graham (1986) has proposed that during Argyll Group times a dextral transcurrent regime prevailed, resulting in pull-apart basin development. The Cruachan Line is thought to represent the north-eastern margin of one such basin. The dextral transcurrent motion has been inferred from the restoration of NW-SE-trending dykes on Jura (Graham & Borradaile 1984). Graham (1986) suggested that during pull-apart development the basins were floored by quasi-oceanic crust, with analogies being drawn with the present situation in the Gulf of California (Graham & Borradaile 1984).

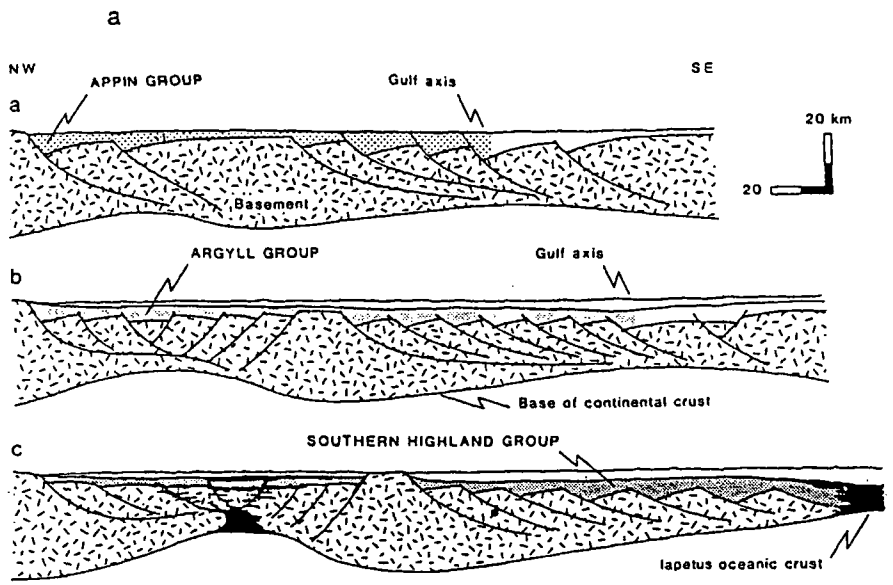

Fig. 9.6. Schematic cross-section of the Dalradian in the SW Highlands to show the tectonic setting in **(a)** late Appin Group times, **(b)** late Argyll Group times and **(c)** Southern Highland Group times. In (c) basaltic intrusions and volcanics are shown in solid ornament. After Anderton (1985).

The role of the Cruachan line in the evolution of the Dalradian cover sequence has been addressed by e.g. Graham 1976, Ashcroft *et al.* 1984, and Harte *et al.* 1984. It is generally believed by many workers that while such a structure may have played a role in the control of Dalradian basin evolution, it exerted no apparent influence in the later structural development of the cover. However, Fettes *et al.* (1986) suggest that such lineaments may have influenced the Dalradian cover sequence during orogenic deformation. They suggest that this is shown by the discontinuity in structural profile of the Tay Nappe as it crosses the Loch Lomond lineament (Mendum & Fettes 1984) and by the change in structure of the NE-SW-trending Ossian/Geal Charn steep belt (Thomas 1979) as it is traced across the Cruachan lineament.

Fettes *et al.* (1986) have distinguished three types of lineament within the Grampian Highlands (Fig. 9.7): (i) those with trans-Caledonoid, NW-SE-trends, e.g. Cruachan-Loch Lomond, Glenlivet, and Rothes; (ii) those with partly Caledonoid trends, e.g. northern part of the Portsoy-Duchray Hill and Fraserburgh-Old Meldrum; and (iii) those with E-W trends, e.g. Insch, and Deeside.

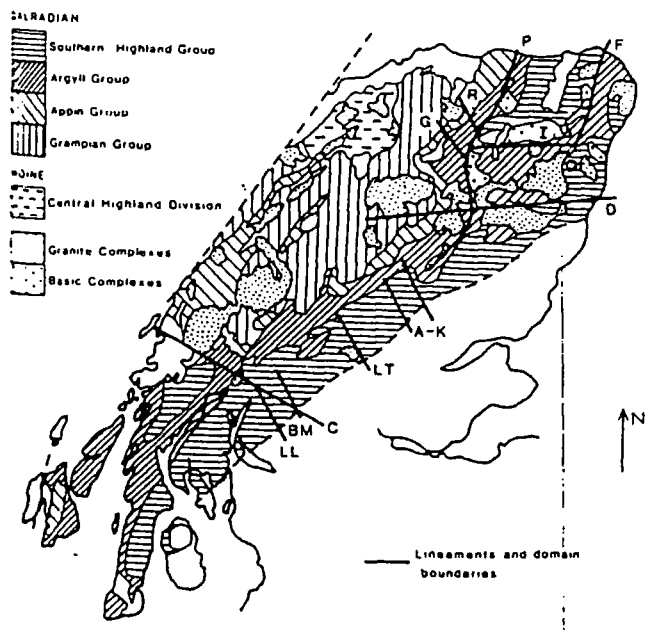

Fig. 9.7. Dalradian lithostratigraphy showing lineaments. LL, Loch Lomond; BM, Ben More; C, Cruachan; LT, Loch Tay; A-K, Aberfeldy-Kirkmichael; D, Deeside; G, Glenlivet; R, Rothes; P, Portsoy-Duchray Hill; F, Fraserburgh-Old Meldrum; I, Insch (in part, after Aschcroft *et al.* (1984)). After Fettes *et al.* (1986).

Recently, Soper (1994) has proposed that the set of NW-SE-trending lineaments in the Grampian Highlands are related to a Vendian rifting event, which originated as a triple junction, with the third arm marked by trans-Caledonoid extensional lineaments (Fig. 9.8).

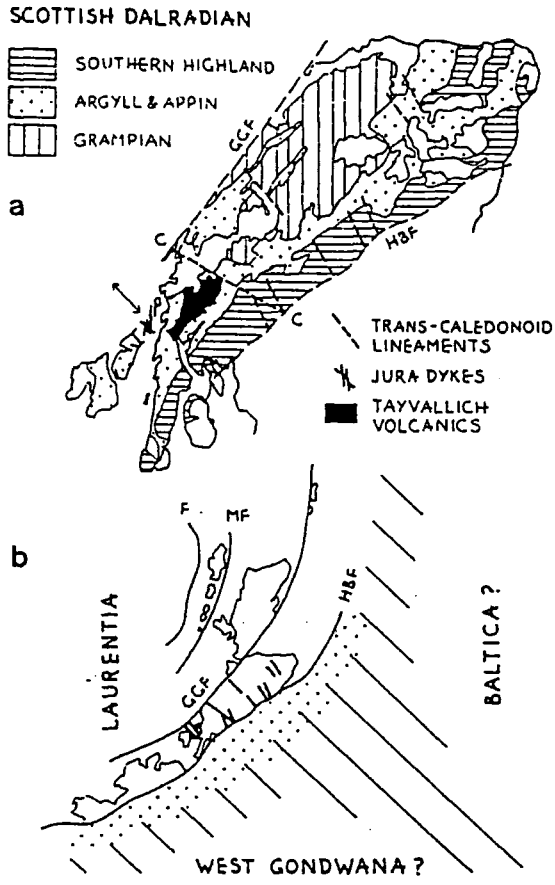

Fig. 9.8. **(a)** Scottish Dalradian terrane showing trans-Caledonoid lineaments, mainly after Fettes *et al.* (1986); C, Cruachan lineament; arrow, pre-deformation trend of Jura dykes after Graham and Borradaile (1984). **(b)** Cartoon showing inferred position of the Dalradian terrane in relation to a pre-Iapetus RRR junction. F, surface projection of Flannan reflector after Snyder and Flack (1990); GGF, HBF, MF, Great Glen, Highland Boundary, and Minch faults. Stipple, youngest Dalradian (Palaeozoic?) prograding onto oceanic crust (diagonal ruling), subsequently removed by Caledonian strike-slip. After Soper (1994).

9.5 INTRUSIVE EVENTS

The result of new mapping undertaken during this current study and the compilation of existing data (Table 9.1; see Fig. 9.4) reveal that within the multiphase intrusions of Etive, Glencoe, Rannoch Moor, Strath Ossian, Ballachulish and Ben Nevis, a comparative

sequence of intrusive phases is broadly applicable to all plutons. The earliest activity is represented by the appinite suite. As mentioned in Chapter 2, appinites are distinctive coarse-grained, ultramafic to intermediate igneous rocks, generally considered to be related to the lamprophyric group of minor intrusions (Hunter & Rock 1987). They are often interpreted as being cumulates from volatile-rich, K-rich basaltic or intermediate magma (French 1966; Hall 1967; Wright & Bowes 1979), and are therefore generally assumed to be sub-crustal in origin and to have been emplaced, often explosively, via deep crustal structures.

Etive Complex	**Rannoch Moor Complex**	**Ballachulish Complex**
After Bailey & Maufe (1916), Anderson (1937), Bailey (1960), Clayburn *et al.* (1983) and Batchelor (1987).	After Hinxman *et al.* (1923), Read 1961) and Leighton (1985).	After Bailey (1960) and Weiss & Troll (1989).
G1, Quarry Intrusion and isolated bodies of quartz-diorite and dioritic material. G2, Cruachan facies (major intrusive component). Essentially a fine-grained felsic monzodiorite. Reversely zoned. G3, Meall Odhar Granite. Sheets of monzogranite and syenogranite. Etive Dyke Swarm. Suite of NE-SW-trending porphyrite and microdiorite dykes. G4, Porphyritic Starav facies. Coarsely porphyritic monzogranite (K-feldspar megacrysts up to 3 cm). G5, Central Starav facies. Monzogranite.	G1, Monzodiorites through to quartz-diorites. G2, Heterogeneous granodioritic facies. Shows evidence of reverse zonation (major intrusive component). G3, Series of monzogranite and syenogranite sheets (minor phase). G4, Coarsely porphyritic monzogranite-syenogranite, consisting of large K-feldspar and plagioclase megacrysts (1-3 cm) in a fine-grained granodioritic groundmass. G5, Non-porphyritic monzogranite.	G1, Quartz-diorite. G2, Heterogeneous monzodioritic facies. Reversely zoned. G3, Series of monzogranite sheets (minor phase). G4, Coarsely porphyritic monzogranite containing large K-feldspar megacrysts in a granodioritic groundmass. G5, Non-porphyritic leucocratic monzogranite.
Ben Nevis Complex	**Strath Ossian Complex**	**Glencoe Complex**
After Maufe (1910), Anderson (1935) and Haslam (1968).	After Hinxman *et al.* (1923), Anderson (1956), Clayburn (1981), Henderson (1982) and Key *et al.* (1993).	After Bailey & Maufe (1916), Anderson (1937), Bailey 1960, Clayburn *et al.* (1983) and Batchelor (1987).
G1, Outer Quartz-Diorite. G2, Inner Quartz-Diorite. Heterogeneous granodioritic phase. G3, Series of microgranite sheets (minor phase). G4, Porphyritic Outer Granite. Homogeneous monzogranite containing megacrysts of K-feldspar and plagioclase. Ben Nevis Dyke Swarm. Suite of NE-SW-trending porphyrite and microdiorite dykes. G5, Inner Granite. Non-porphyritic leucocratic monzogranite.	G1, Quartz-diorite. G2, Medium- to coarse-grained homogeneous granodiorite (major intrusive component). G3, Microgranite sheets. G4, Coarsely porphyritic monzogranite consisting of large (1-3 cm) tabular plagioclase and K-feldspar megacrysts. G5, Microgranite sheets and dykes.	Fault Intrusion. G1/G2? possibly injected along the high-level ring dyke structure. Consists of a number of intrusive phases (main types: grey tonalite, grey and pink porphyrite, pink granite). G2, Coarse-grained monzogranite. Evidence of reverse zonation.

Table 1. Previous research on the complexes studied and distribution of petrographic facies within each pluton.

A high concentration of these small satellite bodies are found around the periphery of the Ballachulish and Etive igneous complexes. A zone of appinites can be traced from the Ardsheal Hill/Ballachulish region south to the Garabal Hill complex along the line of the Cruachan lineament (Fig. 9.2b). Appinite bodies also occur at the northern end of the Strath Ossian complex, along the line of the Strath Ossian lineament (see Ch. 6) (Fig. 9.2b). Following the emplacement of the suite, the first main phase of the complexes is represented by a quartz-diorite G1 which may contain numerous country rock xenoliths and occasional microdioritic/appinitic enclaves. This is followed by G2, a more heterogeneous phase which ranges from monzodiorite through tonalite/granodiorite to monzogranite and contains abundant microgranitoid enclaves. G3 is a minor phase of pink microgranitic dykes and sheets which clearly crosscut the two earlier intrusive events. G4 is a porphyritic monzogranite which contains euhedral megacrysts (1-3 cm long) of K-feldspar and plagioclase, set in a much finer groundmass. The last intrusive phase is a non-porphyritic leucocratic monzogranite G5.

Most of the data is concerned with the Strath Ossian (Ch. 6), Rannoch Moor (Ch. 5), Etive (Ch. 3) and Glencoe (Ch. 4) complexes, however implications for the Ballachulish and Ben Nevis complexes are mentioned where appropriate.

9.5.1 Controls on the Strath Ossian Complex

This linear shaped body which is 30 km by 6 km is markedly transverse to the regional Caledonian strike. The complex is essentially bounded to the north by the Ballachulish-Corrieyairack shear zone and to the south by the Ericht-Laidon shear zone (Fig 9.9). Its long axis runs NW-SE along the Strath Ossian lineament. The Etive-Laggan shear zone runs through the centre of the complex. It is envisaged that the history of Strath Ossian can be explained by reactivation of the Strath Ossian lineament, which functioned as a transtensional Caledonian shear zone, interacting with the other three shear zones. The geometry and depth of the complex indicates a shear zone siting and ascent by sheeting. Data presented in Chapter 6 shows that the sequence of events is as follows. Intrusion of appinite bodies at the intersection of the Strath Ossian lineament and the Ballachulish-Corrieyairack shear zone was followed by emplacement of quartz-diorite which formed a sub-elliptical core to the complex at the intersection of the Strath Ossian lineament and the Etive-Laggan fault. This mass was subsequently rotated and disrupted by the intrusion of G2 resulting in G1 now forming several discrete bodies (Fig. 9.9a). The main mass of the body consists of homogeneous equigranular granodiorite (G2) (Fig. 9.9b). This facies is elongate along the lineament and has a pervasive PFC fabric trending NW-SE parallel with the long axis of the pluton, except at the traces of the Ericht-Laidon and the Etive-Laggan

shear zones. Within the Ericht-Laidon shear zone, this PFC fabric swings into a NE-SW orientation reflecting sinistral movement within the zone. The situation at the trace of the Etive-Laggan shear zone is complicated by the deformation of G1 described above. PFC fabrics within G2 associated with the Etive-Laggan shear zone do exist at several localities, however they are largely overprinted or obliterated by continued deformation induced by the rotation of G1 and the emplacement of subsequent G2 sheets. The general NW-SE-trend of the fabric shows that the lineament was an active shear zone during magma ascent, corroborated by ductile planar fabrics developed within migmatites along the western flank and the reorientation of regional folds (see Ch. 11). The data shows that the shear zone was actively transtensional, allowing intrusion by a process of multiple sheeting combined with sinistral displacements along the NE-SW shear zones, producing a pull-apart structure. Although G2 is largely homogeneous, at some localities internal contacts of individual sheets are observed.

The next apparent activity along the Strath Ossian shear zone is associated with the intrusion of a 30-40 m wide sheet-like marginal facies (regionally G4) of a K-feldspar megacrystic granite along the western flank of G2 (Fig. 9.9c). This again possesses an intense vertical PFC fabric parallel with the contact shown by the preferred orientation of hornblende and biotite clots and microphenocrysts of plagioclase. The megacrysts of microperthitic K-feldspar and plagioclase are generally more randomly orientated, but still possess a general NW-SE alignment. A solid state CPS fabric, shown by ribboned quartz, which is developed in G2 where it is in contact with G4, probably formed at this time. The spatial distribution of G4 and the marked swing in the orientation of its PFC fabric suggests that the Ericht-Laidon shear zone was active during its intrusion. The narrow zone of G4 along the rest of the pluton implies that transtensional deformation across the Strath Ossian shear zone was now limited, due to the cessation of movement on the Etive-Laggan and Ballachulish-Corrieyairack systems. However, the Ericht-Laidon shear zone continued to influence the southern end of the pluton after crystallisation, by displacing it some 8 km to its present position (Fig. 9.9c). The absence of G5 from the complex and the limited occurrence of G4 suggests that no further space was available for emplacement.

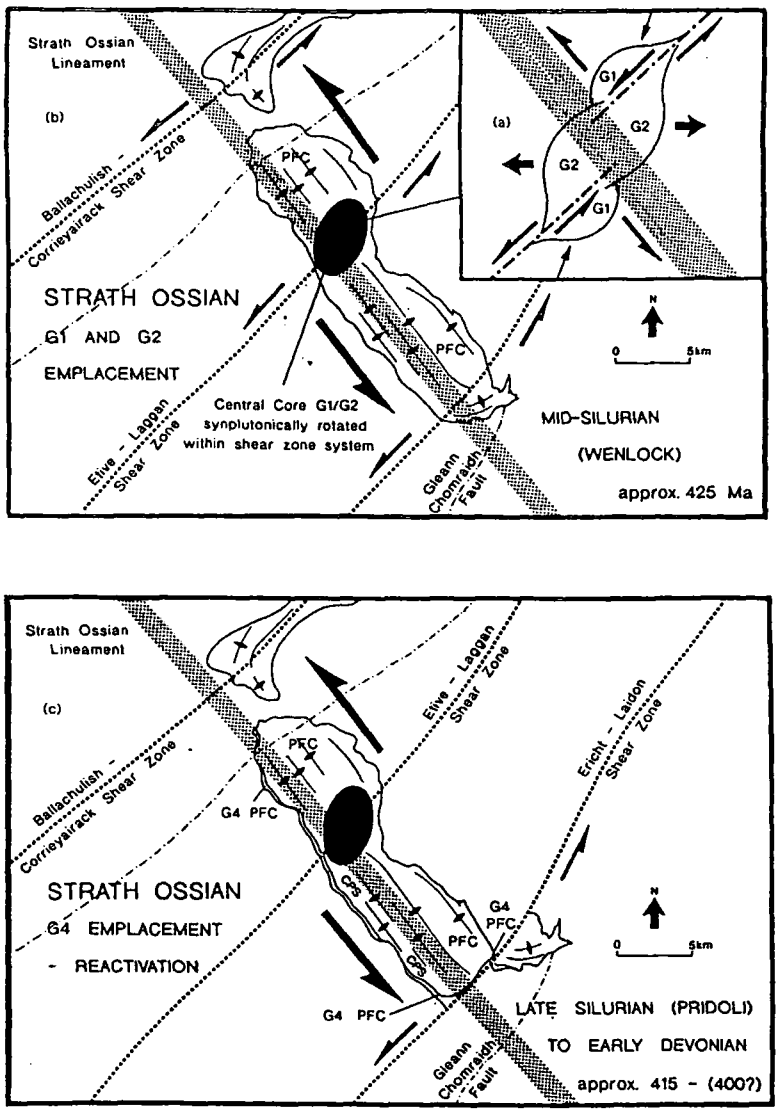

Fig. 9.9. Inset **(a)** shows an idealised model for the initial stages of G1 and G2 emplacement. Generalised model for the emplacement of **(b)** G1 and G2 and **(c)** G4 of the Strath Ossian complex. (N.B. The minor Ciaran-Ossian shear zone is not shown).

9.5.2 Controls on the Rannoch Moor Complex

The Rannoch complex represents magmatism in a different tectonic environment than at Strath Ossian. The use of similar techniques to distinguish successive events can still be applied, however the situation is here complicated by arrival or true emplacement configurations not seen previously which can obscure/obliterate earlier siting/ascent structures.

Rannoch is a somewhat elliptical complex 28 km by 18 km with the long axis along the NE-SW Caledonian strike. It is bounded to the NW by the Etive-Laggan shear zone and in the SE, by the Gleann Chomraidh fault (Fig. 9.10). The major Ericht-Laidon shear zone bisects the complex. Data presented in Chapter 5 shows a similar sequence of intrusive events as at Strath Ossian. G1, quartz-diorite, occurs in the SE along the Gleann Duibhe fault, and takes the form of a narrow elongate sheet with a PFC fabric parallel to its contacts (Fig. 9.10a). G2, a heterogeneous granodiorite, forms the bulk of the complex (Fig. 9.10b). Much of G2 displays an inward-dipping concentric PFC fabric, modified dramatically in certain areas. Figure 9.10a shows the projected orientations of fabric within G2, Figure 9.10b shows the actual present orientations i.e., post G5 emplacement. It is envisaged that the Etive-Laggan and Gleann Chomraidh structures are bounding structures to the complex, causing a gross anti-clockwise rotational strain. Within this system magma was able to rise within a transtensional regime created along the Ericht-Laidon shear zone which was acting as an ascent conduit. The data, showing a sigmoidal swing in the concentric PFC fabric within the trace of the shear zone, coupled with a local weak CPS fabric overprint indicate that magma was allowed to escape from this conduit to undergo *in situ* expansion. These processes created great petrological heterogeneity due to the complexity caused by the interaction and coalescence of successive sheets during pluton construction. This is in contrast to Strath Ossian which exhibits an ascent geometry in which, as described above, individual sheets are preserved. Simultaneous sheeting and stoping along the margins of the pluton occur where magma rose within the zone of maximum constriction of the overall system (Fig. 9.10a). The maximum extension direction of the strain ellipse within this expansion system was orientated in an ENE direction (Fig. 9.10a). As expansion and rotation of G2 continued, early PFC fabrics within this extension direction were progressively modified and overprinted by a CPS fabric. Along this zone of deformation, strain increases progressively from the centre of the complex towards its western margin, deformed mafic enclaves show an increase in X/Z ratios from c.2 to c. 5.5.

In the eastern side, lower strains are observed; generally an intense PFC is only slightly modified by a CPS fabric, the higher strains in the west being a result of the added effect of the adjacent expansion of the Glencoe complex which cuts and obliterates large parts of the SW of Rannoch G2. Blocks of Rannoch G2 which exhibit this fabric are seen as xenoliths within the main phase of the Glencoe ring intrusion, which exhibits a PFC fabric of its own. A minor phase, G3, is represented by a series of monzogranitic and syenogranitic sheets which crosscut G1 and G2. Sheets of Rannoch G4, the typical K-feldspar megacrystic granite, occur along the contact developed between the Glencoe Fault Intrusion and Rannoch G2, and in proximity to the bounding faults of the complex (Fig. 9.10b), which must have been reactivated to allow the intrusion of G4. These sheets display a moderately developed bimodal PFC fabric. The angular relationship of the two

sub-fabrics is indicative of sinistral shear during their development (see Ch. 5). G5, an equigranular monzogranite, occurs in two localities (Fig. 9.10b). One of these is at the centre of the complex (G5a) along the trace of the Ericht-Laidon shear zone, which must again have been active; a weak PFC fabric is seen running E-W suggesting some limited rotational expansion. A smaller sub-elliptical body (G5b) occurs along the Gleann Duibhe structure in the southern part of G2.

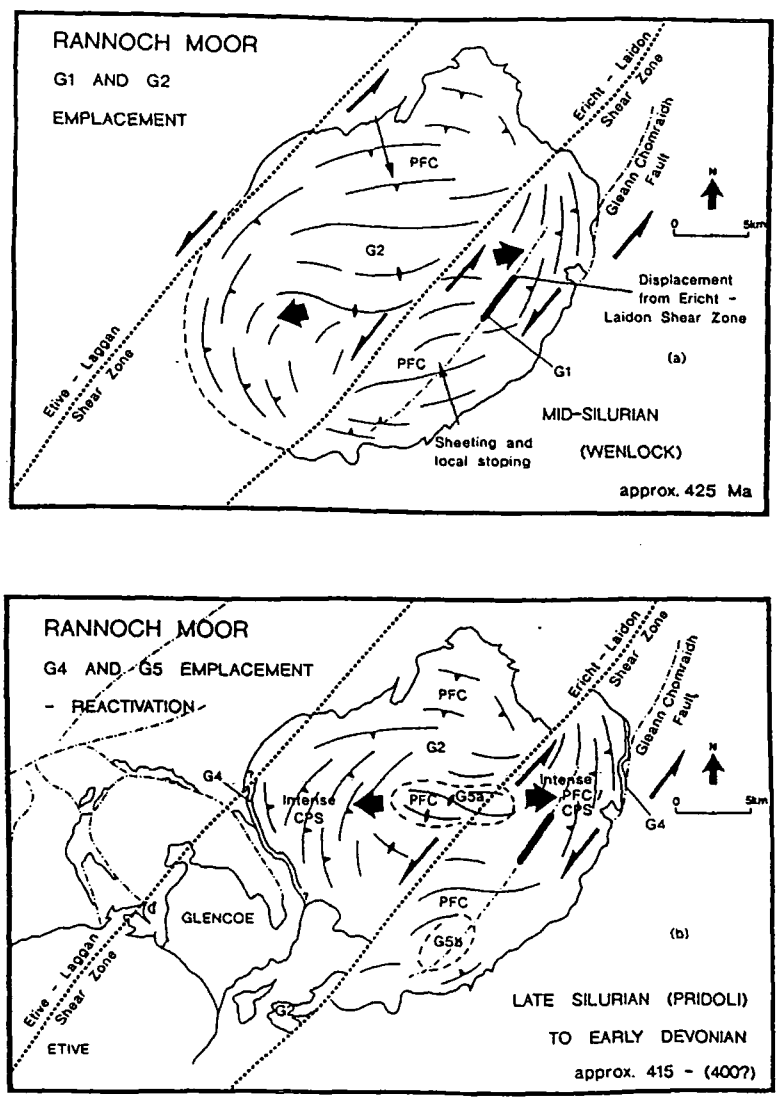

Fig. 9.10. Generalised models for the emplacement of **(a)** G1 and G2 and **(b)** G4 and G5 of the Rannoch Moor complex.

It is apparent from Figure 9.4 that G5a occurs at the centre of the complex in association with the NE-SW-trending Ericht-Laidon shear zone. If a line parallel to the NW-SE-trending Strath Ossian lineament was extrapolated through G5a to the NW, it would intersect the Ballachulish-Corrieyairack shear zone close to the site of the Ben Nevis complex. G5b is associated with the NE-SW-trending Gleann Duibhe fault. If the late offset along the Ericht-Laidon shear zone is restored and the pluton margins are returned to their original positions, another line with a similar trend through G5b would run straight through the centre of the Glencoe and the Mullach nan Coirean complexes. These "lines" are tentatively named the Rannoch Moor line and the Glencoe lines respectively. If these lines actually exist, it is unlikely that they represent deep crustal structures of the scale of the Strath Ossian lineament or the Cruachan line, however the occurrence of activity along them and where they intersect other proven structures is unlikely to be a coincidence and suggests that they may be possible synthetic splays which were initiated during magmatism and played a part in siting activity.

9.5.3 Controls on the Etive and Glencoe Complexes

These complexes represent a higher crustal level of magma emplacement than is seen at Rannoch and Strath Ossian, the distribution of facies seen here are therefore related to high level emplacement phenomenon. Most previous workers (e.g. Anderson 1937) have regarded the Etive complex as consisting of two lobes. However, structural data (Fig. 9.11a) presented in Chapters 3 and 4, together with radiometric and chemical data (Barritt 1983) suggest that these are infact independent intrusive bodies, and that the term Etive complex should only refer to the southern body. The centre of the Etive complex is situated at the intersection of the NE-SW-trending Etive-Laggan shear zone and the NW-SE-trending Cruachan lineament (Fig. 9.4). The northern lobe, which essentially forms part of the Glencoe complex, is centred at the intersection of the Etive-Laggan shear zone and the NW-SE-trending Glencoe line proposed above. Both lobes were emplaced at relatively high crustal levels (3-6 km, Droop & Treloar 1981) and both intrusive complexes show clear structural evidence that they interacted with the free surface during the initial stages of emplacement (see Ch. 7).

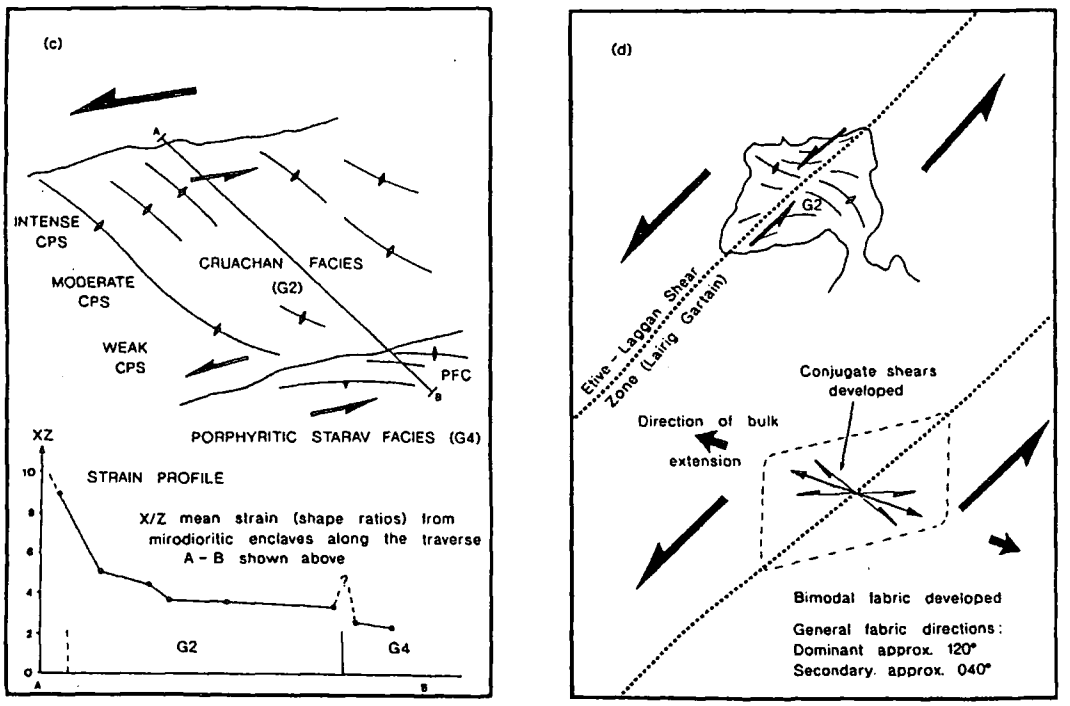

ETIVE AND GLENCOE IGNEOUS COMPLEXES

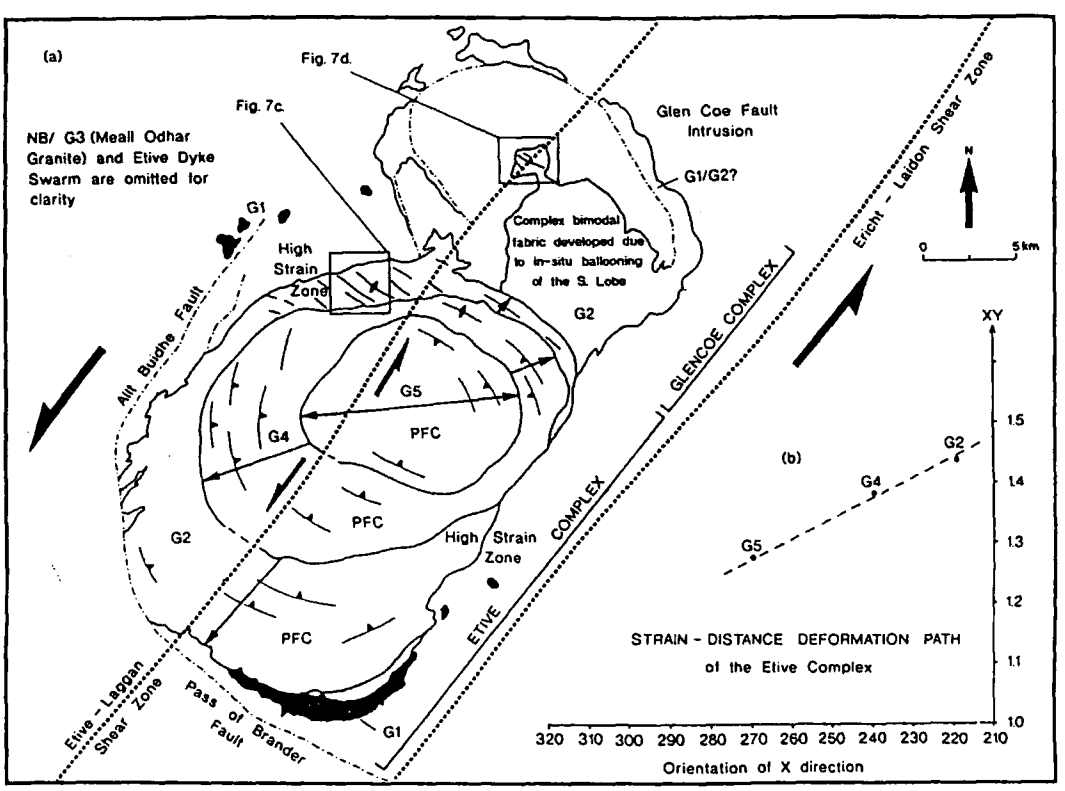

Fig. 9.11. (a) Generalised model for the emplacement of the intrusive phases of the Etive complex and the Glencoe complex. (b) A plot which shows the X/Z ratios for the intrusive phases G2, G4 and G5 against the orientation of the X direction. (c) Sketch map of orientation of fabrics within high strain zone in G2, and associated strain profile. (d) Sketch map of the centre of the Glencoe complex showing orientation of fabric and associated structures during initial stages of *in situ* expansion.

The Etive complex is markedly elliptical (30 km x 15 km) with the long axis trending NE-SW along Caledonian strike (Fig. 9.11a). Running through the adjacent wall rocks and in places partially bounding the pluton are the Allt Buidhe fault (a possible continuation of the Laggan Dam fault) in the NW, the Pass of Brander fault in the SW and the Ericht-Laidon shear zone to the SE. The E, SE and SW margins of the pluton in places show evidence of ring faulting indicating that cauldron subsidence has occurred at relatively high crustal levels similar to that seen in nearby Glencoe (see Ch. 7). It has been established that the southern lobe of Etive lies at the intersection of the NW-SE-trending Cruachan line and the NE-SW-trending Etive-Laggan shear zone. It is believed that the Cruachan line was an important structure in controlling the siting of the Etive complex (and the Ballachulish complex, see below); this follows its earlier role in siting a group of appinitic bodies stretching from Cuil Bay (NW) to Garabal Hill (SE) (Fig. 9.2b).

The major occurrence of G1 (known as the "Quarry Intrusion") takes the form of a "partial ring dyke", intruded along the ring fault which downfaults metavolcanics against Dalradian country rock (Ch. 7). The distribution of G1 may suggest that the NW-SE-trending Pass of Brander fault was influential during its construction (see Ch. 7).

Successive pulses of G2 granodiorite (Cruachan facies), G4 porphyritic granite (Porphyritic Starav facies) and G5 equigranular granite (Starav facies) are all elliptical (Fig. 9.11a). It is envisaged that space created at the intersection of the Etive-Laggan shear zone and the Cruachan lineament allowed magma ascent into what is now the centre of the complex. During high level emplacement, as at Rannoch, successive pulses underwent *in situ* expansion whilst undergoing sinistral transpression, shown by broadly concentric PFC fabrics developed within G2. The centres of each successive pulse (i.e. G2, G4 and G5) appear to have migrated during the constructional phase. The reason for this migration will be addressed elsewhere. However, one possibility is that the site of magma ascent changed possibly due to movements along the NE-SW-trending Starav-Chaorainn fault zone (Fig. 9.12), which has been shown to have been an active sinistral shear zone during Caledonian magmatism (see Rannoch Moor complex; Ch. 5). It is envisaged that movements along this structure may have created an ascent conduit where it intersects with the NW-SE-trending Cruachan lineament, essentially "tapping" the magma supply. Thus, explaining why the centre of the Central Starav facies (G5) occurs directly at the intersection of these two structures (Fig. 9.12). The Starav-Chaorainn fault may also explain the position of the "Chaorainn pulse" within the Glencoe complex (see below).

If the X/Y ratios for the G2, G4 and G5 pulses are plotted against geographical orientation of the X axis (Fig. 9.11b), the resulting straight line implies that the strain imposed remained fairly constant during the expansion process.

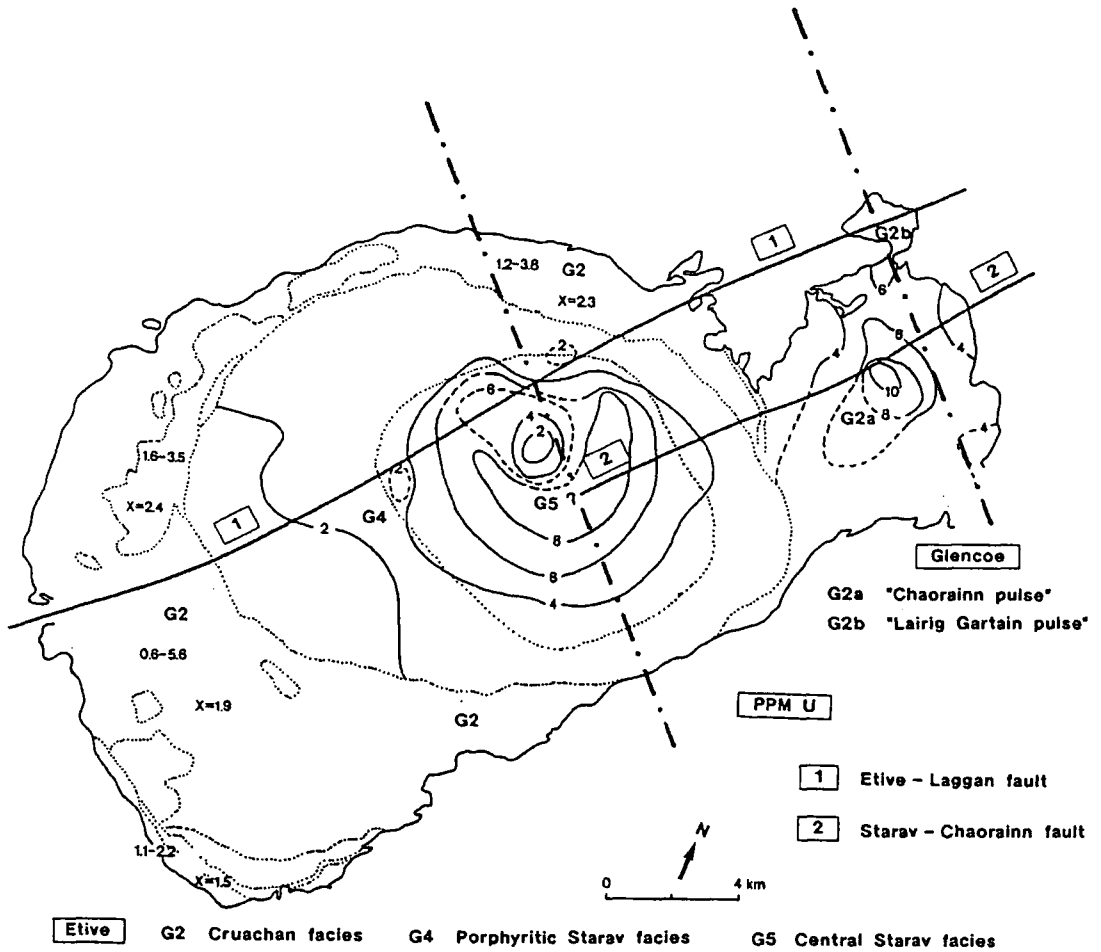

Fig. 9.12. Locality map showing the traces of the NE-SW-trending Starav-Chaorainn and Etive-Laggan faults, and the NW-SE-trending Cruachan lineament and Glencoe line, and their spatial association with the centres of the major intrusive phases within the Etive complex and the Glencoe 'Chaorainn and Lairig Gartain pulses'. The concentric zonation of U/Th by Barritt (1983) is shown to illustrate the position of the two pulses in the Glencoe complex.

The fabric in G2 is locally modified within high strain zones where it is overprinted by a CPS fabric, caused by the synplutonic rotation of G4/G5. Strains are highest near the outer margin of G2 (Fig. 9.11c), where the PFC fabric is obliterated by an intense CPS fabric and microdiorite enclaves show X/Z ratios of approximately 8; against the contact with G4, the PFC fabric shows only slight modification and is weakly overprinted by a CPS fabric, enclaves have X/Z values of 3. This can be explained by the outer parts of G2 being more crystallised than the inner; this outer part, having passed through the "critical melt

percentage" (Arzi 1978) and undergone crystal lockup, was able to develop an intense CPS fabric.

The intrusive phases (G2, G4 and G5) exhibit an early PFC fabric sub-parallel to the margins of each pulse. It is envisaged that successive magma batches being fed into the enlarging body produced steeply inclined sheets parallel to its margins and flattish sheets across the top of S-LS type (Flinn 1965). Within G2, a sub-horizontal stretching lineation is affected by small discrete conjugate ductile shears or "lock-up" shears (Hutton & Ingram 1992) formed during the last stages of PFC deformation, which show a bulk extensional component parallel to the fabric direction. Parts of G2 which generally show no apparent fabric in the field, but possess a weak sub-horizontal S-LS type PFC in thin-section, appear to represent the upper portion of the pluton. The data presented here do not require any cauldron subsidence to account for the emplacement of G2, G4 and G5 as proposed by Anderson (1956). This model thus avoids the space difficulties inherent in having a large sunken block in the vicinity of magma ascent and pluton construction. The present distribution of G3 takes the form of flat-lying sheets exposed on the highest peaks which rest on and cross-cut the upper parts of the G2 'balloon'. The G3 conduit, presumably the intersection of the NE-SW-trending Etive-Laggan shear zone and the NW-SE-trending Cruachan lineament, has now been obliterated by G4 and G5. Such relationships would be impossible if a large sunken block, produced by cauldron subsidence, existed. However the concentric gentle dip of some of the upper G2 sheets suggests some central downwarping during G3 emplacement. This initiated the intrusion of a partial ring dyke of G3 in the NE between the "northern and southern lobe" (i.e. the Etive complex and the Glencoe body) (Fig. 9.11a).

The northern lobe, part of the Glencoe complex, situated at the intersection of the Etive-Laggan shear zone and the possible Glencoe line, consists exclusively of G2 (Fig. 9.11d). Above this lobe, cauldron subsidence occurred which allowed the emplacement of the Fault Intrusion along outer ring faults (see Ch. 7) and was followed by the development of the Glencoe caldera. Fabric analysis over much of the northern lobe suggests that emplacement took place by *in situ* expansion; the structures are largely complicated by overprinting, probably produced by strains related to the construction of the Etive complex and the emplacement of the NE-SW-trending Etive Dyke Swarm. The only area where the fabrics are generally unaffected by this deformation is in the extreme NW within Lairig Gartain, in what has been shown (Barritt 1983) to be a geochemically distinct unit. The PFC fabric preserved here shows a sigmoidal swing into the Etive-Laggan shear zone (Fig. 9.11d). Conjugate shears imply extension towards 120°, the direction of the dominant fabric. A secondary fabric is developed at 040°, parallel with the Etive-Laggan shear zone. This may represent the preservation of a situation where magma is emerging from an ascent conduit and being fed outwards into an incipient balloon.

Generalised orientations of strain: a comparison between the Etive and Rannoch Moor complexes.

It is apparent from the above that the Etive complex shows concentric fabrics whereas, the Rannoch Moor complex shows a combination of overall concentric and sigmoidal fabrics within the Ericht-Laidon shear zone. The lack of deformation along the Etive-Laggan shear zone within the Etive complex might be a result of overall simple shear being applied along the bounding shear zones (Fig. 9.13); this might be the case if the magnitude of strike-slip along the bounding shear zones is considerably greater than along the Etive-Laggan shear zone. If movement along the Etive-Laggan shear zone is at a minimum during the emplacement of the major phases of the Etive complex, the concentric fabrics produced by the expansion process will remain the dominant feature. In the case of the Rannoch Moor complex, the fabrics produced by the expansion have been progressively influenced by movements along the Ericht-Laidon shear zone producing both concentric and sigmoidal fabrics (Fig. 9.13). In this case it is envisaged that movement along the Ericht-Laidon shear zone was at least as important as movements on the bounding shear zones. It is also possible that the complex could have been subjected to a gross general shear rather than simple shear alone.

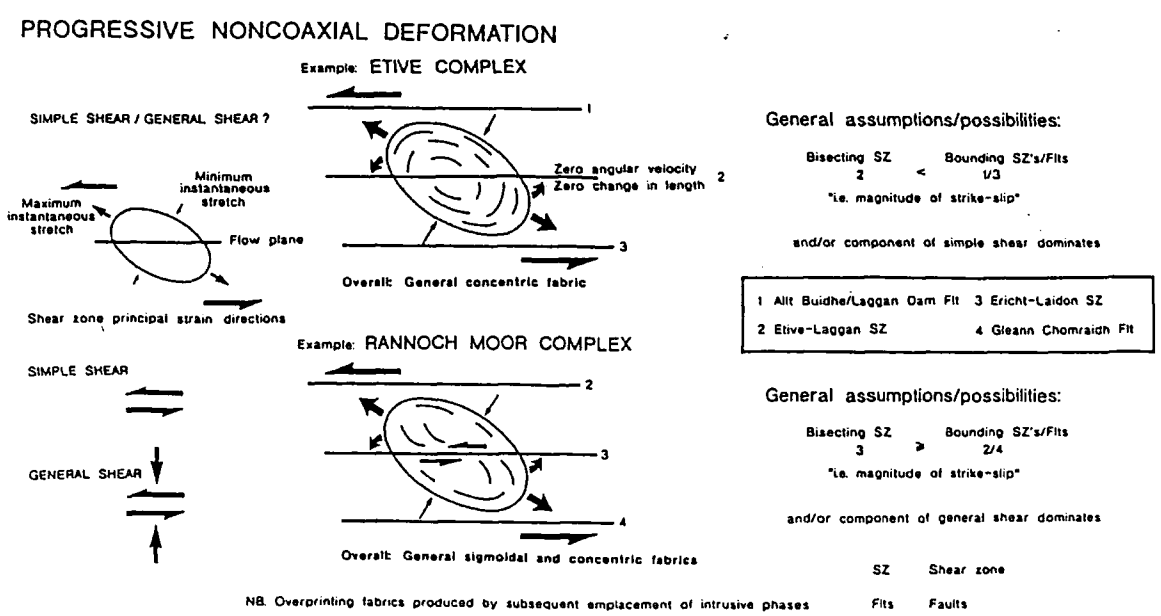

Fig. 9.13. Generalised orientations of strain: a comparison between Etive and Rannoch Moor complexes.

9.5.4 Controls on the Ballachulish and Ben Nevis complexes

Although the data on these complexes is limited, it is apparent that both occur along the NE-SW-trending-Ballachulish-Corrieyairack shear zone and appear to be related to the Cruachan line and the Rannoch Moor line respectively. Intrusive phases, G1 to G5, are shown in Figure 9.4b and Figure 9.4c.

Ballachulish was emplaced at similar depths to Strath Ossian (Weiss & Troll 1989); the distribution of the facies and its overall geometry may indicate that the major control on its emplacement was the Cruachan line. In Fig. 9.14, two zones of sheeting and stoping are shown, these may correspond to similar zones in the Rannoch complex which lay in the compressional direction of the strain ellipse. Based on these, a possible orientation of the strain ellipse at Ballachulish is proposed in relation to rotation and deformation associated with the Cruachan line.

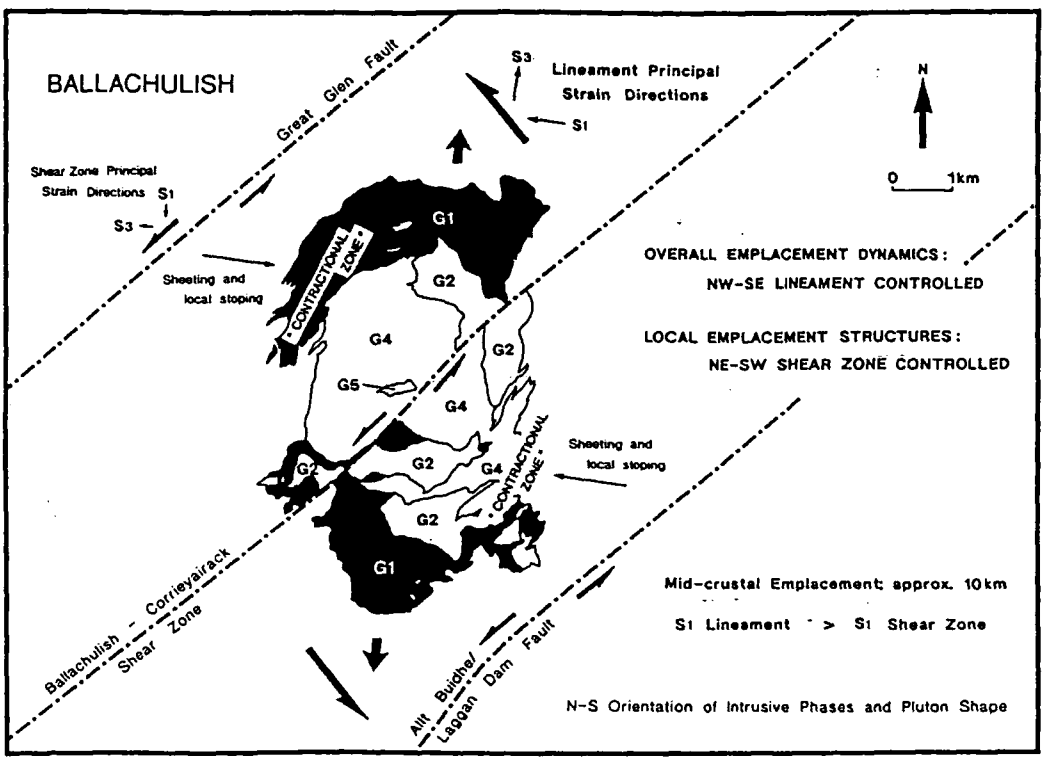

Fig. 9.14. Sketch map showing the principal strain directions controlling the orientation of intrusive phases and emplacement geometry of the Ballachulish complex.

Within the higher level Ben Nevis complex the actual phases appear to be orientated in a general N-S trend (Fig. 9.15), indicating that the Rannoch Moor line may have been the dominant control, however, see below. The overall shape of the complex is not elongate in this direction, suggesting that the Ballachulish-Corrieyairack shear zone was may have also been involved during emplacement. It should be noted that the model proposed for the Ben Nevis complex was tentatively based primarily on the distribution and geometrical orientation of its internal intrusive facies, and their possible relationship to major structural features within the area. A generalised model of its construction was developed from the information obtained from the study of the Etive, Glencoe, Rannoch Moor and Strath Ossian complexes, which involved the mapping of; (i) fabric type and intensity; (ii) strain type, magnitude and distribution; and (iii) local emplacement phenomena. Such an approach is currently being carried out on the Ballachulish pluton and will be subsequently applied to the Ben Nevis complex.

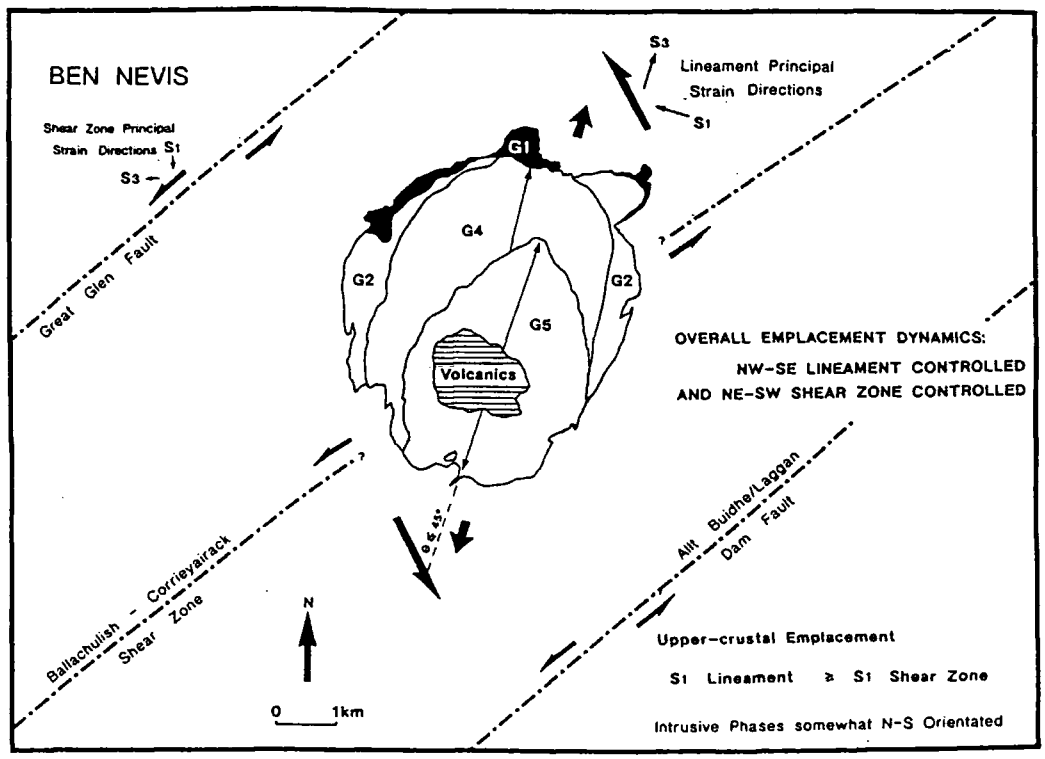

Fig. 9.15. Sketch map showing the principal strain direction controlling the orientation of intrusive phases and emplacement geometry of the Ben Nevis complex.

A sinistral shear component along the Rannoch Moor line is envisaged to account for the orientation of the long axis of subsequent intrusive phases in Ben Nevis, with magma predominantly expanding NNE-SSW into the direction of maximum extension imposed by that structure. This was based upon the apparent X/Z ratios for the intrusive phases and their geometrical orientation of their X axis relative to each other. For a dextral shear component imposed by a structure orientated NE-SW, the geometrical orientation of its internal intrusive facies would indicate that the long axis of subsequent pulses would have been rotated to a greater extent than earlier intrusive phases. This would imply that the later pulses tracked the finite strain ellipsoid faster than their predecessors, which would be an extremely unlikely situation. However, the model proposed was based on the petrographical distribution maps of earlier workers (Maufe 1910; Anderson 1935; Haslam 1968) and as such, if the contacts between individual intrusive phases are somewhat different, revealed by new mapping (Burt & Brown 1996), it obviously questions such a solution. A cautionary note, however, is that for a structure orientated NE-SW possessing a dextral shear component, the directions of maximum extension (orientated NNE-SSW) and shortening (orientated WNW-ESE) would be approximately the same as those imposed by a structure orientated NW-SE possessing a component of sinistral shear. One possible way to solve such a problem would be to analyse the types of fabric and their distribution, and in particular the amount of strain accumulation within G2 and possibly G4 along the eastern flank of the complex. If the complex has been affected by an overall dextral component, the subsequent expansion and synplutonic rotation of G5 at the centre of the complex would presumably have a profound effect on the deformation of G2 and G4 as it essentially "pinches-out" these earlier intrusive phases. It is intended to employ such an approach to the Ben Nevis complex. The most apparent feature of this pluton is that it has a fairly equidimensional form compared to other plutons within this region. This may be because it was emplaced at a crustal level where no one set of structures, i.e. NE-SW-trending Caledonian shear zones or NW-SE-trending lineaments, were clearly dominant; a possible "transitional zone" between the respective strain fields imposed by both sets of structures (see Ch. 10). If the pluton was predominantly controlled by a structure orientated NE-SW, possessing a dextral shear component as proposed by Burt *et al.* (*in press*), it is regarded that such an episode(s) of dextral deformation would surely be overshadowed by the overall gross sinistral transpressional deformation experienced by the whole region during the development of the Caledonian orogenic belt; thus, not effecting the overall regional model presented in Section 9.9.

9.6 NW-SE-TRENDING LINEAMENTS WITHIN THE SW HIGHLANDS

Summarised evidence for the Strath Ossian and Cruachan lineaments, and the minor Rannoch Moor and Glencoe lines

The following information demonstrates the existence of several NW-SE-trending structures within the Argyll region (Fig. 9.4).

The Cruachan lineament:

❶ Small satellite bodies of appinite form a NW-SE-trending zone which can be traced from the Ardsheal Hill/Ballachulish region south to the Garabal Hill complex (Watson 1984) (Fig. 9.2). This ultrabasic suite is generally regarded as being sub-crustal in origin (see Ch. 2 and references within), implying that the lineament must have at least reached lithospheric mantle depths, thus inferring it represents a deep basement structure.

In the south-eastern part of the Etive complex, a number of minor NW-SE-trending faults occur in the vicinity of the Beinn Lurachan dioritic intrusion, spatially associated with the trace of the Cruachan lineament.

❷ The Ballachulish, Etive and Garabal Hill complexes occur along the Cruachan lineament (Fig. 9.2). The Ballachulish complex is sited at the intersection of the NE-SW-trending Ballachulish-Corrieyairack shear zone and the Cruachan lineament. The Etive complex in general appears to have been sited at the intersection of the major NE-SW-trending Etive-Laggan shear zone and the Cruachan lineament. The major intrusive component G2 (Cruachan facies) in particular appears to be sited at this intersection. However, the subsequent change in the position of the centres of the next intrusive phases may be explained by the interaction of the Cruachan lineament with the NE-SW-trending Starav-Chaorainn fault, siting G4 and G5 at its intersection.

The intersection of the Cruachan lineament with the NE-SW-trending Tyndrum and/or Garabal Faults may explain the spatial distribution of the Garabal Hill complex (Fig. 9.2).

❸ The emplacement of the Ballachulish complex appears to have been at a crustal depth where the Cruachan lineament was the dominant control. However, the interaction of strain fields imposed by both sets of structures, i.e. the NE-SW-trending shear zones and the NW-SE-trending Cruachan lineament during the construction of the Ballachulish complex, may have resulted in the development of zones of localised emplacement phenomena ("sheeting and stoping"; see Ch. 10).

❹ If the Cruachan lineament is extended towards the SE it roughly coincides with a zone containing the NW-SE-trending Ben More and Loch Lomond lineaments (Fettes *et al.* 1986) (see Fig. 9.7).

The Strath Ossian lineament:

❶ Appinite bodies occur at the northern end of the Strath Ossian complex, sited at the intersection of the NE-SW-trending Ballachulish-Corrieyairack shear zone and the Strath Ossian lineament (Fig. 9.2). Their 'original' spatial distribution may have been 'obliterated' by the subsequent intrusion of the Strath Ossian granite which forms a NW-SE-trending linear shaped body (30 km x 6 km) sited along part of the Strath Ossian lineament (see below). However, appinites and dioritic bodies are common as dykes and small, irregular shaped bodies within the pluton. They are concentrated in two areas: (i) at the intersection of the NE-SW-trending Etive-Laggan shear zone and the Strath Ossian lineament, forming the earliest intrusive component of the complex, G1; and (ii) at the intersection of the NE-SW-trending Ciaran-Ossian shear zone and the Strath Ossian lineament, forming a small group of bodies which show synplutonic relationships with the Sgòr Choinnich facies (G2) (see Ch. 6).

As with the Cruachan line (see above), the Strath Ossian lineament is likely to represent a major deep seated basement structure which was exploited by ultrabasic magma, facilitating its ascent and controlling its distribution.

❷ The Strath Ossian lineament was first recognised by Forrest and Key (1989) by image analysis of regional geochemical stream sediment data, which produced a NW-SE-trending linear discontinuity.

❸ It has been shown by this current study (see Jacques & Reavy 1994; Ch. 6) that part of the Strath Ossian lineament was an active 'regional-scale', ductile shear zone during the emplacement of the Strath Ossian pluton.

❹ Phillips *et al.* (1994) have also shown that the Strath Ossian pluton may have been intruded along the boundary between two areas of contrasting styles of 'D2' deformation (Fig. 9.16). They suggest that this regional variation in the style of deformation was controlled, at least in part, by activity along the Strath Ossian shear zone. They also show that the location and deep seated nature of this structure can be seen on a regional gravity map of the area (Fig. 9.16a).

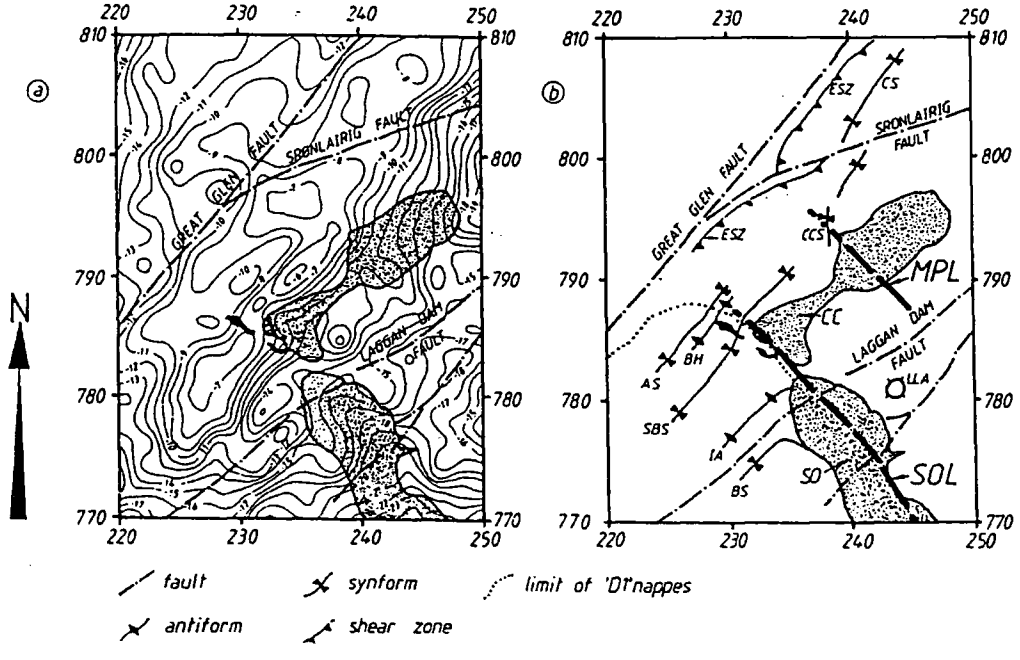

Fig. 9.16. (a) Regional Bouger Gravity Anomaly map of the Glen Roy district with contours at 1 mGal intervals (after Key *et al.* 1993). Heavy lines are major faults. Stippling over major intrusive complexes mentioned in text. Large appinitic bodies are shown in black. (b) Structural map showing the position of the major 'D2' fold structures and position of the proposed Strath Ossian and Meall Ptarmigan lineaments. ESZ, Eilrig Shear Zone; CS, Corrieyairack Synform; CCS, Creag a' Chail Synform; AS, Appin Synform; BH, Bohuntine; LLA, Loch Laggan Antiform; SO, Strath Ossian Lineament; MPL, Meall Ptarmigan Lineament.

❺ If the Strath Ossian lineament is traced south-eastwards it coincides exactly with the centre of the Comrie igneous complex (see Fig. 9.2).

❻ In the SE, it also coincides exactly with the NW-SE-trending Loch Tay Lineament (Fettes *et al.* 1986; see Fig. 9.7).

❼ Recent mapping during this study shows that deformation along the Strath Ossian lineament has influenced fabric development within the south-western part of the Corrieyairack granitic complex. This occurs where the lineament intersects with the NE-SW-trending Ballachulish-Corrieyairack shear zone where there is a gradual change in fabric orientation from a NW-SE-trend to a NE-SW-trending foliation moving NE (see Fig. 9.9).

The Glencoe line:

❶ The Glencoe line passes through the Mullach nan Coirean complex and straight through the centre of the Glencoe pluton, possibly siting activity along the line where it intersects with proven synplutonic NE-SW-trending shear zones (see Fig. 9.4 & 9.12): (i) the Mullach nan Coirean complex may be sited at the intersection of the Ballachulish-Corrieyairack shear zone and the Glencoe line; (ii) the centre of the the Glencoe complex (the "Lairig Gartain pulse", G2) is sited at the intersection of the Etive-Laggan shear zone and the Glencoe line; (iii) if the Glencoe line is continued south-eastwards it intersects with the Starav-Chaorainn fault, which coincides with the centre of the Glencoe "Chaorainn pulse" (G2); and (iv) if the late offset of some 7-8 km along the Ericht-Laidon shear zone is restored and the pluton margins of Rannoch Moor are returned to their original position, the south-eastward continuation of this line would intersect with the NE-SW-trending Gleann Duibhe shear zone, remarkably passing straight through the centre of an isolated, elliptical mass (approximately 3 km x 2 km) of monzogranites and syenogranites (G5b) located within the south-eastern part of the complex.

❷ Cross-cutting the Glencoe Cauldron block, are a number of WNW-trending felsite, quartz-porphyry, "andesite WNW dykes (Glencoe district)" and "monchiquite WNW dykes (Glencoe)" (mapped by British Geological Survey (Sheet 53)) which occur along the general trend of the Glencoe line.

The Rannoch Moor line:

❶ This passes through the centre of the Rannoch Moor complex, and where it has intersected with the NE-SW-trending Ericht-Laidon shear zone it appears to have sited the major intrusive component of the pluton, G2 and a subsequently smaller intrusive body G5a (Fig. 9.4).

❷ Although the dominant tectonic control during the emplacement of the Rannoch Moor complex was the NE-SW-trending shear zones, the development of localised emplacement phenomena (such as "sheeting and stoping") may suggest that strains related to deformation along the Rannoch Moor line were influential during its development (see Ch. 10).

❸ If this line is extrapolated through G5a to the NW, it would intersect the NE-SW-trending Ballachulish-Corrieyairack shear zone close to the site of the Ben Nevis complex.

❹ Mapping by the British Geological Survey (Sheet 53) has revealed a suite of NW-SE-trending dolerite dykes, which are localised directly along the Rannoch Moor line between the Ben Nevis and Rannoch Moor plutons.

The lack of appinitic/dioritic material along both the Glencoe and Rannoch Moor lines, may suggest that these do not represent deep crustal structures of the scale of the Cruachan and Strath Ossian lineaments. However, their importance in siting plutons and their major intrusive components, and a number of groups of dykes localised along these structures, may suggest that they represent synthetic splays developed as a consequence of movements along the NW-SE-trending Strath Ossian and Cruachan lineaments which bound this region.

9.7 THE TERM 'LINEAMENT'

As shown above, a geological lineament may be recognised within the cover by a number of geological features, including:

(1) The linear distribution of small, isolated intrusive bodies, e.g. the appinite suite aligned along the Cruachan lineament (Watson 1984);

(2) The spatial distribution of Caledonian plutons, as shown within the Argyll Suite (see also the control of Caledonian magmatism in the NE and Northern Highlands; see Sections 9.12 & 9.15 respectively);

(3) Major mid-crustal ductile shear zones controlling pluton emplacement, e.g. Strath Ossian complex (see Ch. 6);

(4) The siting and alignment of dyke swarms, e.g. the localised NW-SE-trending dyke swarm along the Rannoch Moor line (see above);

(5) Faults, e.g. Rothes fault, NE Highlands (Fettes *et al.* 1986);

(6) Their influence in the development of regional foliation patterns, e.g. the possible syntectonic rotation of regional fabrics within the Central and SE Sutherland regions, Northern Highlands (see Section 9.19). Possibly leading to the development of strike swings ("gross orogenic flow patterns") along major tectonic structures/boundaries, e.g. Portsoy-Duchray Hill lineament, NE Highlands (see Section 9.12);

(7) Syndepositional faults, e.g. NW-SE-trending Meall Ptarmigan lineament, SW Highlands (Glover *et al.* 1995);

(8) Linear discontinuities in regional geochemical stream patterns, e.g. Strath Ossian lineament, SW Highlands (Forrest & Key 1989), Clova lineament, NE Highlands (Fettes *et al.* 1986);

(9) Regional variation in style of deformation, e.g. contrasting styles of 'D2' deformation across the Strath Ossian lineament (Phillips *et al.* 1994) (see Fig. 9.16);

(10) Regional joint patterns defining 'distinct tectonic domains' (see Section 9.14);

(11) Geochemically- and isotopically-defined boundaries between granitic suites may define basement structures (lineaments) separating 'distinct tectonic domains' (see Section 9.14);

(12) Geophysical anomaly patterns, e.g. the NW-SE-trending Loch Shin line (Bott *et al.* 1972; see Sections 9.15 & 9.19).

Structures such as the NW-SE-trending Loch Shin line (Bott *et al.* 1972) and Cruachan lineament (e.g. Hall 1985, 1986) have been interpreted as representing important tectonic features within the basement, as they can be observed as Bouger anomaly patterns due to density contrasts, separating different tectonic domains. Features such as the Strath Ossian lineament (Forrest & Key 1989; Jacques & Reavy 1994), are clearly trans-Caledonoid, obliquely crossing the strike of the Caledonian orogenic belt, indicating its source is likely to be beneath the cover, of deep basement origin. Lineaments within the basement, defined by Bouger gravity anomalies, can be generated by a number of situations, where such a feature defines a difference in density across or along that structure: (i) This could be produced by the juxtaposition of crustal units with different densities, which could involve both vertical and horizontal components of translation; (ii) The intrusion of granite or basic material into one of the basement domains, possibly confined to that crustal unit by the basement structure. The Scourian-Laxford contact may represent such a situation in Sutherland, where the Loch Shin line is represented by a strong NW-SE-trending gravity gradient, which has been attributed to the localised injection of the Laxford granitic and pegmatic sheets of the foreland (Bott *et al.* 1972). This lineamental feature appears to continue south-eastwards, where the gravity gradient broadens to form an anomaly low centred on the Grudie and Rogart granitic complexes (see below); (iii) The intrusion of igneous material along the basement structure. Such exploitation of a crustal weakness is represented by the construction of the Strath Ossian complex of the Argyll Suite. During its emplacement the NW-SE-trending Strath Ossian lineament actively functioned as a major sinistral transcurrent shear zone, allowing magma to intrude predominantly by a process of multiple sheeting into a transtensional segment created along its length (see Ch. 6); (iv) Defined by variations in basement depth. These features may

include syndepositional faults associated with horsts and grabens of sedimentary basins. Such structures have been identified within the Central Highlands, such as the NW-SE-trending Meall Ptarmigan lineament, which appears to have formed the SW margin of a topographic high during sedimentation of the Grampian and Appin group (Glover *et al.* 1985).

Where these geologically-defined lineaments, observed at the present erosion level, are coincident with geophysically defined lineaments they have often been interpreted as cover rock features sited above and generated by a major pre-existing basement structure. This therefore assumes that such linear features within the upper crust have not been produced by events confined to the cover sequence, but have originated from major tectonic lineaments present within the basement directly below. It is therefore important to be able to distinguish lineamental features confined to the cover from major 'geophysical lineaments' (likely tectonic structures) established within the basement. This can be achieved to some extent by: (i) the examination of the surface geology above a geophysically-defined lineament will reveal features at the erosion level likely to be responsible for patterns within the gravity anomaly field; (ii) geophysically-defined lineaments and geologically-defined lineaments which continue for great lengths across the regional tectonic fabric within the crust/cover, maintaining their along strike continuity across major structural discontinuities, are likely to be related to major tectonic structures present within the basement, e.g. NW-SE-trending lineaments in the SW Highlands appear to cross major NE-SW-trending shear zones and faults without disturbance. Using such methods it is possible to identify 'distinct tectonic domains' characterised to some extent by their own lineament/shear zone systems (see below).

Watterson (1975) made the point that there is good evidence for the longevity of activity along basement structures. This is probably because, as stated by Muehlberger (1986), "major faults do not die; they will move again in whatever direction is necessary to accommodate the new stresses that are being imposed". This explains why many faults show evidence of reactivation, often with an opposite or significantly changed sense of displacement (Prucha 1989). It is therefore not suprising that in the SW Highlands major NW-SE-trending tectonic discontinuities within the basement, such as the Cruachan lineament, have been the focus for subsequent deformation leading to their reactivation during the Caledonian.

9.8 APPLICATIONS TO OTHER AREAS

Within the NW Highlands (see Sections 9.15 & 9.19), the Rogart pluton and an associated NW-SE linear belt of appinites are associated with the Loch Shin line, the continuation of the Laxford front (Watson 1984); the Ratagain complex was controlled by the Strathconan fault and associated NW-SE synthetic splays (Hutton & McErlean 1991). The tectonic setting of the south of Scotland Suite is dominated by major NE-SW-trending Caledonian structures within the transpressionally-thickened Southern Uplands. However, the abundance of plutons here is much less than in the Argyll Suite. Those which do occur may be associated with the trace of a N-S lineament (Woollett 1988) traversing the western side of the Loch Doon pluton intersecting Caledonian shear zones (see Ch. 10, Section 10.6). A number of NW-SE-trending lineaments have been recognised moving from the SW Highlands, across the Central Highlands and into the 'Buchan block' (NE Highlands). However, the situation within the Buchan block and immediate surrounding area, west of the Portsoy-Duchray Hill lineament (see Section 9.11), appears to be much more complicated. In this region, two further sets of lineaments or regional shear zones have been recognised (see Ashcroft *et al.* 1984; Fettes *et al.* 1986): (i) an E-W-trending set; and (ii) a NNE-SSW- to NE-SW-trending set. It has been suggested by Ashcroft *et al.* (1984) that the latter two sets of lineaments and major shear zones may have controlled the siting of pre-orogenic 'Older Basics' and syn-orogenic 'Younger Basics'. Within the Buchan block the E-W-trending lineaments appear to have been the dominant tectonic control in siting Caledonian granitic magmatism, with many plutons occurring where these structures intersect NW-SE-trending lineaments (see Section 9.12).

Moving SW from the Grampians, the Donegal batholith may be an area where similar structural controls to the Argyll Suite exist. The Main Donegal shear zone is a Caledonian structure akin to those described here, and was the dominant control in the emplacement of the Main Donegal Granite (Hutton 1982). A major NNE-SSW lineament is also present in this area (Hutton & Alsop *in press*). This has controlled the orientation and distribution of other plutons in the Donegal batholith as well as the emplacement of the Ardara granite and most of the appinites at the intersection of the Main Donegal Granite shear zone and the lineament.

9.9 DISCUSSION

Data has been presented which shows that the plutons of the Argyll Suite are intimately associated with synplutonic Caledonian NE-SW shear zones and pre-Caledonian re-activated NW-SE lineaments (Fig. 9.17). Hutton & Reavy (1992) have suggested that Caledonian magmatism was caused by anatexis of thickened crust by mantle-derived melts at the lower ends of NE-SW-trending transpressional faults detaching into the Moho, within an overall setting of a thickened lithosphere consequent to the final transpressional Caledonian collision.

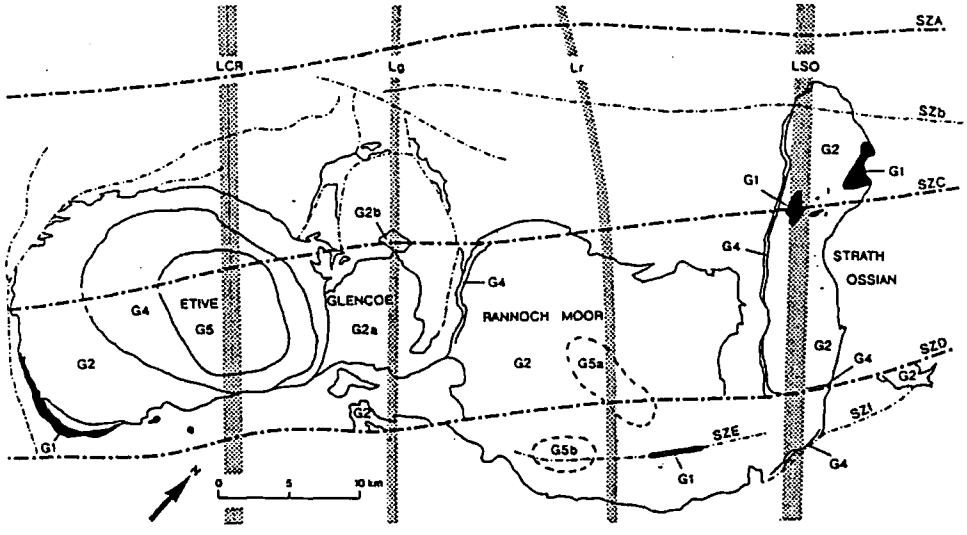

Fig. 9.17 Stuctural controls on the siting of the intrusive phases of the Etive-Glencoe-Rannoch Moor-Strath Ossian complexes. In each case (Table 9.2) an attempt is made to distinguish the structures involved in controlling siting and ascent, and whether ascent or emplacement configurations are recorded in the field.

ETIVE

Siting (at intersection of): SZC/LCR Major bounding structures: SZb and SZD Approx. depth of emplacement: 4-6 km	
Appinites along LCR	
G1: only now seen in NW at LCR and in S Ring dyke structures and small isolated bodies	EMPLACEMENT by ballooning
G2: ascent at SZC/LCR (not seen)	EMPLACEMENT by ballooning
G3: occurs above G2 (flat sheets) ascent SZC/LCR (not seen)	EMPLACEMENT by ballooning
G4: ascent at SZC/LCR (not seen)	ASCENT/ EMPLACEMENT by ballooning
G5: ascent at SZC/LCR (not seen)	

GLENCOE

Siting (at intersection of): SZC/Lg Major bounding structures: SZb and SZD Approx. depth of emplacement: 2-6 km	
G1/G2?: ring fault	EMPLACEMENT
G2a: ascent at SZC/Lg (not seen)	EMPLACEMENT by ballooning
G2b: ascent at SZC/Lg	ASCENT/ EMPLACEMENT

RANNOCH MOOR

Siting (at intersection of): SZD/Lr Major bounding structures: SZC and SZf Approx. depth of emplacement: 6-8 km	
G1: ascent at SZE/Lr	ASCENT
G2: ascent at SZD/Lr	EMPLACMENT by ballooning
G3/G4: sheets	EMPLACEMENT by ballooning
G5a: ascent at SZD/Lr	EMPLACEMENT
G5b: ascent at SZE/Lg	by ballooning
N.B. Displaced approx. 7-8 km by SZD	

STRATH OSSIAN

Siting (at intersection of): SZC/LSO Major bounding structures: SZA and SZD Approx. depth of emplacement: 10 km	
Appinites along LSO	
G1: ascent at SZC/LSO	ASCENT
G2: ascent at LSO	ASCENT
G4: ascent at LSO	ASCENT
LSO/SZD	

Table 9.2. Summary of structural controls on each complex and proposed ascent/emplacement configurations.

It is envisaged that transpressional deformation within the SW Grampians reactivated much older lineaments which may themselves represent former shear zones in the pre-Caledonian basement. As these structures meet at approximately 90°, it is possible to envisage, in what is obviously a very complex situation within the lower crust, a series of mobile blocks bounded by ductile shear zones in two directions. Such a structure is comparable with models of lower crustal seismic profiles (Reston 1988, Sanders 1991)

which suggest that the lower crust can be envisaged as a series of low strain lozenges or mega-augens bounded by anastomosing shear zones (Fig. 9.18a, 9.19a & 9.20a). As these blocks interact within the gross transpressional system, they may rotate to some extent (Fig. 9.20a). Transtensional voids will be created at certain intersections and crustal thickening will be accentuated along the Caledonian shear zones. The establishment of such a pattern of structural interactions within the lower crust could provide the mechanistic framework within which all the relationships described in this paper, i.e. location of anatectic zones, siting and type of ascent pathways (Fig. 9.19b) and any subsequent emplacement phenomena (Fig. 9.19c) can be interpreted. It is apparent from Figure 9.20b that the width of the Grampians between the Great Glen Fault and the Highland Boundary Fault increases towards the NE. The Argyll Suite lies in a convergent zone in the SW where these two structures are closest, the Cairngorm Suite in a divergent zone to the NE. Moreover, within the Cairngorm Suite, the structural controls described in detail for the Argyll Suite can not be recognised with any certainty (however, see Section 9.12), although other lineaments/shear zones have been recognised here (Ashcroft *et al.* 1984; Fettes *et al.* 1986). It is therefore likely that the main cause for the abundance of plutons within the Argyll Suite may be the concentration of closely spaced lineamental intersections within that section of crust. It can be seen from Figure 9.20c that the spatial distribution of these plutons appears to be closely tied to the likely sites of extensional zones between the hypothetical crustal blocks (1-11).

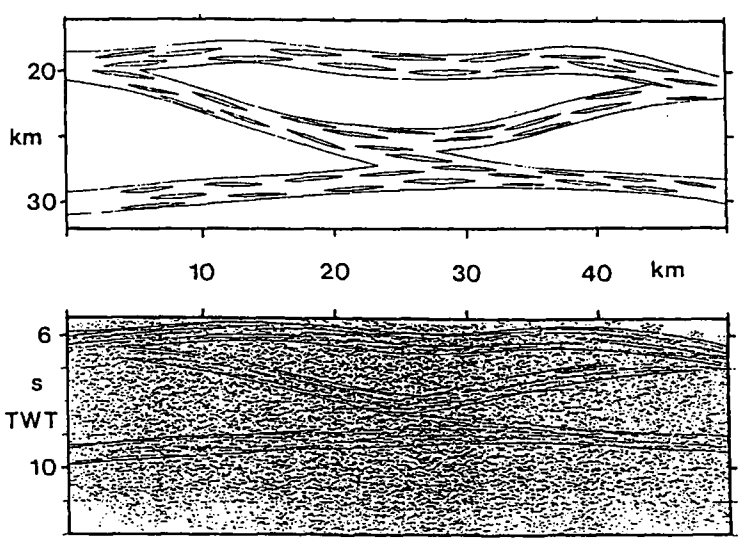

Fig. 9.18. Model and synthetic seismic response of a lower crust divided into low strain lozenges by subhorizontal detatchments and dipping shear zones. Noise has been added to the synthetic section to make it look more realisitc. After Reston (1988).

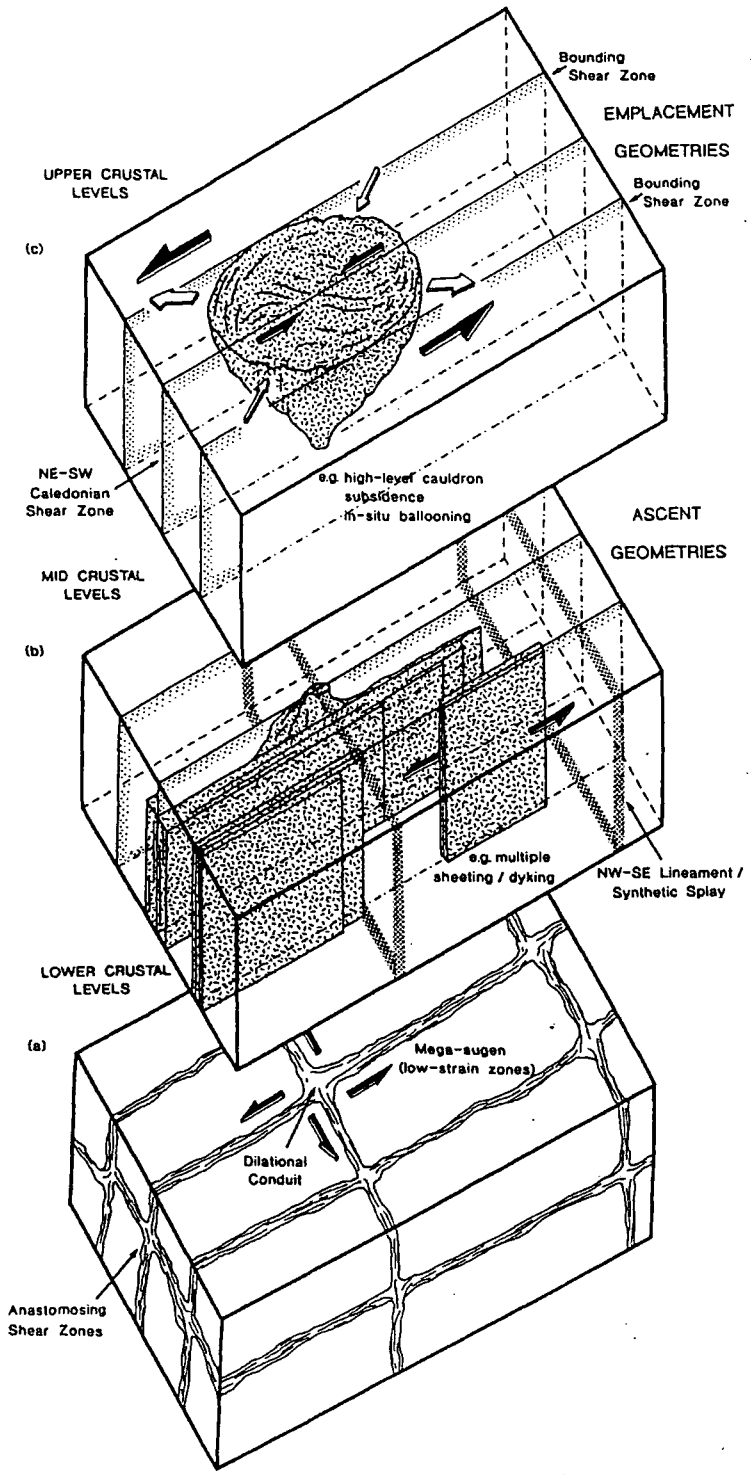

Fig. 9.19. (a) Lower crustal structure showing a series of low strain zones bounded by anastomosing shear zones (modified from Reston & Sanders 1991). (b) Ascent pathways within the mid-crust for granitoid magma by a process of sheeting within shear zones or at transtensional voids at shear zone intersections. (c) Emplacement geometry of a granitoid complex within the upper crust undergoing rotational expansion within a shear zone system. The ascent mechanism is not implicit.

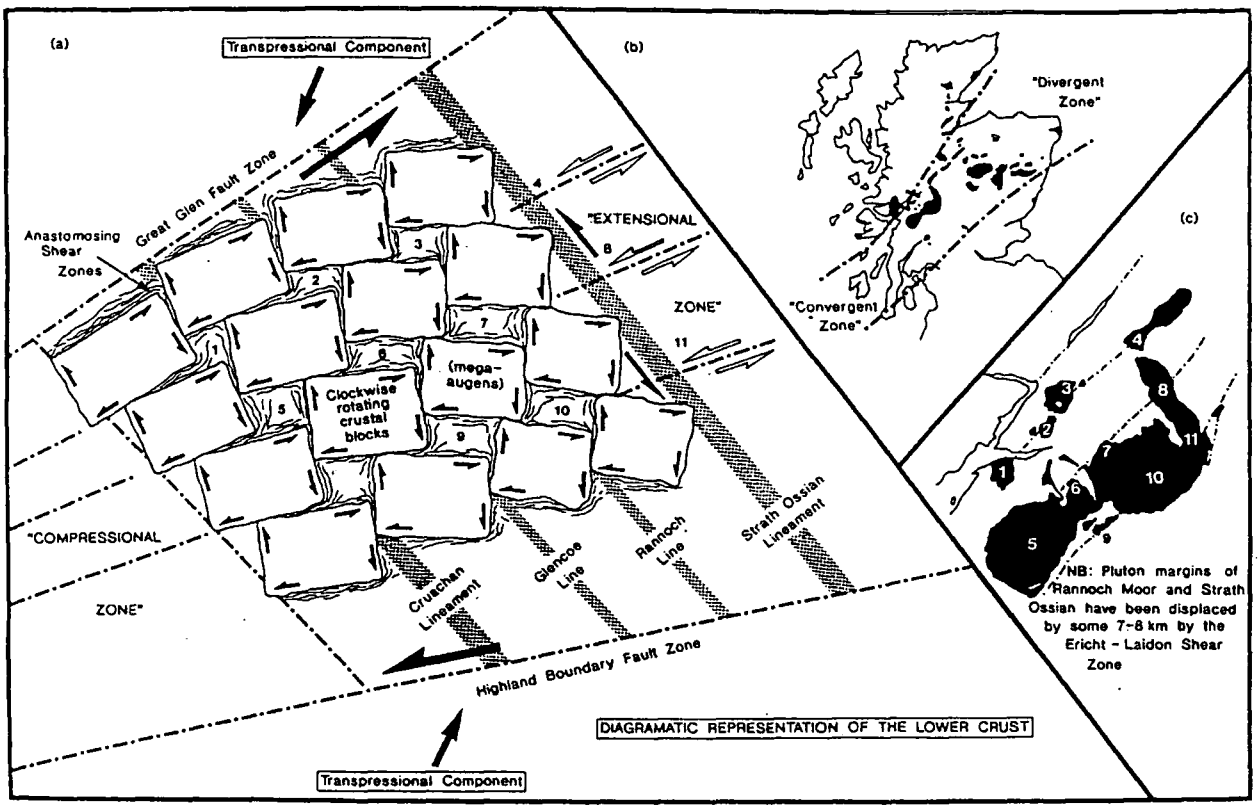

Fig. 9.20. (a) Possible structure of SW Grampian crust showing rotation of 'blocks' at lineamental intersections between the Great Glen Fault and the Highland Boundary Fault. (b) Map showing the positions of the Argyll Suite in a 'convergent zone' in the SW Grampians. (c) Map showing how centres of intrusive activity (numbered) occur above proposed corresponding extensional lineamental intersections (also numbered).

Possible tectonic controls on the differences in petrological and geochemical characteristics between adjacent granitic suites

As already mentioned in Section 9.2, although there are many possible causes for contrasts in geochemistry and petrology between late Caledonian plutons, it is apparent that the Argyll Suite coincides closely with the region where transpressional strike-slip faults are demonstrably present. This is in contrast to the NE Highlands, the area designated as the Cairngorm Suite (Stephens & Halliday 1984), where such faults are less obviously developed. This therefore raises the question, could differences in tectonic environment during granite petrogenesis have a strong effect in determining petrological characteristics ?

Figure 9.20 shows that the Argyll Suite lies in a 'convergent zone' in the SW Grampians, where the width between the Great Glen Fault and the Highland Boundary Fault is at its minimum. However, moving towards the NE the width between these two

faults increases. In the NE Highlands, the Caingorm Suite is located within this 'divergent zone' and raises the possibility that anatexis took place in an "overall regional extensional regime" (an area of "least tectonic thickening in the Dalradian"; Fettes *et al.* 1986); a completely different structural setting to that which may have been established during the development of the Argyll Suite. It is interesting to note that the emplacement of one of the largest granitic bodies in the NE Highlands, the Cairngorm pluton (see Fig. 9.3), has been attributed by Harrison (1986) to have been achieved predominantly by a process of stoping. He suggested that the partially crystallised magma acted as a Bingham fluid, allowing the larger country rock xenoliths to sink due to them exceeding the critical yield strength of the magma. Such "passive-type" emplacement may reflect to some extent the overall tectonic regime prevailing at that time.

It is regarded by many workers (e.g. Ashcroft *et al.* 1984) that the NE Grampian Highlands represents a regional block (known as the 'Buchan block') which is essentially decoupled from the main Dalradian tract by several lineaments or shear zones (discussed below). This work (see Ashcroft *et al.* 1984; Fettes *et al.* 1986) has led to the recognition that the Buchan block contains a system of shear zones or lineaments with different trends to those observed within the SW Highlands. This raises the possibility that if these structures represent basement features, could the lower crust underlying the Buchan block, at least in part (see below), be different from the 'Lewisianoid-type' basement which have been inferred to occur beneath the Central and SW Highlands (see Bamford *et al.* 1978; LISPB profiles). This may explain the geographical position of the boundary inferred by Stephens and Halliday (1984) to separate the Argyll and Cairngorm suites (Fig. 9.3).

9.10 MODEL PROPOSED FOR LINEAMENTS AND SHEAR ZONES WITHIN THE SW HIGHLANDS

Within the SW Grampian Highlands several NE-SW-trending shear zones and faults related to the Caledonian transpressional collision are recognised as being distinct from an intersecting set of NW-SE-trending pre-Caledonian crustal lineaments which were reactivated during Caledonian orogenesis. The geochemical and isotopic characteristics of the 425-400 Ma granitoids of this region show that they were derived by anatexis of the lower crust associated with a mantle component which provided an influx of mantle heat and/or metasomatic fluids; their spatial distribution suggests a close genetic relationship with Caledonian shear zones. Having made the fundamental distinction between ascent

(transport) and emplacement (arrival) configurations possible for granitoid magmas, new data are presented for these plutons which show that: (i) a common modal sequence of intrusive phases can be recognised; (ii) these phases are all sited at shear zone or lineament intersections where transtensional zones allowed and facilitated ascent; (iii) emplacement was often by a process of localised *in situ* expansion.

The existence of such lineaments in these orientations in the SW Highlands may indicate that the structure of the lower crust can be regarded as a series of blocks bounded by intersecting ductile zones of high strain. The establishment of such a pattern of structural interactions within the lower crust could provide a mechanistic framework within which the location of anatectic zones, siting and ascent pathways and any subsequent emplacement phenomena can be explained in orogenic belts.

Models are presented in Appendix A in an attempt to explain the distribution and differences in emplacement style of Caledonian magmatism in the NE and NW Highlands of Scotland.

CHAPTER 10

THE CONTROL ON GRANITE EMPLACEMENT STYLES BY THE INTERACTION OF SHEAR ZONES AND DEEP CRUSTAL LINEAMENTS: the influence of crustal depth and rheology

10.1 INTRODUCTION

As shown in the previous Chapters, magma emplacement during pluton construction in the Argyll Suite occurs within a combination of strain fields which may be "externally derived", resulting from the activity of tectonic structures ('tectonic-related strains') or "internally derived" caused by, for example, lateral expansion during emplacement ('expansion-related strains'). Within the Argyll Suite, a variety of emplacement phenomena are observed. Despite the complexities in deformation produced by pluton expansion, such as fluctuating strain rates, variations in type of strain and pluton expansion rates etc., this Chapter presents data which, it is believed, can help to explain this variation by consideration of (a) relative depths of emplacement and (b) the interactions between regional tectonic and local magmatic strain fields.

It is the intention of this Chapter to show how the overall geometry of pluton shapes, internal distribution of facies and local emplacement phenomenon can be used to determine the directional distribution of tectonically-induced strain fields in relation to depth.

10.2 TECTONIC CONTROLS ON CALEDONIAN MAGMATISM WITHIN THE SW HIGHLANDS

This Section includes a summarised account of both general characteristics of the plutons within the Argyll Suite and the major tectonic structures controlling their siting and emplacement, recognised during this current study (for a more extensive review see Ch. 9).

Within the Argyll Suite (Fig. 10.1), it has been shown (Jacques & Reavy 1994; see Ch. 9) that a common sequence of intrusive phases is broadly applicable to all the plutons. The earliest activity is represented by the volatile-rich appinite suite. These intrusions occur as isolated bodies along the Cruachan line and the Strath Ossian lineament (Fig. 10.1c & 10.2).

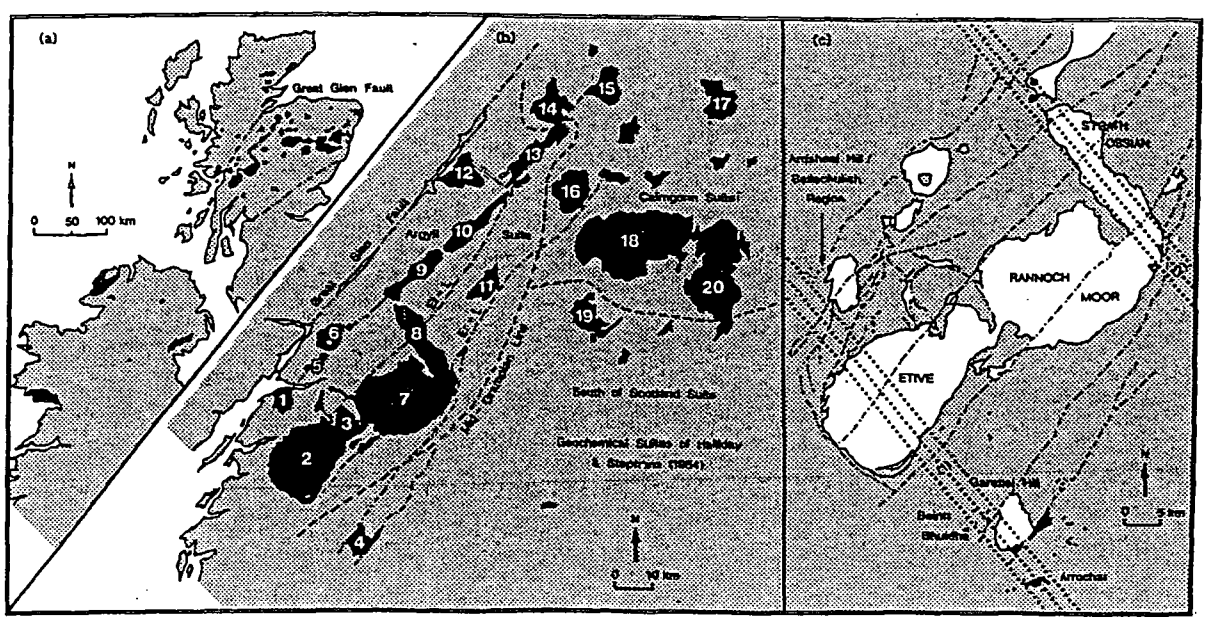

Fig. 10.1. **(a)** Distribution of late Caledonian granites in Scotland and Ireland. **(b)** Distribution of granitoids in the Grampian Highlands; 1. Ballachulish; 2. Etive; 3. Glencoe; 4. Garabal Hill; 5. Mallach Nan Coirean; 6. Ben Nevis; 7. Moor of Rannoch; 8. Strath Ossian; 9. Corrieyairack; 10. Allt Crom; 11. Strathspey; 12. Foyers; 13. Glen Kyllachy/Findhorn; 14. Moy; 15. Ardclach; 16. Monadliath; 17. Ben Rinnes; 18. Cairngorm; 19. Glen Tilt; 20. Lochnagar; in association with major Caledonian faults and shear zones: Et-L Etive-Laggan shear zone; Er-L Ericht-Laidon shear zone; and showing boundaries of geochemical suites of Halliday and Stephens (1984). **(c)** Distribution of appinite bodies along the Cruachan lineament (1) and the Strath Ossian lineament (2).

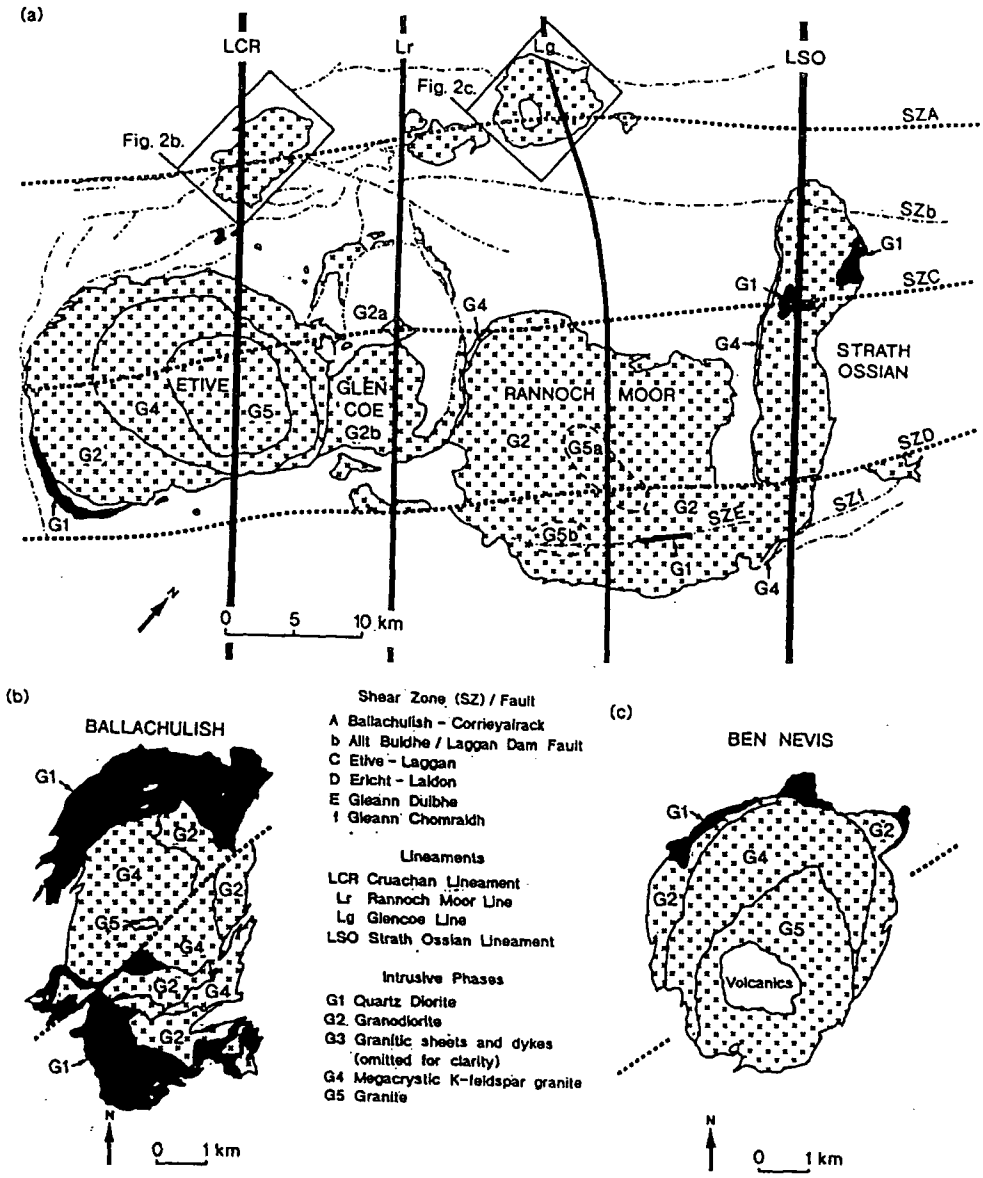

Fig. 10.2. (a) Sketch map of the SW Grampians showing major structural features and the Caledonian plutons under study. Intrusive phases, G1, G2, G4, and G5 (G3 omitted for clarity) within the Etive, Glencoe, Rannoch Moor, Strath Ossian, (b) Ballachulish and (c) Ben Nevis plutons are shown.

The timing of emplacement of the appinite bodies in some cases was contemporaneous (Rogers & Dunning, 1991), but generally closely predates the emplacement of the granitoid complexes. As discussed in Chapter 9 these complexes are generally composite normally-zoned intrusions comprising quartz diorite (G1), heterogeneous monzodiorite-tonalite-granodiorite-monzogranite (G2), minor sheets of

microgranite (G3), megacrystic monzogranite (G4) and equigranular leucocratic monzogranite (G5) (Fig. 10.2). It has been further shown that within the area occupied by the Argyll Suite plutons, two sets of structures are associated with magmatism: (i) the NE-SW-trending Ballachulish-Corrieyairack shear zone, the Allt-Buidhe/Laggan Dam fault, the Etive-Laggan shear zone, the Ericht-Laidon shear zone, the Gleann Chomraidh fault and (ii) the NW-SE-trending Cruachan lineament, the Strath Ossian lineament and the minor Glencoe and Rannoch Moor lines (Fig. 10.2). It has been shown that these structures controlled not only the siting of appinitic magmas (as proposed by Watson (1984)), but also, by interacting with the Caledonian shear zones, were crucial in controlling the siting and ascent of the granitoids (Ch. 9).

Although all the plutons in the Argyll Suite (Stephens & Halliday 1984), SW Grampian Highlands (Fig. 10.1), are currently at the same erosion level, it is well documented that there was considerable variation in the depth of crystallisation (12-2 km, see below). It is also clear that the age range of the plutons is restricted (approximately 425-410 Ma), and that the oldest plutons are the deepest and the youngest plutons are the shallowest. All this implies that exhumation occured during the emplacement history and that the Earth's surface (free surface) was progressively lowered relative to the initial emplacement levels.

10.3 CRUSTAL STRUCTURE WITHIN THE SW GRAMPIANS

During the period under discussion, two sets of structures played a crucial role in controlling most aspects of the magmatism; these have been distinguished (Jacques & Reavy (1994) and in this contribution) by the terms "lineament" and "shear zone". The term "lineament" refers to a series of well defined, deep crustal structures within the mid to lower crust which have a general NW-SE-trend. As shown on the LISPB profile (Fig. 10.3a & b) by Bamford (1979), the pre-Caledonian basement extends from the Caledonian foreland as far south as at least the Southern Uplands with an approximate downthrow to the SE of 3 km at the Great Glen fault. It is therefore probable that the deep crust beneath the Grampian Highlands is "Lewisianoid" in nature, and that the Cruachan and the Strath Ossian lineaments represent some tectonic discontinuity within such a crust. Watterson (1975) noted that there is good evidence for longevity of activity along such major crustal weaknesses.

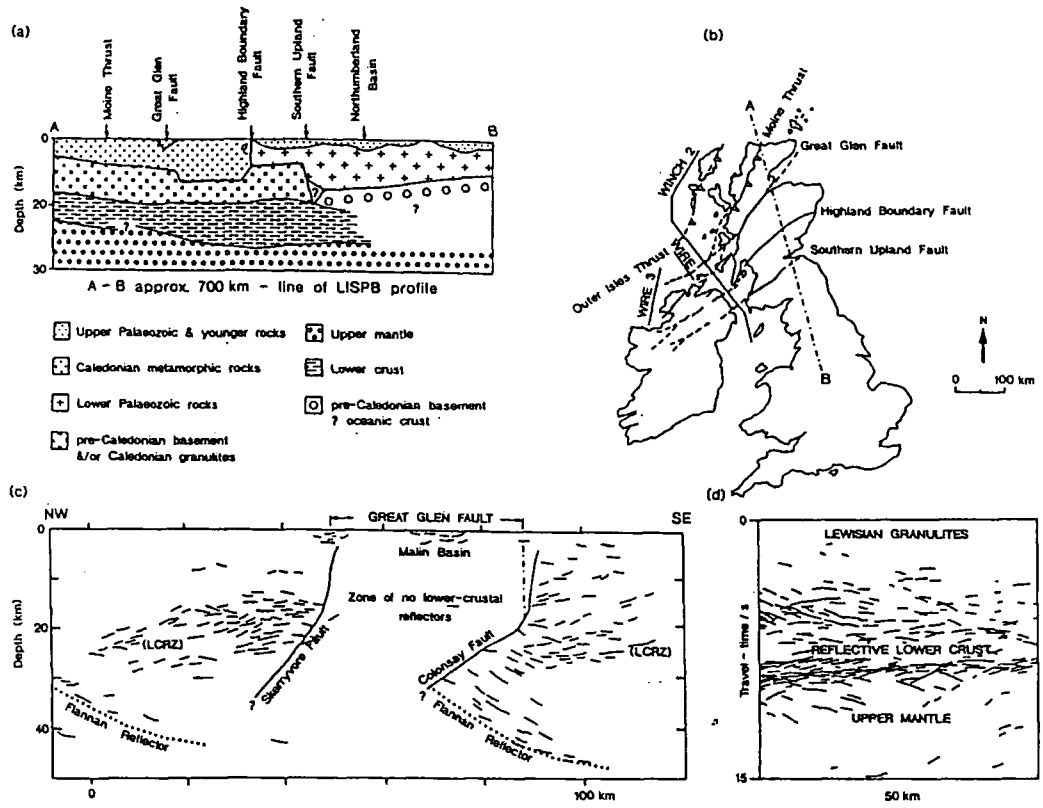

Fig. 10.3. **(a)** Interpretation of LISPB profile (largely after D. Bamford (1979). **(b)** Locality map showing major Caledonian fault systems and position of the LISPB profile and BIRPS surveys. **(c)** Migrated line-drawing of WIRE 4A to show interpretation of lower-crustal reflectors (LCRZ) and mantle reflectors (Flannan Reflector) being truncated by north-dipping Caledonian strike-slip faults. Reproduced from Snyder & Flack (1990). **(d)** Line-drawing of part of WINCH 2 showing position of highly reflective lower crust (LCRZ). Reproduced from Klemperer and the BIRPS Group (1987).

The major structures associated with the magmatism are the NE-SW-trending Ballachulish-Corrieyairack shear zone, the Allt-Buidhe/Laggan Dam fault, the Etive-Laggan shear zone, the Ericht-Laidon shear zone, and the Gleann Chomraidh fault (Fig. 10.2). These structures not only controlled the siting of the plutons but also their emplacement mechanisms (Jacques & Reavy 1994). Movement on the faults and shear zones and timing relative to granite crystallisation has been deduced (see Ch.'s 3, 4, 5, 6 & 7) from the analysis of both 'magmatic state'/pre-full crystallisation (PFC) (Hutton 1988) kinematic indicators, and 'solid state' shear sense indicators developed in crystal plastic strain fabrics (CPS) (Hutton 1988) and the wall rocks. In the 'magmatic state' these

include: (i) overall gross fabric trajectories; (ii) fabric obliquity to wall rocks; (iii) imbricate tiling; (iv) the angular relationship of sub-fabrics produced by strain partitioning; and (v) minor ductile shear zones. 'Solid state' shear sense indicators in the granitic and the wall rocks include: (i) brittle-ductile shears; (ii) the form and internal deformation features of synthetic splays; (iii) quartz ribbons and highly elongate swathes of biotite; (iv) the sense of obliquity of CPS fabrics in relation to earlier 'pre-existing' (PFC) fabrics; (v) asymmetric extensional shear bands; and (vi) porphyroblasts, porphyroclasts and asymmetric pressure shadows. This data set suggests a significant sinistral strike-slip component on these synplutonic NE-SW structures during the late Caledonian. However, the amount of movement on these structures remains unclear, and the magnitude of strain associated with deformation on these faults and shear zones appears to be relatively low.

Jacques & Reavy (1994) have proposed, in addition, and using the same methodology, that major old deep seated lineaments orientated NW-SE, at a high angle to the Caledonian faults, were sinistrally reactivated during the Caledonian and were a further major control, at their mutual intersections, on the siting and emplacement mechanisms of the Caledonian granitic plutons. The NW-SE-trending structures (lineaments) have a variety of geological expressions at the current erosion level: (i) many are the sites of the deeply sourced (sub-crustal) mafic, shoshonitic-type magmas of the Appinite Suite (Watson 1984) (see Fig. 10.1c); (ii) they may control the location of mafic dyke swarms; (iii) they may be the locus of sedimentary facies changes in the Dalradian country rocks *al.* 1986), forming syndepositional faults (e.g. Meall Ptarmigan lineament (Glover et al. 1995)); (iv) they may separate different zones of regional metamorphism; (v) the lineaments can be associated with changes in deformation style in the Dalradian (Phillips *et al.* 1994); (vi) they may have deep seated, long wavelength gravity and magnetic anomalies; (v) they can occur as major faults in the cover (e.g. Rothes fault (Fettes et al. 1986)); (vi) such transverse basement faults (lineaments) may.have controlled the uprise of mineralised hydrothermal fluids, siting base metal (i.e. lead, zinc, copper etc.) sulphide deposits (Horne 1974; 1975).

A preferred model for these lineaments (see also Hutton & Alsop 1996) is that they are deep, early, major faults that formed in the basement beneath the Dalradian before Dalradian deposition. The subsequent "activity" on these faults varies from actual movement in the overlying cover to other forms of expression. Jacques and Reavy (1994) showed that all the major plutons of the Caledonian granitic suite in this area lie at the intersections of the deep seated faults (lineaments) and NE-SW Caledonian sinistral faults and shear zones (Fig. 10.2). They also showed from internal deformation features of these plutons that both sets of the major structures were invariably active during granite emplacement (see also Ch.'s 9 & 10).

If as claimed by Jacques & Reavy (1994) the two sets of structures were synchronously active during granite emplacement, then the strain pattern of a

contemporaneous pluton should reflect the relative interaction of the two major structures as well as emplacement processes related to the proximity of the free surface. For the simple case of a pluton ballooning at depths of less than 8 km (a situation applicable to many of the plutons that will be discussed, see below), the likely patterns of strain produced by the relative interaction of sinistral shear on both NE-SW and NW-SE structures is as shown (Fig. 10.4). At its simplest, a NE-SW sinistral transcurrent or transpressional structure could be expected to have the maximum principal strain directions aligned approximately N-S and the minimum principal strain directions aligned approximately E-W (Fig. 10.4a). In the case of a NW-SE structure possessing a sinistral shear component, these principal strain directions would be reversed (Fig. 10.4b).

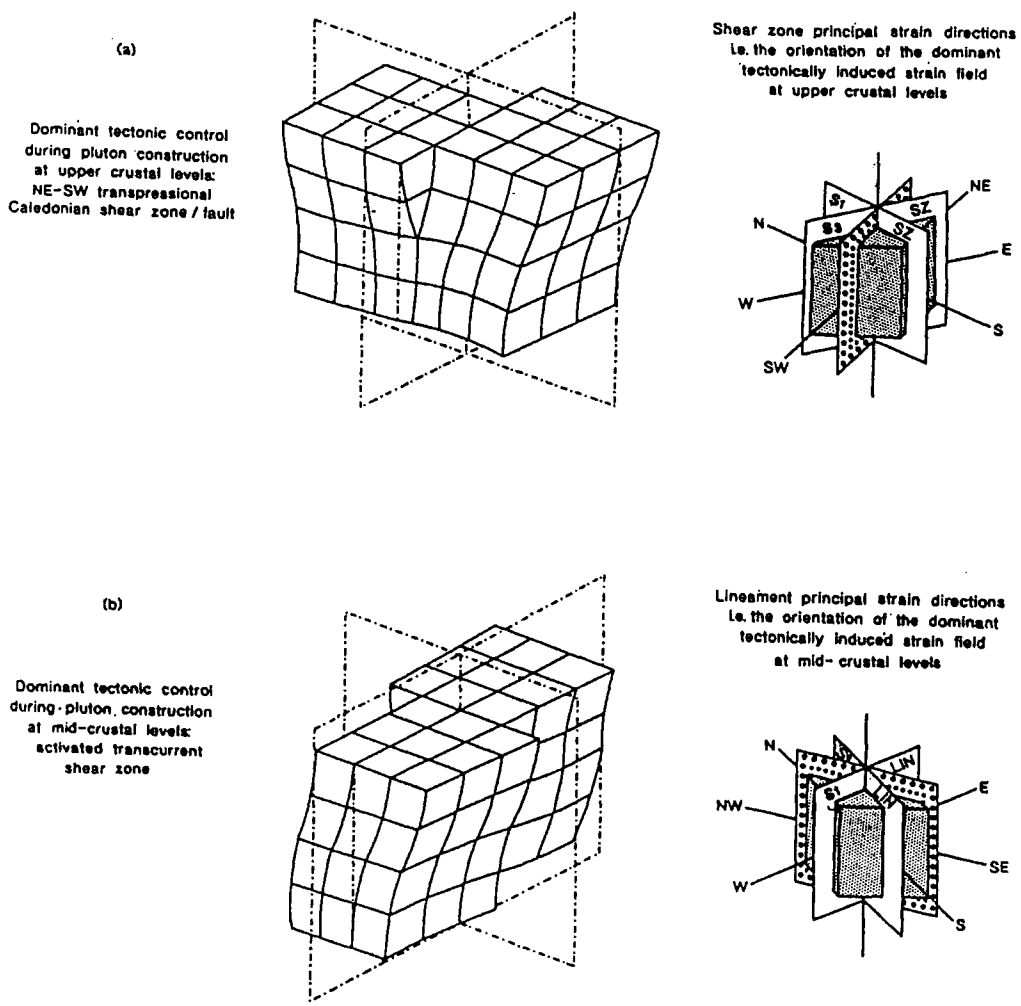

Fig. 10.4. The orientation of the principal strain directions associated with the dominant controlling tectonic structure at upper crustal levels, **(a)** and mid-crustal levels **(b)**. Both sets of structures within this region possess a sinistral shear component.

Mutual interference at the intersections between these two sets will result in the superposition of approximately orthogonal N-S, and E-W principal strain axes which, depending on the relative strain magnitude of either major structure will result in a predictable finite strain pattern (Fig. 10.5). One of the main aims of this Chapter is to identify from such patterns the relative importance of one set of structures with respect to the other, and to examine any correlation between this and crustal depth of emplacement.

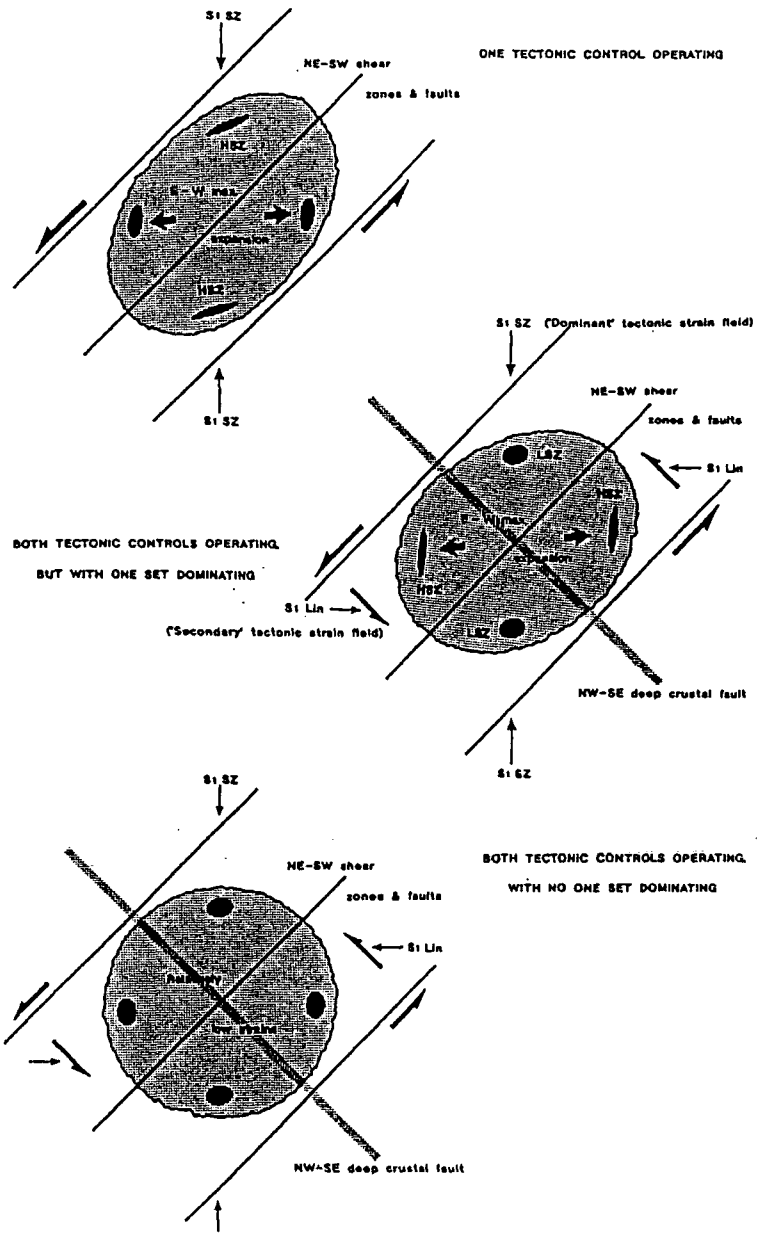

Fig. 10.5. Simple two dimensional strain models showing how strain patterns could vary in a ballooning pluton emplacing where (top), sinistral shear on a NE-SW shear zone is occurring, (middle), where NE-SW sinistral shear dominates over sinistral shear on an orthogonal NW-SE shear zone, and (bottom) where sinistral shear on both sets is of equal magnitude.

In what follows is an attempt to identify these, and similar patterns, in the five plutons under discussion. Following this we will discuss the relationship of the depth control and crustal rheology on the activation of major interfering fault systems responsible for siting and emplacement mechanisms of the granitoid plutons in this area.

10.4 EMPLACEMENT MECHANISMS AND STRAIN PATTERNS

10.4.1 The Etive complex:

The Etive complex represents pluton construction at a relatively high crustal level, approximately 2-4 km (Droop & Treloar 1981). The complex is markedly elliptical (30 km x 15 km) with the long axis trending NE-SW. It is sited at the intersection of the NE-SW-trending Etive-Laggan shear zone and the NW-SE-trending Cruachan lineament (Fig. 10.6a), and it is bounded by the Allt-Buidhe/Laggan Dam fault and the Ericht-Laidon shear zone on its NW and SE sides. The E, SE and SW margins of the pluton show evidence of ring faulting and associated cauldron subsidence, related to the Quarry Intrusion (G1), which is interpreted as a partially disrupted ring dyke (Anderson 1956).

The major intrusive phases G2 (Cruachan facies), G4 (Porphyritic Starav facies), and G5 (Starav facies) are all elliptical units which exhibit, in general, pseudoconcentric, steeply inclined fabrics and flattened microdioritic enclaves ($K \approx 0$) which are interpreted as the result of emplacement by an expansion ('ballooning') process (see Ch. 3). These three successive expanding pulses have been affected by contemporaneous sinistral shear on the NE-SW shear zones/faults, with the earlier units more deformed and sinistrally rotated than the later units (Jacques & Reavy 1994) (Fig. 10.6b). Within the north and south of the complex, G2 is locally modified within high strain zones where it is overprinted by a moderate to intensely developed CPS fabric (Fig. 10.6b). It is suggested that higher strains are developed within these regions due to the combined effects of: (i) the angle between pluton expansion-related strains and the direction of S_1 of the NE-SW-trending shear zones is low, resulting in opposing strain fields, which produce higher finite strain magnitudes (see Fig. 10.5a); and (ii) the effect of subsequent expansion and synplutonic rotation of G4 and G5 against G2 (Fig. 10.6b & 10.7).

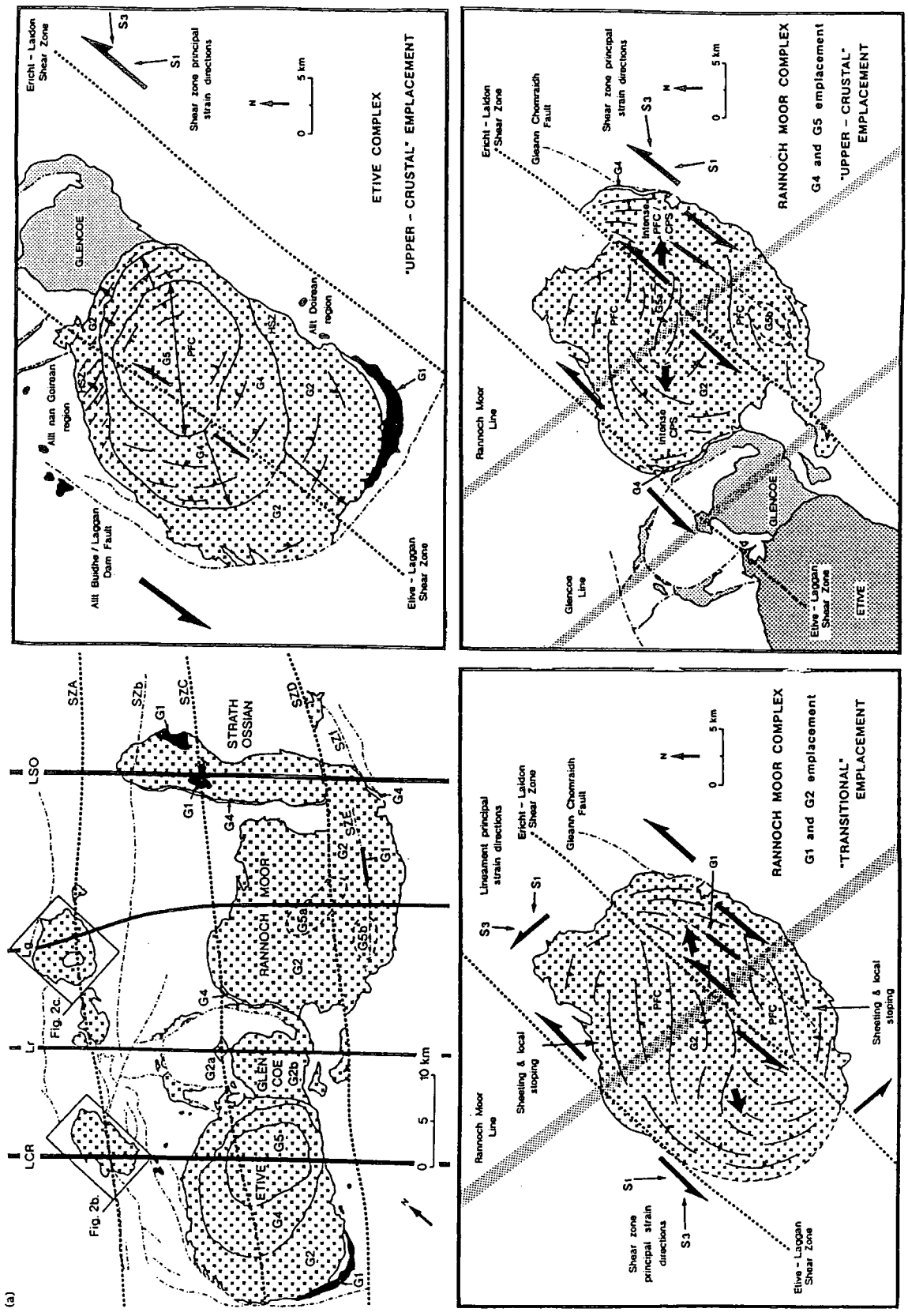

Fig. 10.6. **(a)** The Caledonian plutons and the major tectonic structures in the SW Highlands. Generalised models for the emplacement of: **(b)** the Etive complex (G3, a minor phase of pink microgranitic sheets and dykes, and the Etive Dyke Swarm are omitted for clarity); **(c)** G1 and G2, and **(d)** G4 and G5 of the Rannoch Moor complex. The distribution of tectonic-related strains are shown.

In summary, the construction of the major intrusive phases G2, G4 and G5 at this high crustal level, were controlled by expansion and tectonic-related strains imposed by the major Caledonian NE-SW-trending shear zones (Fig. 10.6b & 10.7). The strain field imposition by the Cruachan lineament (Fig. 10.6a) was of little, or of no importance to the overall construction of all the major intrusive components of this plutonic complex.

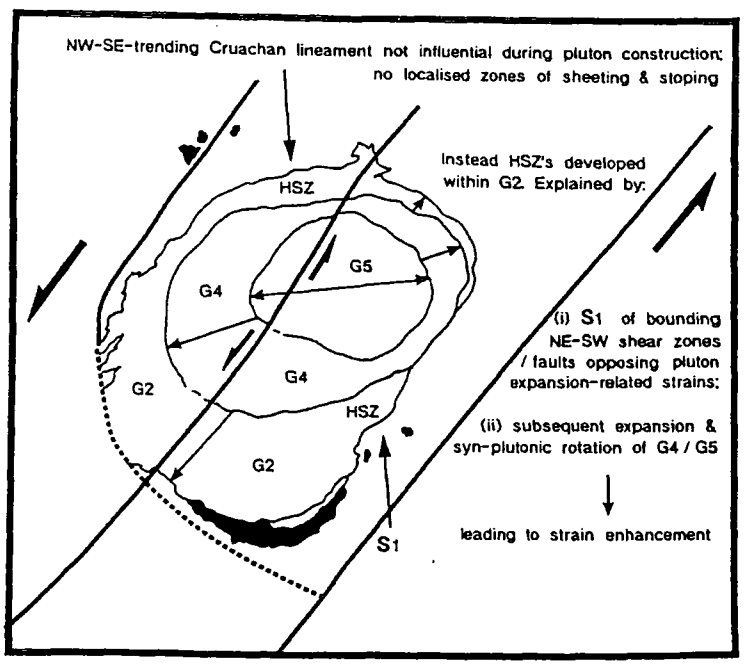

Fig. 10.7. Possible model explaining the distribution of high strain zones (HSZ) within the Etive complex.

10.4.2 The Rannoch Moor complex:

The Rannoch Moor complex is somewhat elliptical (28 km x 18 km), with a NE-SW long axis. It is sited at the intersection of the NW-SE Rannoch Moor lineament and the NE-SW Ericht-Laidon shear zone and is bounded to the NW and SE by the NE-SW Etive-Laggan shear zone and the Gleann Chomraidh fault (Fig. 10.6a). Fabric development and cross-cutting relationships suggest that this pluton was constructed by two distinct magmatic episodes (see Ch. 5): (i) an earlier, deeper level event involving the intrusion of G1 and the major intrusive component G2 (Fig. 10.6c); and (ii) the later, higher level emplacement of G4 and G5 (Fig. 10.6d). Evidence is presented below which shows that the regional strain fields pertaining at the level of crystallisation were different in each case due to the relative level of the free surface.

As with Etive, the Rannoch Moor complex is an elliptical body orientated NE-SW, and its major intrusive components (G2 and G5) have also been emplaced by a process of *in situ* expansion during contemporaneous sinistral shear on the NE-SW-trending shear zones/faults. The general concentric fabric has been deflected in the magmatic state by sinistral movement on the Ericht-Laidon shear zone. However, unlike Etive, the north and south pluton contacts are characterised by low strains and abundant sheeting and stoping (Fig. 10.6c). These zones correspond to the overall constrictional direction imposed by the NE-SW-trending shear zones, with localised transtension occurring as a result of the interaction of the maximum principal strain directions of the bounding shear zones and the NW-SE Rannoch Moor lineament (Fig. 10.6c), interacting at a high angle and possibly resulting in their cancellation (see Fig. 5b & 10.8). In contrast, at the east and west ends of the pluton, intense ductile flattening strains are observed. This corresponds to the direction of maximum expansion imposed by the controlling NE-SW-trending structures. It is possible that higher strains accumulated within these two regions due to the combined effect of strains related to pluton expansion opposing strains related to a small, but significant component of sinistral shear on the NW-SE Rannoch Moor lineament (with its maximum principal strain direction (S_1) orientated E-W) (see Fig. 10.5b & 10.8).

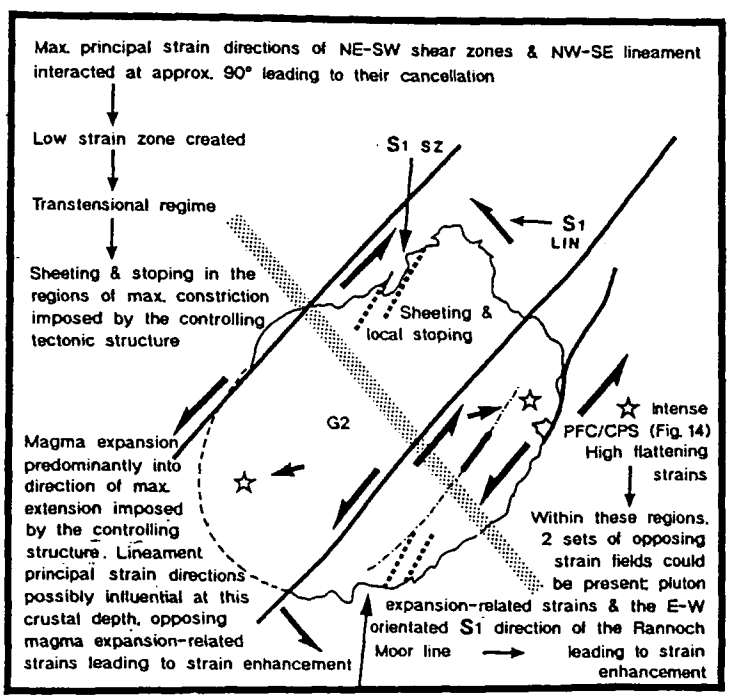

Fig. 10.8. Possible model explaining localised emplacement phenomena of sheeting and stoping, and zones of high strain within the Rannoch Moor complex.

The adjacent Glencoe body (Fig. 10.6a & d), which was emplaced at a higher crustal level (2-4 km) and is associated with ring dykes and ring faults, cross-cuts and obliterates a significant portion of the Rannoch Moor pluton, allowing the contemporaneous intrusion of G4 along this contact (Fig. 10.6d). G4 also occurs as a sheet-like marginal facies at the east and west ends of the body. Displacement along the bounding NE-SW structures created space for G4 at the outer margins of the crystallised G2 (Fig. 10.6d). The major phase of G5 occurs at the centre of the complex and appears to have expanded towards the S_3 direction of the NE-SW shear zone system (Fig. 10.6d).

The actual depth of emplacement of G1 and G2 is not well constrained. However, since uplift occurred before G4 was emplaced it must be greater than 2-4 km. It is suggested by comparison with deeper plutons e.g. Strath Ossian/Ballachulish (emplaced at depths > 8 km (see Key *et al.* (1993) and Weiss & Troll (1989) respectively)), and the absence of high level emplacement phenomena such as ring dykes which can be related to the earlier phase of emplacement (G1/G2), it is likely that the main construction of the pluton (G2) was at a crustal depth between 2/4 km and 8 km (say 6 km).

In summary, the NE-SW-trending shear zones and faults were obviously the dominant controlling structures during the emplacement of the Rannoch Moor pluton, a situation similar to the Etive complex. However, the suggestion is that the strain fields interfered during G1/G2 times, with imposition of NW-SE lineament and NE-SW shear zone movements, to produce a strain field in which E-W S_1 associated with the lineament(s) is opposed by maximum expansion direction of the pluton (see Fig. 10.5b & 10.8). This, led to high strains in the east and west, and strains being cancelled out in the north and south of the body, explaining the locallised emplacement phenomena of sheeting and stoping. A period of uplift and erosion, between the emplacement of G1/G2 and G4/G5, then followed. During the later magmatic event, strains were much less at the east and west ends of the pluton allowing the 'passive' emplacement of G4 sheets as a marginal facies, possibly the result of a lack of E-W compression and the influence of NW-SE structure(s).

Geometrical form and emplacement dynamics: a comparison between the Etive and Rannoch Moor complexes.

It is apparent that the geometrical form of the Rannoch Moor and Etive (Fig. 10.6a) complexes are somewhat different. The Rannoch Moor complex is only slightly elliptical with a somewhat irregular margin, whereas the Etive complex is clearly elliptical. There are two possibilities, or a combination of these factors to account for the contrast. In the case of Rannoch Moor, its more equidimensional form may be attributed to: (i) during main phase construction (i.e. G1/G2) both the NE-SW shear zone and NW-SE lineament

tectonic-related strain fields were operating; (ii) expansion-related strains were greater than the rate of tectonic deformation (Fig. 10.9a). Whereas during the construction of the Etive complex: (i) it crystallised at a crustal depth at which only strain fields associated with NE-SW-trending shear zones were influential; (ii) tectonic deformation may have been greater than the rate of pluton expansion (Fig. 10.9b). Emplacement dynamics and the structural features of both complexes are also different. Although both complexes have been constructed by a process of *in situ* lateral expansion, with magma expansion being predominantly into the direction of maximum extension imposed by the NE-SW-trending shear zone systems, the distribution of strain magnitude is clearly different. High strains developed within these zones in the Rannoch Moor pluton is primarily attributed to magma expansion being opposed by the maximum principal strain direction (S_1) of the NW-SE-trending Rannoch Moor line; interaction occurring at a low angle resulting in an increase in strain magnitude (Fig. 10.9a). As the Etive complex was constructed at a higher crustal level and clearly was not affected by strains related to the NW-SE-trending Cruachan lineament during its construction, strain magnitudes within these regions are low to moderate (Fig. 10.9b).

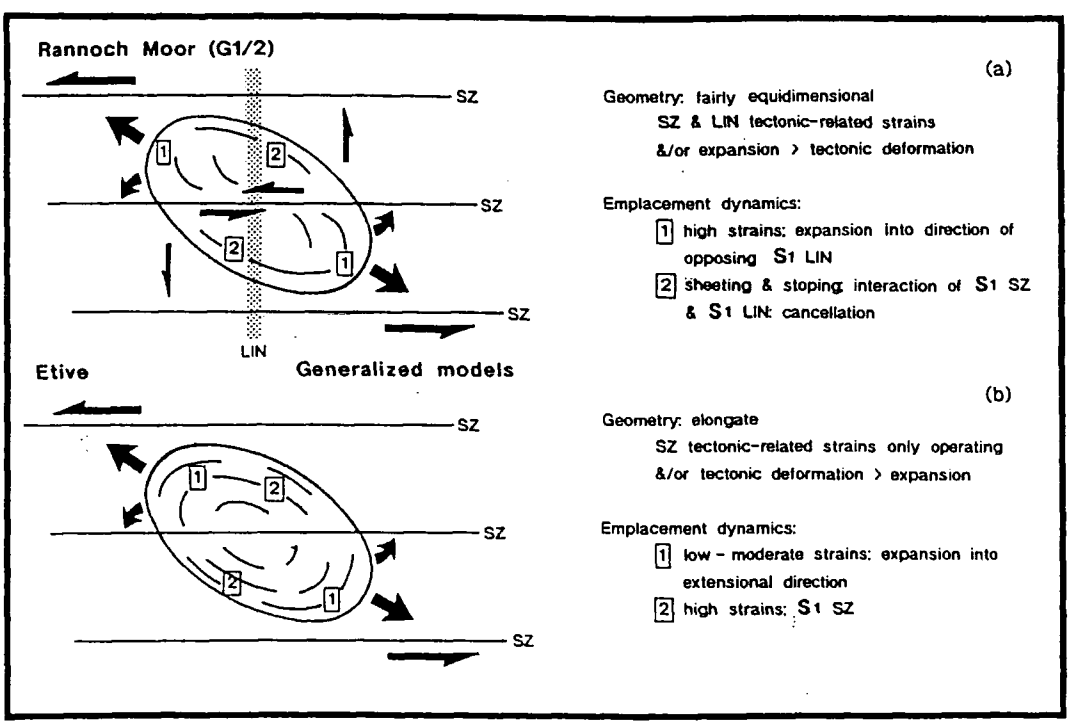

Fig. 10.9. Generalised model explaining the differences in fabric orientation, strain distribution and the development of local emplacement phenomena (sheeting and stoping) between the Rannoch Moor **(a)** and Etive **(b)** complexes.

The development of multiple sheeting and stoping in the northern and southern regions of the Rannoch Moor complex (zones of maximum constriction) appear to be due to the interaction of strain fields imposed by both the shear zone and lineament regional tectonic structures. Interaction of S_1 of both structures occurring at a high angle (approximately 90°) leading to their cancellation and the development of a low strain zone (see discussion above). This is in contrast to the Etive complex, as the equivalent zones exhibit extremely high strains created by the imposition of S_1 of the NE-SW shear zones (Fig. 10.9b), combined with the synplutonic rotation and expansion of subsequent intrusive phases (G4/G5) (see discussion above).

10.4.3 The Ben Nevis complex:

The Ben Nevis complex crystallised at approximately 1.5 kb (pers. comm. P. E. Brown 1995), indicating an apparent depth of approximately 5-6 km, with part of the roof zone preserved. It is possibly bounded to the north by the Great Glen fault and to the south by the Allt-Buidhe/Laggan Dam fault (Fig. 10.2). It is sited at the intersection of the NE-SW-trending Ballachulish-Corrieyairack shear zone and the trace of the Rannoch Moor lineament (see Jacques & Reavy 1996) (Fig. 10.6a). The most apparent feature of this pluton is that it is fairly equidimensional (approximately 6 km x 5 km), although the long axes of individual facies, especially G4 and G5, are orientated somewhat NE-SW/N-S (Fig. 10.10a).

The pluton as a whole possesses weak pseudoconcentric fabrics. The maximum expansion direction appears to have been orientated NNE-SSW (Fig. 10.10a), which may suggest a sinistral shear component on the NW-SE Rannoch Moor lineament (however see discussion by Burt & Brown 1996). No major zones of sheeting and stoping occur around the periphery of the pluton and in general strains are very low. These features may imply that at these crustal levels strain interference created a situation in which there was no overall dominance of either NE-SW- or NW-SE-trending structures (see Fig. 10.5c), both being approximately equal in magnitude. This crustal depth may represent some type of transition zone between the influence of the two different types (see below) (see Fig. 10.5c).

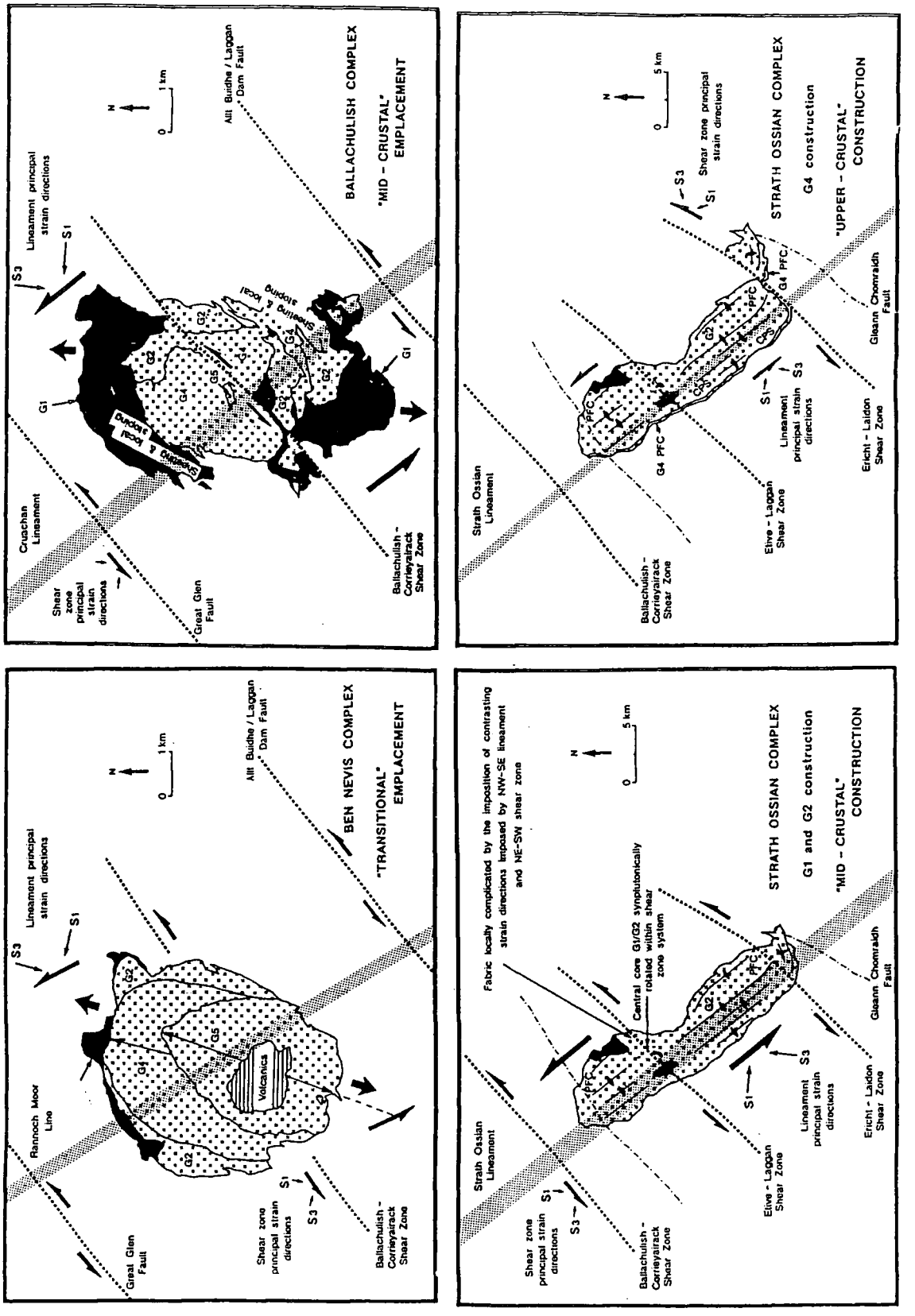

Fig. 10.10. Generalised models for the emplacement of: (a) the Ben Nevis complex; (b) the Ballachulish complex; (c) G1 and G2, and (d) G4 of the Strath Ossian complex, showing the possible distribution of tectonic-related strains.

10.4.4 The Ballachulish complex:

The Ballachulish complex crystallised at a crustal depth of approximately 10 km (Weiss & Troll 1989). When the offset of the margins of 0.8 km along the NE-SW-trending Ballachulish-Corrieyairack shear zone is restored, it has dimensions of approximately 8 km by 3 km and is elongate N-S. It is sited at the intersection of the NW-SE-trending Cruachan lineament and the Ballachulish-Corrieyairack shear zone, and it is possibly bounded by the Great Glen fault in the NW and the Allt-Buidhe/Laggan Dam fault in the SE (Fig. 10.6a).

In general, pseudoconcentric fabrics and microdioritic enclaves indicate expansion-related strains during emplacement of the Ballachulish pluton. As indicated by the common presence of minor sinistral shears, and offset mafic enclaves along the NW-SE margins of the body it is likely that expansion related strains were affected by contemporaneous sinistral shear associated with the NW-SE-trending Cruachan lineament (Fig. 10.10b). The pluton is characterised by sheeting and stoping on the opposite NW and SE sides, and intense ductile flattening fabrics at its north and south ends. As with Rannoch Moor, this is consistent with the simultaneous operation of NW-SE and NE-SW structures, but in this case with NW-SE shear dominating and producing N-S pluton expansion; the localised emplacement phenomena of sheeting and stoping being produced due to the cancellation of contractional strains by mutual interferance of two strain fields (Fig. 10.11).

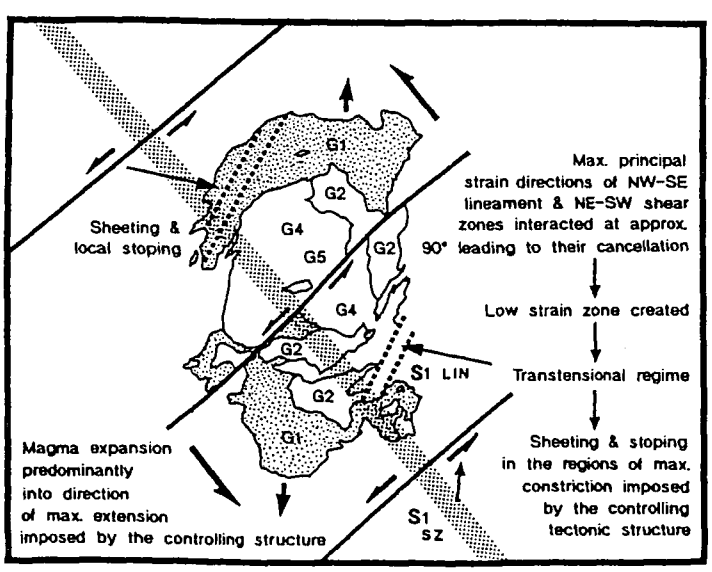

Fig. 10.11. Possible model explaining localised emplacement phenomena of sheeting and stoping within the Ballachulish complex.

The reasons for the contrasts between Ballachulish and Ben Nevis may be:

(i) the Rannoch Moor line is less significant than the Cruachan lineament in terms of crustal structure;

(ii) its higher level of crystallisation means that the NE-SW-trending shear zones were more influential;

(iii) the pluton expansion rate may have been greater than rates of tectonic deformation. The lack of obvious local emplacement phenomena, such as sheeting and stoping, possibly indicates that crystallisation occurred at a depth where no one set of structures were obviously dominant.

10.4.5 The Strath Ossian complex:

The Strath Ossian complex is known to have crystallised at a depth in excess of 10 km (Key *et al.* 1993). It is sited at the cross-over of the NW-SE-trending Strath Ossian lineament and the NE-SW-trending Etive-Laggan shear zone (Fig. 10.6a). The body is essentially bounded to the north and south by the Ballachulish-Corrieyairach and Ericht-Laidon shear zones, respectively (Fig. 10.6a & 10.10c). It is markedly linear in shape (30 km x 6 km), elongated NW-SE along the Strath Ossian lineament. There is abundant evidence in G1 and G2 of sinistral synmagmatic shear orientated NW-SE parallel to the walls and sheets in the main G2 phase (Jacques & Reavy 1994, Ch. 6). There is also evidence (Jacques & Reavy 1994) of synmagmatic sinistral shear along the Etive-Laggan and Ericht-Laidon shear zones in G1 and G2. This suggests the simultaneous operation of the NW-SE- and NE-SW-trending shear zones during the construction of the Strath Ossian pluton, but with the NW-SE-trending Strath Ossian lineament dominating (Fig. 10.10c).

G4 has been emplaced along both major directions, as thin, sheet-like bodies along the western flank of the complex, parallel to the NW-SE Strath Ossian lineament, and along the NE-SW Ericht-Laidon shear zone (Fig. 10.10d). G4 contains a contact parallel PFC fabric, but strong CPS fabrics in adjacent G2 implies a significant time difference in crystallisation, with G4 intruding significantly later than the main deformation in G2. This suggests either a later, independant phase of movement occured along the NE-SW structures or uplift in the interveening period resulted in the deformation associated with the NE-SW faults and shear zones to become more dominant. This may imply the increasing significance of the NE-SW structures with time, and since uplift was occuring, with decreasing crustal depth.

10.5 COMPUTER MODELLING OF PLUTON EXPANSION DURING TECTONIC DEFORMATION

Mathematical modelling of the interference between non-coaxial tectonic strain fields and pluton ballooning strain fields has been carried out by Brun and Pons (1981), producing two-dimensional kinematic simulations. They used the models to predict fabric trajectories, finite strain variations and position of triple points, both within the expanding pluton and around its periphery. These simple models show that when an expanding circular plutonic body is combined with a component of shear, the resultant shape of the pluton is elliptical. As described above, the geometrical form of the plutons within the Argyll Suite is a consequence of such strain imposition. When pluton expansion is non-circular, that is elliptical, Bruns and Pons (1981) concluded that complex shapes can be produced and the position of triple points become asymmetrical. An example of such emplacement could be the Loch Doon complex of the Southern Uplands. This pluton is bisected and bounded to the N and S by major NE-SW-trending Caledonian structures which may have interacted with a NNW-SSE lineament (Woolett 1988) which traverses the plutons western flank (Fig. 10.12). This may have sited and provided the necessary ascent pathways for pluton construction. Field observations show the pluton to possess *in situ* ballooning characteristics, in which its overall geometrical shape could be attributable to non-circular expansion within a complex regime of tectonic strain field interaction. *In situ* expansion within such an environment has produced an unusual 'peanut' type form (Fig. 10.12). Such a process of construction was envisaged by Oertel (1955) who attributed the fabric orientation within the pluton to forceful lateral expansion.

The models of Brun and Pons (1981) also show that triple points, narrow zones of constrictive strain, can be internal or external to the pluton. An external position occurs when pluton expansion-related strain rates are greater than tectonic-related strain rates. As mentioned previously, based on its fairly equidimensional form, probably as a result of the implied tectonic deformation rate only being slightly higher than the expansion rate and the development of local emplacement phenomena, the Rannoch Moor complex appears to fall within this category. At the ends of the pluton, intense pseudoconcentric PFC and CPS fabrics occur, exhibiting flattening type strains (Fig. 10.6d) Externally, within the adjacent country rock, zones of constriction may occur. An example of triple point development occurring internally, is represented by the Etive complex. Here, tectonic-related strain rates are clearly greater than expansion-related strain rates, producing an elliptical pluton with high strain magnitudes at the sides. This has been further complicated by subsequent

ballooning and rotation of later intrusive phases and in the NE of the complex by the *in situ* expansion of the adjacent Glencoe complex (Fig. 10.6a).

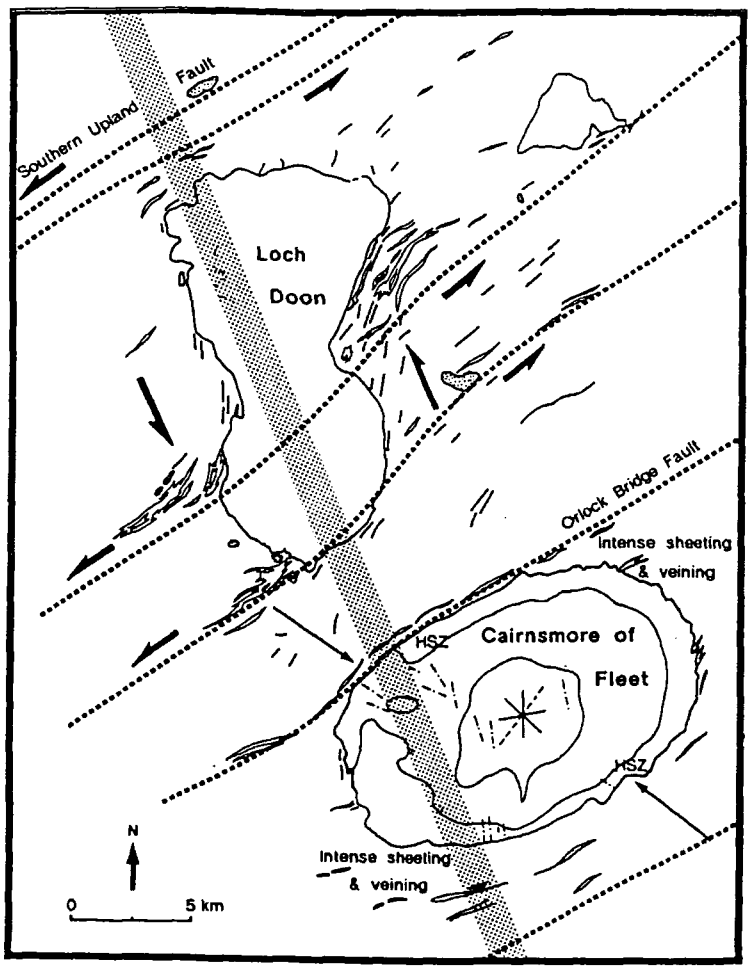

Fig. 10.12. Generalised model showing the tectonic structures associated with the construction of the Loch Doon and Cairnsmore of Fleet plutons. Joint and vein orientations related to a postulated late/post-magmatic regional stress field by Parslow (1968; 1971) are shown for the Cairnsmore of Fleet complex.

Computer modelling of pluton expansion within both non-coaxial and coaxial tectonic environments, has been recently produced by Guglielmo (1993, 1994). These are three-dimensional kinematic simulations, which show how the form of the pluton and its

internal and external distribution of strain magnitude change as the ratio of strain intensity between tectonic and pluton expansion-related fields vary. The models show that the resultant deformation from the combination of these strain fields can be complex. This complexity can further increase, if during pluton construction, strain rates vary, the type of tectonic deformation changes and as shown by plutons within the Argyll Suite, a number of interacting tectonically induced strain fields may exist. As shown within this Chapter, this can have a great influence on overall pluton geometry, local emplacement phenomena, strain intensity and distribution. It has also been shown that with time, what was the dominant controlling tectonic structure during one particular phase of pluton construction, may become less influential or of little importance compared to the establishment of a tectonically induced strain field with a different orientation. Modelled strain magnitude patterns of a pluton expanding within an environment undergoing non-coaxial tectonic deformation (Guglielmo 1993), show that two distinct zones are developed. Ellipsoidal low strain zones at the ends of the pluton, approximately parallel to the major axis of the pluton and zones of high strain, which are in three-dimensions convex lens shaped, occurring at the sides of the pluton.

As shown above, the overall geometry of the Etive complex and its internal distribution of strain closely resembles that predicted by computer modelling of pluton expansion during non-coaxial deformation. This becomes more complicated when more than one tectonically induced strain field is present, as seen within the Argyll Suite. In this situation, there is not only the interaction between tectonic and pluton expansion-related strain fields to consider, but also the imposition of tectonic strain fields with different orientations, leading to complex strain patterns and the development of local emplacement phenomena, e.g. Rannoch Moor. It is therefore possible, with the combination of field observations and computer modelling of pluton construction, that three-dimensional kinematic simulations of the structural evolution of a region can be established using such methods as described in this Chapter.

10.6 APPLICATIONS TO OTHER AREAS:

As previously mentioned, the Loch Doon pluton within the Southern Uplands of Scotland, may have also been principally controlled during its construction by a deep basement structure with an approximate northwesterly trend (named here as the Loch Doon lineament; Fig. 10.12). The lineament, may have not only controlled the overall geometry of the pluton (N-S orientation) and its internal distribution of structural features, but also affected the Ordovician cover sequence by the synplutonic rotation of regional fabrics. Such features, together with field data suggests a sinistral shear component along the lineament. Interestingly, this sense of motion may account for the late/post-magmatic features observed by Parslow (1968; 1971) within the Cairnsmore of Fleet complex, which may be traversed by the Loch Doon lineament to the south of the Loch Doon pluton (Fig. 10.12). It is an elliptical pluton, approximately 19 km by 12 km, with its long axis parallel to the regional Caledonian trend (ENE-WSW). As with the plutons within the Argyll Suite it is bounded by major NE-SW-trending Caledonian structures. It is concentrically zoned and recent mapping during this study shows that it possesses a roughly pseudoconcentric pre-full crystallisation fabric (see Parslow 1968 for fabric trajectories), with an increase in flattening strains towards the pluton margin. Emplacement features are consistent with a predominant process of *in situ* expansion, deforming to some degree the surrounding Lower Palaeozoic rocks. As with the Ballachulish and Rannoch Moor complexes within the Argyll Suite, intense zones of sheeting and veining occur in corresponding zones along its outer margin. Such localised emplacement phenomena may also be attributable to the interaction of tectonically induced strain fields imposed by the NE-SW-trending bounding structures and the NNW-SSE-trending Loch Doon lineament. The position of these zones in the NE and SW of the complex suggests that the dominant controlling structures during the main phase of construction was the Caledonian NE-SW-trending structures. This would account for the geometrical orientation of the pluton, with the zones of sheeting and veining occurring in the regions of maximum constriction imposed by the dominant controlling structures. Zones of high strain (HSZ; Fig. 10.12) occur in the NE and SW of the complex, corresponding to the directions of maximum expansion into the regions of maximum extension created by the controlling tectonic structures, i.e. the NE-SW-trending structures. Due to pluton expansion-related strains being opposed by S_1 of the NNW-SSE Loch Doon lineament, an increase in strain magnitude occurred, leading to the development of zones of high strain.

The Rannoch Moor complex exhibits very similar emplacement characteristics and the model developed for its construction (see Fig. 10.6a & 10.8) may account for the observed emplacement phenomena of the Cairnsmore of Fleet pluton during its main phase of emplacement. However, unlike the Rannoch Moor complex, there appears to have been a change in the dominance of the controlling tectonic structures during the latter stages of construction; with the NNW-SSE-trending Loch Doon lineament becoming the dominant tectonic control, probably leading to further strain enhancement within the high strain zones, producing extremely intense crystal plastic strain fabrics (termed by Parslow (1968) as a "shear foliation") and the emplacement of quartz veins (3-4 m wide) into a series of *en echelon* shear planes. The latter were interpreted by Parslow (1968) as representing tension-gash type structures, postulating a regional stress system orientated approximately NW-SE (see Fig. 10.12). This would correspond to a sinistral sense of shear along the Loch Doon lineament, accounting for the constructional characteristics observed. Such an orientation of a late/post-magmatic regional stress system was also envisaged by Parslow (1968) to account for the orientation of joints and veins within the complex (see Fig. 10.12). As he noted, this is substantiated by Blyth's work on the sheared porphyrite dykes of South Galloway (1949) and on the Clints of Dromore, where quartz gash-veins displaced the contact along the southern margin in a sinistral manner (1954), concluding the stress field pertaining at that time had an approximate 135° orientation.

It is therefore possible that the techniques could be used to identify the orientation and distribution of individual strain fields tectonically imposed on and in a region, leading to the identification of the major mechanisms operating during its structural evolution.

10.7 DEPTH OF GRANITE INTRUSION

As shown by Figures 10.1 and 10.2, a large number of granitic plutons and associated minor intrusive bodies are currently exposed at the present level of erosion within the Argyll Suite. This geographically high concentration of intrusives, which represents a range of ages and significantly different relative depths of crystallisation (Figs. 10.13 & 10.14), all appear to have been emplaced at approximately the same relative level within the crust. This means that during Caledonian magmatism the level of crystallisation for subsequent intrusive events was approximately the same throughout the region. Figure 10.14 diagramatically represents the dominant controlling tectonic-related strain fields

pertaining at the time of pluton construction; explaining the overall geometrical form of the plutons, internal distribution of facies and local emplacement phenomena. It is therefore apparent that with increasing depth of pluton construction, the NE-SW crustal shear zones become progressively more dominant (Fig.10.13 & 10.14). However, as documented above, there is considerable variation in depth of crystallisation, explained as a function of relative pluton age and an erosion rate of approximately 10 km / 10 Ma during this period of plutonism. It is envisaged that the upper crustal NE-SW-trending shear zones essentially only operate to a certain depth below the free surface, therefore during this period of granite magmatism, the free surface was progressively lowered and hence the effective depth at which these shear zones controlled pluton construction was also lowered. This explains why the construction of: (i) the older, mid-crustal plutons have been predominantly controlled by the NW-SE deep crustal lineaments (e.g. Strath Ossian); (ii) the youngest, upper crustal plutons have been essentially controlled by the NE-SW upper crustal shear zones (e.g. Etive) and; (iii) the intermediate- to upper crustal plutons (e.g. Ben Nevis) have fairly equidimensional forms, i.e. no preferred geometrical orientation indicating their construction was at a relative crustal depth at which no one set of tectonic-related strain fields were clearly dominant ("transitional zone"; Fig. 10.13 & 10.14).

The reason why ascending granitic magma should stop at a particular level within the crust and not continue in great quantities to the free surface may be attributed to the concept that the magma will essentially stop at its level of neutral buoyancy (LNB) within the crust (see Lister & Kerr 1991). Lister and Kerr (1991) also suggest that once the magma has reached its LNB it will accumulate and form lateral dykes and sills along this horizon, driven laterally away from the site where magma emerges from the ascent conduit by its own buoyancy forces. Other theories put forward to account for why magma should stop at a particular level within the crust are addressed in Chapter 11, together with comments about the actual three-dimensional form of these plutons and the mechanisms by which space has been created to accommodate such bodies, which have crystallised at different relative depths.

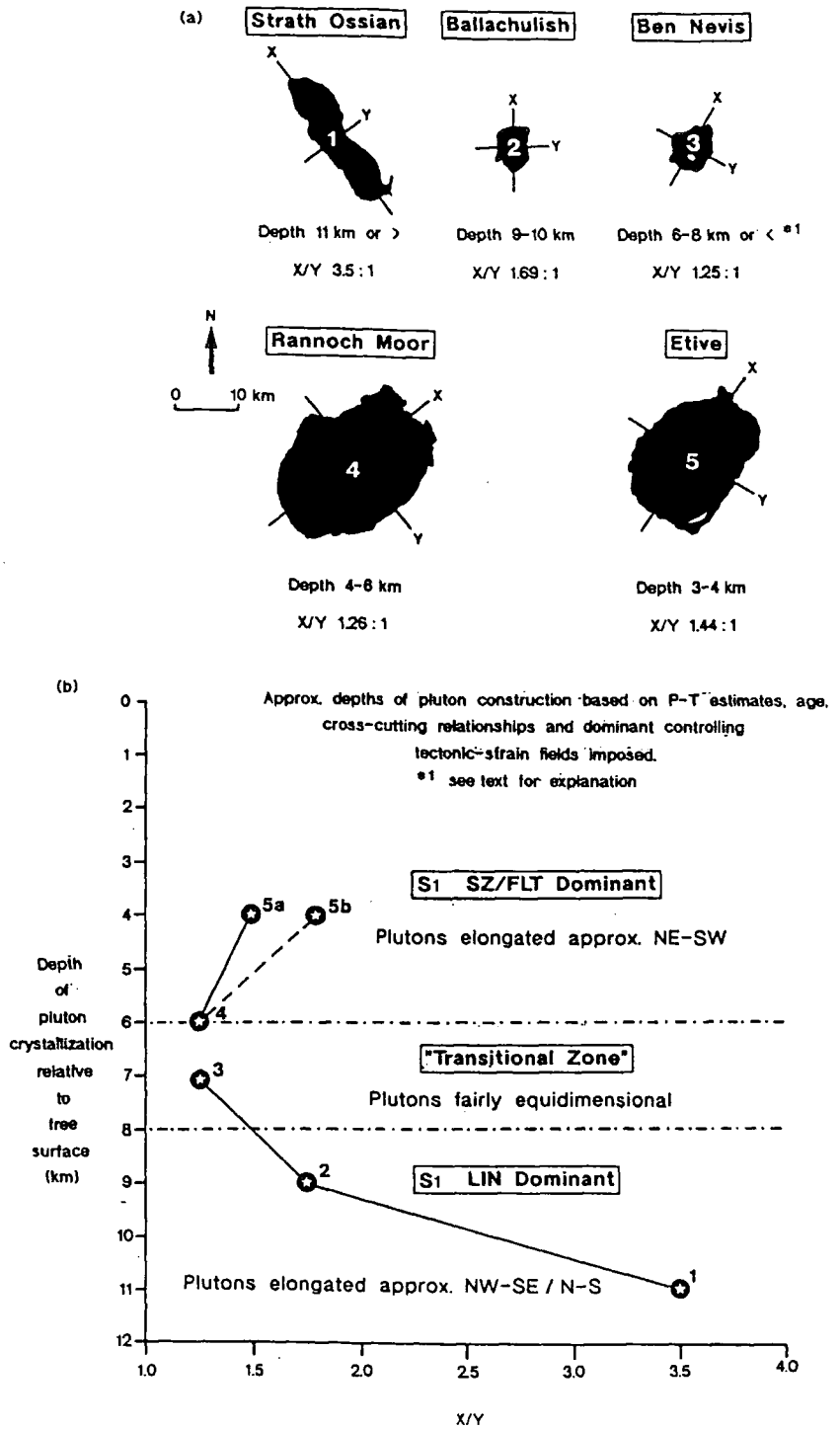

Fig. 10.13. **(a)** Shows the geometrical form of the plutons and the geographical orientations of their long axis (X). Relative depths of the major phase of pluton construction are shown, together with X/Y ratios of the plutons. **(b)** A plot which shows the X/Y ratios of the plutons against the relative depth of pluton construction in relation to the free surface at that time. For the Etive complex, 5a represents the actual X/Y ratio, whereas 5b is the restored X/Y ratio after removing the effects of the Etive Dyke Swarm.

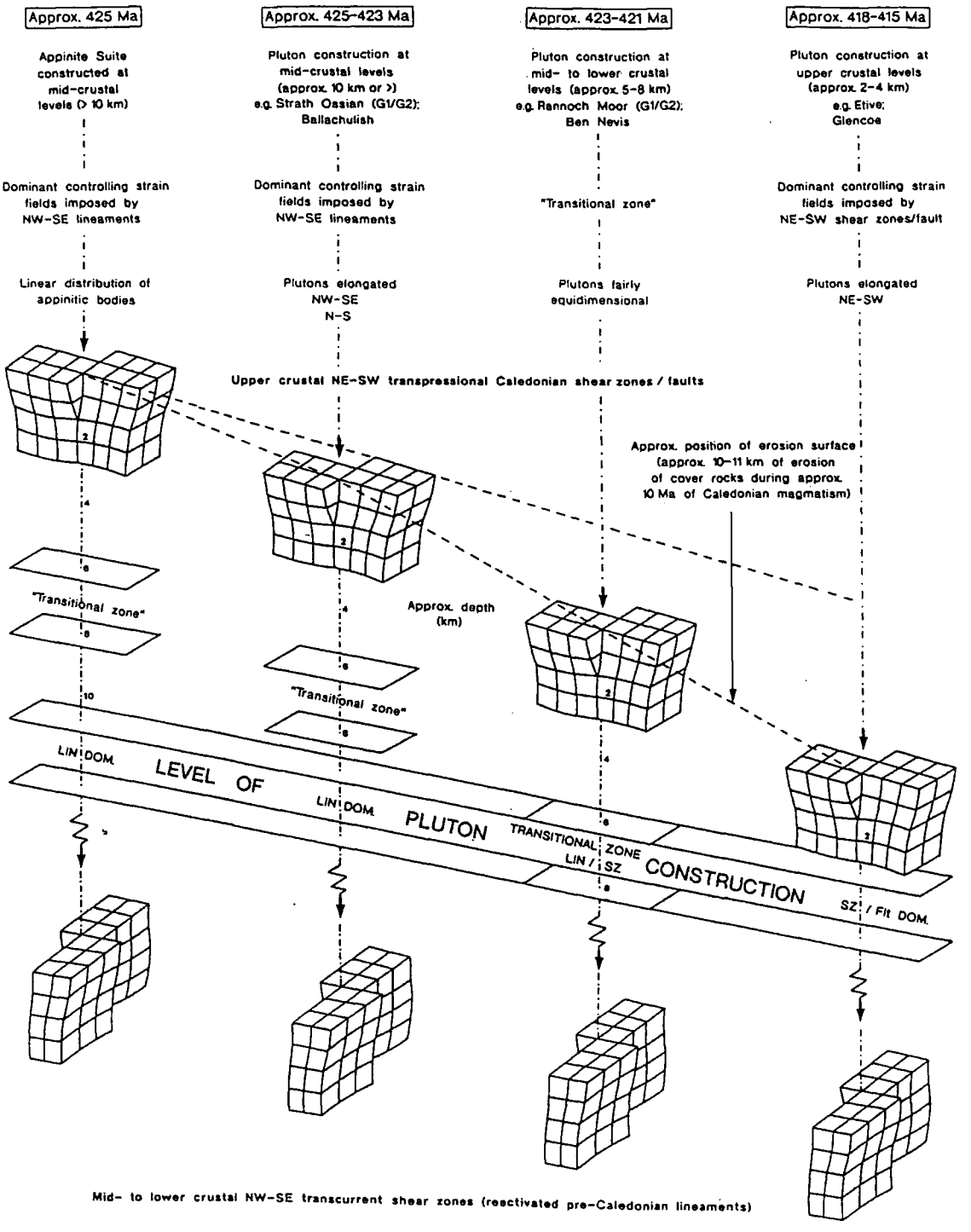

Fig. 10.14. Generalised model explaining how the dominant controlling tectonic-related strain fields pertaining at the time of the intrusion of the Appinite Suite and during pluton construction, was controlled by the relative position of the free surface.

10.8 CONCLUSIONS

The integration of data, such as the overall geometry, shape and distribution of intrusive facies, fabric orientation and intensities, strain distribution and local emplacement phenomena of the syntectonic plutons, of the Argyll Suite, has led to a number of observations:

❶ The deeper level plutons are elongated parallel to the NW-SE lineaments, whereas the higher level plutons are elongated parallel to the NE-SW shear zones and faults. Intermediate level plutons are the least elongate (Fig.10.13 & 10.14).

❷ The fabric patterns and strain distribution show that the deeper level plutons were more affected by sinistral shear on the NW-SE deep crustal faults and equally, the higher level plutons were clearly more affected by sinistral movement on the NE-SW shear zones and faults.

❸ Between these two end-members it is believed that the shapes, elongations, fabric patterns and internal structures reflect the combination and varying dominance of both sets of structures. Thus, at intermediate levels plutons are characterised by low degrees of elongation (Fig. 10.14).

❹ Interference of strain fields produces quadrants in the plutons where diametrically opposite sides are characterised by "passive" sheeting and stoping and the sides at right angles to these by high ductile flattening. At upper crustal levels (Etive, Rannoch Moor) this arrangement indicates the dominance of NE-SW sinistral shear and E-W pluton expansion. Whereas at deeper levels (Strath Ossian, Ballachulish) this indicates the dominance of NW-SE sinistral shear with N-S pluton expansion. This effect is least with the intermediate level, near-equant Ben Nevis pluton which is associated with very low strains.

❺ Pluton expansion with concentric fabrics has occurred in all these plutons with the exception of the deepest (Strath Ossian), and in the highest crustal level granites (Etive, Rannoch Moor and Ben Nevis) the influence of the free surface is clearly

seen with the various preservation of ring dykes, ring faults and contemporaneous volcanics in the roof.

❻ The interaction of tectonically induced strain fields with pluton expansion-related strains increases the complexity of strain patterns. Combined strain fields may enhance strains imposed or cancel them out, leading to the development of local emplacement phenomena;

❼ Many of these plutons have crystallised at different relative depths but, occur at approximately the same position within the crust. This is attributed to plutonism occurring over a significant time span of at least 10 Ma, where the ascending magma of each plutonic event has essentially stoped and laterally migrated, possibly along its LNB, during which time the free surface has been progressively lowered by approximately 10 km;

❽ Magma expansion during the construction of the elliptical/sub-elliptical plutons is predominantly into the direction of least tectonic strain (S_3) imposed by the major controlling tectonic structure(s);

❾ The results of computer modelling of pluton expansion within an environment of non-coaxial deformation, producing both two- and three-dimensional kinematic simulations, show great similarities to the observed structural characteristics of the Argyll plutons;

❿ The structural study of syntectonic plutonism may make it possible to identify the orientation and distribution of individual strain fields tectonically imposed on and in a region, leading to the identification of the major mechanisms operating during its structural evolution. This could then be used to obtain a detailed understanding of the regions internal structure and to the building of a three-dimensional kinematic simulation of how this particular part of the crust has structurally developed during regional deformation.

It is therefore concluded that this data set shows that the deep level, deeply seated lineamental faults are the dominant control on granite emplacement up to depths of about 8 km (Fig. 10.13 & 10.14), and that their influence diminishes above this level. Above say 6

km, the NE-SW Caledonian faults and shear zones become progressively more important (Fig. 10.13 & 10.14), although the strains and displacements associated with them are not that large. The direct influence of the free surface on emplacement extends down to about 6 km, and that ballooning/expansion is important only above 10 km and therefore may be a deeper level expression of the influence of the free surface. Below 10 km this influence is absent and the emplacement style has changed to the formation of granitic sheeted complexes.

This data shows that during the history of emplacement of these granitic bodies that uplift was occurring. With uplift the free surface migrates down through the crust towards the older, more deeply emplaced plutons. It has been well documented that there was considerable variation in depth of crystallisation, which can be largely explained as a function of relative pluton age and an erosion rate of approximately 10 km / 10 Ma during this period of granite magmatism (Fig. 10.13). This resulted in younger, shallower level plutons being emplaced at the same level as older, more deeply emplaced bodies. Thus preserving the influence of depth on the emplacement styles of the plutons. This data reinforces H. H. Read's Granite Series except that it has been shown how different crustal faults, originating at different crustal levels can also influence emplacement style.

Discussion: Crustal structure within the SW Highlands and relationship to emplacement mechanism

One important matter remains to be considered: why are the lineamental NW-SE faults more important at depths below about 8km and the NE-SW faults more significant above this? To answer this we need to consider the depths at which the faults originated and the likely rheological controls exerted by the crust.

As suggested by many authors (Watson 1984, Fettes 1986), and as evidenced by the siting control on deeply sourced magmatic rocks (appinites etc), the NW-SE lineamental faults are likely to have formed in the deep old continental crust although variously reactivated since in the overlying cover. The NE-SW structures on the other hand are likely to be transcrustal; Brewer et al 1983, and Synder & Flack 1990 having shown from deep crustal reflection data that major reflectors in the uppermost mantle are offset by splays of the Great Glen Fault.

The strength of the crust is determined by the weakest major mineral component, probably wet quartz in the upper crust (Kusznir & Park 1987). Within the lower crust, many workers (Meissner & Kusznir 1987; Kusznir & Park 1987; Hall 1986; Cheadle *et al.* 1987) have suggested that there is insufficient quartz and that the rheology may here be controlled by feldspar (Meissner & Kusznir 1987; Kusznir & Park 1987). These workers

predict that a zone of weakness would be expected just above the transition from quartz to feldspar controlled rheology. This zone would define the upper decoupling surface (Reston 1988) of the LCRZ (Fig. 10.15a). A lower detachment zone would occur just above the crust-mantle transition (CMT), below which the rheology is dominated by olivine (Fig. 10.15a; Kusznir & Park 1987). The two detachment surfaces bounding the LCRZ have been identified by seismic modelling (Meissner & Kusznir 1987) as two crustal reflectivity bands. Reston (1988) proposed that the two decoupling surfaces occur at depths of 20 km and 30 km. Within the context of the Grampians, the upper detachment surface may be close to, but not necessarily parallel with, the base of the Lewisian. These studies provide a rationale for suggesting that there are major sub-horizontal strength variations within the continental crust. When combined with the two sets of major steep faults this will create a series of crustal blocks between the two decoupling surfaces at depths between 20 and 30 km (Jacques & Reavy 1994). This zone may correspond to the LCRZ described for this depth range by Reston(1988), comprising low strain "lozenges" or "mega-augen" bounded by intersecting zones of high strain (see Fig. 10.16).

Although orthogonal (NW-SE and NE-SW), the two sets of structures, in the Caledonian, were synchronous but not conjugate; both being apparently sinistral. Jacques & Reavy (1994) explained this as the result of dextral vorticity of the lower crustal blocks between the major bounding faults of the Great Glen Fault and the Highland Boundary Fault, whose slight divergence towards the NE causes an increase in the vorticity and hence intra-block sinistral displacement in that part of the Highlands. For rotation of blocks to occur most easily dilation of the lower crust should occur. However this would be opposed by regional transpressive tectonoics envisaged for this period (Hutton 1987, Hutton & Reavy 1992). It may be that the amount of block rotation is relatively small and is in effect buffered by the transpressional regime. In addition we note that Robin & Cruden (1994) propose that upper crustal transpression may be transfered downwards into non-transpressional flat lying detachments in the deeper continental crust, perhaps corresponding to the upper detachment which bounds the LCRZ.

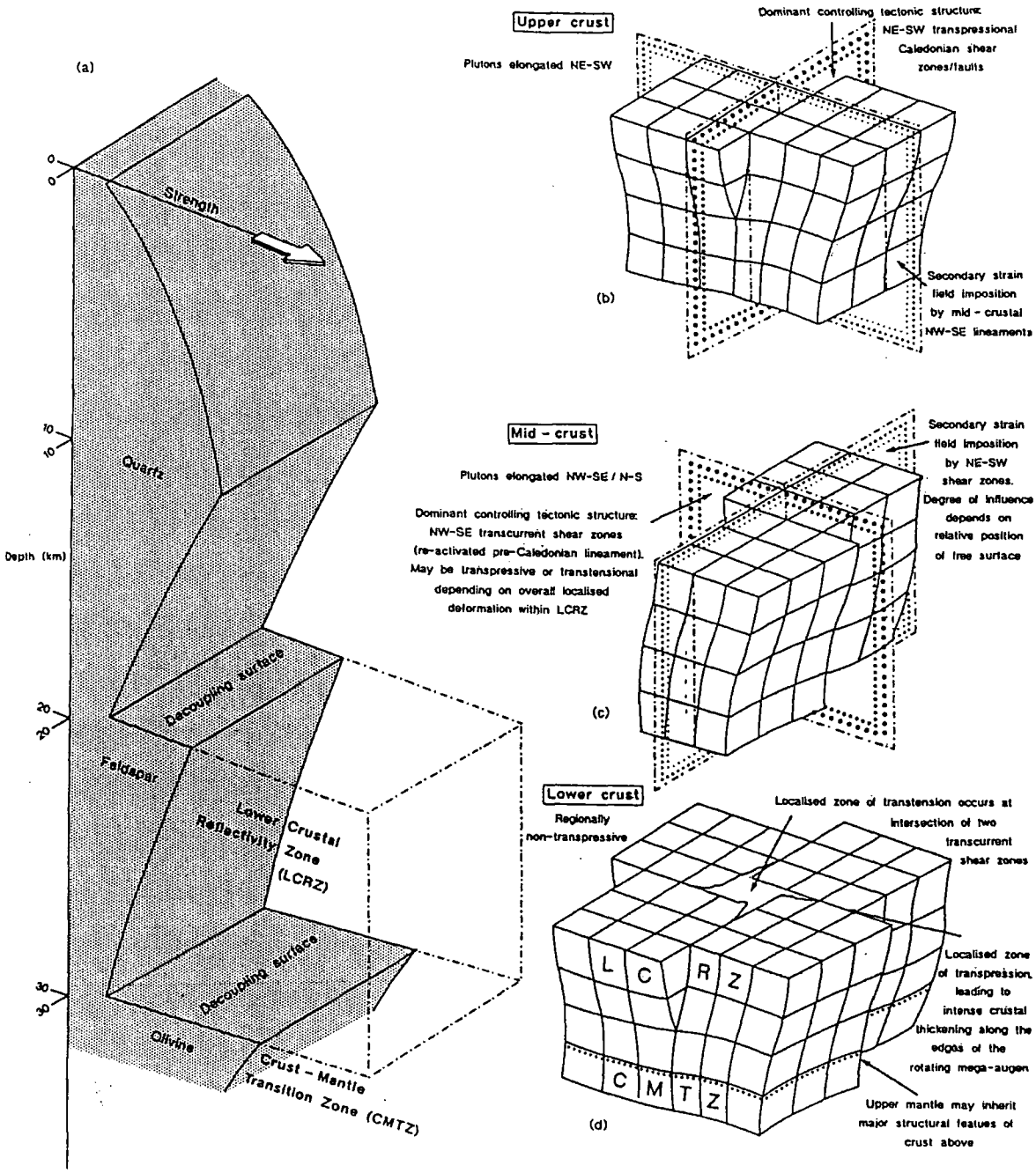

Fig. 10.15. **(a)** Diagrammatic representation of the variation of crustal strength with depth (modified after Meissner *et al.* 1987; Reston 1988), showing decoupling surfaces, produced by the rheological changes from quartz to feldspar and from feldspar to olivine. These zones of weakness, decouple the lower crust from the upper crust and the mantle, essentially bounding the Lower Crustal Reflectivity Zone (LCRZ). **(b)** Structure of the LCRZ showing the development of a low strain zone bounded by anastomosing shear zones. **(c)** The dominant controlling tectonic structure at mid-crustal levels; NW-SE-trending lineaments. **(d)** The dominant controlling tectonic structure at upper crustal levels; NE-SW-trending shear zones and faults.

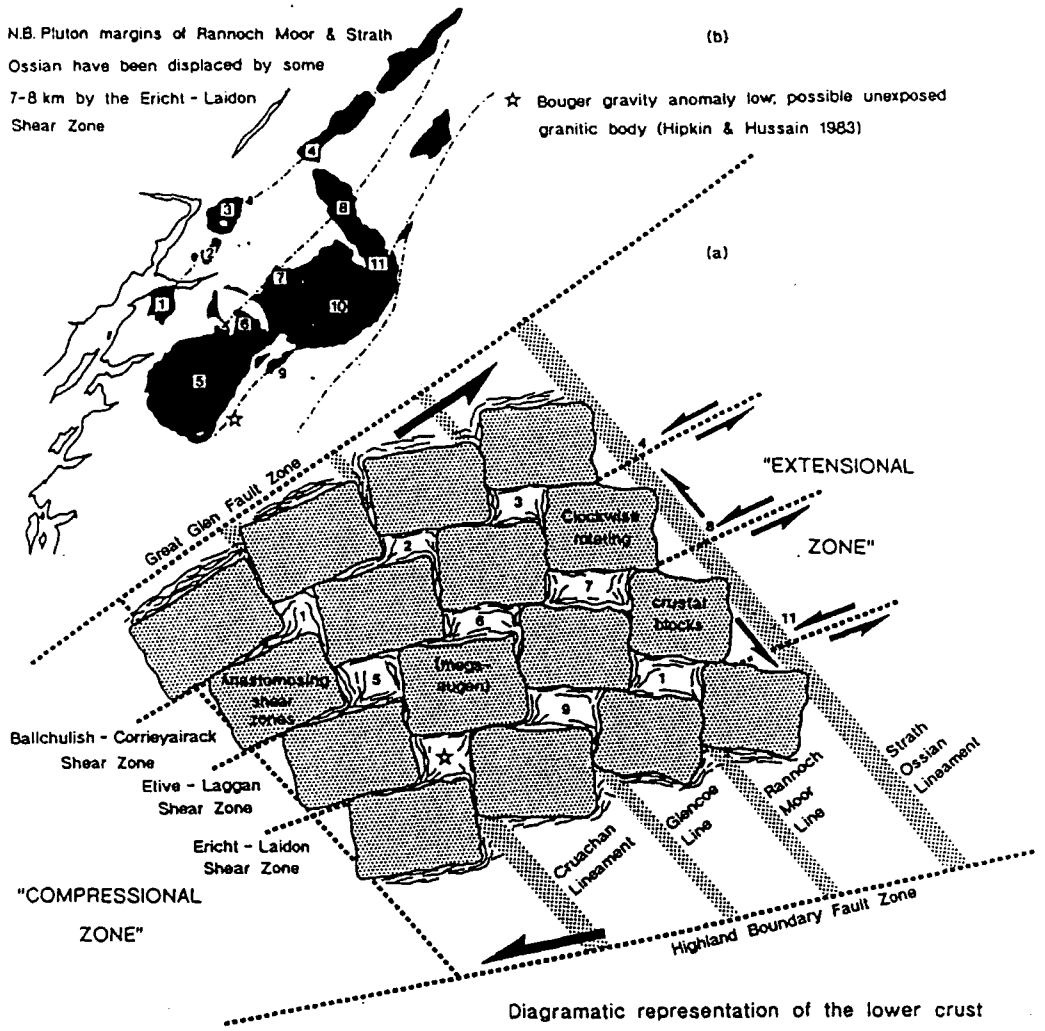

Fig. 10.16. **(a)** Possible structure of SW Grampian crust showing rotation of 'blocks' and lineamental intersections between the Great Glen Fault and the Highland Boundary Fault. **(b)** Map showing how centres of intrusive activity (numbered) occur above proposed corresponding extensional lineamental intersections (also numbered).

To summarise: the NW-SE lineaments by their very nature are deep seated structures. When the crust is affected by younger through-going faults (due to external plate tectonics) we would expect blocks to be formed in the lower crust where lineaments are seated (Fig.10.15b & 10.16). The NW-SE faults (lineaments) are fundamentally located in the feldspar-rich, strong lower crust, and only move in the Caledonian by reactivation. The prediction is that they will dissipate displacements up (and down) across the

sandwiching weak zone(s) (mid- to upper crust and underlying mantle) (Fig. 10.15). The NE-SW Caledonian faults and shear zones on the other hand are contemporary trans-crustal structures created by contemporaneous far field plate tectonics. These structures occur throughout the crust, although they are probably not so important in the rheologically weaker parts. This suggests that the NE-SW structures are influential throughout the crust, but are most dominant in the upper cover sequence, whereas deformation (movements) on the deep crustal NW-SE faults diminishes upwards. This implies that as exhumation was occuring during the emplacement history, leading to the Earth's surface (free surface) being progressively lowered relative to the initial emplacement levels, the effective depth at which the NE-SW structures were the dominant control on magmatism was also lowered (Fig. 10.13).

This explains the pattern of emplacement styles relative to depth of crystallisation (Fig. 10.14). It also explains the more general features of lineaments, with activities and movements on these reactivated lower crustal structures only occuring in rocks above this by propagation of the original fault. If this propagation has to take place through weaker materials, the movements on these structures will diminish explaining the typical 'non-fault' nature of many lineaments within the cover. This is directly reflected in the emplacement styles of the granites within the SW Highlands which have crystallised at significantly different crustal depths. Thus granite emplacement mechanisms.may reflect, in addition to tectonic controls and proximity to the free surface, gross crustal structure and crustal rheology.

Model proposed

Five Caledonian granitic plutons in the SW Scottish Highlands show emplacement styles which vary according to depth of crystallisation. The plutons are associated with two types of major crustal structures: NE-SW steep, sinistral, transcurrent faults of Caledonian age and NW-SE steep, sinistral, lineamental faults which originated in the deep crust probably during the Proterozoic. Plutons are found at the intersection of these structures, and their shapes and internal deformation features are controlled by the relative intensity of movement on either structure, as well as by proximity to the (Earth's) free surface. Thus, at high crustal levels (< 6 km) ring dyking and ballooning combine with dominant displacements on the sinistral NE-SW Caledonian shear zones and faults, and only minor activity on the NW-SE structures. This produces plutons that are elongated NE-SW. Below this the influence of the NW-SE structures becomes more important, with at intermediate levels (approx. 6-8 km) approximate cancellation of the two respective strain

fields and the production of equant shaped plutons. At the deepest levels (> 8 km), activity of the NE-SW structures is minimal and influence of the NW-SE structures is dominant; the remoteness from the influence of the free surface being indicated by the absence of ring dyking and ballooning, and the presence of granite sheeted complexes.

I interpret the depth controlled influence of the two sets of major structures to reflect the primary vertical strength profile in the continental crust of this area. This suggests that the older NW-SE deeper structures were formed in the feldspar-rich mid- to lower crust and during Caledonian reactivation their displacements diminished upwards in the quartz dominated mid- to upper crust. The contemporaneous NE-SW Caledonian structures are transcrustal and so become relatively more important in the mid- to upper crust as the affect of the NW-SE faults diminishes. Combination of the two sets of structures in the mid- to lower crust high strength zone may generate large crustal blocks seperated by the faults together with upper and lower rheological detatchments; a zone which may correspond to the Lower Crustal Reflectivity Zone. Regional sinistral shear on the bounding Great Glen and Highland Boundary faults may concentrate deformation in these mid- to lower crustal rocks, where, by rotation of the crustal blocks, primary ascent and siting mechanisms are created.

CHAPTER 11

MECHANISMS OF SPACE CREATION DURING PLUTON CONSTRUCTION

11.1 INTRODUCTION

It is the aim of this Chapter, to present field data from the Argyll Suite, Scotland, in order to show not only how the interaction of tectonic-related and pluton expansion-related strain fields locally controlled pluton geometry and type of emplacement mechanisms operating, but also how the overall construction of a pluton at mid-crustal levels may have been controlled by the structural architecture and kinematic evolution of the lower crust.

11.2 TECTONIC CONTROLS DURING PLUTON EMPLACEMENT

It has been shown in Chapter 10 that these plutons have been emplaced into crust within which it is possible to distinguish tectonically induced strain fields established by the interaction of intersecting shear zones from strain fields caused by emplacement or arrival phenomena, principally *in situ* lateral expansion. In many cases the cause of the relative dominance of one of these controls is principally a function of depth of emplacement. This has led to the recognition of two distinct tectonically-induced strain fields: (i) strain fields imposed by NE-SW-trending shear zones and faults related to Caledonian transpressional collision and; (ii) strain fields associated with an intersecting set of NW-SE-trending pre-Caledonian crustal lineaments which were reactivated during Caledonian orogenesis. This fundamental distinction has led to the recognition that pluton

construction at relative depths of approximately 10 km or greater is dominantly controlled by NW-SE-trending structures, whereas pluton emplacement near to the free surface and up to approximately 6 km in depth is dominantly controlled by NE-SW-trending faults and shear zones.

Although a pluton constructed at mid-crustal levels (10 km or greater) has been shown to be dominantly controlled by NW-SE-trending structures, bodies emplaced at this crustal level may show considerable differences in the way they were constructed and the mechanisms by which space was created for them, e.g. Strath Ossian and Ballachulish. It is shown below, how the structural characteristics of the lower crust and its evolution may have controlled the type of emplacement at mid-crustal levels.

11.3 PLUTON CONSTRUCTION

For an account of field observations, analysis, and interpretations, including: (i) the distribution of intrusive component facies; (ii) the internal structural characteristics (e.g. fabric trajectories, fabric type, strain distribution); (iii) local emplacement phenomena; (iv) the overall geometrical form and; (v) the major controlling tectonic structure(s) during the construction of the Etive, Glencoe, Ben Nevis, Rannoch Moor, Ballachulish and Strath Ossian plutons, see Chapters 9 and 10. Some of this information is summarised below for each plutonic complex, together with new data which helps to explain how space was created during their construction.

11.3.1 The Strath Ossian complex: Summarised information from Chapters 6, 9 and 10 illustrating the dominant mechanisms operating to create space during its construction.

The Strath Ossian complex is markedly linear in shape (30 km x 6 km) and has crystallised at a depth in excess of 10 km (Key *et al.* 1993). Construction of the complex involved the interaction of the NW-SE-trending Strath Ossian lineament, which traverses the western flank of the pluton, with three NE-SW-trending Caledonian shear zones (Fig. 11.1). The Ballachulish-Corrieyairack shear zone bounds the complex to the north and the Ericht-Laidon shear zone essentially bounds it to the south. The Etive-Laggan shear zone runs through the centre of the complex.

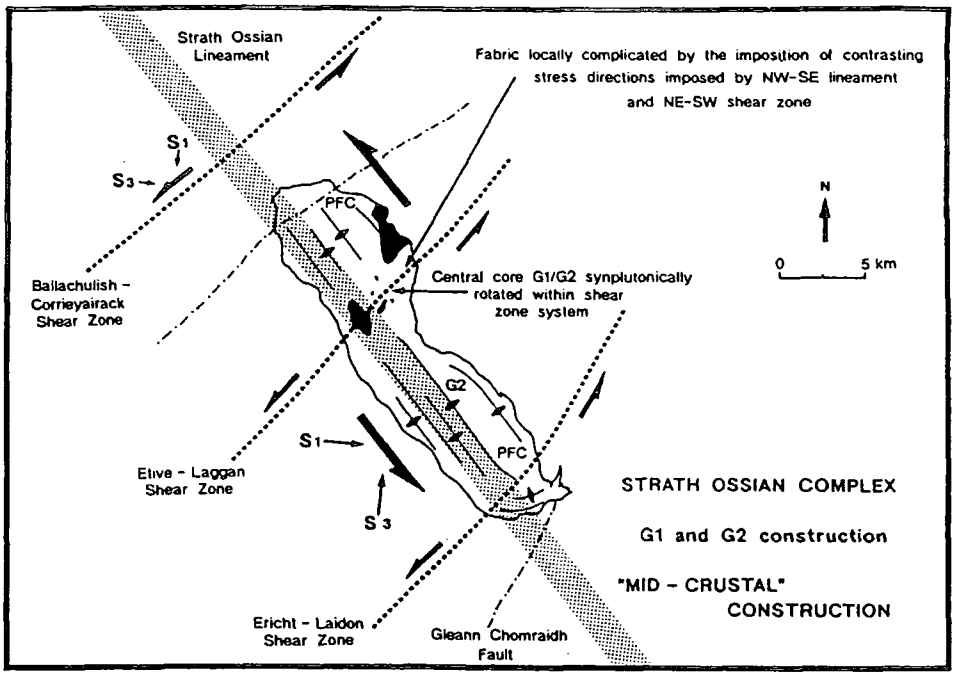

Fig. 11.1. Generalised model for the construction of G1 and G2 of the Strath Ossian complex at "mid-crustal" levels; showing strain fields associated with the Strath Ossian lineament were the dominant control and the NE-SW-trending and bisecting shear zones were of secondary importance.

During both intrusive episodes, i.e. the intrusion of G1/G2 and then the subsequent emplacement of G4, it is apparent that the Strath Ossian lineament was reactivated to form an actively transtensional shear zone. Combined with sinistral displacements along the Caledonian NE-SW shear zones, this interaction led to the development of a pull-apart structure allowing the intrusion of granite magma by a process of multiple sheeting. It was noted by Hinxman *et al.* (1923), that both the northern summit of Beinn Pharlagain, and to the north of the head of Loch Ossian, along the western contact of the pluton (Fig. 11.2), G2 forms a sheeted complex, enveloping large, undisturbed xenolithic units of schist, whose regional fabrics lie parallel to that of the schists outside the intrusion.

As shown by the model proposed by Jacques and Reavy (1994; see Ch. 9 & 10), part of the lower crust, the lower crustal reflectivity zone (LCRZ), could be regarded as a series of blocks or mega-augen bounded by intersecting ductile shear zones of high strain. Due to the geometrical relationships and transcurrent components of the Great Glen Fault and the Highland Boundary Fault systems, it is possible that within the lower crust, the pattern of structural interactions between these blocks could provide a locally developed 'extensional' regime; also influencing structures within the crust above. It is therefore possible that the structure and the kinematic evolution of the LCRZ initiated the

reactivation of the lineament and ultimately controlled the resultant development of this transcurrent shear zone. At mid-crustal levels, this may have resulted in the development of a transtensional pull-apart structure (Fig. 11.3). However, in other parts of the region, where the interaction of blocks causes an overall 'compressional' regime within the LCRZ (Fig. 11.3), the reactivation of structures such as the Cruachan lineament, may lead to the development of actively transpressional shear zones at mid-crustal levels. This may explain why, although the Ballachulish complex appears to have been constructed at a similar depth to that of the Strath Ossian complex, it clearly shows evidence of a different constructional process (see below); *in situ* expansion whilst undergoing sinistral transpression imposed by the strain fields associated with the Cruachan lineament (see Ch. 9). This may therefore demonstrate that the architecture and kinematics within the lower crust may influence the overall mechanism of pluton construction at mid-crustal levels.

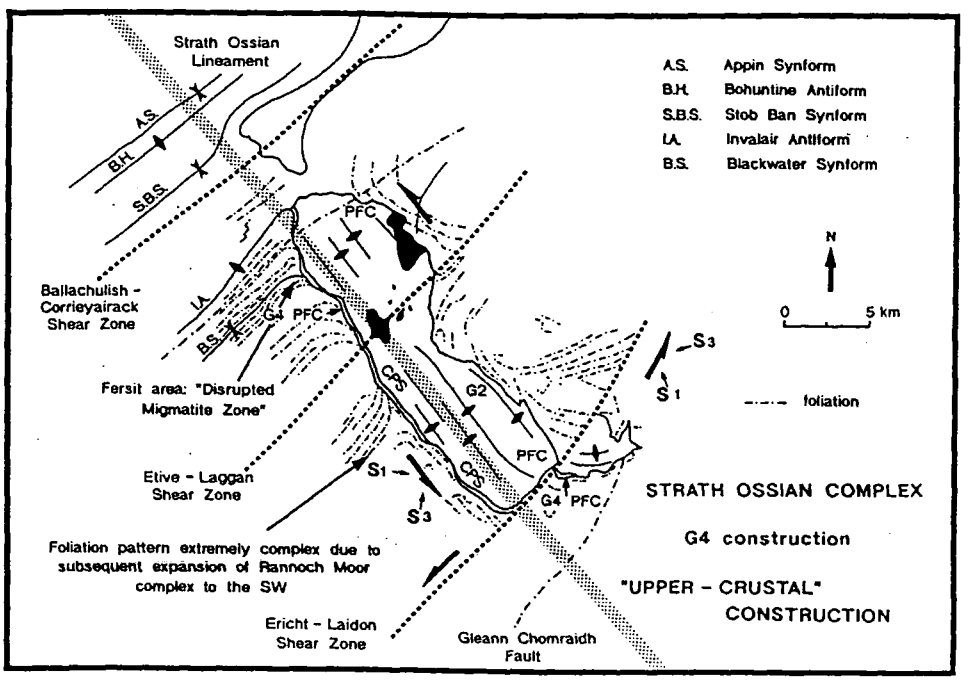

Fig. 11.2. Generalised model for the construction of G4 of the Strath Ossian complex at "upper crustal" levels; the distribution and structural features of G4 suggests that at this crustal level no one set of strain fields were obviously dominant, indicating the free surface was lowered and the lineament was re-activated. Shows the pattern of fold axial traces and regional foliations.

It is apparent, from above, that the major space creation process operating during the construction of the Strath Ossian complex, was the rigid translation of the adjacent country wall rocks. Another important mechanism facilitating the process of magma accommodation, was the ductile flow of the wall rocks during this pull-apart development.

Regional fold structures such as the axis of the Loch Laggan Antiform have been synplutonically rotated, from an original WSW-plunge to a steep southerly plunge as the eastern flank of the pluton is reached (Fig. 11.2; see Key *et al.* 1993). Fold axial traces and regional foliations on both the eastern and western flanks of the pluton have been synplutonically rotated (Fig. 11.2). This ductile deformation produced a partially concordant contact aureole, together with the possible development of slightly asymmetrical external triple points, identified by regional foliation patterns and variations of finite strain (Fig. 11.2). These narrow zones of constrictive strain may have developed as a consequence of the strain fields imposed by the *in situ* expansion of G1/G2 at the centre of the complex, combined with the interaction of tectonic-related strain fields associated with the transcurrent motion along the Strath Ossian lineament and the Etive-Laggan shear zone. These triple points were probably further enhanced during the major phase of pluton construction (G2). The rotational sense of these regional structures, from kilometre scale folds to planar fabrics, complies with the kinematic information obtained from the granitic rocks of the Strath Ossian complex; a major sinistral component along the lineament.

Ductile deformation of the wall rocks is clearly evident along the north-western flank of the pluton, within the Fersit area (Fig. 11.2). This zone, termed here the 'Disrupted Migmatite Zone', has very similar petrological and structural characteristics to that of the 'Chaotic Zone' of the Ballachulish complex (see Pattison & Harte 1988). The 'Disrupted Migmatite Zone' extends for approximately 2 km and is generally between 200-300 m wide. The zone is composed of Leven Schists, which have undergone extensive migmatisation and disruption, forming angular, semipelitic and psammitic xenoliths set in a matrix of semipelitic composition. The matrix possesses an intense ductile planar fabric, trending NW-SE parallel to the contact of the pluton. Most angular xenoliths are randomly orientated, whereas some rectilinear raft type units exhibit a preferred orientation, parallel to the ductile planar fabric developed within the matrix. A sinistral sense of rotation is implied for a large number of these xenoliths, inferred by the way the ductile planar fabric within the matrix has been deflected around them.

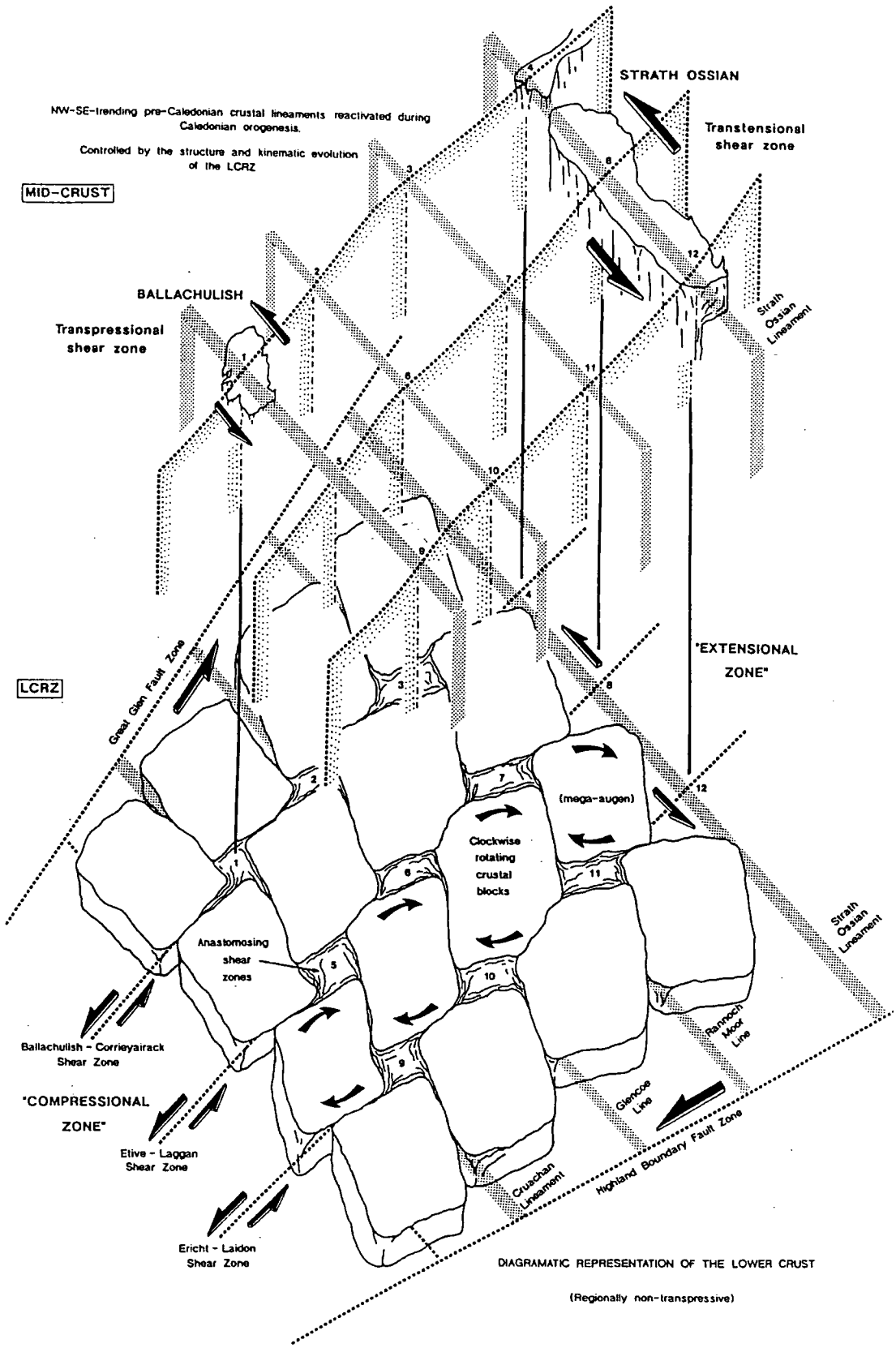

Fig. 11.3. A generalised model showing how the architecture and kinematic evolution of the LCRZ could have initiated and ultimately controlled the development of the Cruachan and Strath Ossian lineaments at mid-crustal levels.

In summary, the syn-kinematic rotation of regional structures and the development of ductile planar fabrics within the aureole of the Strath Ossian pluton, are consistent with sinistral transcurrent motion along the Strath Ossian lineament during its construction. The development of these structures indicates the importance of ductile flow type processes as a mechanism of space creation at mid-crustal levels. Estimates of bulk wall rock shortening, i.e. ductile flow type processes within the adjacent wall rocks, suggest up to 70-80 % may have been created by this process during the construction of the Strath Ossian pluton. The rest may have been accommodated by the rigid translation of the country rock by the bounding shear zone system. An interesting point, based on the synplutonic rotation of the regional fabrics is that it would appear that only a lateral displacement of 1.75-2.0 km would be needed along the Strath Ossian lineament to produce a NW-SE-trending linear shaped body approximately 120 km^2; with a larger translation component occurring along the NE-SE-trending Caledonian shear zone system.

The architectural development and subsequent deformation of the lower crust may control the type of constructional process operating during pluton development at mid-crustal depths. The localised development of an 'extensional' regime within the lower crust may have initiated and controlled the resultant transtensional component along the Strath Ossian lineament.

11.3.2 The Ballachulish complex: Summarised information from Chapters 9 and 10 illustrating the dominant mechanisms operating to create space during its construction.

The Ballachulish complex is sited at the intersection of the Cruachan lineament and the Ballachulish-Corrieyairack shear zone. It is possibly bounded to the north by the Great Glen Fault and to the south by the Allt Buidhe/Laggan Dam fault (Fig. 11.4). The Ballachulish-Corrieyairack shear zone offsets the margins of the pluton by approximately 0.8 km. When this is restored, the pluton occupies an area of approximately 8 km by 3 km and is elongated N-S. The major phases of the pluton crystallised at a slightly higher crustal level than Strath Ossian at approximately 10 km (Weiss & Troll 1989), which appears to be reflected in its constructional characteristics. It has been shown (Ch.'s 9 & 10) that the dominant controlling structure during its construction was the NW-SE-trending Cruachan lineament. The strain fields imposed by this structure caused the magma to intrude towards the N and S, into the direction of least tectonic strain (S_3). This is shown by the internal distribution of its intrusive phases (G1, G2, G4 and G5; Fig. 11.4). Although controlled essentially by a structure very similar to the NW-SE-trending Strath Ossian lineament, it has been shown that this reactivated structure did not act as a transtensional shear zone as in the development of the Strath Ossian pluton. The resultant

overall geometry is a sub-elliptical complex, compared to the well defined, linear shaped Strath Ossian complex. Internal distribution of intrusive facies, fabric types and trajectories, strain distribution and local emplacement phenomena suggests that the Ballachulish complex was essentially constructed by a process of localised *in situ* expansion whilst undergoing sinistral transpression. The process is clearly different from the one envisaged for the Strath Ossian complex (as mentioned above), in which the major component (G2), was intruded by a process of multiple sheeting into a transtensional regime (Fig.11.1). As mentioned previously, the difference in the way these lineaments have functioned, and the overall process by which these plutons were constructed at mid-crustal levels, may have been controlled by the deformational processes occurring at that time within the LCRZ of the lower crust (Fig. 11.3).

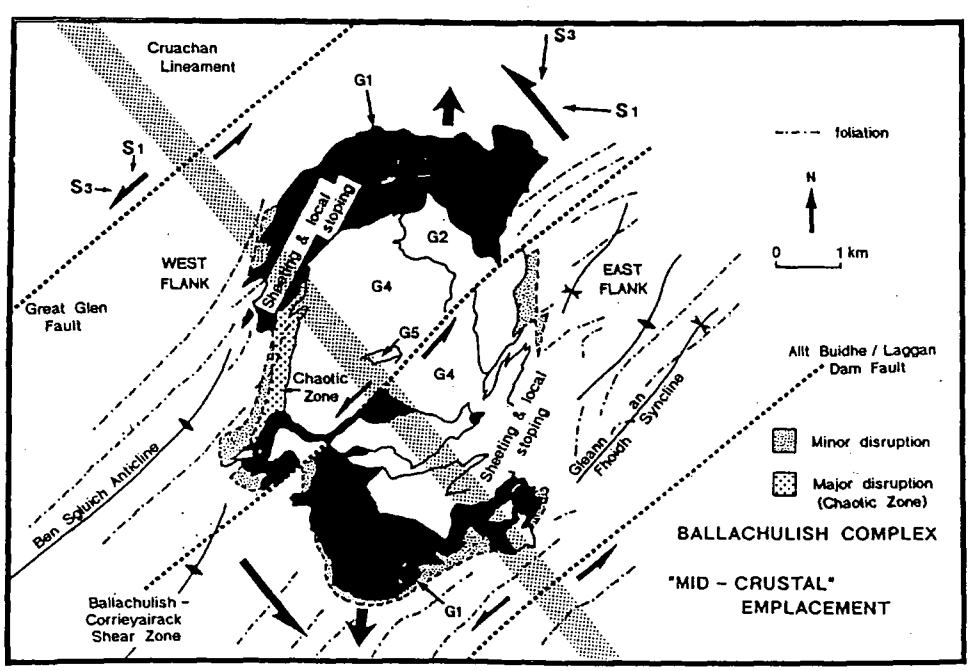

Fig. 11.4. Generalised model for the emplacement of the Ballachulish complex, at a "mid-crustal" depth at which the Cruachan lineament was the dominant controlling structure. Shows the occurrence of migmatitic pelitic rocks of the "Chaotic Zone" and zones of minor disruption (after Pattison & Harte 1988). Regional fold structures and foliations around the pluton are shown.

Reflecting the slightly higher level of crystallisation of the Ballachulish complex, compared to that of Strath Ossian, is the development of local emplacement phenomena, in the form of stoping and sheeting. These zones occur on the NW and SE sides of the complex (Fig. 11.4) and indicate a greater influence by the NE-SW shear zones. This is explained by the interaction of strain fields imposed by the Cruachan lineament and the less dominant NE-SW bounding shear zones (see Ch. 10). A transtensional zone is created by the combined effects of the imposed constriction on the pluton by S_1 of the lineament and WNW-ESE extension resulting from the shear zone motion. The resultant transtensional voids lie approximately parallel to S_1 of the NE-SW-trending bounding shear zones, allowing the magma to be intruded by a process of multiple sheeting into these 'tension gash' type structures (Fig. 11.5). It is envisaged that this extensional environment was further enhanced, due to the rate of tectonic deformation being greater than the rate of pluton expansion, as indicated by its markedly elongate sub-elliptical shape. This is in contrast with the development of the sheeting and stoping zones associated with the Rannoch Moor complex (see below).

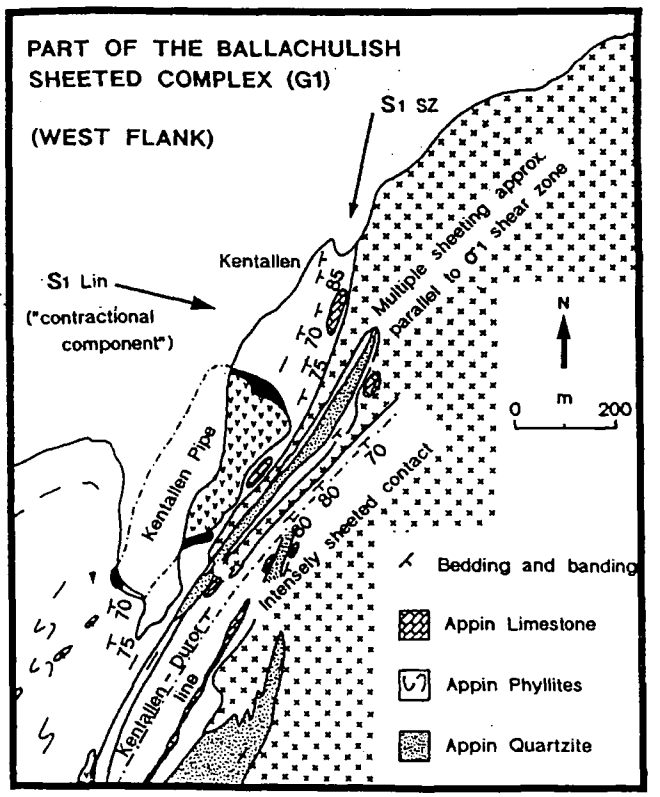

Fig. 11.5. Model of multiple sheeting into transtensional fractures created parallel to S_1 of the NE-SW-trending shear zones; northern zone of sheeting and stoping of the Ballachulish complex (modified after Bowes & Wright 1979).

Within the aureole of the Ballachulish complex, synplutonic ductile flow type processes are observed on a variety of scales, very similar to those developed on the east and west margins of the Strath Ossian pluton. On the western flank, it is apparent that fold axial traces, e.g. the Ben Sgluich Anticline and regional foliations have been rotated into sub-parallelism with the contact of the pluton (Fig. 11.4). Such relationships within the eastern aureole are unclear, however, partially concordant contacts are not uncommon. The resultant pattern developed appears to be consistent with that expected to be produced by the rotation and deflection of regional fabrics during expansion and synplutonic rotation of the complex (Fig. 11.4). As previously mentioned, a local zone of extensive migmatisation and disruption, known as the 'Chaotic Zone' (Pattison & Harte 1988), occurs within the aureole of the Ballachulish complex (Fig. 11.4). As with the 'Disrupted Migmatite Zone' of Strath Ossian, the zone is composed of semi-pelites and quartz-rich pelites of the Leven Schists and occurs on the western flank, adjacent to the pluton contact. The zone extends for approximately 2 km and is generally between 350-400 m wide. The petrological and structural characteristics of this zone, such as the development of an intense planar fabric within the matrix, parallel to the igneous contact, is essentially the same as that described for the 'Disrupted Migmatite Zone' of Strath Ossian (see above). On the eastern flank, and along parts of the southern margin of the Ballachulish pluton, small-scale local migmitisation has occurred within approximately 100 m of the igneous contact (Fig. 11.4). Migmatitic features and large scale disruption is absent and the zones are characterised by leucocratic segregations of quartz and K-feldspar. However, at the pluton contact, G1 has intruded the more competent layers of the wall rock, causing fragmentation. The resultant rock is a hybrid of partially digested pelitic xenoliths and quartz diorite (see Pattison & Harte 1988). Deformed incompetent layers (semi-pelites) exhibit internal, ductile flow structures. This migmatisation along the eastern and southern margins, has been attributed to localised partial remelting, in which the source of water was internal (Pattison & Harte 1988). Whereas within the 'Chaotic Zone', the lack of segregated leucosomes and restites and the presence of sharp contacts between the migmatites and quartz diorite, suggests that the melt did not segregate from the protolith (Pattison & Harte 1988). It is possible that an external source of water could have been derived via the Cruachan lineament, also explaining the development of the 'Disrupted Migmatite Zone' which occurs along the western flank of the Strath Ossian pluton where the Strath Ossian lineament traverses.

It is apparent from field evidence that the major mechanism operating to create space for the Ballachulish complex was clearly different from that operating during the construction of the Strath Ossian pluton. Although it is possible that the Cruachan lineament produced a significant component of space, with the combined effects of transcurrent motion along the bounding NE-SW shear zones (deduced by the ductile deformation experienced by the surrounding wall rocks) during the emplacement of the

Ballachulish pluton, geometrical considerations on the three-dimensional shape of the granitic body indicates space must have been predominantly achieved by a different process. It is likely that such a process involved the ductile deformation and uplift of the overlying country rock and the possible downward displacement of the pluton floor. It will be shown in the following discussions, on the Rannoch Moor, Ben Nevis, Etive and Glencoe complexes, that with decreasing depth of pluton crystallisation, the free surface becomes increasingly influential during their construction.

11.3.3 The Ben Nevis complex: Summarised information from Chapters 9 and 10 illustrating the dominant mechanisms operating to create space during its construction.

The Ben Nevis complex is possibly bounded to the north by the Great Glen Fault and to the south by the Allt-Buidhe/Laggan Dam Fault (Fig. 11.6). It is sited at the intersection of the Ballachulish-Corrieyairack shear zone and the possible trace of the Rannoch Moor line, which may be a minor NW-SE-trending structure; a possible synthetic splay developed between the Cruachan and Strath Ossian lineaments. It crystallised at approximately 1.5 Kb (pers. comm. P. E. Brown), indicating an apparent depth of approximately 5-6 km. Field observations indicate that the pluton was constructed by a process of *in situ* expansion, at a depth in which no one set of structures were obviously dominant (see Ch. 10). This is suggested by its overall equidimensional form and the lack of obvious local emplacement phenomena, such as sheeting and stoping. However, the N-S orientation of the long axes of individual facies, especially G4 and G5 (Fig. 11.6), may indicate that the Rannoch Moor line was of greater influence during its construction (however, see Ch. 9, sub-section 9.5.4).

The most striking feature of this pluton is the presence of a sub-circular mass, consisting of rhyolitic lavas and agglomerates, at the centre of the complex (Fig. 11.6). The country rock block is steep-sided and completely surrounded by G5. Field observations suggest that during construction the complex was sub-volcanic, influencing the free surface to some degree. Such interaction, possibly leading to the development of peripheral ring fault-type structures, as a consequence of pluton expansion-related strains causing roof doming and uplift. However, during periods of little or no magma input (possibly during the interval between subsequent major intrusive events) lithostatic pressure (Pl) of the roof zone may have exceeded the internal magmatic pressure (Pm) of the pluton, causing the downward displacement of the crustal block along such translatory structures; initially developed during pluton expansion. Such a process would lead to cauldron subsidence and the possible development of high level emplacement phenomena such as ring dykes (see below). It is envisaged that during such a period of Pl > Pm, part of the roof zone of the

Ben Nevis pluton subsided as a coherent block into the plutonic complex below, as with the *en bloc* or piston-like caldera collapse models of Clough and others (1909); Smith and Bailey (1968); and Lipman (1984). This resulted in G5 developing a chilled margin against the cooler roof block. Such situations may provide invaluable information on the way the roof zone was deformed and the resultant development of such features as bounding ring fractures and processes of cauldera collapse. Such studies can lead to the identification of structures produced by pluton expansion and associated emplacement phenomena; volcanotectonic faults (see Lipman 1976; Kokelaar 1992; and Branney & Kokelaar 1994), from purely regional tectonic faults and shear zones. As noted by Branney and Kokelaar (1994), it is likely that some regional tectonic stress is accommodated by such structures initiated by magma movement. During regional transpression, it is envisaged that these volcanotectonic structures may accommodate some of the resultant tectonic stress, causing roof uplift and the possible subsidence of the pluton floor, providing a major space creation mechanism during pluton construction (see below).

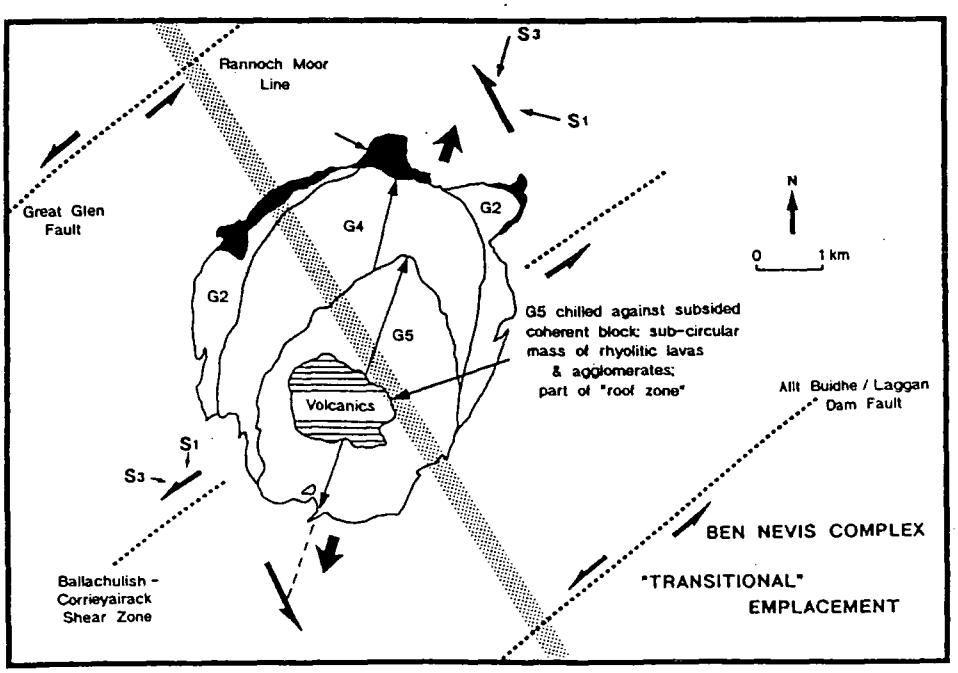

Fig. 11.6. Generalised model for the emplacement of the Ben Nevis complex.

11.3.4 The Rannoch Moor complex: Summarised information from Chapters 5, 9 and 10 illustrating the dominant mechanisms operating to create space during its construction.

The Rannoch Moor complex is bounded to the north and south by the Etive-Laggan shear zone and the Gleann Chomraidh fault and is sited at the intersection of the proposed Rannoch Moor line and the Ericht-Laidon shear zone (Fig. 11.7).

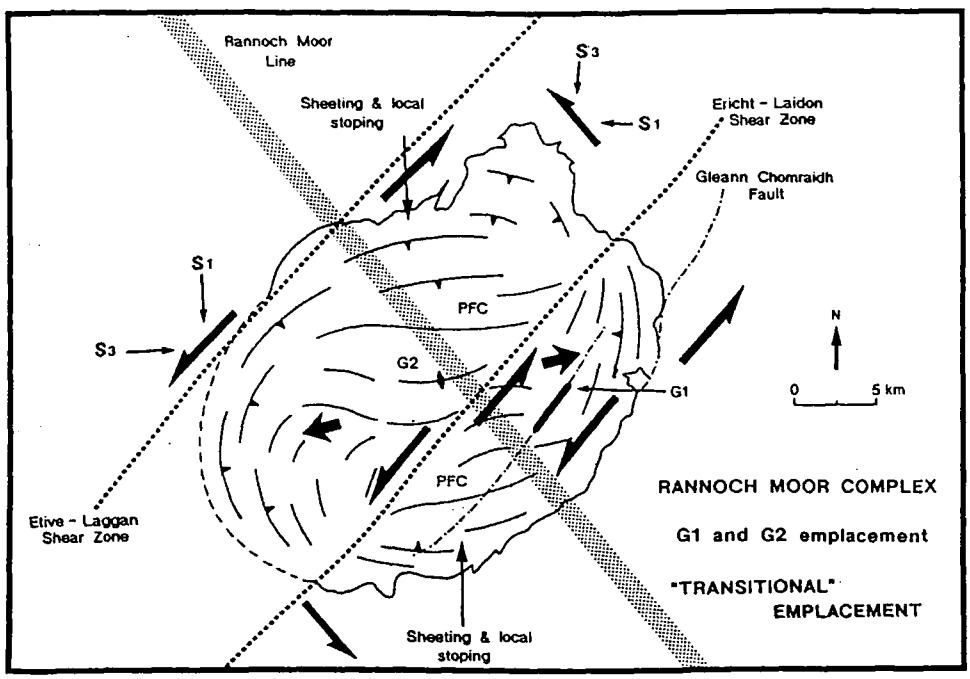

Fig. 11.7. Generalised model for the emplacement of G1 and G2 of the Rannoch Moor complex.

As with the Strath Ossian pluton, field evidence suggests that the complex was constructed in two distinct phases (G1, G2, and G4 & G5), in which the relative interaction of strain fields pertaining at that level of crystallisation were different in each case due to the relative level of the free surface. G1 and G2 were assembled principally under the influence of the NE-SW shear zones (Fig. 11.7), although there is evidence (see below) that the NW-SE-trending Rannoch Moor line exerted some effect at this level of crystallisation. As with the other elliptical/sub-elliptical plutons, i.e. Ballachulish and Ben Nevis, the major intrusive components (in the case of Rannoch Moor, G2 and G5) have been emplaced by a process of *in situ* lateral expansion, predominantly into the direction of least tectonic strain S_3 imposed by the dominant controlling structure(s). It is apparent from figures 11.7 and 11.8 that the dominant expansion direction of the intruding magma during the construction of the Rannoch Moor complex was approximately ESE and WNW, controlled by the NE-

SW shear zones. Within these regions, two sets of opposing strain fields are present (see Ch. 10); pluton expansion-related strains and the E-W orientated S_1 direction of the Rannoch Moor line. This resulted in the development of high flattening strains shown by highly strained enclaves and intense pseudoconcentric fabrics. Also within the adjacent wall rocks to these regions, a component of ductile shortening is clearly evident. Within both zones, the pluton margin has been essentially controlled by the bounding NE-SW-trending Etive-Laggan shear zone in the NW and the Gleann Chomraidh fault in the SE (Fig. 11.8).

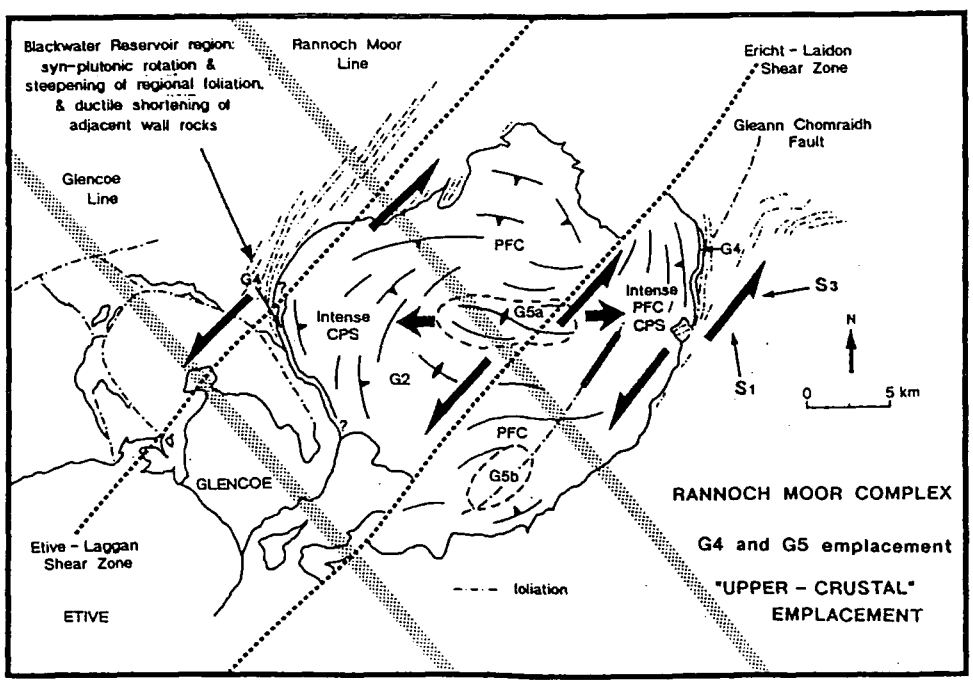

Fig. 11.8. Generalised model for the emplacement of G4 and G5 of the Rannoch Moor complex at "upper crustal" levels at which the NE-SW-trending Caledonian shear zones were the dominant controlling structures. Regional fabrics within the NW and SE of the complex are shown.

As described by Read (1956; 1961), in the south-eastern part of the complex, a 1000 m traverse from the faulted contact (Gleann Chomraidh fault) into the adjacent country rocks shows that the regional foliation has been synplutonically rotated and steepened towards the pluton margin (Fig. 11.8). Such features led Read (1956; 1961) to describe the pluton as exhibiting predominantly forceful characteristics, where significant ductile flow type processes have occurred within the contact aureole. As mentioned above, such processes have occurred within the wall rocks of the Strath Ossian and Ballachulish complexes,

suggesting that such ductile deformation of the surrounding country rock may provide a small but significant component of space creation during pluton construction at mid-crustal levels. However, at higher levels of pluton construction , e.g. Etive, Glencoe, such ductile processes are clearly of less magnitude, where instead brittle type deformational processes dominate, such as peripheral ring fault development (see below); explaining why such high level plutons have been described as being 'passive' or 'permitted' intrusives (Read 1956; 1961), although all the elliptical/sub-elliptical plutons within the Argyll Suite have been essentially constructed by a process of *in situ* lateral expansion during transcurrent shear. Ductile deformation of the wall rocks within the NW region of the complex, show similar characteristics and magnitudes of strain to that exhibited by the SE region. Within the western aureole, in the vicinity of Blackwater Reservoir, regional foliations and the trace of the NE-SW-trending fold structures, appear to have been synplutonically rotated into a NNE orientation forming a partly concordant contact aureole (Fig. 11.8 & 11.9). This ductile deformation has led to the development of a zone of approximately 600-800 m wide, the majority of which is composed of grey pelitic gneisses (Reservoir Schists). Following the contact of the pluton is a zone approximately 150-200 m wide of fine-grained quartzites (Reservoir Quartzite) and a banded psammitic gneiss with micaceous laminae (Reservoir Flags). Developed within the latter lithological unit are large, metre scale shear sense indicators in the form of σ- and δ-type structures (see Ch. 5, sub-section 5.6: Plates 5.27 & 5.28), kinematically consistent with a gross sinistral rotation of the complex during its expansion.

Such ductile deformational structures indicate that along the NW and SE external contacts of the pluton, sinistral transcurrent motion along the bounding NE-SW-trending shear zones was a significant process of space creation during pluton construction. This combined with the strains imposed by magma expansion, produced a component of shortening both internal and external to the plutons margin. It is envisaged that the transcurrent motion along the bisecting NE-SW shear zones was an additional space creation mechanism during the lateral expansion of the magma, causing the rigid, lateral displacement of the surrounding country rock. However, as with the Ballachulish and Ben Nevis plutons, the amount of space which could be achieved by the combined effects of laterally translating the wall rocks and by ductile flow type processes within their aureoles, would not produce by any means the space required to accommodate such volumes of magma within the crust. It is therefore likely that the major mechanism of space creation was actually achieved by the deformation and vertical translation of the overlying and/or underlying country rock, explaining why magnitudes of strain are relatively low around such plutons which have clearly been dominantly constructed by a process of *in situ* expansion. The presence of the bounding NE-SW shear zones, essentially forming the pluton contact in the NW and SE of the Rannoch Moor complex (Fig. 11.7 & 11.8), and its

moderately shallow depth of crystallisation, possibly around 4-6 km depth (see Jacques & Reavy 1995) suggests this complex was sub-volcanic. It is therefore possible that the free surface was influenced directly by the upward translation of the roof zone along peripherally developed ring fault type structures.

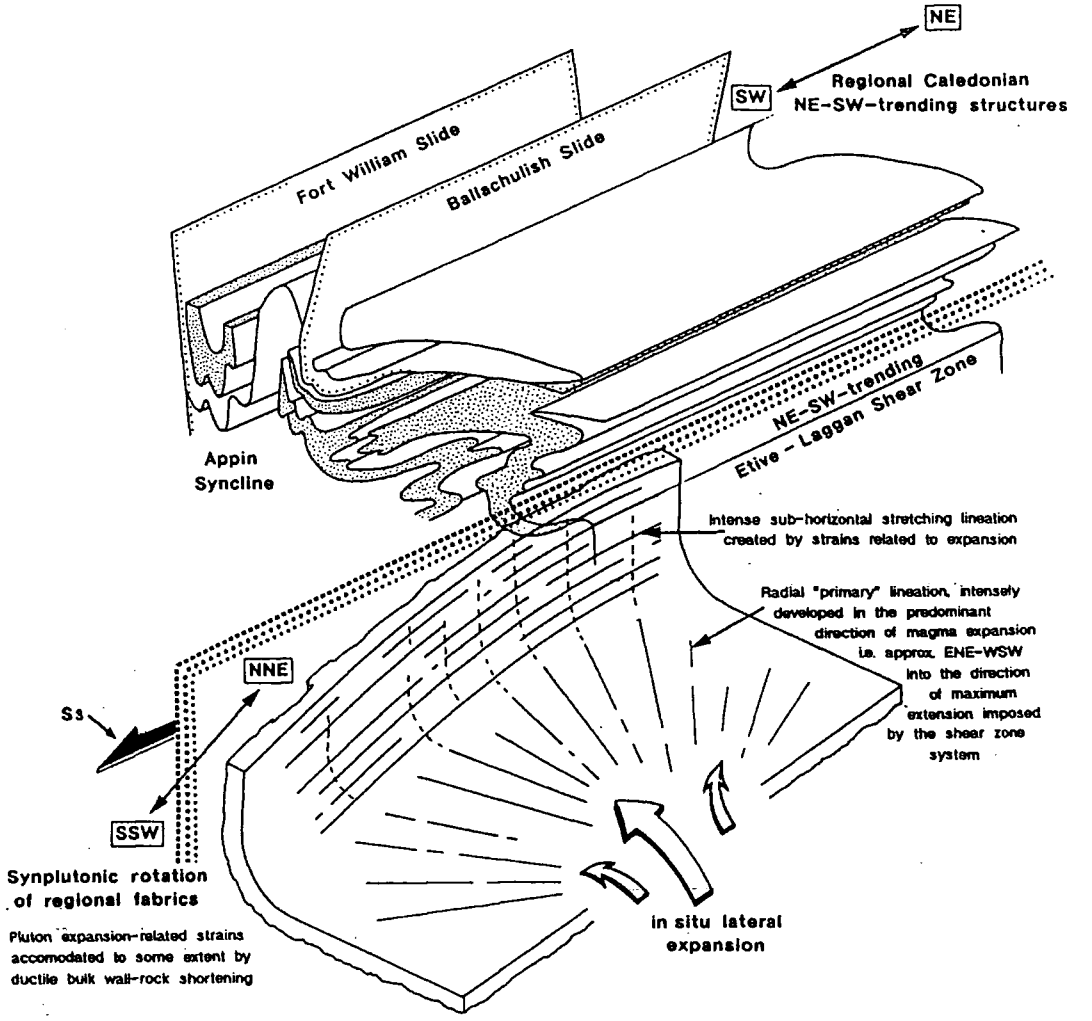

Fig. 11.9. Generalised model showing the development of primary sub-radial lineations and an overprinting sub-horizontal stretching lineation. A schematic cross-section (not to scale) projected above and below the present level of erosion, showing regional Caledonian NE-SW-trending fold structures and slides (following Bailey 1934, as revised by Treagus 1974) and the synplutonic rotation of regional fabrics within the Blackwater Reservoir region.

In the north and south of the complex, two zones of sheeting and stoping occur (Fig. 11.7), which are possibly attributable to the influence of the Rannoch Moor line during pluton construction. As already mentioned, such emplacement phenomena occurs within

the Ballachulish complex as a result of such interaction between strain fields imposed by regional tectonic structures with different orientations. The nature of the southern zone of the Rannoch Moor complex, has been previously addressed by Hinxman *et al.* (1923) and France (1971), both commenting on the intricate intrusion complex developed, in which the foliation of the larger xenolithic rafts can be traced without disturbance into the surrounding country rock. The zone is approximately 400-500 km wide from the 'main' pluton contact. In the Guala Moor region (Fig. 11.10), a large percentage of the granitic sheets are sub-parallel to the regional foliation within the *in situ*, psammitic screens, trending approximately NE-SW. It is envisaged that the interaction of strain fields imposed by the NE-SW shear zones and the NW-SE Rannoch Moor line, in which the principal stress directions (S_1) of both structures interacted at approximately 90° resulting in partial cancellation (see Ch. 10), producing a zone of low strain. Transcurrent motion along the bounding NE-SW shear zones, which were the dominant controlling structures at this depth of crystallisation, created an overall transtensional regime similar to that developed within the Ballachulish complex (Fig. 11.4). As shown by Figure 11. 10, the trend of the regional foliation of the *in situ* xenoliths and the granitic sheets have been rotated in a sigmoidal fashion, from a NE-SW orientation into sub-parallelism with the "main" pluton contact. The orientation and geometrical form of the granitic sheets suggests they represent transtensional fractures ('tension-gash' type structures) approximately parallel to S_1 of the NE-SW shear zones. During their emplacement they were progressively modified and subsequent sheets were reorientated as a consequence of pluton expansion and synplutonic rotation of the complex. Structural characteristics of the northern zone of sheeting and stoping (Fig. 11.7; Leum Uilleim and Carn Dearg (see Hinxman *et al.* 1923)) are very similar to that described for the southern zone and so the model proposed above to account for such localised emplacement phenomena appears to be the same. However, as shown by Figures 11.5 and 11.10, the emplacement and synplutonic rotation of granitic sheets during the construction and deformation of the Rannoch Moor and Ballachulish complexes appears to be somewhat different. This is attributed to the ratio of strain imposed by the interacting structures, and more importantly the rate of pluton expansion in relation to the rate of tectonic deformation being different for both complexes.

By the time G4 and G5 were assembled, the free surface had been lowered and the Rannoch Moor line had minimum influence (Fig. 11.8). Part of G4 forms along the contact between the Glencoe complex and the Rannoch Moor pluton, close to the bounding Etive-Laggan shear zone in the NW. It appears from Figure 11.8 that the emplacement of the Fault Intrusion, a high level emplacement phenomena associated with the Glencoe complex (see below), has removed a large part of the Rannoch Moor pluton. Wall rock deformation around the Fault Intrusion, within both G2 of Rannoch Moor and to the north within adjacent country rocks, is generally of low magnitude and sharp contacts are observed.

Such absence of deformation suggests that the 'missing' part of the Rannoch Moor complex was removed by brittle type processes, possibly involving such a mechanism as peripheral ring fault development, allowing roof uplift. This then subsequently led to cauldron subsidence forming the ring dyke complex of the Fault Intrusion, involving localised stoping (see below). G4 also occurs as a sheet-like body in the proximity of the bounding Gleann Chomraidh fault in the SE (Fig. 11.8). It is therefore envisaged that the controlling structures were the NE-SW shear zones at this crustal level. Displacement along the bounding structures created space for G4 at the outer margins of the crystallised G2. The major phase of G5 occurs at the centre of the complex and appears to have expanded towards the S_3 direction of the NE-SW shear zone system, enhancing strains within the adjacent G2 regions.

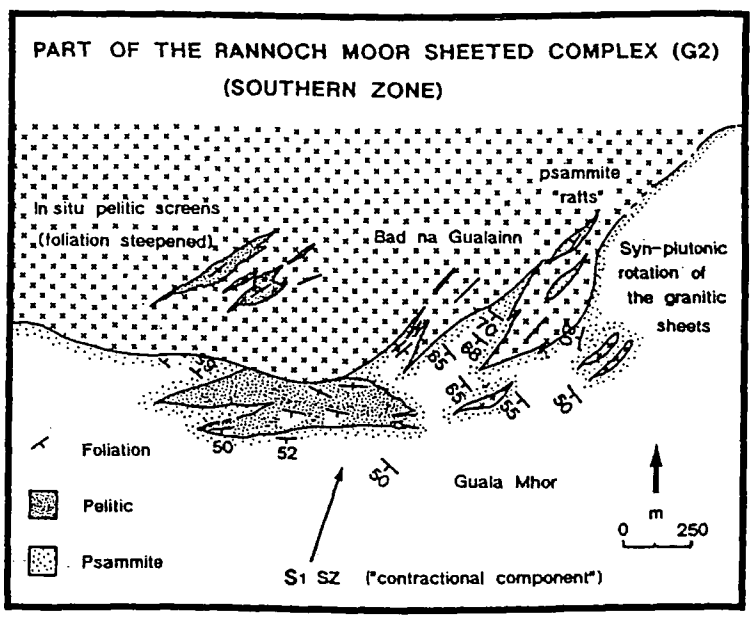

Fig. 11.10. Model of multiple sheeting into transtensional fractures created parallel to S_1 of the NE-SW shear zones; southern zone of sheeting and stoping of the Rannoch Moor complex (modified after France 1971).

Field observations suggest that the other elliptical/sub-elliptical plutons of the Argyll Suite, i.e. Ballachulish, Ben Nevis, Glencoe, and Etive, are exposed at a level of erosion which exhibits their upper to central parts of the granite body. It is believed that the Rannoch Moor complex however, represents a less common situation, where the erosion level exposes the lower portion of the pluton. This is based on direct field observations which include steeper dipping pseudoconcentric fabrics in the most outer parts of the pluton, to much more moderate dips towards the pluton centre; overall implying that

moving from the steep side walls of the pluton towards its centre, the floor must start to flatten out quite rapidly. Other evidence includes the development of bimodal fabrics, which have been generally preserved in zones of relatively low strain. These are interpreted as representing a situation where both a pseudoconcentric foliation and a 'primary' lineation has been preserved (Fig. 11.9). The lineation is sub-radial and generally becomes steeper in inclination towards the centre of the complex. The strongest lineations occur in two corresponding zones within the NW and SE of the complex and appear to represent the direction of magma movement from the ascent conduit and subsequent expansion into the direction of least tectonic stress (S_3). In higher strain zones, especially in the outer portions of the pluton, this 'primary' lineation is generally overprinted by a sub-horizontal stretching lineation associated with pluton expansion-related strains (Fig. 11.8 & 11.9).

In summary, bulk wall rock shortening by ductile flow type processes are clearly evident in the NE and SW of the complex. This has been confined to regions adjacent to the zones of high strain developed within G2 as a consequence of *in situ* lateral expansion into the direction of least tectonic stress (S_3) imposed during its construction. In the north and south of the complex, interaction of regional tectonic-related strain fields resulted in the development of a transtensional regime, allowing the intrusion of G2 into transtensional fractures orientated parallel to S_1 of the NE-SW shear zones, by a process of multiple sheeting. The Rannoch Moor complex represents crystallisation at a relatively higher crustal level than is seen at Strath Ossian and Ballachulish. This is possibly reflected in the relative importance of different space creation mechanisms operating during its construction, as ductile shortening within its aureole is of less magnitude and only occurs in localised zones. In the NW and SE, the pluton margin has been essentially peripherally bounded and controlled by major NE-SW shear zones, which possibly interacted with the free surface to produce a sub-volcanic complex similar to the Ben Nevis complex. It is envisaged that pluton expansion-related strains were dominantly accommodated along these regional tectonic structures and volcanotectonic faults developed within the overlying country rock, allowing space to be principally created by a process of roof uplift, possibly combined with the displacement of the pluton floor; explaining why the apparent total magnitude of strain within its aureole is remarkably low for a pluton which has dominantly been constructed by a forceful type process of *in situ* expansion.

11.3.5 The Etive complex: Summarised information from Chapters 3, 9 and 10 illustrating the dominant mechanisms operating to create space during its construction.

The Etive complex was emplaced at a relatively high crustal level of approximately 2-4 km (Droop & Treloar 1981) and can be shown to have been controlled by upper crustal

NE-SW-trending shear zones during its construction (Fig. 11.11). The complex is markedly elliptical (30 km x 15 km) with the long axis trending NE-SW. It is sited at the intersection of the Etive-Laggan shear zone and the Cruachan lineament. This elliptical pluton also shows clear evidence, that its major intrusive phases were constructed by a process of *in situ* expansion whilst undergoing sinistral transpression. Data indicates that the dominant expansion direction of the intruding magma for each major pulse (G2, G4 and G5) was approximately E-W, corresponding to the theoretical S_3 orientation of the strain ellipse established by the NE-SW shear zones (see Ch. 10).

Running through the adjacent wall rocks and in places partially bounding the pluton are the Allt Buidhe fault (a possible continuation of the Laggan Dam fault) in the NW, the Pass of Brander fault in the SW, and the Ericht-Laidon shear zone in the SE. An important feature of this complex is that the E, SE and SW margins of the pluton show clear evidence of peripheral ring fault development and associated high level emplacement phenomena (Quarry Intrusion; Ch. 7); indicating the free surface was influenced directly (Fig. 11.11).

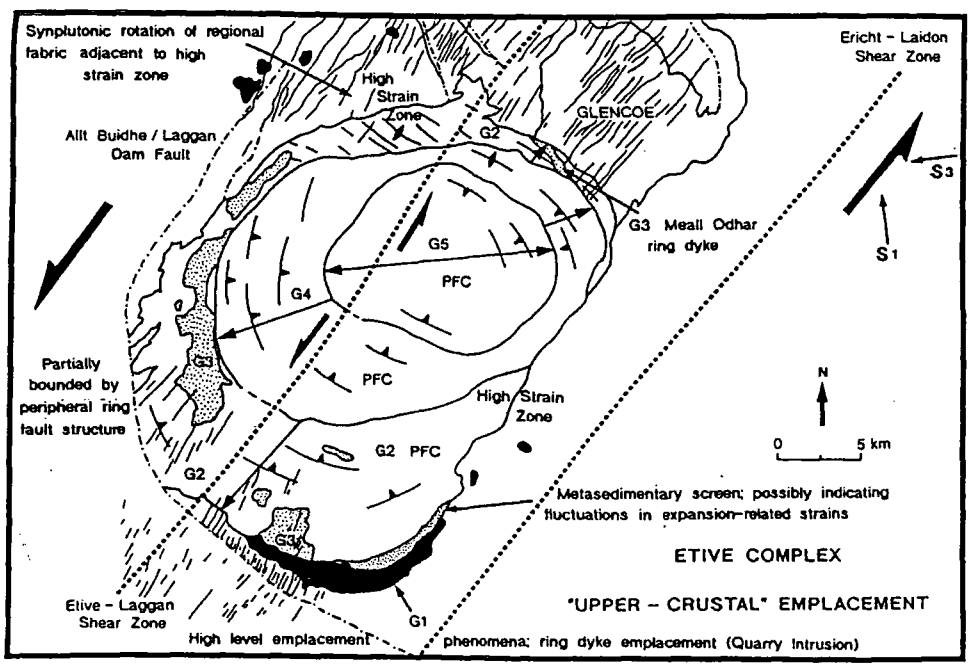

Fig. 11.11. Generalised model for the emplacement of the intrusive phases of the Etive complex at "upper crustal" levels at which the NE-SW-trending Caledonian shear zones were the dominant controlling structures.

Overall, country rock deformation around the pluton is remarkably low, except in the vicinity of the bounding ductile shear zones and in the wall rocks adjacent to the high

strain zones developed within G2, in the N and S of the complex (Fig. 11.11). In the latter zones, G2 has been locally modified, being overprinted by an intense crystal plastic strain (CPS) fabric (Hutton 1988). It is envisaged that the higher strains are developed within these G2 regions due to the combined effects of: (i) the angle between pluton expansion-related strains and the direction of S_1 of the NE-SW shear zones is low, resulting in opposing strain fields which accumulate to give higher strain magnitudes; (ii) the effect of subsequent expansion and synplutonic rotation of G4 and G5 (see Ch.'s 3 & 10). During this deformation, strain was also accommodated within the adjacent wall rocks by ductile flow type processes, reorientating regional fabrics to form a locallised partially concordant aureole. It should be noted that the magnitude of bulk rock shortening within these wall rocks does not appear to be as high as those observed within the aureoles of the sub-elliptical, Ballachulish and elliptical, Rannoch Moor complexes, which were constructed at deeper crustal levels. Also, unlike these mid-crustal plutons, regional structures within other parts of the aureole have generally not been deflected, producing sharp, discordant contacts.

It is envisaged that during the initial stages of pluton construction, expansion-related strains deformed the roof zone, leading to the development of peripheral ring faults which interacted with the Earth's surface. It is likely that during emplacement magma buoyancy and internal magmatic-related forces moved the resultant crustal block upwards towards the free surface ($Pl < Pm$), accommodated along the volcanotectonic faults developed. Such a process of transposition of a coherent block would provide a major component for space creation at upper crustal levels. However, during episodes of little or no magma input expansion-related strains may be exceeded by the lithostatic pressure of the crustal block ($Pl > Pm$), allowing the block to descend. Such an event could lead to cauldron subsidence, such as seen within the SW of the complex; the Quarry Intrusion (G1), which takes the form of a "partial ring dyke", intruded along the ring fault which downfaults metavolcanics against Dalradian country rock (Fig. 11.11). The emplacement of G3 within the complex also suggests that during pluton construction expansion-related strains may be reduced or completely removed, causing the complex as a whole to experience some degree of subsidence. This is shown by some of the upper G2 sheets which possess a concentric gentle dip suggesting some central downwarping during G3 emplacement. G3 takes the form of flat-lying sheets resting on and cross-cutting the upper parts of G2 (Fig. 11.11). This subsidence also initiated the intrusion of a partial ring dyke of G3 in the NE along the complexes northeastern margin (Fig. 11.11; Meall Odhar ring dyke (Anderson 1937)). A large number of G3 sheets, of moderate to steep, inwardly dipping attitudes, cross-cut G2 and parts of the surrounding country rock. These may have been intruded during periods of high magmatic pressure, producing cone sheet type structures. Their intrusive relationship to the flat-lying sheets (G3) is complex, as they clearly post-date an earlier phase and have

themselves been subsequently cross-cut by a later intrusive event of sub-horizontal sheets. They have varying attitudes and cross-cut one another. Such relationships may indicate that during the period of G3 emplacement, there were a number of significant fluctuations between positive and negative buoyancy-related forces within the pluton body and applied to its overlying country rocks. It therefore appears likely that during pluton construction, the magnitude of pluton expansion-related strains may vary quite considerably during subsequent intrusive events. For example, after the emplacement of G3 within the Etive complex, it is envisaged that forces imposed primarily by magma buoyancy, induced by the ascent of G4 and possibly G5, increased greatly as porphyritic and microdioritic material proceeded these major intrusive phases. This probably had the effect of updoming the upper country rock cap and creating an overall transtensional environment, both within the igneous complex as a whole and within the adjacent country rocks. Subsequent intrusion of the 'proceeding' magma into this environment led to the development of the Etive Dyke Swarm (Ch. 8) (Fig. 11.11). Other evidence for sequential uplift and subsidence, is apparent within the SW of the Etive complex. Here it is possible that after the emplacement of the Quarry Intrusion, produced as a result of cauldron subsidence, subsequent intrusion of G2 into the complex created high expansion-related strains, uplifting the cauldron block back towards the free surface. Part of the block remains as a relict metasedimentary screen between the "partial ring dyke" and G2 (Fig. 11.11).

In summary, the adjacent wall rocks around large parts of the Etive pluton show in general extremely low amounts of bulk rock shortening, compared to plutons constructed at mid-crustal levels in which ductile flow type processes are clearly evident within their aureoles. Exceptions to this occur where the bounding NE-SW shear zones run through the adjacent wall rocks, in places partially bounding the pluton and within the aureole in contact with the high strain zones developed in G2. Within these zones, the combined effects of pluton expansion and synplutonic rotation of the complex during non-coaxial deformation, resulted in the syn-kinematic rotation of regional foliations and the possible reorientation of fabrics such as bedding. It is therefore apparent from the general lack of deformation to the adjacent wall rocks that a major mechanism for space creation is needed to account for pluton construction at upper-crustal levels. From the field evidence presented above, it is clearly evident that the interaction with the Earth's surface was a crucial process during the development of the complex. It is envisaged that pluton expansion-related strains from the *in situ* expansion of the major intrusive phases (G2, G4 and G5) were accommodated to a large extent by vertical uplift and deformation of the roof zone. Transposition of the overlying crust being accommodated along the peripheral ring faults probably developed during the initial stages of pluton construction. It is conceivable that fluctuations in magmatic pressure during the emplacement of the Etive complex, may account for a number of different emplacement phenomena, developed throughout its

history. These include: (i) high level "ring dyke formation" associated with cauldron subsidence, i.e. the Quarry Intrusion; (ii) central downwarping of the complex leading to the intrusion of flat-lying granitic sheets (G3), forming a marginal facies at the top of the pluton; (iii) the intrusion of the Meall Odhar ring dyke (G3), during an episode of reduced magmatic pressure which probably coincided with the central downwarping event; (iv) cone sheet type structures (G3); (v) increased magma buoyancy forces induced by the ascent of G4 and probably G5, could have created a transtensional environment within the complex and the overlying country rocks, resulting in the intrusion of the Etive Dyke Swarm.

11.3.6 Glencoe complex: Summarised information from Chapters 4, 9 and 10 illustrating the dominant mechanisms operating to create space during its construction.

The Glencoe complex was emplaced at a relatively high crustal level (2-4 km) and shows clear structural evidence that it interacted with the free surface during emplacement. The Glencoe pluton is situated at the intersection of the Etive-Laggan shear zone and the possible Glencoe line (Fig. 11.12).

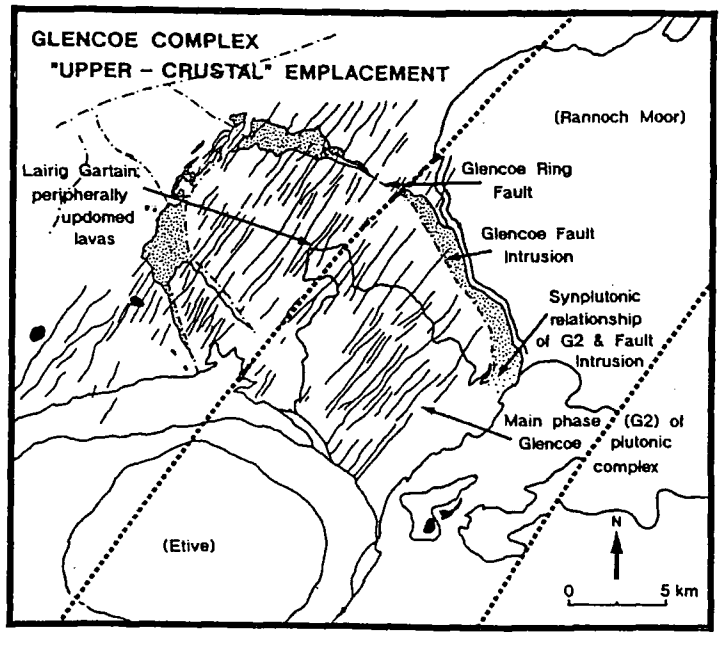

Fig. 11.12. Map of the Glencoe plutonic complex and associated high level Glencoe Fault Intrusion. Distribution of the Etive Dyke Swarm is also shown.

Above the pluton, cauldron subsidence occurred which allowed the emplacement of the Fault Intrusion along outer ring faults and was followed by the development of the cauldron caldera. Within the SE of the complex (Fig. 11.12), along the River Ba, synplutonic sheeting of the main phase of the pluton (G2) and tonalitic material of the Fault Intrusion is clearly visible. This indicates that the development of this high level emplacement phenomena must have occurred simultaneously with the main phase of pluton construction. Fabric and strain analysis over much of the Glencoe pluton suggests that emplacement took place by a process of *in situ* lateral expansion; largely complicated by expansion-related strains imposed by the adjacent Etive complex. In the extreme NW within Lairig Gartain (Fig. 11.12), fabrics have been almost unaffected by this deformation. The orientation of the PFC fabric may represent the preservation of a situation where magma is emerging from an ascent conduit and being fed outwards, predominantly into the direction of least tectonic strain (S_3) imposed by the NE-SW shear zones which dominate at this crustal level. The upper surface of G2 at this locality appears to have a steeply domed form (Bailey & Maufe 1916) and the peripheral exposures of Old Red Sandstone Lorne Lava Suite around this zone show evidence of updoming, possibly reflecting roof deformation by strains related to expansion.

The field observations above suggest that during construction of the plutonic complex, strains associated with expansion caused roof updoming and brittle ring fault development. Space was created for the intrusion of G2 by the upward translation of the resultant crustal block towards the free surface. During a period of reduced magmatic pressure, the block subsided (Pl > Pm), leading to the emplacement of the Fault Intrusion along parts of the peripheral ring fault structure.

11.4 DEPTH OF GRANITE INTRUSION

As seen within the Argyll region, a large number of granitic plutons and associated minor intrusive bodies are now exposed at the present level of erosion. An important point is that these intrusives not only represent a range of ages, but also represent crystallisation at significantly different relative depths, e.g. Strath Ossian approx. 10 km; Etive approx. 4 km and interaction with the free surface. This means that during Caledonian magmatism the level of crystallisation for subsequent intrusive events was approximately the same throughout this region. As pointed out by Leake (1990) and Leake and Cobbing (1993) for

Caledonian granites throughout the British Isles, this level of crystallisation and their subsequent exposure appears to be an unlikely coincidence. They also make the point that geophysical evidence suggests that any unexposed granitic bodies are generally concentrated near to the free surface, within approximately 3 km of the present land surface. They also comment that the lower parts of granites are rarely exposed (an exception being Rannoch Moor; this study) and the majority of plutons which can be seen at the current level of erosion generally represent the upper portion or roof zone of the complex. Examples of direct field evidence which can be used to identify the proximity of a roof zone and may indicate the fundamental processes operating in creating space for pluton construction, include:

(i) peripheral exposures of updomed country rock e.g. Lairig Gartain, Glencoe complex, indicating deformation of the roof zone by expansion-related strains;

(ii) xenolithic rafts in which their foliation can be traced without disturbance into the surrounding country rock, suggesting these may represent roof pendants e.g. existence of country rock xenoliths or 'ghost statigraphy' in the Main Donegal Granite (Pitcher & Read 1959). The lack of deformation to these *in situ* 'raft trains' indicates a process of pluton construction in which the roof zone was essentially unaffected by expansion-related strains. It is therefore probable that such construction would involve the lateral displacement and deformation of the adjacent wall rocks, allowing the resultant transtensional zone to be infilled by a process as multiple sheeting. Such a constructional process has been proposed for the Main Donegal Granite (Hutton 1982; 1992) and a similar process is envisaged for the Strath Ossian complex;

(iii) sub-horizontal marginal facies, which clearly cross-cut and rest upon earlier intrusive phases, e.g. Meall Odhar facies (G3) of the Etive complex. Such intrusive behaviour may indicate the prevailing, internal stress conditions during that particular time of pluton construction;

(iv) interaction with the free surface, forming high level emplacement phenomena such as ring dykes, e.g. the Fault Intrusion of the Glencoe complex, the Quarry Intrusion of the Etive complex. Volcanotectonic faults associated with such intrusive phenomena, may have been developed during the initial stages of pluton expansion, providing a mechanism for space creation by roof uplift along such translatory structures;

(v) fabric orientation, type of strain and its intensity.

The distribution of Caledonian granites raises the questions, why has granitic crystallisation been concentrated at a particular level within the crust and why are the majority of these intrusive bodies exposed near to or at the present land surface? Why ascending magma should stop at a particular level and not continue to the free surface has been questioned by a number of workers, e.g. Pollard and Holzhausen (1979) and has been

recently addressed by Brown (1992), in which he details the current theories for this phenomena. These include:

(i) ascent being halted at the brittle-ductile transition. This seems unlikely, as granitic complexes throughout the world show evidence that they have intruded into the continental crust at a range of depths, typically from 3-12 km. This therefore indicates that the position of the free surface has obviously changed. This change in thickness of the continental crust would generally have the effect of changing the relative position of the brittle-ductile zone and thus crystallisation would not occur at one particular level;

(ii) granitic magma exploiting horizontal décollements within the crust. Within the Argyll region, for example, major sub-horizontal anisotropies do occur such as the low angle parts of slides which, in theory, could be utilised as detachment surfaces. Although it is possible within this region that such structures could be exploited, it seems unlikely that these have fundamentally controlled the level of emplacement, as there are many plutonic complexes throughout the British Isles that have crystallised at the same relative position within the crust and are clearly not associated with such structural features. However, it is possible that other types of décollement have been exploited, such as lithological contacts related to stratigraphy, etc.;

(iii) pluton construction occurring at a level of neutral buoyancy (LNB). Physical constraints determining the level to which magma will rise within the crust has been addressed by Lister and Kerr (1991), who conclude that local density differences within the crust primarily controls the height to which magma will ascend and pluton construction will occur. They have calculated that there will be a small overshoot, in the order of a few kms, beyond the magma's LNB. They also suggest that it is likely that once the magma has reached this LNB it will accumulate and form lateral dykes and sills along this horizon, driven laterally away from the site of magma ascent by its own buoyancy forces. Such a process may well tend to 'concentrate' granitic magma within a particular part of the continental crust, where the magma may laterally intrude itself along any favourable décollements.

11.5 PLUTON GEOMETRY

In order to obtain an understanding of the processes operating to create space during pluton construction, it is obviously important to consider the resultant geometrical form of these granitic bodies. Numerical modelling by Emerman and Marrett (1990) has shown that sheet-like forms are most preferred for typical granitic viscosities. This complies with field evidence from the Argyll region, in which a large number of the plutons with elliptical/sub-elliptical plan shapes appear to have undergone lateral expansion, possibly forming relatively thin, flat lying bodies (Fig. 11.13). Such evidence includes flat-lying sheets resting upon steeply inclined sheets of earlier intrusive facies (e.g. Etive) at the top of the complex, and fabric inclination as seen within the Rannoch Moor pluton, indicating that as you move from the side walls of the pluton towards its centre the floor shallows rapidly. It is further envisaged that with an applied tectonic strain field this lateral migration of magma will be predominantly directed into the region of least principal stress of a crust undergoing non-coaxial deformation.

Further evidence that many plutons may be laterally extensive is given by detailed geophysical surveys (e.g. Hipkin & Hussain 1983) carried out across the British Isles. These show that many topographical features are largely compensated by lateral density variations within or below the crust. A crude calculation of the buoyancy effects of the granites in the Grampian Highlands, suggests this may support their high elevation and lateral extent, making them an important contribution to the isostatic balance of the crust during and after their emplacement into a region undergoing intense crustal thickening.

It is therefore conceivable that many granitic plutons throughout the British Isles are laterally extensive and more importantly limited in vertical thickness. Recently Brown (1992) has highlighted this phenomena, giving examples of thin, tabular shaped plutons, in which their lateral dimensions far exceed their vertical thickness. He quotes examples in which geophysical data was used in order to establish the three-dimensional form of plutons from south-central Maine (Sweeney 1975, 1976), northern New England (Neilson *et al.* 1976; Hodge *et al.* 1982) and NW France (Vigneresse 1988, 1990).

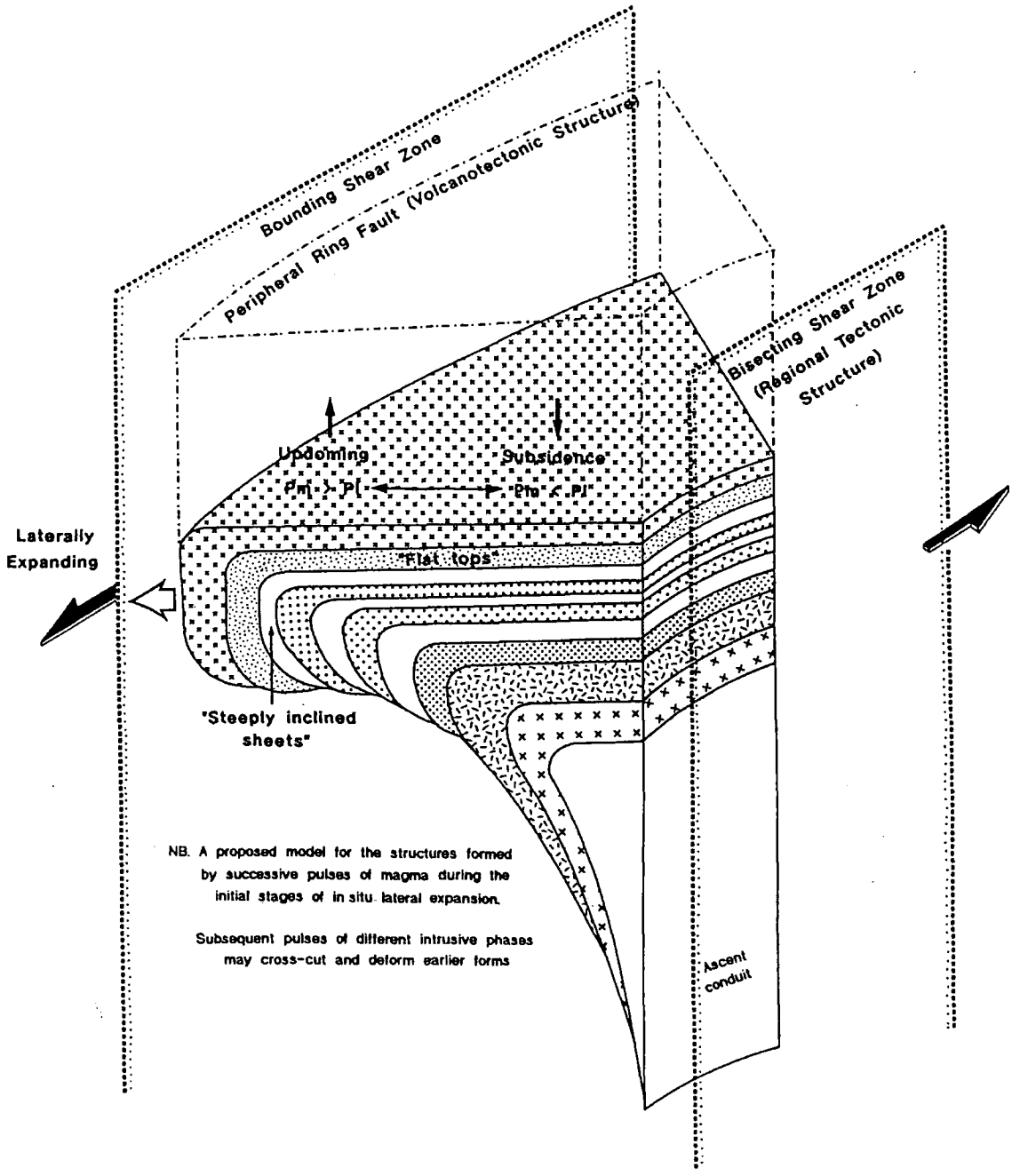

Fig. 11.13. A generalised model showing the development of sub-horizontal and steeply inclined sheets during the initial stages of *in situ* lateral expansion. Regional tectonic and volcanotectonic structures are shown.

	Emplacement mechanism	Approximate depth of emplacement	% of bulk wall rock shortening
Strath Ossian	Multiple sheeting within a transtensional shear zone	10-11 km	70(5)-80(5) %
Ballachulish	*In situ* expansion	9-10 km	35-45 %
Rannoch Moor	*In situ* expansion	5-6 km	8-20 %
Etive	*In situ* expansion	2-4 km	4-16 %

The maximum value determined for any one part of the aureole is given, which is generally considerably lower around the rest of the pluton.

Table 11.1. Estimates of bulk wall rock shortening, i.e. ductile flow type processes within the adajcent wall rocks, are presented for some of the plutons under discussion:

Table 11.1 shows that with decreasing depth of pluton crystallisation, space creation by ductile flow type processes is dramatically reduced. As described above, field observations suggest that with decreasing depth the surface becomes increasingly influential, probably providing a major component for space creation.

11.6 SPACE CREATION FOR PLUTON CONSTRUCTION

Recently Paterson and Fowler (1993a) have considered a number of important issues regarding the viability and importance of different mechanisms for obtaining space for pluton construction. They use the term 'material transfer', sub-dividing it into 'near-field' and 'far-field' mechanisms. The former covers processes which are confined to the structural aureole of the pluton and are concerned with moving country rock material away from the immediate path of the intruding magma. Such processes include ductile flow and rigid translation along faults, as seen within the Argyll Suite. The reassessment of the importance of ductile flow type processes has been investigated by the above authors, who have concluded that previous estimates by other workers of bulk rock shortening for a

number of plutons throughout the world have been considerably overestimated. Paterson and Fowler (1993a) regard a value of approximately 25% or less to be a more realistic average value for local space created by wall rock flow. This complies with the observed estimates throughout the aureoles of the elliptical plutons of the Argyll Suite, described above. If this is the case, it clearly shows the need for other space creation mechanisms. This leads to the latter term, 'far-field material transfer', which covers processes in which material is transported away from the vicinity of pluton construction towards the Earth's surface or back towards the region of granite petrogenesis. At mid-crustal levels this is probably achieved by ductile movements along major bounding shear zones and the deformation of the roof zone and/or pluton floor (e.g. Strath Ossian, Ballachulish), and at upper crustal levels by more brittle translatory mechanisms along such structures as ring faults (e.g. Etive, Glencoe). The latter type structures would influence the free surface directly leading to the initiation and development of a crustal block which would represent the upper crustal expression of far-field material transfer from an expanding pluton below. This in turn could lead to such emplacement phenomena as cone sheet and ring dyke formation. It is apparent from direct field observations and geometrical considerations on the construction of the plutons within the Argyll Suite, that there are fundamental differences in the way space has been created for plutons at mid-crustal levels, compared to those constructed at higher crustal levels, which have clearly interacted with the free surface.

11.6.1 Pluton construction at high crustal levels

In the Argyll Suite, the plutons which have been emplaced at relatively high crustal levels (approximately 2-6 km) are in places peripherally bounded by ring fault structures and show evidence of their association with cauldron subsidence, e.g. synplutonic relationships between the emplacement of the high level ring dyke structures of the Glencoe Fault Intrusion and the Glencoe plutonic complex. Within the Argyll region, field observations and geometrical considerations on creating space for pluton construction at these crustal levels could suggest that the dominant mechanism for far-field material transfer was achieved by roof uplift. Vertical translation being accommodated along the major bounding NE-SW-trending regional tectonic faults and shear zones which partially bound the plutons and the contemporaneous development of volcanotectonic structures, such as peripheral ring faults. As described above, the Glencoe complex affords the best example, with clear syn-magmatic and overlapping intrusive relationships between the main phases of the pluton and the higher level emplacement phenomena of the Fault Intrusion.

For the Argyll Suite the following scenario may be envisaged for pluton construction at relatively high crustal levels: (i) ascending magma stops and laterally migrates along a "zone" of neutral buoyancy (LNB), possibly exploiting localised sub-horizontal décollements; (ii) a laterally extensive sill-like body forms, essentially bounded by NE-SW shear zones/faults; (iii) magma undergoes *in situ* lateral expansion predominantly into the direction of least tectonic strain (S_3) imposed on the complex; (iv) pluton expansion-related strains cause roof updoming, (e.g. Lairig Gartain, Glencoe complex) and possible pluton floor subsidence towards the source region (Fig. 11.14a); (v) continued expansion initiates the development of volcanotectonic faults such as peripheral ring fault type structures which interact with the free surface, e.g. Ring Fault of Glencoe; (vi) crustal block above the pluton is driven upwards by buoyancy driven forces; (vii) during episodes of little or no magma input lithostatic pressure of the crustal block may exceed magmatic pressure ($Pl > Pm$)
allowing the block to descend (Fig. 11.14b). This may lead to classic cauldron subsidence in which high level emplacement phenomena, such as ring dykes are produced, e.g. Etive Quarry Intrusion, and the Glencoe Fault Intrusion. During these episodes of reduced magmatic pressure the complex as a whole may experience some degree of subsidence, e.g. Meall Odhar ring dyke and horizontal sheets of G3 within the Etive complex.

The field evidence above suggests that during pluton construction at high crustal levels, the combination of roof updoming, brittle fault development, and subsequent roof uplift provide a major component for space creation. Pluton expansion-related strains are therefore to a large extent accommodated by vertical uplift and deformation of the overlying country rock, explaining why the overall country rock deformation around such plutons appears to be extremely low. As stated by Paterson and Fowler (1993) more detail is needed to determine the amount and type of deformation to the roof zone of plutonic complexes. They have quoted several studies, e.g. Buddington (1959); Hopson and Dellinger (1987), in which the nature of the contact aureole forming the roof zone, differed considerably from the side walls of the pluton.

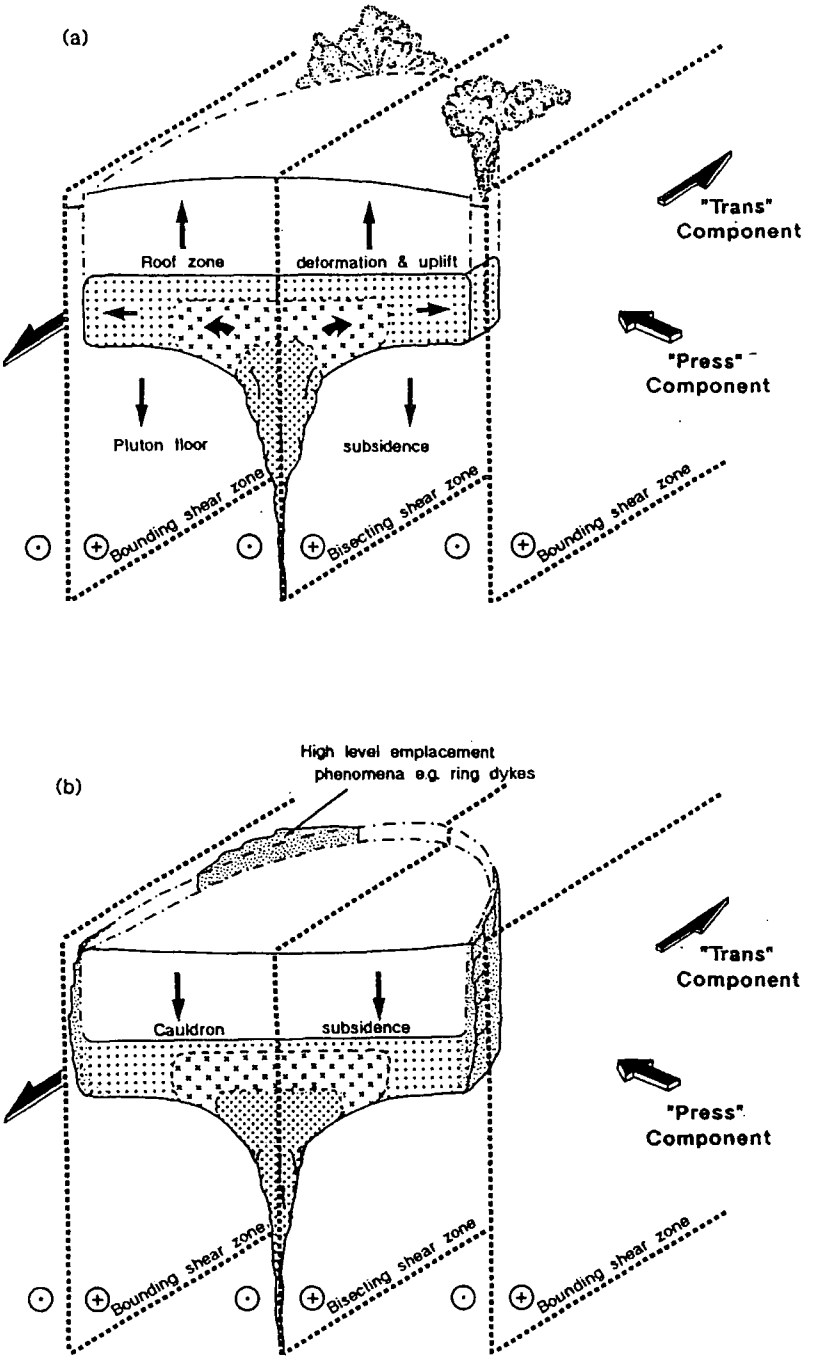

Fig. 11.14. (a) Generalised model showing that the major component of space creation during *in situ* lateral expansion of an elliptical pluton is probably achieved by roof deformation and uplift, and/or pluton floor subsidence. (b) Generalised model for the intrusion of high level emplacement phenomena and caldera development.

11.6.2 Pluton construction at mid-crustal levels

A somewhat different situation is observed within the relatively deeper constructed granites of the Argyll Suite. These mid-crustal plutons, such as the Strath Ossian, Ballachulish and Rannoch Moor complexes, show evidence that space creation has been achieved to a greater extent, than at higher levels, by ductile flow type mechanisms within the adjacent wall rocks. All these plutons show evidence of syn-kinematic rotation of regional folds and fabrics within their aureoles. These plutons are bounded and bisected by major shear zones which appear, as in the case of upper crustal pluton construction, to have aided far-field material transfer. These granites however lack the peripherally developed ring fault structures common to the higher level complexes within the Argyll Suite. Rannoch Moor may be somewhat of an exception, having been emplaced at a somewhat higher crustal level and later reactivated even closer to the free surface. This complex pluton probably represents a sub-volcanic complex being partially bounded within its internal margins by major NE-SW Caledonian shear zones. Such structures may have allowed some amount of roof uplift to be achieved. Such features are not observed with pluton construction at mid-crustal levels, which may indicate in the case of the sub-elliptical Ballachulish complex that transposition of the crust was predominantly achieved by the ductile deformation of the roof zone and the downward displacement of the pluton floor.

11.7 DISCUSSION

It is therefore conceivable, that the elliptical plutons of the Argyll Suite, which topographically are laterally extensive (e.g. Rannoch Moor 28 km x 18 km) and give the impression they are large voluminous bodies, are probably in fact in three-dimensions, thin, tabular, sill-like bodies (Fig. 11.13 & 11.14). The form of these bodies suggests that the amount of vertical transposition of the crust needed to accommodate such plutons is therefore considerably smaller than might have been envisaged. This would explain why with many plutons which have *in situ* expansion type characteristics, the magnitude of strain accumulation at the outer parts of the complex is considerably lower than might be expected. It should be noted that a consequence of the crust undergoing non-coaxial deformation, during a collisional event such as the Caledonian orogeny, is that material is

both shortened horizontally and extends or extrudes vertically (Sanderson & Marchini 1984). This overall process inducing granite petrogenesis (Hutton & Reavy 1992) and aiding the fundamental mechanisms for space creation during pluton construction, i.e. the vertical movement of crust bounding the top and bottom of these plutons. The introduction of granitic magma into the crust during transpressive deformation may well be an essential process in order to stabilize major topographical features consequently produced. It may also aid the deformation process, especially in the latter stages, providing a medium within the crust in which deformation can be focused.

Model proposed

Within the Argyll Suite, SW Grampian Highlands, a large number of Caledonian granitic plutons and associated minor intrusive bodies are now exposed at the present level of erosion; not only representing a range of ages, but also a range of significantly different relative depths of crystallisation. The reason why ascending granitic magma should stop and concentrate at this particular level within the crust may be attributed to it reaching a "zone" of neutral buoyancy (LNB), and possibly exploiting major sub-horizontal detatchment surfaces. If pluton construction occurs along a major transcurrent shear zone, a process of dyke-like sheeting is envisaged; maintaining ascent type characteristics. However, if the ascending magma is confined to an ascent conduit, a localised zone of transtension developed at the intersection of two major shear zones, it may accumulate and be driven laterally away from the site of magma ascent, by the imposition of tectonic-related and its own buoyancy-related forces; creating emplacement geometries which may overprint and/or obliterate structures associated with ascent processes. Integration of data suggests that the resultant elliptical/sub-elliptical plutons have been principally constructed by a process of *in situ* lateral expansion, predominantly into the direction of least tectonic strain (S_3); forming in three-dimensions, relatively thin, tabular shaped bodies in which their lateral extent far exceeds its vertical thickness. At depths of approximately 6-10 km the interaction of tectonically induced strain fields, associated with the NE-SW-trending shear zones and faults related to Caledonian transpressional collision and an intersecting set of NW-SE-trending pre-Caledonian crustal lineaments, during pluton construction has led to the development of localised zones of sheeting and stoping; a process of multiple sheeting into transtensional fractures.

At mid-crustal levels, country rock material is probably transported away from the vicinity of pluton construction by the combined effects of: (i) ductile movements along major regional shear zones; (ii) the deformation and uplift of the roof zone and/or the downward displacement of the pluton floor; and (iii) bulk wall rock shortening by ductile

flow. It is possible that the architecture and kinematic evolution of the lower crustal reflectivity zone (LCRZ) initiated the reactivation of lineaments and ultimately controlled their development, influencing the overall mechanism of pluton construction at mid-crustal levels. At high crustal levels, the combination of roof updoming and brittle translatory mechanisms, such as peripheral ring fault development and subsequent roof uplift, provide a major component for space creation. Pluton expansion-related strains are therefore to a large extent accommodated by vertical uplift and deformation of the overlying country rock, which may explain why the overall wall rock deformation around the periphery of such plutons is relatively low. During regional transpression, it is envisaged that some of the resultant tectonic stress is accommodated along these volcanotectonic faults and regional structures, aiding the space creation process by the deformation and vertical transposition of the crust above and possibly below the expanding pluton.

APPENDIX 1

MAJOR LINEAMENTS WITHIN THE NE HIGHLANDS

The following Sections, based on the information obtained during this current study of Caledonian granitic magmatism in the SW Highlands, and the compilation of existing data, will address the question: Were similar tectonic controls operating in the NE Highlands during Caledonian plutonism?

Models are presented in an attempt to explain the distribution of Caledonian magmatism in the NE Highlands and any possible differences between the magmatism in this region from that occurring throughout the rest of the Grampians and Northern Highlands.

9.11 MAJOR TECTONIC STRUCTURES WITHIN THE NE HIGHLANDS

Several lineaments/shear zones have been recognised within the NE Highlands (e.g. Ashcroft *et al.* 1984; Fettes *et al.* 1986; Fettes *et al.* 1991; see review by Goodman 1994) (Fig. 9.8 & 9.21):

(i) those with trans-Caledonide NW-SE-trends, including Glenlivet and Rothes; (ii) those with partly Caledonide trends, e.g. Frasenburgh-Old Meldrum and the northern part of the Portsoy-Duchray Hill lineament; and (iii) a major set of E-W lineaments or shear zones, e.g. Deeside and Insch.

Anomalous gravity values over this region ("Buchan block") led Ashcroft *et al.* (1984) to suggest that these lineaments/shear zones may separate the Buchan block from the main Dalradian tract (Fig. 9.21). This possibly coincides with a lineament or zone of discontinuities which they traced roughly NNE from Portsoy on the Moray Firth,

southwards to the Cabrach intrusive body (Fig. 9.22) near Duchray Hill (Tayside region) (Fig. 9.9); they referred to this as the Portsoy-Duchray Hill lineament (see Fig. 9.7). Fettes *et al.* (1986) extended the zone further southwards. The southern end of the lineament runs along the eastern side of the Lochnagar granitic pluton and the Duchray Hill gneiss, forming part of the Glen Doll fault (Barrow 1912). There is evidence of a sedimentary facies variation across this structure (Harte 1979), with Ashcroft *et al.* (1984) suggesting that part of the lineament (northern part of the Duchray Hill lineament) may have acted as a syndepositional fault. Combined with changes in stratigraphy, there is also a pronounced change in metamorphic style across the Portsoy-Duchray Hill zone (e.g. Harte 1988; Baker 1987; Beddoe-Stephens 1990).

It still remains unclear what the Portsoy-Duchray Hill lineament represents. Various models have been proposed for its existance, which include: (i) Ashcroft *et al.* (1984) suggested that the lineament (the "Portsoy Line") may have initially been part of a syndepositional fault system. This model was supported by Fettes *et al.* (1986) who suggested that it may represent one of a set of major trans-Caledonoid structures present in the Dalradian (see Fig. 9.8); (ii) Based on metamorphic studies, the lineament has been interpreted as representing a zone of sub-horizontal displacements, which thrusted a higher level nappe towards the NW over the western area. This was subsequently steepened to a sub-vertical attitude by late deformational movements probably related to folding (Baker 1987; Beddoe-Stephens 1990).

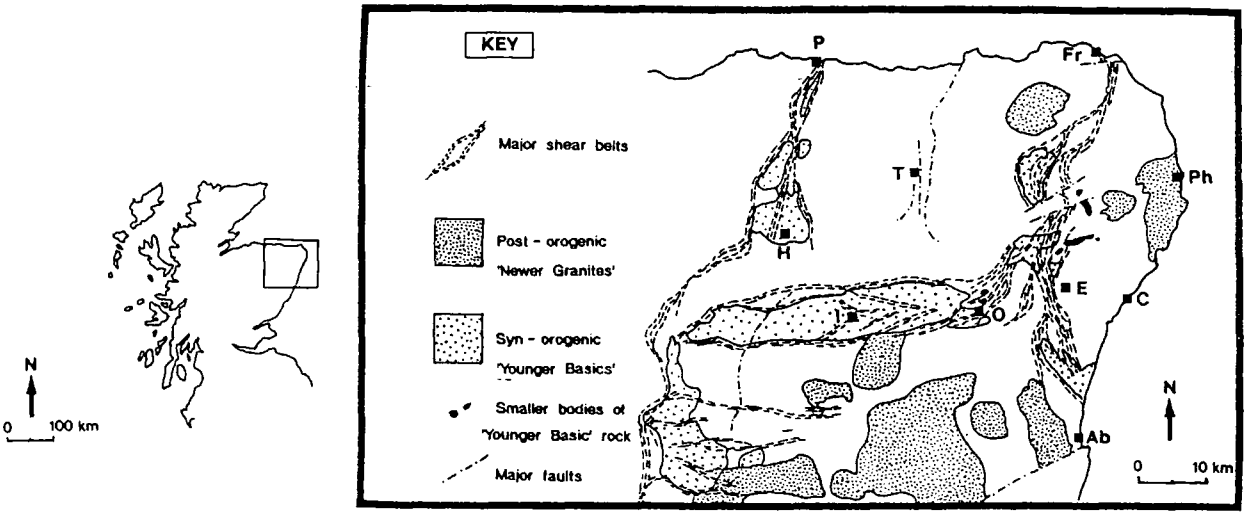

Fig. 9.21. Distribution of major shear belts in NE Scotland. Also shown, principal younger basic (syn-orogenic) masses, newer granites (post-orogenic). Ab, Aberdeen; C, Collieston; E, Ellon; Fr, Fraserburgh; H, Huntly; I, Insch; O, Old-Meldrum; P, Portsoy; Ph, Peterhead; T, Turriff. Largely after Ashcroft et al. (1984).

9.12 IGNEOUS ACTIVITY WITHIN THE NE HIGHLANDS

Along the whole length of the Portsoy-Duchray Hill lineament occur lenses, sheets and dykes of amphibolite, metagabbro and serpentinite, and basic and ultramafic lavas. Some of these bodies are pre-metamorphic, and their occurrence along this lineament may suggest that it was a major early tectonic boundary (Fettes *et al.* 1986). This suite was sub-divided by Read (1919) into two groups: (i) the 'Older Basic Intrusions' which were pre-deformational; and (ii) the 'Younger Basic Intrusions' which were believed to be mainly post-deformational. However, recent work (e.g. Allan 1970; Munro & Gallagher 1984; Fettes & Munro 1989) shows that the deformation was polyphasal, and the magnitude of deformation was extremely variable, post-dating the 'younger basic' group. It was also shown that many of the so called "older basics" are in fact equivalents of the 'younger basic' group, having simply undergone a greater intensity of deformation.

A number of basic and ultrabasic intrusive complexes occur north of the E-W trending Deeside lineament, where they show a strong spatial association with major shear zones and lineaments developed within the region. It has been suggested by Ashcroft *et al.* (1984) that the ascent and siting of these basic intrusives may have been controlled by the Fraserburgh-Old Meldrum lineament, the northern part of the Portsoy-Duchray Hill lineament, and the Insch lineament. These intrusive bodies were subsequently disrupted and deformed by tectonic activity along these zones, resulting in the large scale shear zone system now observed (Fig. 9.21). As mentioned above, basic and ultrabasic bodies occur along the whole length of the Portsoy-Duchray Hill lineament. Their exact age is uncertain, but they probably represent a series of intrusives with different ages suggesting that the zone may have been reactivated several times during magmatism.

As shown by Fig. 9.23, a number of Caledonian granitic plutons within the NE Highlands appear to be also spatially associated with these major lineaments or shear zones. The emplacement of the East Grampian batholith has been suggested by Watson (1984) to have been controlled by the E-W-trending Deeside lineament. It is apparent from Figure 9.23 that in general, many of the granitic plutons may occur along these lineaments or at the intersection of two of these structures with different orientations. The establishment of such a pattern of structural interactions shows great similarities to the mechanistic framework established within the SW Highlands, which may explain the location of anatectic zones, siting and ascent pathways and any subsequent emplacement phenomena. However, the fundamental difference in tectonic control between the NE and SW Highlands (corresponding to the Cairngorm and Argyll suites, respectively) appears to be that in the

case of the SW Highlands the situation appears to be less complicated, with the establishment of only two sets of major structures. This includes several NE-SW-trending shear zones and faults related to the Caledonian transpressional collision, which intersect with a set of trans-Caledonoid NW-SE-trending crustal lineaments. In the NE Highlands however, four possible sets may occur (Fig. 9.23): (i) NE-SW-trending Caledonian structures (e.g. Etive-Laggan fault and Ericht-Laidon fault); (ii) lineaments possessing NW-SE trends (e.g. Rothes and Glenlivet), similar to those described in the Argyll region; (iii) a major set of E-W lineaments or shear zones (e.g. Insch and Deeside); and (iv) lineaments with partly Caledonoid trends (e.g. Fraserburgh-Old Meldrum). The latter set includes the Portsoy-Duchray Hill lineament, which as discussed above, may form a major shear zone system along the western boundary of the Buchan block, essentially decoupling it from the rest of the main Dalradian tract (Ashcroft *et al.* 1984; Fettes *et al.* 1986). It is interesting to note that NE of this lineament the major tectonic structures observed within this particular part of the region appear to be the NW-SE-trending Rothes and Glenlivet lineaments (Fig. 9.22). When traced south-eastwards, both lineaments appear to stop abruptly against the Portsoy-Duchray Hill lineament, as shown by Fettes *et al.* (1986). East of the latter structure, essentially within the 'Buchan block domain', the dominant lineaments or shear zones appear to be the E-W-trending Insch and Deeside lineaments, and the NNE-SSW-trending Fraserburgh-Old Meldrum lineament (Fig. 9.23).

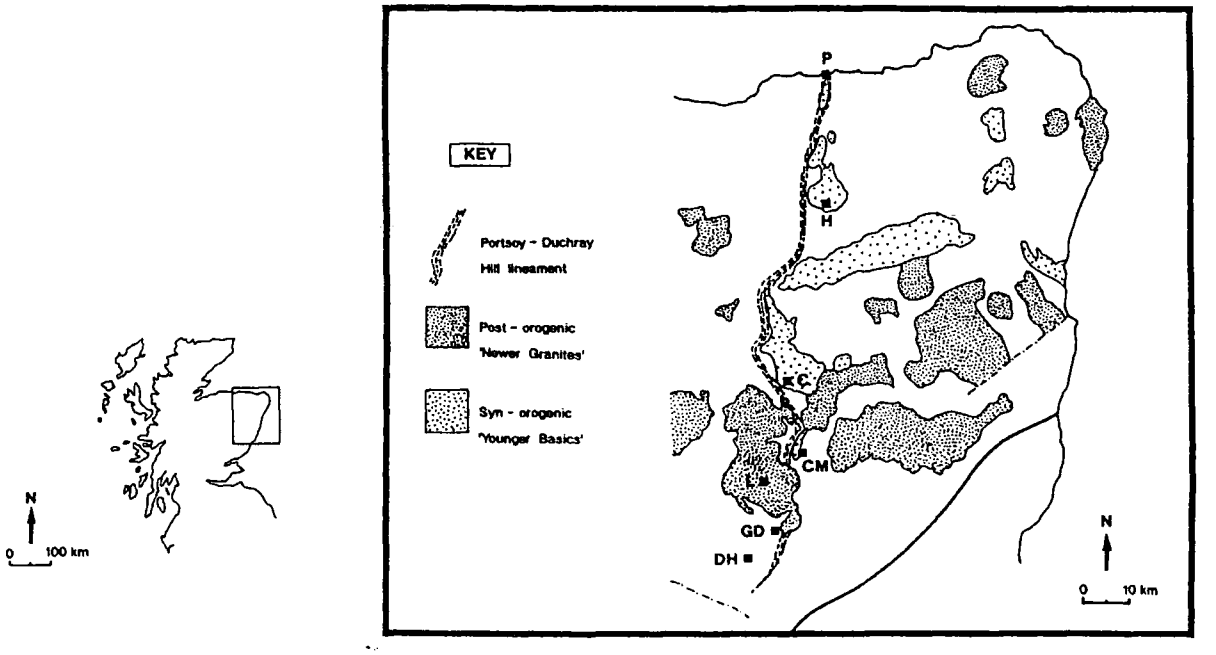

Fig. 9.22. Generalised geological map of the NE Highlands showing the position of the Portsoy-Duchray Hill lineament. P, Portsoy; H, Huntly; C, Corbrack; CM, Coyle of Muick; L, Lochnaggar; GD, Glen Doll; DH, Duchray Hill.

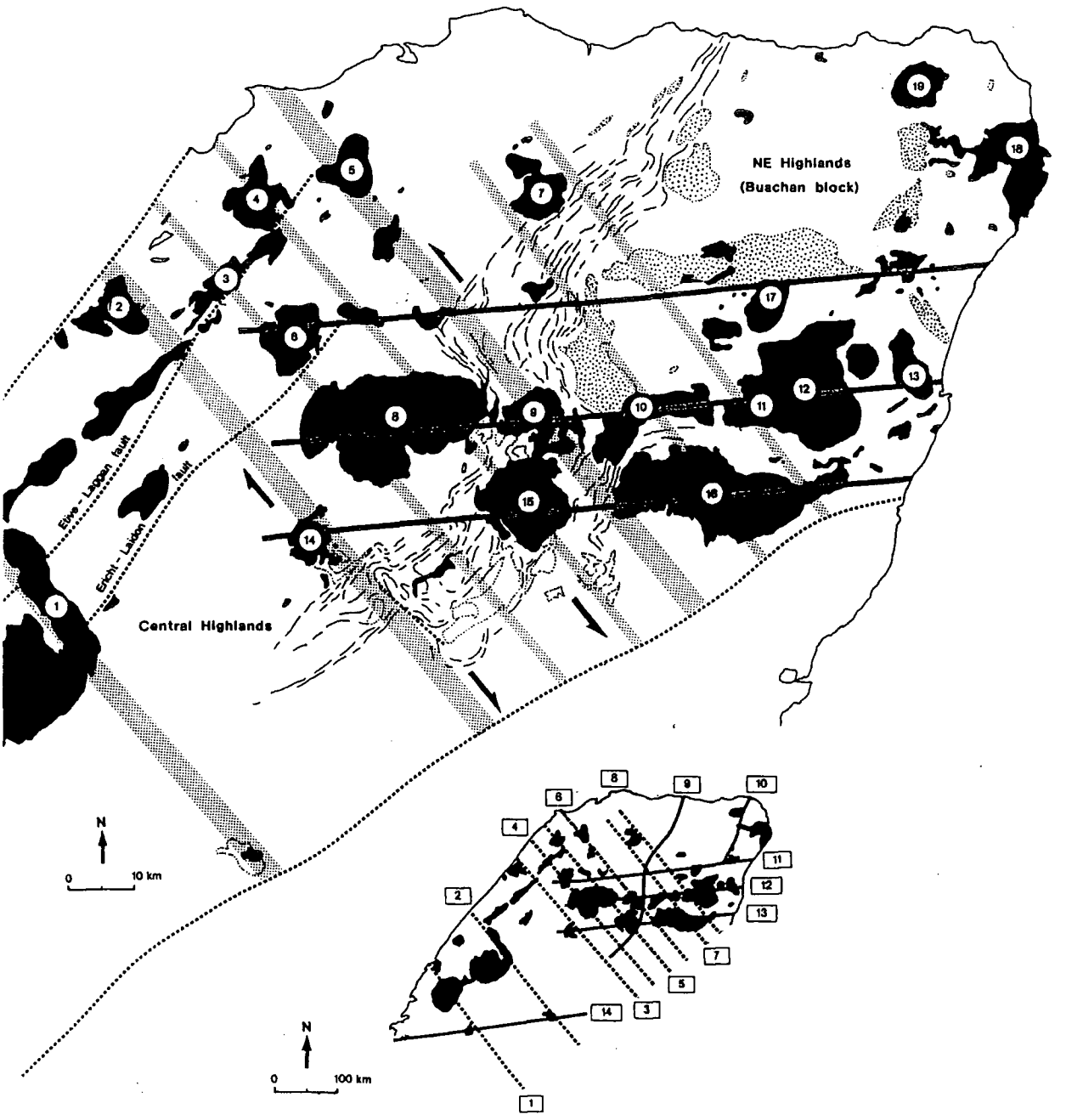

Fig. 9.23. Sketch map of the NE Highlands showing (a) major structural features and the distribution of Caledonian plutons: 1, Strath Ossian; 2, Foyers; 3, Glen Kyllachy/Findhorn; 4, Moy; 5, Ardclach; 6, Monadliath; 7, Ben Rinnes; 8, Cairngorm; 9, Glen Cairn; 10, Ballater; 11, Hill of Fare; 12, Skene complex; 13, Aberdeen; 14, Glen Tilt; 15, Lochnagar; 16, Kincardine (Mt. Battock). (b) Position of the inferred NW-SE-, E-W- and partly Caledonoid-trending lineaments in the SW, Central and NE Highlands: 1, Cruachan; 2, Strath Ossian; 3, Foyers-Glen Tilt; 4, Monadliath; 5, Moy-Lochnagar; 6, Ardclach-Glen Cairn; 7, Glenlivet; 8, Rothes; 9, Portsoy-Duchray Hill; 10, Fraserburgh-Old Meldrum; 11, Insch; 12, "northern" Deeside; 13, "southern" Deeside; 14, Kilmelford-Comrie.

As shown in Figure 9.23 many granitic plutons are sited along, or in close proximity to the major E-W-trending lineaments. At least six granitic plutons of various sizes occur along the E-W-trending Insch lineament, including the large, somewhat E-W elongated Kennethmont complex. If this lineament is extended westwards across the Portsoy-Duchray Hill lineament, a further three granitic bodies occur on the line, and all appear to be sited where NW-SE-trending lineaments (discussed below) intersect it. (Fig. 9.22). The same situation appears to occur to the south along the E-W-trending Deeside lineament. This lineament forms an extremely broad geological feature and has been placed at the centre of the E-W-trending East Grampian batholith (see Fettes *et al.* 1986). Plutons are not sited directly along this line, but occur as two well defined E-W alignments slightly to the north and south of its position (Fig. 9.23). Along the "northern Deeside lineament" at least five extremely large plutons occur, including the Cairngorm, Glen Cairn, Ballater, Hill of Fare, Skene and possibly the Aberdeen and Auchlee complexes. Along the "southern Deeside lineament" the centres of the Lochnagar and the extremely large E-W elongated Kincardine (Mt. Battock) complexes are found, and if this line is extended eastwards across the Portsoy-Duchray Hill lineament it coincides exactly with the Glen Tilt complex where it intersects with the NW-SE-trending Foyers-Glen Tilt lineament (see below). Again, the same NW-SE-trending lineaments which obliquely traverse the E-W-trending Insch lineament, possibly siting plutons along that structure, may continue south-eastwards across both the E-W-trending "Deeside lineaments". Where the two sets of structures intersect, they again coincide with sites of major intrusive activity (see Fig. 9.23), possibly siting at least seven granitic plutons.

As mentioned above, east of the Portsoy-Duchray Hill lineament (the possible western margin of the Buchan block) the E-W-trending Insch and Deeside lineaments are the most dominant feature in this part of the NE Highlands. However, as shown above, the NW-SE-trending lineaments may continue south-eastwards, having a 'real' existence in determining sites of Caledonian magmatism, but possibly having no great importance in the structural development of the region. The reverse may be true NE of the Portsoy-Duchray Hill lineament, where a number of NW-SE-trending lineaments have been recognised (e.g. Rothes and Glenlivet (Fettes *et al.* 1986; see below)). Whereas, the E-W-trending lineaments do not appear to continue any further westwards once they reach the major NE-SW-trending Ericht-Laidon and Etive-Laggan shear zones/faults (see discussion below), and do not have any apparent effect within the structural development of the upper cover sequence. This is in contrast with the NW-SE-trending lineaments, which when traced south-eastwards into the Buchan block area they coincide exactly with major "deflections" or strike swings which occur along the Portsoy-Duchray Hill lineament (Fig. 9.22). The largest strike swing occurs between Tomintoul and a few km's SE of Ballater, where the general NE-SW-trend of the Portsoy-Duchray Hill zone is "deflected" into a NW-SE-trend

for approximately 20 km. SE of the Glen Tilt complex, a similar situation may occur, but of slightly lesser 'magnitude', and possibly accommodated to some extent by brittle deformation, with the development of a NW-SE-trending fault along this zone (Fig. 9.22). These two major NW-SE-trending lineaments may represent deep basement structures of a similar scale to that of the Strath Ossian and Cruachan lineaments observed within the SW Highlands. Within the Tomintoul-Ballater area a further three possible NW-SE-trending lineaments may represent minor structures similar to the Rannoch Moor and Glencoe lines identified within the SW Highlands (see Section 9.6).

Within the NE Highlands a number of geologically-defined NW-SE-trending lineaments may occur. These include:

The Foyers-Glen Tilt lineament:

One of these major lineaments, as mentioned above, appears to modify the strike swing of the Portsoy-Duchray Hill lineament to the SE of the Glen Tilt complex. This NW-SE-trending lineament will be referred to as the Foyers-Glen Tilt lineament. It coincides with an area containing a number of minor NW-SE-lineaments, termed the Aberfeldy-Kirkmichael zone (Fig. 9.8), identified by Fettes *et al.* (1986) from variations in metasedimentary chemistry. If this lineament is traced SE, towards the Highland Boundary Fault zone, it coincides with a Bouger gravity anomaly high located NW of Alyth, which has been interpreted by Woollett (1988) as probably being produced by the local occurrence of unexposed ultrabasic rocks. He also recognised a similar local high near Comrie, which coincides with the Strath Ossian lineament where this structure meets the Highland Boundary Fault zone.

From the Highland Boundary Fault (NW of Alyth), the Foyers-Glen Tilt lineament can be traced NW up to the Great Glen Fault (Fig. 9.23). Two large plutons, the Foyers and Glen Tilt complexes occur along this zone, together with several smaller granitic bodies (see Fig. 9.23). The relatively large amount of appinitic material associated with the Glen Tilt complex may suggest the lineament reached at least lithospheric mantle depths during this period of magmatism.

Ardclach-Glen Cairn lineament:

The other major NW-SE-trending lineament, which may have been responsible for the gross strike swing along the Portsoy-Duchray Hill lineament in the Tomintoul-Ballater area, will be referred to as the Ardclach-Glen Cairn lineament. Sited along this lineament

are at least five granitic plutons including the Ardclach, Grantown, Dorback, and Glen Cairn complexes, and a small body SW of Nairn, in the extreme NW (see Fig. 9.23).

Two minor NW-SE-trending lineaments occur between the Foyers-Glen Tilt line and the Ardclach-Glen Cairn lineament. These may represent synthetic splays between these two major structures, as with the Rannoch Moor and Glencoe lines in the SW Highlands (see Section 9.6). Both may cause a local variation in strike swing where they pass through the Portsoy-Duchray Hill lineament, and are defined by the alignment of granitic plutons and sites of major intrusive activity.

The Monadliath line:

One of these lineaments, named here the Monadliath line passes through the centre of the Glen Kyllachy and Monadliath complexes and a small granitic body near Devil's Elbow (Fig. 9.23). Where it passes through the Cairngorm pluton it coincides with a localised, N-S-trending, somewhat linear body referred to as the Carn Bàn Mór Granite (see Harrison 1986).

The Moy-Lochnagar line:

The other lineament, named here the Moy-Lochnagar line, passes straight through the centres of the Moy, Boat of Gartain and Lochnagar granitic complexes. Where it passes through the Cairngorm pluton, as with the Monadliath line, it is coincident with a site of intrusive activity again coinciding with a N-S-trending, linear shaped body known as the Beinn Bhreac Granite (see Harrison 1986).

If the line is continued south-eastwards, past the Lochnagar pluton, it may coincide with the NW-SE-trending Clova lineament, identified by Fettes *et al.* (1986) from variations in metasedimentary chemistry. Within this area the Glen Clova 'older granites' occur. These have been identified by Harry (1958b) as consisting of two distinct phases: (i) bodies of migmatitic gneiss; and (ii) later discrete masses of microcline granite. Their origin remains poorly understood, but they also occur along the Moy-Lochnagar line.

These features may suggest that these NW-SE-trending lineaments not only controlled the siting of Caledonian magmatism, as seen further west in the SW Highlands,

but may have also had a profound effect during the structural development of the NE Highlands cover sequence. As seen by the major strike swings along the Portsoy-Duchray Hill lineament where these NW-SE-trending lineaments cross. If this is the case, it suggests that deformation (or movements) along these structures in the NE Highlands was of a greater magnitude than that experienced along the same set of lineaments to the SW of this region, i.e. within the SW Highlands where no such clear deformational features are apparent. It is interesting to note, that the hypothetical highly idealised 'rotating block model' of the lower crust presented in Section 9.9, infers that the SW Highlands lies in a "convergent zone" between the Great Glen Fault and the Highland Boundary Fault, whereas, the NE Highlands occurs in a "divergent zone" between these two structures. Within this system, it is envisaged that the lower crust is composed of a series of mobile blocks bounded by anastomosing shear zones. Movements along the two bounding structures, essentially causes the blocks to undergo a gross clockwise rotation. Due to the geometry of the whole system, it appears necessary that movements along the NW-SE-trending lineaments would have to increase in magnitude moving towards the NE, thus possibly explaining why the lineaments in the NE Highlands may have had such an influence during Dalradian deformation. It should be noted that such processes occurring within the lower crust are likely to have been operating some time before the onset of Caledonian granitic magmatism, as it is forseen that interaction between the rotating blocks would have caused crustal thickening, which would have eventually led to the development of anatectic zones and the production of 'granitic' melt.

9.13 LINEAMENTS AND SHEAR ZONES CONTROLLING THE SITING OF CALEDONIAN MAGMATISM IN THE NE HIGHLANDS

As shown above, regional shear zones and lineaments within the Buchan block, including the Portsoy-Duchray Hill zone may have not only controlled the siting and ascent of pre-orogenic 'Older Basics' and syn-orogenic 'Younger Basics' as suggested by Ashcroft *et al.* (1984), but may have also been responsible for the siting of granitic plutons at shear zone or lineament intersections. As proposed within the SW Highlands, it is envisaged that at these intersections transtensional zones were created allowing and facilitating their ascent.

In summary, this synthesis led to the recognition of a number of possible lineaments or shear zones which may have been active during Caledonian granitic magmatism in the

NE Highlands of Scotland. These include (Fig. 9.22): (i) the E-W-trending Insch and Deeside lineaments; (ii) the NNE-SSW-trending Portsoy-Duchray Hill and Fraserburgh-Old Meldrum lineaments; and (iii) NW-SE-trending lineaments, including the Foyers-Glen Tilt lineament, the Ardclach-Glen Cairn lineament, the Moy-Lochnagar line, the Monadliath line, and the Rothes and Glenlivet lineaments.

Sixteen granitic bodies, at least, occur along the E-W-trending structures, thirteen are sited along the NW-SE-trending lineaments, and a minimum of five granitic plutons are spatially coincident with the NNW-SSE-trending lineaments. This means out of approximately twenty-seven moderately sized granitic bodies exposed within the NE Highlands, only five plutons do not appear to be sited along major recognised lineaments. This infers that around 75-80 % of all granitic masses within the NE Highlands are sited directly along one of these sets of structures. Out of twenty-two plutons aligned along these lineaments, at least ten (around 45 %) are sited at the intersection of the E-W- and NW-SE-trending lineaments (Fig. 9.22). West of the apparent influence of the E-W Insch and Deeside lineaments, the NE-SW-trending Etive-Laggan and Ericht-Laidon shear zones/faults may have sited at least four granitic plutons where they intersect with the NW-SE-trending lineaments (Fig. 9.22). Several bodies may also occur at the intersection of the NNE-SSW-trending lineaments/shear zones and the E-W-trending structures. *This may imply that at least 50 % of the granitic plutons observed within the NE Highlands are sited at the intersection of two major lineaments with different orientations, with 75-80 % occurring along at least one major lineament.*

9.14 DISTINCT TECTONIC DOMAINS

It is apparent from Figure 9.23 that the spatial distribution of the granitic plutons in the Buchan block may suggest that the E-W-trending lineaments were the dominant controlling structures. However, as suggested above, NW-SE-trending lineaments identified within the 'main Dalradian tract' may continue south-eastwards into this region (Buchan block). Although they are not observed as major lineaments or regional scale shear zones in the cover sequence to the east of the Portsoy-Duchray Hill lineament, they appear to have (i) had a profound affect on the strike of this 'tectonic boundary', causing significant bends or strike swings where they cross it; and (ii) controlled the siting of granitic bodies where they intersect with the E-W-trending Insch and Deeside lineaments.

The reverse is true west of the Portsoy-Duchray Hill lineament as the regional scale E-W- and NNE-SSW-trending shear zone system developed within the Buchan block does not appear to be apparent in the cover rocks of this adjacent area. Instead, within this part of the Highlands (moving into the Central Highland region) NE-SW-trending shear zones and faults related to the Caledonian transpressional collision (e.g. Etive-Laggan and Ericht-Laidon) and NW-SE-trending lineaments (as recognised further SW in the Argyll region) appear to be the dominant tectonic structures. One possible solution to account for such features is that the 'structural architecture' of the basement underlying the Buchan block is fundamentally different to that occuring beneath the Central and SW Highland regions. Ashcroft *et al.* (1984) have suggested that the Buchan area represents a distinct crustal segment, partly decoupled from the terranes to the south and west by relative movements along the regional shear zone/lineament system; thus, accounting for the unique style of deformation within the Buchan area. However, the continuation of NW-SE-trending lineaments across the Portsoy-Duchray Hill lineament and into the Buchan block may suggest that at least part of the basement beneath this area possesses similar structural characteristics to those identified for the SW Highlands, i.e. a set of NW-SE-trending deep basement structures (a possible "Lewisianoid-type basement"). A simple, possible solution to explain such features is that a 'distinct continental crustal unit', characterised by major E-W-trending lineaments, was thrusted into this region. This may have created a situation in which the NE Highlands is essentially underlain by a basement composed of two tectonically distinct units: (i) ancient "Lewisianoid-type crust" characterised by NW-SE-trending lineaments; and (ii) a continental crust which predominantly contains E-W-trending structures. Such a simple model may explain the 'superimposition' of one set of structures over another, either side of the Portsoy-Duchray Hill zone.

The continuation of the E-W-trending Deeside and Insch lineaments across the Portsoy-Duchray Hill lineament, may suggest thrusting occured up to, but not past a 'zone' now occupied by the NE-SW-trending Ericht-Laidon and Etive-Laggan shear zones/faults (see below). This may account for the approximate position of the boundary inferred by Stephens and Halliday (1984) to separate the Cairngorm Suite from the Argyll Suite (Fig. 9.3). It is therefore possible that the geochemically- and isotopically-defined boundaries separating the Argyll, South of Scotland and Cairngorm Suites of Stephens and Halliday (1984), may roughly coincide with such changes. It is interesting to note that the inferred position of the boundary between the Argyll and Cairngorm Suites does not occur along the Portsoy-Duchray Hill lineament (the possible western margin of the Buchan block), but significantly west of this zone, so as to include for example, the Cairngorm and Monadliath plutons which are sited along the E-W-trending Deeside and Insch lineaments respectively.

Implications for basement structure south of the 'Mid-Grampian Line'

The southern boundary of the Argyll Suite is the isotopically defined 'Mid-Grampian Line' (Halliday & Stephens 1984), north of which ε_{Nd} in the granitoids is always < -6, compared to higher values to the south. This change across the 'Mid-Grampian Line' has been interpreted by Halliday (1984) as representing a 'thrust boundary', separating ancient crust to the NW from younger continental crust to the SE. This rapid change in trace-element abundance occurs between the Arrochar, Comrie and Garaball Hill plutons in the south and the granites of the SW Highlands (e.g. Etive, Glencoe, Rannoch Moor, Ballachulish, Strath Ossian). The precise course of the boundary is uncertain, but is interesting to note that the southern most plutons of the Argyll Suite (e.g. Rannoch Moor, Glencoe, Etive) occur along the NE-SW-trending Etive-Laggan and Ericht-Laidon shear zones, sited where these structures intersect NW-SE-trending lineaments. This contrasts with the Southern Highlands where plutons such as Garabal Hill and Comrie may occur along an E-W-trending lineament (Fettes *et al.* 1986) and at the intersection of the NE-SW- and NW-SE-trending sets of structures (see Fig.9.24). If this possible E-W-trending lineament is traced westwards it passes directly through the Kilmelford complex (see Fig. 9.24), and directly along this zone is a high concentration of E-W-trending late Carboniferous quartz-dolerite dykes (see below). The Kilmelford complex, which comprises of at least ten individual intrusive bodies over an area of approximately 50 km^2, is cut by two major E-W-trending faults. The siting of this body along a major E-W-trending lineament is also suggested by a statement made by Zhou (1987), that "E-W structural lines are particularly important because they appear to control the distribution of the igneous bodies".

Throughout the Southern Highlands an E-W-trending fracture set is well established (Fig. 9.25). These appear to have been exploited by a Carboniferous to early Permian Suite of tholeiitic dykes and sills which form a belt some 200 km wide and 300 km long (see below). As mentioned above, both the Comrie and Garabal Hill complexes may be sited where these E-W-trending structures intersect major NW-SE-trending lineaments and NE-SW-trending faults. This may therefore suggest that the basement beneath these plutons is similar in 'structural architecture' to that underlying the Buchan block to the NE. This may be clearly demonstrated by the distribution and orientation of the major, late Carboniferous (Fitch & Miller 1967; De Souza 1979; Fitch *et al.* 1970) quartz-dolerite dyke swarm (Fig. 9.26a; Smythe 1994). Recent modelling by Smythe *et al.* (1995) shows that this intra-continental dyke swarm has an overall arcuate trend, which they interpret from stress pattern analysis as suggesting that the focus for this relative tensile stress was centred on the West Shetland Shelf region. As Smythe *et al.* (1985) state, "its trend is little affected

by local inhomogeneties in the upper crust", but as shown by Figure 9.26a, the distribution of the suite may have been profoundly influenced by basement 'architecture', with the tensile stress component only being established in the regions possessing an E-W fracture/lineament/shear zone system (see Fig. 9.26a). This may explain why, within the Grampian region (see Fig. 9.26), this suite: (i) occurs in the NE Highlands (essentially east of the Portsoy-Duchray Hill lineament), where a high concentration occurs in the vicinity of the E-W-trending Deeside and Insch lineaments; (ii) a high percentage of dykes occur south of the Mid-Grampian Line (Halliday & Stephens 1984), forming an extremely high concentration exactly coincident with the trace of a possible E-W-trending lineament which passes through the Kilmelford, Garabal Hill and Comrie granitic plutons (see above; which will be referred to as the Kilmelford-Comrie line); and (iii) the SW and Central Highlands are essentially devoid of such bodies.

The differences in geochemistry between the South of Scotland Suite and the Cairngorm Suite may reflect the tectonic regime prevailing during granite petrogenesis. As mentioned in Section 9.9, the Cairngorm Suite may lie in a 'divergent zone', essentially within an "extensional regime", whereas, the plutons under discussion within the "South of Scotland Suite" (Stephens & Halliday 1984) and as with the Argyll Suite lie in a 'convergent zone', a region of crustal thickening. Within the latter region, NE-SW-trending faults and shear zones are an expression of this transpressional component, and are demonstrably present. However, moving NE into the Buchan area this 'regional fabric' diminishes and such major structures do not occur. This therefore may demonstrate again that differences in tectonic environment during anatexis and magma emplacement could have been a strong influencing factor in determining pertrological characteristics between adjacent suites.

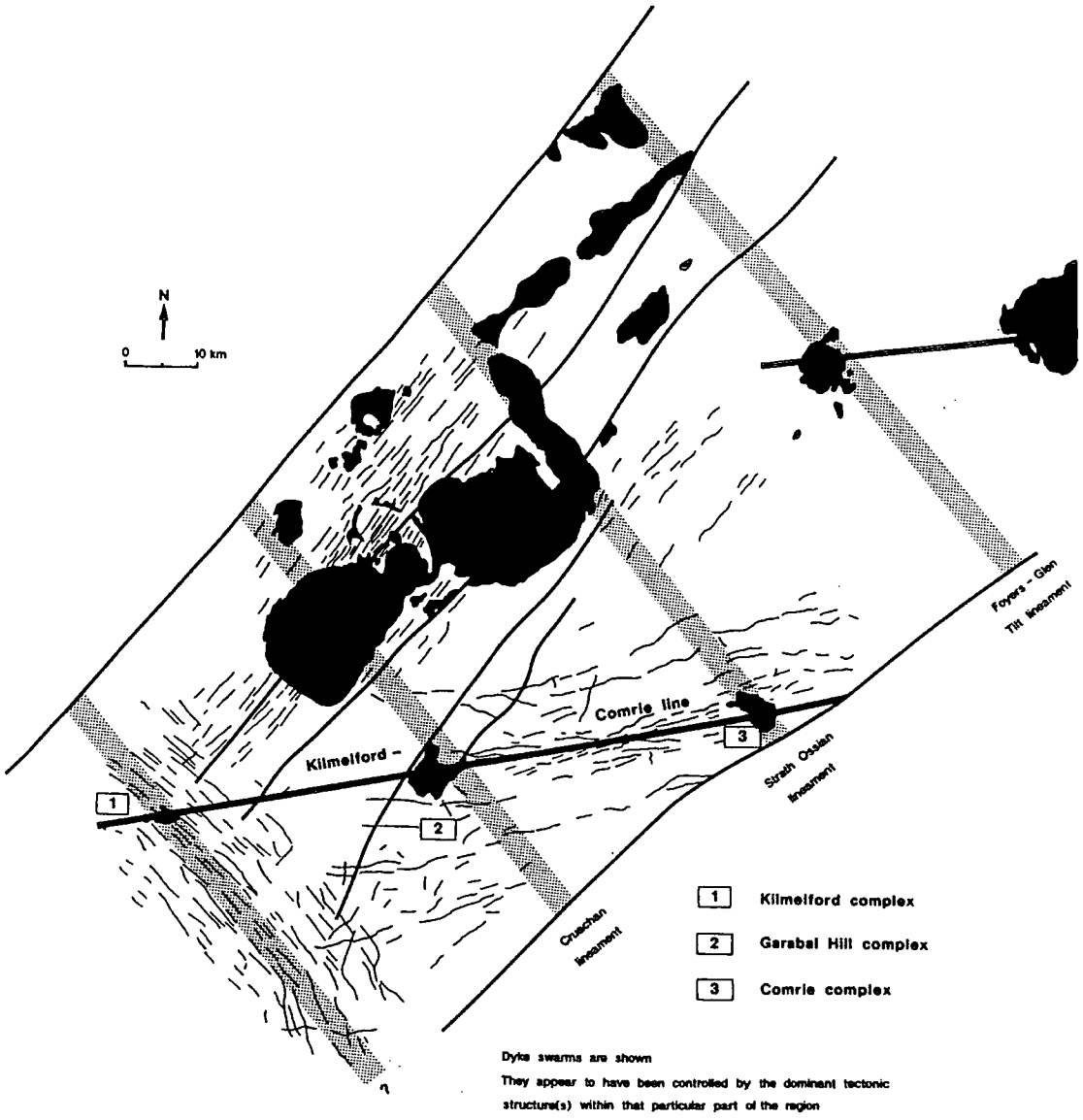

Fig. 9.24. Sketch map showing the possible structural controls on the siting of Caledonian magmatism in the SW and Southern Highlands.

Fig. 9.25. East-west fracture set. After Francis *in* Craig (1991).

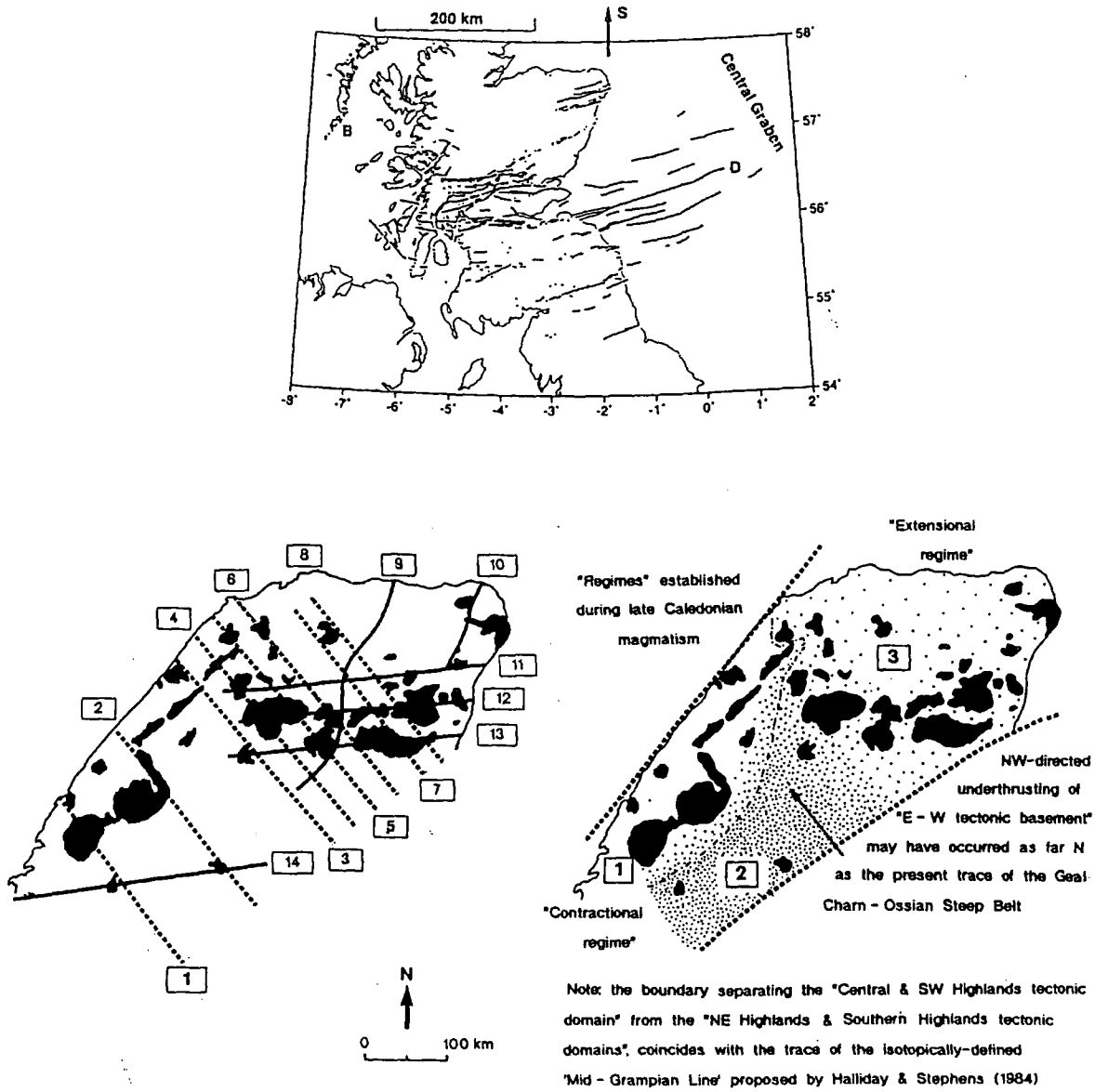

Fig. 9.26. (a) Stephanian (300 Ma) quartz-dolerite dykes of northern Britain, after Smythe (1994). B, Barra; S, towards Shetland; D, Dunbar dyke anomalies. UTM projection, central meridian 3_W. (b) Position of the inferred NE-SW-, E-W-, and partly Caledonoid-trending lineaments: 1, Cruachan; 2, Strath Ossian; 3, Foyers-Glen Tilt; 4, Monadliath; 5, Moy-Lochnagar; 6, Ardclach-Glen Cairn; 7, Glenlivet; 8, Rothes; 9, Portsoy-Duchray Hill; 10, Fraserburgh-Old Meldrum; 11, Insch; 12, "northern" Deeside; 13, "southern" Deeside; 14, Kilmelford-Comrie. (c) Generalised sketch map showing the approximate position of the inferred boundaries separating regions with different structural characteristics ('basement architecture').

MAJOR LINEAMENTS WITHIN THE NW HIGHLANDS

The following Sections will attempt to explain the distribution of late Caledonian magmatism in the NW Highlands. It is based on information obtained from the study of Caledonian magmatism in the SW Highlands during this current study, the result of new mapping undertaken during part of this present study (Rogart granitic complex), and the compilation of existing data (where referenced). It will also address: (i) the problem of what these deep crustal penetrating trans-Caledonoid lineaments may 'represent'; (ii) whether processes operating within the Grampians, leading to the production of Caledonian granitic melt, be responsible for the initiation and development of the Moine Thrust Zone in the Northern Highlands? and (iii) could the position and orientation of lineaments recognised explain "gross orogenic flow patterns" (major strike swings)? Models are presented in an attempt to shed light on these questions.

9.15 MAJOR TECTONIC STRUCTURES WITHIN THE NW HIGHLANDS

Within the NW Highlands, the Rogart granitic complex and an associated NW-SE linear belt of appinites are associated with the Loch Shin line (Watson 1984; Fig. 9.2). This NW-SE-trending lineament can be observed as a major feature on Bouger anomaly maps, and has been interpreted by Bott *et al.* (1972) as representing an important tectonic feature within the basement, possibly representing the Scourian-Laxford contact, separating two different tectonic domains. Within the Precambrian Lewisian foreland region several major NW-SE-trending shear zones (see Section 9.17) have been recognised. One of these, the Laxford shear zone, may continue south-eastwards beneath the Moine Thrust sheet, where it might be represented as a geological feature in the overthrusted Cambro-Ordovician cover sequence by the linear distribution of appinites and its influence in the development of the region (see Section 9.19).

The majority of these NW-SE-trending shear zones within the Lewisian complex represent old tectonic structures possibly formed shortly after the Main Badcallian metamorphism event (c. 2700 Ma; Humphries & Cliff 1982; Pidgeon & Bowes 1972; Chapman & Moorbath 1977), and have had a complex history of reactivation (see Section 9.17). The orientation, size and age of these Lewisian shear zones may suggest that similar structures represent the deep basement NW-SE-trending lineaments observed within the SW, Central and NE Highlands. This would infer that these regions are underlain, at least in part, by "Lewisianoid-type" basement possessing structural characteristics similar to those observed within the Lewisian foreland region. Such a basement has been inferred on the LISPB profile by Bamford (1979), showing that pre-Caledonian basement extends from the Caledonian foreland as far south as at least the Southern Uplands (Fig. 9.27; see Ch. 10, Section 10.3). An account of the main features of these Lewisian shear zones is presented in Section 9.17 which may shed some light on the possibility that some of these pre-Caledonian NW-SE-trending lineaments observed within the Grampian region represent Lewisian shear zones within the basement.

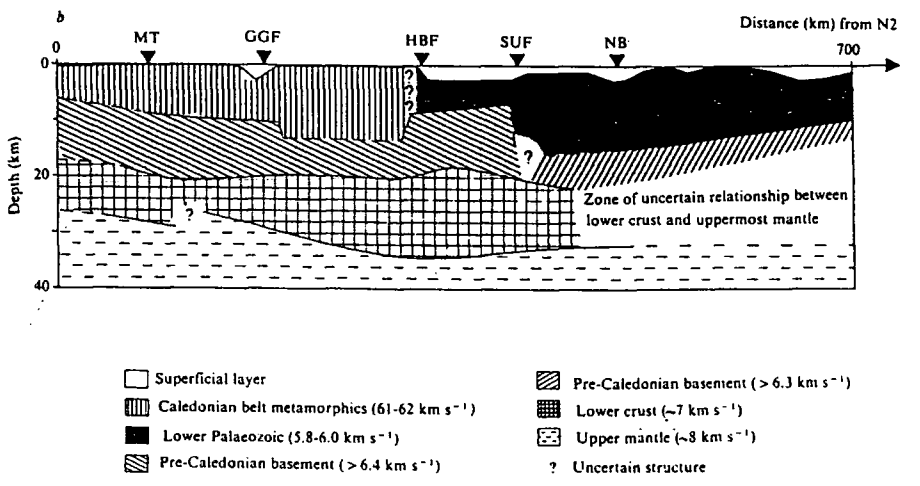

Fig. 9.27. Schematic seismic cross-section through the crust and uppermost mantle of northern Britain. MT, Moine Thrust; GGF, Great Glen Fault; HBF, Highland Boundary Fault; SUF, Southern Uplands Fault; NB, Northumberland Basin. After Bamford *et al.* (1979) *in* Hutton *et al.* (1980).

It has been established that Caledonian magmatism within the SW Highlands has been controlled by a set of NW-SE-trending pre-Caledonian crustal lineaments. These tectonic structures may have also controlled, to some extent, the distribution of Caledonian plutons in the NE Highlands. As mentioned above, a similar NW-SE-trending lineament, the Loch Shin line, has been recognised within the NW Highlands as a major geophysical lineament (Bott *et al.* 1972), and within the cover sequence by several geological features (Watson 1984; see Section 9.19). It is the aim of this Section to show not only how such NW-SE-trending lineaments may have controlled the siting of Caledonian magmatism within the NW Highlands, but also how such structures may have had an important influence in the structural development of the Cambro-Ordovician cover sequence during the north-westward propagation of the Moine Thrust sheet.

9.16 REGIONAL GEOLOGY OF THE NORTHERN HIGHLANDS

The Moine Thrust Zone of the Northern Highlands of Scotland (Fig. 9.28) was first described by Peach *et al.* (1907). The foreland stratigraphy was mainly described by Peach *et al.* (1907) and Sutton & Watson (1951). A high-grade Archean-Lower Palaeozoic gneiss terrane, referred to as the Lewisian complex, forms a metamorphic basement to this foreland region (reviewed in Park & Tarney (1987); Fettes & Mendum 1987). This basement is locally overlain unconformably by a cover sequence comprising of late Proterozoic (Torridonian) rocks, which are themselves unconformably covered by a succession of Cambro-Ordovician sediments. Both the Precambrian foreland and Cambro-Ordovician cover sequence were overthrust by metamorphic rocks of the Caledonian orthotectonic province. This assemblage includes middle to late Proterozoic (Brook *et al.* 1977) metamorphosed psammites and pelites, referred to as the Moine 'Series', together with discontinuous slices of re-worked Lewisian basement, which form inliers within the Moine cover succession (Rathbone & Harris 1979; Strachan & Holdsworth 1988).

The Moine assemblage was initially sub-divided into three tectonostratigraphical sequences (Johnstone *et al.* 1969): the Morar, Glenfinnan and Loch Eil divisions. This has been revised by Rathbone *et al.* (1983) and other workers, e.g. Stoker (1983), Roberts *et al.* (1984; 1987), Strachan (1985), and Holdsworth *et al.* (1987), indicating the Northern Highland succession may form a lithostratigraphic 'Supergroup' consisting of three

divisions and several formations. The original relationship of the Archean to early Proterozoic Lewisian basement to the Moine cover sequence has been largely obscured by subsequent deformation, only locally represented by highly strained conglomerates at the base of the Moine assemblage (Ramsay 1958). The first phase of deformation to effect both the basement and the cover has been previously regarded to have occurred approximately 1000 Ma (1028 +/- 43 Ma (age of Ardgour gneiss) Brook *et al.* 1976; Brook *et al.* 1977; Brewer *et al.* 1979; Powell *et al.* 1983) resulting in the development of major isoclinal folds. However, more recent age determinations suggest an emplacement age for the Ardgour gneiss of 574 +/- 30 Ma and 556 +/- 8 Ma (reviewed by Rogers & Pankhaust 1993), suggesting that this deformational event was much later. This event resulted in the formation of para-autochlothonous sheets of Lewisian in the cores of these structures (Ramsay 1958; Powell 1974; Rathbone & Harris 1979). Further work by Strachan & Holdsworth (1988) on the development of the Lewisian inliers in Central and SE Sutherland has revealed that the basement crops out in two distinct settings within these regions: (i) as allochthonous slices which rest on major Caledonian ductile thrusts; (ii) in the cores of verging intensely curvilinear sheath folds of Caledonian age. Strachan & Holdsworth (1988) also concluded that both the Lewisian basement and the Moine Succession had been affected by two major tectonic events: (i) the first probably occurring during the late Proterozoic, represented by minor folding and upper greenschist to upper amphibolite facies metamorphism, which was subsequently overprinted by: (ii) a widespread low- to mid-amphibolite facies metamorphism, as a consequence of ductile thrusting and folding during the Caledonian orogeny (c. 470-425 Ma).

It is generally regarded that the predominant structures within the Moine cover sequence are D2 in age, believed to have been formed during the initial and main stages of regional Caledonian deformation. This is based on these structures deforming the Cairn Chuineag granite in Ross-Shire (Shepherd 1973; Wilson & Shepherd 1979) which has been dated at 550 +/- 10 Ma (Powell & Phillips 1985). Structures which pre-date the emplacement of the granite are generally regarded as being Precambrian in age.

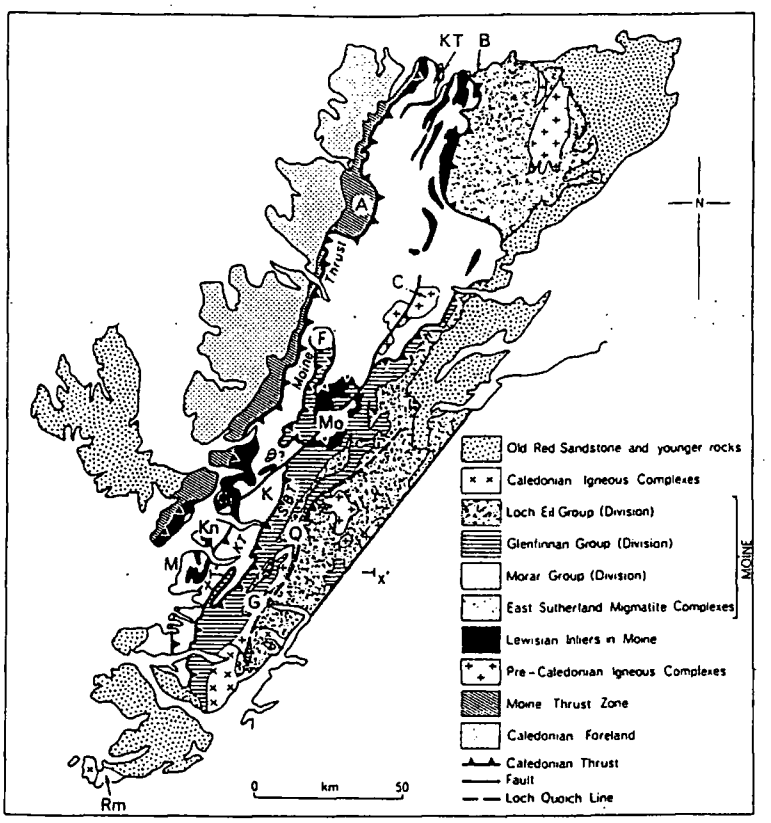

Fig. 9.28. Western Highlands showing the distribution of divisions of groups of the Moine, Lewisian inliers and major Caledonian structures. A, Assynt; B, Bettyhill; C, Carn Chuinneag; F, Fannich; G, Glenfinnan; K, Kintail; Kn, Knoydart; KT, Kyle of Tongue; M, Morar; Mo, Monar; Q, Quoich; Rm, Ross of Mull; S.B.T., Sgurr Beag thrust (Slide). X-X', Line of section in Fig. 9.45. After Harris & Johnson *in* Craig (1991).

9.17 THE FORELAND REGION: LEWISIAN SHEAR ZONES

If the majority or some of the NW-SE-trending deep crustal lineaments observed within the Grampian Highlands are pre-Caledonian in age and the region as a whole is underlain, at least in part, by a "Lewisianoid-type basement" (see LISPB profile (Bamford *et al.* 1978; Bamford 1979); Fig. 9.27), it seems logical to look at the Precambrian Lewisian foreland region (Fig. 9.28) for similar structural features.

Mainland Inverian/Laxfordian shear zones possessing an approximate NW-SE-trend have been identified in the Lewisian basement (Fig. 9.29). These major structures possibly forming shortly after the Main Badcallian high-grade granulite-facies metamorphic event (c. 2700 Ma; Humphries & Cliff 1982; Pidgeon & Bowes 1972; Chapman & Moorbath 1977) which occurred in the deeper parts of the Lewisian crust. Deformation focused along the shear zones and into adjacent parts of the Lewisian basement together with subsequent movements along these structures led to the juxtaposition of crust of different levels. Essentially three tectonic domains have been identified (see Park & Tarney 1987; Fig. 9.29):

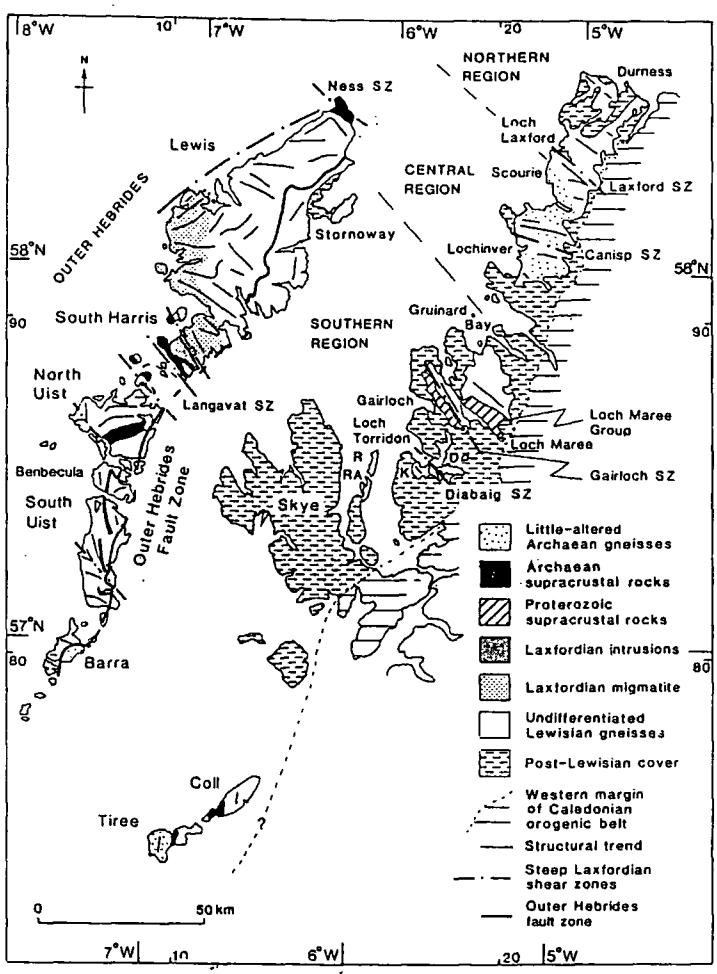

Fig. 9.29. Simplified map of the Lewisian complex showing main rock units and structures, and the regional sub-division. After Park and Tarney (1987) and Fettes and Mendum (1987) *in* Craig (1991).

(i) A 'Northern Region' of high Inverian strain, extending from Loch Laxford to Durness (Fig. 9.29). The block is essentially bounded to the SW by a major, steep NW-SE-trending broad shear zone, with a minimum width of 4 km (see Beach *et al.* 1974; Davies 1978). The zone occurs between Scourie and Loch Laxford, separating undeformed Badcallian structures to the southwest, from strong Laxfordian deformation in the north-eastern part of the shear zone. This zone is generally referred to as the Laxford shear zone, corresponding to the Foindle and Claisfearn zones of deformation described by Sutton & Watson (1951). Interestingly, an intense zone of Laxford granitic sheets occur along and adjacent to this broad zone of shear (Fig. 9.30), showing that this zone has been exploited by at least one phase of granitic magmatism;

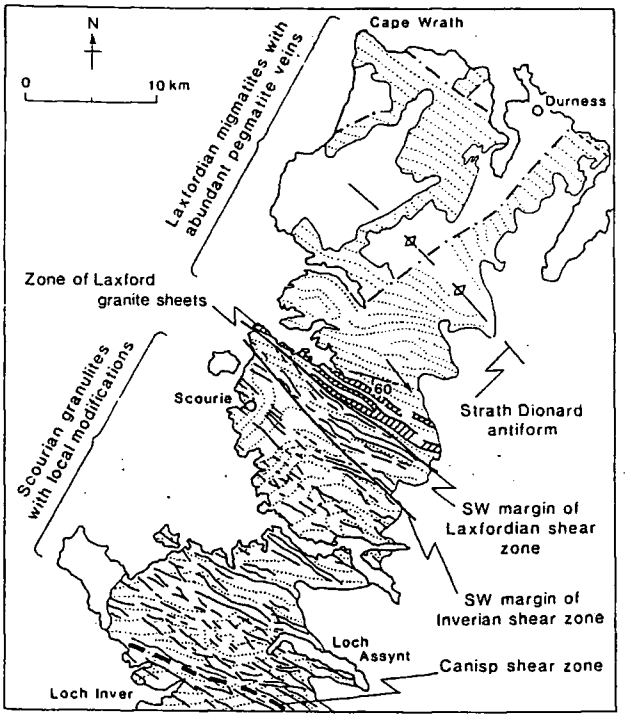

Fig. 9.30. Simplified map of the Northern region and the transitional zone in the N of the Central region, showing the principal structures and the boundaries of the major Inverian and Laxfordian shear zones. Dotted lines represent trend of banding; Scourie dykes in black; Laxfordian granite sheets hachured. Note the generalised dip of the planar fabric and plunge of linear fabric in the Laxford shear zone. After Watson (1983) *in* Craig (1991).

(ii) A 'Central Region' which largely escaped Laxfordian deformation (Fig. 9.29). Laxfordian strain was however focused along a major Inverian shear zone, the Canisp shear zone (Tarney 1963; Evans 1965; Attfield 1987; Coward & Park 1987), which cuts through

the centre of this central block. The zone is approximately 1.5 km wide, steep and WNW-ESE-trending. Deformation within this zone is extremely heterogeneous (Attfield 1987), producing lenses of low-strain gneisses, varying in size from a few centimetres to several metres across. They are bounded by anastomosing zones of high strain represented by highly deformed sheared gneisses. At least two major phases of movement have occurred along this zone (Attfield 1987): (1) an Inverian dip-slip movement with downthrow to the north, and a small component of dextral strike-slip. The zone was then the focus for the sub-parallel emplacement of a suite of NW-SE-trending ultrabasic and quartz-epidiorite dykes; (2) a later reactivation stage during the Laxfordian. Again this consisted of a dominantly dextral strike-slip sense of motion, but with a smaller component of dip-slip movement, again with downthrow to the north. This latter event was however, focused into narrower zones of high strain. This together with the change from an Inverian, dominantly dip-slip, to a Laxfordian, dominantly strike-slip event may have occurred in other parts of the Lewisian (see Coward & Park 1987). A number of relatively minor, steep shear zones with an approximate NW-SE-trend also occur;

(iii) a 'Southern Region' (Fig. 9.29). As with the Northern Region, this zone appears to represent a belt of Inverian high-strain. The Southern and Central Regions are separated by a zone of approximately 8 km width, occurring between the Gruinard River and Fionn Loch. This zone is again steep and NW-SE-trending. It has been referred to as a 'minor image' of the Claisfearn Zone (Park & Tarney 1987), being overprinted and deformed by major Laxfordian strain along its southwestern side, which continues southwards through the region (see Park *et al.* 1987).

During the Inverian, the Lewisian foreland region has been envisaged by Park and Tarney (1987) as consisting of a central stable region, flanked by major steep NW-SE-trending shear zones, which may link to a flat-lying mid-crustal shear zone (see Coward & Park 1987), underlying the resultant block (Fig. 9.31). Sense of movement on the bounding NW-SE zones of shear, indicate a general overthrust regime with a small component of dextral motion (Coward & Park 1987); indicating an apparent dextral transpressional regime. The Inverian shear zones were the focus for amphibolite-facies metamorphism, combined with the injection of volatiles (see Beach 1976, Beach & Tarney 1978), leading to extensive retrogression of the Archean granulite. Contemporaneous with probably the latter stages of this deformation and after, was the intrusion of the NW-SE- to E-W-trending Scourie dyke suite (c. 2400 Ma; Chapman 1979).

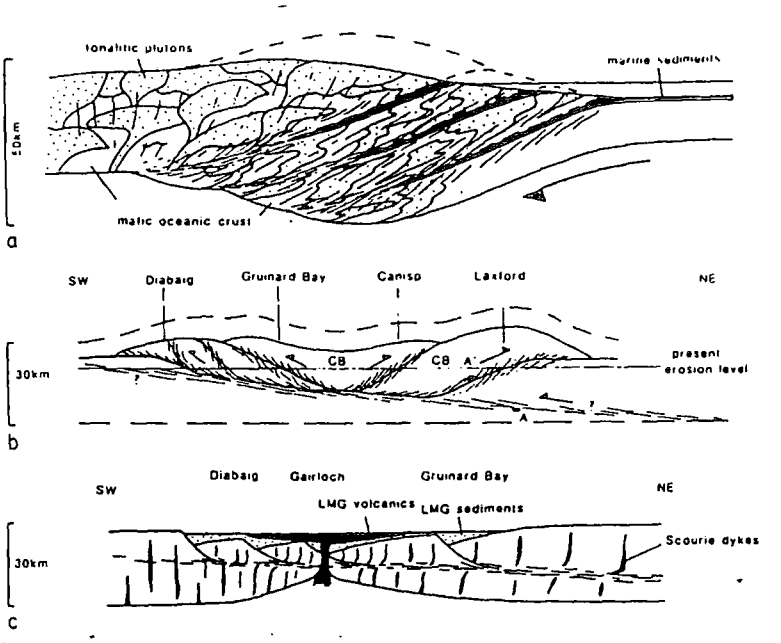

Fig. 9.31. Schematic profiles illustrating the tectonic evolution of the Lewisian complex. (a) Badcallian; (b) Inverian; (c) emplacement of Scourie dykes and Loch Maree Group. CB, central block; LMG, Loch Maree Group. After Park and Tarney (1987) *in* Craig (1991).

In the summary above, it is interesting to note that once established these major NW-SE-trending shear zones have been reactivated a number of times during distinct tectonic episodes and have often been the focus for magmatism during such events. It is therefore concievable that if such structures exist beneath the cover sequences of the Northern and Grampian Highlands they are likely to show a long history of reactivation, accommodating deformation during major tectonic events, as such "major faults do not die" (Muehlberger 1986; see Section 9.7).

The Lewisian foreland may provide an analysis through the lower crust possibly providing information regarding the structural framework of the basement underlying such regions as the SW Highlands. This is because a Scourian crust of some 70 km thick for the NW Highlands has been suggested by Watson (1984), based on the fact that the Moho occured somewhere near its present position. With an estimated overburden of 45 km occuring above the present day surface deduced by Scourian metamorphic assemblages which are themselves approximately 25 km above the present position of the Moho (Watson 1984) indicates that the Lewisian crust now exposed was once part of the (mid- to) lower crust.

The structural characteristics of the Lewisian crust bears great similarities to those proposed for the 'structural architecture' of the lower crust beneath the SW Highlands (see Section 9.9). It is envisaged that the lower crust within the SW Highlands during Caledonian magmatism can be regarded as being composed of a series of crustal blocks ('low strain mega-augen') bounded by anastomosing zones of high strain. This pattern of structural interactions reflecting the major tectonic structures, i.e. the intersecting set of NW-SE-trending lineaments and NE-SW-trending shear zones developed at mid- to upper crustal levels respectively. The Lewisian foreland region may provide such an insight as the NW-SE-trending shear zones observed within this basement have been interpreted by Park and Tarney (1987) to be essentially bounding structures to major crustal blocks (see Fig. 2.31). Not only are the orientations and scale of these Lewisian shear zones comparable with those envisaged within the lower crust during Caledonian magmatism in the SW Highlands, but also the dimensions of the crustal blocks bounded by such structures. Park and Tarney (1987) and Coward (1987) also suggest that the Lewisian shear zones may link to flat lying crustal shear zones. This appears to be remarkably similar to the models proposed by Reston (1988) and Sanders (1991) from lower crustal seismic profiles which suggest that the lower crust can be envisaged as comprising of a series of low strain lozenges or mega augen bounded by anastomosing shear zones (see Section 9.9).

Although such structures may continue beneath the Moine, it appears to be very difficult to be able correlate them with major geologically-defined lineaments observed within the cover sequence (see Section 9.19). One possibility for this may lie in the fact that the Moine Thrust sheet was propagated towards the NW to WNW, possibly slightly displacing geologically-defined lineaments within the cover from their "parent" basement structures.

9.18 THE MOINE THRUST ZONE

9.18.1 Introduction

The Caledonian thrust zone of the NW Highlands shows many features typical of foreland fold-and-thrust belts (see Coward 1983). It has been traditionally regarded as the front of the Caledonian orogenic belt in Scotland. The direction of thrusting towards the foreland is strongly supported by the development of folded thrusts (e.g. Elliott & Johnson

1980; Butler & Coward 1984), and that, lower, later thrusts cut up through higher thrusts. The latter results in the older thrusts being carried in a "piggyback" fashion by displacements on lower thrusts. These relationships show that the most westerly thrust, the Moine Thrust (see Fig. 9.28), is the youngest of a system of Caledonian thrusts. This includes two major further thrusts, the Naver and Swordly thrusts which divide the Moine metasediments into three nappes incorporating slices of Lewisian basement which have been brought to the surface. As mentioned above, the thrust system has been interpreted as a foreland propagating sequence, in which older more ductile thrusts progressively gave way to younger more brittle thrusts (see Barr *et al.* 1986; Butler 1986). Active motion on the Moine Thrust is regarded to have occured between 430-425 Ma based on radiometric dates for igneous intrusions within the Assynt area (van Breeman *et al.* 1979; Halliday *et al.* 1986). In terms of the regional structural framework of the NW Highlands, this thrust has been interpreted as being syn- or post-D3 (Kelley & Powell 1985).

9.18.2 The internal structure of the Moine Thrust sheet

The Moine Thrust belt is characterised by a number of major structural features. These include:

(i) The thrust surfaces are rarely planar, often showing a staircase geometry of "flats" and "frontal ramps". The flats are generally developed along bedding planes ("easy-slip horizons") and are connected to ramps which cut up stratigraphic section in the direction of transport. Assymetric folds are commonly developed above these ramps (see Berger & Johnson 1980; Coward & Potts 1983; Coward 1983);

(ii) Low angle extensional faults occur along the whole length of the Moine Thrust belt, but are exceptionally common in the Assynt region (Fig. 9.28). These structures, together with contractional imbricate faults and strike-slip faults, essentially enclose a system which has been termed a "surge zone" (Coward 1982; Coward 1983), used to describe a fault bounded unit which has propagated faster than the surrounding parts of the sheet. This leads to the development of these extensional faults at the rear of the zone and arcuate imbricate contractional faults at the leading edge. One such surge zone in north Assynt has been displaced 1.75 km NW than its neighbouring rocks (Coward 1982). The position of these structures and how their development may relate to NW-SE-trending lineaments is discussed in Section 9.19;

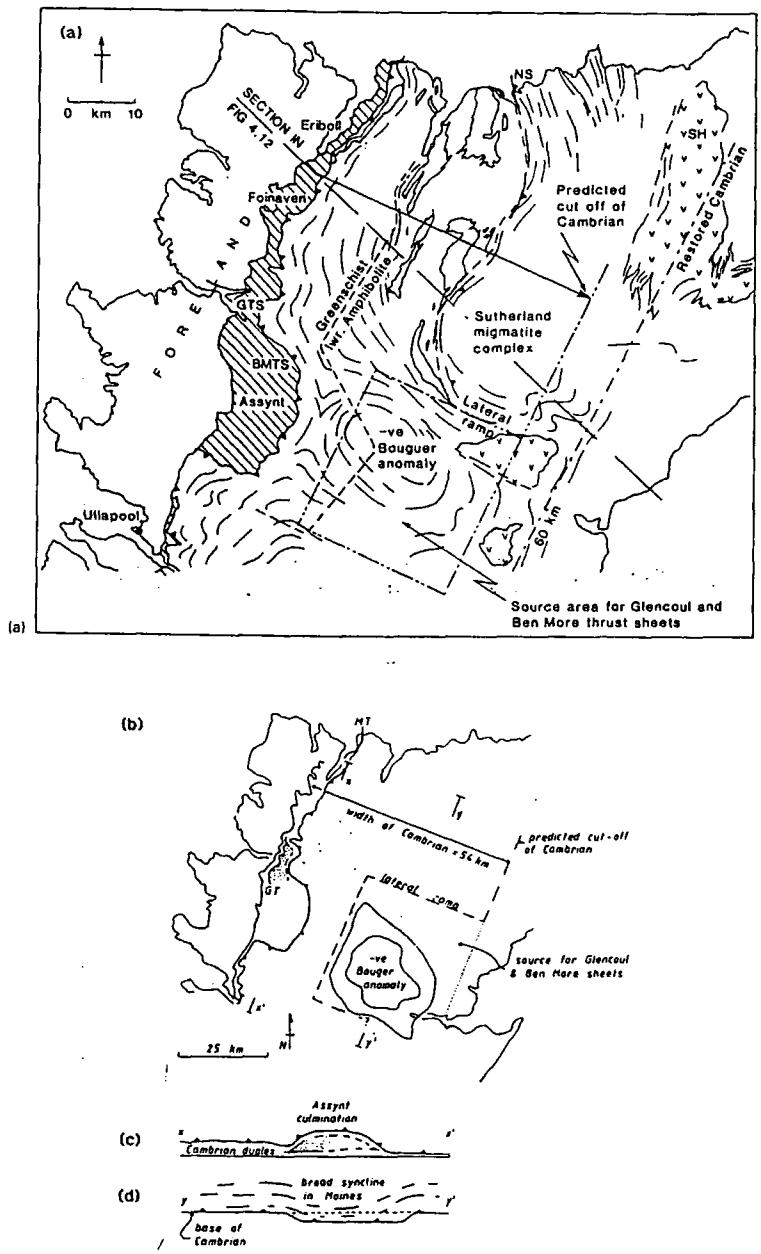

Fig. 9.32. **(a)** Interpretation of crustal structure in northern part of Moine Thrust sheet based on geophysical data and restored sections. Foliation trends define culminations or bulges in the footwall of the Moine Thrust. The approximate width (≈54 km) of the Cambrian shelf is indicated by the showing cut-off of Cambrian in the footwall of the Moine Thrust. In a restored section of the thrust belt Cambrian would lie S of the line marked 'Restored Cambrian'. GTS, Glencoul thrust sheet; BMTS, Ben More thrust sheet; NS, Never slide; SH, Strath Halladale granite. Lewisian inliers are stipled. After Butler and Coward (1986). A model for gravity data shown by: **(b)** Sketch map of northern Scotland; **(c)** longitudinal section; and **(d)** longitudinal section. After Butler and Coward (1986).

(iii) Several places occur along the Moine Thrust Zone where the thrust sheet has been thickened causing a culmination (upwarp or bulge) in the Moine Thrust. The differential uplift is caused by a laterally fault bounded block (or "horse") becoming accreated onto the developing thrust belt (Boyer & Elliott 1982; Butler & Coward 1984). The classic example of a culmination is Assynt, represented topographically by the "Assynt Window" (Fig. 9.32). The Assynt culmination appears to be essentially bounded by NW-SE-trending crustal lineaments, and several smaller culminations may be associated with such structures. This may suggest that movements along these NW-SE-trending lineaments were at least in part responsible for the development of these 'upwarps' (see Section 9.19);
(iv) Layer-parallel ductile shortening results in the development of buckle folds (plane strain features). However, in more brittle conditions along the development of frontal ramps, back thrusts may develop and the eventual formation of the frontal ramp will result in an isolated fault-bounded 'unit' which is uplifted relative to its surrounding rocks (see Butler & Coward 1984). These are referred to as "pop-up" structures (Elliott 1981). In north Assynt a different zone of deformation has been recognised by Coward and Kim (1981) comprising of oblique folds and finite strains in Cambrian metasediments (Pipe Rock). This has been interpreted as being produced by differential movement, leading to the development of a left-lateral couple resulting in the northern part of the zone being displaced by some 3-5 km NW with respect to the southern part. It is also interesting to note that this anomalous zone of deformation corresponds to the trace of the NW-SE-trending Loch Shin line (see Section 9.19).

9.18.3 Models proposed for the initiation and driving mechanism of the Moine Thrust Zone

Two possible models for the initiation and driving mechanism of the Moine thrusts have been considered by Coward (1983):

① A model based on a late period of regional compression, resulting in crustal uplift and thickening of the cover sequence (Fig. 9.33). During this phase it is envisaged that the early thrusts were developed, with late movements possibly due to gravitational spreading from the uplifted region. The latter event possibly explaining the development of the late low-angle extensional faults as described above.

② Another model which does not entail any late phase of crustal compression, but considers the driving mechanism to have been produced by a process of gravity spreading from the Central Highlands (Fig. 9.33). The thickening of the Central

Highlands originally being caused by the Grampian orogeny and then subsequently by the intrusion of the late Caledonian granitic masses.

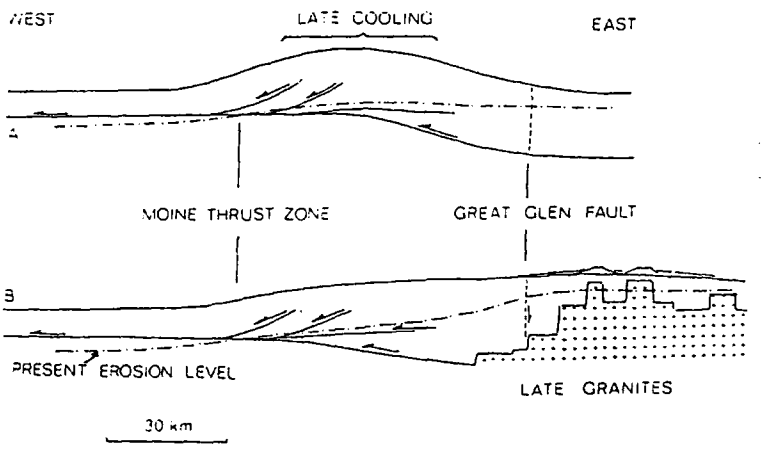

Fig. 9.34. Two models for the development of the Moine Thrust zone. Mainly after Coward (1983).

There are several problems with both models (see Coward 1983). In the first, involving crustal compression, the main problem is that during the period of active motion on the Moine thrust (approximately 430-425 Ma; see above) there was no apparent collision in Scotland which could be attributed to such deformation, and the Grampian deformation within the Central Highlands had finished. The major problem with the gravity spreading model is that for such a mechanism to have been operating throughout the Moine thrust belt, the average dip of the Moine Thrust must be low so as not to hinder gravitational forces. However, work by e.g. Soper and Barber (1982), Brewer and Smythe (1983, 1984) suggest that along parts of the Moine Thrust, the fault is steep and may form a ramp structure. However, more recently McBride and England (1994) have proposed that the Moine Thrust is a more or less planar surface which penetrates the entire crust (see also Andrews 1985).

An alternative model for the development of the Moine Thrust Zone

An alternative model which basically encompasses both types of process proposed by Coward (1983), but may overcome the problems inherent in both models, is proposed below.

It is proposed that the cover sequence in the south-eastern Northern Highlands was underthrust by a 'basement wedge' which is charcterised by E-W-trending lineaments (see

Sections 9.20 & 9.23). It is envisaged that this NW-directed thrusting resulted in the elevation and thickening of the Moine in its hanging wall. The actual initiation and driving mechanism of the early Moine Thrust system is envisaged to have been produced by a late period of regional compression associated with deformation in the Grampian Highlands induced by movements along the NE-SW-trending shear/fault system and the NW-SE-trending lineaments. In the NE Highlands a third set of E-W-trending lineaments may have also been operating during this event. As discussed in Section 9.9 the Grampian lower crust could be regarded as comprising a series of 'blocks' bounded by anastomosing shear zones related to the shear zone/lineament system established within the mid- to upper-crust and major tectonic structures within the underlying mantle. The whole system is essentially bounded by the Great Glen fault in the north and the Highland Boundary fault zone in the south. It is envisaged that transpressive motion along the Caledonian NE-SW-trending bounding structures and along associated sub-parallel shear zones developed within the Grampian region, is transferred to non-transpressive motion at lower crustal levels (see Ch. 10, Section 10.3). This allows the 'blocks' in the lower crust to undergo a gross clockwise rotation in order to accommodate the overall sinistral deformational component imposed on the whole system; thus, explaining the development and distribution of granitic suites within the Grampian Highlands, with the Argyll Suite occuring in a "convergent zone" (a region of intense crustal thickening), whereas the Cairngorm Suite in the NE Highlands lies in an overall "extensional zone" (corresponding to the region of least tectonic thickening within the Grampians). Due to the geometry of the whole system, with increasing deformation it would seem necessary that movements along the NW-SE-trending lineaments would have to increase in magnitude towards the NE. It is apparent from Figure 9.34 that this overall deformation may have resulted in an increased separation of the Great Glen fault and the Highland Boundary faults in the NE. Although this is an extremely simple model, in what is obviously a very complex situation, the "extensional component" which increases towards the NE Highlands could in theory provide "crustal compression" needed to initiate and drive the Moine Thrust sheet. This "divergence component" would initiate the collapse of the 'Moine wedge' and the development of the Moine Thrust Zone. Such a model would explain why the direction of thrusting changed with time from an approximate NW trend to a WNW orientation (Bart et al. 1986; Strachan & Holdsworth 1988; Holdsworth 1989) (see Fig. 9.34).

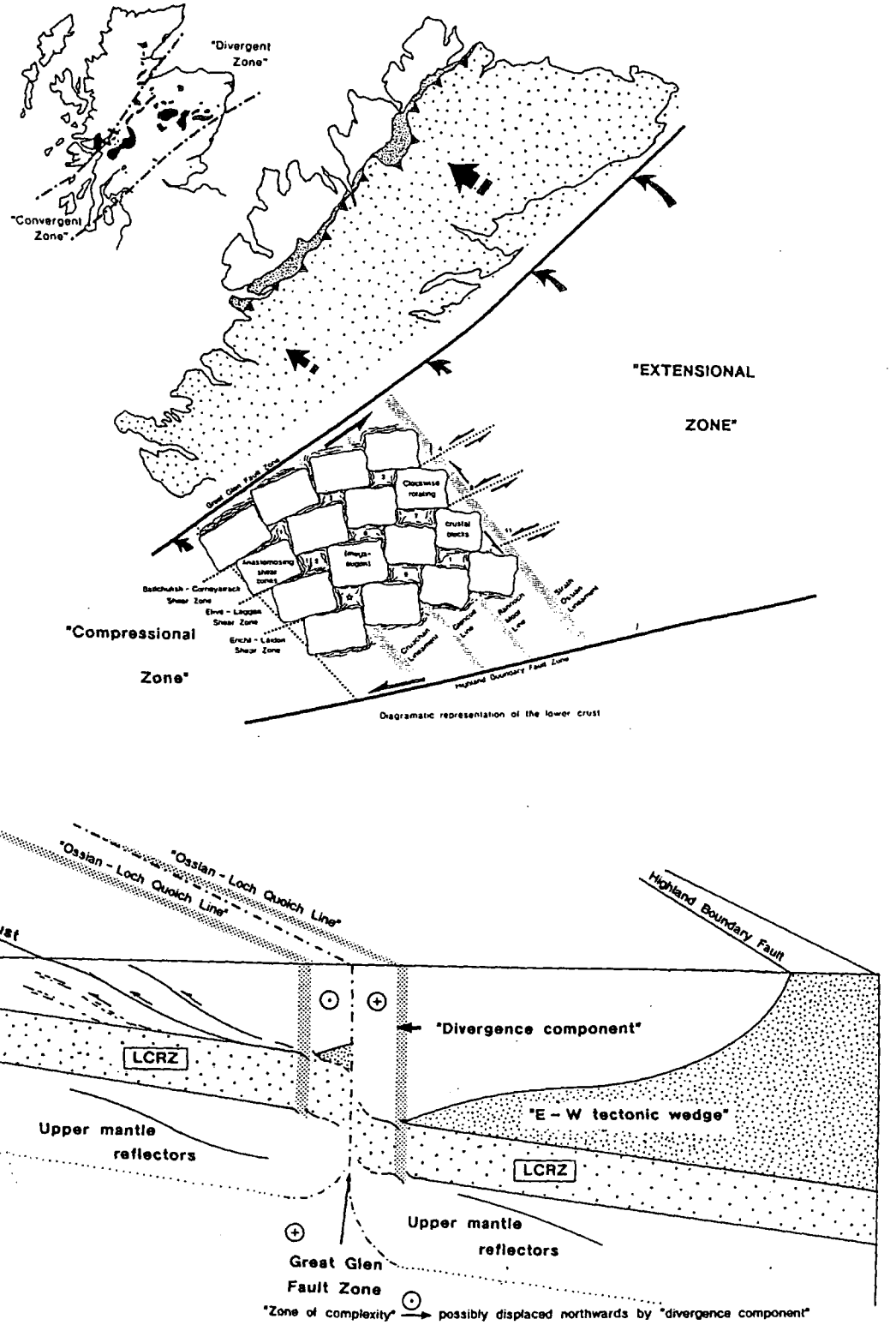

Fig. 9.34. (a) Possible structure of the SW Grampian crust showing rotation of 'blocks' at lineamental intersections between the Great Glen Fault and the Highland Boundary Fault. (b) Map showing the positions of the Argyll Suite in a 'convergent zone' and the Cairngorm Suite in a 'divergent zone' in the SW Grampians. (c) Generalised model showing the possible structure of the crust in northern Scotland and the possible initiation and development of the Moine Thrust zone.

The reason why thrusting should occur only to the north of the Great Glen fault and not to the south of the Highland Boundary fault may be due to the relative position of the lower crust on either side of the Great Glen fault. As shown on the LISPB profile (Bamford *et al.* 1978; Bamford 1979) (Fig. 9.27) there is an apparent downthrow to the SE of 3 km at the Great Glen fault. It is possible, because of the relative position of the upper detatchment zone of the lower crust (corresponding to the "Lower Crustal Reflectivity Zone"; see Ch. 10, Section 10.3), it may have acted as a decoupling surface which accommodated the "divergence component" produced within the Grampian Highlands and consequently initiated the development of the Moine Thrust system; developing into the floor thrust of the Moine Thrust belt (see Fig. 9.34).

9.19 LINEAMENTS CONTROLLING THE SITING OF CALEDONIAN MAGMATISM AND "GROSS OROGENIC FLOW PATTERNS" AND ASSOCIATED STRUCTURES IN THE NORTHERN HIGHLANDS

A number of geological features both within the 'Cambro-Ordovician cover sequence' (Moine Thrust sheet) and the Lewisian foreland region in the NW Highlands may suggest the presence of a number of major NW-SE-trending lineaments (see below). Such features include: (i) the linear distribution of appinitic intrusions; (ii) the distribution of late Caledonian plutons; (iii) the localisation of dyke swarms; (iv) the trend and location of major faults; (v) the geometry of regional fabrics ("gross orogenic flow patterns") and the possible development and distribution of certain types of structures, such as culminations, sheath folds, and back thrusts formed during the north-westward propagation of the Moine Thrust sheet; and (vi) the location and trend of major Lewisian shear zones within the foreland region, which when traced south-eastwards beneath the Moine Thrust sheet may roughly coincide with major geologically-defined lineaments present within the cover sequence.

It is proposed that these structures not only controlled Caledonian magmatism, such as: (i) the distribution of appinitic bodies; (ii) the siting of Caledonian plutons; and (iii) the possible control of emplacement dynamics, e.g. Rogart complex (see below), but also had a profound effect within the cover sequence during the development of the Moine Thrust zone. As shown by Figure 9.35 several geologically-defined NW-SE-trending lineaments may occur, including the Loch Shin line recognised by Bott *et al.* (1972) and Watson (1984).

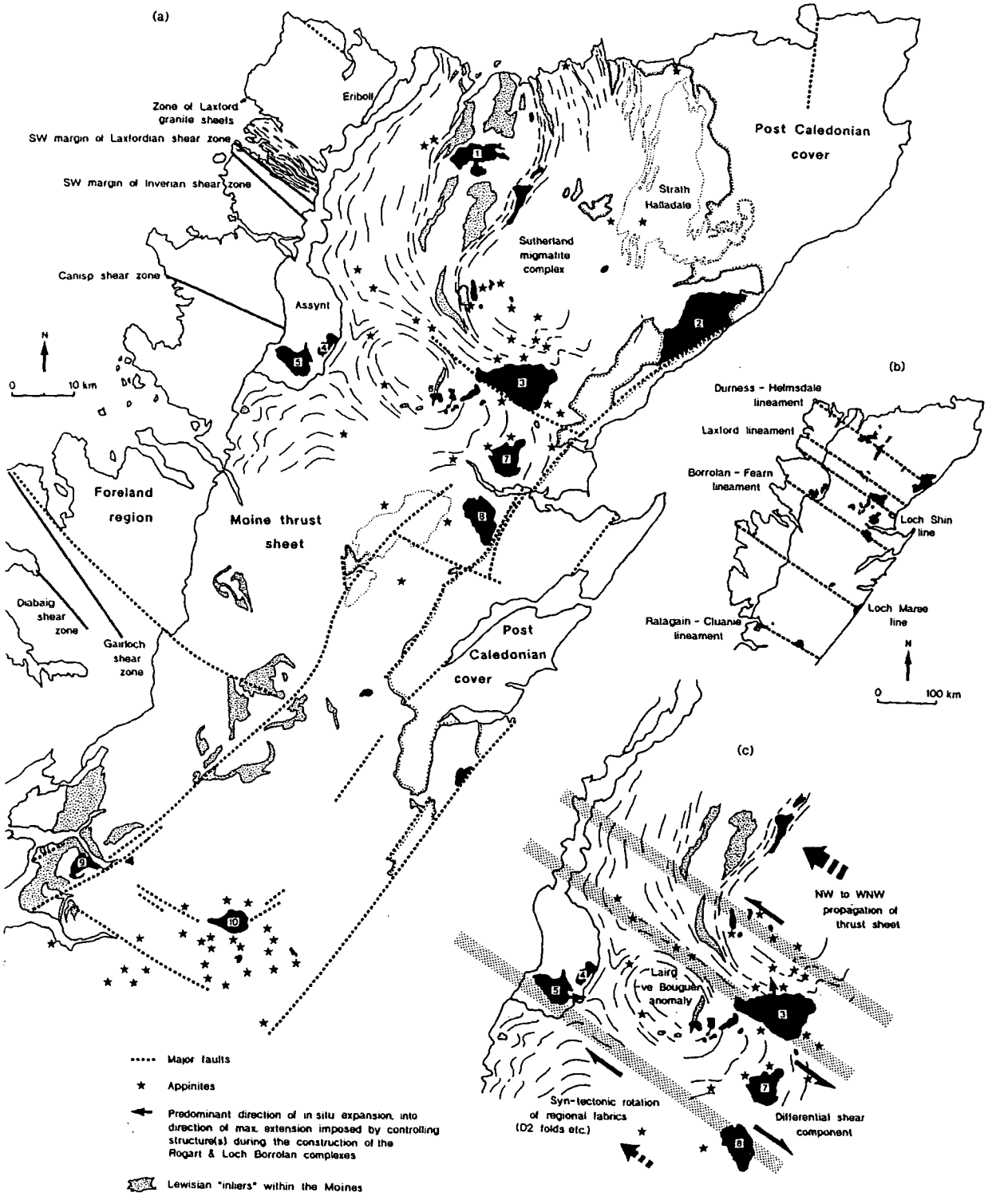

Fig. 9.35. **(a)** A map showing the distribution of appinitic bodies (after Smith 1979) and late Caledonian plutons within the Northern Highlands. Major faults and shear zones within the cover sequence and foreland region (after Park & Tarney 1987) are shown, together with foliation trends within the Moine Thrust sheet. **(b)** Position of the inferred NW-SE-trending lineaments in the Northern Highlands. **(c)** Sketch map showing the distribution of late Caledonian magmatism in association with major structural features. Sense of shear along major NW-SE-trending structures are shown, explaining foliation trajectory patterns within the northern region of the Moine Thrust sheet. Distribution of granitoids in the Northern Highlands: 1. Ben Loyal; 2. Helmsdale; 3. Rogart; 4. Loch Ailsh; 5. Borralan; 6. Grudie; 7. Migdale; 8. Fearn; 9. Ratagain; 10. Cluanie.

Moving from the NE to the SW these newly identified lineaments are named here as the Durness-Helmsdale, Laxford and Borralan-Fearn lineaments, the Loch Maree line, and the Ratagain-Cluanie lineament. The following information may demonstrate that these lineaments represent major basement penetrating structures:

The Durness-Helmsdale lineament

A NW-SE-trending lineament may pass directly through several late Caledonian igneous bodies (Fig. 9.35), the Ben Loyal syenite complex (including the Ben Loyal intrusion and two satellite bodies known as the Cnoc nan Cuillean and Ben Stumanadh syenites), a sizeable complex exposed in Strathnaver, a small body approximately 5 km SSW of Kinlorace which occurs directly along the lineament, and the large Helmsdale granitic complex. Several appinitic/ultrabasic intrusions (see Smith 1979) appear to be localised along this zone. Traced north-westwards into the Lewisian foreland region, the proposed crustal lineament coincides exactly with a major NW-SE-trending fault near Cape Wrath.

The Laxford lineament

If the trace of the NW-SE-trending Laxford shear zone (see Section 9.17) present within the Lewisian foreland region is continued beneath the Moine Thrust sheet it appears to coincide with several features within the cover sequence. A large number of appinitic/ultrabasic bodies (see Smith 1979) occur along part of this zone (Fig. 9.35). The lineament also coincides with several small, late Caledonian granitic bodies. A major geological feature in this area, is the marked change in the foliation trajectory pattern, with F2 folds modified into a curvilinear geometry (see Strachan & Holdsworth 1988). This change may be coincident with this NW-SE-trending zone. To the north of the Laxford lineament this "regional fabric" has a general NE-SW trend, but as the lineament is approached the 'fabric' undergoes a marked strike swing to a NW-SE orientation, parallel to and coincident with the lineament for some 10 kms or so (see Fig. 9.35).

The Loch Shin line

The NW-SE-trending Loch Shin line is expressed by both 'geologically- and geophysically-defined lineaments'. Geophysically it is defined by a strong gravity gradient, which has been related to the Laxford granite sheets and Laxford shear zone of the Lewisian foreland (Bott *et al.* 1972). The Laxford shear zone and associated granite sheets

however, occur approximately 10 km further NW, and appear to be coincident with the NW-SE-trending Laxford lineament defined above. The Loch Shin line is well defined 'geologically' by a number of features developed within the cover sequence (see below; see also Watson 1984), and raises the possibilty that either: (i) two distinct geologically-defined lineaments occur above two independent deep crustal lineaments; or (ii) one major NW-SE-trending basement fracture zone occurs, but has produced two geologically-defined lineaments within the cover sequence. The latter possibly resulting because the "original cover sequence lineament" was displaced by the north-north-westward propagation of the Moine Thrust sheet, and then the deep basement lineament within the underlying autochthon being reactivated to produce another geologically-defined lineament directly above it. During the latter reactivation of the basement it is possible that both 'geologically-defined cover sequence lineaments' were reactivated to give the impression that both occur directly above two idependent shear zones in the autochthonous basement. A model presented in Section 9.23 may suggest that two major independent crustal lineaments do exist.

A number of geological features within the cover sequence may define the position of the Loch Shin line. These include: (i) The linear distribution of a suite of appinitic/ultrabasic bodies (see Smith 1979; Watson 1984) (Fig. 9.36), known as the Ach' uaine hybrids (Read & Phemister 1925; Read, Phemister & Ross 1926). As with the volatile-rich shoshonitic-type appinitic bodies within the SW Highlands (French 1966; Wright & Bowes 1979; see Ch. 2), the Ach' uaine hybrids suggest that they have also been derived from a sub-crustal source indicating that the lineament must have at least reached lithospheric mantle depths. The siting of appinitic bodies along the Durness-Helmsdale lineament and the large concentration of appinites in the vicinity of the Ratagain-Cluanie lineament (see below) may suggest that these two geologically-defined lineaments are also sited above deep basement structures, possibly old shear zones within the underlying autochthon; (ii) The southern edge of the Rogart granitic complex (see Soper 1963) occurs along the trace of the NW-SE-trending Loch Shin line (Fig.'s 9.35 & 9.36, essentially bounded in the south by a series of NW-SE-trending faults, including the Muie fault and the major Strath Fleet fault (Fig. 9.37; see Soper 1963). The latter structure can be traced some 20 km at least along the Loch Shin line. An extremely high percentage of appinitic/ultrabasic bodies and dykes within this area occur within this fault system. The emplacement of the Rogart complex is discussed below, providing important implications for the sense of movement along the Loch Shin line during its construction.

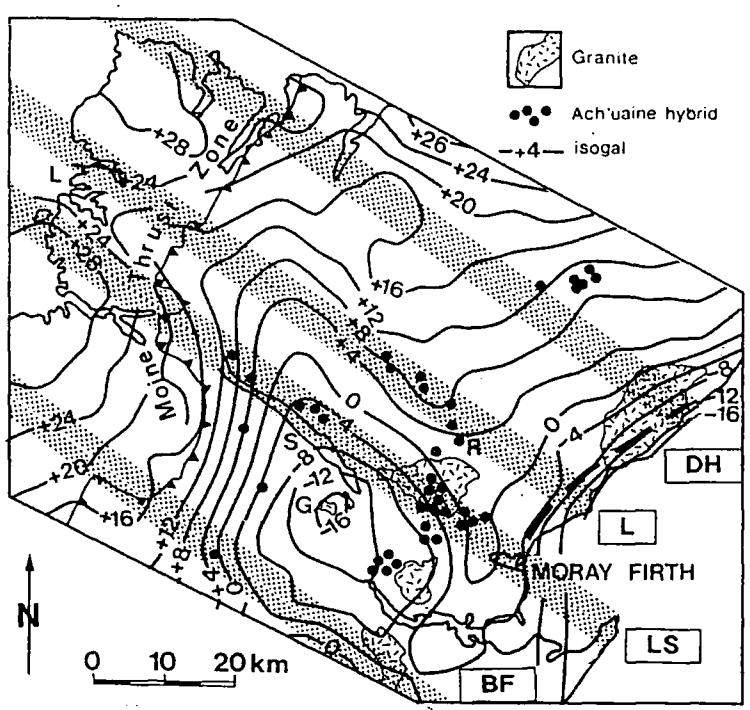

Fig. 9.36. Distribution of appinites (Ach'uaine hybrids) and late Caledonian granites in relation to the negative gravity anomaly centred on the Grudie granite (G). The Durness-Helmsdale, Laxford and Borralan-Fearn lineaments and Loch Shin line have been superimposed from Figure 9.35 onto this diagram. Modified after Watson (1984).

The Rogart complex: implications for sense of shear along the Loch Shin line

Rogart is one of the largest (approximately 65 km^2) late Caledonian granitic complexes in the Northern Highlands (Fig. 9.37). The complex was first surveyed by Hugh Miller in 1890 to 1894 (*quoted in* Read & Phemister 1925), and then subsequently by Read and Phemister (1925; BGS Sheet 103), followed by Read, Phemister and Ross (1926; BGS Sheet 102). A more comprehensive study of the petrological distribution of intrusive phases, their internal deformational characteristics and country rock structures related to the emplacement of the pluton was carried out by Soper (1963).

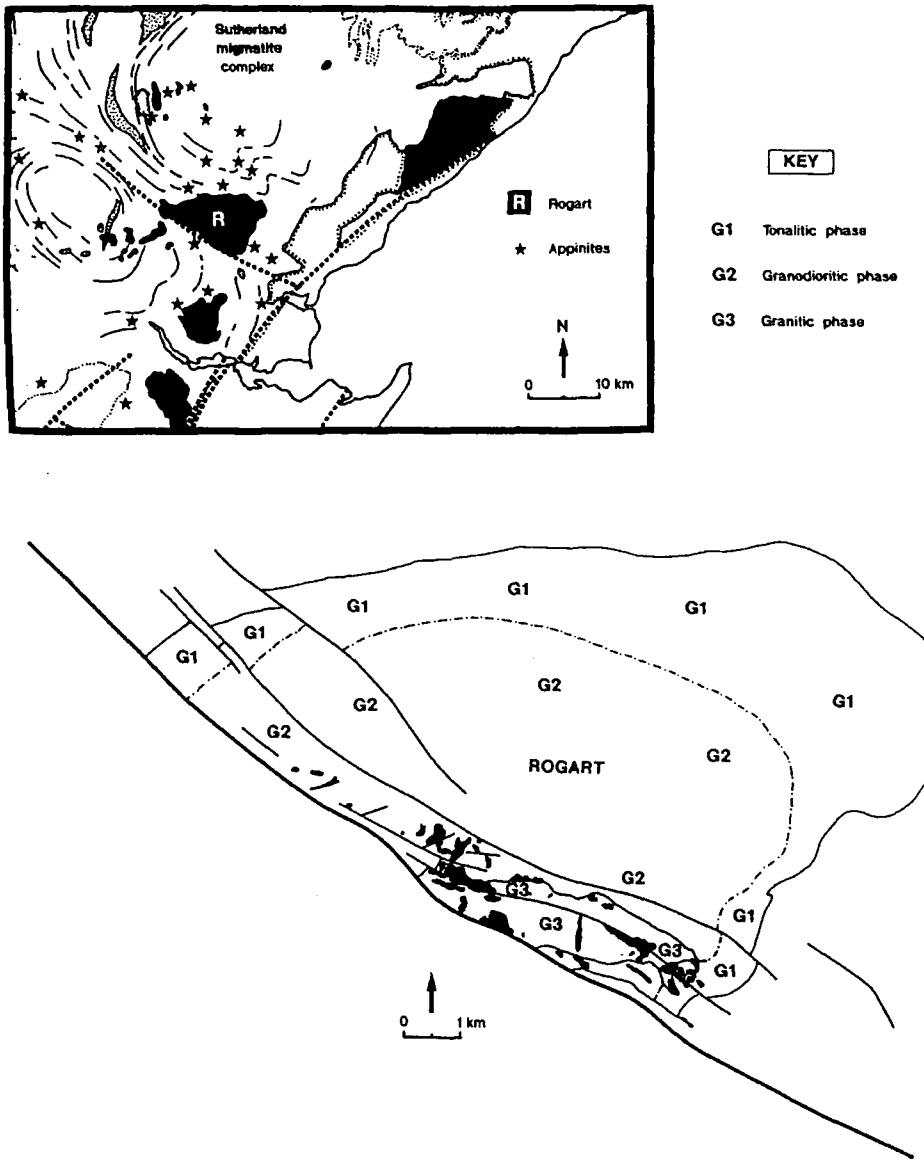

Fig. 9.37. Sketch map of SE Sutherland showing the position of the Rogart granitic complex, the distribution of its major intrusive components, and the major tectonic structures within the region. Largely after Soper (1963).

Based on the detailed petrological distribution maps, and foliation trajectory and lineation maps produced by Soper (1963), the microstructural characteristics of the fabrics developed within the major internal intrusive phases of the complex were studied during this current investigation by the author and J. R. Reavy. The aim of this study was not only to investigate the emplacement processes operating during its construction, but more importantly to test the hypothesis that the NW-SE-trending Loch Shin line had been a major influencing structure during its intrusion, and if so what was the shear sense ?

Detailed descriptions of the internal deformational characteristics, including fabric type, strain distribution and local emplacement phenomena of the pluton will be discussed elsewhere. However a summarised account of the emplacement characteristics of the pluton (Fig. 9.38) is provided below: (i) Rogart is a normally zoned pluton consisting of three major intrusive components (Fig. 9.37 & 9.38; see Soper 1963):

G1: a tonalitic phase;
G2: a granodioritic phase;
G3: a granitic unit.

❶ The boundary between the tonalite (G1) and granodiorite (G2) is transitional, suggesting fairly contemporaneous emplacement. However, the contacts between these two intrusive phases (G1/G2) and the later granitic phase G3 is sharp, and microstructural evidence suggests a significant time lapse, with the granitic magma being emplaced into the complex after both the tonalite and granodioritic units had fully crystallised.

❷ The pluton is bounded in the SW, and sited along the NW-SE-trending Strath Fleet fault system (corresponding to the trace of the Loch Shin line) (Fig. 9.37). In the NE, running through the adjacent country rocks, the NW-SE-trending Laxford lineament may essentially bound the complex in the north (see below).

❸ The deformation fabric throughout all three intrusive phases can be generally described as being pseudoconcentric, with the planar fabric in the tonalite (G1) and the granodiorite (G2) being somewhat contact parallel with the pluton margin, and the fabric in the granitic phase being sub-parallel to its contact with the two earlier intrusive units (Fig. 9.38).

In the north and east of the complex, the tonalite and granodiorite phases possess a weak to moderately developed pre-full crystallisation (PFC) fabric which intensifies towards the pluton margin. In the east the PFC fabric is steep to moderate (50-85°) outward-dipping, and becomes progressively less steep (around 40-50°) in the NE. Moving from the north-eastern part of the complex towards the north the inclination of the PFC fabric, in general, slightly increases to approximately 50-60°. This is combined with a progressive increase in fabric intensity and a slight modification by a relatively high temperature, coplanar solid state deformational overprint. This crystal plastic strain (CPS) deformation

increases moving towards the west of the complex, coeval with a rapid change in the dip direction of the fabric from outwards-dips to steeply inward-dipping.

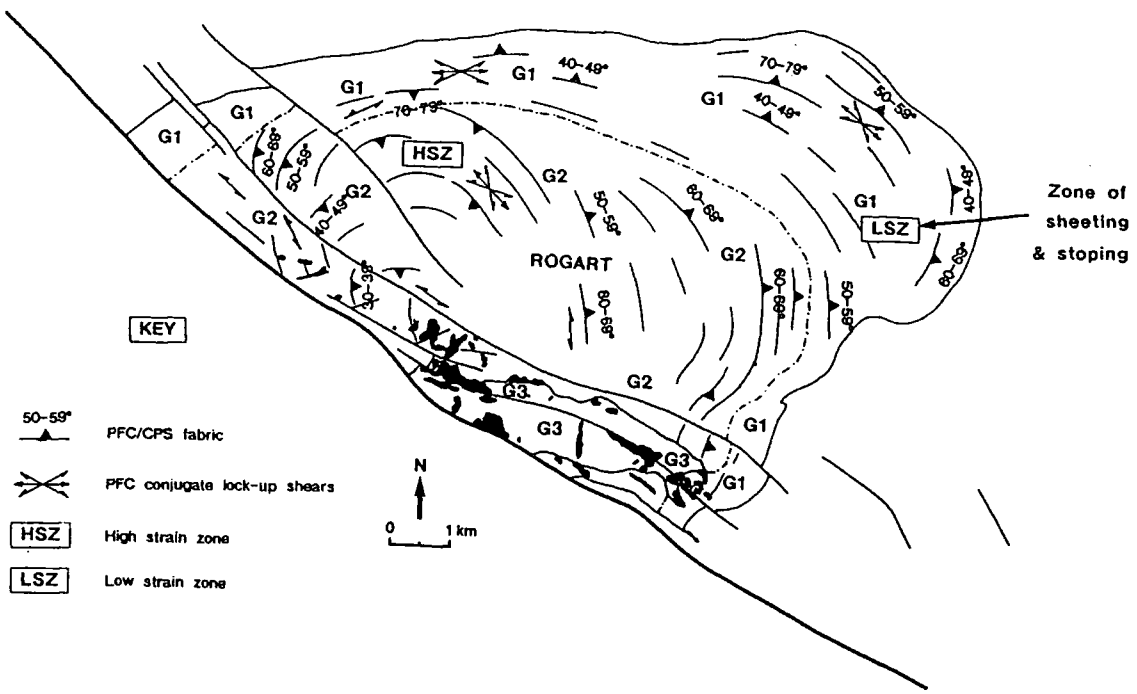

Fig. 9.38. Generalised sketch map showing fabric orientation, PFC conjugate shears and localised emplacement phenomena throughout the Rogart granitic complex. Partly after Soper (1963).

The type of fabrics, their intensity, and X/Z ratios of microdioritic enclaves (where observed) in both the tonalite (G1) and granodiorite (G2) units suggests that deformation within the complex can be divided into two zones: a low strain zone in the east and NE of the complex, and a high strain zone in the west (Fig. 9.38). The low strain zone is characterised by weak to moderately developed, outward-dipping PFC fabrics and the presence of a large amount of country rock material, including small xenoliths (cm's to m's across) and large "raft units" (up to several m's in length). This zone bears great similarities to the "zones of sheeting and stoping" within the Rannoch Moor (see Ch. 5) and Ballachulish (see Ch. 9) complexes, and raises the possibility that this too represents a localised emplacement phenomena (see below). However, in the area designated "the high strain zone" (see Fig. 9.38) in the west, it is envisaged that the deformation within this part of the complex was

of a much higher magnitude and continued for a short period into the solid state regime. Thus resulting in the development of a moderately developed high temperature CPS fabric (Plate 9.1).

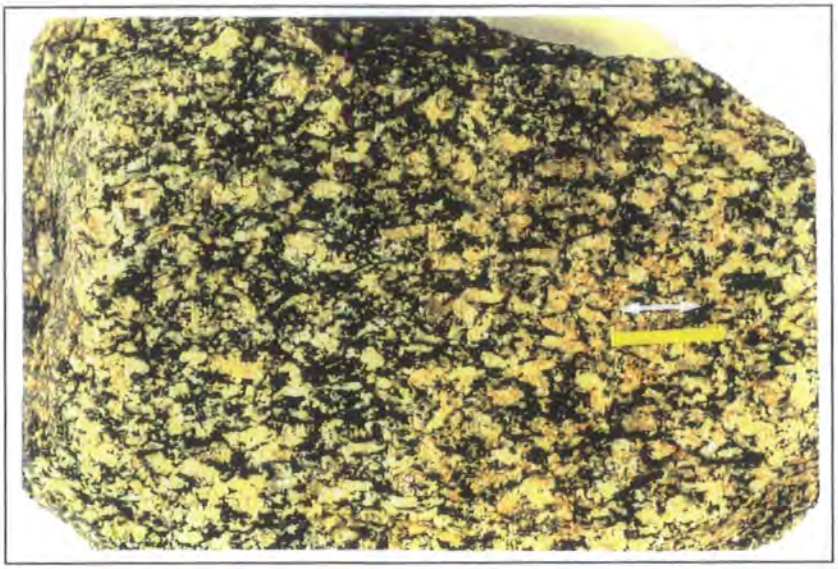

Plate 9.1. Hand-specimen of tonalitic phase from the western part of the Rogart complex ("High Strain Zone") showing an intense PFC fabric which has been overprinted by a relatively moderately developed, high temperature CPS fabric. (Yellow 'bar' approximately 2 cm long).

The later emplacement of the granitic phase (G3) is shown by: (i) the way it cuts across both the granodiorite-tonalite (G1/G2) "transitional" boundary; (ii) the way it has cut across both PFC and CPS fabrics within the two earlier phases; and (iii) the development of high to moderate temperature CPS fabrics within the granodioritic phase (G2) along the granite contact, suggesting that the granodiorite had fully crystallised and cooled significantly for the deformation related to the emplacement of the granite to occur in the solid state regime. The majority of the granite phase possesses an extremely weak fabric. Exceptions occur within the south of the complex, along the NW-SE-trending Strath Fleet fault and some of the associated minor faults (Plate 9.2). Fabric trajectory patterns and microstructural observations suggest that the Strath Fleet fault and possibly some associated minor structures were active shear zones during magma emplacement. The localised development of high to low temperature solid state fabrics along these structures suggest that the deformation (movement) continued down-temperature into the solid

state regime (Plate 9.2 & 9.3). Shear sense indicators within the resultant CPS fabrics suggest a sinistral component of shear during their development, which is consistent with an overall environment of sinistral deformation during the construction of the complex (see below). However, breccias and cataclasites along many of the structures associated with the 'Strath Fleet fault system' suggest a later period of reactivation with a reverse sense of motion (a dextral component).

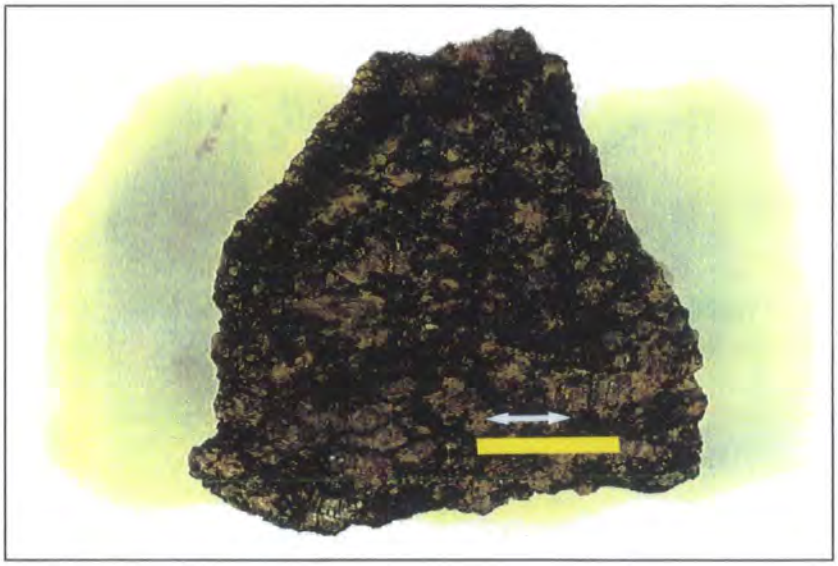

Plate 9.2. Hand-specimen of granodioritic material from the south-western part of the Rogart complex. It possesses a relatively moderately developed, moderate to low temperature CPS fabric. (Yellow 'bar' approximately 2 cm long).

❹ The tonalite (G1) and granodiorite (G2) possess a sub-horizontal mineral stretching lineation which generally increases in intensity towards the pluton margin. The tonalite phase, in general, contains the most intense lineation defined by both prismatic hornblende and euhedral sphene. The lineation is generally horizontal, or pitches gently (up to 20°) towards the south (Fig. 9.38).

The axis of both microdioritic enclaves (where observed) and lenticular country rock xenoliths lie parallel to the sub-horizontal mineral stretching lineation.

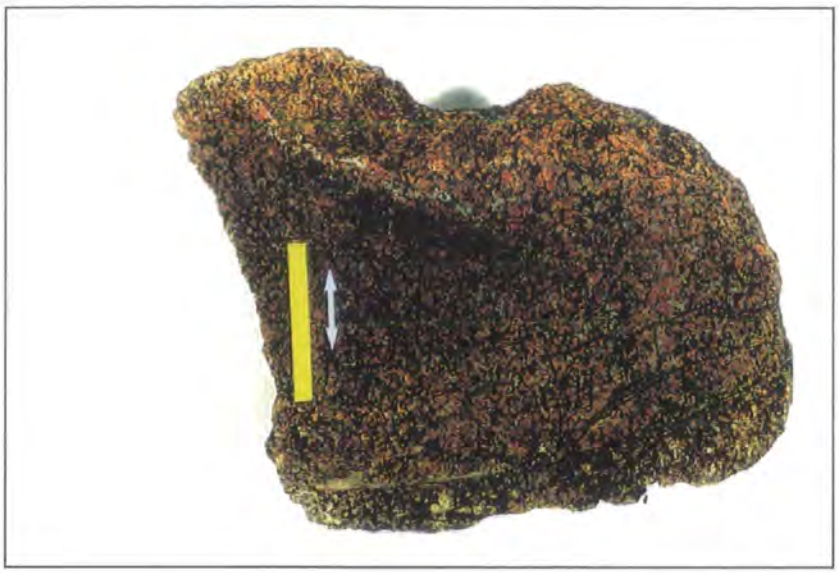

Plate 9.3. Hand-specimen of granitic material from the south-western part of the Rogart complex. It possesses a low temperature CPS fabric, which has developed within a localised zone along the Strath Fleet fault. (Yellow 'bar' is approximately 2 cm long).

❺ The three-dimensional shapes of microdioritic enclaves where observed within G1 and G2, suggest an overall bulk shortening component. X/Z ratios of the enclaves show an apparent slight increase in strain towards the pluton margin, and K-values consistently between 0 and 1 ("flattening strains").

❻ Discrete PFC conjugate, ductile 'lock-up' shears developed within both G1 and G2 show a bulk horizontal extensional component parallel to the fabric direction.

❼ Within the surrounding country wall rocks a sub-horizontal extensional component is also seen. Around certain parts of the complex the country rock possesses a ductile planar fabric. Where thick semi-pelitic horizons occur the deformation has often produced boudins (see Soper 1963).

Model proposed

A simple model to account for all these features could be:

❶ The complex as a whole, including G1, G2 and G3, was constructed by a process of *in situ* expansion (Fig. 9.39). This led to the development of a pervasive, weak to moderately developed, fairly pseudoconcentric PFC fabric due to the imposition of predominantly "flattening-type strains". This is verified by : (i) the three-dimensional analysis of microdioritic enclaves (where observed); (ii) the moderate to intensely developed sub-horizontal stretching lineation (Fig. 9.38); (iii) boudinage formation in the country wall rocks; (iv) the development of PFC conjugate ductile shears which show that the imposition of expansion-related strains continued during the last stages of pre-full crystallisation deformation; and (v) a progressive increase in fabric intensity towards the pluton margin. "Forceful" emplacement of both the tonalite (G1) and granodiorite (G2) was proposed by Read and Phemister (1925). This was confirmed by Soper (1963), concluding "that the central granodioritic complex is of magmatic origin and that the tonolite-granodiorite portion was emplaced forcefully". Also substantiated by "analysis of the deformation of 'regional' linear structures around the complex confirms the forcefully intrusive nature of the igneous mass" (Soper 1963).

❷ As the pluton body continued to 'inflate' and earlier intrusive components crystallised, localised, high to moderate temperature CPS fabrics were produced at petrological contacts (as seen along parts of the contact between G2 and G3) as the imposed deformation proceeded into the solid state regime.

❸ It is envisaged that a major NW-SE-trending ductile shear zone was active along the south-western margin of the complex during its construction (Fig. 9.39). It is sited directly along the trace of the proposed Loch Shin line, and is represented by the Strath Fleet fault system. It is proposed that the Loch Shin line represents a major basement penetrating structure which was reactivated during late Caledonian magmatism. The occurrence of numerous small appinitic/ultrabasic bodies (Plate 9.4) within the south of the complex (essentially within the Strath Fleet system), occasionally showing synplutonic relationships with the granodiorite (G2) and granitic (G3) phases, suggest that the 'Loch Shin line' was operating throughout the construction of the Rogart complex, "tapping" appinitic/ultrabasic magmas of sub-crustal origin.

Plate 9.4. Hand-specimen of ultrabasic material (Ach'uaine hybrids) from the south of the complex (essentially within the "Strath Fleet Fault system"). It may possess a weak to moderate PFC fabric which is defined by mafic crystals. (Yellow 'bar' is approximately 2 cm long).

❹ The close proximity of the NW-SE-trending Laxford lineament may suggest that the Rogart complex was essentially bounded to the north by this structure (Fig. 9.39). The possible syntectonic rotation of regional fabrics along both the Laxford lineament (see above) and the Loch Shin line (see Fig. 9.35) may suggest that both structures possessed a sinistral component of shear during the north-westward propogation of the Moine thrust sheet. It is envisaged that this deformational component along both lineaments was also operational during the construction of the Rogart pluton. This would explain: (i) the overall distribution of strain throughout the complex; (ii) the localised emplacement phenomena of sheeting and stoping within the eastern part of the complex; and (iii) the high to low temperature solid state fabrics which suggest a sinistral sense of deformation along parts of the Strath Fleet fault system.

It is suggested that the NW-SE-trending Loch Shin line was a major sinistral ductile shear zone during the construction of the Rogart complex. The first major phase of activity was the intrusion of the Ach' uaine hybrids which were emplaced into the cover sequence via this deep crustal lineament. The Loch Shin line not only sited and controlled granitic magma, but also controlled the emplacement dynamics of the pluton. It is envisaged that sinistral transcurrent motion along this structure,

and possibly the Laxford lineament in the north, which may have been acting as a bounding structure, allowed magma to laterally expand into the direction of maximum extension imposed by this system (Fig. 9.39). The maximum expansion direction would have been orientated approximately NNW, explaining the development of the high strain zone in this part of the complex. As 'ballooning' continued, early PFC fabrics within this extension direction were progressively modified and overprinted by a solid state overprint. However, in the eastern part of the complex, strains are considerably lower and it appears that simultaneous sheeting and stoping within this region occur where magma rose within the zone of maximum construction of the overall system (Fig. 9.39).

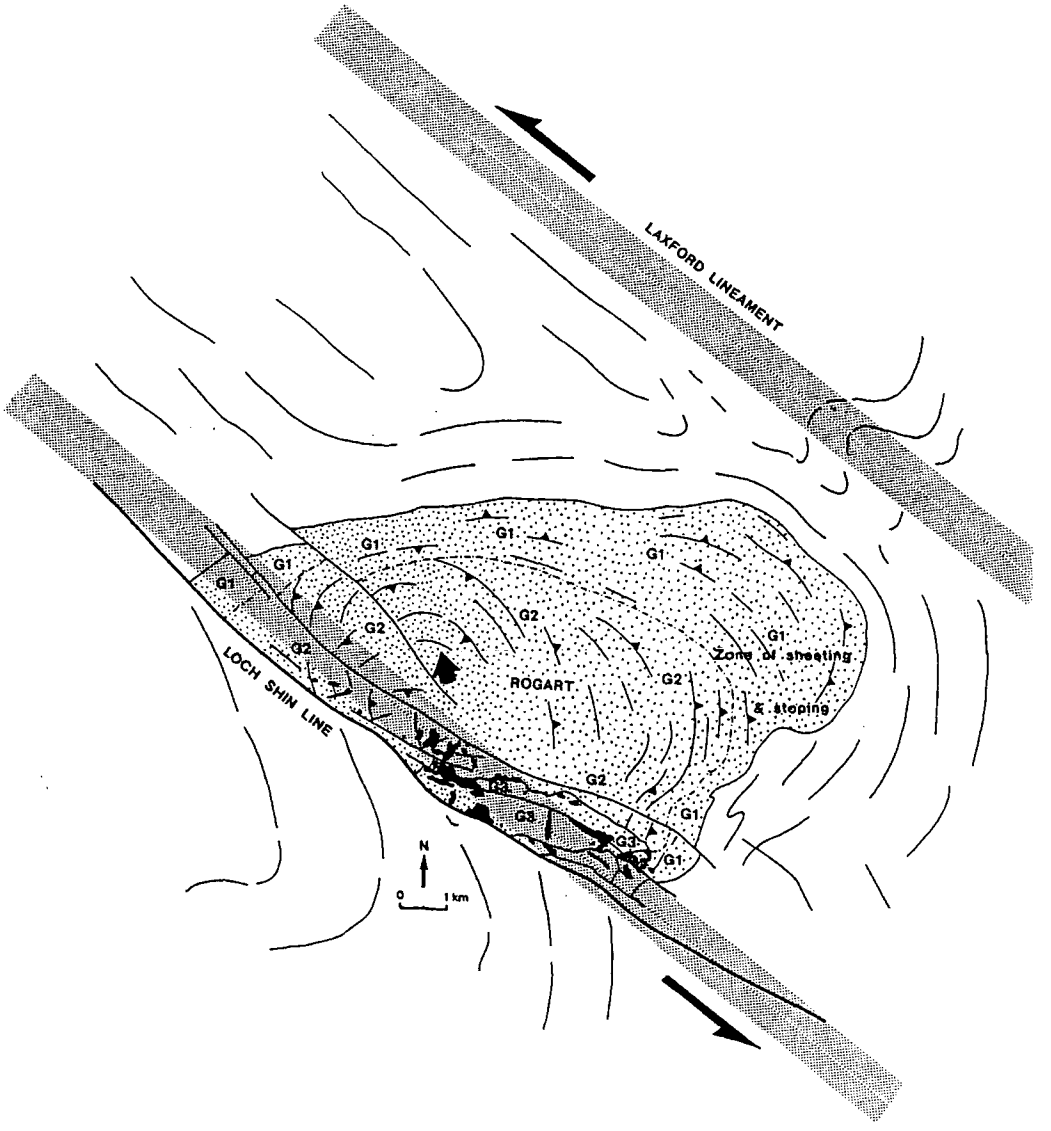

Fig. 9.39. Generalised model for the emplacement of G1 (tonalitic phase), G2 (granodioritic phase), and G3 (granitic unit) of the Rogart granitic complex.

In summary : a sinistral sense of shear along the NW-SE-trending Loch Shin line and possibly along the Laxford lineament is inferred to have occured during the construction of the Rogart complex. A sinistral component of deformation along these lineaments may not only explain the pluton's emplacement characteristics, but also the gross regional strike-swing which occurs in the vicinity of these two proposed structures (see Fig. 9.35). As previously mentioned, it is also interesting to note that in north Assynt an anomalous zone of deformation, comprising oblique folds and finite strains (Coward & Kim 1981), occurs within the vicinity of the Loch Shin line. Coward and Kim (1981) have proposed that its development was due to differential movement during the north-westward propagation of the Moine Thrust sheet, leading to the development of a left-lateral couple which resulted in the northern part of the zone being displaced some 3-5 km NW with respect to the southern part. It is therefore possible that this left-lateral couple is associated with the sinistral shear component established along the Loch Shin line during this period of deformation.

The Borralan-Fearn lineament

As with the Loch Shin line, the Borralan-Fearn lineament is expressed by both 'geologically- and geophysically-defined lineaments'. Geophysically both are defined by a strong gravity gradient, which essentially bounds the Assynt culmination (Fig. 9.36; see below).

The Borralan-Fearn lineament is defined geologically by a gross change in the "orogenic flow pattern" (Fig. 9.35). As with the Laxford lineament and Loch Shin line, this lineament appears to mark a major strike swing in the regional fabric pattern, with F2 folds modified into a curvilinear geometry (see Strachan & Holdsworth 1988). A dextral shear component along the Borralan-Fearn lineament may explain this regional fabric geometry (Fig. 9.35). The Borralan-Fearn lineament may coincide with the south-western flank of the Borralan complex and to the south, pass directly through the Fearn pluton. Very few appinitic bodies occur directly along the lineament, but instead several large NW-SE-trending lamprophyric dykes (or 'minette' dykes; see Smith 1979 (see below)) are localised along its trace, marking the north-western edge of the "Assynt window". This minor intrusive phase has been related to the appinitic suite (see Hunter & Rock 1987); thus assumed to be sub-crustal in origin. Smith (1979) made an interesting comment about faulted lamprophres recorded from the Strath Fleet fault, "that this fault marks the north east edge of the Assynt culmination, while the south west margin is defined by a local concentration of thick minette dykes, presumably intruded along fissures, which extend almost across the full width of the Moine outcrop". Both NW-SE-trending zones of

lamprophyre ('minette') dykes correspond to the Loch Shin line and Borralan-Fearn lineament. This may suggest that the geologically-defined Borralan-Fearn lineament represents a structure which reached at least lithospheric mantle depths, explaining the distribution of NW-SE-trending lamprophyric dykes along this zone.

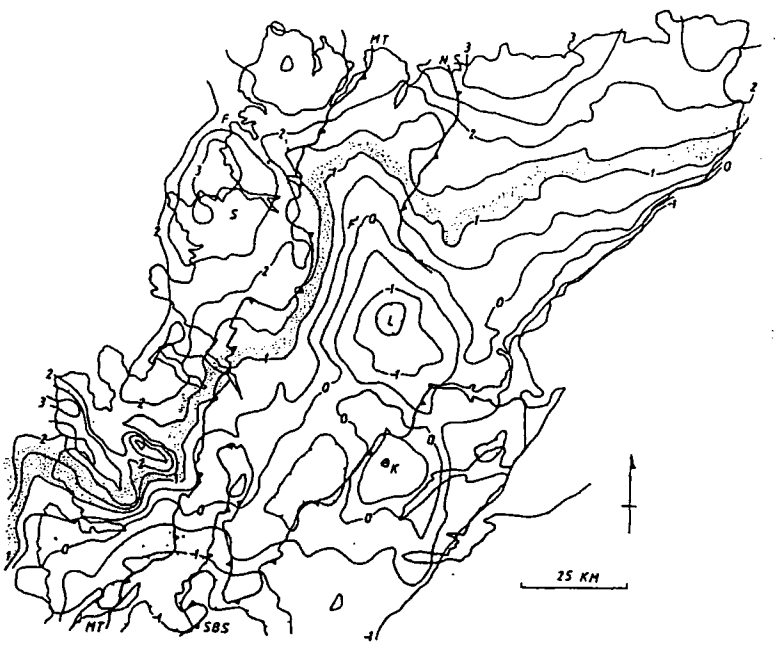

Fig. 9.40. Bouger gravity anomaly map of northern Scotland (after Hussain & Hipkin 1981). Contours are in 5 mGals. Major displacement zones are marked; MT, Moine Thrust; SBS, Sgurr Beag slide; NS, Naver slide. F-F', Laxford front anomaly; S, positive gravity anomaly associated with Scourian granulites; L, negative gravity anomaly around Lairig; K, positive gravity anomaly. After Butler and Coward (1984).

The Borralan-Fearn lineament and the Loch Shin line appear to bound a prominent Bouger gravity anaomaly low (see Hussain & Hipkin 1981) (Fig. 9.40) which is centred on the Grudie granite pluton (Fig. 9.36). This negative gravity anaomaly occurs directly behind the Assynt culmination and has been interpreted by Butler and Coward (1984) as representing a zone of thicker metasediments which has been produced by a process of downwarping (Fig. 9.33). Equally likely, is that the anomaly represents a large, relatively unexposed granitic mass (see Woollett 1988), represented at the surface by a few smaller bodies (the Grudie pluton). The magnetic anomaly over this area has also been interpreted as representing a granite intrusion (Powell 1970). It could be possible that the "downwarping" process proposed by Butler and Coward (1984) could have, in some way, provided the space for granite magma to exploit. The Loch Shin line and Borralan-Fearn lineament may therefore essentially bound a large granitic complex. The sense of shear

along these structures, inferred from the apparent rotation of regional fabrics (D2 folds etc; see Fig. 9.35), and the construction of the Rogart pluton along the Loch Shin line, may suggest that a 'differential shear component' was established across this region, during the north-westward propagation of the Moine Thrust sheet and emplacement of the many late Caledonian plutons localised within this area. This 'differential shear component' may help to explain the development and distribution of certain types of structures such as culminations, sheath folds, back thrusts, anomalous zones of deformation (e.g. oblique folds), and "surge zones" which are common within this region (see sub-section 9.18.2).

The Loch Maree line

Geologically this lineament is defined by the NW-SE-trending Loch Maree fault, which extends some 60 km or so, across both the Lewisian foreland region and the cover sequence of the Moine thrust sheet (Fig. 9.35). In the foreland region, the Loch Maree fault is coincident with a broad NW-SE-trending zone of Laxfordian deformation referred to as the Gairloch shear zone (see Park & Tarney 1987; Park *et al.* 1987; Lei Shihe & Park 1993). Within this zone are the supracrustal rocks of the Loch Maree Group which have been interpreted (see Park & Tarney 1987) as representing the metasedimentary infill of an early Proterozoic extensional rift basin (Fig. 9.31c), associated with the extrusion of primitive tholeiitic basalts.

If the trace of the Loch Maree fault is continued south-eastwards it would pass directly through a relatively small, late Caledonian granitic pluton which is sited along the north-western edge of the Great Glen Fault (Fig. 9.35), approximately 13 km SW of Inverness, near Abriachan. The lineament may also pass through the location of the Glen Urquhart 'inlier', an anomalous zone of supposed high grade Moine and Lewisian rocks and ultramafic bodies (pers. comm. R. E. Holdsworth 1996).

The Ratagain-Cluanie lineament

The Ratagain-Cluanie lineament is geologically-defined by several features (Fig. 9.35): (i) NW-SE-trending faults extend some distance (approximately 5-15 km) along the trace of the lineament; (ii) A large concentration of appinitic bodies occur within the vicinity of the lineament, suggesting it represents a major basement penetrating structure which "tapped" shoshonitic-type magma of sub-crustal origin (see Ch. 2); and (iii) The late Caledonian Ratagain and Cluanie granite plutons are sited directly along the lineament. The Ratagain complex (Nicholls 1951; Hutton & McErlean 1991; McErlean 1993) is a small (approximately 17 km^2) body which has been emplaced along the Moine Thrust sheet

some 5 km SE of the Moine Fault trace (Fig. 9.35). It is of particular interest as its internal deformational features have been studied in detail by Hutton and McErlean (1991), who have shown that the construction of the pluton was controlled by the NE-SW-trending synthetic splays (Fig. 9.41). Centred on the Ratagain complex is a regional suite of lamprophyre (minette), felsite and porphyrite dykes (Smith 1979). Hutton and McErlean (1991) have shown: (a) that they are "late stage", as they post-date the early deformation experienced by the pluton, and are penecontemporaneous with later 'brittle' deformational events; and (b) where the dykes cut the complex they may form two main WNW-ESE-trending swarms (Fig. 9.42), possibly confined to the synthetic splays associated with the early deformation (Fig. 9.41). This led them to suggest "that these splays, possibly as basement faults of the WNW-ESE-trending Loch Maree-Kinlochhourn fault set, were partially reactivated during the late deformation to control the dyke locations and orientations" (Hutton & McErlean 1991).

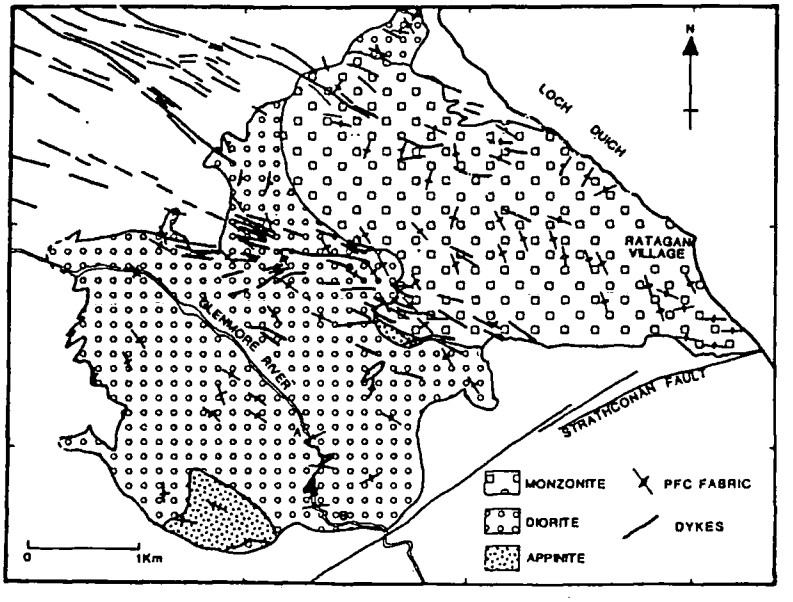

Fig. 9.41. Geological map of the Ratagain complex simplified after Hutton *et al.* (1991). Regional dyke swarms after Clough (1910). PFC, pre-full crystallisation deformation. After Hutton and McErlean (1991).

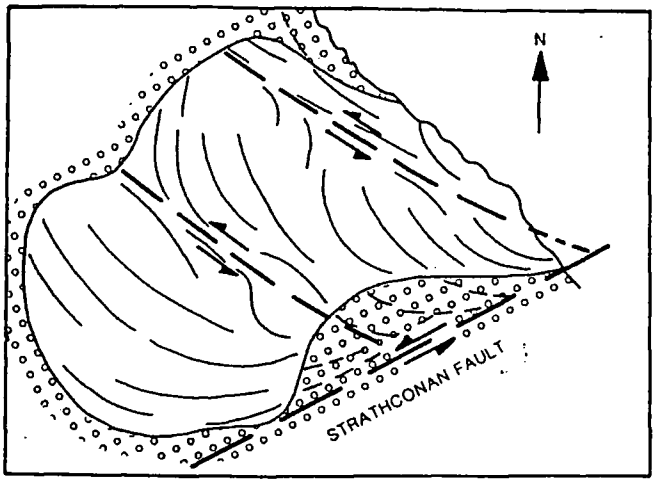

Fig. 9.42. Summary and interpretation of pre-full crystallisation deformation in the Ratagain pluton. Circle ornament indicates country rocks around pluton. Thin dashed lines in the south show interpolated swing of fabrics beneath gently inclined roof contact. After Hutton and McErlean (1991).

9.20 DISTINCT TECTONIC DOMAINS WITHIN THE NORTHERN HIGHLANDS

As shown above, a number of major NW-SE-trending deep basement structures may occur in the Northern Highlands. These lineaments appear to have not only controlled the distribution of late Caledonian magmatism, but may have also had a profound affect on the structural development of the Caledonian cover sequence during the NW directed movements along the Moine Thrust Zone. However, within the southern part of the Northern Highlands, essentially south of the structurally-defined NE-SW-trending Loch Quoich Line (see below), geological features defining the position of the NW-SE-trending lineaments are less well defined or lost completely. Instead, particularly within the Loch Gary-Loch Arkaig-Loch Eil area, the predominant 'tectonic basement fabric' may have an E-W-trend (see below); a situation possibly very similar to that proposed for the "NE Highlands tectonic domain" (Buchan block area) and the "Southern Highlands tectonic domain" (see Section 9.14) where an E-W set of lineaments appear to have 'superimposed' themselves over the NW-SE-trending set, resulting in the E-W set controlling the siting of late Caledonian magmatism and subsequent intrusive events. Within the southern Northern

Highlands intra-continental dyke swarms appear to have exploited this E-W-trending 'tectonic fabric', as depicted by the distribution of the late Carboniferous quartz-dolerite dyke swarm in the Grampian Highlands (see Section 9.14). In the southern Northern Highlands, the Permo-Carboniferous swarms of basic alkaline dykes, generally referred to as the 'Camptonite-Monchiquite Suite', have been recognised as consisting of nine dyke swarms (Rock 1983). Within the mainland four out of five swarms are essentially E-W-trending (see Fig. 9.43; Rock 1983), leading Baxter and Mitchell (1984) to suggest that these "Visean east-west dykes may have utilised a pre-existing late Caledonian fracture system". It is interesting to note that the only dyke swarm with a different orientation, the NW-SE-trending Ardgour swarm, may be centred west of the Loch Quoich Line, within the 'tectonic domain' characterised by NW-SE-trending basement structures (see below).

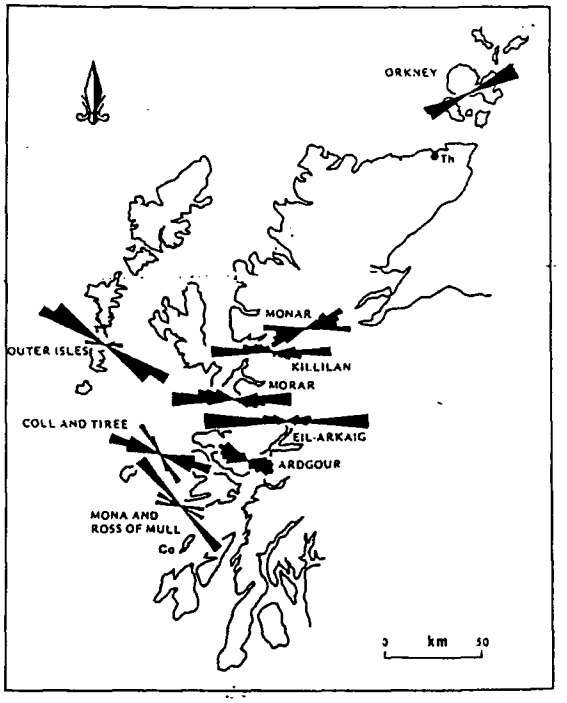

Fig. 9.43. Location and azimuth distributions of the main camptonite-monchiquite dyke swarms in the Scottish Highlands. After Rock (1983) in Baxter and Mitchell (1984).

Baxter and Mitchell (1984) also made the point that the "east-west trend for minor intrusions seems to be a persistent late-Proterozoic feature", not only controlling the orientation of the Permo-Carboniferous dyke swarms, but also the preceeding late Caledonian lamprophyre (minette) dyke suite (Richey 1939; Smith 1979), concluding that "net extension normal to those E-W lines of lithospheric weakness during periods of regional extension and their exploitation of ascending magma could explain the orientation

of both swarms". These features may suggest that the Northern Highlands can be roughly divided, possibly within the vicinity of the Loch Quoich Line (extending its trace towards the NE, possibly coinciding with the Northern Highlands steep belt ; see Section 9.22), into two 'distinct tectonic basement domains' which will be referred to as: (i) the "north-western Northern Highlands tectonic domain" which is characterised by major NW-SE-trending lineaments; and (ii) the "south-eastern Northern Highlands tectonic domain" which appears to contain an E-W-trending 'tectonic fabric'. Geochemical analysis of xenoliths and megacrysts encorporated within the Permo-Carboniferous dykes suggests they contain a mantle component (Upton *et al.* 1984), which may imply that as with the NW-SE-trending lineaments, the E-W set represent deep basement penetrating structures.

The Loch Quoich Line

As discussed above, the position of the Loch Quoich Line (Fig. 9.44) may represent or roughly coincide with the boundary which separates the two proposed tectonic domains: the "north-western Northern Highlands" from the "south-eastern Northern Highlands". A model is presented in Section 9.21 which may show that restoration along the Great Glen Fault could account for the differences in 'structural architecture' of the basement underlying the regions on either side of the Loch Quoich Line. This simple model suggests that a 'tectonically distinct crustal unit' characterised by E-W-trending lineaments was thrusted as far north as the approximate position of the 'Loch Quoich Line' (see below). This may have created a situation in which the southern Northern Highlands is essentially underlain by a basement composed of two tectonically distinct crustal units: (i) ancient "Lewisianoid-type crust" characterised by NW-SE-trending lineaments; and (ii) a continental crust which predominantly contains E-W-trending structures. This model may explain the 'superimposition' of the E-W set of structures over the NW-SE-trending lineaments within the south-eastern part of the Northern Highlands ("south-eastern Northern Highlands tectonic domain").

The Loch Quoich Line is a 'structurally-defined', NE-SW-trending linear zone. The 'line' forms the eastern limit of a steep belt of psammitic and pelitic gneisses, some 12 km wide, from regionally 'flat lying' psammites in the east (Fig. 9.45). It can be traced approximately 60 km from Loch Quoich, south-eastwards into the Loch Arkaig area (Fig. 9.44). The zone was originally described by Leedal (1952), and was subsequently defined and named by Clifford (1957). Various suggestions have been made to explain its development, including: (i) a possible root zone (Clifford 1957); (ii) a zone of early ductile upthrusting (Dalziel 1966); (iii) a zone containing an unconformity which seperates Glenfinnan Division basement, which has been affected by the Grenville orogeny (Brook *et*

al. 1977), from the Loch Eil Division which has been interpreted as a post-Grenville cover sequence (Lambert *et al.* 1979; Piasecki & van Breeman 1979; Piasecki 1980); and (iv) as the eastern limit of intense, upright Caledonian reworking of the Grenville belt (Fig. 9.45; Roberts & Harris 1983). The latter authors concluding that the Loch Quoich Line simply represents the eastern limit of a zone of intense D_3 (early Palaeozoic) deformation, with rocks either side of the line experiencing the same deformational history. This D_3 event has been given a maximum age of 456 +/- 5 Ma, the age of the Glen Dessary Syenite which has been strongly deformed by this event (Roberts *et al.* 1984); thus providing a constraint on the formation of the 'line'.

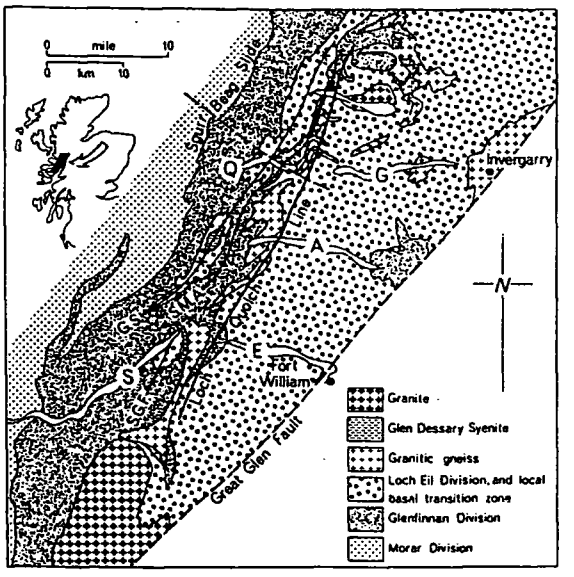

Fig. 9.44. Distribution of the Moine tectonostratigraphic divisions in central Inverness-shire. Some regional correlations are shown: GS, Gleouraich Synform; SGF, Sgurr Ghiubhsachain folds and SMA, Spidean Mialach Antiform. A, Loch Arkaig; E, Loch Eil; G, Loch Garry; Q, Loch Quoich; and S, Loch Spiel. Inset shows regional position of main map.

The reason why there should be an eastern limit on intense D_3 deformation across the width of the Moine outcrop is unclear, but it may be related to and show the approximate position of a major terrane boundary which extended south-eastwards as a continuous structure across the Grampian Highlands, before being displaced by movements along the Great Glen Fault (see Section 9.21). In the Grampian Highlands, the Geal Charn-Ossian Steep Belt (see Ch. 2) may roughly mark the trace of this boundary. It is envisaged

that during the Grampian orogeny, Dalradian deformation was focussed along part of this major tectonic boundary (within the Grampian Highlands), leading to the development of the Geal Charn-Ossian Steep Belt. However, it still remains unclear why the apparent ages of the deformational events and the Caledonian structural style on either side of the Great Glen Fault are so different, preventing their correlation.

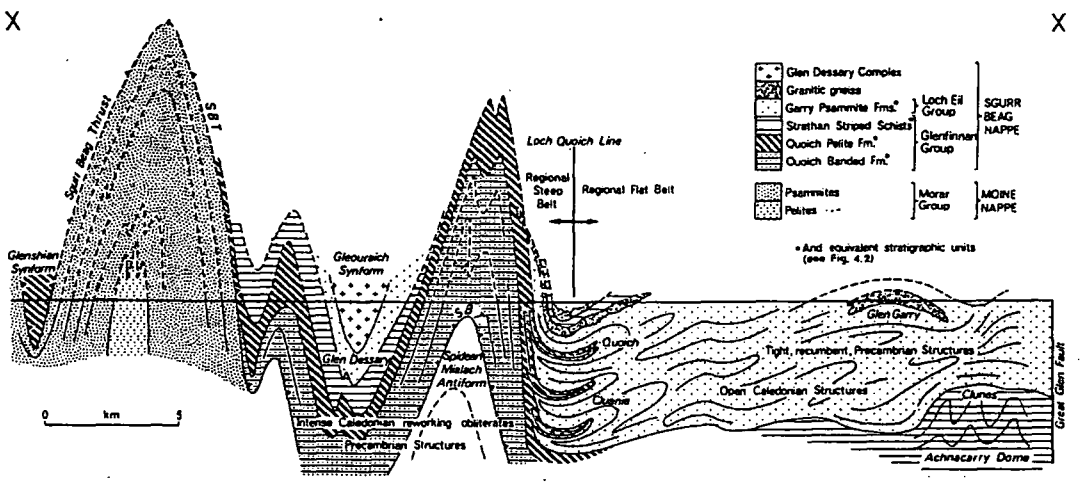

Fig. 9.45. Section X-X' (see Fig. 9.28) showing the steep and flat belts, the Loch Quoich Line and folding of the Sgurr Beag thrust (SBT). After Roberts *et al.* (1984) *in* Craig (1991).

The following Section attempts to: (i) define the position of this terrane boundary; (ii) comment on its probable age and what it seperates; and (iii) determine important movement phases along the Great Glen Fault with respect to its displacement.

A MAJOR TECTONIC BOUNDARY:
the northern margin of a major deep crustal terrane ?

9.21 INTRODUCTION

It is envisaged that the 'Mid-Grampian Line' proposed by Stephens and Halliday (1984) to separate the Argyll and South of Scotland Suites, is in fact likely to represent a 'thrust boundary' (see Section 9.14), separating ancient crust to the NW from younger continental crust to the SE (Halliday 1984). The distribution of Caledonian plutons and associated magmatism in the Grampians has led to the identification of several major sets of lineaments or shear zones, suggesting that the boundaries inferred by Stephens and Halliday (1984) to separate the Argyll, Cairngorm, and South of Scotland Suites may roughly coincide with the boundaries of three 'distinct tectonic domains'. These will be referred to as: (i) the "Central and SE Highlands tectonic domain"; (ii) the "NE Highlands tectonic domain"; and (iii) the "Southern Highlands tectonic domain". These roughly coincide with the Argyll, Cairngorm and part of the South of Scotland Suite, respectively.

An actual tectonic boundary separating the Southern Highlands and NE Highlands tectonic domains may not exist. Both 'domains' may comprise a basement composed of two tectonically distinct units: (i) ancient "Lewisianoid-type" crust characterised by NW-SE-trending lineaments; and (ii) a continental crust which contains E-W structures. As mentioned in Section 9.14, the relative dominance of one set of lineaments over another may be governed by the tectonic regime prevailing at that time. In the NE Highlands it is envisaged that during Caledonian magmatism this region could be regarded as an "extensional regime" with respect to the tectonic environment established further SW. This possibly explains why this area (i.e. the NE Highlands) represents a zone of least tectonic thickening within the Dalradian, and consequently the lack of major NE-SW-trending faults and shear zones. In contrast, the Southern Highlands tectonic domain lies in a "contractional zone" where NE-SW-trending faults are well developed.

The boundary separating the Southern and NE Highlands tectonic domains from the Central and SE Highlands domain may actually represent a tectonic discontinuity (a 'thrust boundary'). A number of features suggest (see below) that this may lie close to the trace of the Geal Charn-Ossian Steep Belt, and may continue north-eastwards close to the trace of the Grampian Steep Belt (see Piasecki 1975). This does not infer that both steep belts can be linked to form a zone of 'structural continuity' as proposed by van Breemen and Piasecki

(1983). However, it may suggest that strain was focussed along this 'thrust boundary' leading to the development of both steep belts. As shown on Figure 9.46a this 'boundary' may continue in an arcuate trace into and across the Northern Highlands. This is again defined by a change in the orientation and dominance of lineaments across this zone, and as within the Grampian Highlands this may have influenced the distribution of deformation, possibly explaining the spatial coincidence of the Loch Quoich Line and the Northern Highlands Steep Belt. This boundary will be referred to as the "Ossian-Loch Quoich Line" (Fig. 9.46).

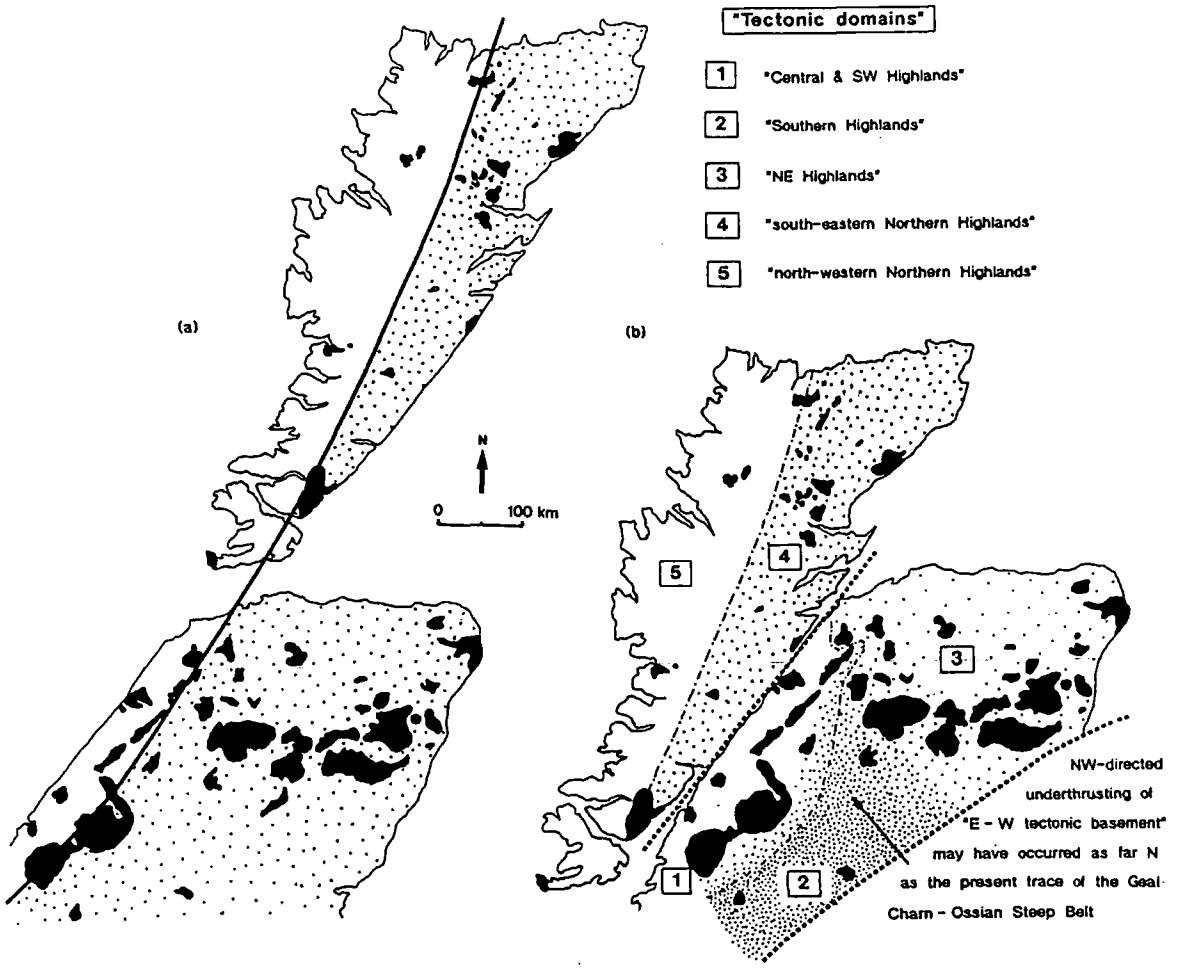

Fig. 9.46. A generalised sketch map of the Northern Highlands showing **(a)** the position and continuation of the 'Ossian-Loch Quoich Line' if the sinistral offset across the Great Glen Fault is restored, and **(b)** the present position of the Northern Highlands and Grampians explaining the distribution of the "tectonic domains" now observed.

This structure may therefore represent a major tectonic boundary subsequently crosscut and displaced by the Great Glen fault, suggesting it represents a Palaeozoic or older structure. The 'boundary' appears to have been the focus for intense deformation and repeated intrusive activity along the whole of its length (see Section 9.22). The age of these events may suggest that this lineament represents the northern margin of a major deep crustal terrane. The trend and geographical position of this tectonic boundary may suggest that it represents part of the position of a continental margin separating Early Proterozoic crust in the SE from older Archean crust in the NW. Isotopic analysis of Caledonian granites from the Northern and Grampian Highlands suggest Archean and Early Proterozoic crustal sources respectively (Pidgeon & Aftalion 1978; Blaxland *et al.* 1979). It has been suggested by Menuge and Daly (1991) that the northern margin of the Ketilidian terrane (see Sutton & Watson 1987; Marcantonio *et al.* 1988; Winchester 1988; Menuge & Daly 1989) may continue from NW Ireland across the Grampian Highlands. However, the problem with the trace of the 'Ossian-Loch Quoich Line' as the position of the northern margin of the Ketilidian terrane, is that it would not apparently explain the position of the Rhinns Complex (Colonsay-West Islay block) (Fig. 9.47), as this has been shown to be of early Proterozoic age (Marcantonio *et al.* 1988) and occurs to the north of the 'Line'.

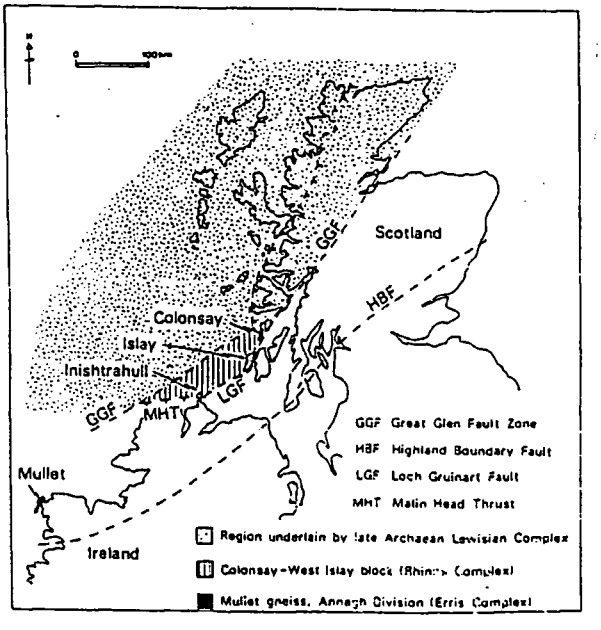

Fig. 9.47. Regional sketch geological map of Scotland and northern Ireland (after Dunning 1985, *in* Daly *et al.* 1991) showing the regional setting of Inishtrahull.

The concept that the Geal Charn-Ossian Steep Belt in the Grampians may mark the position of a terrane boundary separating the Northern and Grampian Highlands, rather than the Great Glen Fault, has been previously suggested by Powell *et al.* (1988). They suggested that contrasts in peak metamorphic timing between the Northern and Grampian Highlands could be used as evidence to support its existence. Thirlwall (1988) has questioned such a model on the basis that if it was true, terrane juxtaposition must have taken place after Caledonian peak metamorphism (approximately 460 Ma) in the Northern Highlands. This is because the development of Dalradian nappes either side of the Geal Charn-Ossian Steep Belt appears to have occurred before 500 Ma, suggesting that no major movement along the boundary could have occurred since at least 500 Ma. A solution to this problem may however lie in the timing of displacements along the Great Glen Fault. Hutton (1987) made the point that the Great Glen Fault was not likely to be a major terrane boundary, although it may have constituted part of such a boundary during 460-410 Ma. The importance of the Great Glen Fault in separating the Northern Highlands and Grampian terranes has been questioned by Lindsay *et al.* (1989) on the basis that: (i) the relative age of deposition, deformation and metamorphism of the Moine rocks to the NW of the Great Glen Fault and of Dalradian metasediments to the SE of the fault depends on the validity of tentative structural conclusions; and (ii) the reliability of radiometric age determinations on a small number of metamorphosed and deformed intrusive bodies. An alternative position for the terrane boundary, the 'Ossian-Loch Quoich Line', is discussed below.

9.22 THE OSSIAN-LOCH QUOICH LINE

There are several lines of evidence to suggest that the 'Ossian-Loch Quoich Line' represents the approximate position of a major terrane boundary separating the Northern Highlands terrane from the Grampian terrane:

- Within both the Northern and Grampian Highlands, the 'line' appears to aproximately separate regions underlain by basement with different 'structural characteristics'. North of the 'line', only one set of major basement structures have been recognised. These are NW-SE-trending lineaments. However, south of the 'line', two sets occur: (i) an E-W 'tectonic fabric'; and (ii) the NW-SE set of lineaments. An important feature is that it might be possible to trace the NW-SE-

trending lineaments across the Ossian-Loch Quoich Line (see Section 9.23), implying that they developed either during or after terrane accretion. A model is presented in Section 9.23 in which the lower crust is essentially decoupled from the mid- to upper crust and the uppermost mantle. It is envisaged that a 'tectonically distinct crustal unit', characterised by E-W-trending structures, was thrusted northwards along possibly the upper detatchment zone as far as the Ossian-Loch Quoich Line. Therefore, south of the 'line' the cover sequence is underlain by a basement composed of two tectonically distinct units: (i) ancient "Lewisianoid-type crust" characterised by NW-SE-trending lineaments; and (ii) a continental crust containing E-W structures (Fig. 9.46a). Subsequent displacement along the Great Glen Fault and deformational events within the Grampian Highlands led to the development of three distinct domains (Fig. 9.46b) which are characterised by an E-W 'tectonic fabric': (a) the "south-eastern Northern Highlands tectonic domain"; (b) the "NE Highlands tectonic domain"; and (c) the "Southern Highlands tectonic domain".

❷ In the Northern Highlands part of the 'line', from Ardgour to Glen Doe (roughly coinciding with the 'Loch Quoich Line'), is defined by a somewhat linear array of granitic gneiss bodies (Fig. 9.48). These are generally referred to as the "West Highland Granitic Gneiss". The age of the suite is controversial, relying on a radiometric (Rb/Sr) age of 1028 +/- 43 Ma (Brook *et al.* 1976) for the Ardgour granitic gneiss body. More recent age determinations (reviewed by Rogers & Pankhurst 1993) suggest an emplacement age of 574 +/- 30 Ma and 556 +/- 8 Ma. They have been generally interpreted as metasomatic in origin (e.g. Harry 1954; Dalziel 1963, 1966; Johnstone *et al.* 1969) or magmatic (Mercy 1963), with recent geochemical analysis suggesting the latter (Barr *et al.* 1985; Highton 1994). Barr *et al.* (1985) concluded that these gneisses represented a series of S-type granitic sheets emplaced either before or during Moine D_1 deformation (possible synorogenic emplacement). This therefore infers, taking the most recent age determinations at face value, that major differences in the age of metamorphic basement on either side of the Great Glen Fault may not occur.

The distribution and form of these bodies may therefore suggest that the 'Ossian-Loch Quoich Line' was a focus for and controlled the intrusion of the West Highland Granite Gneiss Suite.

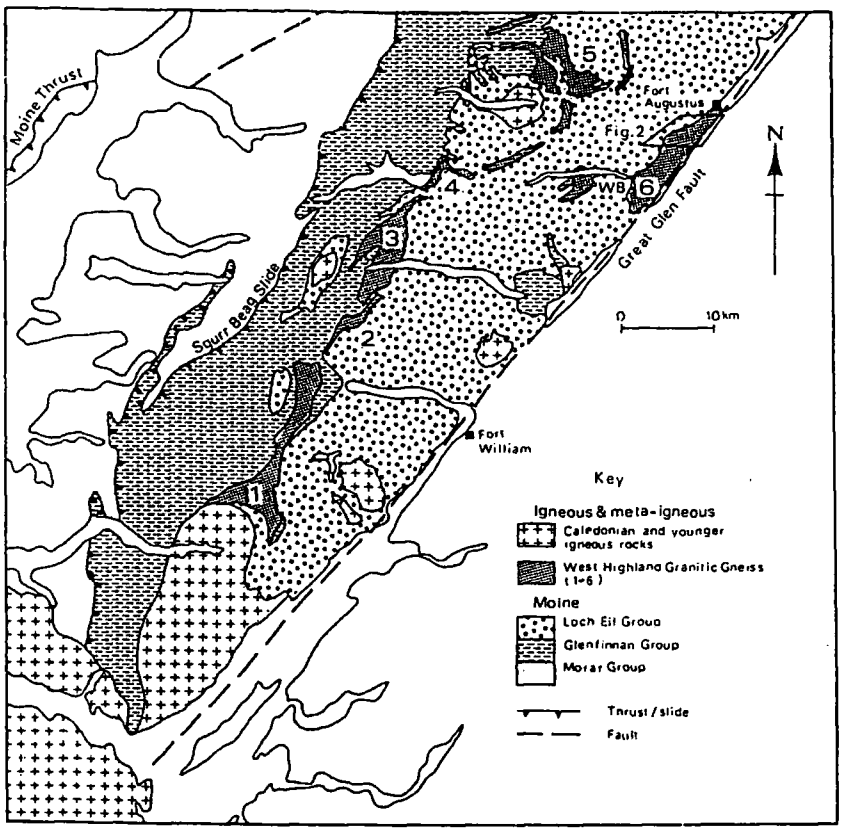

Fig. 9.48. Distribution of component masses of the West Highland Granitic Gneiss in numerical order: 1. Ardgour, 2. Gulvain, 3. Loch Arkaig, 4. Loch Quoich, 5. Glen Doe, 6. Fort Augustus. WB marks the locality of the White Bridge hornblendic rocks (Rock 1984). After Highton (1994).

Possibly penecontemporaneous with this event was the intrusion of a suite of minor basic intrusives. These have been referred to as the 'amphibolite suite' (Smith 1979), but more recently have been termed the 'metabasites' (Rock *et al.* 1985). Their age is uncertain, possibly forming a number of suites with different ages. Rock *et al.* (1985) have shown that the suite cuts the West Highland Granitic Gneiss, suggesting a syn-D_1 age and that they represent tholeiitic magmas intruded as part of a differential sill complex. The regional distribution of these metabasites ('amphibolite suite') has been described by Smith (1979), commenting on the fact that they form a remarkably straight feature coinciding with the trace of the 'Loch Quoich Line' for over 100 km. If this phase of magmatism was concentrated to some degree along the Ossian-Loch Quoich Line, its distribution would have been significantly modified by subsequent deformational events. This may have occurred to a greater extent in the north of the Northern Highlands, where Smith's (1979) 'northern zone of metabasites' "is conspicuously sinuous following round the large,

late-stage cross-folds which affected the full width of the Moine outcrop" (Smith 1979). This sinuosity may possibly illustrate major strike swings related to crossing NW-SE-trending lineaments (see Fig. 9.35). It is therefore likely the metabasites may have originally formed a fairly contionuous, broad linear feature along the whole length of this part of the Ossian-Loch Quoich Line.

It has also been described by Smith (1979) that late NE-SW-trending Caledonian felsic porphyrite dykes (of the Cluanie complex) and microdioritic dykes are concentrated along the trace of the Loch Quoich Line. It is also apparent from Figure 9.49 that when the trace of the Ossian-Loch Quoich Line is restored across the Great Glen, that a high number of the larger, late Caledonian granitic plutons both within the Grampians and Northern Highlands are sited close to the trace of this proposed tectonic boundary. Woollett (1988) suggested that the poor definition of the Great Glen Fault on Bouger anomaly maps suggests that it does not control the subsurface distribution of any significant intrusions. However, along the proposed trace of the "Ketilidian northern margin", three major lineaments recognised by digital image analysis of Bouger gravity data (Woollett 1988) are coincident. This therefore suggests that even after the displacement of the Ossian-Loch Quoich Line by movements along the Great Glen Fault, the 'line' may have been utilised by subsequent granitic magma, and/or more likely was the focus of intense crustal thickening (e.g. Geal Charn-Ossian Steep Belt, Grampian Steep Belt) leading to anatexis and the production of granitic melt (see Hutton & Reavy 1992; Ch. 2, Section 2.3). The siting of Caledonian plutons along this zone has been previously described by van Breeman and Piasecki (1983), stating that "All the granitic intrusions of the Upper Findhorn region were emplaced within the broad zone of the Grampian Steep Belt and have a north-easterly elongation. This steep belt may have acted as a zone of weakness along which repeated phases of granitic magma were funnelled. On the larger scale, it may have controlled the rise of magmas on both sides of the Great Glen Fault, from the complexes of Etive and Glen Coe in the SW, with their associated NE-trending microdiorite dykes, to beyond the Cluanie Granite north of the Great Glen Fault" (van Breeman & Piasecki 1983).

The large concentration of major granitic plutons in the NE Highlands (Cairngorm Suite; Stephens & Halliday 1984), some distance away from the Ossian-Loch Quoich Line, appear to represent granite petrogenesis and emplacement in a completely different tectonic setting; a possible "extensional regime" (see Sections 9.9 & 9.14).

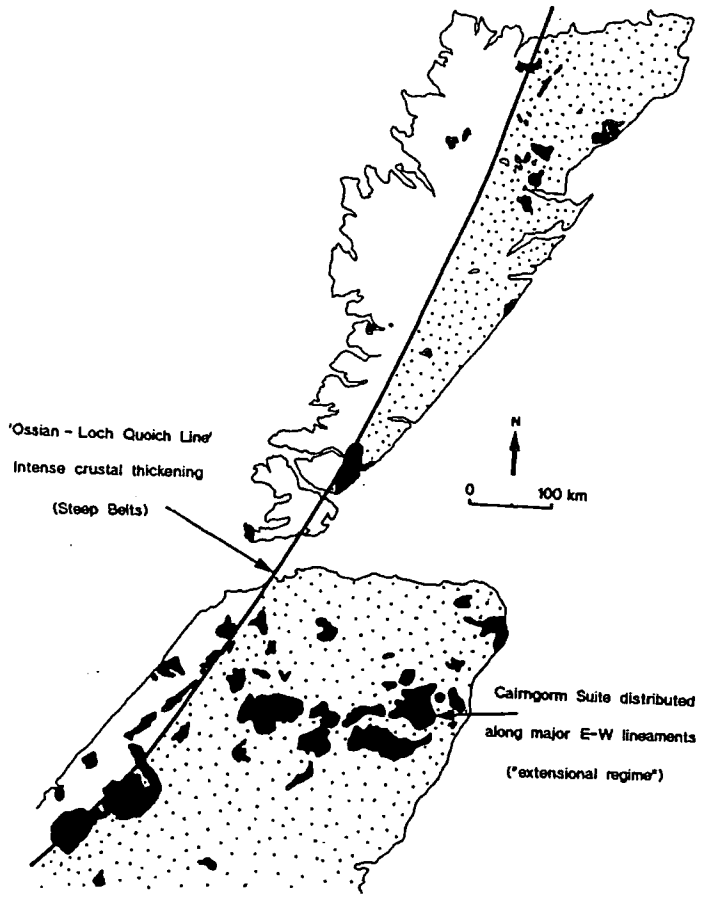

Fig. 9.49. The distribution of the late Caledonian plutons when the 'Ossian-Loch Quoich Line' is restored across the Great Glen Fault.

❸ The position of the Ossian-Loch Quoich Line may also help to explain the distribution of chemical and isotopic characteristics of Caledonian intrusive rocks on either side of the Great Glen Fault. A progressive WNW increase in Sr across the Grampians and into the Northern Highlands (Fig. 9.50) has been related by Thirlwall (1981) to a WNW-dipping subduction zone, suggesting continuity of the high-Sr magmatic zone across the Great Glen Fault (see Thirlwall 1989). Whatever the mechanism was for the genesis of these magmas (see discussion in Ch. 2, Section 2.3), it is clear from Figure 9.50 that 'restoring' the Ossian-Loch Quoich Line would clearly give a progressive increase in Sr concentrations towards the NW, perpendicular to the trace of the 'line'.

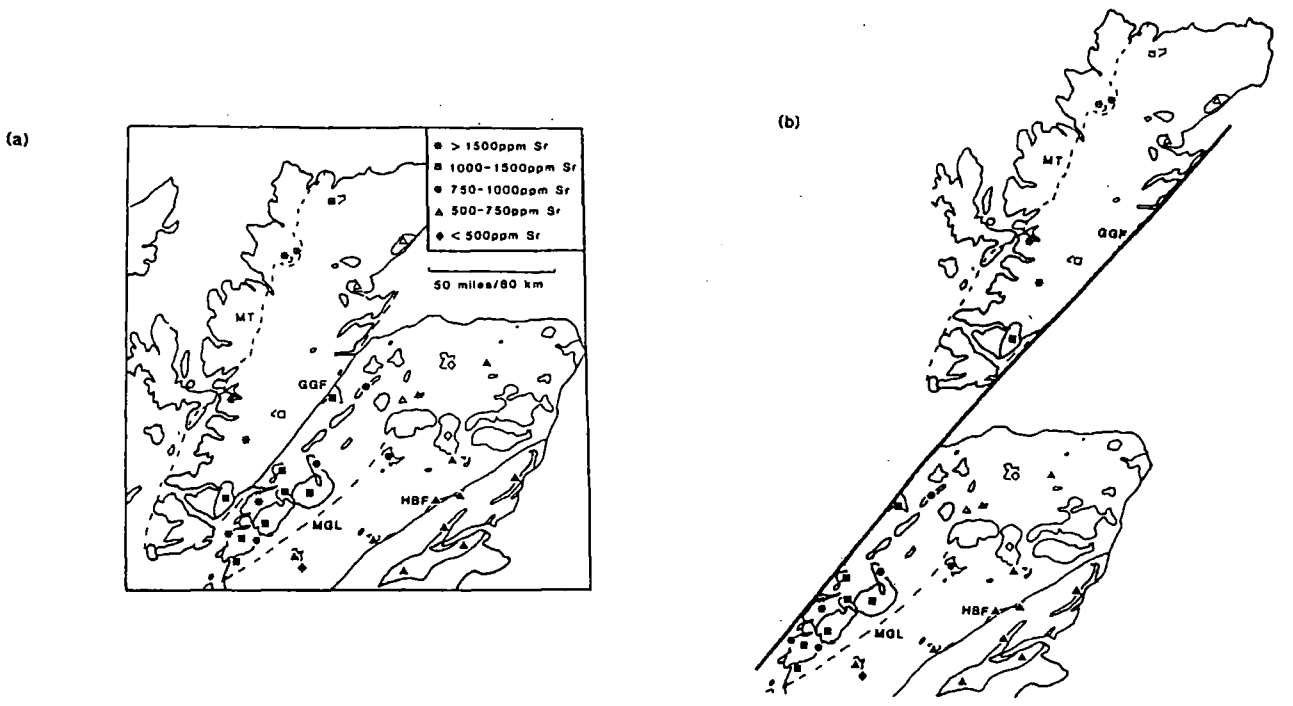

Fig. 9.50. **(a)** Typical Sr concentrations in magmas with less than 65 % SiO_2 (solid symbols) or with 65-70 % SiO_2 (open symbols) in northern Scotland. MT, Moine Thrust; GGF, Great Glen Fault; MGL, Mid-Grampian Line; HBF, Highland Boundary Fault. Data sources: Stephens & Halliday (1984), Thirlwall (1979, 1982), Thompson & Fowler (1986). Areas of igneous rock with no symbols have no published data for rocks with < 70 % SiO_2. After Thirwall (1989). **(b)** The distribution of Sr after restoration of the 'Ossian-Loch Quoich Line' across the Great Glen Fault. Modified after Thirlwall (1989).

❹ It is possible that deformation was focussed and/or distributed along parts of the Ossian-Loch Quoich Line during different deformational episodes. This may explain the development of the Geal Charn-Ossian Steep Belt and the Grampian Steep Belt along the trace of the 'line' in the Grampian Highlands, and the Loch Quoich Line and the Northern Highlands Steep Belt in the Northern Highlands.

❺ It has also been noted by Thirlwall (1989) that Old Red Sandstone lavas in the SW Highlands have a mantle source component with a distinctive Sr-Nd-Pb isotopic signature (Thirlwall 1982, 1986), which is almost identical to the isotopic composition of mafic syenites from the Borralan complex situated in the northern part of the Northern Highlands. Although some 160 km apart at their present position, and approximately 300-320 km apart if the Ossian-Loch Quoich Line is

restored, they both occur approximately 10 to 20 km north of the proposed trace of the terrane boundary. This is different from the regional Caledonian NE-SW-trend, in which the Borralan complex is some 70 to 80 km NW of the Great Glen Fault, whereas the SW Highland, Old Red Sandstone lavas are on the opposite side, only some 5 to 15 km SW of the fault zone.

❻ Faber and Bamford (1979, 1981) have shown that on the LISPB profile, which was approximately NNW-SSE across Britain (Fig.'s 9.51, 9.52 & 9.53), two well defined, local structural offsets occur beneath northern Scotland. One occurs at the Moho in the Northern Highlands, and the other in the lower lithosphere, observed as a sub-Moho lateral variation, located in the Central Highlands. The inferred surface positions of these two offsets coincides exactly with the proposed trace of the Ossian-Loch Quoich Line, suggesting that this geologically-defined 'line' does indeed represent a major tectonic boundary which penetrates so far down as to cause a step in the Moho and an offset in the sub-crustal lithosphere.

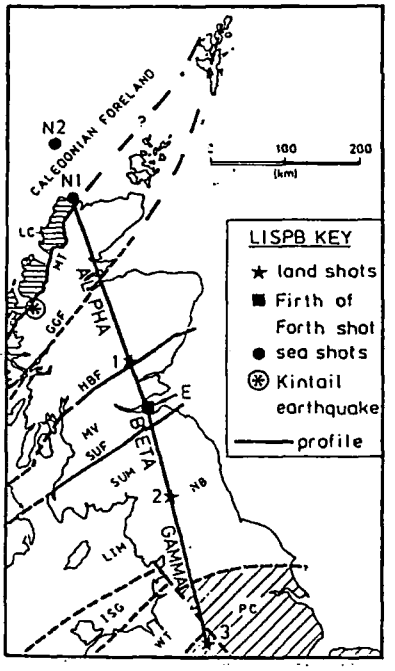

Fig. 9.51. LISPB shots and profiles with geological summary. (Details of the LISPB experiment are given in Bamford *et al.* 1976). Key to geological features: LC, Lewisian Complex; MT, Moine Thrust; GGF, Great Glen Fault; HBF, Highland Boundary Fault; MV, Midland Valley; SUF, Southern Uplands Fault; SUM, Southern Uplands Massif; NB, Northumberland Basin; LIM, Lake District - Isle of Man Massif; ISG, Irish Sea Geanticline; WT, Welsh Trough; PC, Pre-Cambrian Craton of England and Wales. After Faber and Bamford (1981).

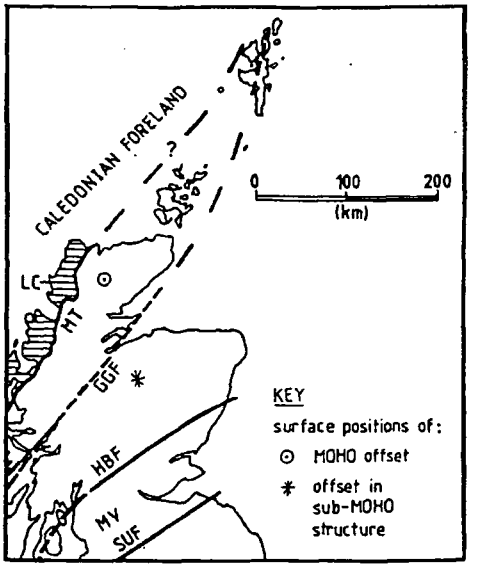

Fig. 9.52. Tectonic map of Scotland with the approximate surface positions of structural offsets at the Moho and in the lower lithosphere (for key to geological features see Figure 9.51). After Faber and Bamford (1981).

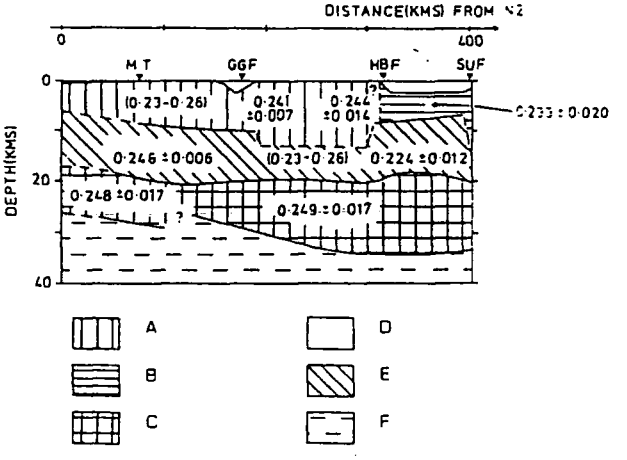

Fig. 9.53. Schematic cross-section of the crust and Moho of Scotland from LISPB shotpoint N2 to the Southern Upland Fault (Fig. 9.51), summarising P velocities and layering, and Poisson's ratio. Geological features are as in Figure 9.51. Key to seismic layers: A, Caledonian belt metamorphics (6.1-6.2 km s^{-1}); B, Lower Palaeozoic (5.8-6.0 km s^{-1}); C, Lower crust (≈7 km s^{-1}); D, Superficial layers (Cromaty-Moray ORS; Midland Valley); E, Pre-Caledonian basement (> 6.4 km s^{-1}); F, Uppermost mantle (≈8 km s^{-1}); ?, Uncertain structure. After Faber and Bamford (1981).

9.23 DISPLACEMENT OF THE OSSIAN-LOCH QUOICH LINE BY THE GREAT GLEN FAULT

The amount of displacement along the Great Glen Fault has long been the subject of debate. A number of proposed correlations across this structure have been made, including:

(1) The first work was by Kennedy (1946), who re-interpreted the structure as a strike-slip fault; before this work it had been regarded as a dip-slip structure (Bailey & Maufe 1916). Kennedy (1946) proposed a lateral sinistral displacement of some 100 km (65 miles), based on the present position of the Foyers and Strontian granite bodies, which he believed were formerly one single pluton, and the correlation of metamorphic zones and of regional injection complexes on either side of the fault.

(2) A detailed structural study of the Foyers pluton by Marston (1971) appeared to verify this assumption, as this subsequent work suggested that the Foyers and Strontian (Sabine 1963; Munro 1965) plutons could be explained by a difference in the relative erosion level on either side of the Great Glen Fault. This however has been disputed on two main grounds: (a) isotopic data and rare-earth elements suggest that the two bodies cannot be correlated (Pankhurst 1979); and (b) a detailed study of both the Foyers and Strontian thermal aureoles to deduce P/T estimates (Tylor & Ashworth 1983) suggests that metamorphism took place at around 4 kbar for both bodies.

(3) Flinn (1961) suggested that the Great Glen Fault could be traced NE to the Shetlands, where it was represented by the Walls Boundary Fault. Subsequent work by Flinn (1969) on the amount of displacement along the Walls Boundary Fault indicated a dextral component of 65 km. This was recently revised by Flinn (1988), concluding that the fault system has an overall 200 km sinistral offset, suggesting that a post-Hercynian dextral component observed along the Walls Boundary Fault had essentially been 'superimposed' on the site of the Great Glen Fault.

Correlating dyke swarms:

(4) Correlating dyke swarms across the Great Glen was first proposed by Holgate (1969), proposing a 30 km post-Tertiary dextral component. However, this was critised by Speight and Mitchell (1978), stating that Holgate (1969) had failed to distinguish between Permo-Carboniferous and Tertiary Dyke Swarms. By comparing the percentage of dilation of the Permo-Carboniferous dykes on either side of the fault, Speight and Mitchell (1978)

suggested a dextral displacement of 7-8 km, with an approximate 500 m downthrow to the SE. The Tertiary Dyke Swarm cross the Great Glen Fault without displacement, constraining the timing of this event to pre-Tertiary.

The results of Speight and Mitchell (1978) have been disputed on the basis that some of the dykes used for correlation may be of different age (Morrison *et al.* 1987) and it has been suggested that the dykes may have utilised previously offset weaknesses (Rogers *et al.* 1989).

'Geomorphological' correlation:

(5) An 88 km dextral component was suggested by Garson and Plant (1972) to align the approximately E-W-trending north coastlines of the Northern Highlands (Sutherland) and NE Highlands (Morayshire).

Correlating metamorphic isograds:

(6) A year later, the correlation of metamorphic isograds across the fault led Winchester (1973) to propose a sinistral displacement of approximately 160 km.

Palaeomagnetic correlations:

(7) Again, this was modified a year later, with Storetvedt (1974) proposing a 300 km sinistral component, which had been followed by a late Devonian 50 km dextral displacement. These findings were based on palaeomagnetic data, correlating Old Red Sandstone rocks of NW Scotland and Norway.

(8) A large sinistral component of several thousand kilometres has been proposed by Morris (1976), Piper (1979) and van der Voo and Scotese (1982). This has been based on correlating palaeomagnetic data between NW Scotland/N America and SE Scotland/Europe. Van der Voo and Scotese (1982) suggested a Carboniferous, approximately 2000 km, sinistral displacement. This was however, disputed on both palaeomagnetic and geological grounds (see Donovan *et al.* 1976; Parnell 1982). Briden *et al.* (1982), however, suggested that although the 2000 km sinistral displacement could not be applied to the Great Glen Fault, it may have occurred elsewhere in the Caledonides.

More recently Storetvedt (1987), using palaeomagnetic data from Ordovician-Devonian rocks of northern Scotland, has proposed an approximately 600 km, possibly late Middle Devonian to Upper Devonian, sinistral phase. He suggested that this was subsequently followed by a Hercynian 300 km dextral component, resulting in an 'overall' sinistral displacement of some 300 km. This author suggested that the surface position of the Moine Thrust could be continued across the Great Glen Fault, where it was represented by the Loch Skerrols Thrust on Islay. This was however disputed by Fitches and Maltman

(1984), stating that the amount of movement experienced by the thrusts on either side of the fault was not compatable. Instead, Fitches and Maltman (1984) suggested the Loch Skerrols structure was a zone of regional D_2 high strain, with little evidence of local movement.

Tectonic, metamorphic and sedimentary correlations:

(9) Piasecki and van Breeman (1979b) suggested: (a) the Grampian slide in the Central Highlands may be represented by the Sgurr Beag slide in the Northern Highlands; (b) their 'Central Highland Division' could be correlated with the higher grade parts of the Loch Eil Division in the Northern Highlands; and (c) the Grampian Group represents the equivalent of the lower grade parts of the Loch Eil Division. This was followed by Piasecki (1980) correlating approximately 750 Ma pegmatites across the Great Glen Fault. These two studies (Piasecki & van Breeman 1979b; Piasecki 1980) suggested an apparent 160 km sinistral component along the Great Glen Fault.

(10) Thomas (1980) suggested that the Geal Charn-Ossian Steep Belt in the Central/SW Highlands could be traced across the Great Glen Fault where it was represented by the Loch Quoich Line. This was upheld by Piasecki *et al.* (1981), who suggested that their Grampian Steep Belt in the Central Highlands could be correlated with the Northern Highlands Steep Belt. It should be noted, that the trace of the 'Ossian-Loch Quoich Line', proposed in this study to represent the approximate surface position of a major tectonic boundary, possibly separating old Archean crust in the NW from younger, Early Proterozoic crust in the SE (the northern margin of the Kentilidian terrane), is coincident with the Geal Charn-Ossian Steep Belt, the Grampian Steep Belt, the Loch Quoich Line and the Northern Highlands Steep Belt. This does not however, imply that these zones may be 'structurally continuous' (as proposed by Piasecki and van Breeman (1979b), Thomas (1980) and Piasecki *et al.* (1981)), as there appears to be a pronounced contrast in the age of deformation and 'structural style' on either side of the Great Glen Fault. It has generally been regarded that deformation in the Grampian Highlands reached a metamorphic climax at around 500 Ma (e.g. 520-490 Ma, McKerrow & Lambert 1976), significantly earlier than the development of the Northern Highlands Steep Belt/Loch Quoich Line which appear(s) to be of Caledonian age, deforming the Glen Dessary Syenite (456 +/- 5 Ma; Roberts *et al.* 1984) during their development (see Section 9.20). The structural style between the Geal Charn-Ossian Steep Belt and the Loch Quoich Line is also different, making correlation between the two improbable (Roberts 1984). This is based on the fact that the Loch Quoich Line/Northern Highland Steep Belt has an 'asymmetric form' (see Roberts 1984), compared to the Geal Charn-Ossian Steep Belt which has been shown by Thomas (1980) to have a 'symmetrical structure' (see Ch. 2, sub-section 2.4.3). It is envisaged that these

"deformation zones" are localised along the Ossian-Loch Quoich Line because this tectonic boundary was a focus for deformation during major orogenic events. Leading to crustal thickening and the 'line' repeatedly exploited by magmatism.

(11) More recently, Rogers *et al.* (1989) suggest that any late Caledonian sinistral movements along the Great Glen Fault must have ceased by late Emsian (upper Lower Devonian, c. 390 Ma). On the Scottish mainland the Great Glen Fault displaces the Emsian to Frasnian (upper Lower Devonian to lower Upper Devonian) Old Red Sandstone by a dextral component of 25-29 km (Rogers 1987; Rogers *et al.* 1989). An earlier dextral phase of motion along the Great Glen Fault during the late Caledonian has been proposed by Hutton (1988) to account for the 'emplacement dynamics' of the Strontian granite (435 +/- 10 Ma; Pidgeon & Aftalion 1978).

As shown by Figure 9.54, deformational features and the distribution of late Caledonian plutons both along and between the NW-SE-trending Borralan-Fearn and Laxford lineaments in the Assynt region of the Northern Highlands (Fig. 9.54a), show remarkable similarities to geological features which define the position of the NW-SE-trending Foyers-Glen Tilt and Ardclach-Glen Cairn lineaments in the Central/NE Highlands (Fig. 9.54b). A tentative correlation is made based on the apparent sense of rotation of regional fabrics along these structures, the relative scale of these regional strike swings and the siting of late Caledonian plutons along these lineaments (Fig. 9.54c).

The most apparent feature is the overall "gross orogenic flow pattern" which occurs across these NW-SE-trending lineaments on both sides of the Great Glen Fault (Fig. 9.54c). The largest 'deflection' in the regional fabric appears to be along the Laxford lineament in the Northern Highlands and the Ardclach-Glen Cairn lineament in the Grampians. A major sinistral component along both structures has been proposed to account for the major strike swings across them (see Section 9.12 and 9.19). If these two lineaments are aligned across the Great Glen Fault, this also brings into alignment the Borralan-Fearn and Foyers-Glen Tilt lineaments (see Fig. 9.54c). Regional fabric geometries across the latter two structures however, appear to suggest a dextral shear component across both. It is also apparent that this correlation would also bring into alignment the Loch Shin and Moy-Lochnagar lines. It is also interesting to note that the well defined NW-SE-trending Monadliath line, when traced from the Central/NE Highlands across the Great Glen Fault and into the Northern Highlands may explain the siting of both appinitic and late Caledonian granitic bodies. It appears to pass directly through the Migdale and Loch Ailsh plutons, and if it is continued into the Lewisian foreland region it is coincident with the NW-SE-trending Canisp shear zone (Fig. 9.54c). The differential shear component produced by movements along the Foyers-Glen Tilt and Ardclach-Glen Cairn lineaments may account for the development of

the Cairngorm pluton, which is essentially bounded by these structures, and is one of the largest plutons in the Grampian Highlands. A similar situation may have occurred in the Northern Highlands, between the Borralan-Fearn and Laxford lineaments, explaining the 'Lairig Bouger anomaly low'; the small granitic bodies of Grudie possibly representing the upper parts of an extremely large unexposed pluton.

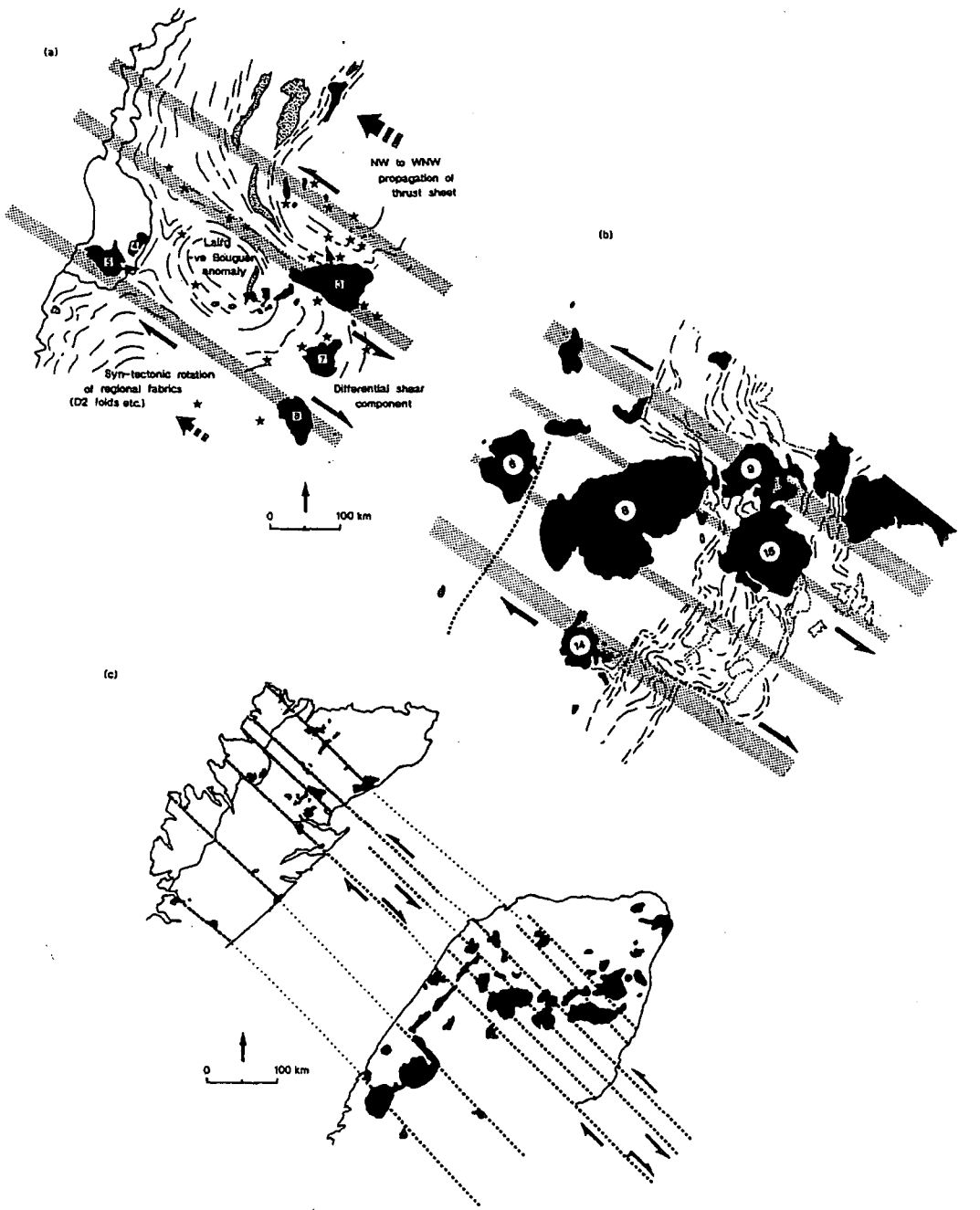

Fig. 9.54. Generalised models showing the siting and distribution of late Caledonian plutons along major lineaments in **(a)** the Northern Highlands and **(b)** the Central/NE Highlands. **(c)** Sketch map showing the possible position of the Northern Highlands relative to the Grampians during late Caledonian magmatism, based on a tentative correlation of structural similarities across the Great Glen Fault.

If such a situation did exist during the late Caledonian, several questions arise (see below). To create such a situation a 200-240 km sinistral component along the Great Glen Fault would have to have occurred; estimated from the displacement of the Ossian-Loch Quoich Line. However, this would presumably imply that the Great Glen Fault would displace the NW-SE-trending lineaments which cross it. To overcome this problem at least three possible scenarios may exist: (i) these lineaments were developed after the main phase of sinistral displacement along the Great Glen Fault, suggesting they developed during the late Caledonian. However, as shown in Section 9.19, some of the geologically-defined, cover lineaments within the Northern Highlands closely coincide with the south-eastward continuation of foreland Lewisian shear zones (see_Section 9.17) beneath the Moine thrust sheet; thus, suggesting that these basement structures were responsible for their development. Also their influence during Dalradian deposition in the Grampian terrane is well documented (see Fettes *et al.* 1986). It has been recently proposed by Soper (1994) that they represent Early Proterozoic structures related to a triple rift (RRR) junction between Laurentia and two other continents (possibly Baltica and West Gondwana), with the third arm marked by these lineaments (see Section 9.24). He proposes that both Vendian sedimentation and MORB-type volcanicity (e.g. Tayvallich Volcanics dated at 595 +/- 5 Ma (Halliday *et al.* 1989)) were controlled by trans-Caledonoid extensional lineaments; (ii) the displacement across the Great Glen Fault brought lineaments of the same orientation into perfect alignment. This however, would seem to be a highly unlikely situation, considering the quite wide uniform spacing (approximately 40-45 km wide) of the major lineaments and the amount of displacement along the Great Glen Fault; and (iii) Brewer *et al.* (1983) have shown that major reflectors within the mantle are offset within the zone bounded by the Skerryvore and Colonsay faults. As this zone is thought to represent the Great Glen fault system, these offsets were taken as evidence that the Great Glen fault penetrates into the uppermost mantle. More recently, Snyder & Flack (1990) have shown in detail that dipping reflectors within the upper mantle (known as the Flannan reflector) are dismembered by late Caledonian faulting (Fig. 9.55b & c), again implying that the Great Glen fault reaches the mantle. This implies that the Flannan reflector is a Palaeozoic or older feature. Although therefore there is clear evidence that deformation on crustal structures does influence the uppermost mantle, Reston (1988) pointed out that nowhere on BIRP profiles is the linkage actually observed; no single crustal shear zone has been successfully traced across the Moho (Matthews *et al.* 1987). Instead, most profiles show a zone within the lower crust of intense sub-horizontal reflectors known as the lower crustal reflectivity zone (LCRZ) (Fig. 9.55d). It is generally regarded that this lower-crustal zone of sub-horizontal reflectors may represent a weak, ductile lower crust which essentially decouples the brittle upper crust from a relatively high strength zone in the uppermost mantle (e.g. Mathews & Hirn 1984; Mathews 1986, 1988; Kusznir & Park 1987;

Meissner & Kusznir 1987; Meissner 1989). Reston (1988) has suggested that although the LCRZ may tectonically decouple the upper crust from the mantle, it may however, transfer deformation between the overlying crust and the underlying mantle. The upper surface of the lower crust ("Lower Crustal Reflectivity Zone"; LCRZ) could be regarded as a 'detatchment zone' (see Ch. 10, sub-section 10.3), essentially decoupling the LCRZ from the Grampian and Moine cover sequence. This could imply that movements along the Great Glen Fault would laterally displace the cover sequence on either side of this structure, but may not actually displace the LCRZ. Although NW-SE-trending lineaments within the pre-Caledonian basement ("Lewisianoid-type crust") may become offset across the Great Glen Fault, major NW-SE-trending structures established within the lower crust may be unaffected. For such a model to be valid it would have to take into account the "terrane accretion episode" proposed, which it is envisaged may have resulted in a tectonically distinct 'crustal wedge' (characterised by an E-W 'tectonic fabric') being thrusted into the region from the south. The northern limit of the thrusting appears to coincide with the Ossian-Loch Quoich Line. It is unclear when this event may have taken place, but it could be related to early to mid-Ordovician collision ("Grampian orogeny"), or a significantly older event. North of the Great Glen Fault the "southern Northern Highlands terrain" is characterised by an E-W-trending 'fabric'. This suggests that during the displacement of the Loch Quoich Line, the Great Glen Fault also laterally offset part of this 'tectonic wedge', implying that this crustal unit was initially thrusted along the upper detatchment surface of the lower crust (LCRZ), underthrusting part of the Grampian and Moine cover sequence (see Fig. 9.34).

However, as mentioned above, the Flannan reflector within the upper mantle has been shown to have been offset by displacements along the Great Glen Fault (Brewer *et al.* 1983; Synder & Flack 1990). This may imply that the LCRZ transferred this "displacement component" from the brittle upper crust into the strong uppermost mantle, but was not itself displaced. This would suggest that major tectonic discontinuities within the lower crust (LCRZ) would not be offset by deformation associated with the Great Glen fault system. However, this would be an extremely unlikely situation, as the displacement of structures within the uppermost mantle (such as the Flannan reflector), suggest that there must have been regional-scale coupling between faulting in the upper crust and deformation within the uppermost mantle; thus affecting the lower crust (LCRZ). An alternative, more attractive model, is that the geologically-defined lineaments within the cover are related to much deeper mantle structures, which are decoupled from the crust and brittle, uppermost mantle. This would imply that deformation along the Great Glen fault system was transferred along a major detatchment zone/décollement horizon between the uppermost mantle/crust and the underlying mantle. This would suggest that crustal faulting would displace structures within the cover sequence, basement and uppermost mantle on either

side of the Great Glen Fault, but not affect major discontinuities within the underlying mantle (i.e. major NW-SE-trending lineaments) (Fig. 9.34).

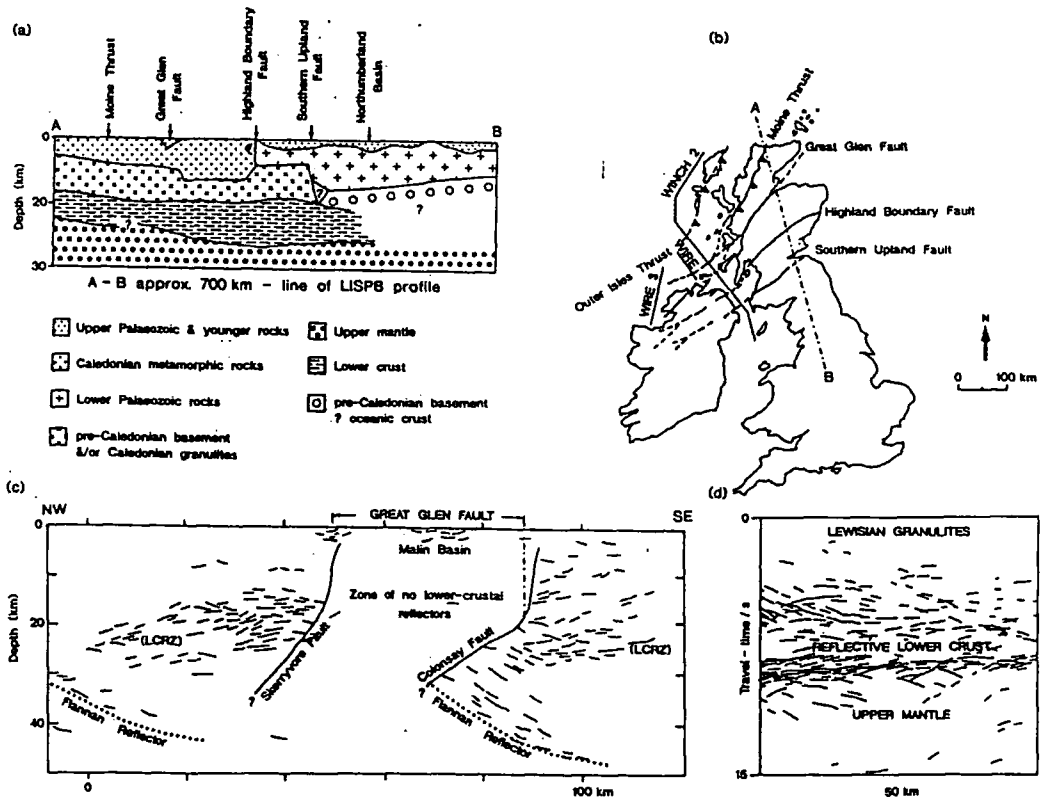

Fig. 9.55. **(a)** Interpretation of LISPB profile (largely after D. Bamford (1979). **(b)** Locality map showing major Caledonian fault systems and position of the LISPB profile and BIRPS surveys. **(c)** Migrated line-drawing of WIRE 4A to show interpretation of lower-crustal reflectors (LCRZ) and mantle reflectors (Flannan Reflector) being truncated by north-dipping Caledonian strike-slip faults. Reproduced from Snyder & Flack (1990). **(d)** Line-drawing of part of WINCH 2 showing position of highly reflective lower crust (LCRZ). Reproduced from Klemperer & the BIRPS Group (1987).

Evidence which suggests that these lineaments do represent deep mantle structures is shown by the geochemical and isotopic characteristics of many of the intrusive bodies which geologically-define the position of these lineaments within the cover. It has been shown that some of these lineaments have controlled MORB-type magmatism (e.g. Graham 1976; Graham & Borradaile 1984), and many have been shown during this study to be

defined by the distribution of appinites/ultrabasic bodies and lamprophyre dykes. The latter intrusives are shoshonitic-type magmas (Wright & Bowes 1979; Hamidullah & Bowes 1987; Hunter & Rock 1987; Rogers & Dunning 1991) derived from a sub-crustal source, which indicates that the lineaments must have at least reached lithospheric mantle depths. Many granitic plutons which are sited along major lineaments also possess mantle components (see Stephens & Halliday 1984).

If this model is accepted, restoration of the Loch Quoich Line would imply an 'overall' sinistral component across the Great Glen Fault of approximately 200-240 km. This would agree with estimates made by Snyder and Flack (1990), based on the dismemberment of the Flannan reflector, which must have formed a continuous structure over 700 km long prior to displacements across the Great Glen Fault. They suggest that late Caledonian, left-lateral offsets of over 200 km have disrupted this structure. As shown by Figure 9.56 their restoration of the Flannan reflector would also restore the trace of the Ossian-Loch Quoich Line across the Great Glen Fault. This would have to have occurred before active motion on the Moine Thrust, which is thought to have occurred between 430-425 Ma (van Breeman *et al.* 1979; Halliday *et al.* 1986), and the intrusion of appinites (c. 425 Ma; Rodgers & Dunning 1991) and lamprophyres which often geologically-define the lineaments. If this was the relative position of the cover sequences on either side of the Great Glen Fault during late Caledonian magmatism, it is extremely interesting to note that the post-Old Red Sandstone (Devonian) 25-29 km dextral offset along the Great Glen Fault (Fig. 9.57), proposed by Rogers (1987) and Rogers *et al.* (1989), would be exactly the amount and sense of displacement required to produce the present day position of the Grampian and Northern terranes.

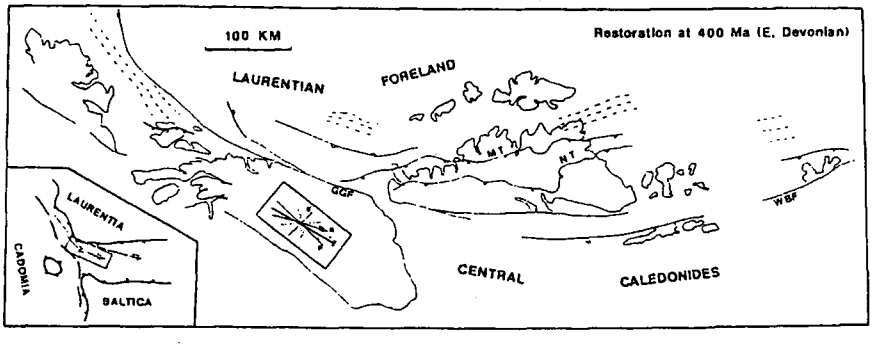

Fig. 9.56. Map with Devonian to Eocene extension and Late Caledonian left-lateral offsets restored. Note semicircles on faults indicating assumed offsets. Dashed lines are contours on the dipping mantle reflector. Small inset shows structures associated with a Riedal shear model: P, thrust sheas; wiggly line, compression axis; hachures, extension axis. Larger inset shows setting in three-plate tectonic model of Soper (1988); dashed line indicates furthest extent of terranes with Gonwana affinity. After Snyder and Flack (1990).

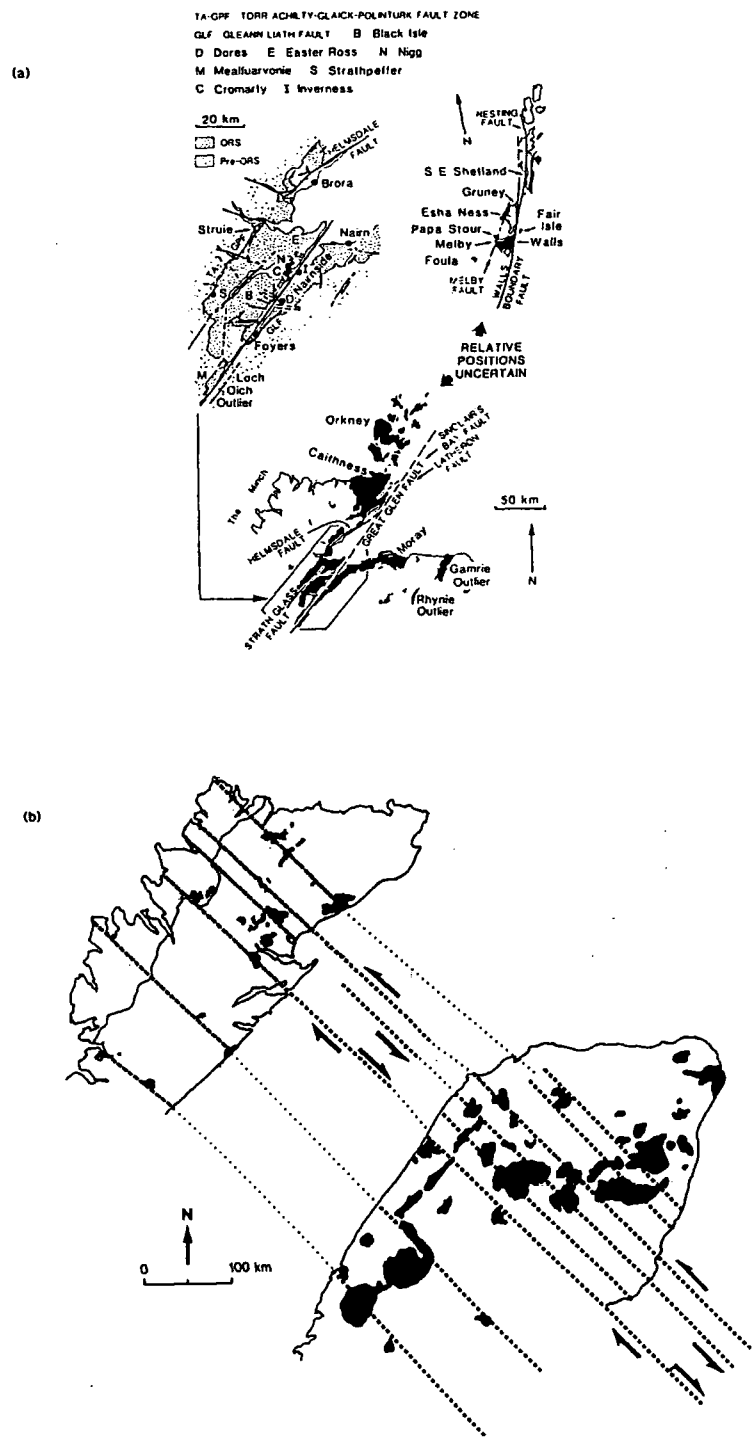

Fig. 9.57. **(a)** Reconstruction of the original configuration of onshore outcrops of the Orcadian ORS. After Rogers *et al.* (1989). **(b)** Generalised model showing the position of the Grampians relative to the Northern Highlands during the late Caledonian when the 25-29 km dextral displacement proposed by Rogers *et al.* (1989) is restored. Major NW-SE-trending (geologically-defined) lineaments are shown: 1, Cruachan; 2, Strath Ossian; 3, Foyers-Glen Tilt; 4, Monadliath; 5, Moy-Lochnagar; 6, Ardclach-Glen Cairn; 7, Glenlivet; 8, Rothes; 9, Portsoy-Duchray Hill; 10, Fraserburgh-Old Meldrum; 11, Insch; 12, "northern" Deeside; 13, "southern" Deeside; 14, Kilmelford-Comrie.

9.24 CONCLUSIONS

- In northern Scotland it may be possible to sub-divide the underlying basement into several 'distinct tectonic domains'. These 'domains' are characterised by the orientation of geologically-defined lineaments (or shear zones) which are interpreted as representing the approximate position of deep crustal penetrating structures.

  In the Grampian Highlands, three 'tectonically distinct domains' have been recognised:

  (1) In the SW and Central Grampian Highlands (the "Central and SW Highlands tectonic domain"), several NE-SW-trending shear zones and faults related to the Caledonian transpressional collision are recognised as being distinct from an intersecting set of NW-SE-trending pre-Caledonian crustal lineaments which were reactivated during Caledonian orogenesis. Where these structures intersect they have controlled the siting and ascent of late Caledonian magmatism;

  (2) In the NE Highlands (Buchan block: "NE Highlands tectonic domain") an E-W- and NNE-SSW-trending shear zone/lineament system (Ashcroft *et al.* 1984) may dominate over a NW-SE-trending set of lineaments. Many late Caledonian granitic plutons appear to be sited at shear zone or lineament intersections where transtensional zones allowed and facilitated their ascent;

  (3) In the Southern Highlands (the "Southern Highlands tectonic domain") three sets of major tectonic structures may have been responsible for the siting of Caledonian plutons where they intersect each other. Several NE-SW-trending faults related to Caledonian transpression are distinct from two intersecting sets of NW-SE- and E-W-trending lineaments.

  In the Northern Highlands, two 'tectonically distinct domains' may occur:

  (1) The "north-western Northern Highlands tectonic domain". This is characterised by major NW-SE-trending lineaments which appear to have controlled the siting of late Caledonian magmatism;

(2) The "south-eastern Northern Highlands tectonic domain". This however, is characterised by a predomiant E-W-trending 'tectonic fabric' which may have controlled the localisation and orientation of Permo-Carboniferous dyke swarms.

❷ A major deep crustal lineament, named here the "Ossian-Loch Quoich Line", may represent the approximate position of a major terrane boundary. Before major movements along the Great Glen Fault, it may have controlled the northern limit of NW-directed underthrusting of a tectonically distinct basement unit (characterised by an E-W 'tectonic fabric') beneath the Dalradian and part of the southern Moine cover sequence. It is defined by a change in the orientation and dominance of lineaments across this zone, and appears to have been the focus for regional deformation, localised along parts of this structure, and repeatedly exploited by magmatism. When the offset along the Great Glen Fault is restored, the terrane boundary has an arcuate form passing through the Geal-Charn Ossian Steep Belt and Grampian Steep Belt in the SW and Central Highlands, and is spatially coincident with the Loch Quoich Line and Northern Highlands Steep Belt in the Northern Highlands.

❸ A tentative model is presented below which may help to explain the relative timing and initiation of deformational events within both the Grampians and the Northern Highlands during the development of several distinct tectonic domains.

Initial stages of Caledonian deformation in the Grampian terrane involved the across-strike shortening of the Dalradian cover during the Grampian orogeny. The first "phase" of deformation (D1) occurred at approximately 590 Ma, which may have been produced by the thrusting in of a basement wedge which is characterised by an E-W fracture/lineament/shear zone system, beneath part of the Dalradian and Moine cover sequences. This underthrusting possibly occurred during the collision of continental fragment terranes against the Dalradian passive margin sequence (Dalradian Miogeocline). The northern limit of this underthrusting appears to have been controlled by a major, pre-existing tectonic boundary; the 'Ossian-Loch Quoich Line'. This event leading to the elevation and thickening of the Dalradian and Moine in the hanging wall of the thrust.

In the NE Highlands (Buchan block), the emplacement of the 'Younger Basic' intrusives along the E-W-trending shear zone system suggests that the thrusting in of the basement wedge must have occurred before the emplacement of these intrusive bodies. The suite of gabbros is regarded to have been intruded into the Dalradian about peak metamorphism (post-D2; Fettes 1970; Ashworth 1975; Kneller & Leslie 1984), with the Insch Intrusion dated at 489 +/- 17 Ma (Pankhurst

1970). The emplacement of the Aberdeen granitic pluton at 470 +/- 1 Ma (Kneller & Aftalion 1987) suggests that the 'Younger Basics' were emplaced before D3 regional deformation.

It is regarded that the Grampian lower crust (LCRZ) comprises a series of 'blocks' bounded by anastomosing shear zones related to the shear zone/lineament system established within the mid- to upper-crust and major tectonic structures within the underlying mantle. The whole system is essentially bounded by the Great Glen Fault in the north and the Highland Boundary Fault in the south. It is envisaged that the final oblique closure of Iapetus led to a gross sinistral transpressional deformation which initiated sinistral movement along the Great Glen and Highland Boundary fault systems. The resultant transpressive motion along the Caledonian NE-SW-trending bounding structures is transferred to non-transpressive motion at lower crustal levels. This allows the 'blocks' in the lower crust to undergo a gross clockwise rotation in order to accommodate the overall sinistral deformational component imposed on the whole system. Due to the geometry of the whole system, with increasing deformation it would seem necessary that movements along the NW-SE-trending lineaments would have to increase in magnitude towards the NE. The NE Highlands may therefore lie in an overall "extensional zone", leading to the activation of the E-W-trending lineament/shear zone system established within the basement wedge. This may explain the distribution and relative timing of emplacement of the 'Younger Basics' and the subsequent intrusion of the Grampian (Ordovician) Granites in the NE Highlands. During this episode, regional compression associated with the "divergent system" established within the NE Highlands, initiated the collapse of the Moine wedge in the Northern Highlands, providing the driving mechanism of the early Moine Thrust system.

It is suggested that an overall sinistral component of approximately 200-240 km occurred along the Great Glen Fault, leading to the displacement of the crust and uppermost mantle on either side of this structure. However, this deformation was decoupled from the underlying mantle, preventing the displacement of major mantle tectonic structures (i.e. NW-SE-trending lineaments).

During the late Caledonian, the NW-SE-trending deep crustal lineaments controlled the siting and distribution of late Caledonian magmatism. This produced a set of geologically-defined lineaments within the Dalradian and Moine cover sequences, which maintained their along strike continuity across the Great Glen Fault with relatively little disturbance.

A late Caledonian dextral component of approximately 25-30 km displaced the cover lineaments across the Great Glen Fault to their present position, but as before, possibly not affecting major mantle lineaments.

APPENDIX 2

MAFIC ENCLAVE STRAIN DATA:

SHAPE RATIOS AND LOG MEANS

STRAIN ANALYSIS FROM MICROGRANITOID ENCLAVES

At a particular locality, the determination of strain involved the measurement of the long and short axes of individual microgranitoid enclaves on two sets of mutually perpendicular joint surfaces which were approximately parallel to two of the principal strain planes. The most commonly exposed surfaces, available for the measurement of enclaves, are sub-horizontal, perpendicular to the foliation, but parallel to the lineation (X/Z strain planes). From vertical joint surfaces, perpendicular to the X direction, Y/Z values were obtained. Due to the nature of the exposure, vertical surfaces are uncommon, and so the amount of Y/Z values measured at any one locality are limited, and have thus been generally omitted from the data sets shown in this Appendix. In areas where the number of Y/Z values obtained were >20, the Y/Z ratio has been commented upon in the relevant text and the location shown on the relevant figures. The shape ratio can be calculated for each principal plane. For a population of enclaves (generally between 20-60) the mean shape ratio can be logarithmically (geometrically) calculated for each strain plane. The number of X/Z values measured for the granitic complexes observed in this thesis are as follows: the Etive Complex (including the (high level) Quarry Intrusion), approximately 3700; the Rannoch Moor Complex, approximately 5350; the Glencoe Complex (including the high level Glencoe Fault Intrusion), approximately 2700; the Strath Ossian Complex, approximately 1200.

Due to the number of values collected, only data sets with population sizes generally greater than 30 are presented in this Appendix; approximately 30% of the total data collected for each granitic complex. All mean shape ratios are, however, represented on the relevant figures and enclosure maps for each granitic complex. Frequency distributions of

the microgranitoid X/Z ratios from individual localities are shown. They show well defined (slightly skewed), log-normal distributions with well defined means. The standard deviation for each population has been calculated.

Values shown are for microgranitoid enclaves, unless otherwise stated, i.e. country rock xenoliths (C.R.Xenolith).

Etive Complex: Allt Ceitlein
Intrusive Phase: The Cruachan facies (G2)

Location [148 477]

X	Z	X/Z	log(X/Z)	log(X×Zπ/4)
8.00	3.50	2.29	0.36	1.34
15.60	6.20	2.52	0.40	1.88
7.20	3.10	2.32	0.37	1.24
2.10	0.70	3.00	0.48	0.06
4.10	1.60	2.56	0.41	0.71
3.30	0.80	4.13	0.62	0.32
9.00	4.50	2.00	0.30	1.50
4.80	2.30	2.09	0.32	0.94
6.10	2.00	3.05	0.48	0.98
9.10	4.60	1.98	0.30	1.52
4.90	2.40	2.04	0.31	0.97
8.30	4.40	1.89	0.28	1.46
8.20	4.10	2.00	0.30	1.42
7.20	2.70	2.67	0.43	1.18
7.00	3.90	1.79	0.25	1.33
3.10	0.60	5.17	0.71	0.16
9.20	4.70	1.96	0.29	1.53
3.40	0.90	3.78	0.58	0.38
2.30	2.20	1.05	0.02	0.60
6.80	2.50	2.72	0.43	1.13
7.10	2.60	2.73	0.44	1.16
8.80	4.40	2.00	0.30	1.48

X	Z	X/Z	log(X/Z)	log(X×Zπ/4)
6.80	2.30	2.96	0.47	1.09
6.40	2.30	2.78	0.44	1.06
5.30	2.80	1.89	0.28	1.07
6.20	2.10	2.95	0.47	1.01
7.00	2.50	2.80	0.45	1.14
5.40	2.90	1.86	0.27	1.09
8.90	4.40	2.02	0.31	1.49
8.10	4.00	2.03	0.31	1.41
3.30	0.80	4.13	0.62	0.32
5.10	2.60	1.96	0.29	1.02
8.40	4.30	1.95	0.29	1.45
6.90	2.00	3.45	0.54	1.03

sum	13.10	36.47
sum/N	0.39	1.07
average	2.43	11.82
wlog	0.69	1.82
N	34	34
S.D.	0.13	0.43
max	0.71	1.88
min	0.02	0.06

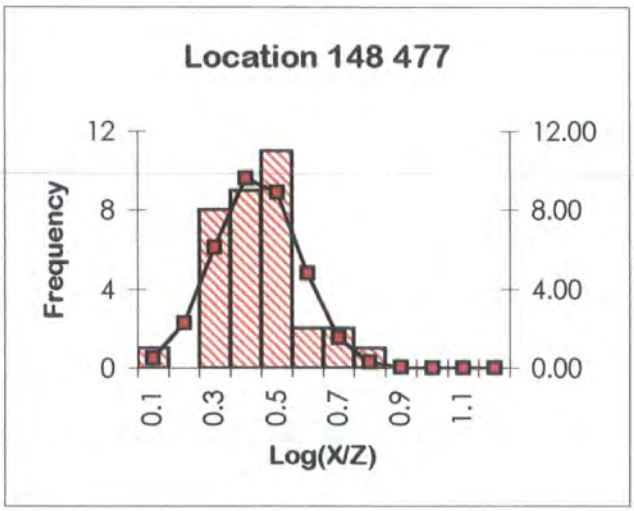

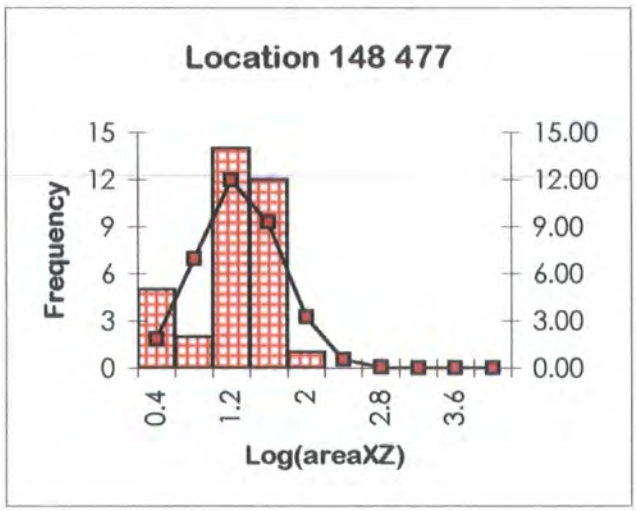

Etive Complex: Allt Ceitlein
Intrusive Phase: The Cruachan facies (G2)

Location [151 477]

X	Z	X/Z	log(X/Z)	log (X×Zπ/4)
10.00	2.10	4.76	0.68	1.22
8.30	2.80	2.96	0.47	1.26
7.20	1.70	4.24	0.63	0.98
8.50	3.00	2.83	0.45	1.30
6.80	1.10	6.18	0.79	0.77
10.40	4.40	2.36	0.37	1.56
12.60	2.90	4.34	0.64	1.46
7.00	4.00	1.75	0.24	1.34
4.10	0.90	4.56	0.66	0.46
4.30	1.70	2.53	0.40	0.76
5.90	2.70	2.19	0.34	1.10
3.70	0.50	7.40	0.87	0.16
11.00	2.80	3.93	0.59	1.38
11.20	3.30	3.39	0.53	1.46
5.00	0.50	10.00	1.00	0.29
5.20	2.20	2.36	0.37	0.95
8.10	4.00	2.03	0.31	1.41
6.90	2.20	3.14	0.50	1.08
9.00	3.00	3.00	0.48	1.33
9.80	3.80	2.58	0.41	1.47
14.50	4.60	3.15	0.50	1.72
4.80	1.80	2.67	0.43	0.83
5.20	0.70	7.43	0.87	0.46
5.40	1.10	4.91	0.69	0.67
7.90	3.20	2.47	0.39	1.30
4.20	1.10	3.82	0.58	0.56
15.70	6.10	2.57	0.41	1.88
4.70	1.50	3.13	0.50	0.74
3.50	0.30	11.67	1.07	-0.08
4.70	1.00	4.70	0.67	0.57
5.90	1.80	3.28	0.52	0.92
8.00	2.50	3.20	0.51	1.20
3.20	0.60	5.33	0.73	0.18
3.60	0.60	6.00	0.78	0.23
13.20	5.60	2.36	0.37	1.76
6.10	2.00	3.05	0.48	0.98
9.00	1.10	8.18	0.91	0.89
8.00	2.00	4.00	0.60	1.10
4.30	1.20	3.58	0.55	0.61
7.00	1.50	4.67	0.67	0.92
5.00	1.50	3.33	0.52	0.77
7.80	3.50	2.23	0.35	1.33
14.90	5.00	2.98	0.47	1.77
6.30	2.20	2.86	0.46	1.04
8.80	0.90	9.78	0.99	0.79
7.20	4.20	1.71	0.23	1.38
7.60	3.30	2.30	0.36	1.29
7.00	3.50	2.00	0.30	1.28
5.70	1.00	5.70	0.76	0.65

X	Z	X/Z	log(X/Z)	log (X×Zπ/4)
13.00	4.80	2.71	0.43	1.69
3.00	0.70	4.29	0.63	0.22
5.80	2.30	2.52	0.40	1.02
6.50	1.00	6.50	0.81	0.71
5.60	1.30	4.31	0.63	0.76
4.10	0.90	4.56	0.66	0.46
7.40	3.10	2.39	0.38	1.26
12.50	2.60	4.81	0.68	1.41
6.80	1.30	5.23	0.72	0.84
7.90	3.80	2.08	0.32	1.37
4.40	0.90	4.89	0.69	0.49
9.20	3.70	2.49	0.40	1.43
8.30	4.20	1.98	0.30	1.44
6.20	2.70	2.30	0.36	1.12
6.10	2.90	2.10	0.32	1.14
5.70	2.50	2.28	0.36	1.05
5.90	2.70	2.19	0.34	1.10
5.90	1.20	4.92	0.69	0.75
6.80	3.30	2.06	0.31	1.25
12.90	3.00	4.30	0.63	1.48
10.20	4.20	2.43	0.39	1.53
8.80	3.30	2.67	0.43	1.36
9.20	1.30	7.08	0.85	0.97
11.10	3.10	3.58	0.55	1.43
5.10	1.80	2.83	0.45	0.86
7.10	3.00	2.37	0.37	1.22
6.00	3.00	2.00	0.30	1.15
6.60	2.70	2.44	0.39	1.15
4.50	0.50	9.00	0.95	0.25
5.00	1.50	3.33	0.52	0.77
5.80	2.40	2.42	0.38	1.04
4.80	0.70	6.86	0.84	0.42
2.50	0.70	3.57	0.55	0.14
5.20	1.20	4.33	0.64	0.69
4.80	1.30	3.69	0.57	0.69
5.30	1.40	3.79	0.58	0.77
4.30	1.50	2.87	0.46	0.70
8.10	3.40	2.38	0.38	1.34
6.60	3.10	2.13	0.33	1.21
4.80	0.30	16.00	1.20	0.05
5.60	1.70	3.29	0.52	0.87
4.60	1.10	4.18	0.62	0.60
4.90	1.70	2.88	0.46	0.82
4.60	1.30	3.54	0.55	0.67
14.80	4.70	3.15	0.50	1.74
11.00	3.10	3.55	0.55	1.43
6.70	3.00	2.23	0.35	1.20
5.00	2.00	2.50	0.40	0.90
3.90	0.70	5.57	0.75	0.33

6.60	2.30	2.87	0.46	1.08
5.50	1.00	5.50	0.74	0.64
7.50	2.00	3.75	0.57	1.07
12.20	4.00	3.05	0.48	1.58
11.40	3.20	3.56	0.55	1.46
4.30	0.60	7.17	0.86	0.31
6.30	0.80	7.88	0.90	0.60
5.80	1.50	3.87	0.59	0.83
6.10	1.40	4.36	0.64	0.83
6.00	2.50	2.40	0.38	1.07
13.70	3.80	3.61	0.56	1.61
13.30	4.90	2.71	0.43	1.71
9.00	3.50	2.57	0.41	1.39
6.30	2.60	2.42	0.38	1.11
8.70	3.20	2.72	0.43	1.34
10.80	2.90	3.72	0.57	1.39

3.90	0.60	6.50	0.81	0.26
8.20	2.20	3.73	0.57	1.15
7.80	1.80	4.33	0.64	1.04
6.80	3.80	1.79	0.25	1.31
5.50	2.30	2.39	0.38	1.00
6.70	1.20	5.58	0.75	0.80
7.70	3.00	2.57	0.41	1.26

sum	65.38	120.33
sum/N	0.54	0.99
average	3.47	9.87
wlog	0.97	1.96
N	121	121
S.D.	0.19	0.43
max	1.20	1.88
min	0.23	-0.08

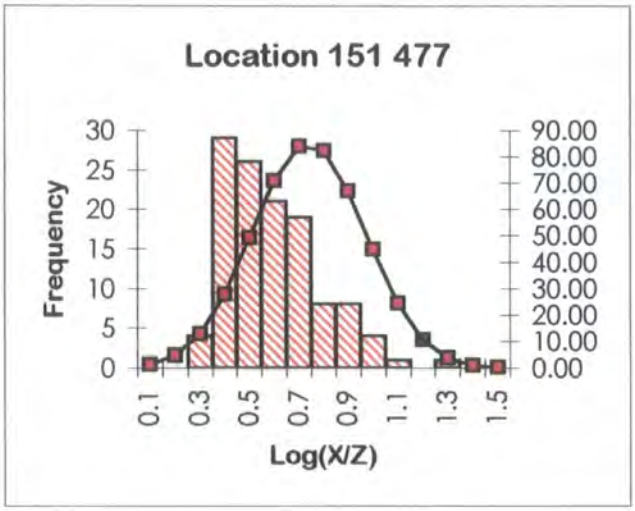

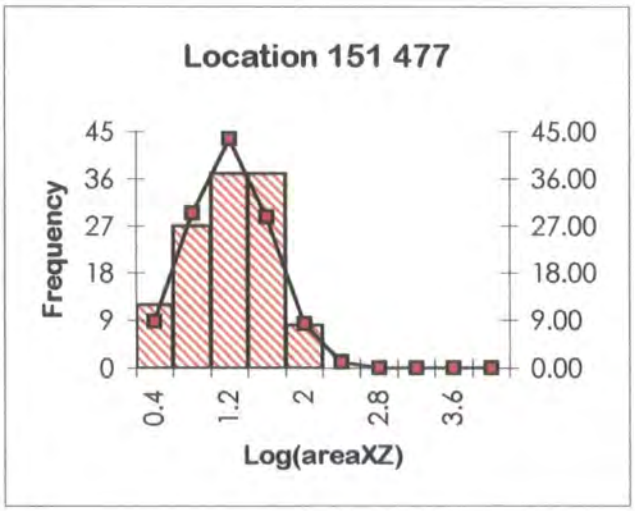

Etive Complex: Allt nan Gaoirean High Strain Zone
Intrusive Phase: The Cruachan facies (G2) (near to country rock contact)

Location [116 495]

X	Z	X/Z	log(X/Z)	log(X×Zπ/4)
23.00	2.50	9.20	0.96	1.65
12.90	3.30	3.91	0.59	1.52
20.70	1.30	15.92	1.20	1.33
15.60	4.00	3.90	0.59	1.69
21.80	1.30	16.77	1.22	1.35
11.00	1.40	7.86	0.90	1.08
21.70	2.30	9.43	0.97	1.59
15.20	4.00	3.80	0.58	1.68
22.80	3.60	6.33	0.80	1.81
13.00	1.80	7.22	0.86	1.26
10.80	1.00	10.80	1.03	0.93
23.60	3.50	6.74	0.83	1.81
22.20	1.70	13.06	1.12	1.47
13.10	3.50	3.74	0.57	1.56
13.60	2.00	6.80	0.83	1.33
11.20	1.60	7.00	0.85	1.15
21.10	1.40	15.07	1.18	1.37
13.40	1.80	7.44	0.87	1.28
22.50	3.50	6.43	0.81	1.79
24.10	3.70	6.51	0.81	1.85
11.40	1.80	6.33	0.80	1.21

X	Z	X/Z	log(X/Z)	log(X×Zπ/4)
20.50	1.10	18.64	1.27	1.25
12.80	3.10	4.13	0.62	1.49
15.20	3.60	4.22	0.63	1.63
23.80	3.70	6.43	0.81	1.84
10.00	0.80	12.50	1.10	0.80
11.30	1.10	10.27	1.01	0.99
12.00	2.20	5.45	0.74	1.32
11.00	1.20	9.17	0.96	1.02
21.00	1.40	15.00	1.18	1.36
22.30	3.30	6.76	0.83	1.76
11.40	1.20	9.50	0.98	1.03
14.20	3.00	4.73	0.68	1.52

sum	29.17	46.72
sum/N	0.88	1.42
average	7.66	26.05
wlog	0.70	1.05
N	33.00	33.00
S.D.	0.20	0.29
max	1.27	1.85
min	0.57	0.80

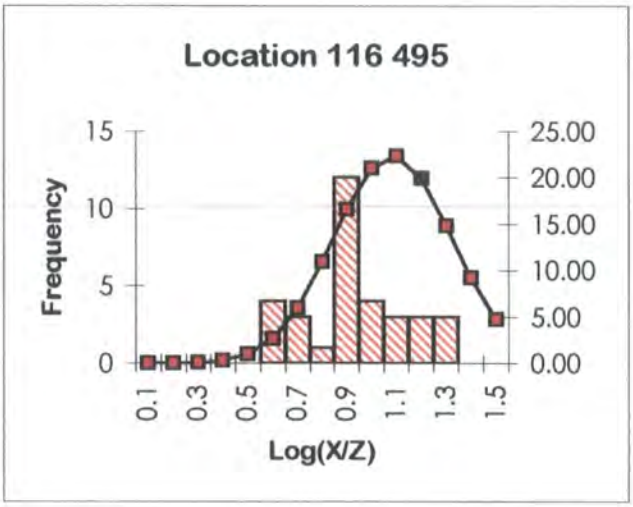

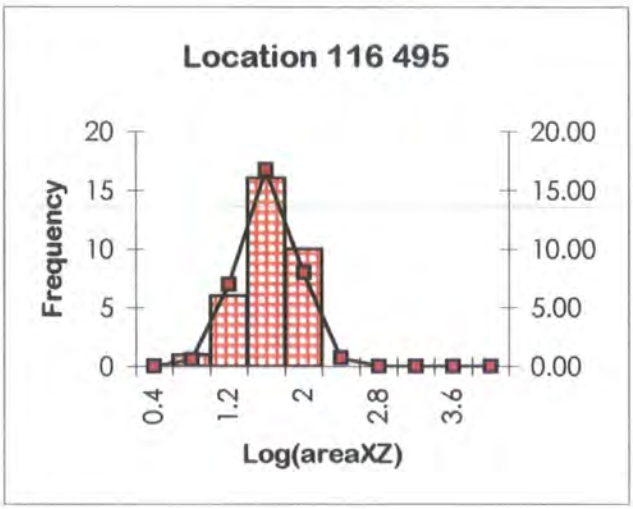

Etive Complex: Allt nan Gaoirean High Strain Zone
Intrusive Phase: The Cruachan facies (G2)

Location [120 486]

X	Z	X/Z	log(x/z)	log (X×Zπ/4)
5.00	1.50	3.33	0.52	0.77
5.40	2.30	2.35	0.37	0.99
8.30	0.60	13.83	1.14	0.59
9.50	2.00	4.75	0.68	1.17
5.60	2.00	2.80	0.45	0.94
11.50	2.80	4.11	0.61	1.40
5.80	2.90	2.00	0.30	1.12
5.30	2.00	2.65	0.42	0.92
5.70	2.40	2.38	0.38	1.03
9.60	2.50	3.84	0.58	1.28
4.40	0.70	6.29	0.80	0.38
10.80	2.10	5.14	0.71	1.25
9.20	0.50	18.40	1.26	0.56
9.80	2.70	3.63	0.56	1.32
4.00	0.60	6.67	0.82	0.28
4.40	1.30	3.38	0.53	0.65
13.60	2.90	3.66	0.56	1.38
10.60	1.70	6.24	0.79	1.15
4.30	1.30	3.31	0.52	0.64
4.80	1.40	3.43	0.54	0.72
9.80	2.30	4.26	0.63	1.25
11.00	2.30	4.78	0.68	1.30
8.10	0.40	20.25	1.31	0.41
10.30	2.60	3.96	0.60	1.32
4.00	0.30	13.33	1.12	-0.03
17.20	2.50	4.48	0.65	1.34
5.00	1.60	3.13	0.49	0.80
6.00	2.90	2.07	0.32	1.14

X	Z	X/Z	log(x/z)	log (X×Zπ/4)
15.20	2.30	6.61	0.82	1.44
4.20	0.70	6.00	0.78	0.36
5.90	2.60	2.27	0.36	1.08
9.00	1.30	7.69	0.89	1.01
8.90	1.60	5.56	0.75	1.05
3.40	0.30	11.33	1.05	-0.10
5.10	1.90	2.68	0.43	0.88
7.70	0.40	19.25	1.28	0.38
10.10	2.80	3.61	0.56	1.35
3.70	0.40	9.25	0.97	0.07
5.60	2.50	2.24	0.35	1.04
8.00	0.50	16.00	1.20	0.50
8.10	0.80	10.13	1.01	0.71
10.15	2.40	4.21	0.62	1.28
9.00	0.30	30.00	1.48	0.33
4.10	0.60	6.83	0.83	0.29
9.10	1.40	6.50	0.81	1.00
5.10	1.60	3.19	0.50	0.81

sum	24.81	27.13
sum/N	0.54	0.59
average	3.46	3.89
wlog	1.16	1.53
N	46.00	46.00
S.D.	0.30	0.42
max	1.48	1.44
min	0.32	-0.10

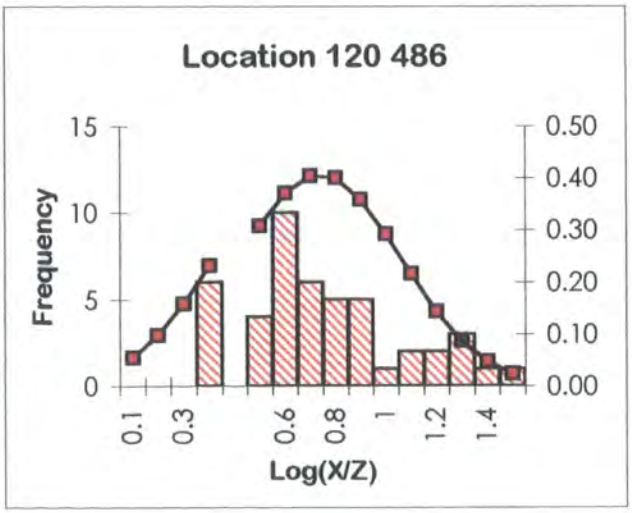

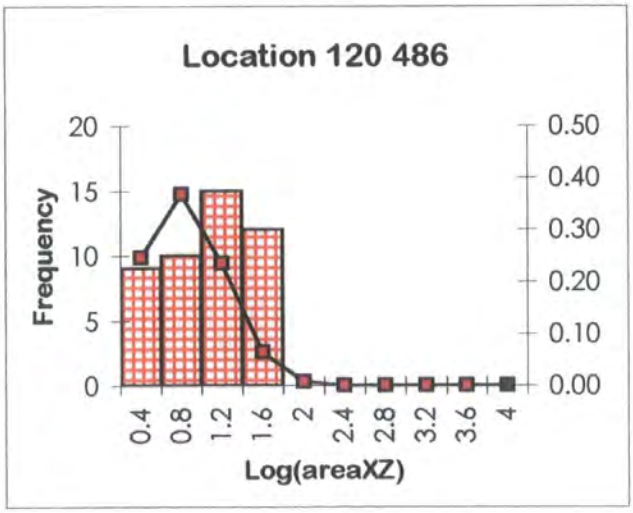

Etive Complex: Allt nan Gaoirean High Strain Zone
Intrusive Phase: The Cruachan facies (G2)

Location [123 482]

X	Z	X/Z	log(X/Z)	log(X×Zπ/4)
30.10	6.90	4.36	0.64	2.21
27.10	5.10	5.31	0.73	2.04
8.10	2.00	4.05	0.61	1.10
8.50	3.40	2.50	0.40	1.36
8.30	2.20	3.77	0.58	1.16
10.70	2.40	4.46	0.65	1.30
28.70	5.90	4.86	0.69	2.12
9.80	3.90	2.51	0.40	1.48
26.70	7.30	4.21	0.62	2.25
7.60	1.50	5.07	0.70	0.95
13.50	5.00	2.70	0.43	1.72
8.60	2.50	3.44	0.54	1.23
11.40	3.10	3.68	0.57	1.44
9.50	3.60	2.64	0.42	1.43
29.10	6.30	4.62	0.66	2.16
5.80	1.86	3.12	0.49	0.93
7.90	1.80	4.39	0.64	1.05
5.90	1.30	4.54	0.66	0.78
24.10	5.90	4.93	0.69	2.13
12.00	3.50	3.43	0.54	1.52
5.20	0.60	8.67	0.94	0.39
6.20	0.80	7.75	0.89	0.59
10.00	4.10	2.44	0.39	1.51
31.40	8.00	3.93	0.59	2.30
8.10	3.00	2.70	0.43	1.28
7.80	2.70	2.89	0.46	1.22
28.60	6.40	4.47	0.65	2.16
6.70	2.10	3.19	0.50	1.04
8.80	3.70	2.38	0.38	1.41
6.00	1.60	3.75	0.57	0.88
11.10	2.80	3.96	0.60	1.39

X	Z	X/Z	log(X/Z)	log(X×Zπ/4)
12.80	4.30	2.98	0.47	1.64
10.10	4.40	2.30	0.36	1.54
31.20	7.80	4.00	0.60	2.28
8.30	3.20	2.59	0.41	1.32
15.70	7.10	2.21	0.34	1.94
11.00	2.50	4.40	0.64	1.33
10.40	4.70	2.21	0.34	1.58
5.50	1.10	5.00	0.70	0.68
5.60	1.20	4.67	0.67	0.72
29.40	6.60	4.45	0.65	2.18
31.10	7.50	4.15	0.62	2.26
13.20	4.70	2.81	0.45	1.69
6.30	1.70	3.71	0.57	0.92
12.80	4.70	2.72	0.44	1.67
9.00	3.10	2.90	0.46	1.34
6.10	1.70	3.59	0.55	0.91
10.50	2.00	5.25	0.72	1.22
22.70	8.30	3.82	0.58	2.32
7.10	2.50	2.84	0.45	1.14
6.40	1.80	3.56	0.55	0.96
6.60	2.00	3.30	0.52	1.02
12.70	4.20	3.02	0.48	1.62

sum	18.00	46.45
sum/N	0.34	0.88
average	2.19	7.52
wlog	0.59	1.93
N	53.00	53.00
S.D.	0.13	0.51
max	0.94	2.32
min	0.34	0.39

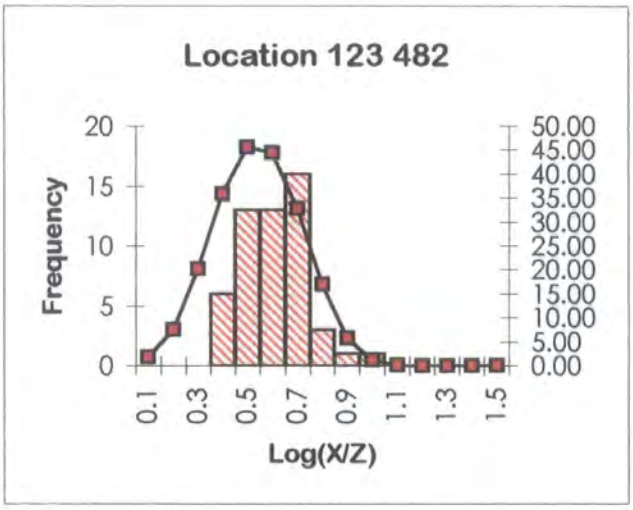
Location 123 482
Frequency
20
15
10
5
0
50.00
45.00
40.00
35.00
30.00
25.00
20.00
15.00
10.00
5.00
0.00
0.1
0.3
0.5
0.7
0.9
1.1
1.3
1.5
Log(X/Z)

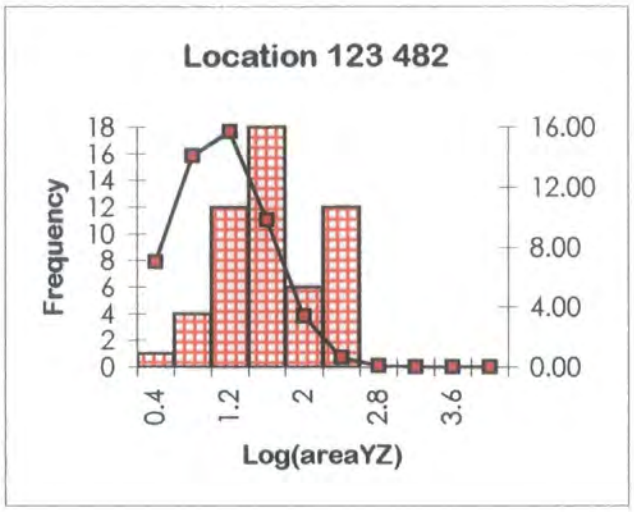
Location 123 482
Frequency
18
16
14
12
10
8
6
4
2
0
16.00
12.00
8.00
4.00
0.00
0.4
1.2
2
2.8
3.6
Log(areaYZ)

Etive Complex: Allt nan Gaoirean High Strain Zone
Intrusive Phase: The Cruachan facies (G2)

Location [123 483]

X	Z	X/Z	log(X/Z)	log(X×Zπ/4)
11.00	1.50	7.33	0.87	1.11
17.50	6.50	2.69	0.43	1.95
18.70	5.40	3.46	0.54	1.90
9.60	0.50	19.20	1.28	0.58
12.00	3.20	3.75	0.57	1.48
8.20	2.80	2.93	0.47	1.26
15.50	1.90	8.16	0.91	1.36
16.20	3.50	4.63	0.67	1.65
11.50	0.60	19.17	1.28	0.73
10.00	0.40	25.00	1.40	0.50
12.10	2.60	4.65	0.67	1.39
17.30	4.40	3.93	0.59	1.78
6.00	0.60	10.00	1.00	0.45
14.20	4.50	3.16	0.50	1.70
8.70	4.20	2.07	0.32	1.46
11.20	1.30	8.62	0.94	1.06
22.50	6.00	3.75	0.57	2.03
5.90	2.20	2.68	0.43	1.01
7.70	2.50	3.08	0.49	1.18
16.20	3.10	5.23	0.72	1.60
15.00	2.00	7.50	0.88	1.37
13.10	3.60	3.64	0.56	1.57
4.10	1.00	4.10	0.61	0.51
12.20	2.30	5.30	0.72	1.34
7.10	1.00	7.10	0.85	0.75
6.20	0.80	7.75	0.89	0.59
18.20	5.10	3.57	0.55	1.86
12.00	2.10	5.71	0.76	1.30
13.10	4.00	3.28	0.52	1.61
17.70	6.70	2.64	0.42	1.97
17.20	4.20	4.10	0.61	1.75
14.30	4.00	3.58	0.55	1.65
8.50	4.00	2.13	0.33	1.43
6.30	2.60	2.42	0.38	1.11
19.80	3.90	5.08	0.71	1.78
15.50	4.10	3.78	0.58	1.70
9.80	0.70	14.00	1.15	0.73
9.90	0.90	11.00	1.04	0.84
17.00	4.00	4.25	0.63	1.73
7.30	3.20	2.28	0.36	1.26
8.20	1.30	6.31	0.80	0.92
15.70	4.70	3.34	0.52	1.76
11.10	0.20	55.50	1.74	0.24
17.00	6.60	2.58	0.41	1.95
14.00	3.90	3.59	0.56	1.63
8.30	3.80	2.18	0.34	1.39
12.10	2.20	5.50	0.74	1.32
16.50	5.50	3.00	0.48	1.85
18.90	5.80	3.26	0.51	1.93

X	Z	X/Z	log(X/Z)	log(X×Zπ/4)
14.80	4.50	3.29	0.52	1.72
17.50	6.50	2.69	0.43	1.95
10.30	1.20	8.58	0.93	0.99
12.20	0.80	15.25	1.18	0.88
9.00	4.50	2.00	0.30	1.50
19.40	3.70	5.24	0.72	1.75
12.20	2.30	5.30	0.72	1.34
10.00	0.90	11.11	1.05	0.85
11.60	2.80	4.14	0.62	1.41
16.60	4.00	4.15	0.62	1.72
12.30	2.50	4.92	0.69	1.38
11.30	1.60	7.06	0.85	1.15
11.90	2.00	5.95	0.77	1.27
16.30	3.80	4.29	0.63	1.69
5.70	0.50	11.40	1.06	0.35
10.00	1.20	8.33	0.92	0.97
12.80	3.50	3.66	0.56	1.55
11.80	3.00	3.93	0.59	1.44
11.20	0.50	22.40	1.35	0.64
18.40	5.30	3.47	0.54	1.88
7.80	2.80	2.79	0.44	1.23
4.80	1.20	4.00	0.60	0.66
4.00	0.70	5.71	0.76	0.34
21.00	5.10	4.12	0.61	1.92
6.70	0.50	13.40	1.13	0.42
10.90	1.90	5.74	0.76	1.21
5.20	1.20	4.33	0.64	0.69
13.20	3.10	4.26	0.63	1.51
15.70	4.30	3.65	0.56	1.72
14.90	1.70	8.76	0.94	1.30
10.70	1.40	7.64	0.88	1.07
13.30	2.80	4.75	0.68	1.47
13.50	3.40	3.97	0.60	1.56
19.90	4.60	4.33	0.64	1.86
21.80	5.90	3.69	0.57	2.00
12.60	2.30	5.48	0.74	1.36
13.20	3.30	4.00	0.60	1.53
22.10	6.00	3.68	0.57	2.02
19.50	6.50	3.00	0.48	2.00
24.70	8.10	3.05	0.48	2.20
16.00	3.00	5.33	0.73	1.58
7.10	1.20	5.92	0.77	0.83
7.00	1.60	4.38	0.64	0.94
6.10	2.40	2.54	0.41	1.06
17.80	4.90	3.63	0.56	1.84
9.00	0.50	18.00	1.26	0.55
17.30	4.70	3.68	0.57	1.81
20.10	5.00	4.02	0.60	1.90
11.40	1.90	6.00	0.78	1.23

11.60	2.20	5.27	0.72	1.30
12.70	2.80	4.54	0.66	1.45
16.50	3.50	4.71	0.67	1.66
13.60	1.90	7.16	0.85	1.31
15.80	3.40	4.65	0.67	1.63
11.70	1.80	6.50	0.81	1.22
17.90	7.10	2.52	0.40	2.00
12.70	2.60	4.88	0.69	1.41
5.50	2.00	2.75	0.44	0.94
8.60	3.40	2.53	0.40	1.36
12.40	3.40	3.65	0.56	1.52
6.90	2.60	2.65	0.42	1.15

14.00	3.30	4.24	0.63	1.56
16.90	3.80	4.45	0.65	1.70

sum	21.99	46.46
sum/N	0.20	0.41
average	1.57	2.60
wlog	0.85	1.85
N	112.00	112.00
S.D.	0.25	0.46
max	1.26	2.20
min	0.41	0.34

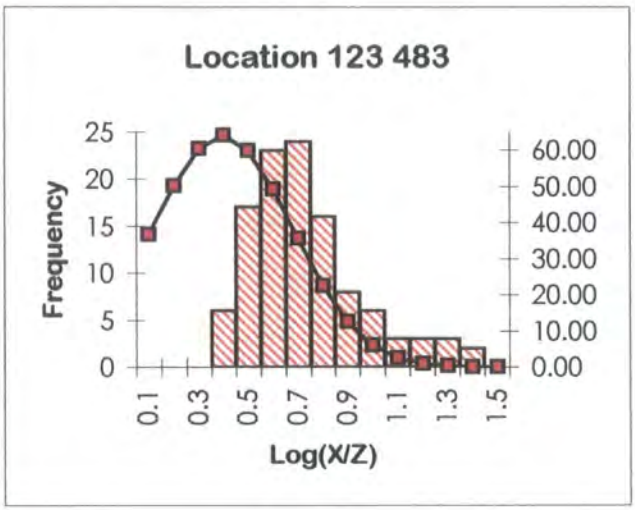

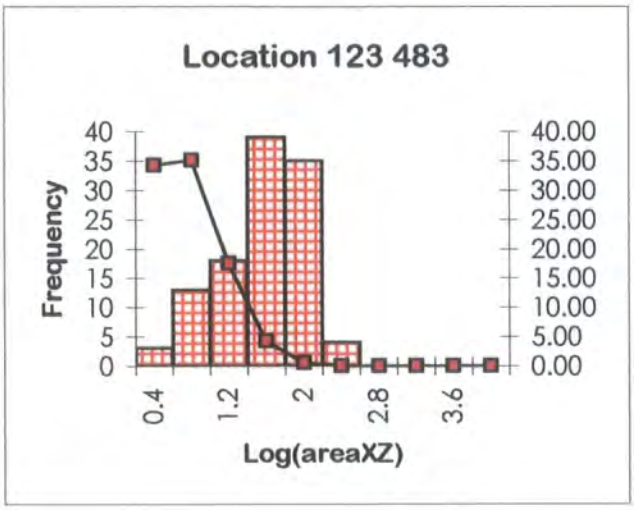

Etive Complex: Allt nan Gaoirean High Strain Zone
Intrusive Phase: The Cruachan facies (G2)

Location [132 477]

X	Z	X/Z	log(X/Z)	log(X×Zπ/4)
10.40	3.50	2.97	0.47	1.46
7.40	1.50	4.93	0.69	0.94
8.80	4.00	2.20	0.34	1.44
11.20	4.50	2.49	0.40	1.60
8.40	1.50	5.60	0.75	1.00
11.00	3.70	2.97	0.47	1.50
9.00	2.30	3.91	0.59	1.21
9.60	3.70	2.59	0.41	1.45
7.30	1.10	6.64	0.82	0.80
7.90	3.20	2.47	0.39	1.30
9.20	2.30	4.00	0.60	1.22
6.80	2.10	3.24	0.51	1.05
9.80	3.90	2.51	0.40	1.48
8.00	1.10	7.27	0.86	0.84
8.80	2.10	4.19	0.62	1.16
8.70	2.00	4.35	0.64	1.14
10.10	2.30	4.39	0.64	1.26
9.30	3.40	2.74	0.44	1.40
10.70	3.40	3.15	0.50	1.46
11.30	4.00	2.83	0.45	1.55
10.50	3.60	2.92	0.46	1.47
18.20	7.50	2.43	0.39	2.03
5.60	1.00	5.60	0.75	0.64
8.60	2.70	3.19	0.50	1.26
7.20	2.50	2.88	0.46	1.15
3.60	0.60	6.00	0.78	0.23
10.00	3.10	3.23	0.51	1.39
10.80	4.20	2.57	0.41	1.55
11.30	4.60	2.46	0.39	1.61
9.00	4.10	2.20	0.34	1.46
7.60	1.70	4.47	0.65	1.01
10.00	3.30	3.03	0.48	1.41
8.00	3.10	2.58	0.41	1.29
7.90	2.00	3.95	0.60	1.09
10.30	3.20	3.22	0.51	1.41

X	Z	X/Z	log(X/Z)	log(X×Zπ/4)
7.40	1.50	4.93	0.69	0.94
7.00	2.50	2.80	0.45	1.14
6.60	1.90	3.47	0.54	0.99
8.50	1.60	5.31	0.73	1.03
7.30	1.40	5.21	0.72	0.90
9.30	3.00	3.10	0.49	1.34
11.00	4.30	2.56	0.41	1.57
7.60	1.70	4.47	0.65	1.01
8.10	1.40	5.79	0.76	0.95
7.80	1.90	4.11	0.61	1.07
10.80	3.50	3.09	0.49	1.47
9.30	2.60	3.58	0.55	1.28
9.90	4.00	2.48	0.39	1.49
7.30	1.40	5.21	0.72	0.90
9.40	3.50	2.69	0.43	1.41
6.80	1.90	3.58	0.55	1.01
7.40	1.90	3.89	0.59	1.04
9.20	2.50	3.68	0.57	1.26
11.20	3.90	2.87	0.46	1.54
8.60	3.90	2.21	0.34	1.42
7.90	2.00	3.95	0.60	1.09
9.90	1.00	9.90	1.00	0.89
9.20	3.20	2.88	0.46	1.36
9.20	4.50	2.04	0.31	1.51
10.70	4.00	2.68	0.43	1.53

sum	32.58	74.40
sum/N	0.54	1.24
average	3.49	17.38
wlog	0.69	1.80
N	60.00	60.00
S.D.	0.15	0.29
max	1.00	2.03
min	0.31	0.23

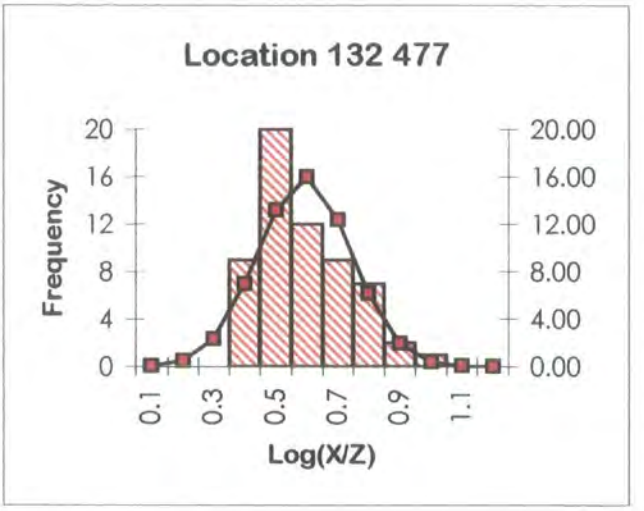
Location 132 477
Frequency
20
16
12
8
4
0
20.00
16.00
12.00
8.00
4.00
0.00
0.1
0.3
0.5
0.7
0.9
1.1
Log(X/Z)

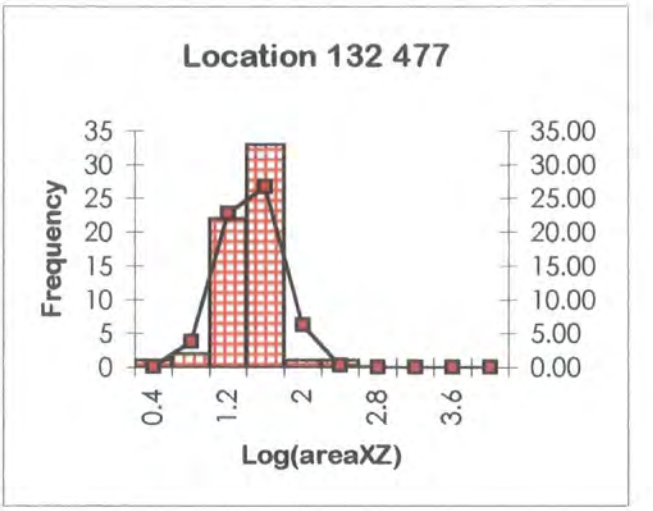
Location 132 477
Frequency
35
30
25
20
15
10
5
0
35.00
30.00
25.00
20.00
15.00
10.00
5.00
0.00
0.4
1.2
2
2.8
3.6
Log(areaXZ)

Glencoe Complex: An t-Sron: Allt Fionn Ghleann
Intrusive Phase: Glencoe Fault Intrusion (G1?)

Location [124 548]

X Orientation	X	Z	X/Z	log(x/z)	log (X×Zπ/4)
C. R. Xenolith 098	10.40	1.20	8.67	0.94	0.99
C. R. Xenolith 104	7.30	2.30	3.17	0.50	1.12
C. R. Xenolith 090	3.50	1.10	3.18	0.50	0.48
C. R. Xenolith 150	20.30	4.70	4.32	0.64	1.87
C. R. Xenolith 087	3.60	0.80	4.50	0.65	0.35
C. R. Xenolith 091	4.20	0.40	10.50	1.02	0.12
C. R. Xenolith 132	7.80	2.90	2.69	0.43	1.25
C. R. Xenolith 078	8.20	2.50	3.28	0.52	1.21
C. R. Xenolith 149	8.60	2.30	3.74	0.57	1.19
C. R. Xenolith 097	8.30	2.50	3.32	0.52	1.21
C. R. Xenolith 090	4.00	0.50	8.00	0.90	0.20
C. R. Xenolith 084	2.70	0.20	13.50	1.13	-0.37
C. R. Xenolith 093	4.50	2.20	2.05	0.31	0.89
C. R. Xenolith 097	9.30	0.30	31.00	1.49	0.34
C. R. Xenolith 095	8.30	3.00	2.77	0.44	1.29

sum	10.57	12.15
sum/N	0.70	0.51
average	5.07	3.21
wlog	1.18	2.25
N	15.00	24.00
S.D.	0.32	0.59
max	1.49	1.87
min	0.31	-0.37

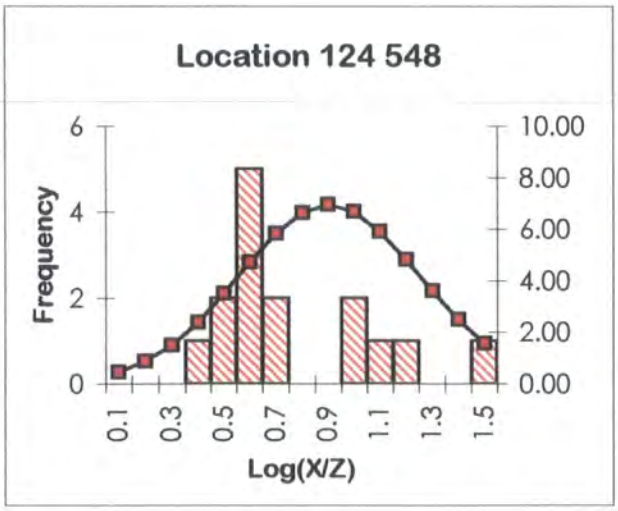

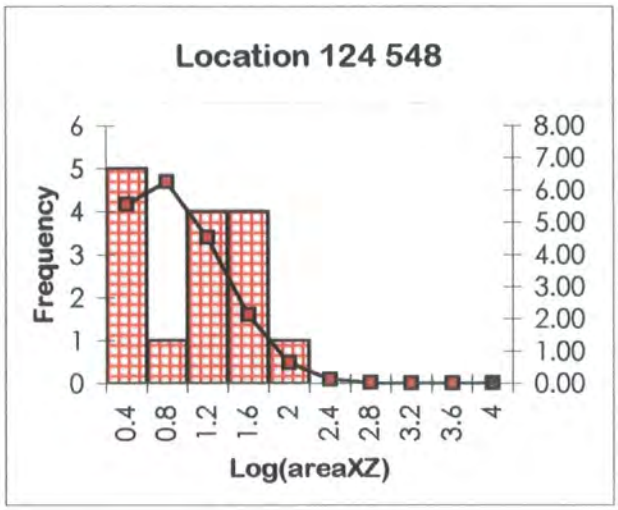

Glencoe Complex: An t-Sron: Allt Fionn Ghleann
Intrusive Phase: Glencoe Fault Intrusion (G1?)

Location [125 544]A

X Orientation	X	Z	X/Z	log(x/z)	log (X×Zπ/4)
C. R. Xenolith 066	10.80	1.20	9.00	0.95	1.01
C. R. Xenolith 026	3.20	1.20	2.67	0.43	0.48
C. R. Xenolith 155	6.70	3.20	2.09	0.32	1.23
C. R. Xenolith 010	7.40	1.60	4.63	0.67	0.97
C. R. Xenolith 036	3.10	0.70	4.43	0.65	0.23
C. R. Xenolith 150	3.00	0.60	5.00	0.70	0.15
C. R. Xenolith 060	3.80	1.20	3.17	0.50	0.55
C. R. Xenolith 023	4.40	1.70	2.59	0.41	0.77
C. R. Xenolith 130	3.20	1.40	2.29	0.36	0.55
C. R. Xenolith 043	6.00	3.20	1.88	0.27	1.18
C. R. Xenolith 147	5.50	1.10	5.00	0.70	0.68
C. R. Xenolith 140	4.60	2.00	2.30	0.36	0.86
C. R. Xenolith 133	11.50	3.30	3.48	0.54	1.47
C. R. Xenolith 172	2.50	1.00	2.50	0.40	0.29
C. R. Xenolith 143	3.20	0.90	3.56	0.55	0.35
C. R. Xenolith 141	3.20	1.90	1.68	0.23	0.68
C. R. Xenolith 114	3.30	1.00	3.30	0.52	0.41
C. R. Xenolith 192	5.30	0.50	10.60	1.03	0.32
187	6.00	5.10	1.18	0.07	1.38
C. R. Xenolith 037	5.00	2.20	2.27	0.36	0.94
C. R. Xenolith 082	5.00	1.50	3.33	0.52	0.77
C. R. Xenolith 192	2.80	0.30	9.33	0.97	-0.18
C. R. Xenolith 040	5.70	2.10	2.71	0.43	0.97
C. R. Xenolith 072	2.70	1.20	2.25	0.35	0.41
C. R. Xenolith 196	29.00	9.50	3.05	0.48	2.34
C. R. Xenolith 192	6.10	1.60	3.81	0.58	0.88
C. R. Xenolith 027	3.00	1.70	1.76	0.25	0.60
C. R. Xenolith 178	4.50	0.60	7.50	0.88	0.33
C. R. Xenolith 192	3.90	1.70	2.29	0.36	0.72
C. R. Xenolith 072	10.20	1.10	9.27	0.97	0.95
C. R. Xenolith 118	5.40	3.20	1.69	0.23	1.13
096	5.60	2.50	2.24	0.35	1.04
C. R. Xenolith 058	4.10	1.10	3.73	0.57	0.55
C. R. Xenolith 014	3.50	1.80	1.94	0.29	0.69
C. R. Xenolith 122	8.10	2.70	3.00	0.48	1.23
C. R. Xenolith 161	12.30	3.90	3.15	0.50	1.58
C. R. Xenolith 017	4.30	1.10	3.91	0.59	0.57
C. R. Xenolith 184	4.00	1.40	2.86	0.46	0.64
C. R. Xenolith 126	3.70	1.00	3.70	0.57	0.46
175	7.00	4.60	1.52	0.18	1.40
C. R. Xenolith 127	6.00	3.00	2.00	0.30	1.15

sum	20.31	32.73
sum/N	0.50	0.80
average	3.13	6.29
wlog	0.95	2.52
N	41.00	41.00
S.D.	0.23	0.46
max	1.03	2.34
min	0.07	-0.18

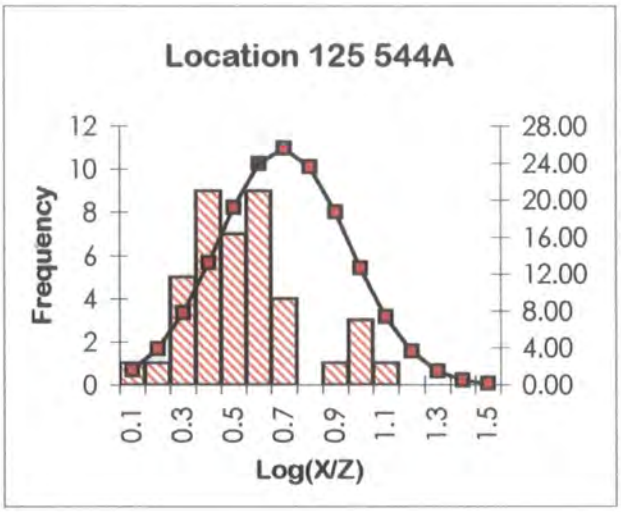

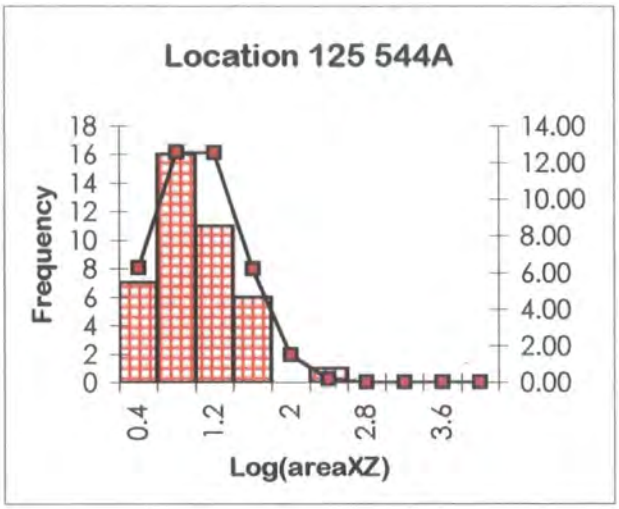

Glencoe Complex: An t-Sron: Allt Fionn Ghleann
Intrusive Phase: Glencoe Fault Intrusion (G1?)

Location [125 544]B

X Orientation	X	Z	X/Z	log(x/z)	log (X×Zπ/4)
C. R. Xenolith 024	7.20	1.70	4.24	0.63	0.98
C. R. Xenolith 020	4.50	2.60	1.73	0.24	0.96
C. R. Xenolith 014	3.70	1.10	3.36	0.53	0.50
C. R. Xenolith 050	6.00	3.00	2.00	0.30	1.15
C. R. Xenolith 042	2.60	1.20	2.17	0.34	0.39
C. R. Xenolith 028	3.40	1.20	2.83	0.45	0.51
C. R. Xenolith 142	9.40	1.20	7.83	0.89	0.95
C. R. Xenolith 110	5.30	2.20	2.41	0.38	0.96
C. R. Xenolith 138	9.50	1.40	6.79	0.83	1.02
C. R. Xenolith 008	4.10	1.20	3.42	0.53	0.59
C. R. Xenolith 008	4.20	2.10	2.00	0.30	0.84
C. R. Xenolith 143	3.50	1.30	2.69	0.43	0.55
C. R. Xenolith 090	2.50	1.20	2.08	0.32	0.37
C. R. Xenolith 148	3.50	0.70	5.00	0.70	0.28
C. R. Xenolith 102	4.00	3.60	1.11	0.05	1.05
C. R. Xenolith 190	11.10	1.30	8.54	0.93	1.05
C. R. Xenolith 124	6.50	6.00	1.08	0.03	1.49
C. R. Xenolith 020	12.50	1.10	11.36	1.06	1.03
C. R. Xenolith 020	5.10	2.50	2.04	0.31	1.00
C. R. Xenolith 010	5.50	2.00	2.75	0.44	0.94
C. R. Xenolith 002	11.60	5.50	2.11	0.32	1.70
C. R. Xenolith 104	7.00	1.10	6.36	0.80	0.78
C. R. Xenolith 116	3.50	1.10	3.18	0.50	0.48
C. R. Xenolith 158	4.40	1.10	4.00	0.60	0.58
C. R. Xenolith 118	10.00	2.10	4.76	0.68	1.22
C. R. Xenolith 138	4.10	0.60	6.83	0.83	0.29
C. R. Xenolith 138	3.50	0.80	4.38	0.64	0.34
C. R. Xenolith 138	4.00	1.90	2.11	0.32	0.78
C. R. Xenolith 095	6.00	1.50	4.00	0.60	0.85
C. R. Xenolith 110	5.30	1.20	4.42	0.65	0.70
C. R. Xenolith 041	2.70	1.00	2.70	0.43	0.33
C. R. Xenolith 022	6.40	0.40	16.00	1.20	0.30
C. R. Xenolith 101	6.70	1.80	3.72	0.57	0.98
C. R. Xenolith 013	4.40	0.60	7.33	0.87	0.32
C. R. Xenolith 024	3.20	1.00	3.20	0.51	0.40
C. R. Xenolith 156	19.80	4.30	4.60	0.66	1.83
C. R. Xenolith 052	9.60	1.20	8.00	0.90	0.96
C. R. Xenolith 034	4.00	1.70	2.35	0.37	0.73
C. R. Xenolith 044	5.50	1.50	3.67	0.56	0.81
C. R. Xenolith 006	5.30	1.50	3.53	0.55	0.80
C. R. Xenolith 036	3.10	1.00	3.10	0.49	0.39
C. R. Xenolith 014	8.50	6.20	1.37	0.14	1.62
C. R. Xenolith 012	4.50	0.60	7.50	0.88	0.33
C. R. Xenolith 020	7.00	3.20	2.19	0.34	1.25
C. R. Xenolith 088	3.00	0.50	6.00	0.78	0.07
C. R. Xenolith 140	2.50	0.40	6.25	0.80	-0.10
C. R. Xenolith 027	3.00	0.50	6.00	0.78	0.07
C. R. Xenolith 052	2.80	0.30	9.33	0.97	-0.18
C. R. Xenolith 016	25.50	5.90	4.32	0.64	2.07

sum	28.07	37.28
sum/N	0.57	0.76
average	3.74	5.77
wlog	1.17	2.25
N	49.00	49.00
S.D.	0.26	0.48
max	1.20	2.07
min	0.03	-0.18

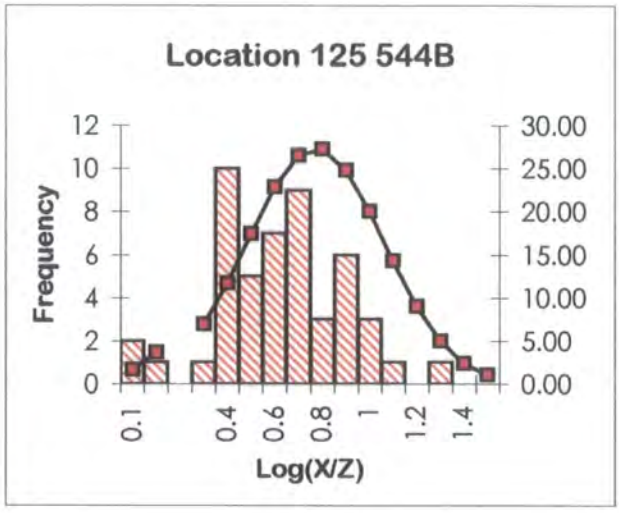

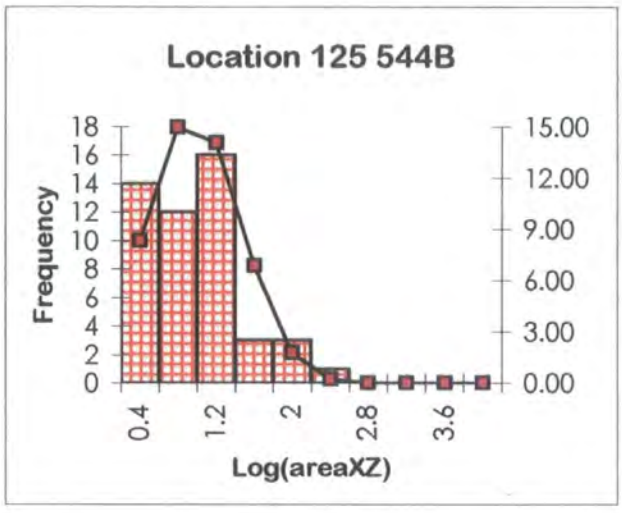

Glencoe Complex: An t-Sron: Allt Fionn Ghleann
Intrusive Phase: Glencoe Fault Intrusion (G1?)

Location [125 544]C

X Orientation	X	Z	X/Z	log(x/z)	log (X×Zπ/4)
C. R. Xenolith 036	3.70	0.40	9.25	0.97	0.07
C. R. Xenolith 047	11.70	0.70	16.71	1.22	0.81
C. R. Xenolith 034	6.10	0.80	7.63	0.88	0.58
C. R. Xenolith 034	3.40	0.40	8.50	0.93	0.03
C. R. Xenolith 142	4.50	1.80	2.50	0.40	0.80
C. R. Xenolith 082	2.00	1.00	2.00	0.30	0.20
C. R. Xenolith 080	3.30	1.60	2.06	0.31	0.62
C. R. Xenolith 072	2.40	0.50	4.80	0.68	-0.03
C. R. Xenolith 116	3.40	1.30	2.62	0.42	0.54
C. R. Xenolith 037	8.60	0.70	12.29	1.09	0.67
C. R. Xenolith 022	7.00	3.80	1.84	0.27	1.32
C. R. Xenolith 070	5.00	1.90	2.63	0.42	0.87
C. R. Xenolith 128	4.90	1.00	4.90	0.69	0.59
C. R. Xenolith 128	4.00	0.90	4.44	0.65	0.45
C. R. Xenolith 087	4.40	0.50	8.80	0.94	0.24
C. R. Xenolith 087	2.20	0.90	2.44	0.39	0.19
C. R. Xenolith 136	4.00	0.90	4.44	0.65	0.45
C. R. Xenolith 062	2.40	0.80	3.00	0.48	0.18
C. R. Xenolith 092	5.20	0.70	7.43	0.87	0.46
112	3.50	1.30	2.69	0.43	0.55
C. R. Xenolith 143	6.00	0.60	10.00	1.00	0.45
C. R. Xenolith 027	11.40	3.90	2.92	0.47	1.54
C. R. Xenolith 036	4.00	2.70	1.48	0.17	0.93
C. R. Xenolith 144	6.00	2.80	2.14	0.33	1.12
C. R. Xenolith 174	5.50	0.80	6.88	0.84	0.54

sum	15.79	14.17
sum/N	0.63	0.57
average	4.28	3.69
wlog	1.05	1.57
N	25.00	25.00
S.D.	0.30	0.39
max	1.22	1.54
min	0.17	-0.03

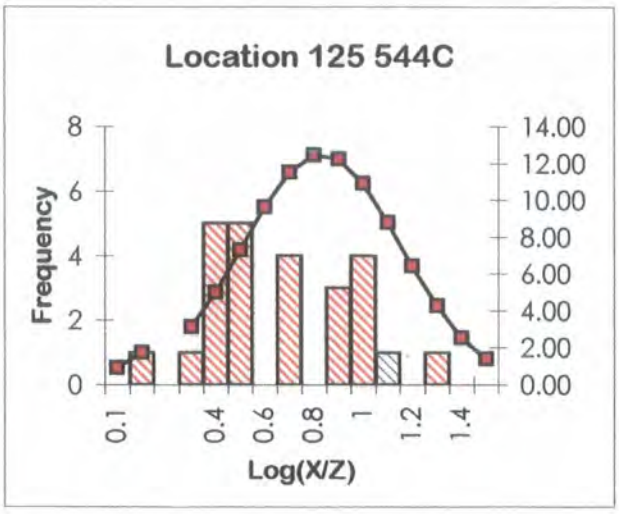
Location 125 544C
Frequency
Log(X/Z)
0.1
0.4
0.6
0.8
1
1.2
1.4
0
2
4
6
8
0.00
2.00
4.00
6.00
8.00
10.00
12.00
14.00

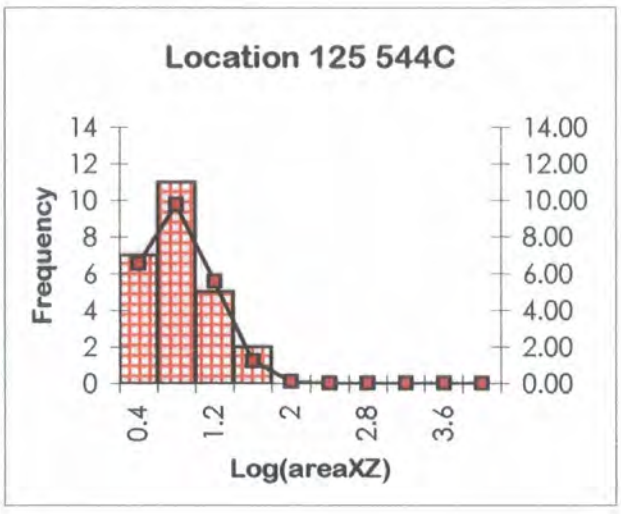
Location 125 544C
Frequency
Log(areaXZ)
0.4
1.2
2
2.8
3.6
0
2
4
6
8
10
12
14
0.00
2.00
4.00
6.00
8.00
10.00
12.00
14.00

Glencoe Complex: An t-Sron: Allt Fionn Ghleann
Intrusive Phase: Glencoe Fault Intrusion (G1?)

Location [125 545]

X Orientation	X	Z	X/Z	log(x/z)	log (X×Zπ/4)
C. R. Xenolith 124	5.20	1.40	3.71	0.57	0.76
C. R. Xenolith 066	13.20	2.70	4.89	0.69	1.45
C. R. Xenolith 110	22.60	3.30	6.85	0.84	1.77
128	6.90	3.60	1.92	0.28	1.29
C. R. Xenolith 140	7.20	3.10	2.32	0.37	1.24
C. R. Xenolith 140	5.50	1.40	3.93	0.59	0.78
C. R. Xenolith 060	4.10	1.50	2.73	0.44	0.68
C. R. Xenolith 130	10.70	2.30	4.65	0.67	1.29
C. R. Xenolith 140	13.70	2.40	5.71	0.76	1.41
C. R. Xenolith 143	4.90	1.50	3.27	0.51	0.76
C. R. Xenolith 137	6.40	4.10	1.56	0.19	1.31
C. R. Xenolith 139	5.10	1.80	2.83	0.45	0.86
C. R. Xenolith 145	4.50	1.20	3.75	0.57	0.63
C. R. Xenolith 141	10.80	2.20	4.91	0.69	1.27
C. R. Xenolith 067	11.70	3.20	3.66	0.56	1.47

sum	8.19	16.97
sum/N	0.55	0.71
average	3.51	5.09
wlog	0.64	1.14
N	15.00	24.00
S.D.	0.18	0.35
max	0.84	1.77
min	0.19	0.63

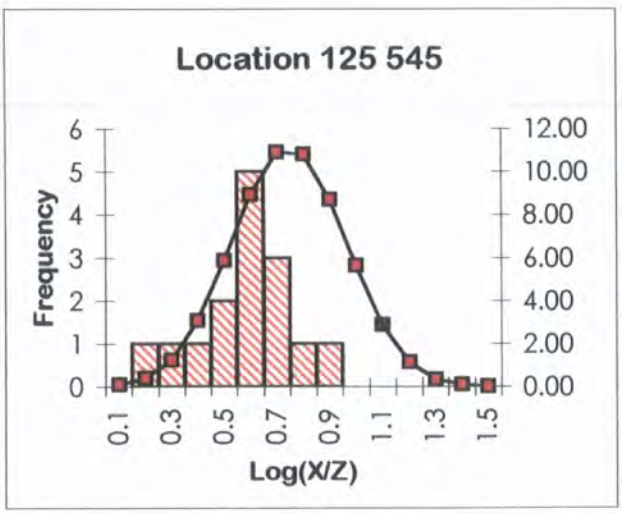

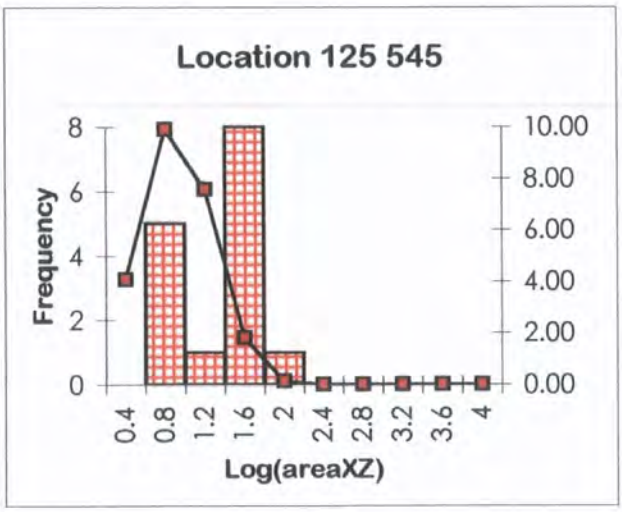

Glencoe Complex: An t-Sron: Allt Fionn Ghleann
Intrusive Phase: Glencoe Fault Intrusion (G1?)

Location [126 539]A

X Orientation	X	Z	X/Z	log(x/z)	log (X×Zπ/4)
C. R. Xenolith 064	6.70	1.20	5.58	0.75	0.80
C. R. Xenolith 104	6.00	2.00	3.00	0.48	0.97
C. R. Xenolith 110	5.00	1.50	3.33	0.52	0.77
C. R. Xenolith 140	3.50	0.90	3.89	0.59	0.39
C. R. Xenolith 290	4.10	1.50	2.73	0.44	0.68
C. R. Xenolith 115	11.50	2.30	5.00	0.70	1.32
C. R. Xenolith 120	4.20	0.60	7.00	0.85	0.30
C. R. Xenolith 152	7.20	2.00	3.60	0.56	1.05
C. R. Xenolith 090	5.60	1.00	5.60	0.75	0.64
C. R. Xenolith 070	4.00	2.50	1.60	0.20	0.90
C. R. Xenolith 070	2.00	0.80	2.50	0.40	0.10
C. R. Xenolith 094	6.00	1.80	3.33	0.52	0.93
C. R. Xenolith 026	2.50	1.50	1.67	0.22	0.47
C. R. Xenolith 080	10.00	1.30	7.69	0.89	1.01
C. R. Xenolith 117	3.30	0.80	4.13	0.62	0.32
C. R. Xenolith 107	17.50	5.20	3.37	0.53	1.85
C. R. Xenolith 125	19.00	5.60	3.39	0.53	1.92
C. R. Xenolith 116	3.20	1.80	1.78	0.25	0.66
C. R. Xenolith 108	6.00	1.80	3.33	0.52	0.93
C. R. Xenolith 138	21.50	10.00	2.15	0.33	2.23
C. R. Xenolith 098	5.50	2.50	2.20	0.34	1.03
C. R. Xenolith 098	19.50	4.80	4.06	0.61	1.87
C. R. Xenolith 026	2.20	0.80	2.75	0.44	0.14
C. R. Xenolith 090	2.80	0.60	4.67	0.67	0.12
C. R. Xenolith 068	12.00	7.20	1.67	0.22	1.83
C. R. Xenolith 068	5.60	2.70	2.07	0.32	1.07
C. R. Xenolith 124	2.50	0.70	3.57	0.55	0.14
C. R. Xenolith 124	11.30	4.00	2.83	0.45	1.55
C. R. Xenolith 172	3.00	1.50	2.00	0.30	0.55
C. R. Xenolith 090	4.80	2.60	1.85	0.27	0.99
C. R. Xenolith 088	13.20	5.80	2.28	0.36	1.78
C. R. Xenolith 084	6.20	2.10	2.95	0.47	1.01
C. R. Xenolith 125	9.60	3.70	2.59	0.41	1.45
C. R. Xenolith 090	21.50	9.80	2.19	0.34	2.22
C. R. Xenolith 078	16.00	4.00	4.00	0.60	1.70
C. R. Xenolith 080	6.20	2.10	2.95	0.47	1.01
C. R. Xenolith 153	5.50	1.50	3.67	0.56	0.81
C. R. Xenolith 148	10.00	1.20	8.33	0.92	0.97
C. R. Xenolith 025	20.00	0.80	25.00	1.40	1.10
C. R. Xenolith 136	5.80	0.90	6.44	0.81	0.61
C. R. Xenolith 160	11.30	4.10	2.76	0.44	1.56
C. R. Xenolith 086	12.50	0.80	15.63	1.19	0.90
C. R. Xenolith 128	91.50	10.50	8.71	0.94	2.88

sum	23.72	45.53
sum/N	0.55	1.06
average	3.56	11.45
wlog	1.19	2.78
N	43.00	43.00
S.D.	0.25	0.64
max	1.40	2.88
min	0.20	0.10

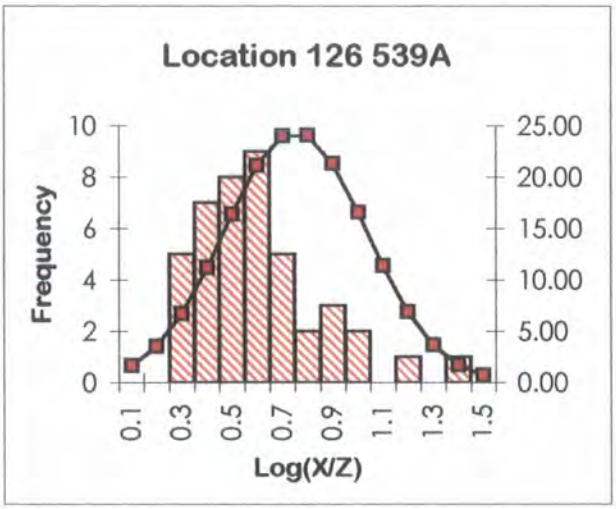

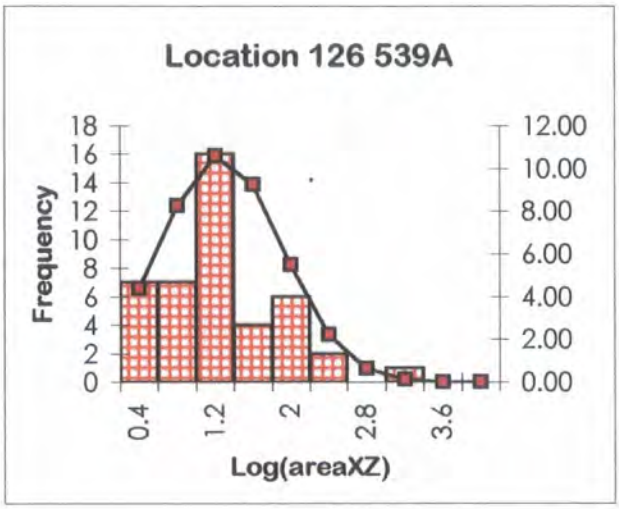

Glencoe Complex: An t-Sron: Allt Fionn Ghleann
Intrusive Phase: Glencoe Fault Intrusion (G1?)

Location [126 539]B

X Orientation	X	Z	X/Z	log(x/z)	log (X×Zπ/4)
C. R. Xenolith 184	8.50	3.50	2.43	0.39	1.37
C. R. Xenolith 112	12.00	2.50	4.80	0.68	1.37
C. R. Xenolith 136	7.70	2.10	3.67	0.56	1.10
C. R. Xenolith 118	7.00	2.80	2.50	0.40	1.19
C. R. Xenolith 115	7.00	3.20	2.19	0.34	1.25
C. R. Xenolith 133	9.00	3.90	2.31	0.36	1.44
C. R. Xenolith 110	24.50	5.80	4.22	0.63	2.05
C. R. Xenolith 070	6.20	3.50	1.77	0.25	1.23
C. R. Xenolith 052	2.60	0.60	4.33	0.64	0.09
C. R. Xenolith 010	8.40	5.30	1.58	0.20	1.54
C. R. Xenolith 152	21.50	2.20	9.77	0.99	1.57
C. R. Xenolith 158	12.50	5.50	2.27	0.36	1.73
C. R. Xenolith 008	5.00	1.60	3.13	0.49	0.80
C. R. Xenolith 116	4.50	1.20	3.75	0.57	0.63
C. R. Xenolith 120	3.70	0.80	4.63	0.67	0.37
C. R. Xenolith 040	6.00	0.60	10.00	1.00	0.45
C. R. Xenolith 121	4.10	0.70	5.86	0.77	0.35
C. R. Xenolith 124	4.60	1.60	2.88	0.46	0.76
C. R. Xenolith 132	25.50	6.00	4.25	0.63	2.08
C. R. Xenolith 124	11.80	2.60	4.54	0.66	1.38
C. R. Xenolith 148	5.50	2.50	2.20	0.34	1.03
C. R. Xenolith 117	12.10	7.50	1.61	0.21	1.85
C. R. Xenolith 008	3.10	1.20	2.58	0.41	0.47
C. R. Xenolith 132	6.70	1.40	4.79	0.68	0.87
C. R. Xenolith 098	2.90	2.60	1.12	0.05	0.77
C. R. Xenolith 138	5.00	1.70	2.94	0.47	0.82
C. R. Xenolith 158	4.70	3.00	1.57	0.19	1.04
C. R. Xenolith 008	3.30	0.50	6.60	0.82	0.11
C. R. Xenolith 018	30.20	2.50	12.08	1.08	1.77
C. R. Xenolith 068	16.00	2.80	5.71	0.76	1.55
C. R. Xenolith 096	19.50	10.00	1.95	0.29	2.19
C. R. Xenolith 126	4.20	1.70	2.47	0.39	0.75
C. R. Xenolith 150	3.20	0.80	4.00	0.60	0.30
C. R. Xenolith 157	4.80	0.70	6.86	0.84	0.42
C. R. Xenolith 157	3.50	1.50	2.33	0.37	0.62
C. R. Xenolith 160	11.00	2.10	5.24	0.72	1.26
C. R. Xenolith 130	18.00	7.60	2.37	0.37	2.03
C. R. Xenolith 178	12.00	5.10	2.35	0.37	1.68

sum	18.37	38.44
sum/N	0.48	1.01
average	3.04	10.27
wlog	1.03	2.10
N	38.00	38.00
S.D.	0.25	0.61
max	1.08	2.19
min	0.05	0.09

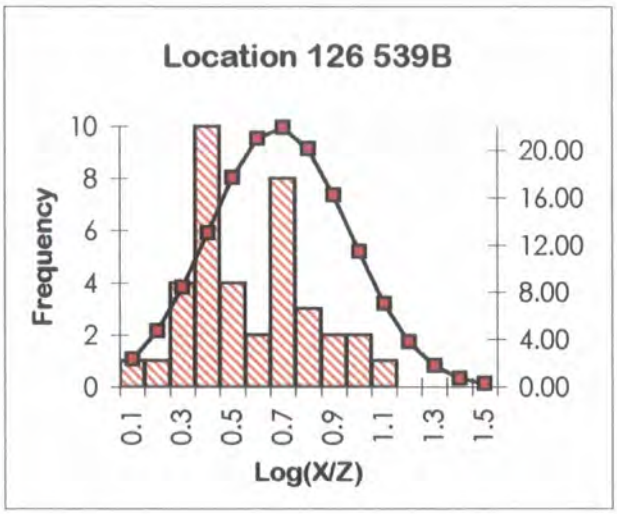

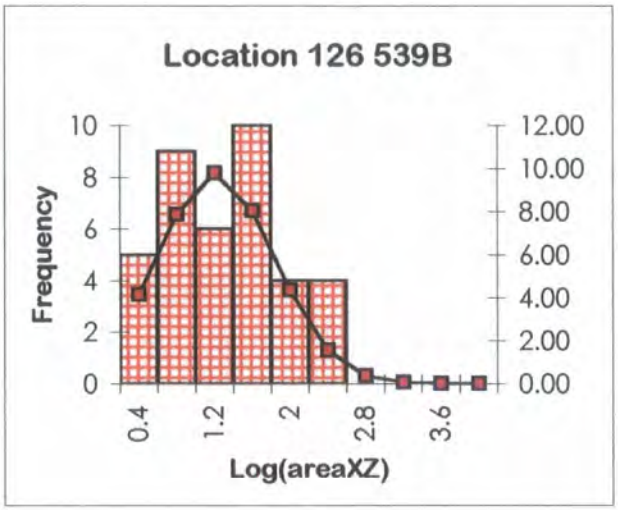

Glencoe Complex: Glen Etive: Allt Fionn Ghleann
Intrusive Phase: The Clach Leathad facies (G2)

Location [227 517]

X	Z	X/Z	log(X/Z)	log(X×Zπ/4)
5.60	9.90	1.77	0.25	1.64
11.50	5.00	2.30	0.36	1.65
8.20	5.50	1.49	0.17	1.55
10.30	4.80	2.15	0.33	1.59
10.90	6.20	1.76	0.25	1.72
10.20	3.90	2.62	0.42	1.49
5.50	2.80	1.96	0.29	1.08
9.00	3.50	2.57	0.41	1.39
10.80	6.70	1.61	0.21	1.75
8.60	3.70	2.32	0.37	1.40
9.40	4.70	2.00	0.30	1.54
10.00	5.00	2.00	0.30	1.59
9.00	5.00	1.80	0.26	1.55
9.10	4.40	2.07	0.32	1.50
8.70	3.20	2.72	0.43	1.34
14.90	9.20	1.62	0.21	2.03
8.00	5.30	1.51	0.18	1.52
12.50	8.00	1.56	0.19	1.90
9.90	5.20	1.90	0.28	1.61
8.10	3.20	2.53	0.40	1.31
11.20	6.90	1.62	0.21	1.78
10.70	6.00	1.78	0.25	1.70
14.60	8.90	1.64	0.21	2.01
8.50	5.80	1.47	0.17	1.59
10.40	5.70	1.82	0.26	1.67
10.90	4.60	2.37	0.37	1.60
12.40	7.10	1.75	0.24	1.84
14.10	9.40	1.50	0.18	2.02
13.40	8.10	1.65	0.22	1.93
6.50	3.80	1.71	0.23	1.29
8.40	3.70	2.27	0.36	1.39
13.80	9.10	1.52	0.18	1.99
10.50	5.00	2.10	0.32	1.62
9.10	4.20	2.17	0.34	1.48
10.10	5.20	1.94	0.29	1.62
11.10	6.40	1.73	0.24	1.75
12.40	5.70	2.18	0.34	1.74
11.00	6.00	1.83	0.26	1.71
7.50	3.50	2.14	0.33	1.31
11.80	5.70	2.07	0.32	1.72
10.60	5.70	1.86	0.27	1.68
8.30	3.40	2.44	0.39	1.35
8.00	2.50	3.20	0.51	1.20

X	Z	X/Z	log(X/Z)	log(X×Zπ/4)
7.90	3.00	2.63	0.42	1.27
12.70	7.40	1.72	0.23	1.87
10.70	5.20	2.06	0.31	1.64
4.00	8.50	2.13	0.33	1.43
7.00	4.30	1.63	0.21	1.37
12.60	5.90	2.14	0.33	1.77
8.70	4.00	2.18	0.34	1.44
7.80	5.10	1.53	0.18	1.49
10.40	4.10	2.54	0.40	1.52
8.50	3.00	2.83	0.45	1.30
15.30	9.60	1.59	0.20	2.06
5.80	3.10	1.87	0.27	1.15
10.60	4.30	2.47	0.39	1.55
14.20	7.30	1.95	0.29	1.91
13.20	8.30	1.59	0.20	1.93
11.40	6.70	1.70	0.23	1.78
9.50	4.00	2.38	0.38	1.47
12.90	7.90	1.63	0.21	1.90
6.20	3.50	1.77	0.25	1.23
12.80	6.10	2.10	0.32	1.79
10.30	5.40	1.91	0.28	1.64
8.30	2.80	2.96	0.47	1.26
13.10	7.80	1.68	0.23	1.90
8.90	4.20	2.12	0.33	1.47
11.90	7.60	1.57	0.19	1.85
9.70	4.70	2.06	0.31	1.55
13.10	6.40	2.05	0.31	1.82
7.50	4.80	1.56	0.19	1.45
14.40	8.70	1.66	0.22	1.99
11.60	7.30	1.59	0.20	1.82
13.60	8.90	1.53	0.18	1.98
15.10	9.40	1.61	0.21	2.05
11.40	7.10	1.61	0.21	1.80

sum	21.70	123.62
sum/N	0.29	1.63
average	1.93	42.32
wlog	0.34	0.98
N	76	76
S.D.	0.08	0.24
max	0.51	2.06
min	0.17	1.08

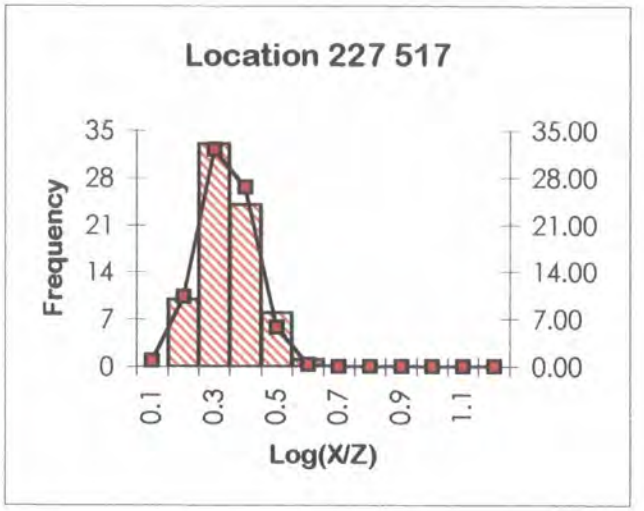
Location 227 517
Frequency
35
28
21
14
7
0
35.00
28.00
21.00
14.00
7.00
0.00
0.1
0.3
0.5
0.7
0.9
1.1
Log(X/Z)

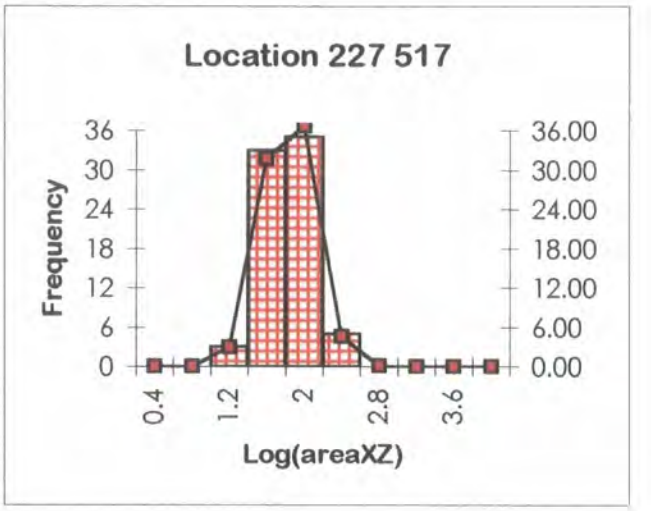
Location 227 517
Frequency
36
30
24
18
12
6
0
36.00
30.00
24.00
18.00
12.00
6.00
0.00
0.4
1.2
2
2.8
3.6
Log(areaXZ)

Glencoe Complex: Glen Etive: Allt Fionn Ghleann
Intrusive Phase: The Clach Leathad facies (G2)

Location [228 522]

X	Z	X/Z	log(X/Z)	log (X×Zπ/4)
12.50	4.50	2.78	0.44	1.65
8.60	3.50	2.46	0.39	1.37
5.60	3.80	1.47	0.17	1.22
8.20	4.70	1.74	0.24	1.48
13.70	6.90	1.99	0.30	1.87
3.80	2.00	1.90	0.28	0.78
18.30	9.10	2.01	0.30	2.12
14.50	7.80	1.86	0.27	1.95
19.00	8.50	2.24	0.35	2.10
8.00	4.50	1.78	0.25	1.45
4.00	2.20	1.82	0.26	0.84
13.20	5.40	2.44	0.39	1.75
15.70	9.00	1.74	0.24	2.05
6.60	3.60	1.83	0.26	1.27
6.20	2.70	2.30	0.36	1.12
13.60	5.80	2.34	0.37	1.79
5.80	2.00	2.90	0.46	0.96
18.00	7.50	2.40	0.38	2.03
5.50	2.00	2.75	0.44	0.94
13.40	5.60	2.39	0.38	1.77
6.60	1.10	6.00	0.78	0.76
5.70	4.10	1.39	0.14	1.26
4.30	1.50	2.87	0.46	0.70
7.60	3.80	2.00	0.30	1.36
6.40	0.90	7.11	0.85	0.66
7.80	4.30	1.81	0.26	1.42
7.30	3.80	1.92	0.28	1.34
17.80	7.30	2.44	0.39	2.01
5.80	2.30	2.52	0.40	1.02
11.40	3.20	3.56	0.55	1.46
6.00	4.20	1.43	0.15	1.30
8.00	4.20	1.90	0.28	1.42
20.20	9.70	2.08	0.32	2.19
6.10	2.40	2.54	0.41	1.06
6.00	4.20	1.43	0.15	1.30
11.80	3.60	3.28	0.52	1.52
13.30	6.50	2.05	0.31	1.83
4.20	1.20	3.50	0.54	0.60
3.60	1.80	2.00	0.30	0.71
7.00	3.50	2.00	0.30	1.28
6.50	3.30	1.97	0.29	1.23
18.20	7.70	2.36	0.37	2.04
6.00	2.20	2.73	0.44	1.02
4.60	1.60	2.88	0.46	0.76
15.30	8.60	1.78	0.25	2.01
6.20	3.20	1.94	0.29	1.19
11.60	3.40	3.41	0.53	1.49
2.80	1.20	2.33	0.37	0.42
1.50	0.80	1.88	0.27	-0.03

X	Z	X/Z	log(X/Z)	log (X×Zπ/4)
19.80	9.30	2.13	0.33	2.16
5.60	3.80	1.47	0.17	1.22
13.60	6.60	2.06	0.31	1.85
6.50	3.00	2.17	0.34	1.19
5.40	2.40	2.25	0.35	1.01
7.50	2.20	3.41	0.53	1.11
20.00	9.50	2.11	0.32	2.17
3.70	2.10	1.76	0.25	0.79
1.70	0.90	1.89	0.28	0.08
4.80	3.00	1.60	0.20	1.05
7.50	4.00	1.88	0.27	1.37
6.80	3.00	2.27	0.36	1.20
13.90	6.10	2.28	0.36	1.82
5.30	1.50	3.53	0.55	0.80
5.00	1.50	3.33	0.52	0.77
25.60	13.50	1.90	0.28	2.43
3.90	0.90	4.33	0.64	0.44
6.10	0.60	10.17	1.01	0.46
13.00	6.20	2.10	0.32	1.80
4.90	1.90	2.58	0.41	0.86
6.30	2.50	2.52	0.40	1.09
5.30	3.50	1.51	0.18	1.16
8.00	4.50	1.78	0.25	1.45
11.20	2.80	4.00	0.60	1.39
15.00	8.30	1.81	0.26	1.99
5.90	2.90	2.03	0.31	1.13
7.10	1.60	4.44	0.65	0.95
6.50	3.00	2.17	0.34	1.19
6.30	4.50	1.40	0.15	1.35
7.00	3.50	2.00	0.30	1.28
7.40	4.10	1.80	0.26	1.38
7.30	3.50	2.09	0.32	1.30
7.80	2.90	2.69	0.43	1.25
14.00	7.20	1.94	0.29	1.90
6.30	4.50	1.40	0.15	1.35
6.90	3.90	1.77	0.25	1.33
5.60	1.90	2.95	0.47	0.92
17.40	7.10	2.45	0.39	1.99
19.60	8.90	2.20	0.34	2.14
3.30	1.50	2.20	0.34	0.59
20.50	10.00	2.05	0.31	2.21
22.70	11.10	2.05	0.31	2.30
8.50	5.00	1.70	0.23	1.52
18.50	8.00	2.31	0.36	2.07
6.00	2.50	2.40	0.38	1.07
8.30	4.50	1.84	0.27	1.47
3.20	1.60	2.00	0.30	0.60
12.90	5.10	2.53	0.40	1.71
5.40	3.40	1.59	0.20	1.16

7.70	4.10	1.88	0.27	1.39
6.80	1.30	5.23	0.72	0.84
5.60	1.80	3.11	0.49	0.90
5.30	1.80	2.94	0.47	0.87
5.70	2.20	2.59	0.41	0.99
4.00	2.20	1.82	0.26	0.84
5.90	3.90	1.51	0.18	1.26
3.70	2.10	1.76	0.25	0.79
22.70	11.50	1.97	0.30	2.31
15.50	8.80	1.76	0.25	2.03
8.40	3.40	2.47	0.39	1.35
7.70	4.20	1.83	0.26	1.40
8.20	3.10	2.65	0.42	1.30
3.60	1.80	2.00	0.30	0.71

4.30	2.50	1.72	0.24	0.93
4.30	2.70	1.59	0.20	0.96
12.10	3.90	3.10	0.49	1.57
8.90	3.80	2.34	0.37	1.42
16.00	9.30	1.72	0.24	2.07

sum	41.24	155.58
sum/N	0.35	1.33
average	2.25	21.37
wlog	0.86	2.46
N	117	117
S.D.	0.14	0.51
max	1.01	2.43
min	0.14	-0.03

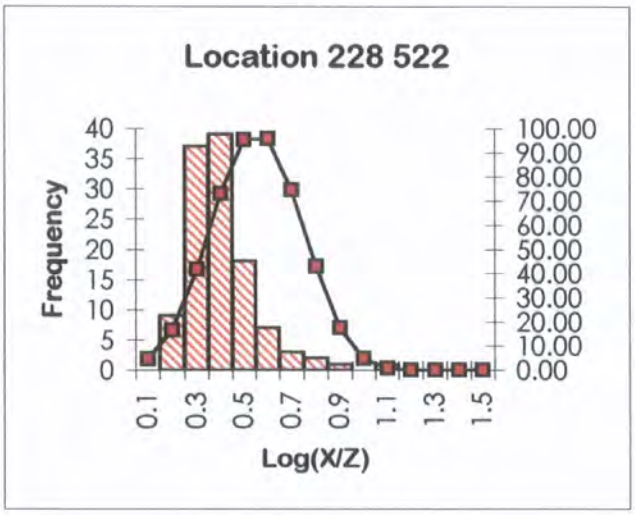

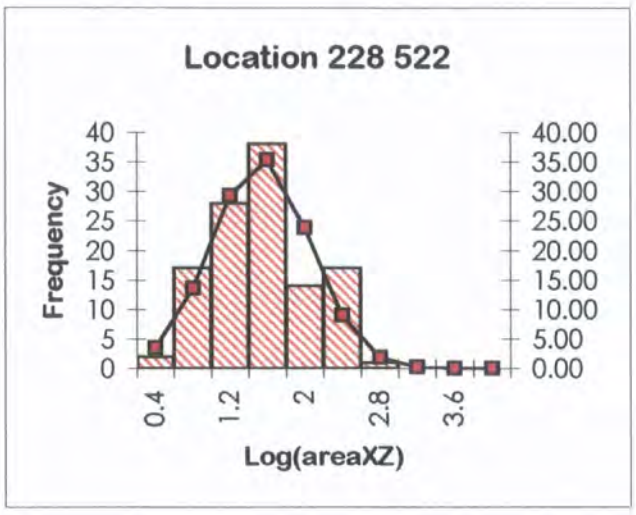

Glencoe Complex: Glen Etive: Allt Fionn Ghleann
Intrusive Phase: The Clach Leathad facies (G2)

Location [229 517]

X	Z	X/Z	log(X/Z)	log(X×Zπ/4)
9.40	5.20	1.81	0.26	1.58
7.90	3.10	2.55	0.41	1.28
10.80	6.00	1.80	0.26	1.71
8.90	3.90	2.28	0.36	1.44
10.50	5.70	1.84	0.27	1.67
8.50	4.80	1.77	0.25	1.51
7.90	4.10	1.93	0.28	1.41
6.90	3.40	2.03	0.31	1.27
12.00	7.00	1.71	0.23	1.82
9.80	5.60	1.75	0.24	1.63
8.20	4.50	1.82	0.26	1.46
8.00	4.30	1.86	0.27	1.43
9.60	4.80	2.00	0.30	1.56
14.20	9.20	1.54	0.19	2.01
10.00	5.20	1.92	0.28	1.61
14.00	9.00	1.56	0.19	2.00
7.60	3.80	2.00	0.30	1.36
10.50	5.90	1.78	0.25	1.69
11.80	6.80	1.74	0.24	1.80
9.80	5.20	1.88	0.28	1.60
8.30	3.50	2.37	0.38	1.36
7.40	3.60	2.06	0.31	1.32
10.00	5.40	1.85	0.27	1.63
12.20	7.20	1.69	0.23	1.84
8.60	3.60	2.39	0.38	1.39
13.60	8.40	1.62	0.21	1.95
14.50	9.50	1.53	0.18	2.03
6.20	3.00	2.07	0.32	1.16
11.50	6.70	1.72	0.23	1.78
6.00	2.70	2.22	0.35	1.10
11.00	2.20	5.00	0.70	1.28
5.80	2.50	2.32	0.37	1.06
13.80	8.80	1.57	0.20	1.98

X	Z	X/Z	log(X/Z)	log(X×Zπ/4)
7.20	3.40	2.12	0.33	1.28
10.20	5.60	1.82	0.26	1.65
5.60	2.30	2.43	0.39	1.01
9.10	4.10	2.22	0.35	1.47
8.60	3.80	2.26	0.35	1.41
9.60	4.60	2.09	0.32	1.54
10.10	5.90	1.71	0.23	1.67
7.50	2.90	2.59	0.41	1.23
11.20	6.40	1.75	0.24	1.75
8.50	4.50	1.89	0.28	1.48
8.10	3.30	2.45	0.39	1.32
2.70	0.90	3.00	0.48	0.28
9.10	4.30	2.12	0.33	1.49
9.60	5.40	1.78	0.25	1.61
18.60	10.20	1.82	0.26	2.17
13.00	8.00	1.63	0.21	1.91
12.50	7.50	1.67	0.22	1.87
5.20	2.00	2.60	0.41	0.91
7.50	3.80	1.97	0.30	1.35
6.90	3.10	2.23	0.35	1.23
11.40	6.60	1.73	0.24	1.77
7.80	4.10	1.90	0.28	1.40
9.10	4.90	1.86	0.27	1.54
9.30	4.30	2.16	0.34	1.50

sum	17.01	86.55
sum/N	0.30	1.52
average	1.99	33.00
wlog	0.52	1.89
N	57	57
S.D.	0.08	0.32
max	0.70	2.17
min	0.18	0.28

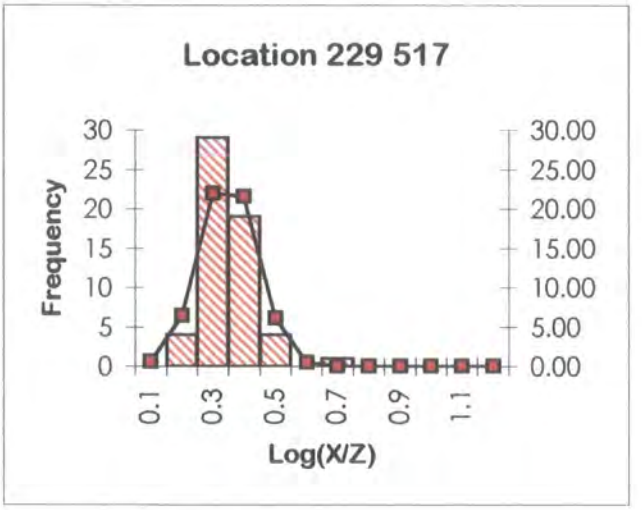
Location 229 517
Frequency
30
25
20
15
10
5
0
30.00
25.00
20.00
15.00
10.00
5.00
0.00
0.1
0.3
0.5
0.7
0.9
1.1
Log(X/Z)

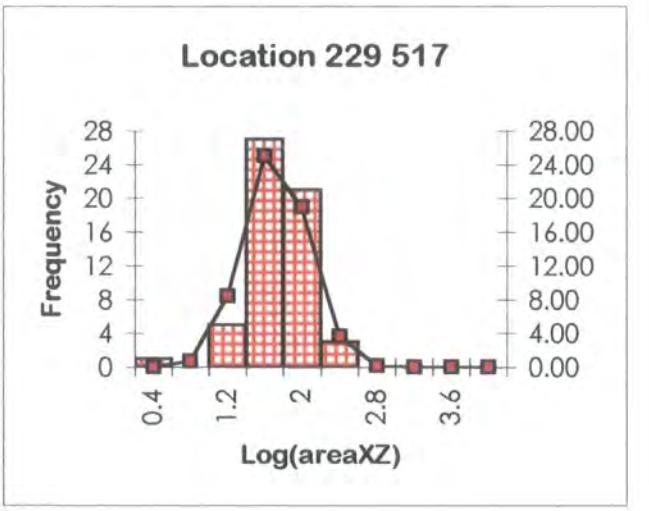
Location 229 517
Frequency
28
24
20
16
12
8
4
0
28.00
24.00
20.00
16.00
12.00
8.00
4.00
0.00
0.4
1.2
2
2.8
3.6
Log(areaXZ)

Glencoe Complex: Glen Etive: Allt Fionn Ghleann
Intrusive Phase: The Clach Leathad facies (G2)

Location [229 520]

X	Z	X/Z	log(X/Z)	log(X×Zπ/4)
12.00	4.00	3.00	0.48	1.58
15.80	3.70	4.27	0.63	1.66
3.30	1.80	1.83	0.26	0.67
12.00	5.50	2.18	0.34	1.71
17.10	5.90	2.90	0.46	1.90
11.10	4.30	2.58	0.41	1.57
3.00	1.50	2.00	0.30	0.55
16.30	4.20	3.88	0.59	1.73
10.50	2.50	4.20	0.62	1.31
13.10	5.90	2.22	0.35	1.78
11.30	3.30	3.42	0.53	1.47
16.90	5.70	2.96	0.47	1.88
11.40	4.60	2.48	0.39	1.61
17.60	6.40	2.75	0.44	1.95
9.00	1.00	9.00	0.95	0.85
19.10	7.90	2.42	0.38	2.07
18.30	5.80	3.16	0.50	1.92
4.50	3.00	1.50	0.18	1.03
11.70	3.70	3.16	0.50	1.53
5.60	4.30	1.30	0.11	1.28
18.50	6.00	3.08	0.49	1.94
3.50	2.00	1.75	0.24	0.74
19.60	8.40	2.33	0.37	2.11
10.10	1.90	5.32	0.73	1.18
10.70	5.30	2.02	0.31	1.65
7.90	5.60	1.41	0.15	1.54
5.90	4.60	1.28	0.11	1.33
17.30	6.10	2.84	0.45	1.92
5.20	3.90	1.33	0.12	1.20
10.90	4.10	2.66	0.42	1.55
17.40	5.10	3.41	0.53	1.84
13.30	6.10	2.18	0.34	1.80
16.50	4.40	3.75	0.57	1.76

X	Z	X/Z	log(X/Z)	log(X×Zπ/4)
10.70	3.90	2.74	0.44	1.52
9.40	1.20	7.83	0.89	0.95
18.60	7.40	2.51	0.40	2.03
16.80	4.70	3.57	0.55	1.79
5.40	4.10	1.32	0.12	1.24
9.60	1.40	6.86	0.84	1.02
19.30	8.10	2.38	0.38	2.09
3.70	2.20	1.68	0.23	0.81
9.80	1.60	6.13	0.79	1.09
18.90	7.70	2.45	0.39	2.06
16.10	4.00	4.03	0.60	1.70
16.70	5.30	3.15	0.50	1.84
4.00	2.50	1.60	0.20	0.90
11.10	2.90	3.83	0.58	1.40
10.30	3.70	2.78	0.44	1.48
19.00	6.50	2.92	0.47	1.99
4.90	3.60	1.36	0.13	1.14
12.90	5.70	2.26	0.35	1.76
18.10	6.90	2.62	0.42	1.99
23.20	6.10	3.80	0.58	2.05
3.20	1.70	1.88	0.27	0.63
13.60	6.40	2.13	0.33	1.83
11.50	3.50	3.29	0.52	1.50

sum	24.18	85.42
sum/N	0.43	1.53
average	2.70	33.53
wlog	0.85	1.56
N	56	56
S.D.	0.19	0.43
max	0.95	2.11
min	0.11	0.55

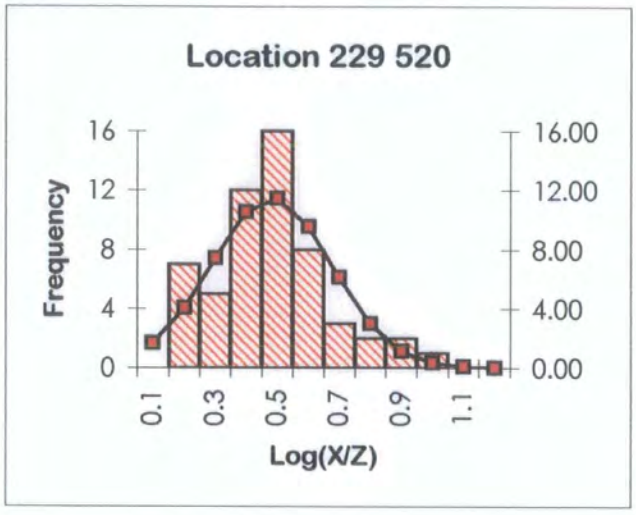
Location 229 520
Frequency
16
12
8
4
0
16.00
12.00
8.00
4.00
0.00
0.1
0.3
0.5
0.7
0.9
1.1
Log(X/Z)

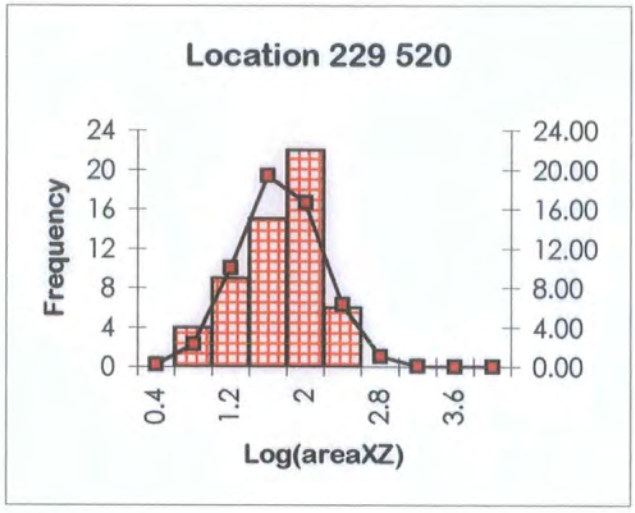
Location 229 520
Frequency
24
20
16
12
8
4
0
24.00
20.00
16.00
12.00
8.00
4.00
0.00
0.4
1.2
2
2.8
3.6
Log(areaXZ)

Glencoe Complex: Glen Etive
Intrusive Phase: The Clach Leathad facies (G2)

Location [228 518]

X	Z	X/Z	log(x/z)	log (X×Zπ/4)
17.00	6.50	2.62	0.42	1.94
7.00	4.50	1.56	0.19	1.39
8.00	5.00	1.60	0.20	1.50
5.30	4.10	1.29	0.11	1.23
2.70	1.50	1.80	0.26	0.50
7.70	1.90	4.05	0.61	1.06
16.30	9.30	1.75	0.24	2.08
13.90	7.10	1.96	0.29	1.89
19.10	8.40	2.27	0.36	2.10
11.00	7.50	1.47	0.17	1.81
8.00	3.50	2.29	0.36	1.34
4.40	3.10	1.42	0.15	1.03
24.80	17.30	1.43	0.16	2.53
16.30	7.80	2.09	0.32	2.00
16.70	6.30	2.65	0.42	1.92
13.70	6.70	2.04	0.31	1.86
8.40	5.20	1.62	0.21	1.54
7.20	4.40	1.64	0.21	1.40
2.00	0.80	2.50	0.40	0.10
11.00	6.50	1.69	0.23	1.75
4.90	2.10	2.33	0.37	0.91
3.00	1.80	1.67	0.22	0.63
10.00	4.20	2.38	0.38	1.52
10.50	5.50	1.91	0.28	1.66
24.50	17.00	1.44	0.16	2.51
9.00	2.80	3.21	0.51	1.30
2.30	0.90	2.56	0.41	0.21
15.00	8.00	1.88	0.27	1.97
18.00	7.50	2.40	0.38	2.03
5.50	4.00	1.38	0.14	1.24
8.00	4.80	1.67	0.22	1.48
3.50	1.50	2.33	0.37	0.62
10.00	3.80	2.63	0.42	1.47
5.50	3.00	1.83	0.26	1.11
8.50	3.50	2.43	0.39	1.37
17.30	6.80	2.54	0.41	1.97
11.20	7.90	1.42	0.15	1.84
8.30	3.80	2.18	0.34	1.39
9.30	3.10	3.00	0.48	1.35
6.20	3.70	1.68	0.22	1.26
9.70	5.20	1.87	0.27	1.60
10.20	5.20	1.96	0.29	1.62
9.70	4.70	2.06	0.31	1.55
3.30	2.10	1.57	0.20	0.74
11.30	6.80	1.66	0.22	1.78
1.40	0.20	7.00	0.85	-0.66
4.00	2.80	1.43	0.15	0.94
9.00	4.50	2.00	0.30	1.50
9.10	5.40	1.69	0.23	1.59

X	Z	X/Z	log(x/z)	log (X×Zπ/4)
12.20	5.40	2.26	0.35	1.71
10.10	4.70	2.15	0.33	1.57
8.50	2.30	3.70	0.57	1.19
8.70	3.90	2.23	0.35	1.43
10.00	6.50	1.54	0.19	1.71
25.50	18.00	1.42	0.15	2.56
5.00	3.80	1.32	0.12	1.17
7.10	3.90	1.82	0.26	1.34
6.00	3.00	2.00	0.30	1.15
2.70	1.50	1.80	0.26	0.50
11.00	6.00	1.83	0.26	1.71
9.00	3.20	2.81	0.45	1.35
9.40	4.70	2.00	0.30	1.54
11.90	5.10	2.33	0.37	1.68
9.50	4.50	2.11	0.32	1.53
13.90	5.60	2.48	0.39	1.79
4.70	2.40	1.96	0.29	0.95
2.20	0.20	11.00	1.04	-0.46
7.20	4.20	1.71	0.23	1.38
9.00	5.80	1.55	0.19	1.61
9.20	6.20	1.48	0.17	1.65
8.70	2.50	3.48	0.54	1.23
24.20	16.70	1.45	0.16	2.50
7.70	3.20	2.41	0.38	1.29
10.60	7.30	1.45	0.16	1.78
9.70	3.90	2.49	0.40	1.47
4.70	3.50	1.34	0.13	1.11
10.70	6.20	1.73	0.24	1.72
7.70	5.20	1.48	0.17	1.50
3.40	2.20	1.55	0.19	0.77
4.00	2.80	1.43	0.15	0.94
14.10	6.90	2.04	0.31	1.88
6.60	3.90	1.69	0.23	1.31
4.40	2.10	2.10	0.32	0.86
4.40	1.60	2.75	0.44	0.74
7.40	4.60	1.61	0.21	1.43
8.70	5.50	1.58	0.20	1.57
4.20	1.70	2.47	0.39	0.75
4.80	2.80	1.71	0.23	1.02
6.40	4.50	1.42	0.15	1.35
4.00	2.20	1.82	0.26	0.84
7.50	4.90	1.53	0.18	1.46
15.70	8.70	1.80	0.26	2.03
13.60	6.80	2.00	0.30	1.86
8.80	5.10	1.73	0.24	1.55
6.20	3.20	1.94	0.29	1.19
10.00	4.50	2.22	0.35	1.55
1.70	0.50	3.40	0.53	-0.18
8.30	5.80	1.43	0.16	1.58

3.70	2.50	1.48	0.17	0.86
4.50	2.50	1.80	0.26	0.95
9.30	6.10	1.52	0.18	1.65
2.50	0.50	5.00	0.70	-0.01
7.00	3.80	1.84	0.27	1.32
6.90	3.70	1.86	0.27	1.30
4.20	1.20	3.50	0.54	0.60
26.20	18.70	1.40	0.15	2.59
15.70	7.20	2.18	0.34	1.95
10.70	4.50	2.38	0.38	1.58
13.70	5.20	2.63	0.42	1.75
6.80	4.30	1.58	0.20	1.36
4.80	1.80	2.67	0.43	0.83
2.80	0.80	3.50	0.54	0.25
5.70	2.70	2.11	0.32	1.08
11.90	4.50	2.64	0.42	1.62
4.80	1.60	3.00	0.48	0.78
8.80	4.10	2.15	0.33	1.45
6.30	3.30	1.91	0.28	1.21
10.30	5.30	1.94	0.29	1.63
10.90	5.70	1.91	0.28	1.69
19.30	8.80	2.19	0.34	2.13
9.40	5.70	1.65	0.22	1.62
26.80	19.30	1.39	0.14	2.61
11.00	4.80	2.29	0.36	1.62
26.50	19.00	1.39	0.14	2.60
6.60	4.90	1.35	0.13	1.40
16.90	6.60	2.56	0.41	1.94
8.00	2.20	3.64	0.56	1.14
9.90	5.10	1.94	0.29	1.60
6.00	3.00	2.00	0.30	1.15
12.10	6.90	1.75	0.24	1.82
16.10	8.90	1.81	0.26	2.05
12.30	7.30	1.68	0.23	1.85
8.20	3.20	2.56	0.41	1.31
18.70	8.30	2.25	0.35	2.09
11.70	6.70	1.75	0.24	1.79
5.40	2.20	2.45	0.39	0.97

5.70	3.20	1.78	0.25	1.16
14.20	7.40	1.92	0.28	1.92
6.30	3.80	1.66	0.22	1.27
9.00	4.50	2.00	0.30	1.50
9.60	6.40	1.50	0.18	1.68
14.30	5.80	2.47	0.39	1.81
11.30	5.10	2.22	0.35	1.66
6.60	5.50	1.20	0.08	1.45
4.20	2.20	1.91	0.28	0.86
10.30	5.80	1.78	0.25	1.67
14.30	7.80	1.83	0.26	1.94
6.60	3.80	1.74	0.24	1.29
8.10	5.40	1.50	0.18	1.54
24.20	17.70	1.37	0.14	2.53
8.50	5.50	1.55	0.19	1.56
7.30	4.10	1.78	0.25	1.37
9.90	5.60	1.77	0.25	1.64
15.00	6.50	2.31	0.36	1.88
13.00	6.00	2.17	0.34	1.79
2.50	1.20	2.08	0.32	0.37
16.10	7.40	2.18	0.34	1.97
9.80	6.80	1.44	0.16	1.72
5.90	3.60	1.64	0.21	1.22
6.60	3.40	1.94	0.29	1.25
7.00	4.00	1.75	0.24	1.34
7.80	4.80	1.63	0.21	1.47
10.00	5.50	1.82	0.26	1.64
5.50	2.50	2.20	0.34	1.03
5.00	3.10	1.61	0.21	1.09

sum	48.90	235.38
sum/N	0.30	1.43
average	1.98	26.70
wlog	0.96	3.27
N	165	165
S.D.	0.13	0.55
max	1.04	2.61
min	0.08	-0.66

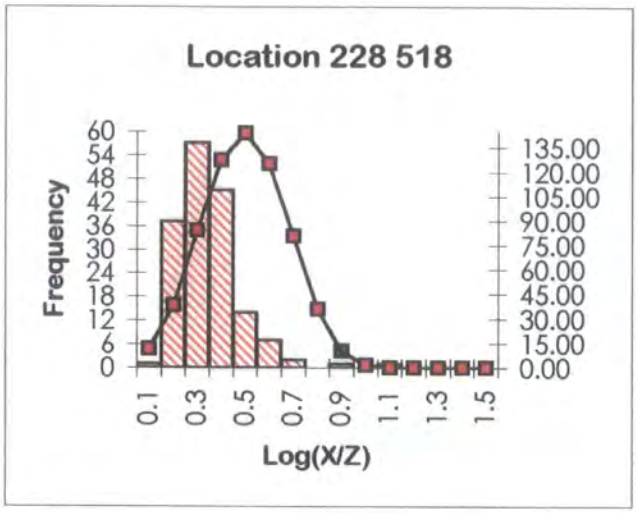
Location 228 518
Frequency
60
54
48
42
36
30
24
18
12
6
0
135.00
120.00
105.00
90.00
75.00
60.00
45.00
30.00
15.00
0.00
0.1
0.3
0.5
0.7
0.9
1.1
1.3
1.5
Log(X/Z)

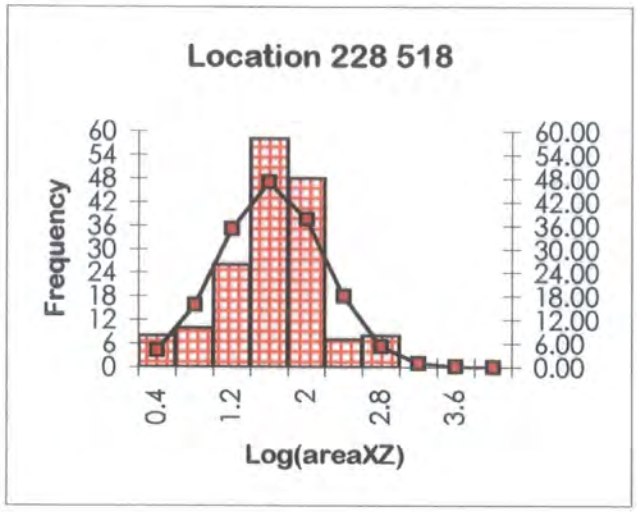
Location 228 518
Frequency
60
54
48
42
36
30
24
18
12
6
0
60.00
54.00
48.00
42.00
36.00
30.00
24.00
18.00
12.00
6.00
0.00
0.4
1.2
2
2.8
3.6
Log(areaXZ)

Glencoe Complex: Glen Etive
Intrusive Phase: The Clach Leathad facies (G2)

Location [228 519]

X	Z	X/Z	log(X/Z)	log(X×Zπ/4)
16.10	7.90	2.04	0.31	2.00
15.00	11.00	1.36	0.13	2.11
9.00	4.50	2.00	0.30	1.50
5.20	4.70	1.11	0.04	1.28
4.80	3.30	1.45	0.16	1.09
7.60	4.60	1.65	0.22	1.44
4.80	3.10	1.55	0.19	1.07
5.00	3.50	1.43	0.15	1.14
10.50	8.00	1.31	0.12	1.82
6.70	4.20	1.60	0.20	1.34
9.70	6.00	1.62	0.21	1.66
10.30	7.80	1.32	0.12	1.80
4.20	1.70	2.47	0.39	0.75
6.30	4.80	1.31	0.12	1.38
12.70	8.70	1.46	0.16	1.94
10.30	5.80	1.78	0.25	1.67
6.00	3.00	2.00	0.30	1.15
12.50	10.00	1.25	0.10	1.99
14.00	5.00	2.80	0.45	1.74
11.50	9.00	1.28	0.11	1.91
8.00	5.00	1.60	0.20	1.50
4.40	2.10	2.10	0.32	0.86
7.50	3.80	1.97	0.30	1.35
13.00	4.00	3.25	0.51	1.61
9.30	5.60	1.66	0.22	1.61
12.30	9.80	1.26	0.10	1.98
6.20	3.20	1.94	0.29	1.19
13.30	9.30	1.43	0.16	1.99
16.20	8.20	1.98	0.30	2.02
18.30	13.70	1.34	0.13	2.29
3.00	1.50	2.00	0.30	0.55
6.60	4.90	1.35	0.13	1.40
3.20	1.70	1.88	0.27	0.63
4.80	3.30	1.45	0.16	1.09
8.20	3.70	2.22	0.35	1.38
4.20	2.70	1.56	0.19	0.95
7.30	3.60	2.03	0.31	1.31
13.00	3.60	3.61	0.56	1.57
15.00	6.00	2.50	0.40	1.85
12.80	10.30	1.24	0.09	2.02
5.20	3.70	1.41	0.15	1.18
5.80	2.80	2.07	0.32	1.11
15.80	7.80	2.03	0.31	1.99
15.20	6.20	2.45	0.39	1.87
13.70	5.70	2.40	0.38	1.79

X	Z	X/Z	log(X/Z)	log(X×Zπ/4)
14.60	10.60	1.38	0.14	2.08
7.80	3.30	2.36	0.37	1.31
7.00	6.50	1.08	0.03	1.55
10.10	5.40	1.87	0.27	1.63
10.1	5.4	1.87	0.27	1.63
5.00	4.50	1.11	0.05	1.25
9.50	5.80	1.64	0.21	1.64
6.60	3.90	1.69	0.23	1.31
6.00	5.50	1.09	0.04	1.41
4.00	2.50	1.60	0.20	0.90
6.70	5.20	1.29	0.11	1.44
13.00	9.00	1.44	0.16	1.96
8.50	4.80	1.77	0.25	1.51
5.50	3.00	1.83	0.26	1.11
7.00	4.00	1.75	0.24	1.34
13.90	6.90	2.01	0.30	1.88
14.00	10.00	1.40	0.15	2.04
8.40	5.40	1.56	0.19	1.55
7.20	6.70	1.07	0.03	1.58
15.00	7.00	2.14	0.33	1.92
5.50	4.00	1.38	0.14	1.24
20.10	14.20	1.42	0.15	2.35
7.90	3.60	2.19	0.34	1.35
4.40	3.10	1.42	0.15	1.03
3.30	1.50	2.20	0.34	0.59
10.70	8.20	1.30	0.12	1.84
9.70	5.20	1.87	0.27	1.60
14.30	6.30	2.27	0.36	1.85
15.40	11.40	1.35	0.13	2.14
6.80	6.30	1.08	0.03	1.53
2.80	1.30	2.15	0.33	0.46
6.30	3.80	1.66	0.22	1.27
7.70	4.00	1.93	0.28	1.38
14.60	6.00	2.43	0.39	1.84
4.80	2.30	2.09	0.32	0.94

sum	18.28	120.29
sum/N	0.23	1.50
average	1.69	31.89
wlog	0.53	1.89
N	80	80
S.D.	0.11	0.42
max	0.56	2.35
min	0.03	0.46

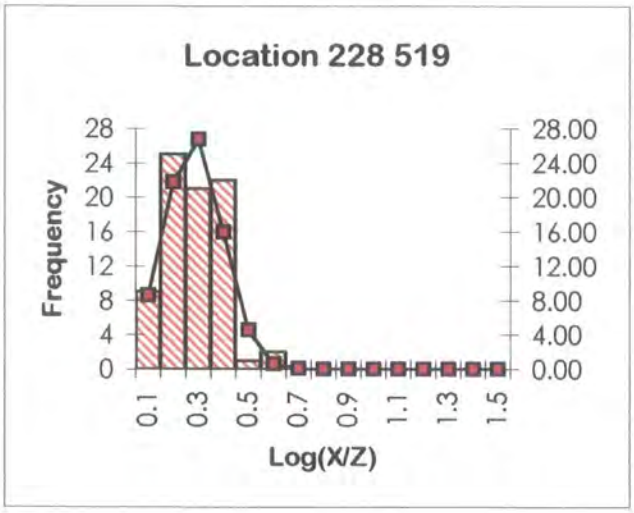
Location 228 519
Frequency
28
24
20
16
12
8
4
0
28.00
24.00
20.00
16.00
12.00
8.00
4.00
0.00
0.1
0.3
0.5
0.7
0.9
1.1
1.3
1.5
Log(X/Z)

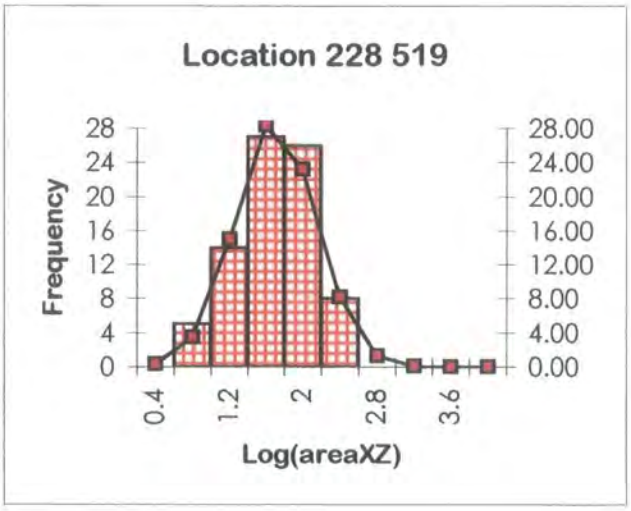
Location 228 519
Frequency
28
24
20
16
12
8
4
0
28.00
24.00
20.00
16.00
12.00
8.00
4.00
0.00
0.4
1.2
2
2.8
3.6
Log(areaXZ)

Glencoe Complex: Glen Etive
Intrusive Phase: The Clach Leathad facies (G2)

Location [229 519]

X	Z	X/Z	log(X/Z)	log(X×Zπ/4)
18.00	16.00	1.13	0.05	2.35
5.70	4.90	1.16	0.07	1.34
9.70	6.70	1.45	0.16	1.71
6.10	5.30	1.15	0.06	1.40
6.00	4.10	1.46	0.17	1.29
5.30	4.50	1.18	0.07	1.27
16.00	14.00	1.14	0.06	2.25
6.30	4.80	1.31	0.12	1.38
6.50	5.00	1.30	0.11	1.41
6.80	3.80	1.79	0.25	1.31
15.70	4.70	3.34	0.52	1.76
16.80	14.80	1.14	0.06	2.29
4.10	2.60	1.58	0.20	0.92
4.10	3.30	1.24	0.09	1.03
7.60	4.40	1.73	0.24	1.42
3.40	2.80	1.21	0.08	0.87
17.00	15.00	1.13	0.05	2.30
22.30	17.00	1.31	0.12	2.47
7.60	4.60	1.65	0.22	1.44
4.30	3.50	1.23	0.09	1.07
9.50	6.50	1.46	0.16	1.69
16.80	14.80	1.14	0.06	2.29
9.30	6.30	1.48	0.17	1.66
8.40	5.40	1.56	0.19	1.55
4.50	3.00	1.50	0.18	1.03
7.70	4.70	1.64	0.21	1.45
17.20	15.20	1.13	0.05	2.31
15.20	13.20	1.15	0.06	2.20
13.70	3.70	3.70	0.57	1.60
4.30	2.80	1.54	0.19	0.98
6.70	5.20	1.29	0.11	1.44
16.10	5.10	3.16	0.50	1.81
6.50	5.00	1.30	0.11	1.41
13.90	2.90	4.79	0.68	1.50
17.00	15.60	1.09	0.04	2.32
8.50	5.70	1.49	0.17	1.58
5.30	3.80	1.39	0.14	1.20
8.50	5.50	1.55	0.19	1.56
19.20	17.20	1.12	0.05	2.41
6.50	5.70	1.14	0.06	1.46
4.50	3.70	1.22	0.09	1.12
3.70	2.90	1.28	0.11	0.93
5.30	4.50	1.18	0.07	1.27
6.10	4.60	1.33	0.12	1.34
7.30	4.30	1.70	0.23	1.39
14.80	12.80	1.16	0.06	2.17
19.60	17.00	1.15	0.06	2.42
5.60	4.60	1.22	0.09	1.31
6.20	5.60	1.11	0.04	1.44

Y	Z	Y/Z	log(Y/Z)	log(Y×Zπ/4)
15.00	14.00	1.07	0.03	2.22
8.00	7.00	1.14	0.06	1.64
3.10	2.00	1.55	0.19	0.69
6.10	6.00	1.02	0.01	1.46
15.20	14.50	1.05	0.02	2.24
9.20	8.10	1.14	0.06	1.77
1.40	1.20	1.17	0.07	0.12
15.80	14.80	1.07	0.03	2.26
16.30	15.10	1.08	0.03	2.29
19.10	16.50	1.16	0.06	2.39
14.20	13.30	1.07	0.03	2.17
10.30	9.30	1.11	0.04	1.88
1.80	1.60	1.13	0.05	0.35
6.30	6.20	1.02	0.01	1.49
4.50	4.20	1.07	0.03	1.17
17.30	16.20	1.07	0.03	2.34
15.20	14.20	1.07	0.03	2.23
7.30	6.20	1.18	0.07	1.55
9.70	8.50	1.14	0.06	1.81
13.70	12.70	1.08	0.03	2.14
3.40	3.20	1.06	0.03	0.93
7.80	6.70	1.16	0.07	1.61
3.80	3.60	1.06	0.02	1.03
8.90	7.00	1.27	0.10	1.69
3.70	3.50	1.06	0.02	1.01
16.90	15.00	1.13	0.05	2.30
14.00	13.00	1.08	0.03	2.16
1.60	1.50	1.07	0.03	0.28
17.00	16.10	1.06	0.02	2.33
9.00	8.00	1.13	0.05	1.75
7.40	6.50	1.14	0.06	1.58
16.00	15.00	1.07	0.03	2.28
3.90	3.70	1.05	0.02	1.05
8.20	7.40	1.11	0.04	1.68
16.50	15.30	1.08	0.03	2.30
14.80	13.30	1.11	0.05	2.19
8.80	7.80	1.13	0.05	1.73
10.00	9.00	1.11	0.05	1.85
2.70	1.60	1.69	0.23	0.53
9.00	8.00	1.13	0.05	1.75
17.00	14.00	1.21	0.08	2.27
6.70	5.60	1.20	0.08	1.47

4.40	2.70	1.63	0.21	0.97

sum	7.77	79.09
sum/N	0.16	1.58
average	1.43	38.17
wlog	0.64	1.60
N	50	50
S.D.	0.14	0.47
max	0.68	2.47
min	0.04	0.87

sum	2.13	69.97
sum/N	0.05	1.67
average	1.12	46.34
wlog	0.22	2.27
N	42	42
S.D.	0.04	0.63
max	0.23	2.39
min	0.01	0.12

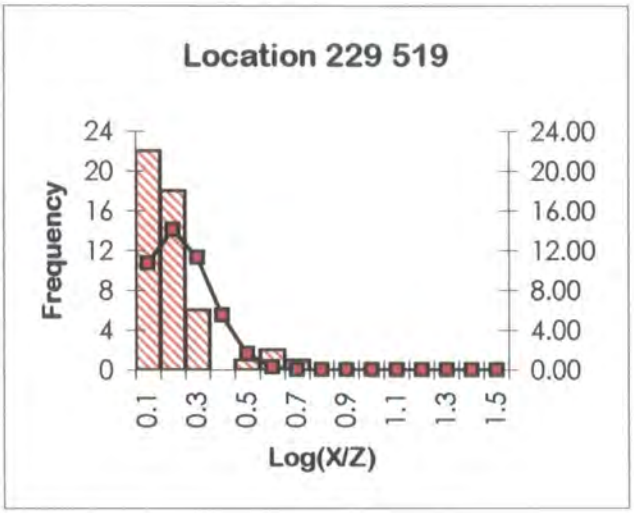

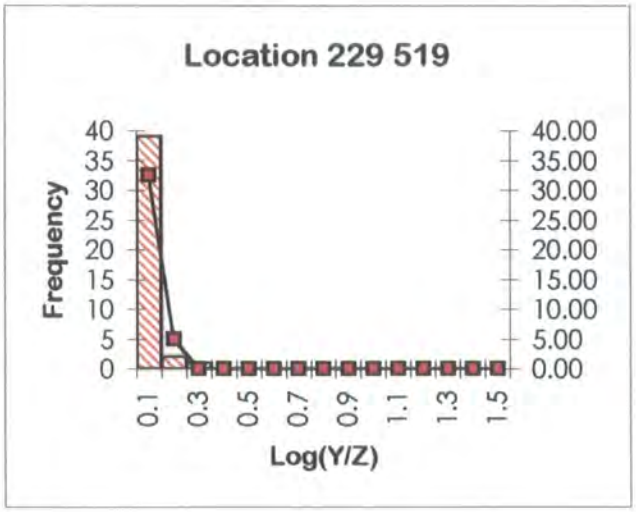

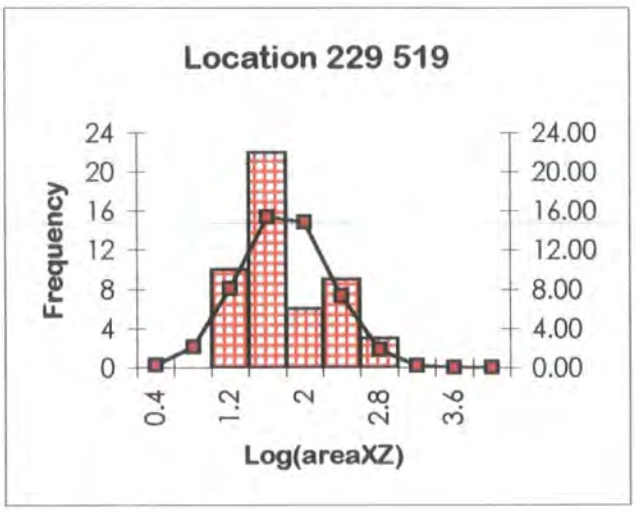

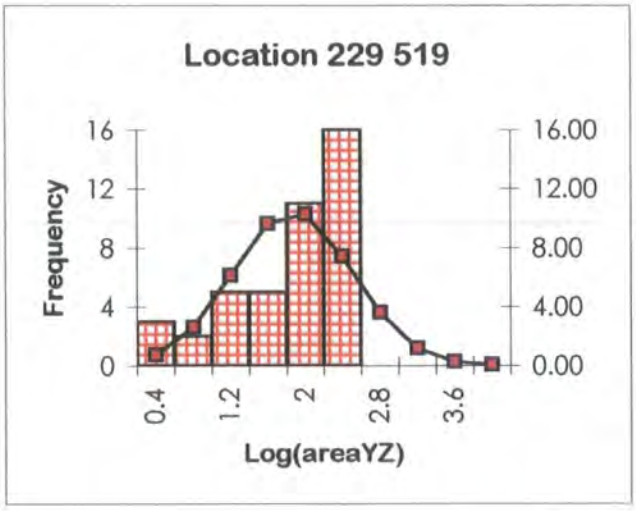

Glencoe Complex: Lairig Gartain
Intrusive Phase: The Clach Leathad facies (G2)

Location [193 540]

X	Z	X/Z	log(X/Z)	log(X×Zπ/4)
11.10	3.70	3.00	0.48	1.51
14.90	4.70	3.17	0.50	1.74
13.00	5.40	2.41	0.38	1.74
11.50	4.10	2.80	0.45	1.57
15.20	5.00	3.04	0.48	1.78
17.30	6.70	2.58	0.41	1.96
24.20	10.50	2.30	0.36	2.30
2.30	1.20	1.92	0.28	0.34
2.70	0.80	3.38	0.53	0.23
13.20	6.00	2.20	0.34	1.79
17.20	6.60	2.61	0.42	1.95
3.70	0.50	7.40	0.87	0.16
6.40	3.40	1.88	0.27	1.23
13.60	6.40	2.13	0.33	1.83
17.10	6.50	2.63	0.42	1.94
6.20	3.20	1.94	0.29	1.19
13.40	6.20	2.16	0.33	1.81
6.00	3.00	2.00	0.30	1.15
15.10	4.90	3.08	0.49	1.76
5.00	2.00	2.50	0.40	0.90
18.60	7.20	2.58	0.41	2.02
4.30	1.10	3.91	0.59	0.57
12.40	4.80	2.58	0.41	1.67
13.00	5.80	2.24	0.35	1.77
12.60	5.00	2.52	0.40	1.69
11.70	4.30	2.72	0.43	1.60
12.80	5.20	2.46	0.39	1.72

X	Z	X/Z	log(X/Z)	log(X×Zπ/4)
4.10	0.90	4.56	0.66	0.46
16.20	5.80	2.79	0.45	1.87
11.80	4.20	2.81	0.45	1.59
12.50	5.10	2.45	0.39	1.70
3.90	0.70	5.57	0.75	0.33
15.00	4.80	3.13	0.49	1.75
5.60	2.60	2.15	0.33	1.06
13.80	6.60	2.09	0.32	1.85
17.40	6.80	2.56	0.41	1.97
13.10	5.50	2.38	0.38	1.75
4.50	1.30	3.46	0.54	0.66
5.80	2.80	2.07	0.32	1.11
11.30	3.90	2.90	0.46	1.54
17.50	6.90	2.54	0.40	1.98
15.30	5.10	3.00	0.48	1.79
11.90	4.50	2.64	0.42	1.62
22.30	9.70	2.30	0.36	2.23
2.90	1.00	2.90	0.46	0.36

sum	19.40	65.56
sum/N	0.43	1.46
average	2.70	28.63
wlog	0.59	2.14
N	45	45
S.D.	0.12	0.58
max	0.87	2.30
min	0.27	0.16

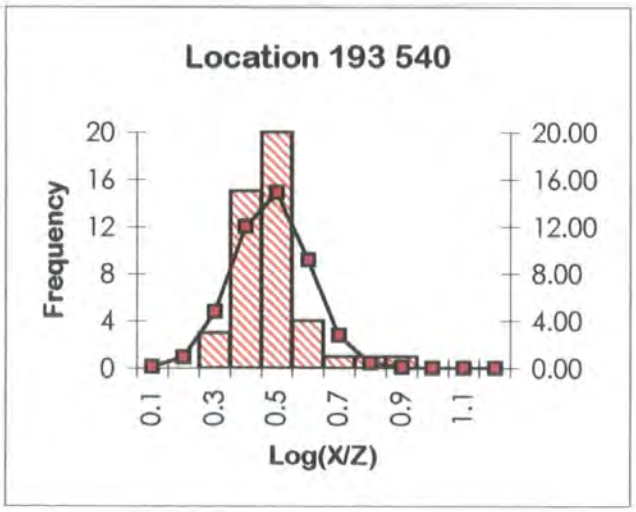

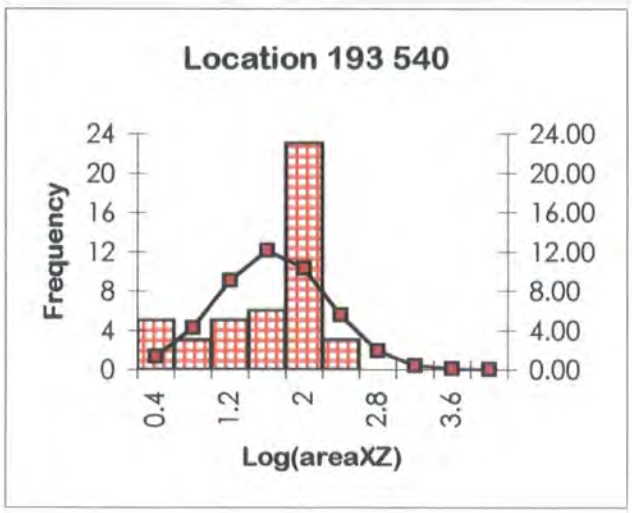

Glencoe Complex: Lairig Gartain
Intrusive Phase: The Clach Leathad facies (G2)

Location [194 535]

X	Z	X/Z	log(X/Z)	log(X×Zπ/4)
7.20	2.70	2.67	0.43	1.18
8.50	5.20	1.63	0.21	1.54
21.70	12.30	1.76	0.25	2.32
13.80	7.80	1.77	0.25	1.93
5.00	3.00	1.67	0.22	1.07
8.70	5.40	1.61	0.21	1.57
5.50	3.50	1.57	0.20	1.18
6.20	2.90	2.14	0.33	1.15
6.50	3.30	1.97	0.29	1.23
8.80	4.40	2.00	0.30	1.48
10.80	7.30	1.48	0.17	1.79
7.00	3.80	1.84	0.27	1.32
4.80	1.60	3.00	0.48	0.78
16.30	10.30	1.58	0.20	2.12
8.80	5.50	1.60	0.20	1.58
13.70	7.70	1.78	0.25	1.92
8.70	5.20	1.67	0.22	1.55
7.30	2.80	2.61	0.42	1.21
1.70	0.80	2.13	0.33	0.03
5.30	3.10	1.71	0.23	1.11
16.20	10.20	1.59	0.20	2.11
6.30	3.00	2.10	0.32	1.17
6.80	2.30	2.96	0.47	1.09
11.00	7.50	1.47	0.17	1.81
2.20	0.90	2.44	0.39	0.19
6.90	2.60	2.65	0.42	1.15
9.00	5.50	1.64	0.21	1.59
16.10	9.90	1.63	0.21	2.10
3.10	1.30	2.38	0.38	0.50
5.80	2.60	2.23	0.35	1.07
13.30	8.30	1.60	0.20	1.94
4.50	1.30	3.46	0.54	0.66
3.00	1.00	3.00	0.48	0.37
9.20	5.70	1.61	0.21	1.61
14.20	8.20	1.73	0.24	1.96
4.60	1.40	3.29	0.52	0.70
5.40	3.40	1.59	0.20	1.16
6.80	3.60	1.89	0.28	1.28
15.00	9.00	1.67	0.22	2.03
10.70	7.20	1.49	0.17	1.78
8.00	3.50	2.29	0.36	1.34

X	Z	X/Z	log(X/Z)	log(X×Zπ/4)
4.20	2.20	1.91	0.28	0.86
17.50	9.60	1.82	0.26	2.12
1.90	1.00	1.90	0.28	0.17
6.50	3.20	2.03	0.31	1.21
9.20	4.70	1.96	0.29	1.53
8.30	5.00	1.66	0.22	1.51
6.60	3.40	1.94	0.29	1.25
11.30	7.80	1.45	0.16	1.84
2.90	0.90	3.22	0.51	0.31
6.80	3.50	1.94	0.29	1.27
6.70	2.20	3.05	0.48	1.06
3.50	1.50	2.33	0.37	0.62
13.90	8.10	1.72	0.23	1.95
10.00	6.50	1.54	0.19	1.71
26.70	13.20	1.80	0.25	2.39
7.50	4.20	1.79	0.25	1.39
9.10	4.40	2.07	0.32	1.50
5.00	2.00	2.50	0.40	0.90
15.70	9.70	1.62	0.21	2.08
15.80	9.80	1.61	0.21	2.08
8.80	5.30	1.66	0.22	1.56
11.20	7.70	1.45	0.16	1.83
5.00	1.80	2.78	0.44	0.85
3.40	1.40	2.43	0.39	0.57
6.70	3.40	1.97	0.29	1.25
9.40	5.70	1.65	0.22	1.62
8.20	4.90	1.67	0.22	1.50
4.90	2.90	1.69	0.23	1.05
7.20	3.80	1.89	0.28	1.33
9.20	4.90	1.88	0.27	1.55
8.70	4.20	2.07	0.32	1.46

sum	20.83	98.02
sum/N	0.29	1.36
average	1.95	22.98
wlog	0.38	2.36
N	72	72
S.D.	0.10	0.54
max	0.54	2.39
min	0.16	0.03

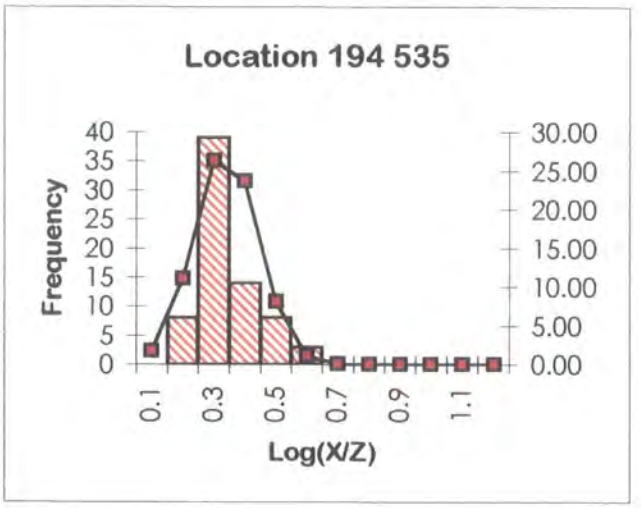
Location 194 535
Frequency
40
35
30
25
20
15
10
5
0
30.00
25.00
20.00
15.00
10.00
5.00
0.00
0.1
0.3
0.5
0.7
0.9
1.1
Log(X/Z)

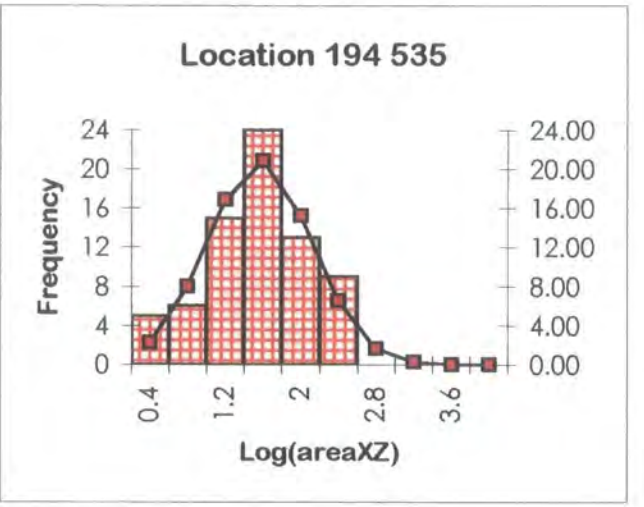
Location 194 535
Frequency
24
20
16
12
8
4
0
24.00
20.00
16.00
12.00
8.00
4.00
0.00
0.4
1.2
2
2.8
3.6
Log(areaXZ)

Glencoe Complex: Lairig Gartain
Intrusive Phase: The Clach Leathad facies (G2)

Location [200 538]

X	Z	X/Z	log(x/z)	log (X×Zπ/4)
6.20	3.70	1.68	0.22	1.26
5.90	3.40	1.74	0.24	1.20
9.10	5.00	1.82	0.26	1.55
6.90	3.00	2.30	0.36	1.21
7.80	5.30	1.47	0.17	1.51
9.30	5.40	1.72	0.24	1.60
6.30	3.80	1.66	0.22	1.27
6.10	3.80	1.61	0.21	1.26
15.10	12.40	1.22	0.09	2.17
8.00	4.10	1.95	0.29	1.41
1.50	0.60	2.50	0.40	-0.15
8.10	5.60	1.45	0.16	1.55
7.20	3.30	2.18	0.34	1.27
6.00	3.50	1.71	0.23	1.22
8.70	4.80	1.81	0.26	1.52
7.90	5.40	1.46	0.17	1.53
8.10	5.80	1.40	0.15	1.57
6.90	3.20	2.16	0.33	1.24

X	Z	X/Z	log(x/z)	log (X×Zπ/4)
2.30	1.20	1.92	0.28	0.34
12.30	8.60	1.43	0.16	1.92
9.20	5.30	1.74	0.24	1.58
6.80	2.90	2.34	0.37	1.19
7.10	3.20	2.22	0.35	1.25
8.80	4.90	1.80	0.25	1.53
7.10	4.60	1.54	0.19	1.41
8.40	5.90	1.42	0.15	1.59

sum	6.31	34.98
sum/N	0.24	1.35
average	1.75	22.16
wlog	0.31	2.32
N	26	26
S.D.	0.08	0.44
max	0.40	2.17
min	0.09	-0.15

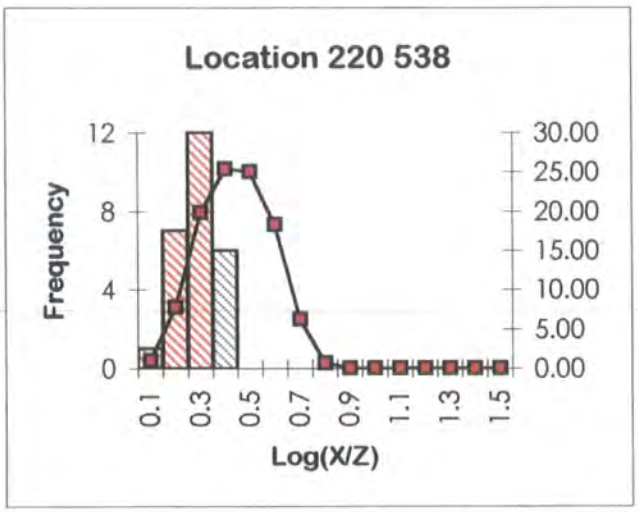

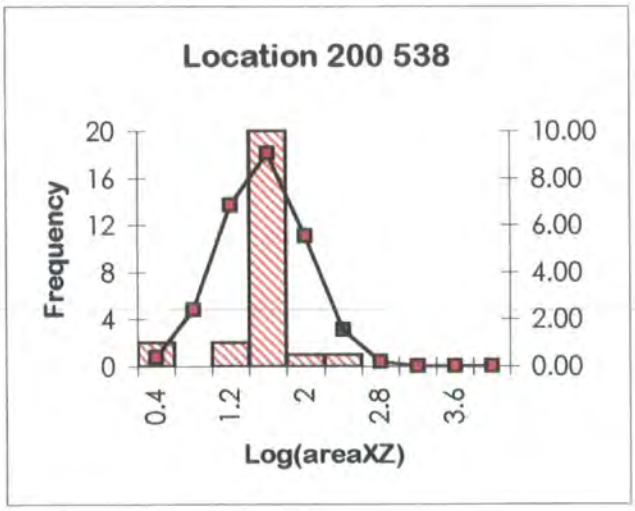

Glencoe Complex: River Coupall
Intrusive Phase: Glencoe Fault Intrusion (G1?)

Location [234 552]

X Orientation	X	Z	X/Z	log(x/z)	log (X×Zπ/4)
C. R. Xenolith 176	9.50	2.50	3.80	0.58	1.27
C. R. Xenolith 155	3.70	0.90	4.11	0.61	0.42
C. R. Xenolith 050	5.50	1.30	4.23	0.63	0.75
C. R. Xenolith 050	6.10	1.20	5.08	0.71	0.76
016	7.90	2.80	2.82	0.45	1.24
028	6.50	4.70	1.38	0.14	1.38
072	4.20	2.10	2.00	0.30	0.84
C. R. Xenolith 160	6.30	1.30	4.85	0.69	0.81
C. R. Xenolith 048	3.40	0.70	4.86	0.69	0.27
C. R. Xenolith 178	8.20	3.50	2.34	0.37	1.35
C. R. Xenolith 178	22.40	8.90	2.52	0.40	2.19
170	13.20	7.30	1.81	0.26	1.88
036	4.60	2.10	2.19	0.34	0.88
068	3.70	2.60	1.42	0.15	0.88
171	13.70	6.80	2.01	0.30	1.86
040	5.00	1.80	2.78	0.44	0.85
016	7.20	3.20	2.25	0.35	1.26
C. R. Xenolith 175	8.60	1.50	5.73	0.76	1.01
C. R. Xenolith 158	4.70	1.70	2.76	0.44	0.80
C. R. Xenolith 045	7.70	2.30	3.35	0.52	1.14
C. R. Xenolith 047	5.10	0.30	17.00	1.23	0.08
C. R. Xenolith 162	6.00	1.00	6.00	0.78	0.67
C. R. Xenolith 049	3.30	0.50	6.60	0.82	0.11
C. R. Xenolith 176	8.40	3.60	2.33	0.37	1.38

sum	12.33	24.08
sum/N	0.51	1.00
average	3.26	10.08
wlog	1.09	2.11
N	24.00	24.00
S.D.	0.25	0.53
max	1.23	2.19
min	0.14	0.08

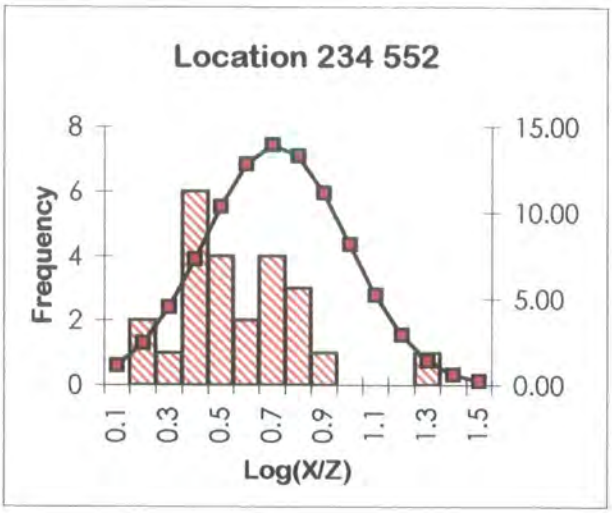
Location 234 552
Frequency
8
6
4
2
0
15.00
10.00
5.00
0.00
0.1
0.3
0.5
0.7
0.9
1.1
1.3
1.5
Log(X/Z)

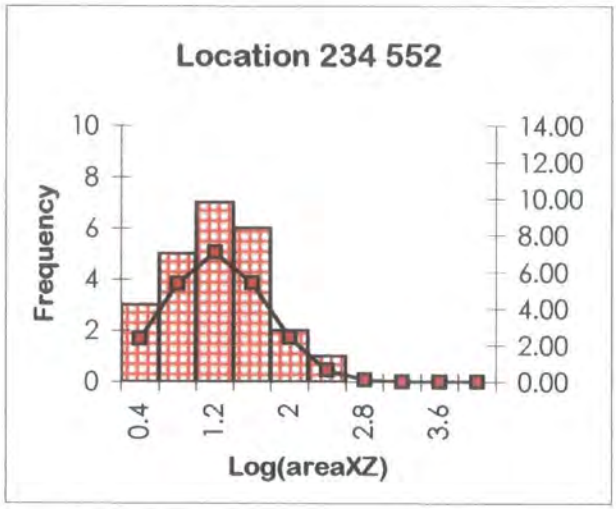
Location 234 552
Frequency
10
8
6
4
2
0
14.00
12.00
10.00
8.00
6.00
4.00
2.00
0.00
0.4
1.2
2
2.8
3.6
Log(areaXZ)

Glencoe Complex: River Coupall
Intrusive Phase: Glencoe Fault Intrusion (G1?)

Location [242 546]

X Orientation	X	Z	X/Z	log(x/z)	log (X×Zπ/4)
C. R. Xenolith 046	4.20	2.30	1.83	0.26	0.88
C. R. Xenolith 040	10.20	3.60	2.83	0.45	1.46
C. R. Xenolith 065	8.20	3.20	2.56	0.41	1.31
C. R. Xenolith 172	5.30	1.30	4.08	0.61	0.73
C. R. Xenolith 070	13.40	3.70	3.62	0.56	1.59
C. R. Xenolith 070	14.30	2.20	6.50	0.81	1.39
C. R. Xenolith 071	7.20	2.10	3.43	0.54	1.07
C. R. Xenolith 076	6.10	0.60	10.17	1.01	0.46
C. R. Xenolith 060	6.30	2.90	2.17	0.34	1.16
C. R. Xenolith 060	7.10	1.50	4.73	0.68	0.92
C. R. Xenolith 180	9.50	1.60	5.94	0.77	1.08
C. R. Xenolith 090	5.10	1.50	3.40	0.53	0.78
C. R. Xenolith 146	4.40	1.30	3.38	0.53	0.65
C. R. Xenolith 138	3.50	1.50	2.33	0.37	0.62
164	6.90	3.20	2.16	0.33	1.24
074	8.10	3.20	2.53	0.40	1.31
090	4.50	3.10	1.45	0.16	1.04
073	4.70	2.80	1.68	0.22	1.01
006	3.10	1.30	2.38	0.38	0.50

sum	9.36	19.21
sum/N	0.49	0.80
average	3.11	6.31
wlog	0.85	1.13
N	19.00	24.00
S.D.	0.21	0.33
max	1.01	1.59
min	0.16	0.46

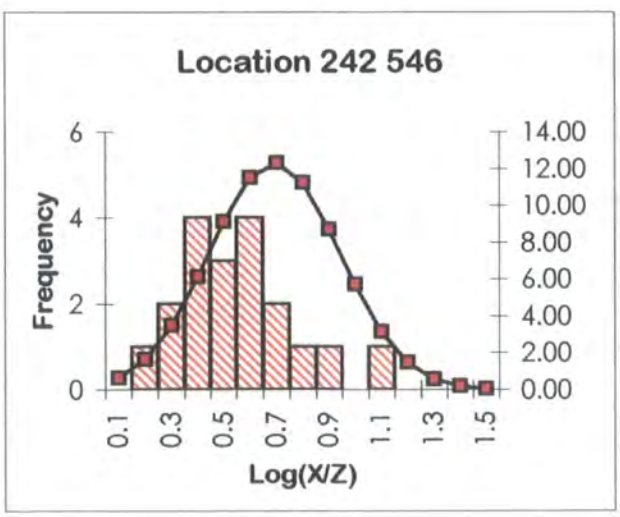

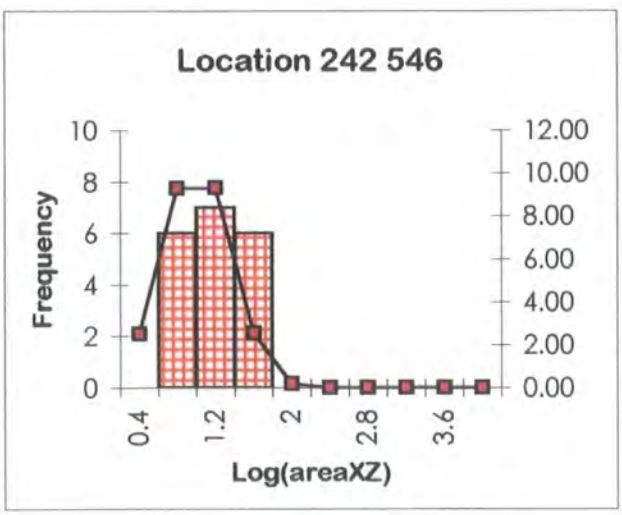

Glencoe Complex: River Coupall
Intrusive Phase: Glencoe Fault Intrusion (G1?)

Location [243 543]

X Orientation	X	Z	X/Z	log(x/z)	log (X×Zπ/4)
C. R. Xenolith 120	13.20	4.30	3.07	0.49	1.65
C. R. Xenolith 160	2.50	0.60	4.17	0.62	0.07
C. R. Xenolith 030	9.30	3.10	3.00	0.48	1.35
C. R. Xenolith 020	4.60	2.10	2.19	0.34	0.88
C. R. Xenolith 064	6.50	0.50	13.00	1.11	0.41
C. R. Xenolith 020	5.70	1.50	3.80	0.58	0.83
C. R. Xenolith 038	3.50	2.90	1.21	0.08	0.90
C. R. Xenolith 180	4.20	1.50	2.80	0.45	0.69
C. R. Xenolith 050	9.80	3.90	2.51	0.40	1.48
C. R. Xenolith 180	9.00	5.50	1.64	0.21	1.59
C. R. Xenolith 090	6.70	1.80	3.72	0.57	0.98
C. R. Xenolith 024	4.50	1.60	2.81	0.45	0.75
C. R. Xenolith 042	13.40	4.70	2.85	0.46	1.69
C. R. Xenolith 021	20.10	6.30	3.19	0.50	2.00
C. R. Xenolith 023	4.20	1.40	3.00	0.48	0.66
C. R. Xenolith 021	18.30	10.70	1.71	0.23	2.19
C. R. Xenolith 020	3.20	1.10	2.91	0.46	0.44
C. R. Xenolith 021	3.80	2.30	1.65	0.22	0.84
C. R. Xenolith 002	7.40	1.50	4.93	0.69	0.94
120	4.60	4.00	1.15	0.06	1.16
022	7.50	2.20	3.41	0.53	1.11
140	14.20	6.30	2.25	0.35	1.85
031	5.10	2.30	2.22	0.35	0.96
033	6.50	3.10	2.10	0.32	1.20
013	9.40	2.70	3.48	0.54	1.30
015	10.10	2.20	4.59	0.66	1.24
010	10.20	5.90	1.73	0.24	1.67

sum	11.88	30.84
sum/N	0.44	1.29
average	2.75	19.28
wlog	1.05	2.12
N	27.00	24.00
S.D.	0.21	0.51
max	1.11	2.19
min	0.06	0.07

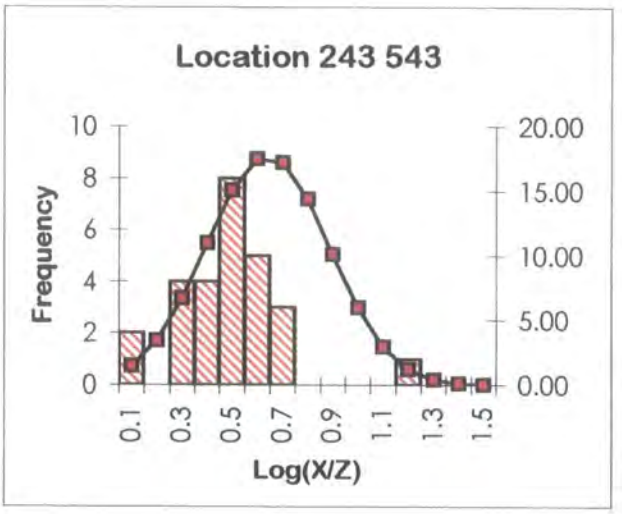
Location 243 543
Frequency
10
8
6
4
2
0
20.00
15.00
10.00
5.00
0.00
0.1
0.3
0.5
0.7
0.9
1.1
1.3
1.5
Log(X/Z)

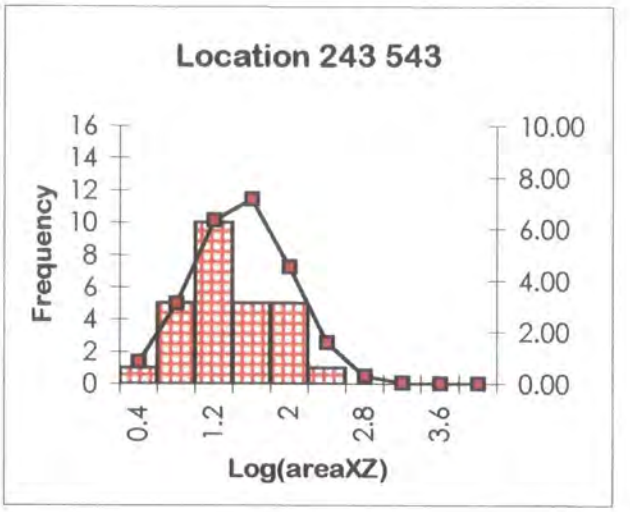
Location 243 543
Frequency
16
14
12
10
8
6
4
2
0
10.00
8.00
6.00
4.00
2.00
0.00
0.4
1.2
2
2.8
3.6
Log(areaXZ)

Rannoch Moor Complex: Old Military Road
Intrusive Phase: The Blackwater facies (G2)

Location [273 519]

X	Z	X/Z	log(X/Z)	log(X×Zπ/4)
13.90	2.50	5.56	0.75	1.44
16.20	3.40	4.76	0.68	1.64
11.40	3.00	3.80	0.58	1.43
7.00	1.00	7.00	0.85	0.74
8.00	2.00	4.00	0.60	1.10
6.50	1.80	3.61	0.56	0.96
13.00	1.80	7.22	0.86	1.26
21.50	5.50	3.91	0.59	1.97
19.70	3.70	5.32	0.73	1.76
29.00	1.60	18.13	1.26	1.56
13.90	1.10	12.64	1.10	1.08
9.00	3.00	3.00	0.48	1.33
22.30	3.30	6.76	0.83	1.76
7.30	2.60	2.81	0.45	1.17
12.90	2.20	5.86	0.77	1.35
30.80	3.30	9.33	0.97	1.90
9.20	3.20	2.88	0.46	1.36
13.30	2.60	5.12	0.71	1.43
17.50	4.70	3.72	0.57	1.81
4.10	3.30	1.24	0.09	1.03
19.80	4.70	4.21	0.62	1.86
22.70	3.80	5.97	0.78	1.83
10.90	0.60	18.17	1.26	0.71
10.20	1.80	5.67	0.75	1.16
10.50	4.50	2.33	0.37	1.57
29.40	2.00	14.70	1.17	1.66
8.80	2.80	3.14	0.50	1.29
17.50	2.60	6.73	0.83	1.55
19.70	4.40	4.48	0.65	1.83
7.70	3.00	2.57	0.41	1.26
15.30	1.50	10.20	1.01	1.26
18.70	9.80	1.91	0.28	2.16
7.50	2.80	2.68	0.43	1.22
7.20	1.20	6.00	0.78	0.83
17.10	4.30	3.98	0.60	1.76
5.30	0.60	8.83	0.95	0.40
20.10	4.80	4.19	0.62	1.88
19.50	3.50	5.57	0.75	1.73
11.90	0.90	13.22	1.12	0.92
23.00	1.80	16.22	1.21	1.62
17.90	3.00	5.97	0.78	1.63
15.20	1.20	12.67	1.10	1.16
5.70	1.00	5.70	0.76	0.65
14.00	3.00	4.67	0.67	1.52
23.90	5.00	4.78	0.68	1.97
24.10	3.50	6.89	0.84	1.82
23.50	4.60	5.11	0.71	1.93
16.90	5.40	3.13	0.50	1.86

X	Z	X/Z	log(X/Z)	log(X×Zπ/4)
13.10	2.40	5.46	0.74	1.39
23.00	2.40	9.58	0.98	1.64
9.20	0.80	11.50	1.06	0.76
16.30	4.70	3.47	0.54	1.78
11.80	0.80	14.75	1.17	0.87
13.70	2.90	4.72	0.67	1.49
11.10	0.80	13.88	1.14	0.84
18.80	3.70	5.08	0.71	1.74
7.50	1.50	5.00	0.70	0.95
31.50	4.50	7.00	0.85	2.05
11.40	0.40	28.50	1.45	0.55
22.70	2.80	8.11	0.91	1.70
15.20	3.80	4.00	0.60	1.66
12.40	1.40	8.86	0.95	1.13
6.50	0.50	13.00	1.11	0.41
21.00	5.00	4.20	0.62	1.92
23.70	4.80	4.94	0.69	1.95
22.90	3.00	7.63	0.88	1.73
15.00	3.60	4.17	0.62	1.63
24.30	3.70	6.57	0.82	1.85
24.30	5.20	4.67	0.67	2.00
15.80	3.00	5.27	0.72	1.57
27.00	4.00	7.75	0.89	1.99
14.10	2.70	5.22	0.72	1.48
14.00	1.20	11.67	1.07	1.12
12.00	1.00	12.00	1.08	0.97
21.00	2.30	9.13	0.96	1.58
15.00	2.20	6.82	0.83	1.41
30.10	2.90	10.38	1.02	1.84
14.20	1.40	10.14	1.01	1.19
10.70	0.40	26.75	1.43	0.53
11.00	2.60	4.23	0.63	1.35
13.80	1.00	13.80	1.14	1.03
9.40	1.00	9.40	0.97	0.87
20.00	1.70	11.76	1.07	1.43
15.60	1.60	9.75	0.99	1.29
5.50	0.80	6.88	0.84	0.54
16.00	3.20	5.00	0.70	1.60
13.00	2.00	6.50	0.81	1.31
14.30	2.90	4.93	0.69	1.51
21.30	5.30	4.02	0.60	1.95
6.80	0.80	8.50	0.93	0.63
12.10	1.10	11.00	1.04	1.02
19.30	3.30	5.85	0.77	1.70
11.20	2.80	4.00	0.60	1.39
17.80	2.70	6.59	0.82	1.58
17.30	4.50	3.84	0.58	1.79
11.70	0.70	16.71	1.22	0.81

8.00	3.30	2.42	0.38	1.32
17.30	5.80	2.98	0.47	1.90
29.70	2.30	12.91	1.11	1.73
13.60	1.90	7.16	0.85	1.31
20.40	5.10	4.00	0.60	1.91
21.90	1.50	14.60	1.16	1.41
15.40	4.00	3.85	0.59	1.68
22.50	2.60	8.65	0.94	1.66
13.60	2.20	6.18	0.79	1.37
19.00	3.00	6.33	0.80	1.65
9.50	3.50	2.71	0.43	1.42
18.20	3.30	5.52	0.74	1.67
19.40	0.90	21.56	1.33	1.14
7.00	2.30	3.04	0.48	1.10
15.80	2.00	7.90	0.90	1.39
16.60	5.10	3.25	0.51	1.82
23.60	3.00	7.87	0.90	1.75
15.70	4.30	3.65	0.56	1.72
21.60	2.70	8.00	0.90	1.66
22.10	1.70	13.00	1.11	1.47
17.10	5.60	3.05	0.48	1.88
21.70	1.30	16.69	1.22	1.35
13.50	0.70	19.29	1.29	0.87
10.70	2.30	4.65	0.67	1.29
20.40	1.90	10.74	1.03	1.48
13.50	2.50	5.40	0.73	1.42
14.70	3.30	4.45	0.65	1.58
24.60	4.00	6.15	0.79	1.89
21.40	1.00	21.40	1.33	1.23
12.40	1.60	7.75	0.89	1.19
11.70	3.30	3.55	0.55	1.48
10.20	4.30	2.37	0.38	1.54
16.60	3.60	4.61	0.66	1.67
26.00	3.50	8.71	0.94	1.92
31.20	4.20	7.43	0.87	2.01
14.80	1.00	14.80	1.17	1.07
21.70	5.70	3.81	0.58	1.99
12.20	1.20	10.17	1.01	1.06

9.00	0.60	15.00	1.18	0.63
12.00	1.50	8.00	0.90	1.15
16.30	3.50	4.66	0.67	1.65
22.10	3.20	6.91	0.84	1.74
19.70	1.20	16.42	1.22	1.27
21.90	3.00	7.30	0.86	1.71
19.90	1.40	14.21	1.15	1.34
16.80	3.90	4.31	0.63	1.71
11.50	0.50	23.00	1.36	0.65
17.60	6.10	2.89	0.46	1.93
14.60	3.20	4.56	0.66	1.56
23.90	3.30	7.24	0.86	1.79
13.60	2.90	4.69	0.67	1.49
22.60	3.70	6.11	0.79	1.82
14.40	1.80	8.00	0.90	1.31
19.90	4.10	4.85	0.69	1.81
8.50	2.50	3.40	0.53	1.22
21.10	5.90	3.58	0.55	1.99
17.30	2.20	7.86	0.90	1.48
17.80	4.90	3.63	0.56	1.84
22.40	2.00	11.20	1.05	1.55
23.20	4.30	5.40	0.73	1.89
19.30	4.20	4.60	0.66	1.80
28.70	1.30	22.08	1.34	1.47
15.50	2.70	5.74	0.76	1.52
23.10	3.40	6.79	0.83	1.79
22.20	2.30	9.65	0.98	1.60
14.60	3.40	4.29	0.63	1.59

sum	131.19	235.93
sum/N	0.81	1.46
average	6.45	28.60
wlog	1.36	1.76
N	162	162
S.D.	0.25	0.39
max	1.45	2.16
min	0.09	0.40

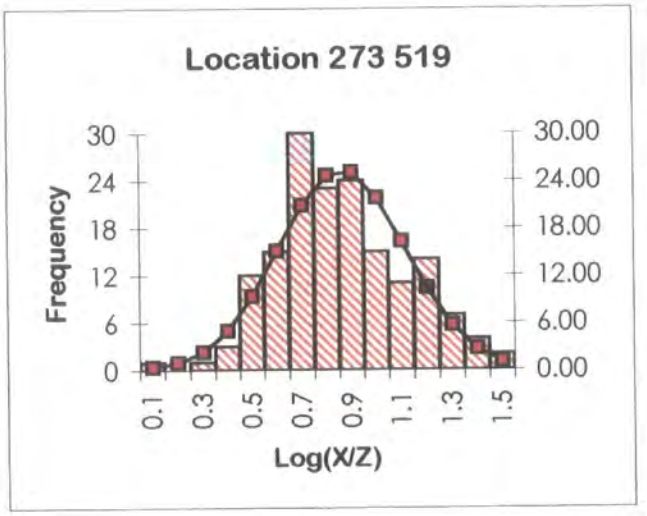
Location 273 519
Frequency
30
24
18
12
6
0
30.00
24.00
18.00
12.00
6.00
0.00
0.1
0.3
0.5
0.7
0.9
1.1
1.3
1.5
Log(X/Z)

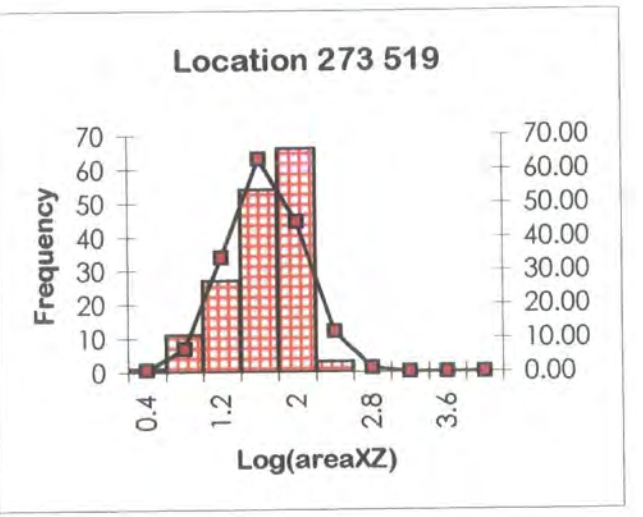
Location 273 519
Frequency
70
60
50
40
30
20
10
0
70.00
60.00
50.00
40.00
30.00
20.00
10.00
0.00
0.4
1.2
2
2.8
3.6
Log(areaXZ)

Rannoch Moor Complex: Kigshouse (River Etive)
Intrusive Phase: The Blackwater facies (G2)

Location [266 551]

X	Z	X/Z	log(x/z)	log (X×Zπ/4)
10.20	1.40	7.29	0.86	1.05
21.20	4.50	4.71	0.67	1.87
8.80	2.80	3.14	0.50	1.29
17.90	4.90	3.65	0.56	1.84
19.30	3.80	5.08	0.71	1.76
6.10	1.30	4.69	0.67	0.79
9.40	3.60	2.61	0.42	1.42
22.80	4.80	4.75	0.68	1.93
9.40	0.80	11.75	1.07	0.77
9.00	3.10	2.90	0.46	1.34
6.90	1.10	6.27	0.80	0.78
10.40	3.30	3.15	0.50	1.43
7.20	1.00	7.20	0.86	0.75
9.10	2.70	3.37	0.53	1.29
17.30	4.50	3.84	0.58	1.79
12.30	2.20	5.59	0.75	1.33
4.40	0.50	8.80	0.94	0.24
10.20	2.60	3.92	0.59	1.32
8.50	2.50	3.40	0.53	1.22
15.90	0.80	19.88	1.30	1.00
9.70	4.00	2.43	0.38	1.48
7.00	0.90	7.78	0.89	0.69
12.20	1.10	11.09	1.04	1.02
13.10	0.90	14.56	1.16	0.97
12.50	1.70	7.35	0.87	1.22
9.20	2.90	3.17	0.50	1.32
14.10	1.90	7.42	0.87	1.32
9.90	2.90	3.41	0.53	1.35
6.50	0.60	10.83	1.03	0.49
21.50	5.60	3.84	0.58	1.98
7.20	1.90	3.79	0.58	1.03
6.60	0.90	7.33	0.87	0.67
18.90	5.30	3.57	0.55	1.90
10.50	3.60	2.92	0.46	1.47
8.60	3.40	2.53	0.40	1.36
7.00	1.70	4.12	0.61	0.97
16.30	1.40	11.64	1.07	1.25
9.20	3.20	2.88	0.46	1.36
9.00	2.00	4.50	0.65	1.15
9.50	3.60	2.64	0.42	1.43
21.50	5.00	4.30	0.63	1.93
8.70	2.80	3.11	0.49	1.28
12.10	2.50	4.84	0.68	1.38
8.20	2.50	3.28	0.52	1.21
9.50	2.70	3.52	0.55	1.30
34.10	5.50	6.20	0.79	2.17
11.10	2.10	5.29	0.72	1.26
7.50	1.60	4.69	0.67	0.97

X	Z	X/Z	log(x/z)	log (X×Zπ/4)
23.40	5.20	4.50	0.65	1.98
11.60	0.70	16.57	1.22	0.80
6.00	0.30	20.00	1.30	0.15
10.90	3.60	3.03	0.48	1.49
6.50	0.60	10.83	1.03	0.49
7.50	1.60	4.69	0.67	0.97
7.60	2.80	2.71	0.43	1.22
7.20	1.60	4.50	0.65	0.96
19.00	3.40	5.59	0.75	1.71
8.90	2.80	3.18	0.50	1.29
10.60	0.70	15.14	1.18	0.77
17.00	1.70	10.00	1.00	1.36
7.20	2.20	3.27	0.51	1.09
9.40	3.30	2.85	0.45	1.39
6.00	0.50	12.00	1.08	0.37
7.00	1.50	4.67	0.67	0.92
7.30	1.30	5.62	0.75	0.87
10.50	2.80	3.75	0.57	1.36
48.20	10.20	4.73	0.67	2.59
7.50	2.40	3.13	0.49	1.15
8.50	2.20	3.86	0.59	1.17
20.70	4.40	4.70	0.67	1.85
8.20	1.90	4.32	0.64	1.09
13.90	3.90	3.56	0.55	1.63
23.70	5.90	4.02	0.60	2.04
8.60	2.20	3.91	0.59	1.17
16.60	4.20	3.95	0.60	1.74
19.00	5.80	3.28	0.52	1.94
16.30	1.60	10.19	1.01	1.31
13.60	1.60	8.50	0.93	1.23
14.10	4.30	3.28	0.52	1.68
6.50	0.20	32.50	1.51	0.01
18.30	5.10	3.59	0.55	1.87
16.10	4.10	3.93	0.59	1.71
6.90	1.90	3.63	0.56	1.01
11.60	1.10	10.55	1.02	1.00
23.10	5.20	4.44	0.65	1.97
13.40	1.20	11.17	1.05	1.10
14.50	4.70	3.09	0.49	1.73
27.30	3.70	7.38	0.87	1.90
18.40	5.40	3.41	0.53	1.89
7.30	0.10	73.00	1.86	-0.24
8.70	3.60	2.42	0.38	1.39
23.00	5.20	4.42	0.65	1.97
6.30	0.60	10.50	1.02	0.47
18.80	2.30	8.17	0.91	1.53
10.00	3.10	3.23	0.51	1.39
12.50	1.80	6.94	0.84	1.25

7.00	1.80	3.89	0.59	1.00
10.10	1.10	9.18	0.96	0.94
8.80	2.70	3.26	0.51	1.27
6.80	1.50	4.53	0.66	0.90
18.60	3.10	6.00	0.78	1.66
8.30	2.40	3.46	0.54	1.19
16.30	1.00	16.30	1.21	1.11
15.70	3.10	5.06	0.70	1.58
6.30	0.50	12.60	1.10	0.39
6.50	1.20	5.42	0.73	0.79
9.10	3.90	2.33	0.37	1.45
13.60	1.40	9.71	0.99	1.17
22.40	4.20	5.33	0.73	1.87
19.40	2.70	7.19	0.86	1.61
8.10	1.60	5.06	0.70	1.01
20.00	4.10	4.88	0.69	1.81
16.20	3.60	4.50	0.65	1.66
18.80	3.30	5.70	0.76	1.69
11.30	0.60	18.83	1.27	0.73
8.00	2.10	3.81	0.58	1.12
9.80	1.00	9.80	0.99	0.89
21.00	4.90	4.29	0.63	1.91
7.20	0.40	18.00	1.26	0.35
6.60	1.80	3.67	0.56	0.97
9.00	3.00	3.00	0.48	1.33
8.70	2.40	3.63	0.56	1.21
14.20	4.60	3.09	0.49	1.71

8.10	1.50	5.40	0.73	0.98
21.10	3.20	6.59	0.82	1.72
10.30	1.80	5.72	0.76	1.16
12.50	3.20	3.91	0.59	1.50
8.80	3.60	2.44	0.39	1.40
8.30	3.20	2.59	0.41	1.32
8.50	2.80	3.04	0.48	1.27
15.90	3.40	4.68	0.67	1.63
14.80	5.00	2.96	0.47	1.76
7.50	2.20	3.41	0.53	1.11
11.00	4.10	2.68	0.43	1.55
7.40	1.40	5.29	0.72	0.91
9.50	2.60	3.65	0.56	1.29
14.50	2.50	5.80	0.76	1.45
8.50	2.50	3.40	0.53	1.22
7.70	2.80	2.75	0.44	1.23
13.30	3.50	3.80	0.58	1.56

sum	99.53	278.81
sum/N	0.71	1.99
average	5.14	98.07
wlog	1.50	2.83
N	140.00	140.00
S.D.	0.25	0.47
max	1.86	2.59
min	0.37	-0.24

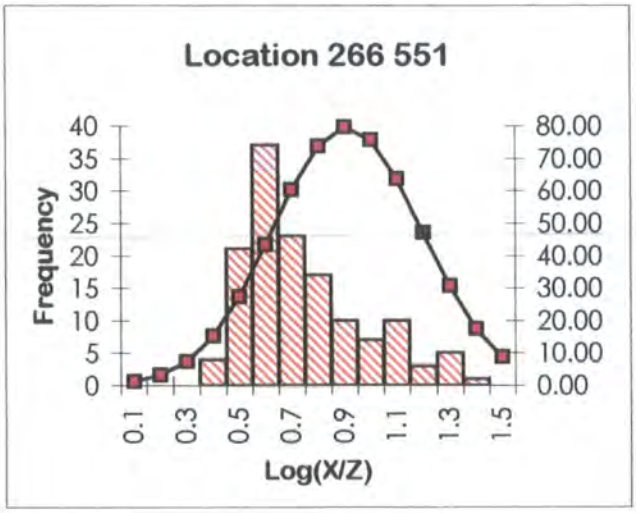

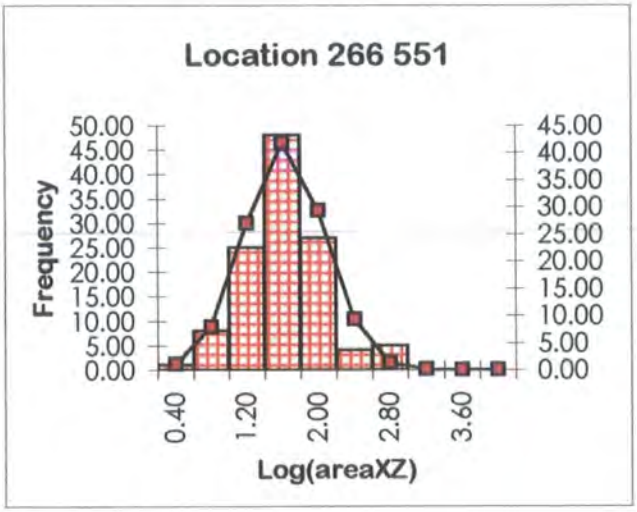

Rannoch Moor Complex: Leacann nam Braonan
Intrusive Phase: The Ciaran/Chomraidh marginal facies (G4)

Location [273 516]

X	Z	X/Z	log(X/Z)	log(X×Zπ/4)
8.50	4.50	1.89	0.28	1.48
29.60	9.40	3.15	0.50	2.34
12.00	1.40	8.57	0.93	1.12
13.00	2.40	5.42	0.73	1.39
31.60	5.50	5.75	0.76	2.14
5.00	0.90	5.56	0.74	0.55
10.30	6.10	1.69	0.23	1.69
14.50	4.50	3.22	0.51	1.71
20.90	6.20	3.37	0.53	2.01
12.50	1.90	6.58	0.82	1.27
31.40	5.10	6.16	0.79	2.10
11.50	2.10	5.48	0.74	1.28
34.20	7.30	4.68	0.67	2.29
14.20	4.20	3.38	0.53	1.67
21.10	6.40	3.30	0.52	2.03
21.60	6.90	3.13	0.50	2.07
11.20	1.80	6.22	0.79	1.20
19.10	4.80	3.98	0.60	1.86
20.00	5.50	3.64	0.56	1.94
21.70	7.20	3.01	0.48	2.09
9.00	5.00	1.80	0.26	1.55
6.50	1.80	3.61	0.56	0.96
7.70	2.60	2.96	0.47	1.20
11.80	1.20	9.83	0.99	1.05
34.00	7.10	4.79	0.68	2.28
5.50	1.20	4.58	0.66	0.71
14.00	4.00	3.50	0.54	1.64
12.20	1.60	7.63	0.88	1.19
27.60	7.40	3.73	0.57	2.21
33.70	6.80	4.96	0.70	2.26
32.30	6.20	5.21	0.72	2.20
11.50	0.90	12.78	1.11	0.91
20.50	6.00	3.42	0.53	1.98
26.90	6.70	4.01	0.60	2.15
8.00	4.00	2.00	0.30	1.40
18.90	4.60	4.11	0.61	1.83
21.30	6.60	3.23	0.51	2.04
21.90	8.90	2.46	0.39	2.18
28.10	7.90	3.56	0.55	2.24
33.00	6.50	5.08	0.71	2.23

X	Z	X/Z	log(X/Z)	log(X×Zπ/4)
10.00	6.00	1.67	0.22	1.67
7.80	3.80	2.05	0.31	1.37
26.30	6.30	4.17	0.62	2.11
9.40	5.70	1.65	0.22	1.62
7.20	2.10	3.43	0.54	1.07
10.50	6.50	1.62	0.21	1.73
12.30	2.70	4.56	0.66	1.42
34.70	7.80	4.45	0.65	2.33
32.00	5.90	5.42	0.73	2.17
12.00	2.40	5.00	0.70	1.35
7.90	2.80	2.82	0.45	1.24
5.30	1.00	5.30	0.72	0.62
31.80	5.70	5.58	0.75	2.15
27.10	6.90	3.93	0.59	2.17
8.10	4.30	1.88	0.28	1.44
9.80	5.80	1.69	0.23	1.65
29.40	9.20	3.20	0.50	2.33
34.40	7.50	4.59	0.66	2.31
11.80	2.20	5.36	0.73	1.31
27.20	7.20	3.78	0.58	2.19
28.90	8.70	3.32	0.52	2.30
7.40	2.50	2.96	0.47	1.16
8.20	3.10	2.65	0.42	1.30
5.80	1.50	3.87	0.59	0.83
7.40	3.60	2.06	0.31	1.32
28.50	8.50	3.35	0.53	2.28
13.60	3.60	3.78	0.58	1.58
18.70	4.40	4.25	0.63	1.81
12.90	3.10	4.16	0.62	1.50
13.70	3.90	3.51	0.55	1.62

sum	40.10	118.37
sum/N	0.57	1.69
average	3.74	49.10
wlog	0.90	1.79
N	70	70
S.D.	0.19	0.49
max	1.11	2.34
min	0.21	0.55

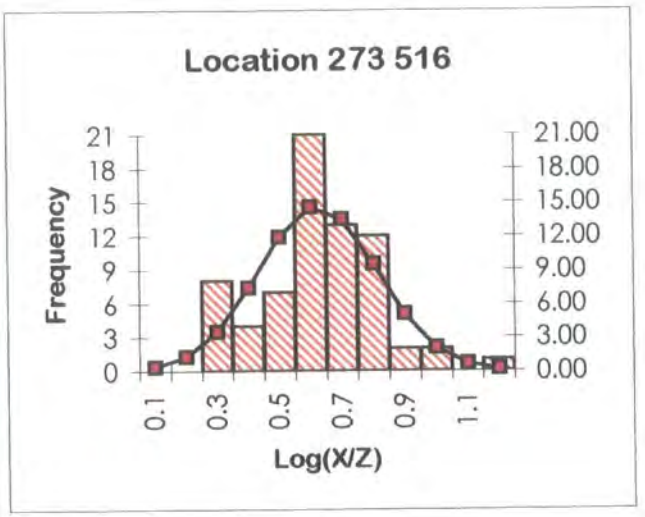
Location 273 516
Frequency
21
18
15
12
9
6
3
0
21.00
18.00
15.00
12.00
9.00
6.00
3.00
0.00
0.1
0.3
0.5
0.7
0.9
1.1
Log(X/Z)

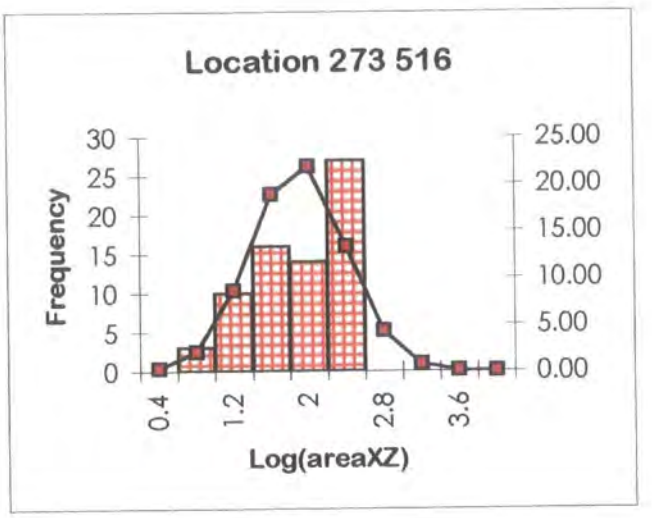
Location 273 516
Frequency
30
25
20
15
10
5
0
25.00
20.00
15.00
10.00
5.00
0.00
0.4
1.2
2
2.8
3.6
Log(areaXZ)

Rannoch Moor Complex: Leacann nam Braonan
Intrusive Phase: The Ciaran/Chomraidh marginal facies (G4)

Location [272 515]

X	Z	X/Z	log(x/z)	log (X×Zπ/4)
11.20	5.70	1.96	0.29	1.70
10.20	2.40	4.25	0.63	1.28
15.90	3.20	4.97	0.70	1.60
5.60	3.20	1.75	0.24	1.15
16.50	3.90	4.23	0.63	1.70
20.30	8.30	2.45	0.39	2.12
13.00	4.00	3.25	0.51	1.61
9.00	3.50	2.57	0.41	1.39
5.00	2.20	2.27	0.36	0.94
10.20	2.30	4.43	0.65	1.27
4.00	1.10	3.64	0.56	0.54
11.70	4.10	2.85	0.46	1.58
11.50	3.30	3.48	0.54	1.47
10.30	3.50	2.94	0.47	1.45
11.40	3.80	3.00	0.48	1.53
14.50	2.50	5.80	0.76	1.45
10.50	2.30	4.57	0.66	1.28
10.70	2.10	5.10	0.71	1.25
8.90	1.10	8.09	0.91	0.89
9.50	4.00	2.38	0.38	1.47
16.00	3.50	4.57	0.66	1.64
18.00	5.00	3.60	0.56	1.85
8.40	3.10	2.71	0.43	1.31
7.30	2.70	2.70	0.43	1.19
6.80	2.20	3.09	0.49	1.07
16.60	3.90	4.26	0.63	1.71
5.70	2.50	2.28	0.36	1.05
11.40	3.40	3.35	0.53	1.48
17.10	4.30	3.98	0.60	1.76
19.80	8.00	2.48	0.39	2.09
10.80	1.80	6.00	0.78	1.18
16.30	3.60	4.53	0.66	1.66
8.10	0.90	9.00	0.95	0.76
9.80	2.00	4.90	0.69	1.19
18.80	5.80	3.24	0.51	1.93
18.00	5.80	3.10	0.49	1.91
10.00	4.50	2.22	0.35	1.55
11.40	2.00	5.70	0.76	1.25
10.80	5.30	2.04	0.31	1.65
13.90	1.70	8.18	0.91	1.27
16.80	3.80	4.42	0.65	1.70
7.00	1.10	6.36	0.80	0.78
19.30	6.10	3.16	0.50	1.97
9.90	2.30	4.30	0.63	1.25
8.50	2.50	3.40	0.53	1.22
7.50	2.50	3.00	0.48	1.17
10.50	2.50	4.20	0.62	1.31
14.10	1.90	7.42	0.87	1.32

X	Z	X/Z	log(x/z)	log (X×Zπ/4)
19.60	7.60	2.58	0.41	2.07
10.80	1.80	6.00	0.78	1.18
10.50	3.00	3.50	0.54	1.39
4.60	1.60	2.88	0.46	0.76
4.00	0.70	5.71	0.76	0.34
17.90	5.20	3.44	0.54	1.86
12.50	3.50	3.57	0.55	1.54
4.20	1.30	3.23	0.51	0.63
20.10	8.10	2.48	0.39	2.11
5.90	3.30	1.79	0.25	1.18
18.20	5.30	3.43	0.54	1.88
9.20	3.70	2.49	0.40	1.43
16.10	3.90	4.13	0.62	1.69
9.80	3.00	3.27	0.51	1.36
13.20	4.20	3.14	0.50	1.64
18.30	5.60	3.27	0.51	1.91
11.00	5.50	2.00	0.30	1.68
11.90	4.30	2.77	0.44	1.60
14.10	2.30	6.13	0.79	1.41
8.60	3.50	2.46	0.39	1.37
9.00	2.00	4.50	0.65	1.15
10.40	2.80	3.71	0.57	1.36
10.60	4.90	2.16	0.34	1.61
9.70	1.80	5.39	0.73	1.14
9.20	3.70	2.49	0.40	1.43
11.10	1.90	5.84	0.77	1.22
18.10	6.10	2.97	0.47	1.94
19.10	7.10	2.69	0.43	2.03
11.00	2.80	3.93	0.59	1.38
8.00	2.50	3.20	0.51	1.20
17.10	4.40	3.89	0.59	1.77
4.20	1.00	4.20	0.62	0.52
12.00	3.00	4.00	0.60	1.45
6.00	3.60	1.67	0.22	1.23
8.80	3.30	2.67	0.43	1.36
15.40	3.60	4.28	0.63	1.64
12.00	4.60	2.61	0.42	1.64
15.10	2.90	5.21	0.72	1.54
19.20	5.80	3.31	0.52	1.94
7.00	1.50	4.67	0.67	0.92
16.80	4.20	4.00	0.60	1.74
7.20	1.70	4.24	0.63	0.98
11.00	2.80	3.93	0.59	1.38
10.90	3.30	3.30	0.52	1.45
4.50	0.70	6.43	0.81	0.39
22.70	11.80	1.92	0.28	2.32
18.30	6.30	2.90	0.46	1.96
24.10	7.90	3.05	0.48	2.17

12.70	3.90	3.26	0.51	1.59
7.90	3.10	2.55	0.41	1.28
18.60	5.40	3.44	0.54	1.90
4.70	1.50	3.13	0.50	0.74
17.50	5.00	3.50	0.54	1.84
17.70	4.30	4.12	0.61	1.78
9.30	2.50	3.72	0.57	1.26
18.60	6.60	2.82	0.45	1.98
11.50	2.50	4.60	0.66	1.35
15.90	3.70	4.30	0.63	1.66

9.00	3.50	2.57	0.41	1.39

sum	58.56	213.18
sum/N	0.55	1.99
average	3.53	98.24
wlog	0.73	2.10
N	107.00	107.00
S.D.	0.15	0.54
max	0.95	2.32
min	0.22	0.22

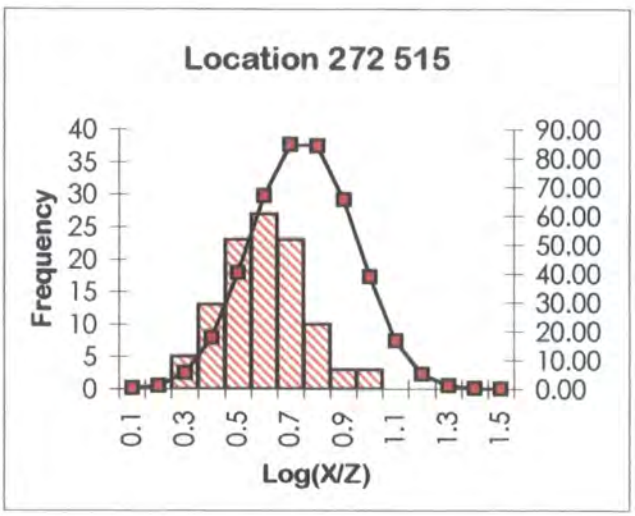

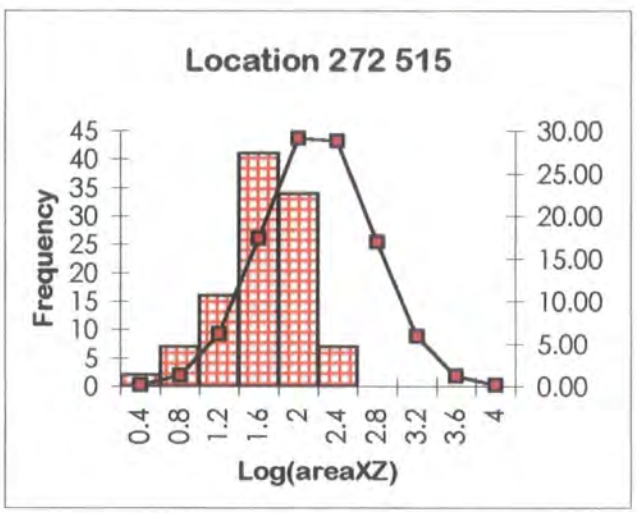

Rannoch Moor Complex: Kingshouse (Allt nan Giubhas)
Intrusive Phase: The Blackwater facies (G2)

Location [264 541]A

X	Z	X/Z	log(x/z)	log (X×Zπ/4)
13.50	4.00	3.38	0.53	1.63
16.40	3.80	4.32	0.64	1.69
12.50	2.50	5.00	0.70	1.39
12.90	3.10	4.16	0.62	1.50
20.70	5.20	3.98	0.60	1.93
45.80	12.60	3.63	0.56	2.66
16.30	3.30	4.94	0.69	1.63
13.10	3.50	3.74	0.57	1.56
14.00	4.90	2.86	0.46	1.73
46.10	12.70	3.63	0.56	2.66
43.40	7.90	5.49	0.74	2.43
45.80	10.50	4.36	0.64	2.58
38.50	12.50	3.08	0.49	2.58
11.80	1.30	9.08	0.96	1.08
12.80	2.80	4.57	0.66	1.45
11.40	22.40	0.51	-0.29	2.30
7.50	43.60	0.17	-0.76	2.41
10.80	10.50	1.03	0.01	1.95
39.00	13.20	2.95	0.47	2.61
8.20	1.30	6.31	0.80	0.92
13.50	3.60	3.75	0.57	1.58
14.60	1.60	9.13	0.96	1.26
13.60	4.50	3.02	0.48	1.68
37.10	11.10	3.34	0.52	2.51
13.90	4.60	3.02	0.48	1.70
15.50	3.60	4.31	0.63	1.64
22.00	6.30	3.49	0.54	2.04
12.00	2.00	6.00	0.78	1.28
11.10	0.90	12.33	1.09	0.89
42.90	7.40	5.80	0.76	2.40
15.10	2.10	7.19	0.86	1.40
13.00	3.00	4.33	0.64	1.49
10.90	0.70	15.57	1.19	0.78
13.90	0.90	15.44	1.19	0.99
39.20	13.40	2.93	0.47	2.62
12.20	2.70	4.52	0.65	1.41
12.50	3.00	4.17	0.62	1.47
13.60	0.60	22.67	1.36	0.81
43.20	10.60	4.08	0.61	2.56
20.50	4.80	4.27	0.63	1.89
43.80	8.50	5.15	0.71	2.47
39.50	13.50	2.93	0.47	2.62
21.10	5.60	3.77	0.58	1.97
45.40	10.00	4.54	0.66	2.55
14.20	3.90	3.64	0.56	1.64
10.70	0.40	26.75	1.43	0.53
45.70	10.00	4.57	0.66	2.56
21.50	5.80	3.71	0.57	1.99

X	Z	X/Z	log(x/z)	log (X×Zπ/4)
15.70	3.10	5.06	0.70	1.58
11.50	2.00	5.75	0.76	1.26
38.90	13.00	2.99	0.48	2.60
37.00	10.80	3.43	0.53	2.50
13.20	3.30	4.00	0.60	1.53
13.80	3.70	3.73	0.57	1.60
44.90	11.90	3.77	0.58	2.62
12.20	2.80	4.36	0.64	1.43
43.70	11.10	3.94	0.60	2.58
11.00	2.00	5.50	0.74	1.24
22.70	7.80	2.91	0.46	2.14
46.70	13.10	3.56	0.55	2.68
43.70	11.50	3.80	0.58	2.60
14.10	1.10	12.82	1.11	1.09
44.30	9.00	4.92	0.69	2.50
13.00	3.50	3.71	0.57	1.55
10.80	1.80	6.00	0.78	1.18
43.20	7.70	5.61	0.75	2.42
36.60	10.60	3.45	0.54	2.48
13.50	3.50	3.86	0.59	1.57
45.10	9.80	4.60	0.66	2.54
11.90	2.20	5.41	0.73	1.31
37.30	11.40	3.27	0.51	2.52
46.30	12.90	3.59	0.55	2.67
16.00	3.20	5.00	0.70	1.60
37.70	11.50	3.28	0.52	2.53
22.00	7.10	3.10	0.49	2.09
11.00	2.50	4.40	0.64	1.33
12.00	2.50	4.80	0.68	1.37
21.00	5.30	3.96	0.60	1.94
45.60	12.20	3.74	0.57	2.64
11.40	2.60	4.38	0.64	1.37
44.80	9.50	4.72	0.67	2.52
21.60	6.90	3.13	0.50	2.07
22.00	7.50	2.93	0.47	2.11
14.30	5.20	2.75	0.44	1.77
44.10	11.70	3.77	0.58	2.61

sum	55.31	223.04
sum/N	0.63	2.53
average	4.25	342.45
wlog	2.19	3.45
N	88.00	88.00
S.D.	0.27	0.79
max	1.43	2.68
min	-0.76	-0.76

14.20	1.40	10.14	1.01	1.19
43.60	8.10	5.38	0.73	2.44
38.00	12.30	3.09	0.49	2.56

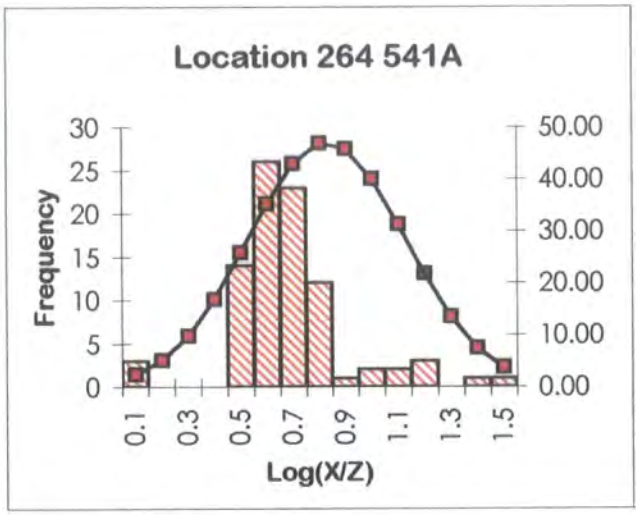

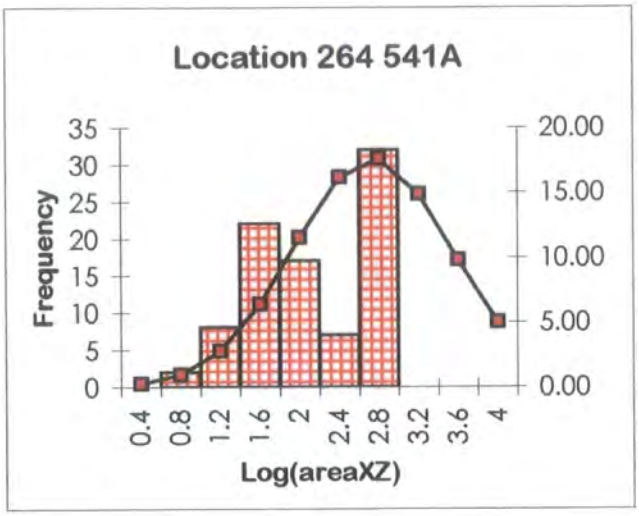

Rannoch Moor Complex: Kingshouse (Allt nan Giubhas)
Intrusive Phase: The Blackwater facies (G2)

Location [264 541]B

X	Z	X/Z	log(x/z)	log (X×Zπ/4)
14.40	2.90	4.97	0.70	1.52
8.50	1.70	5.00	0.70	1.05
10.30	2.50	4.12	0.61	1.31
45.50	13.10	3.47	0.54	2.67
46.10	13.70	3.36	0.53	2.70
45.50	12.40	3.67	0.56	2.65
22.60	5.40	4.19	0.62	1.98
15.70	2.30	6.83	0.83	1.45
44.40	12.40	3.58	0.55	2.64
7.40	2.00	3.70	0.57	1.07
14.70	3.60	4.08	0.61	1.62
8.60	3.80	2.26	0.35	1.41
6.00	1.40	4.29	0.63	0.82
16.70	4.50	3.71	0.57	1.77
20.40	4.60	4.43	0.65	1.87
11.70	1.30	9.00	0.95	1.08
40.10	11.90	3.37	0.53	2.57
69.40	16.80	4.13	0.62	2.96
55.00	6.90	7.97	0.90	2.47
11.80	2.50	4.72	0.67	1.36
14.50	4.00	3.63	0.56	1.66
9.80	4.40	2.23	0.35	1.53
10.00	4.40	2.27	0.36	1.54
16.90	3.20	5.28	0.72	1.63
9.60	2.20	4.36	0.64	1.22
14.70	1.50	9.80	0.99	1.24
10.30	3.40	3.03	0.48	1.44
14.20	3.30	4.30	0.63	1.57
14.10	4.20	3.36	0.53	1.67
13.50	2.60	5.19	0.72	1.44
6.50	1.00	6.50	0.81	0.71
10.10	1.40	7.21	0.86	1.05
11.60	2.90	4.00	0.60	1.42
16.30	2.90	5.62	0.75	1.57
7.80	2.70	2.89	0.46	1.22
7.40	0.50	14.80	1.17	0.46
9.30	4.00	2.33	0.37	1.47
8.00	3.20	2.50	0.40	1.30
13.90	2.90	4.79	0.68	1.50
13.50	2.50	5.40	0.73	1.42
7.50	2.90	2.59	0.41	1.23
15.90	3.30	4.82	0.68	1.62
13.90	2.50	5.56	0.75	1.44
17.80	5.50	3.24	0.51	1.89
11.60	1.70	6.82	0.83	1.19
12.20	1.90	6.42	0.81	1.26
13.90	3.50	3.97	0.60	1.58
12.40	2.70	4.59	0.66	1.42

X	Z	X/Z	log(x/z)	log (X×Zπ/4)
9.50	1.60	5.94	0.77	1.08
15.10	1.90	7.95	0.90	1.35
8.90	3.50	2.54	0.41	1.39
7.80	1.50	5.20	0.72	0.96
10.90	1.70	6.41	0.81	1.16
11.50	1.00	11.50	1.06	0.96
13.00	2.50	5.20	0.72	1.41
5.00	0.50	10.00	1.00	0.29
11.20	2.30	4.87	0.69	1.31
12.80	2.40	5.33	0.73	1.38
24.40	4.50	5.42	0.73	1.94
11.40	1.90	6.00	0.78	1.23
11.80	1.70	6.94	0.84	1.20
13.60	2.90	4.69	0.67	1.49
17.20	4.10	4.20	0.62	1.74
6.40	1.60	4.00	0.60	0.91
47.20	11.40	4.14	0.62	2.63
15.20	8.70	1.75	0.24	2.02
17.80	4.50	3.96	0.60	1.80
21.20	3.50	6.06	0.78	1.77
7.10	2.30	3.09	0.49	1.11
12.20	2.10	5.81	0.76	1.30
9.70	0.80	12.13	1.08	0.78
9.60	3.80	2.53	0.40	1.46
42.90	1.50	28.60	1.46	1.70
8.30	1.20	6.92	0.84	0.89
8.50	1.30	6.54	0.82	0.94
13.00	2.30	5.65	0.75	1.37
22.40	7.60	2.95	0.47	2.13
25.20	3.80	6.63	0.82	1.88
8.50	2.90	2.93	0.47	1.29
8.50	2.70	3.15	0.50	1.26
6.10	0.40	15.25	1.18	0.28
17.50	0.80	21.88	1.34	1.04
16.30	3.90	4.18	0.62	1.70
45.10	9.50	4.75	0.68	2.53
53.20	11.50	4.63	0.67	2.68
23.20	5.60	4.14	0.62	2.01
19.30	3.50	5.51	0.74	1.72
11.40	0.60	19.00	1.28	0.73
21.90	5.10	4.29	0.63	1.94
14.50	3.50	4.14	0.62	1.60
12.40	2.10	5.90	0.77	1.31
11.30	1.10	10.27	1.01	0.99
6.00	0.50	12.00	1.08	0.37
14.80	2.40	6.17	0.79	1.45
10.90	1.50	7.27	0.86	1.11
14.20	0.90	15.78	1.20	1.00

14.90	2.30	6.48	0.81	1.43
21.30	4.70	4.53	0.66	1.90
17.40	4.80	3.63	0.56	1.82
20.00	4.00	5.00	0.70	1.80
6.70	1.70	3.94	0.60	0.95
7.50	0.80	9.38	0.97	0.67
8.90	3.40	2.62	0.42	1.38
12.70	3.80	3.34	0.52	1.58
43.30	12.60	3.44	0.54	2.63

sum	73.76	156.35
sum/N	0.70	1.49
average	5.04	30.84
wlog	1.21	2.72
N	105.00	105.00
S.D.	0.22	0.54
max	1.46	2.96
min	0.24	0.28

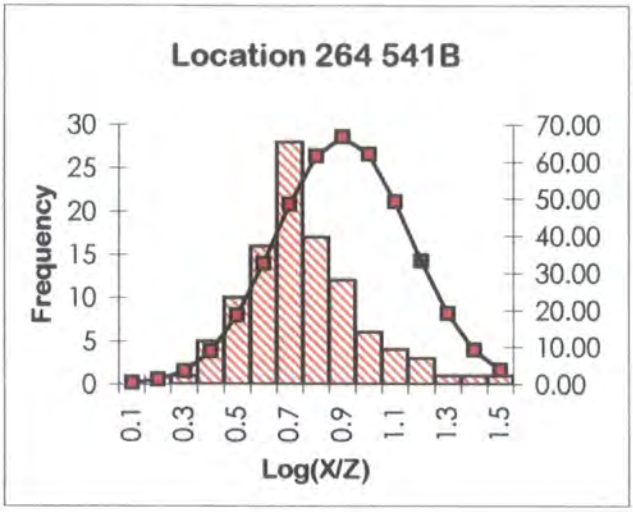

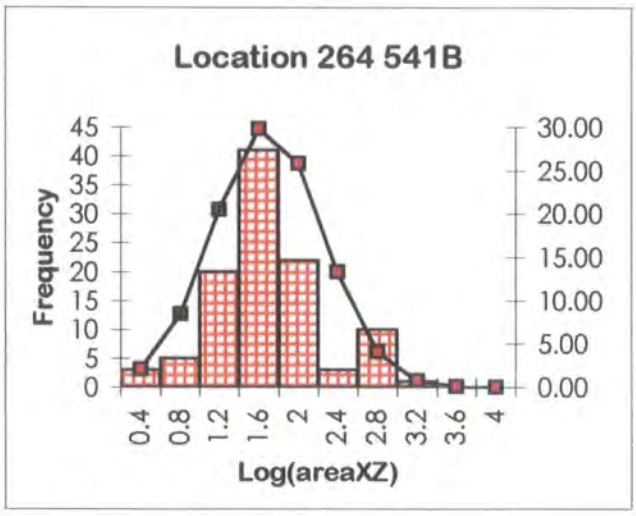

Rannoch Moor Complex: Kingshouse (Allt nan Giubhas)
Intrusive Phase: The Blackwater facies (G2)

Location [260 544]

X	Z	X/Z	log(X/Z)	log (X×Zπ/4)
11.30	2.70	4.19	0.62	1.38
10.50	2.80	3.75	0.57	1.36
10.20	2.00	5.10	0.71	1.20
15.60	3.40	4.59	0.66	1.62
11.90	0.50	23.80	1.38	0.67
10.40	2.20	4.73	0.67	1.25
14.50	2.30	6.30	0.80	1.42
16.20	3.40	4.76	0.68	1.64
13.20	4.70	2.81	0.45	1.69
10.30	2.60	3.96	0.60	1.32
42.20	5.40	7.81	0.89	2.25
15.20	2.50	6.08	0.78	1.47
11.80	2.70	4.37	0.64	1.40
13.70	2.80	4.89	0.69	1.48
17.40	3.60	4.83	0.68	1.69
23.40	5.40	4.33	0.64	2.00
8.00	1.10	7.27	0.86	0.84
14.20	2.00	7.10	0.85	1.35
12.90	4.40	2.93	0.47	1.65
14.60	3.70	3.95	0.60	1.63
16.70	1.60	10.44	1.02	1.32
19.10	3.20	5.97	0.78	1.68
9.90	3.50	2.83	0.45	1.43
12.70	3.20	3.97	0.60	1.50
20.70	3.50	5.91	0.77	1.76
8.00	1.40	5.71	0.76	0.94
13.80	1.80	7.67	0.88	1.29
16.40	3.20	5.13	0.71	1.62
12.50	1.10	11.36	1.06	1.03
12.10	2.50	4.84	0.68	1.38
9.60	2.40	4.00	0.60	1.26
26.00	4.90	5.31	0.72	2.00
25.50	4.90	5.20	0.72	1.99
14.20	2.40	5.92	0.77	1.43
12.10	1.90	6.37	0.80	1.26
14.80	3.70	4.00	0.60	1.63
8.30	1.70	4.88	0.69	1.04
14.30	2.50	5.72	0.76	1.45
10.00	1.60	6.25	0.80	1.10
15.90	3.10	5.13	0.71	1.59
12.40	0.60	20.67	1.32	0.77
10.10	2.90	3.48	0.54	1.36
14.20	1.50	9.47	0.98	1.22
20.50	5.20	3.94	0.60	1.92
14.50	4.70	3.09	0.49	1.73
19.40	4.10	4.73	0.68	1.80
13.30	1.00	13.30	1.12	1.02
15.70	2.60	6.04	0.78	1.51

X	Z	X/Z	log(X/Z)	log (X×Zπ/4)
10.90	3.30	3.30	0.52	1.45
15.20	4.20	3.62	0.56	1.70
11.10	2.70	4.11	0.61	1.37
10.70	3.00	3.57	0.55	1.40
14.70	4.10	3.59	0.55	1.68
7.90	1.50	5.27	0.72	0.97
9.10	0.50	18.20	1.26	0.55
8.50	1.00	8.50	0.93	0.82
14.10	4.10	3.44	0.54	1.66
9.20	2.40	3.83	0.58	1.24
13.70	1.90	7.21	0.86	1.31
13.30	1.10	12.09	1.08	1.06
11.70	2.70	4.33	0.64	1.39
23.10	5.10	4.53	0.66	1.97
15.20	2.80	5.43	0.73	1.52
10.80	3.80	2.84	0.45	1.51
11.30	2.30	4.91	0.69	1.31
8.60	1.80	4.78	0.68	1.08
13.60	3.40	4.00	0.60	1.56
10.10	2.20	4.59	0.66	1.24
7.50	0.80	9.38	0.97	0.67
10.80	2.40	4.50	0.65	1.31
13.90	1.70	8.18	0.91	1.27
12.60	4.10	3.07	0.49	1.61
10.50	2.20	4.77	0.68	1.26
12.60	3.60	3.50	0.54	1.55
21.20	2.20	9.64	0.98	1.56
15.30	0.70	21.86	1.34	0.92
10.00	0.80	12.50	1.10	0.80
14.10	3.30	4.27	0.63	1.56
24.50	2.30	10.65	1.03	1.65
13.50	3.40	3.97	0.60	1.56
9.70	1.50	6.47	0.81	1.06
25.90	2.60	9.96	1.00	1.72
16.30	2.70	6.04	0.78	1.54
11.60	2.60	4.46	0.65	1.37
10.60	1.90	5.58	0.75	1.20
11.90	0.90	13.22	1.12	0.92
10.60	3.00	3.53	0.55	1.40
12.60	1.90	6.63	0.82	1.27
8.60	1.80	4.78	0.68	1.08
18.00	3.50	5.14	0.71	1.69
10.50	1.70	6.18	0.79	1.15
17.10	2.90	5.90	0.77	1.59
9.20	1.90	4.84	0.69	1.14
15.50	2.70	5.74	0.76	1.52
15.00	4.50	3.33	0.52	1.72
11.70	3.60	3.25	0.51	1.52

11.40	4.20	2.71	0.43	1.58
8.90	1.50	5.93	0.77	1.02
8.30	1.40	5.93	0.77	0.96
13.10	1.70	7.71	0.89	1.24
22.30	4.50	4.96	0.70	1.90
13.00	2.40	5.42	0.73	1.39
12.90	1.90	6.79	0.83	1.28
10.70	2.70	3.96	0.60	1.36
21.20	3.60	5.89	0.77	1.78
9.40	2.20	4.27	0.63	1.21
24.00	2.50	9.60	0.98	1.67
29.40	1.70	17.29	1.24	1.59
14.70	2.30	6.39	0.81	1.42
15.40	2.90	5.31	0.73	1.55
12.20	3.40	3.59	0.55	1.51
17.30	3.50	4.94	0.69	1.68
10.40	3.60	2.89	0.46	1.47
13.50	1.50	9.00	0.95	1.20
14.60	2.40	6.08	0.78	1.44
12.80	3.80	3.37	0.53	1.58
9.70	1.70	5.71	0.76	1.11
9.70	1.30	7.46	0.87	1.00
12.00	2.30	5.22	0.72	1.34
15.00	2.10	7.14	0.85	1.39
17.10	3.30	5.18	0.71	1.65
14.40	3.50	4.11	0.61	1.60
7.90	1.10	7.18	0.86	0.83
14.00	2.20	6.36	0.80	1.38
7.70	0.80	9.63	0.98	0.68
8.70	0.50	17.40	1.24	0.53
14.90	2.70	5.52	0.74	1.50
13.50	1.50	9.00	0.95	1.20
4.50	0.60	7.50	0.88	0.33
21.90	3.90	5.62	0.75	1.83
20.50	2.50	8.20	0.91	1.60
9.10	1.80	5.06	0.70	1.11
11.90	3.50	3.40	0.53	1.51
12.40	3.20	3.88	0.59	1.49
8.30	3.50	2.37	0.38	1.36
18.10	3.20	5.66	0.75	1.66
10.40	2.70	3.85	0.59	1.34
8.90	0.90	9.89	1.00	0.80
16.80	3.40	4.94	0.69	1.65
10.00	2.00	5.00	0.70	1.20
12.60	3.40	3.71	0.57	1.53
10.90	3.10	3.52	0.55	1.42
9.00	1.20	7.50	0.88	0.93
18.20	2.70	6.74	0.83	1.59
9.30	2.70	3.44	0.54	1.29
6.50	1.30	5.00	0.70	0.82
11.60	3.20	3.63	0.56	1.46
9.70	1.10	8.82	0.95	0.92
12.80	2.70	4.74	0.68	1.43
17.70	3.90	4.54	0.66	1.73
8.50	1.70	5.00	0.70	1.05

11.10	2.50	4.44	0.65	1.34
19.40	3.60	5.39	0.73	1.74
15.60	4.40	3.55	0.55	1.73
13.20	2.80	4.71	0.67	1.46
8.80	2.00	4.40	0.64	1.14
12.40	1.00	12.40	1.09	0.99
14.80	2.80	5.29	0.72	1.51
11.00	3.60	3.06	0.49	1.49
10.60	3.30	3.21	0.51	1.44
21.40	4.00	5.35	0.73	1.83
23.80	5.60	4.25	0.63	2.02
11.50	0.70	16.43	1.22	0.80
10.00	2.50	4.00	0.60	1.29
11.80	3.20	3.69	0.57	1.47
14.50	1.90	7.63	0.88	1.34
12.30	3.10	3.97	0.60	1.48
12.90	1.70	7.59	0.88	1.24
8.20	1.40	5.86	0.77	0.96
15.50	3.10	5.00	0.70	1.58
7.90	1.00	7.90	0.90	0.79
13.00	3.50	3.71	0.57	1.55
9.40	0.80	11.75	1.07	0.77
13.70	3.90	3.51	0.55	1.62
11.10	2.50	4.44	0.65	1.34
11.30	3.70	3.05	0.48	1.52
15.30	2.40	6.38	0.80	1.46
14.70	4.20	3.50	0.54	1.69
19.30	3.60	5.36	0.73	1.74
17.10	1.80	9.50	0.98	1.38
12.30	2.60	4.73	0.67	1.40
13.10	0.60	21.83	1.34	0.79
8.90	2.10	4.24	0.63	1.17
15.20	1.80	8.44	0.93	1.33
10.60	2.40	4.42	0.65	1.30
14.70	1.70	8.65	0.94	1.29
11.20	3.20	3.50	0.54	1.45
12.60	0.50	25.20	1.40	0.69
12.30	1.60	7.69	0.89	1.19
10.50	2.50	4.20	0.62	1.31
10.50	1.40	7.50	0.88	1.06
13.10	2.10	6.24	0.80	1.33
15.10	4.00	3.78	0.58	1.68
13.50	3.60	3.75	0.57	1.58
8.40	2.20	3.82	0.58	1.16
10.60	2.90	3.66	0.56	1.38
17.40	2.10	8.29	0.92	1.46

sum	150.42	275.98
sum/N	0.74	1.37
average	5.55	23.24
wlog	1.03	1.93
N	202.00	202.00
S.D.	0.20	0.31
max	1.40	2.25
min	0.38	0.33

12.70	1.30	9.77	0.99	1.11
10.90	2.20	4.95	0.70	1.27
12.70	2.40	5.29	0.72	1.38
11.30	2.90	3.90	0.59	1.41
15.90	3.30	4.82	0.68	1.62

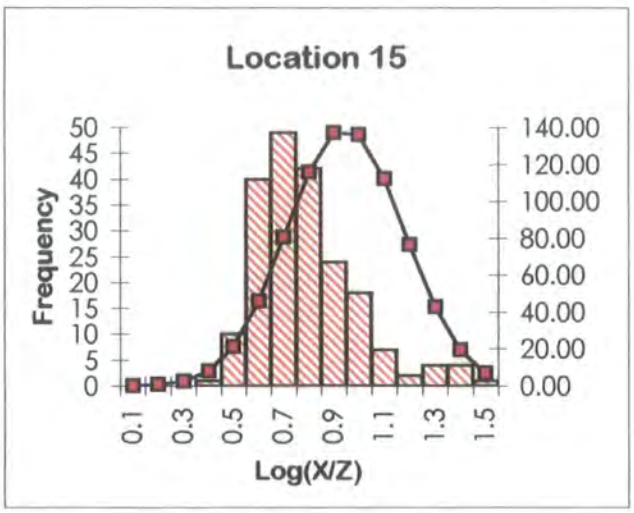

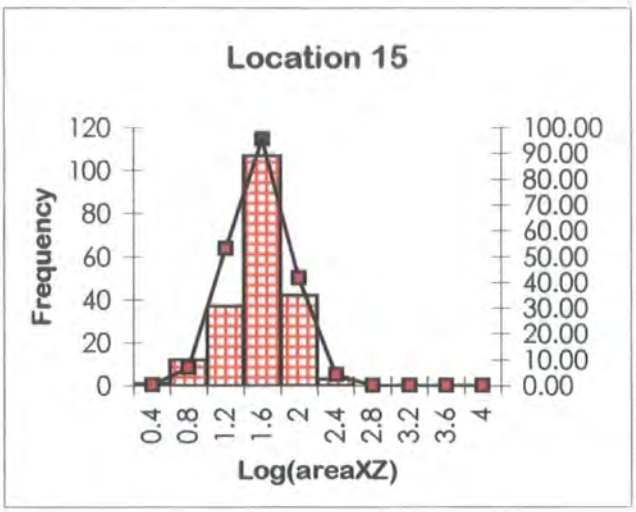

Rannoch Moor Complex: Allt nan Giubhas
Intrusive Phase: The Ciaran / Chomraidh marginal facies (G4)

Location [264 521]

X	Z	X/Z	log(x/z)	log (X×Zπ/4)
11.90	2.90	4.10	0.61	1.43
8.90	1.10	8.09	0.91	0.89
8.10	2.20	3.68	0.57	1.15
7.80	1.90	4.11	0.61	1.07
15.30	5.20	2.94	0.47	1.80
16.60	5.90	2.81	0.45	1.89
10.40	4.70	2.21	0.34	1.58
17.10	6.40	2.67	0.43	1.93
9.30	1.50	6.20	0.79	1.04
10.60	1.80	5.89	0.77	1.18
15.00	4.10	3.66	0.56	1.68
12.90	4.30	3.00	0.48	1.64
11.30	3.10	3.65	0.56	1.44
14.40	4.10	3.51	0.55	1.67
11.40	2.40	4.75	0.68	1.33
11.90	3.50	3.40	0.53	1.51
8.60	0.80	10.75	1.03	0.73
10.80	2.60	4.15	0.62	1.34
13.00	4.80	2.71	0.43	1.69
17.70	6.80	2.60	0.42	1.98
9.60	4.10	2.34	0.37	1.49
10.90	1.90	5.74	0.76	1.21
9.10	3.60	2.53	0.40	1.41
18.30	6.90	2.65	0.42	2.00
17.30	6.60	2.62	0.42	1.95
12.60	3.80	3.32	0.52	1.58
10.60	4.10	2.59	0.41	1.53

X	Z	X/Z	log(x/z)	log (X×Zπ/4)
11.30	1.90	5.95	0.77	1.23
11.10	2.90	3.83	0.58	1.40
15.10	4.80	3.15	0.50	1.76
11.30	3.40	3.32	0.52	1.48
8.30	2.40	3.46	0.54	1.19
10.20	2.20	4.64	0.67	1.25
12.20	3.60	3.39	0.53	1.54
9.10	1.30	7.00	0.85	0.97
12.70	4.10	3.10	0.49	1.61
14.90	4.60	3.24	0.51	1.73
16.00	5.50	2.91	0.46	1.84
10.60	5.10	2.08	0.32	1.63
9.50	1.90	5.00	0.70	1.15
10.40	1.40	7.43	0.87	1.06
16.90	6.20	2.73	0.44	1.92
8.40	2.70	3.11	0.49	1.25
10.10	4.60	2.20	0.34	1.56
9.00	2.70	3.33	0.52	1.28

sum	25.22	91.19
sum/N	0.56	2.03
average	3.63	106.27
wlog	0.71	1.68
N	45.00	45.00
S.D.	0.16	0.52
max	1.03	2.00
min	0.32	0.32

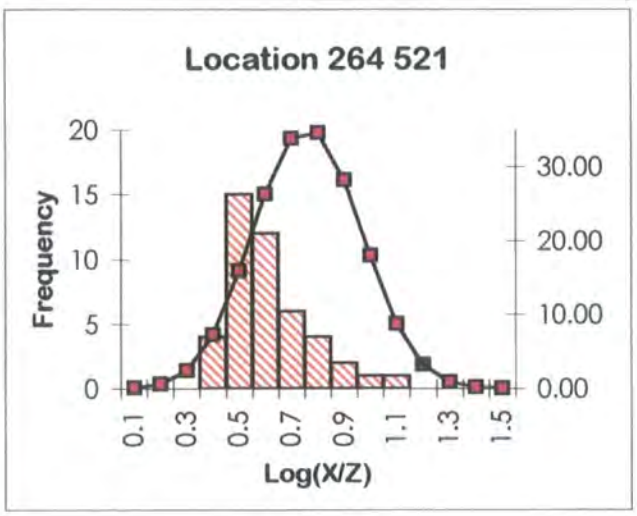

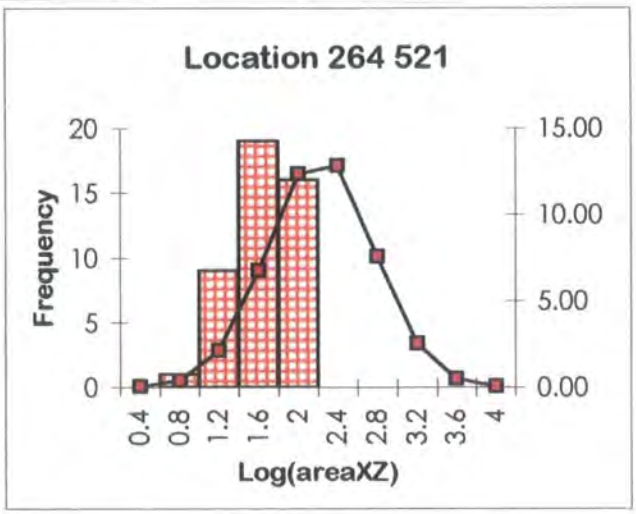

Rannoch Moor Complex: Kingshouse (River Etive)
Intrusive Phase: The Blackwater facies (G2)

Location [262 547]

X	Z	X/Z	log(x/z)	log (X×Zπ/4)
17.00	3.50	4.86	0.69	1.67
14.00	1.50	9.33	0.97	1.22
15.20	3.40	4.47	0.65	1.61
13.00	1.60	8.13	0.91	1.21
18.80	1.80	10.44	1.02	1.42
21.20	2.00	10.60	1.03	1.52
7.30	0.50	14.60	1.16	0.46
11.20	1.40	8.00	0.90	1.09
16.50	1.40	11.79	1.07	1.26
7.20	1.70	4.24	0.63	0.98
10.00	3.30	3.03	0.48	1.41
18.10	2.20	8.23	0.92	1.50
9.30	1.90	4.89	0.69	1.14
20.80	3.20	6.50	0.81	1.72
14.80	3.20	4.63	0.67	1.57
19.90	2.70	7.37	0.87	1.63
11.50	0.80	14.38	1.16	0.86
10.00	1.70	5.88	0.77	1.13
11.40	1.50	7.60	0.88	1.13
12.10	2.50	4.84	0.68	1.38
17.50	2.40	7.29	0.86	1.52
9.30	2.60	3.58	0.55	1.28
12.00	6.30	1.90	0.28	1.77
6.90	1.40	4.93	0.69	0.88
11.40	1.80	6.33	0.80	1.21
7.60	1.90	4.00	0.60	1.05
10.60	3.90	2.72	0.43	1.51
18.80	3.70	5.08	0.71	1.74
27.10	4.50	6.02	0.78	1.98
11.20	1.70	6.59	0.82	1.17
13.10	1.00	13.10	1.12	1.01
14.80	1.60	9.25	0.97	1.27
15.00	1.90	7.89	0.90	1.35
17.50	2.90	6.03	0.78	1.60
16.80	1.70	9.88	0.99	1.35
8.30	1.80	4.61	0.66	1.07
7.50	0.50	15.00	1.18	0.47
18.30	1.70	10.76	1.03	1.39
13.30	1.90	7.00	0.85	1.30
16.80	3.70	4.54	0.66	1.69
15.30	2.70	5.67	0.75	1.51
14.80	1.10	13.45	1.13	1.11
16.70	3.20	5.22	0.72	1.62
17.40	4.20	4.14	0.62	1.76
15.20	2.30	6.61	0.82	1.44
19.40	4.40	4.41	0.64	1.83
19.10	4.10	4.66	0.67	1.79
15.70	1.90	8.26	0.92	1.37

X	Z	X/Z	log(x/z)	log (X×Zπ/4)
18.40	3.50	5.26	0.72	1.70
13.10	3.50	3.74	0.57	1.56
9.70	2.10	4.62	0.66	1.20
23.30	3.90	5.97	0.78	1.85
20.90	1.70	12.29	1.09	1.45
17.40	2.40	7.25	0.86	1.52
12.80	0.70	18.29	1.26	0.85
18.90	2.30	8.22	0.91	1.53
22.00	4.20	5.24	0.72	1.86
5.50	0.80	6.88	0.84	0.54
16.20	2.80	5.79	0.76	1.55
15.50	2.50	6.20	0.79	1.48
4.10	2.50	1.64	0.21	0.91
22.30	3.00	7.43	0.87	1.72
9.30	3.50	2.66	0.42	1.41
16.40	2.50	6.56	0.82	1.51
15.30	1.80	8.50	0.93	1.34
12.50	0.40	31.25	1.49	0.59
17.20	2.00	8.60	0.93	1.43
23.00	3.60	6.39	0.81	1.81
12.90	3.10	4.16	0.62	1.50
21.60	2.20	9.82	0.99	1.57
15.30	3.70	4.14	0.62	1.65
21.30	3.80	5.61	0.75	1.80
19.90	4.50	4.42	0.65	1.85
7.60	0.80	9.50	0.98	0.68
16.00	2.50	6.40	0.81	1.50
13.10	2.60	5.04	0.70	1.43
18.40	3.40	5.41	0.73	1.69
21.70	3.50	6.20	0.79	1.78
9.80	0.60	16.33	1.21	0.66
8.70	2.90	3.00	0.48	1.30
15.20	0.80	19.00	1.28	0.98
17.10	3.90	4.38	0.64	1.72
15.10	1.40	10.79	1.03	1.22
12.70	1.30	9.77	0.99	1.11
21.00	1.60	13.13	1.12	1.42
7.00	0.20	35.00	1.54	0.04
10.80	1.00	10.80	1.03	0.93
16.30	1.00	16.30	1.21	1.11
10.50	1.50	7.00	0.85	1.09
8.50	1.30	6.54	0.82	0.94

17.40	3.70	4.70	0.67	1.70
23.60	4.20	5.62	0.75	1.89
9.80	2.60	3.77	0.58	1.30
13.40	3.80	3.53	0.55	1.60
8.10	3.00	2.70	0.43	1.28
44.10	7.30	6.04	0.78	2.40
9.20	2.50	3.68	0.57	1.26
10.40	3.50	2.97	0.47	1.46

sum	79.98	133.60
sum/N	0.82	1.36
average	6.55	23.08
wlog	1.33	2.36
N	98.00	98.00
S.D.	0.23	0.38
max	1.54	2.40
min	0.21	0.04

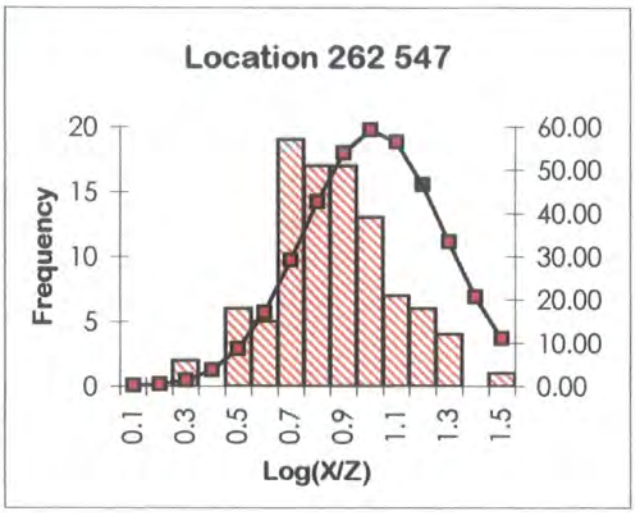

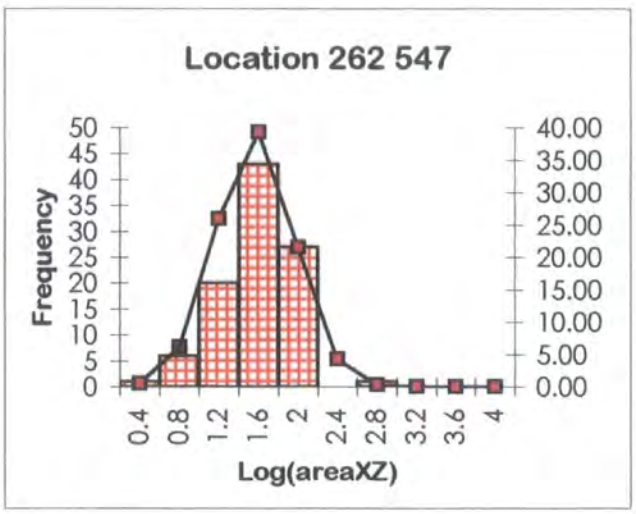

Rannoch Moor Complex: Kingshouse (River Etive)
Intrusive Phase: The Blackwater facies (G2)

Location [275 523]

X	Z	X/Z	log(X/Z)	log(X×Zπ/4)
17.00	2.20	7.73	0.89	1.47
15.60	3.40	4.59	0.66	1.62
14.40	1.50	9.60	0.98	1.23
17.70	3.90	4.54	0.66	1.73
15.00	2.00	7.50	0.88	1.37
16.10	1.50	10.73	1.03	1.28
25.20	2.10	12.00	1.08	1.62
15.30	3.10	4.94	0.69	1.57
27.40	4.30	6.37	0.80	1.97
18.00	4.00	4.50	0.65	1.75
6.20	0.90	6.89	0.84	0.64
15.70	1.10	14.27	1.15	1.13
26.90	3.80	7.08	0.85	1.90
16.40	1.80	9.11	0.96	1.37
17.40	3.50	4.97	0.70	1.68
14.00	2.00	7.00	0.85	1.34
26.40	3.30	8.00	0.90	1.84
12.90	1.10	11.73	1.07	1.05
27.60	4.50	6.13	0.79	1.99
12.70	0.90	14.11	1.15	0.95
12.40	0.60	20.67	1.32	0.77
8.60	3.60	2.39	0.38	1.39
15.60	2.40	6.50	0.81	1.47
24.90	1.80	13.83	1.14	1.55
14.90	2.70	5.52	0.74	1.50
13.10	1.30	10.08	1.00	1.13
15.30	2.10	7.29	0.86	1.40

X	Z	X/Z	log(X/Z)	log(X×Zπ/4)
22.80	4.90	4.65	0.67	1.94
17.60	2.60	6.77	0.83	1.56
14.60	2.40	6.08	0.78	1.44
18.40	4.60	4.00	0.60	1.82
25.40	2.30	11.04	1.04	1.66
18.10	3.10	5.84	0.77	1.64
17.10	3.00	5.70	0.76	1.61
18.30	3.30	5.55	0.74	1.68
18.10	4.30	4.21	0.62	1.79
13.40	1.60	8.38	0.92	1.23
25.60	2.70	9.48	0.98	1.73
17.90	2.60	6.88	0.84	1.56
27.20	4.10	6.63	0.82	1.94
14.90	1.70	8.76	0.94	1.30
15.90	1.30	12.23	1.09	1.21
15.10	2.90	5.21	0.72	1.54
26.00	2.70	9.63	0.98	1.74
15.40	0.80	19.25	1.28	0.99

sum	39.31	67.16
sum/N	0.87	1.49
average	7.47	31.07
wlog	0.94	1.39
N	45	45
S.D.	0.19	0.32
max	1.32	1.99
min	0.38	0.64

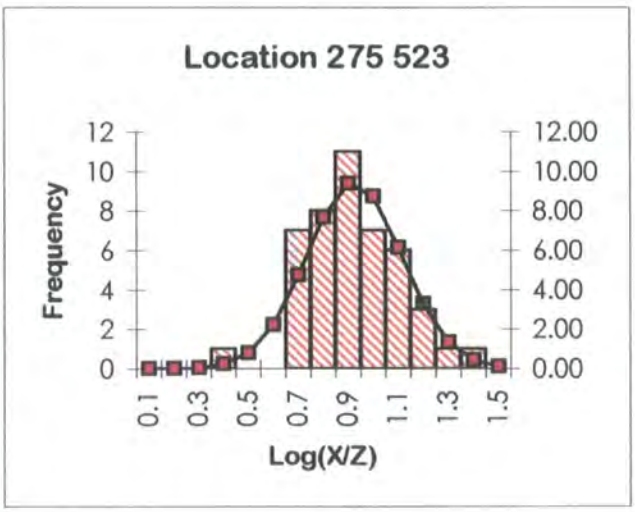

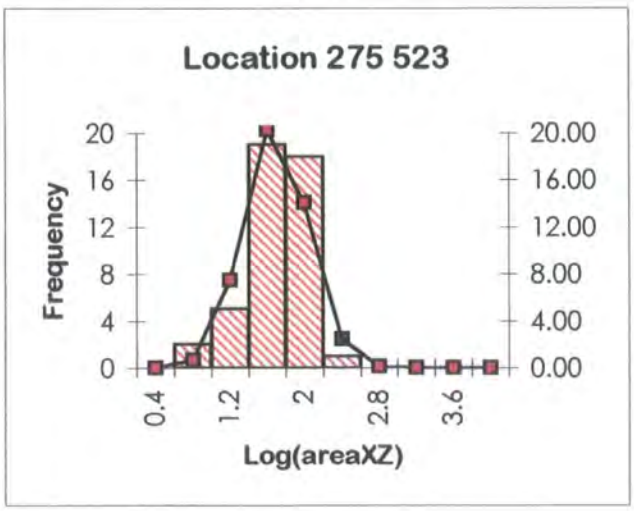

Rannoch Moor Complex: Kingshouse (River Etive)
Intrusive Phase: The Blackwater facies (G2)

Location [264 549]

X	Z	X/Z	log(x/z)	log (X×Zπ/4)
22.10	3.50	6.31	0.80	1.78
6.50	3.30	1.97	0.29	1.23
12.10	0.60	20.17	1.30	0.76
26.90	3.70	7.27	0.86	1.89
8.40	2.30	3.65	0.56	1.18
5.90	4.80	1.23	0.09	1.35
22.50	5.00	4.50	0.65	1.95
11.50	1.20	9.58	0.98	1.03
14.20	4.00	3.55	0.55	1.65
43.70	8.80	4.97	0.70	2.48
23.00	3.90	5.90	0.77	1.85
30.00	3.50	8.57	0.93	1.92
12.50	1.30	9.62	0.98	1.11
4.80	3.90	1.23	0.09	1.17
6.60	0.60	11.00	1.04	0.49
11.70	0.50	23.40	1.37	0.66
10.10	0.60	16.83	1.23	0.68
21.70	3.80	5.71	0.76	1.81
23.90	5.00	4.78	0.68	1.97
10.30	2.20	4.68	0.67	1.25
15.90	1.90	8.37	0.92	1.38
13.70	3.50	3.91	0.59	1.58
43.30	8.20	5.28	0.72	2.45
10.30	2.40	4.29	0.63	1.29
22.00	4.50	4.89	0.69	1.89
10.50	2.70	3.89	0.59	1.35
23.00	5.50	4.18	0.62	2.00
11.30	3.90	2.90	0.46	1.54
12.10	0.70	17.29	1.24	0.82
12.90	4.70	2.74	0.44	1.68
14.00	21.70	0.65	-0.19	2.38
20.60	3.10	6.65	0.82	1.70
16.70	2.30	7.26	0.86	1.48
15.80	1.90	8.32	0.92	1.37
10.80	1.70	6.35	0.80	1.16
10.80	3.40	3.18	0.50	1.46
9.90	1.80	5.50	0.74	1.15
15.20	2.30	6.61	0.82	1.44
20.20	2.50	8.08	0.91	1.60
13.00	3.20	4.06	0.61	1.51
13.50	3.00	4.50	0.65	1.50
10.70	1.90	5.63	0.75	1.20
9.30	1.20	7.75	0.89	0.94
25.90	2.70	9.59	0.98	1.74
13.40	2.80	4.79	0.68	1.47
12.90	3.70	3.49	0.54	1.57
12.00	2.50	4.80	0.68	1.37
15.40	1.40	11.00	1.04	1.23

X	Z	X/Z	log(x/z)	log (X×Zπ/4)
12.60	2.10	6.00	0.78	1.32
4.50	3.20	1.41	0.15	1.05
18.00	4.10	4.39	0.64	1.76
9.30	1.40	6.64	0.82	1.01
22.00	3.20	6.88	0.84	1.74
25.40	4.80	5.29	0.72	1.98
10.50	1.70	6.18	0.79	1.15
17.50	3.50	5.00	0.70	1.68
18.10	2.50	7.24	0.86	1.55
10.80	2.90	3.72	0.57	1.39
11.00	3.60	3.06	0.49	1.49
10.70	1.00	10.70	1.03	0.92
15.10	2.60	5.81	0.76	1.49
26.40	3.20	8.25	0.92	1.82
11.50	4.70	2.45	0.39	1.63
14.20	2.80	5.07	0.71	1.49
12.10	3.50	3.46	0.54	1.52
14.50	2.50	5.80	0.76	1.45
24.40	5.50	4.44	0.65	2.02
22.10	7.60	2.91	0.46	2.12
17.00	3.40	5.00	0.70	1.66
15.70	2.10	7.48	0.87	1.41
11.50	2.20	5.23	0.72	1.30
16.40	2.40	6.83	0.83	1.49
12.50	2.20	5.68	0.75	1.33
25.50	2.30	11.09	1.04	1.66
9.50	1.00	9.50	0.98	0.87
13.10	1.60	8.19	0.91	1.22
12.60	1.10	11.45	1.06	1.04
12.30	2.70	4.56	0.66	1.42
14.90	0.90	16.56	1.22	1.02
7.20	1.30	5.54	0.74	0.87
5.80	3.00	1.93	0.29	1.14
13.10	3.10	4.23	0.63	1.50
42.80	7.70	5.56	0.74	2.41
14.70	2.50	5.88	0.77	1.46
23.50	4.40	5.34	0.73	1.91
8.20	1.00	8.20	0.91	0.81
14.60	1.10	13.27	1.12	1.10
16.20	1.80	9.00	0.95	1.36
11.10	0.60	18.50	1.27	0.72
14.00	4.20	3.33	0.52	1.66
13.30	5.30	2.51	0.40	1.74
7.90	1.80	4.39	0.64	1.05
13.60	3.60	3.78	0.58	1.58
42.20	9.30	4.54	0.66	2.49
28.30	4.50	6.29	0.80	2.00
11.50	2.20	5.23	0.72	1.30

9.70	1.80	5.39	0.73	1.14
7.10	1.50	4.73	0.68	0.92
9.50	2.10	4.52	0.66	1.20
9.10	2.60	3.50	0.54	1.27
8.70	0.80	10.88	1.04	0.74
8.50	2.70	3.15	0.50	1.26
7.50	0.70	10.71	1.03	0.62
10.70	2.90	3.69	0.57	1.39
11.50	2.00	5.75	0.76	1.26
5.40	4.30	1.26	0.10	1.26
18.70	4.50	4.16	0.62	1.82
4.80	4.40	1.09	0.04	1.22
45.00	9.40	4.79	0.68	2.52
6.10	0.50	12.20	1.09	0.38
11.20	2.00	5.60	0.75	1.25
13.00	1.80	7.22	0.86	1.26

19.20	4.50	4.27	0.63	1.83
7.10	3.70	1.92	0.28	1.31
20.50	3.50	5.86	0.77	1.75
9.50	0.70	13.57	1.13	0.72
5.50	2.30	2.39	0.38	1.00
8.50	1.70	5.00	0.70	1.05

sum	85.55	167.73
sum/N	0.73	1.42
average	5.31	26.39
wlog	1.56	2.14
N	118.00	118.00
S.D.	0.27	0.43
max	1.37	2.52
min	-0.19	0.38

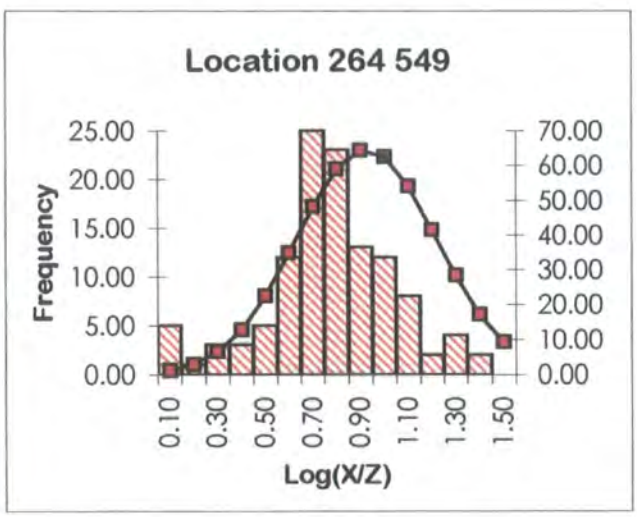

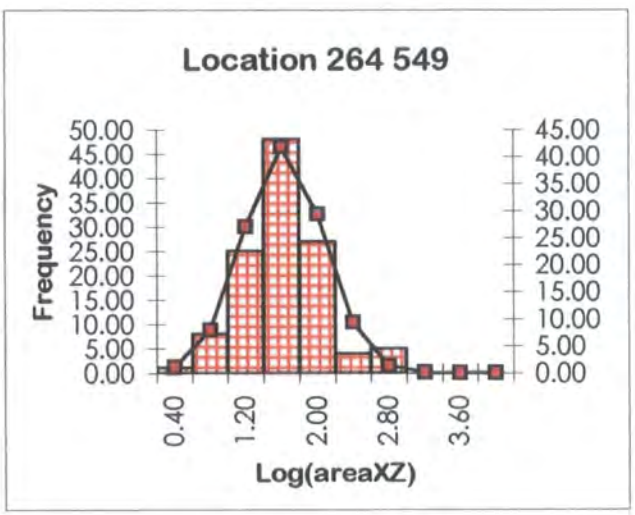

Rannoch Moor Complex: Kingshouse (River Etive)
Intrusive Phase: The Blackwater facies (G2)

Location [266 550]

X	Z	X/Z	log(x/z)	log (X×Zπ/4)
63.20	7.40	8.54	0.93	2.57
26.40	5.30	4.98	0.70	2.04
12.30	2.70	4.56	0.66	1.42
10.60	1.50	7.07	0.85	1.10
6.90	1.20	5.75	0.76	0.81
29.20	5.50	5.31	0.73	2.10
7.10	1.60	4.44	0.65	0.95
13.30	0.90	14.78	1.17	0.97
5.10	1.30	3.92	0.59	0.72
9.90	1.40	7.07	0.85	1.04
9.80	3.90	2.51	0.40	1.48
17.50	2.30	7.61	0.88	1.50
13.30	3.70	3.59	0.56	1.59
12.40	1.30	9.54	0.98	1.10
34.30	12.70	2.70	0.43	2.53
16.00	2.80	5.71	0.76	1.55
7.50	1.80	4.17	0.62	1.03
9.20	1.70	5.41	0.73	1.09
6.70	0.80	8.38	0.92	0.62
9.20	3.30	2.79	0.45	1.38
17.80	2.60	6.85	0.84	1.56
21.50	3.10	6.94	0.84	1.72
11.30	2.00	5.65	0.75	1.25
8.20	0.70	11.71	1.07	0.65
10.00	0.80	12.50	1.10	0.80
10.50	6.20	1.69	0.23	1.71
11.60	1.90	6.11	0.79	1.24
17.20	1.90	9.05	0.96	1.41
10.10	1.60	6.31	0.80	1.10
19.20	4.80	4.00	0.60	1.86
11.20	2.50	4.48	0.65	1.34
9.00	1.20	7.50	0.88	0.93
14.10	3.50	4.03	0.61	1.59
8.70	2.60	3.35	0.52	1.25
12.30	2.40	5.13	0.71	1.37
8.00	0.30	26.67	1.43	0.28
13.20	3.20	4.13	0.62	1.52
13.90	3.00	4.63	0.67	1.52
16.90	2.50	6.76	0.83	1.52
9.50	3.60	2.64	0.42	1.43
13.60	3.60	3.78	0.58	1.58
11.70	2.40	4.88	0.69	1.34
7.80	2.50	3.12	0.49	1.19
4.70	0.70	6.71	0.83	0.41
23.80	2.40	9.92	1.00	1.65
11.20	6.10	1.84	0.26	1.73
20.50	2.70	7.59	0.88	1.64
6.80	1.10	6.18	0.79	0.77

X	Z	X/Z	log(x/z)	log (X×Zπ/4)
14.80	2.40	6.17	0.79	1.45
21.70	4.10	5.29	0.72	1.84
8.50	2.60	3.27	0.51	1.24
23.40	7.90	2.96	0.47	2.16
27.80	3.50	7.94	0.90	1.88
4.70	3.30	1.42	0.15	1.09
32.80	11.60	2.83	0.45	2.48
24.30	2.50	9.72	0.99	1.68
13.80	4.00	3.45	0.54	1.64
10.20	2.00	5.10	0.71	1.20
12.10	3.60	3.36	0.53	1.53
12.30	3.90	3.15	0.50	1.58
7.40	1.60	4.63	0.67	0.97
12.40	4.20	2.95	0.47	1.61
34.60	12.50	2.77	0.44	2.53
7.10	2.50	2.84	0.45	1.14
6.50	1.80	3.61	0.56	0.96
8.30	2.40	3.46	0.54	1.19
11.30	1.40	8.07	0.91	1.09
7.50	1.80	4.17	0.62	1.03
26.10	5.50	4.75	0.68	2.05
38.80	5.50	7.05	0.85	2.22
6.70	2.50	2.68	0.43	1.12
12.30	2.70	4.56	0.66	1.42
11.20	2.90	3.86	0.59	1.41
9.90	1.70	5.82	0.77	1.12
13.70	4.00	3.43	0.53	1.63
13.30	3.30	4.03	0.61	1.54
33.60	12.00	2.80	0.45	2.50
10.10	2.20	4.59	0.66	1.24
5.60	2.20	2.55	0.41	0.99
8.90	3.00	2.97	0.47	1.32
15.30	2.50	6.12	0.79	1.48
18.30	3.50	5.23	0.72	1.70
18.50	3.30	5.61	0.75	1.68
6.90	0.50	13.80	1.14	0.43
34.70	16.30	2.13	0.33	2.65
12.20	4.40	2.77	0.44	1.62
10.70	2.20	4.86	0.69	1.27
6.10	0.60	10.17	1.01	0.46
11.40	6.50	1.75	0.24	1.76
6.40	0.90	7.11	0.85	0.66
21.70	3.50	6.20	0.79	1.78
29.60	5.20	5.69	0.76	2.08
12.50	3.30	3.79	0.58	1.51
13.90	1.50	9.27	0.97	1.21
14.30	3.20	4.47	0.65	1.56
10.70	1.50	7.13	0.85	1.10

8.40	2.30	3.65	0.56	1.18
15.30	3.10	4.94	0.69	1.57
12.30	4.00	3.08	0.49	1.59
13.60	2.70	5.04	0.70	1.46
33.30	11.70	2.85	0.45	2.49
5.50	1.70	3.24	0.51	0.87
13.60	1.20	11.33	1.05	1.11
19.60	4.80	4.08	0.61	1.87
16.00	4.50	3.56	0.55	1.75
24.40	5.50	4.44	0.65	2.02
14.30	1.50	9.53	0.98	1.23
29.20	3.90	7.49	0.87	1.95
23.60	2.10	11.24	1.05	1.59
8.50	1.00	8.50	0.93	0.82
18.80	4.40	4.27	0.63	1.81
10.80	2.70	4.00	0.60	1.36
7.30	2.10	3.48	0.54	1.08
18.50	3.40	5.44	0.74	1.69
38.30	7.50	5.11	0.71	2.35
25.90	6.40	4.05	0.61	2.11
13.10	5.50	2.38	0.38	1.75
18.00	1.30	13.85	1.14	1.26
34.30	12.60	2.72	0.43	2.53
11.20	2.50	4.48	0.65	1.34
11.90	4.10	2.90	0.46	1.58

10.20	2.60	3.92	0.59	1.32
8.10	2.30	3.52	0.55	1.17
7.90	2.20	3.59	0.56	1.14
81.10	22.20	3.65	0.56	3.15
11.70	3.40	3.44	0.54	1.49
12.70	4.30	2.95	0.47	1.63
10.80	2.20	4.91	0.69	1.27
12.50	2.50	5.00	0.70	1.39
12.00	3.50	3.43	0.54	1.52
14.50	2.30	6.30	0.80	1.42
12.50	4.60	2.72	0.43	1.65
12.30	2.70	4.56	0.66	1.42
12.50	2.70	4.63	0.67	1.42
12.60	4.30	2.93	0.47	1.63
24.90	3.30	7.55	0.88	1.81
10.90	1.90	5.74	0.76	1.21

sum	92.83	293.58
sum/N	0.68	2.14
average	4.76	138.98
wlog	1.27	3.00
N	137.00	137.00
S.D.	0.21	0.54
max	1.43	3.15
min	0.15	0.15

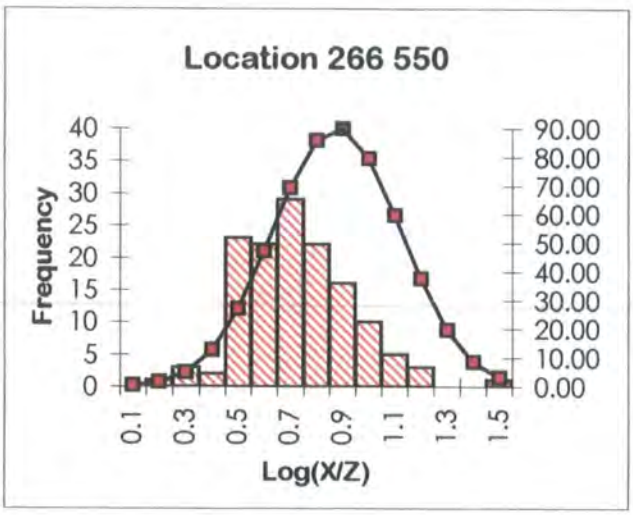

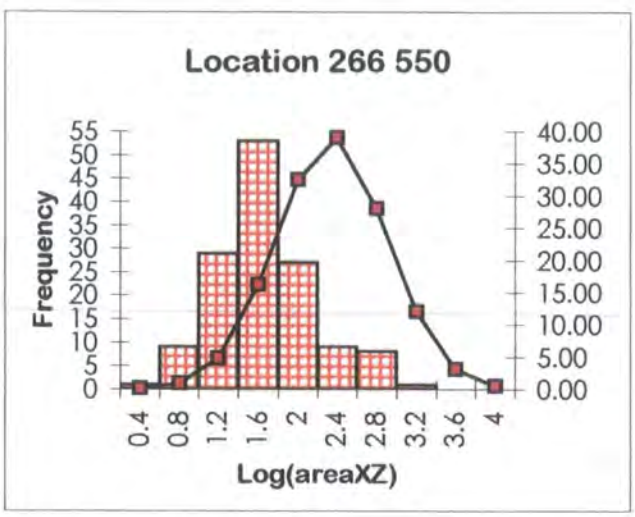

Rannoch Moor Complex: Kingshouse (River Etive)
Intrusive Phase: The Blackwater facies (G2)

Location [268 550]

X	Z	X/Z	log(x/z)	log (X×Zπ/4)
7.20	2.80	2.57	0.41	1.20
11.20	3.40	3.29	0.52	1.48
5.90	1.30	4.54	0.66	0.78
6.10	2.20	2.77	0.44	1.02
15.50	4.40	3.52	0.55	1.73
14.20	5.30	2.68	0.43	1.77
15.80	5.00	3.16	0.50	1.79
8.40	4.60	1.83	0.26	1.48
5.60	1.40	4.00	0.60	0.79
6.70	1.40	4.79	0.68	0.87
9.90	1.70	5.82	0.77	1.12
13.00	4.10	3.17	0.50	1.62
5.70	0.90	6.33	0.80	0.61
6.60	2.10	3.14	0.50	1.04
6.20	2.00	3.10	0.49	0.99
20.80	3.00	6.93	0.84	1.69
11.10	6.20	1.79	0.25	1.73
32.00	6.80	4.71	0.67	2.23
21.30	3.50	6.09	0.78	1.77
12.70	3.40	3.74	0.57	1.53
17.50	4.30	4.07	0.61	1.77
12.30	3.90	3.15	0.50	1.58
23.10	7.40	3.12	0.49	2.13
7.00	2.30	3.04	0.48	1.10
14.80	5.90	2.51	0.40	1.84
7.50	2.20	3.41	0.53	1.11
6.30	2.30	2.74	0.44	1.06
14.20	3.20	4.44	0.65	1.55
10.20	5.50	1.85	0.27	1.64
10.90	3.10	3.52	0.55	1.42
14.80	3.90	3.79	0.58	1.66
12.50	3.00	4.17	0.62	1.47
6.60	2.00	3.30	0.52	1.02
7.20	1.90	3.79	0.58	1.03
8.00	3.60	2.22	0.35	1.35
8.10	3.90	2.08	0.32	1.39
15.50	4.90	3.16	0.50	1.78
9.00	3.90	2.31	0.36	1.44
9.60	1.60	6.00	0.78	1.08
9.40	4.30	2.19	0.34	1.50
7.90	2.80	2.82	0.45	1.24
7.30	3.30	2.21	0.34	1.28
12.40	2.70	4.59	0.66	1.42
14.70	3.60	4.08	0.61	1.62
15.30	2.90	5.28	0.72	1.54
13.50	4.60	2.93	0.47	1.69
8.10	1.20	6.75	0.83	0.88
10.20	2.40	4.25	0.63	1.28

X	Z	X/Z	log(x/z)	log (X×Zπ/4)
15.20	5.90	2.58	0.41	1.85
8.00	2.10	3.81	0.58	1.12
6.80	1.80	3.78	0.58	0.98
8.50	4.10	2.07	0.32	1.44
15.80	4.50	3.51	0.55	1.75
9.40	3.90	2.41	0.38	1.46
22.00	3.80	5.79	0.76	1.82
16.40	4.90	3.35	0.52	1.80
7.20	2.40	3.00	0.48	1.13
6.20	1.20	5.17	0.71	0.77
13.20	3.50	3.77	0.58	1.56
6.50	1.70	3.82	0.58	0.94
8.90	3.40	2.62	0.42	1.38
8.40	3.80	2.21	0.34	1.40
17.10	5.20	3.29	0.52	1.84
9.20	0.40	23.00	1.36	0.46
10.70	2.90	3.69	0.57	1.39
7.70	3.30	2.33	0.37	1.30
5.70	1.70	3.35	0.53	0.88
8.70	3.60	2.42	0.38	1.39
10.80	6.10	1.77	0.25	1.71
8.60	4.00	2.15	0.33	1.43
14.90	4.30	3.47	0.54	1.70
10.60	5.70	1.86	0.27	1.68
9.50	0.50	19.00	1.28	0.57
8.30	4.30	1.93	0.29	1.45
19.90	1.50	13.27	1.12	1.37
8.30	2.80	2.96	0.47	1.26
6.20	1.40	4.43	0.65	0.83
6.90	2.30	3.00	0.48	1.10
19.50	1.30	15.00	1.18	1.30
8.90	4.20	2.12	0.33	1.47
15.20	4.60	3.30	0.52	1.74
9.60	4.70	2.04	0.31	1.55
23.10	5.20	4.44	0.65	1.97
9.70	5.00	1.94	0.29	1.58
10.70	3.20	3.34	0.52	1.43
7.20	2.50	2.88	0.46	1.15
20.30	2.50	8.12	0.91	1.60
8.30	3.40	2.44	0.39	1.35
15.30	4.00	3.83	0.58	1.68
9.50	1.10	8.64	0.94	0.91
8.70	4.00	2.18	0.34	1.44
7.40	2.80	2.64	0.42	1.21
19.30	0.90	21.44	1.33	1.13
17.40	5.30	3.28	0.52	1.86
8.00	3.40	2.35	0.37	1.33
8.40	3.30	2.55	0.41	1.34

30.50	7.30	4.18	0.62	2.24
16.00	3.80	4.21	0.62	1.68
6.20	1.80	3.44	0.54	0.94
17.50	5.80	3.02	0.48	1.90
6.90	1.60	4.31	0.63	0.94
21.00	3.20	6.56	0.82	1.72
7.20	2.60	2.77	0.44	1.17
8.10	4.10	1.98	0.30	1.42
11.50	3.70	3.11	0.49	1.52
17.90	6.00	2.98	0.47	1.93
5.50	1.60	3.44	0.54	0.84
14.70	4.10	3.59	0.55	1.68
6.70	2.30	2.91	0.46	1.08
8.20	3.90	2.10	0.32	1.40
17.70	6.10	2.90	0.46	1.93
14.00	5.10	2.75	0.44	1.75
9.40	4.70	2.00	0.30	1.54
7.60	3.40	2.24	0.35	1.31
8.30	4.20	1.98	0.30	1.44
13.60	2.60	5.23	0.72	1.44
14.20	3.60	3.94	0.60	1.60
11.80	3.80	3.11	0.49	1.55

13.80	3.00	4.60	0.66	1.51
6.10	1.60	3.81	0.58	0.88
8.70	4.50	1.93	0.29	1.49
8.20	2.90	2.83	0.45	1.27
7.90	3.30	2.39	0.38	1.31
14.50	5.60	2.59	0.41	1.80
21.60	3.80	5.68	0.75	1.81
18.90	4.90	3.86	0.59	1.86
9.00	5.20	1.73	0.24	1.57
5.50	1.20	4.58	0.66	0.71
8.20	3.10	2.65	0.42	1.30
9.80	5.50	1.78	0.25	1.63
13.60	2.20	6.18	0.79	1.37

sum	70.29	254.73
sum/N	0.54	1.94
average	3.44	88.01
wlog	1.12	2.00
N	131.00	131.00
S.D.	0.21	0.52
max	1.36	2.24
min	0.24	0.24

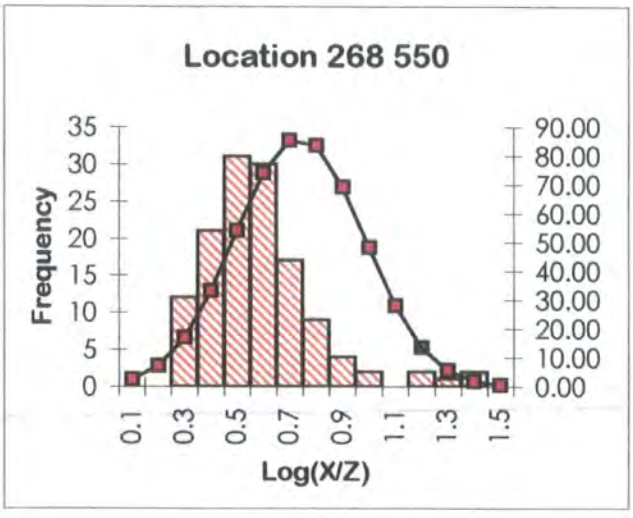

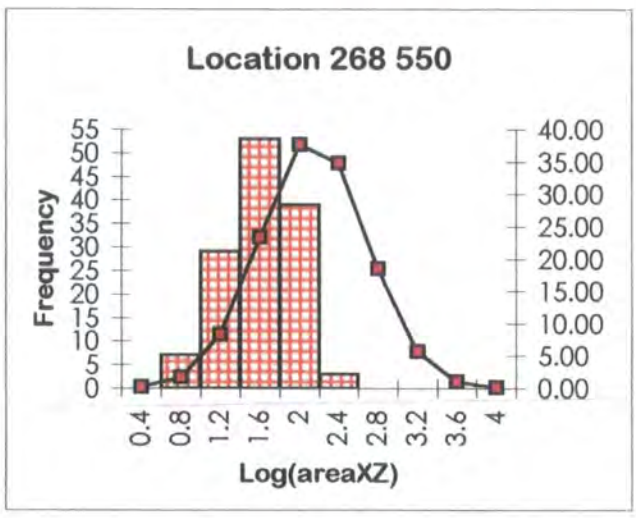

Rannoch Moor Complex: Kingshouse (River Etive)
Intrusive Phase: The Blackwater facies (G2)

Location [269 550]

X	Z	X/Z	log(x/z)	log (X×Zπ/4)
7.70	1.60	4.81	0.68	0.99
7.00	1.60	4.38	0.64	0.94
23.80	6.50	3.66	0.56	2.08
9.20	3.70	2.49	0.40	1.43
21.30	5.40	3.94	0.60	1.96
8.00	3.90	2.05	0.31	1.39
10.40	1.70	6.12	0.79	1.14
9.70	4.20	2.31	0.36	1.51
24.40	6.90	3.54	0.55	2.12
16.40	2.40	6.83	0.83	1.49
9.40	3.80	2.47	0.39	1.45
10.60	2.10	5.05	0.70	1.24
9.80	0.90	10.89	1.04	0.84
12.20	4.30	2.84	0.45	1.61
9.00	3.20	2.81	0.45	1.35
16.20	2.00	8.10	0.91	1.41
11.00	2.80	3.93	0.59	1.38
22.50	5.80	3.88	0.59	2.01
8.20	2.40	3.42	0.53	1.19
10.00	1.30	7.69	0.89	1.01
11.50	3.70	3.11	0.49	1.52
14.00	4.50	3.11	0.49	1.69
6.90	1.00	6.90	0.84	0.73
12.00	2.70	4.44	0.65	1.41
7.30	1.60	4.56	0.66	0.96
14.60	5.30	2.75	0.44	1.78
11.20	3.40	3.29	0.52	1.48
8.00	1.90	4.21	0.62	1.08
13.20	3.50	3.77	0.58	1.56
6.70	1.80	3.72	0.57	0.98
11.80	4.10	2.88	0.46	1.58
6.60	1.00	6.60	0.82	0.71
7.50	3.00	2.50	0.40	1.25
20.50	4.80	4.27	0.63	1.89
10.60	2.60	4.08	0.61	1.34
11.00	3.50	3.14	0.50	1.48
6.80	1.40	4.86	0.69	0.87
15.40	2.00	7.70	0.89	1.38
17.50	3.90	4.49	0.65	1.73
9.30	0.50	18.60	1.27	0.56
9.10	3.40	2.68	0.43	1.39
14.30	4.80	2.98	0.47	1.73
7.20	2.30	3.13	0.50	1.11
7.00	1.50	4.67	0.67	0.92
9.50	1.10	8.64	0.94	0.91
11.80	3.70	3.19	0.50	1.54
10.30	1.40	7.36	0.87	1.05
9.40	3.20	2.94	0.47	1.37

X	Z	X/Z	log(x/z)	log (X×Zπ/4)
7.90	3.20	2.47	0.39	1.30
23.50	5.80	4.05	0.61	2.03
21.60	5.70	3.79	0.58	1.99
8.80	2.80	3.14	0.50	1.29
6.40	1.50	4.27	0.63	0.88
17.80	4.40	4.05	0.61	1.79
12.80	3.30	3.88	0.59	1.52
8.40	4.10	2.05	0.31	1.43
7.60	2.00	3.80	0.58	1.08
15.30	1.50	10.20	1.01	1.26
7.10	1.90	3.74	0.57	1.03
25.20	8.60	2.93	0.47	2.23
24.20	5.30	4.57	0.66	2.00
10.30	1.90	5.42	0.73	1.19
16.60	3.20	5.19	0.71	1.62
13.00	4.50	2.89	0.46	1.66
27.10	5.80	4.67	0.67	2.09
11.40	2.30	4.96	0.70	1.31
6.20	1.30	4.77	0.68	0.80
17.60	4.20	4.19	0.62	1.76
14.80	5.70	2.60	0.41	1.82
8.80	0.40	22.00	1.34	0.44
5.70	0.80	7.13	0.85	0.55
8.10	3.40	2.38	0.38	1.34
15.70	2.10	7.48	0.87	1.41
11.20	3.00	3.73	0.57	1.42
14.20	5.30	2.68	0.43	1.77
8.20	2.70	3.04	0.48	1.24
21.00	4.90	4.29	0.63	1.91
9.70	3.30	2.94	0.47	1.40
18.10	4.70	3.85	0.59	1.82
23.40	6.50	3.60	0.56	2.08
9.40	3.90	2.41	0.38	1.46
21.20	5.10	4.16	0.62	1.93
9.30	0.90	10.33	1.01	0.82
17.10	3.70	4.62	0.66	1.70
8.70	3.20	2.72	0.43	1.34
12.50	3.20	3.91	0.59	1.50

sum	56.60	127.51
sum/N	0.62	1.40
average	4.19	25.19
wlog	1.03	1.79
N	91.00	91.00
S.D.	0.19	0.41
max	1.34	2.23
min	0.31	0.44

12.40	2.90	4.28	0.63	1.45
11.30	3.80	2.97	0.47	1.53
24.10	6.60	3.65	0.56	2.10
9.80	1.40	7.00	0.85	1.03
6.20	0.90	6.89	0.84	0.64

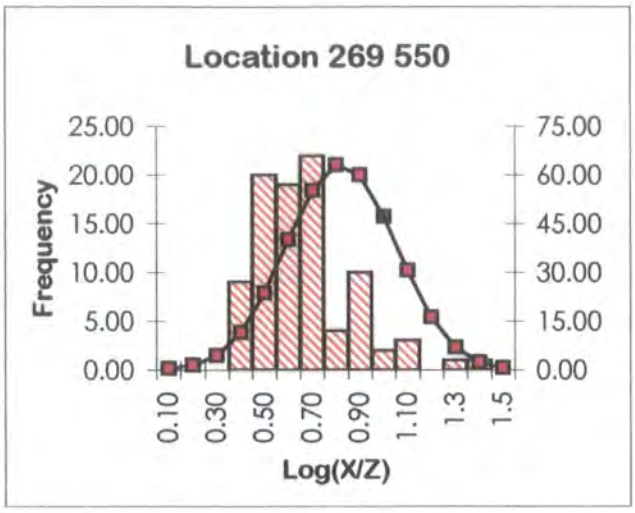

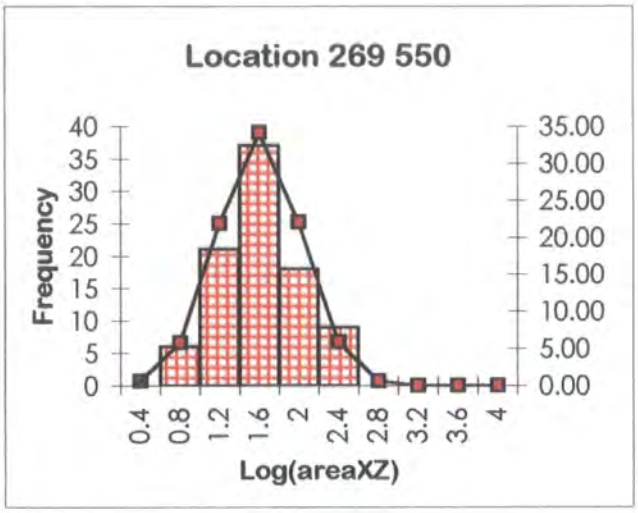

Rannoch Moor Complex: Kingshouse (River Etive)
Intrusive Phase: The Blackwater facies (G2)

Location [277 551]

X	Z	X/Z	log(x/z)	log (X×Zπ/4)
6.90	2.10	3.29	0.52	1.06
10.60	3.40	3.12	0.49	1.45
7.70	3.00	2.57	0.41	1.26
11.60	4.70	2.47	0.39	1.63
8.60	3.50	2.46	0.39	1.37
10.30	2.80	3.68	0.57	1.36
9.40	3.70	2.54	0.40	1.44
5.70	2.00	2.85	0.45	0.95
8.00	2.50	3.20	0.51	1.20
9.90	4.20	2.36	0.37	1.51
22.70	1.70	13.35	1.13	1.48
9.60	2.10	4.57	0.66	1.20
9.70	3.50	2.77	0.44	1.43
6.20	1.30	4.77	0.68	0.80
4.10	2.40	1.71	0.23	0.89
10.10	2.70	3.74	0.57	1.33
6.00	2.20	2.73	0.44	1.02
7.00	2.50	2.80	0.45	1.14
7.80	3.50	2.23	0.35	1.33
23.00	2.00	11.50	1.06	1.56
9.20	3.50	2.63	0.42	1.40
5.70	2.00	2.85	0.45	0.95
5.30	1.60	3.31	0.52	0.82
7.70	2.40	3.21	0.51	1.16
25.10	7.50	3.35	0.52	2.17
5.70	0.40	14.25	1.15	0.25
11.30	5.80	1.95	0.29	1.71
9.60	2.40	4.00	0.60	1.26
11.30	3.60	3.14	0.50	1.50
8.50	3.50	2.43	0.39	1.37
10.40	4.70	2.21	0.34	1.58
6.50	1.80	3.61	0.56	0.96
7.30	4.00	1.83	0.26	1.36
7.30	1.20	6.08	0.78	0.84
11.40	6.30	1.81	0.26	1.75
11.00	4.70	2.34	0.37	1.61
23.50	2.90	8.10	0.91	1.73
10.60	3.10	3.42	0.53	1.41
23.20	2.20	10.55	1.02	1.60
26.30	6.70	3.93	0.59	2.14
10.10	2.60	3.88	0.59	1.31
10.90	3.60	3.03	0.48	1.49
5.90	0.90	6.56	0.82	0.62
9.70	3.60	2.69	0.43	1.44
8.50	1.00	8.50	0.93	0.82
23.20	7.70	3.27	0.51	2.18
9.60	3.90	2.46	0.39	1.47
9.00	3.20	2.81	0.45	1.35

X	Z	X/Z	log(x/z)	log (X×Zπ/4)
10.40	3.20	3.25	0.51	1.42
7.90	4.40	1.80	0.25	1.44
18.00	5.10	2.39	0.38	1.69
9.00	1.40	6.43	0.81	1.00
9.70	4.40	2.20	0.34	1.53
7.00	2.20	3.18	0.50	1.08
24.20	6.40	3.78	0.58	2.09
6.50	3.20	2.03	0.31	1.21
7.30	2.60	2.81	0.45	1.17
24.80	7.80	3.18	0.50	2.18
8.80	2.80	3.14	0.50	1.29
9.90	2.40	4.13	0.62	1.27
8.90	3.20	2.78	0.44	1.35
3.40	1.60	2.13	0.33	0.63
5.40	1.10	4.91	0.69	0.67
24.30	7.70	3.16	0.50	2.17
9.30	3.40	2.74	0.44	1.40
21.50	8.10	3.15	0.50	2.21
8.30	0.50	16.60	1.22	0.51
7.90	2.10	3.76	0.58	1.11
7.00	3.70	1.89	0.28	1.31
7.20	2.60	2.77	0.44	1.17
11.30	3.90	2.90	0.46	1.54
9.30	1.70	5.47	0.74	1.09
15.40	4.30	2.42	0.38	1.55
8.10	3.30	2.45	0.39	1.32
11.50	6.70	1.72	0.23	1.78
4.80	0.50	9.60	0.98	0.28
9.50	3.40	2.79	0.45	1.40
9.10	3.40	2.68	0.43	1.39
7.50	4.20	1.79	0.25	1.39
23.40	2.40	9.75	0.99	1.64
8.30	2.50	3.32	0.52	1.21
6.90	2.40	2.88	0.46	1.11
11.10	5.70	1.95	0.29	1.70
5.60	0.80	7.00	0.85	0.55
7.50	2.80	2.68	0.43	1.22
9.70	4.10	2.37	0.37	1.49
7.40	2.40	3.08	0.49	1.14
8.70	1.30	6.69	0.83	0.95
5.70	1.50	3.80	0.58	0.83
11.90	5.00	2.38	0.38	1.67
8.50	2.90	2.93	0.47	1.29
5.60	1.70	3.29	0.52	0.87

6.90	2.40	2.88	0.46	1.11
6.40	1.10	5.82	0.76	0.74
11.10	5.00	2.22	0.35	1.64
8.00	4.70	1.70	0.23	1.47
8.70	2.90	3.00	0.48	1.30
5.80	2.30	2.52	0.40	1.02
6.90	1.70	4.06	0.61	0.96
12.40	5.40	2.30	0.36	1.72

sum	52.38	130.95
sum/N	0.52	1.31
average	3.34	20.39
wlog	0.99	1.98
N	100.00	100.00
S.D.	0.21	0.40
max	1.22	2.21
min	0.23	0.25

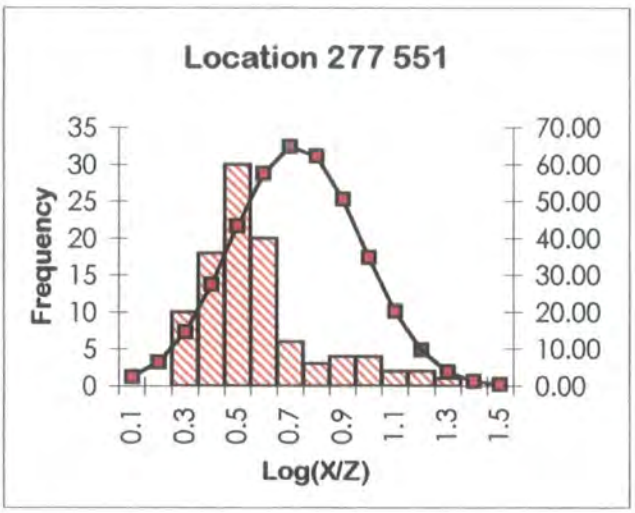

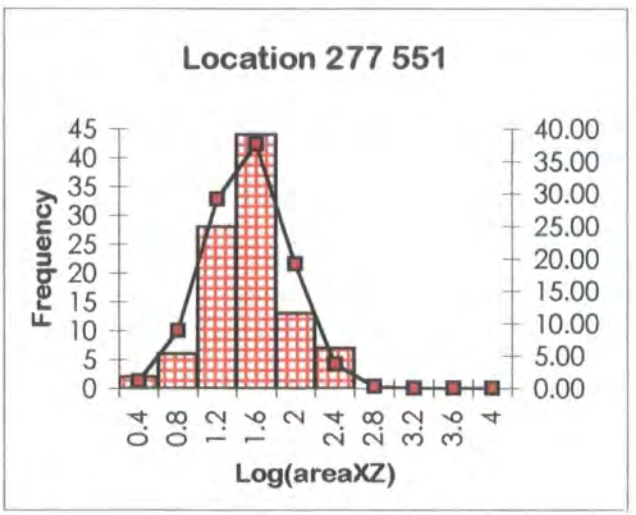

Rannoch Moor Complex: Kingshouse (River Etive)
Intrusive Phase: The Blackwater facies (G2)

Location [282 557] A

X	Z	X/Z	log(x/z)	log (X×Zπ/4)
10.10	3.70	2.73	0.44	1.47
6.70	1.60	4.19	0.62	0.93
11.60	5.20	2.23	0.35	1.68
14.00	2.70	5.19	0.71	1.47
8.60	2.20	3.91	0.59	1.17
14.90	4.20	3.55	0.55	1.69
6.70	1.90	3.53	0.55	1.00
14.80	3.40	4.35	0.64	1.60
13.50	2.20	6.14	0.79	1.37
9.70	2.70	3.59	0.56	1.31
12.60	3.50	3.60	0.56	1.54
11.40	5.00	2.28	0.36	1.65
11.50	3.40	3.38	0.53	1.49
6.20	1.50	4.13	0.62	0.86
15.50	4.80	3.23	0.51	1.77
17.30	3.90	4.44	0.65	1.72
8.30	3.10	2.68	0.43	1.31
17.90	4.70	3.81	0.58	1.82
13.80	2.50	5.52	0.74	1.43
15.30	5.40	2.83	0.45	1.81
14.70	3.10	4.74	0.68	1.55
15.70	5.00	3.14	0.50	1.79
5.90	0.70	8.43	0.93	0.51
12.60	3.20	3.94	0.60	1.50
17.60	5.30	3.32	0.52	1.86
8.90	3.30	2.70	0.43	1.36
13.00	1.80	7.22	0.86	1.26
13.90	3.90	3.56	0.55	1.63
9.90	2.90	3.41	0.53	1.35
10.60	4.20	2.52	0.40	1.54
15.60	6.10	2.56	0.41	1.87
14.50	3.30	4.39	0.64	1.57
7.90	3.10	2.55	0.41	1.28

X	Z	X/Z	log(x/z)	log (X×Zπ/4)
14.10	2.90	4.86	0.69	1.51
15.00	3.70	4.05	0.61	1.64
16.90	3.90	4.33	0.64	1.71
8.60	3.80	2.26	0.35	1.41
5.90	1.20	4.92	0.69	0.75
13.30	1.90	7.00	0.85	1.30
10.70	4.40	2.43	0.39	1.57
9.10	2.00	4.55	0.66	1.16
15.80	5.50	2.87	0.46	1.83
13.20	4.10	3.22	0.51	1.63
15.10	4.90	3.08	0.49	1.76
14.70	3.60	4.08	0.61	1.62
17.30	4.60	3.76	0.58	1.80
15.40	4.40	3.50	0.54	1.73
13.10	3.60	3.64	0.56	1.57
11.10	4.70	2.36	0.37	1.61
9.40	2.50	3.76	0.58	1.27
7.30	2.60	2.81	0.45	1.17
17.20	3.70	4.65	0.67	1.70
14.10	3.10	4.55	0.66	1.54
14.90	4.20	3.55	0.55	1.69
16.10	3.80	4.24	0.63	1.68
14.20	4.50	3.16	0.50	1.70

sum	18.66	48.19
sum/N	0.33	0.86
average	2.15	7.25
wlog	0.58	1.53
N	56.00	56.00
S.D.	0.14	0.31
max	0.93	1.87
min	0.35	0.51

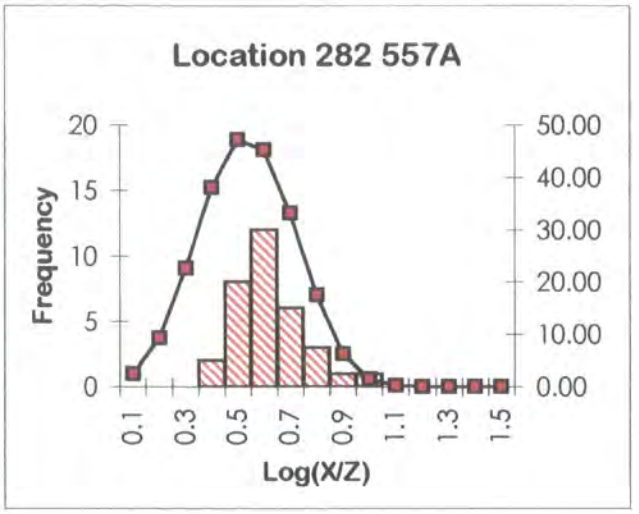
Location 282 557A
Frequency
20
15
10
5
0
50.00
40.00
30.00
20.00
10.00
0.00
0.1
0.3
0.5
0.7
0.9
1.1
1.3
1.5
Log(X/Z)

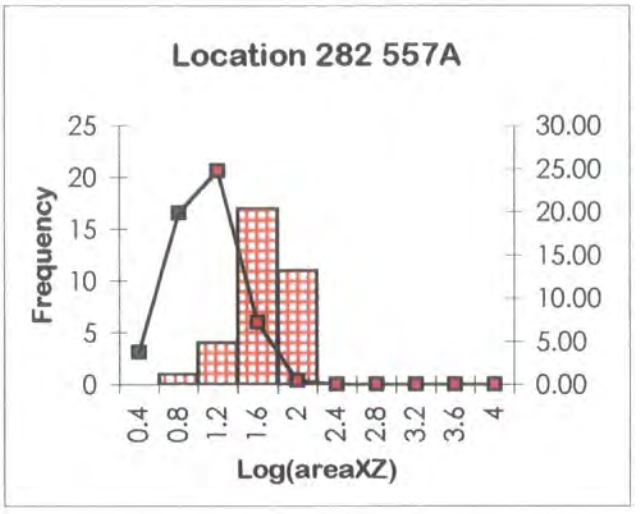
Location 282 557A
Frequency
25
20
15
10
5
0
30.00
25.00
20.00
15.00
10.00
5.00
0.00
0.4
0.8
1.2
1.6
2
2.4
2.8
3.2
3.6
4
Log(areaXZ)

Rannoch Moor Complex: Kingshouse (River Etive)
Intrusive Phase: The Blackwater facies (G2)

Location [282 557] B

X	Z	X/Z	log(x/z)	log (X×Zπ/4)
16.20	5.50	2.95	0.47	1.84
7.20	0.60	12.00	1.08	0.53
5.80	1.20	4.83	0.68	0.74
9.60	5.00	1.92	0.28	1.58
6.20	2.40	2.58	0.41	1.07
7.70	3.50	2.20	0.34	1.33
5.80	2.50	2.32	0.37	1.06
6.70	3.50	1.91	0.28	1.27
5.70	2.70	2.11	0.32	1.08
4.10	1.10	3.73	0.57	0.55
11.70	6.40	1.83	0.26	1.77
11.30	4.30	2.63	0.42	1.58
7.00	0.50	14.00	1.15	0.44
14.60	4.50	3.24	0.51	1.71
3.10	1.50	2.07	0.32	0.56
6.50	1.50	4.33	0.64	0.88
9.20	2.90	3.17	0.50	1.32
4.10	1.90	2.16	0.33	0.79
5.50	3.10	1.77	0.25	1.13
7.60	4.20	1.81	0.26	1.40
9.30	3.50	2.66	0.42	1.41
6.30	2.60	2.42	0.38	1.11
14.90	6.60	1.80	0.26	1.79
8.90	2.90	3.07	0.49	1.31
8.80	7.50	1.17	0.07	1.71
7.30	3.50	2.09	0.32	1.30
5.30	3.50	1.51	0.18	1.16
8.50	3.90	2.18	0.34	1.42
11.40	4.60	2.48	0.39	1.61
15.40	4.70	3.28	0.52	1.75
7.20	3.40	2.12	0.33	1.28
13.20	6.30	2.10	0.32	1.82
5.20	1.50	3.47	0.54	0.79
4.50	1.40	3.21	0.51	0.69
6.20	3.00	2.07	0.32	1.16
3.50	1.50	2.33	0.37	0.62
5.60	3.80	1.47	0.17	1.22
6.20	3.90	1.59	0.20	1.28
17.10	6.00	2.85	0.45	1.91
8.90	2.50	3.56	0.55	1.24
8.90	3.30	2.70	0.43	1.36
13.40	6.90	1.94	0.29	1.86
5.30	2.10	2.52	0.40	0.94
4.50	3.10	1.45	0.16	1.04
16.80	5.90	2.85	0.45	1.89
8.80	5.00	1.76	0.25	1.54
13.80	7.30	1.89	0.28	1.90
11.70	5.30	2.21	0.34	1.69

X	Z	X/Z	log(x/z)	log (X×Zπ/4)
15.70	5.00	3.14	0.50	1.79
7.40	3.60	2.06	0.31	1.32
5.00	2.50	2.00	0.30	0.99
5.60	2.40	2.33	0.37	1.02
7.30	3.60	2.03	0.31	1.31
11.50	4.40	2.61	0.42	1.60
12.50	5.40	2.31	0.36	1.72
9.70	4.80	2.02	0.31	1.56
15.20	4.50	3.38	0.53	1.73
17.30	6.40	2.70	0.43	1.94
15.40	6.50	1.91	0.28	1.80
8.50	2.30	3.70	0.57	1.19
3.00	0.80	3.75	0.57	0.28
11.20	6.40	1.75	0.24	1.75
14.60	4.10	3.56	0.55	1.67
7.80	2.20	3.55	0.55	1.13
5.90	3.70	1.59	0.20	1.23
10.50	3.80	2.76	0.44	1.50
7.10	3.10	2.29	0.36	1.24
3.70	1.70	2.18	0.34	0.69
4.20	1.30	3.23	0.51	0.63
4.10	0.60	6.83	0.83	0.29
6.00	3.50	1.71	0.23	1.22
5.10	0.60	8.50	0.93	0.38
4.90	0.90	5.44	0.74	0.54
24.30	14.10	1.72	0.24	2.43
10.80	5.70	1.89	0.28	1.68
22.60	13.40	1.69	0.23	2.38
8.00	1.80	4.44	0.65	1.05
6.40	2.60	2.46	0.39	1.12
13.30	6.60	2.02	0.30	1.84
4.30	0.80	5.38	0.73	0.43
5.90	3.20	1.84	0.27	1.17
5.60	3.40	1.65	0.22	1.17
5.30	3.00	1.77	0.25	1.10
8.80	4.40	2.00	0.30	1.48
12.80	6.10	2.10	0.32	1.79
5.30	2.10	2.52	0.40	0.94
11.30	3.70	3.05	0.48	1.52
3.90	0.70	5.57	0.75	0.33
4.50	2.00	2.25	0.35	0.85
3.80	2.70	1.41	0.15	0.91
5.80	4.10	1.41	0.15	1.27
5.80	2.90	2.00	0.30	1.12
17.70	6.40	2.77	0.44	1.95
8.50	4.40	1.93	0.29	1.47

12.40	7.10	1.75	0.24	1.84
5.40	1.70	3.18	0.50	0.86
5.50	1.10	5.00	0.70	0.68
9.60	4.30	2.23	0.35	1.51
3.70	0.60	6.17	0.79	0.24
6.00	1.80	3.33	0.52	0.93
6.70	3.10	2.16	0.33	1.21
5.30	1.00	5.30	0.72	0.62
17.90	6.80	2.63	0.42	1.98

sum	42.42	129.83
sum/N	0.41	1.26
average	2.58	18.22
wlog	1.08	2.36
N	103.00	103.00
S.D.	0.19	0.48
max	1.15	2.43
min	0.07	0.24

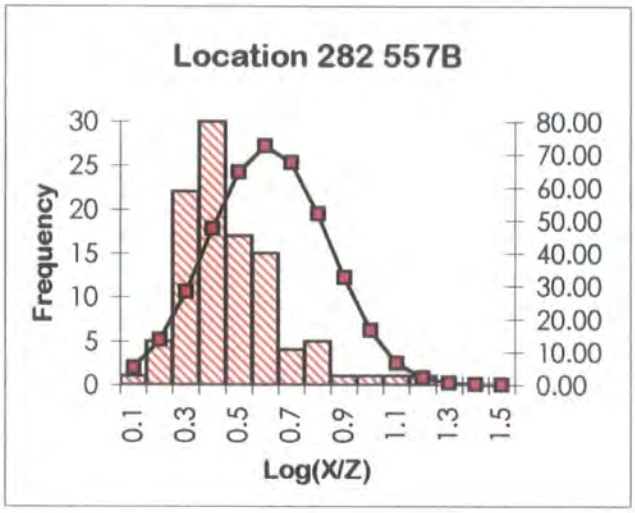

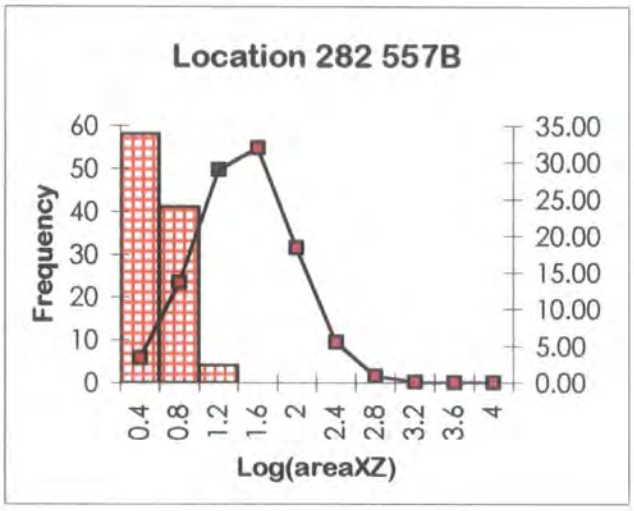

Rannoch Moor Complex: Kingshouse (River Etive)
Intrusive Phase: The Blackwater facies (G2)

Location [282 557]C

X	Z	X/Z	log(x/z)	log (X×Zπ/4)
12.50	3.50	3.57	0.55	1.54
9.50	4.40	2.16	0.33	1.52
6.40	1.30	4.92	0.69	0.82
8.50	1.40	6.07	0.78	0.97
3.60	2.20	1.64	0.21	0.79
4.70	1.80	2.61	0.42	0.82
9.00	5.50	1.64	0.21	1.59
7.90	3.40	2.32	0.37	1.32
3.80	1.10	3.45	0.54	0.52
7.10	2.80	2.54	0.40	1.19
6.50	2.60	2.50	0.40	1.12
7.50	1.50	5.00	0.70	0.95
3.10	1.20	2.58	0.41	0.47
8.50	3.30	2.58	0.41	1.34
9.70	3.10	3.13	0.50	1.37
8.30	4.00	2.08	0.32	1.42
6.90	3.30	2.09	0.32	1.25
5.90	1.80	3.28	0.52	0.92
13.40	2.30	5.83	0.77	1.38
17.30	6.50	2.66	0.43	1.95
6.40	2.00	3.20	0.51	1.00
7.50	0.70	10.71	1.03	0.62
7.70	1.10	7.00	0.85	0.82
9.30	2.80	3.32	0.52	1.31
1.50	0.40	3.75	0.57	-0.33
3.20	1.40	2.29	0.36	0.55
6.90	1.30	5.31	0.72	0.85
8.30	1.10	7.55	0.88	0.86
5.40	2.20	2.45	0.39	0.97
4.90	3.20	1.53	0.19	1.09
8.70	5.40	1.61	0.21	1.57
6.70	3.60	1.86	0.27	1.28
8.30	1.20	6.92	0.84	0.89
7.90	3.40	2.32	0.37	1.32
4.40	1.50	2.93	0.47	0.71
4.30	2.30	1.87	0.27	0.89
9.00	5.70	1.58	0.20	1.61
5.20	1.50	3.47	0.54	0.79
7.60	0.80	9.50	0.98	0.68
1.80	0.90	2.00	0.30	0.10
2.80	1.10	2.55	0.41	0.38
7.70	3.90	1.97	0.30	1.37
19.60	6.70	2.63	0.42	1.97
5.30	1.80	2.94	0.47	0.87
7.40	4.20	1.76	0.25	1.39
5.00	1.70	2.94	0.47	0.82
14.60	4.30	3.40	0.53	1.69
12.80	2.10	6.10	0.78	1.32

X	Z	X/Z	log(x/z)	log (X×Zπ/4)
10.10	3.40	2.97	0.47	1.43
10.40	6.70	1.55	0.19	1.74
8.20	4.90	1.67	0.22	1.50
7.60	3.80	2.00	0.30	1.36
5.70	1.70	3.35	0.53	0.88
7.60	3.10	2.45	0.39	1.27
17.10	6.30	2.71	0.43	1.93
9.30	4.10	2.27	0.36	1.48
15.50	3.90	3.97	0.60	1.68
5.80	1.30	4.46	0.65	0.77
5.50	1.40	3.93	0.59	0.78
15.20	4.50	3.38	0.53	1.73
6.90	3.70	1.86	0.27	1.30
5.80	1.10	5.27	0.72	0.70
2.50	2.10	1.19	0.08	0.62
24.80	6.70	3.70	0.57	2.12
6.40	1.20	5.33	0.73	0.78
21.80	5.50	3.96	0.60	1.97
7.70	2.20	3.50	0.54	1.12
9.50	4.20	2.26	0.35	1.50
6.80	3.60	1.89	0.28	1.28
4.00	1.50	2.67	0.43	0.67
5.10	1.10	4.64	0.67	0.64
7.60	4.40	1.73	0.24	1.42
12.50	1.40	7.50	0.88	1.06
5.90	3.30	1.79	0.25	1.18
7.30	3.60	2.03	0.31	1.31
7.70	2.80	2.75	0.44	1.23
3.80	2.00	1.90	0.28	0.78
6.70	3.20	2.09	0.32	1.23
2.30	1.60	1.44	0.16	0.46
6.30	1.10	5.73	0.76	0.74
21.50	5.40	3.98	0.60	1.96
7.10	1.10	6.45	0.81	0.79
5.30	1.10	4.82	0.68	0.66
5.50	0.60	9.17	0.96	0.41
7.00	3.30	2.12	0.33	1.26
7.80	4.90	1.59	0.20	1.48
5.60	1.40	4.00	0.60	0.79
10.40	6.50	1.60	0.20	1.73
6.80	4.00	1.70	0.23	1.33
6.50	2.90	2.24	0.35	1.17
7.70	2.00	3.85	0.59	1.08
24.60	6.50	3.32	0.52	2.04
3.10	1.50	2.07	0.32	0.56
3.50	0.80	4.38	0.64	0.34
9.70	6.00	1.62	0.21	1.66
9.70	3.00	3.23	0.51	1.36

7.40	3.70	2.00	0.30	1.33
7.30	4.00	1.83	0.26	1.36
5.90	1.80	3.28	0.52	0.92
15.70	4.50	3.49	0.54	1.74
14.10	2.50	5.64	0.75	1.44
10.30	4.20	2.45	0.39	1.53
7.30	3.30	2.21	0.34	1.28
10.40	3.50	2.97	0.47	1.46
7.40	3.30	2.24	0.35	1.28
6.30	1.10	5.73	0.76	0.74
6.90	2.90	2.38	0.38	1.20
8.00	3.90	2.05	0.31	1.39
1.40	0.80	1.75	0.24	-0.06
4.00	2.20	1.82	0.26	0.84
6.10	1.80	3.39	0.53	0.94
24.10	7.10	3.39	0.53	2.13
5.10	2.90	1.76	0.25	1.07
9.50	2.90	3.28	0.52	1.34
6.60	2.70	2.44	0.39	1.15
13.10	2.10	6.24	0.80	1.33
9.70	4.50	2.16	0.33	1.54
9.80	4.60	2.13	0.33	1.55
12.30	3.30	3.73	0.57	1.50
8.40	4.70	1.79	0.25	1.49
9.50	2.60	3.65	0.56	1.29
2.70	1.50	1.80	0.26	0.50
14.00	3.20	4.38	0.64	1.55
18.30	7.80	2.35	0.37	2.05
6.20	2.50	2.48	0.39	1.09
9.30	5.80	1.60	0.21	1.63
8.10	3.70	2.19	0.34	1.37
6.40	2.50	2.56	0.41	1.10
8.50	3.50	2.43	0.39	1.37
7.00	2.50	2.80	0.45	1.14
5.00	2.70	1.85	0.27	1.03
23.00	6.30	3.65	0.56	2.06
8.50	1.90	4.47	0.65	1.10
8.70	1.60	5.44	0.74	1.04
5.60	3.30	1.70	0.23	1.16
10.60	1.10	9.64	0.98	0.96
9.30	4.50	2.07	0.32	1.52
15.40	4.50	3.42	0.53	1.74
14.90	4.20	3.55	0.55	1.69
7.70	3.40	2.26	0.36	1.31
7.20	3.50	2.06	0.31	1.30
8.20	5.50	1.49	0.17	1.55
8.30	3.50	2.37	0.38	1.36
6.00	1.80	3.33	0.52	0.93
10.80	7.30	1.48	0.17	1.79
7.50	2.10	3.57	0.55	1.09
7.70	1.70	4.53	0.66	1.01
9.30	4.30	2.16	0.34	1.50
4.90	2.90	1.69	0.23	1.05
5.10	3.30	1.55	0.19	1.12
8.20	3.20	2.56	0.41	1.31

4.60	1.30	3.54	0.55	0.67
4.40	2.80	1.57	0.20	0.99
8.80	4.00	2.20	0.34	1.44
22.10	6.20	3.56	0.55	2.03
5.90	2.90	2.03	0.31	1.13
8.00	2.70	2.96	0.47	1.23
3.60	1.60	2.25	0.35	0.66
7.30	2.60	2.81	0.45	1.17
8.90	3.80	2.34	0.37	1.42
5.10	0.60	8.50	0.93	0.38
9.70	6.40	1.52	0.18	1.69
6.20	2.20	2.82	0.45	1.03
13.80	2.50	5.52	0.74	1.43
3.60	1.70	2.12	0.33	0.68
6.80	2.20	3.09	0.49	1.07
16.80	6.00	2.80	0.45	1.90
8.10	4.00	2.03	0.31	1.41
6.70	3.00	2.23	0.35	1.20
4.90	2.50	1.96	0.29	0.98
6.80	3.30	2.06	0.31	1.25
10.40	0.60	17.33	1.24	0.69
10.00	4.70	2.13	0.33	1.57
8.00	3.50	2.29	0.36	1.34
12.10	3.00	4.03	0.61	1.45
7.00	4.30	1.63	0.21	1.37
3.60	1.60	2.25	0.35	0.66
9.30	3.50	2.66	0.42	1.41
6.70	2.10	3.19	0.50	1.04
9.00	2.40	3.75	0.57	1.23
15.40	4.70	3.28	0.52	1.75
4.60	1.50	3.07	0.49	0.73
14.80	3.10	4.77	0.68	1.56
14.30	4.30	3.33	0.52	1.68
7.40	3.40	2.18	0.34	1.30
7.90	0.60	13.17	1.12	0.57
8.40	4.40	1.91	0.28	1.46
5.60	1.20	4.67	0.67	0.72
8.00	0.90	8.89	0.95	0.75
10.70	4.00	2.68	0.43	1.53
5.20	2.00	2.60	0.41	0.91
5.00	3.20	1.56	0.19	1.10
6.20	2.90	2.14	0.33	1.15
4.70	2.50	1.88	0.27	0.97
7.20	1.70	4.24	0.63	0.98
23.70	6.60	3.59	0.56	2.09
21.20	5.10	4.16	0.62	1.93
12.40	1.60	7.75	0.89	1.19
5.80	2.30	2.52	0.40	1.02
7.40	2.70	2.74	0.44	1.20
7.80	3.70	2.11	0.32	1.36
24.90	7.20	3.46	0.54	2.15
7.00	1.60	4.38	0.64	0.94
2.30	0.90	2.56	0.41	0.21
2.80	1.20	2.33	0.37	0.42
4.20	1.80	2.33	0.37	0.77

5.20	4.10	1.27	0.10	1.22
5.50	3.20	1.72	0.24	1.14
9.70	4.40	2.20	0.34	1.53
11.50	2.50	4.60	0.66	1.35
4.50	2.30	1.96	0.29	0.91
8.70	3.20	2.72	0.43	1.34
16.30	5.50	2.96	0.47	1.85
17.80	8.30	2.14	0.33	2.06
49.00	3.50	14.00	1.15	2.13
6.00	2.80	2.14	0.33	1.12
4.00	2.20	1.82	0.26	0.84
7.50	2.20	3.41	0.53	1.11
6.50	2.00	3.25	0.51	1.01
3.80	2.40	1.58	0.20	0.86
4.90	1.30	3.77	0.58	0.70
6.30	3.40	1.85	0.27	1.23
9.40	5.90	1.59	0.20	1.64
5.10	3.50	1.46	0.16	1.15
4.90	3.00	1.63	0.21	1.06
11.00	6.70	1.64	0.22	1.76
5.60	1.60	3.50	0.54	0.85
8.70	3.50	2.49	0.40	1.38
10.60	1.90	5.58	0.75	1.20
7.70	3.30	2.33	0.37	1.30
7.90	2.40	3.29	0.52	1.17
5.20	3.60	1.44	0.16	1.17
7.90	3.90	2.03	0.31	1.38
3.50	1.30	2.69	0.43	0.55
3.70	1.70	2.18	0.34	0.69
8.70	3.70	2.35	0.37	1.40
9.30	4.00	2.33	0.37	1.47
3.30	1.10	3.00	0.48	0.45
24.10	6.80	3.54	0.55	2.11
7.70	2.30	3.35	0.52	1.14
3.50	2.70	1.30	0.11	0.87
7.60	2.90	2.62	0.42	1.24
7.70	2.40	3.21	0.51	1.16
16.10	4.70	3.43	0.53	1.77
4.20	2.00	2.10	0.32	0.82

4.70	0.80	5.88	0.77	0.47
8.30	2.60	3.19	0.50	1.23
4.60	1.70	2.71	0.43	0.79
7.20	2.70	2.67	0.43	1.18
8.70	5.20	1.67	0.22	1.55
6.40	3.90	1.64	0.22	1.29
5.90	1.60	3.69	0.57	0.87
10.90	2.10	5.19	0.72	1.25
13.50	3.80	3.55	0.55	1.61
7.60	4.70	1.62	0.21	1.45
5.70	3.50	1.63	0.21	1.20
7.90	2.90	2.72	0.44	1.26
6.30	0.70	9.00	0.95	0.54
5.60	4.40	1.27	0.10	1.29
2.90	2.30	1.26	0.10	0.72
2.50	0.70	3.57	0.55	0.14
9.10	1.80	5.06	0.70	1.11
5.60	1.10	5.09	0.71	0.68
8.00	3.90	2.05	0.31	1.39
10.20	3.10	3.29	0.52	1.40
1.80	1.30	1.38	0.14	0.26
5.60	3.60	1.56	0.19	1.20
9.50	5.10	1.86	0.27	1.58
7.90	1.30	6.08	0.78	0.91
0.80	0.40	2.00	0.30	-0.60
4.40	2.80	1.57	0.20	0.99
7.80	3.10	2.52	0.40	1.28
6.30	2.50	2.52	0.40	1.09
17.60	7.10	2.48	0.39	1.99

sum	122.87	322.32
sum/N	0.45	1.18
average	2.81	15.01
wlog	1.16	2.75
N	274.00	274.00
S.D.	0.21	0.44
max	1.24	2.15
min	0.08	-0.60

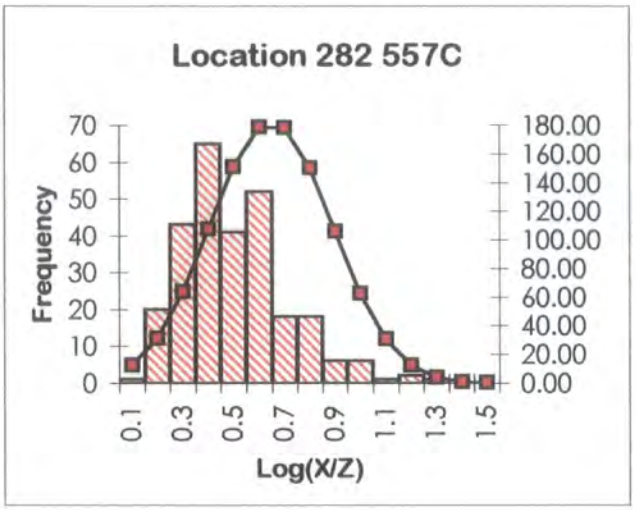
Location 282 557C
Frequency
70
60
50
40
30
20
10
0
180.00
160.00
140.00
120.00
100.00
80.00
60.00
40.00
20.00
0.00
0.1
0.3
0.5
0.7
0.9
1.1
1.3
1.5
Log(X/Z)

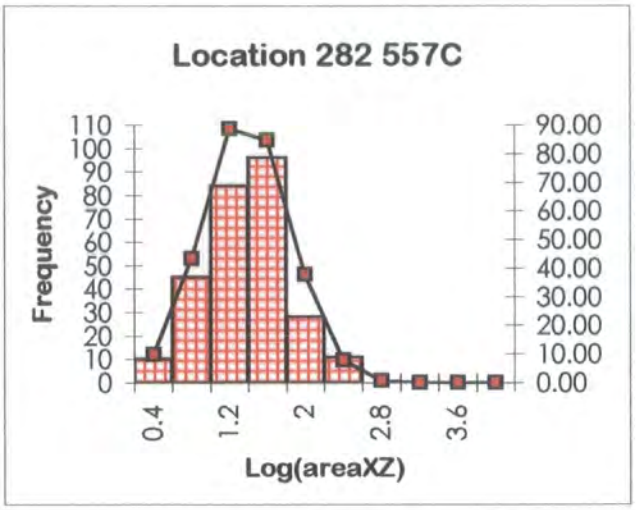
Location 282 557C
Frequency
110
100
90
80
70
60
50
40
30
20
10
0
90.00
80.00
70.00
60.00
50.00
40.00
30.00
20.00
10.00
0.00
0.4
1.2
2
2.8
3.6
Log(areaXZ)

Rannoch Moor Complex: Kingshouse
Intrusive Phase: The Blackwater facies (G2)

Location [263 543]

X	Z	X/Z	log(x/z)	log (X×Zπ/4)
9.20	0.80	11.50	1.06	0.76
4.50	0.70	6.43	0.81	0.39
9.00	1.50	6.00	0.78	1.03
25.30	5.10	4.96	0.70	2.01
12.90	2.30	5.61	0.75	1.37
10.40	2.10	4.95	0.69	1.23
4.90	0.60	8.17	0.91	0.36
9.10	2.50	3.64	0.56	1.25
7.70	0.90	8.56	0.93	0.74
28.50	7.20	3.96	0.60	2.21
6.20	1.30	4.77	0.68	0.80
7.40	1.10	6.73	0.83	0.81
5.50	1.20	4.58	0.66	0.71
9.80	3.00	3.27	0.51	1.36
8.10	2.50	3.24	0.51	1.20
25.80	4.50	5.73	0.76	1.96
10.00	1.50	6.67	0.82	1.07
7.00	1.70	4.12	0.61	0.97
10.90	2.60	4.19	0.62	1.35
7.00	1.40	5.00	0.70	0.89
26.10	4.90	5.33	0.73	2.00
5.50	0.70	7.86	0.90	0.48
8.00	0.60	13.33	1.12	0.58

X	Z	X/Z	log(x/z)	log (X×Zπ/4)
27.30	5.90	4.63	0.67	2.10
6.90	0.70	9.86	0.99	0.58
8.20	1.70	4.82	0.68	1.04
7.30	2.00	3.65	0.56	1.06
4.00	0.50	8.00	0.90	0.20
8.80	1.60	5.50	0.74	1.04
6.00	0.40	15.00	1.18	0.28
9.60	0.80	12.00	1.08	0.78
5.50	0.30	18.33	1.26	0.11
6.30	1.40	4.50	0.65	0.84
8.10	1.50	5.40	0.73	0.98
4.30	0.50	8.60	0.93	0.23
9.10	2.70	3.37	0.53	1.29
7.90	2.40	3.29	0.52	1.17

sum	28.68	37.22
sum/N	0.78	1.01
average	5.96	10.14
wlog	0.75	2.09
N	37.00	37.00
S.D.	0.20	0.54
max	1.26	2.21
min	0.51	0.11

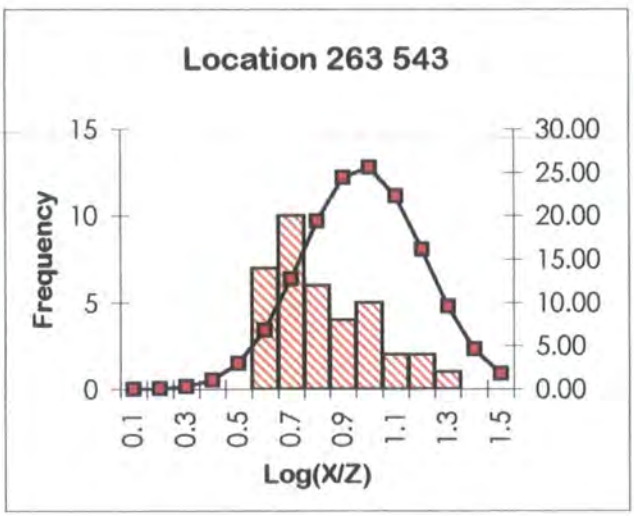

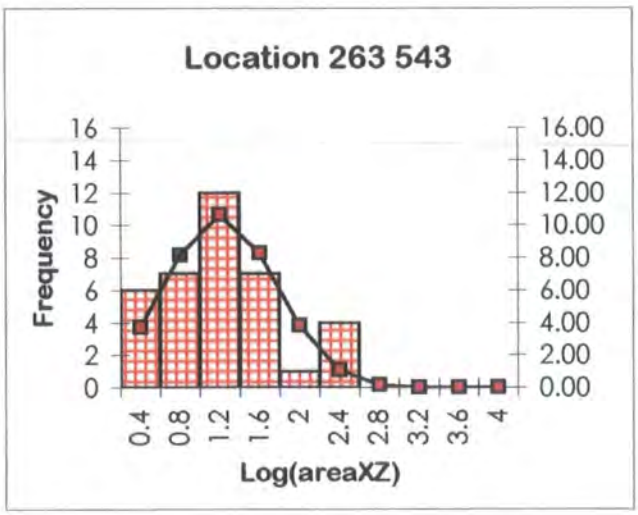

Strath Ossian Complex: Fersit (River Treig)
Intrusive Phase : The Sgòr Choinnich facies (G2)

Location [357 787] A

X	Z	X/Z	log(x/z)	log (X×Zπ/4)
13.50	5.50	2.45	0.39	1.77
9.00	2.20	4.09	0.61	1.19
8.50	3.50	2.43	0.39	1.37
20.00	7.00	2.86	0.46	2.04
6.70	1.60	4.19	0.62	0.93
19.40	6.60	2.94	0.47	2.00
8.50	1.70	5.00	0.70	1.05
24.40	6.50	3.75	0.57	2.10
9.20	3.00	3.07	0.49	1.34
19.70	6.70	2.94	0.47	2.02
17.10	4.00	4.28	0.63	1.73
5.60	1.20	4.67	0.67	0.72
7.60	2.70	2.81	0.45	1.21
14.90	7.50	1.99	0.30	1.94
16.60	3.30	5.03	0.70	1.63
5.30	0.90	5.89	0.77	0.57
7.50	2.40	3.13	0.49	1.15
12.00	2.60	4.62	0.66	1.39
9.70	3.00	3.23	0.51	1.36
8.60	2.00	4.30	0.63	1.13
15.60	8.40	1.86	0.27	2.01
10.30	2.60	3.96	0.60	1.32
13.00	5.00	2.60	0.41	1.71
6.10	1.70	3.59	0.55	0.91
10.70	2.60	4.12	0.61	1.34
11.30	4.70	2.40	0.38	1.62
6.90	1.80	3.83	0.58	0.99
9.40	2.40	3.92	0.59	1.25
20.40	7.20	2.83	0.45	2.06
14.50	7.50	1.93	0.29	1.93
5.30	0.50	10.60	1.03	0.32
13.80	5.80	2.38	0.38	1.80
14.50	4.00	3.63	0.56	1.66
9.00	4.00	2.25	0.35	1.45
14.10	3.40	4.15	0.62	1.58
15.00	4.50	3.33	0.52	1.72
12.00	5.60	2.14	0.33	1.72
20.40	7.60	2.68	0.43	2.09

X	Z	X/Z	log(x/z)	log (X×Zπ/4)
11.50	3.00	3.83	0.58	1.43
7.20	2.10	3.43	0.54	1.07
11.80	5.40	2.19	0.34	1.70
8.00	3.40	2.35	0.37	1.33
12.60	3.20	3.94	0.60	1.50
11.10	4.60	2.41	0.38	1.60
17.30	4.20	4.12	0.61	1.76
8.80	3.80	2.32	0.36	1.42
14.30	3.60	3.97	0.60	1.61
5.90	1.50	3.93	0.59	0.84
10.00	3.30	3.03	0.48	1.41
11.00	2.90	3.79	0.58	1.40
9.30	3.00	3.10	0.49	1.34
16.50	3.00	5.50	0.74	1.59
14.10	5.90	2.39	0.38	1.82
17.00	3.50	4.86	0.69	1.67
10.20	3.70	2.76	0.44	1.47
13.20	5.20	2.54	0.40	1.73
10.80	3.50	3.09	0.49	1.47
11.70	3.20	3.66	0.56	1.47
11.70	2.50	4.68	0.67	1.36
8.20	2.80	2.93	0.47	1.26
15.00	8.00	1.88	0.27	1.97
11.50	5.10	2.25	0.35	1.66
14.80	4.30	3.44	0.54	1.70
15.20	8.40	1.81	0.26	2.00
12.30	2.90	4.24	0.63	1.45
12.80	3.40	3.76	0.58	1.53

sum	33.94	98.69
sum/N	0.51	1.50
average	3.27	31.28
wlog	0.77	1.84
N	66.00	66.00
S.D.	0.14	0.38
max	1.03	2.10
min	0.26	0.32

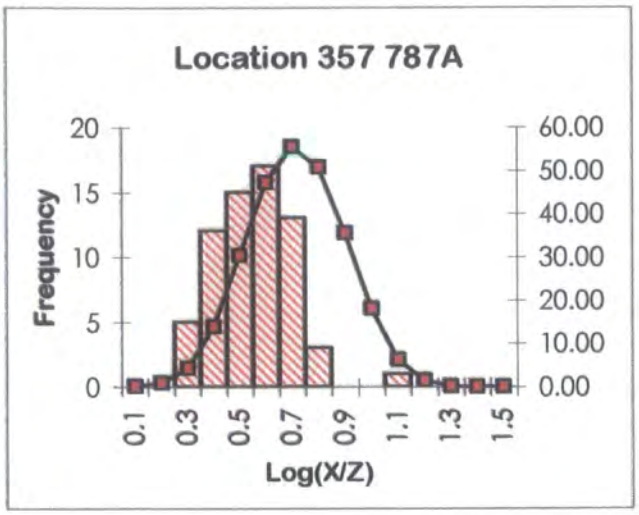
Location 357 787A
Frequency
20
15
10
5
0
60.00
50.00
40.00
30.00
20.00
10.00
0.00
0.1
0.3
0.5
0.7
0.9
1.1
1.3
1.5
Log(X/Z)

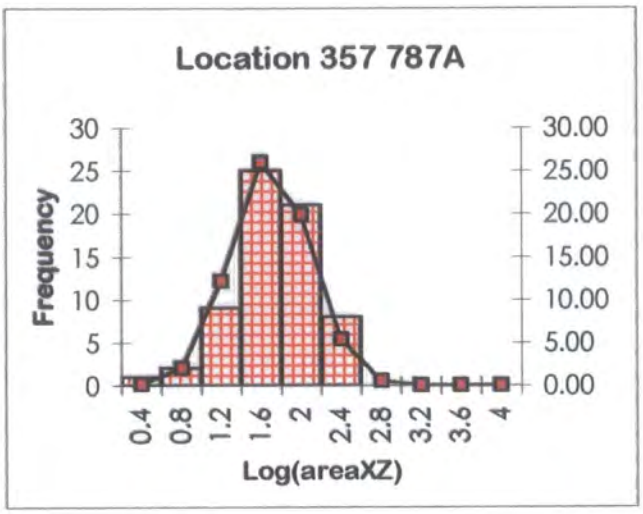
Location 357 787A
Frequency
30
25
20
15
10
5
0
30.00
25.00
20.00
15.00
10.00
5.00
0.00
0.4
0.8
1.2
1.6
2
2.4
2.8
3.2
3.6
4
Log(areaXZ)

Strath Ossian Complex: Fersit (River Treig)
Intrusive Phase : The Sgòr Choinnich facies (G2)

Location [357 787] B

X	Z	X/Z	log(x/z)	log (X×Zπ/4)
13.20	6.20	2.13	0.33	1.81
19.50	5.10	3.82	0.58	1.89
27.00	7.50	3.60	0.56	2.20
3.60	1.70	2.12	0.33	0.68
13.60	7.50	1.81	0.26	1.90
22.80	9.60	2.38	0.38	2.24
7.40	2.50	2.96	0.47	1.16
5.80	2.90	2.00	0.30	1.12
12.90	5.90	2.19	0.34	1.78
23.00	10.00	2.30	0.36	2.26
5.70	2.20	2.59	0.41	0.99
7.50	3.60	2.08	0.32	1.33
9.00	4.00	2.25	0.35	1.45
16.00	9.80	1.63	0.21	2.09
12.70	7.20	1.76	0.25	1.86
7.50	3.00	2.50	0.40	1.25
4.00	1.90	2.11	0.32	0.78
8.90	3.50	2.54	0.41	1.39
17.00	6.50	2.62	0.42	1.94
20.00	5.60	3.57	0.55	1.94
10.50	3.80	2.76	0.44	1.50
10.10	4.40	2.30	0.36	1.54
9.60	6.40	1.50	0.18	1.68
5.70	2.60	2.19	0.34	1.07
13.90	6.50	2.14	0.33	1.85
17.50	7.60	2.30	0.36	2.02
5.60	1.90	2.95	0.47	0.92
17.50	7.00	2.50	0.40	1.98
9.40	4.60	2.04	0.31	1.53
16.30	10.50	1.55	0.19	2.13
12.20	4.50	2.71	0.43	1.63
18.70	8.40	2.23	0.35	2.09
15.70	9.50	1.65	0.22	2.07
10.20	4.70	2.17	0.34	1.58
6.70	3.20	2.09	0.32	1.23
10.70	4.00	2.68	0.43	1.53
9.10	5.90	1.54	0.19	1.62
9.30	4.30	2.16	0.34	1.50
19.30	4.70	4.11	0.61	1.85
9.00	5.40	1.67	0.22	1.58
9.40	6.20	1.52	0.18	1.66
7.00	2.10	3.33	0.52	1.06
16.00	6.20	2.58	0.41	1.89
3.30	1.40	2.36	0.37	0.56
6.50	2.60	2.50	0.40	1.12
11.80	4.50	2.62	0.42	1.62
19.80	5.40	3.67	0.56	1.92
11.20	4.10	2.73	0.44	1.56
23.20	10.40	2.23	0.35	2.28
23.50	10.50	2.24	0.35	2.29
16.60	5.90	2.81	0.45	1.89
8.60	3.40	2.53	0.40	1.36
11.30	3.40	3.32	0.52	1.48
3.00	1.30	2.31	0.36	0.49
21.60	11.40	1.89	0.28	2.29
6.60	3.70	1.78	0.25	1.28
6.50	1.60	4.06	0.61	0.91
6.70	2.80	2.39	0.38	1.17
7.50	2.60	2.88	0.46	1.19
4.00	2.30	1.74	0.24	0.86
7.70	3.80	2.03	0.31	1.36
13.80	7.70	1.79	0.25	1.92
11.10	5.40	2.06	0.31	1.67
18.10	8.00	2.26	0.35	2.06
6.20	2.30	2.70	0.43	1.05
17.20	6.90	2.49	0.40	1.97
17.90	7.60	2.36	0.37	2.03
6.60	3.80	1.74	0.24	1.29
11.10	4.00	2.78	0.44	1.54
21.30	11.30	1.88	0.28	2.28
13.00	7.50	1.73	0.24	1.88
21.00	11.00	1.91	0.28	2.26
18.50	8.20	2.26	0.35	2.08
10.60	5.50	1.93	0.28	1.66
13.60	6.40	2.13	0.33	1.83
7.10	2.60	2.73	0.44	1.16
20.50	10.90	1.88	0.27	2.24
10.50	5.00	2.10	0.32	1.62
6.20	3.10	2.00	0.30	1.18
16.50	9.90	1.67	0.22	2.11
11.40	4.50	2.53	0.40	1.61
7.00	2.50	2.80	0.45	1.14
12.90	5.50	2.35	0.37	1.75
8.50	5.50	1.55	0.19	1.56
19.20	4.40	4.36	0.64	1.82
11.50	4.80	2.40	0.38	1.64

sum	32.72	148.46
sum/N	0.36	1.63
average	2.29	42.80
wlog	0.46	2.11
N	91.00	91.00
S.D.	0.10	0.44
max	0.64	2.29
min	0.18	0.49

15.20	9.60	1.58	0.20	2.06
22.50	9.50	2.37	0.37	2.22
12.30	7.20	1.71	0.23	1.84
20.60	10.40	1.98	0.30	2.23
11.50	4.20	2.74	0.44	1.58

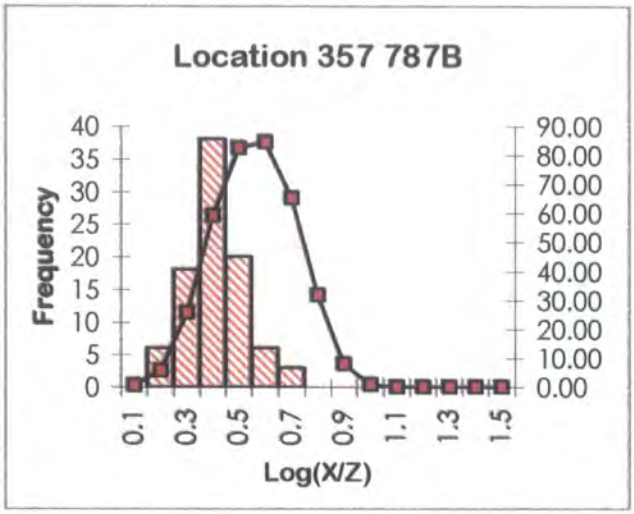

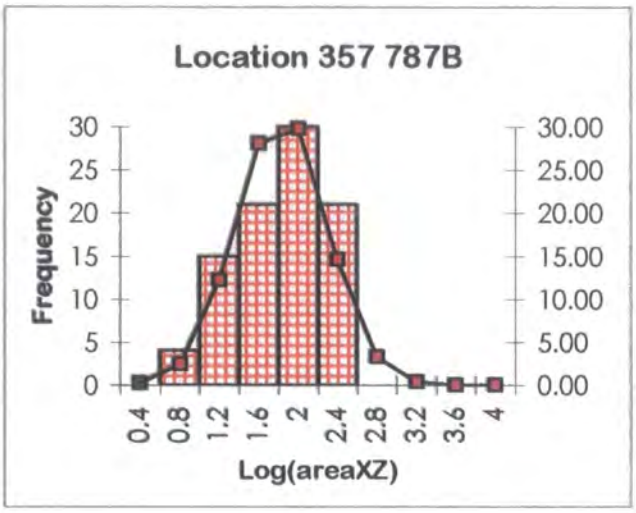

Strath Ossian Complex: Laggan Dam
Intrusive Phase : The Sgòr Choinnich facies (G2)

Location [372 808]

X	Z	X/Z	log(x/z)	log (X×Zπ/4)
8.00	4.20	1.90	0.28	1.42
5.70	2.10	2.71	0.43	0.97
6.50	3.50	1.86	0.27	1.25
6.20	1.80	3.44	0.54	0.94
8.20	2.90	2.83	0.45	1.27
17.80	9.30	1.91	0.28	2.11
8.00	5.00	1.60	0.20	1.50
10.00	5.20	1.92	0.28	1.61
8.30	2.70	3.07	0.49	1.25
18.00	9.00	2.00	0.30	2.10
5.50	1.80	3.06	0.49	0.89
8.90	3.50	2.54	0.41	1.39
16.50	10.80	1.53	0.18	2.15
10.50	4.50	2.33	0.37	1.57
12.20	4.80	2.54	0.41	1.66
13.80	7.00	1.97	0.29	1.88
8.30	4.00	2.08	0.32	1.42
6.20	3.60	1.72	0.24	1.24
8.10	4.70	1.72	0.24	1.48
10.40	4.70	2.21	0.34	1.58
10.70	4.30	2.49	0.40	1.56
5.70	1.70	3.35	0.53	0.88
8.80	3.70	2.38	0.38	1.41

Y	Z	Y/Z	log(Y/Z)	log(Y×Zπ/4)
10.50	3.50	3.00	0.48	1.46
4.20	1.60	2.63	0.42	0.72
10.80	3.00	3.60	0.56	1.41
6.10	1.70	3.59	0.55	0.91
15.80	2.80	5.64	0.75	1.54
10.20	2.70	3.78	0.58	1.34
9.10	1.70	5.35	0.73	1.08
5.60	1.30	4.31	0.63	0.76
8.50	1.10	7.73	0.89	0.87
7.20	2.00	3.60	0.56	1.05
8.30	3.70	2.24	0.35	1.38
4.40	1.80	2.44	0.39	0.79
15.70	7.00	2.24	0.35	1.94
16.30	4.00	4.08	0.61	1.71
19.50	4.20	4.64	0.67	1.81
13.40	5.30	2.53	0.40	1.75
12.20	5.00	2.44	0.39	1.68
12.00	3.20	3.75	0.57	1.48
6.30	1.50	4.20	0.62	0.87
12.40	2.90	4.28	0.63	1.45
22.50	4.50	5.00	0.70	1.90
16.50	5.30	3.11	0.49	1.84

sum	8.10	33.54
sum/N	0.35	1.46
average	2.25	28.72
wlog	0.35	1.96
N	23.00	23.00
S.D.	0.10	0.37
max	0.54	2.15
min	0.18	0.88

sum	12.32	29.73
sum/N	0.56	1.35
average	3.63	22.46
wlog	0.54	1.21
N	22.00	22.00
S.D.	0.14	0.40
max	0.89	1.94
min	0.35	0.72

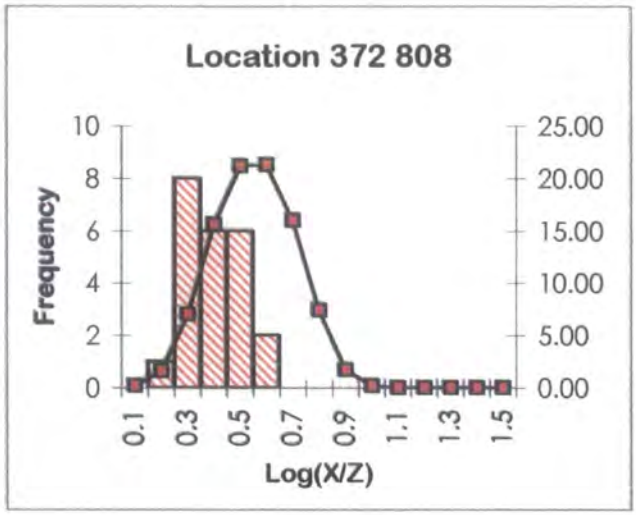
Location 372 808
Frequency
Log(X/Z)
0.1
0.3
0.5
0.7
0.9
1.1
1.3
1.5
0
2
4
6
8
10
0.00
5.00
10.00
15.00
20.00
25.00

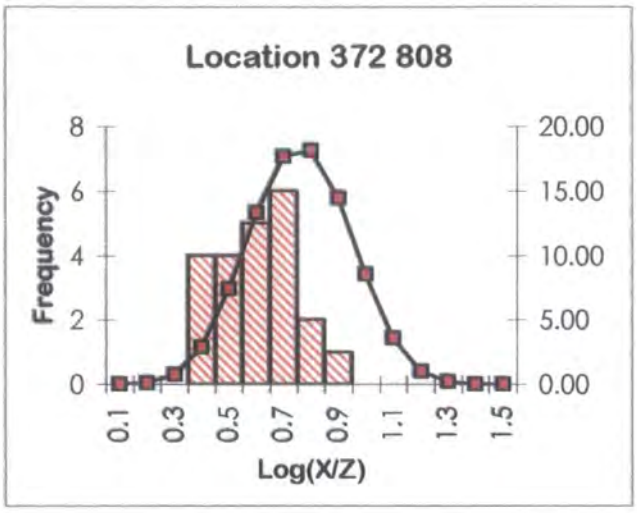
Location 372 808
Frequency
Log(X/Z)
0.1
0.3
0.5
0.7
0.9
1.1
1.3
1.5
0
2
4
6
8
0.00
5.00
10.00
15.00
20.00

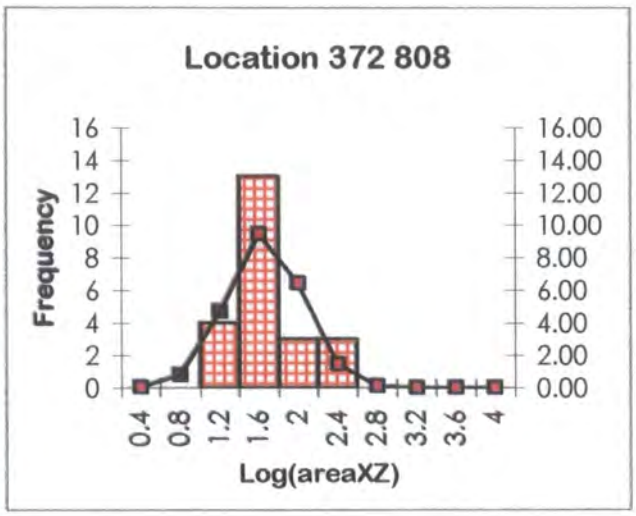
Location 372 808
Frequency
Log(areaXZ)
0.4
0.8
1.2
1.6
2
2.4
2.8
3.2
3.6
4
0
2
4
6
8
10
12
14
16
0.00
2.00
4.00
6.00
8.00
10.00
12.00
14.00
16.00

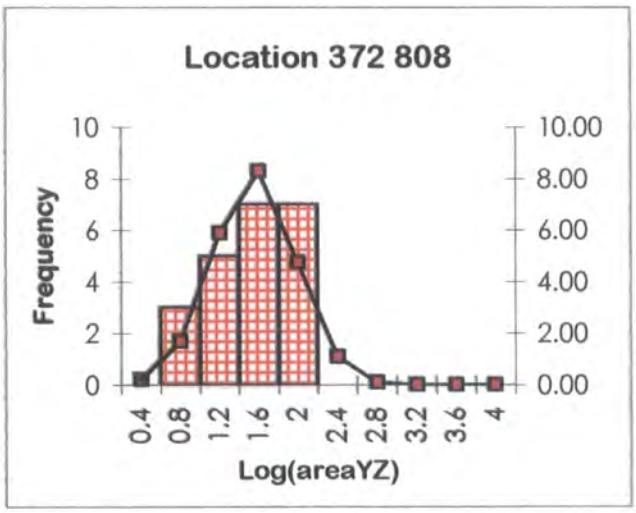
Location 372 808
Frequency
Log(areaYZ)
0.4
0.8
1.2
1.6
2
2.4
2.8
3.2
3.6
4
0
2
4
6
8
10
0.00
2.00
4.00
6.00
8.00
10.00

Strath Ossian Complex: Uisge Labhair
Intrusive Phase : The Sgòr Choinnich facies (G2)

Location [417 701]A

X Orientation	X	Z	X/Z	log(x/z)	log (X×Zπ/4)
045	28.00	17.00	1.65	0.22	2.78
168	21.70	9.40	2.31	0.36	3.09
172	6.00	4.50	1.33	0.12	2.78
163	9.60	5.30	1.81	0.26	2.83
165	5.80	4.10	1.41	0.15	2.73
161	5.60	2.30	2.43	0.39	2.46
161	17.30	3.70	4.68	0.67	2.67
176	10.60	5.00	2.12	0.33	2.84
160	6.00	2.50	2.40	0.38	2.50
160	11.80	4.60	2.57	0.41	2.76
037	4.30	1.60	2.69	0.43	1.67
164	6.10	3.50	1.74	0.24	2.65
102	22.00	13.00	1.69	0.23	3.02
050	12.00	5.00	2.40	0.38	2.29
160	9.90	5.80	1.71	0.23	2.86
164	6.80	3.00	2.27	0.36	2.59
160	9.00	2.20	4.09	0.61	2.44
179	11.00	2.60	4.23	0.63	2.56
047	5.50	2.90	1.90	0.28	2.03
172	12.60	5.00	2.52	0.40	2.83
166	10.50	1.80	5.83	0.77	2.37
169	6.50	2.60	2.50	0.40	2.54
163	18.80	4.90	3.84	0.58	2.80
102	9.10	2.70	3.37	0.53	2.34
108	6.00	3.00	2.00	0.30	2.41
C. R. Xenolith 032	11.00	2.00	5.50	0.74	1.70
036	4.40	2.10	2.10	0.32	1.77
166	17.00	3.40	5.00	0.70	2.65
167	8.60	2.00	4.30	0.63	2.42
167	22.40	13.20	1.70	0.23	3.24
170	21.40	8.50	2.52	0.40	3.05
164	6.50	4.60	1.41	0.15	2.77
140	21.50	9.00	2.39	0.38	3.00
170	9.40	4.90	1.92	0.28	2.82
176	7.20	6.00	1.20	0.08	2.92
188	16.50	9.30	1.77	0.25	3.14
160	5.90	2.70	2.19	0.34	2.53
048	9.30	5.60	1.66	0.22	2.32
160	4.20	2.60	1.62	0.21	2.51
162	4.90	2.20	2.23	0.35	2.45
172	21.50	12.90	1.67	0.22	3.24
169	9.30	5.00	1.86	0.27	2.82
173	3.70	3.10	1.19	0.08	2.62

sum	15.49	112.82
sum/N	0.36	2.62
average	2.29	420.36
wlog	0.69	1.57
N	43	43
S.D.	0.18	0.37
max	0.77	3.24
min	0.08	1.67

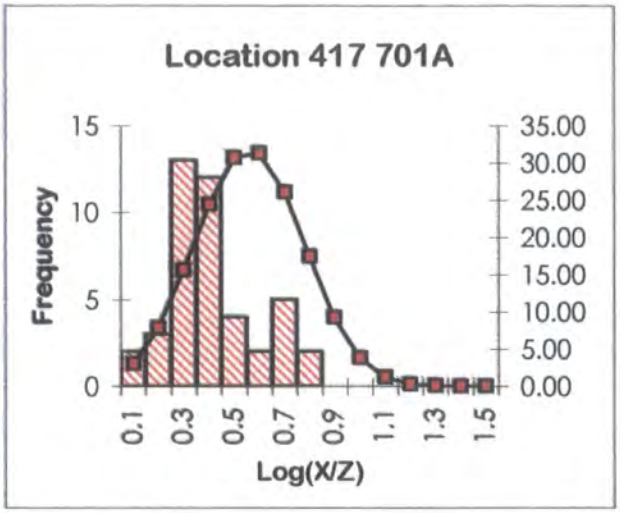

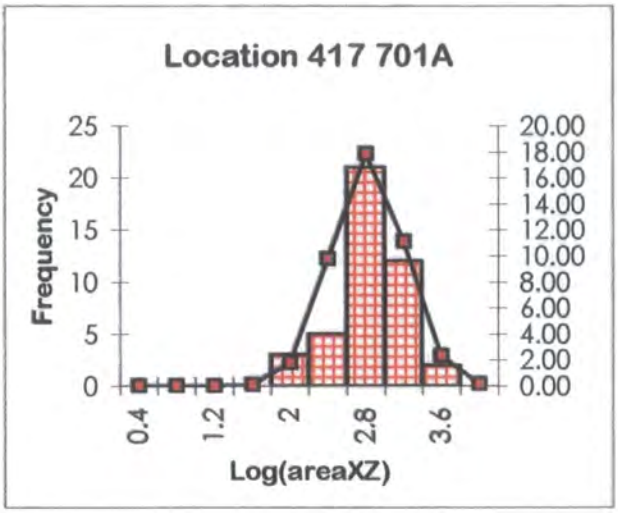

Strath Ossian Complex: Uisge Labhair
Intrusive Phase : The Sgòr Choinnich facies (G2)

Location [417 701]B

X Orientation	X	Z	X/Z	log(x/z)	log (X×Zπ/4)
168	5.40	1.70	3.18	0.50	2.35
025	10.00	3.80	2.63	0.42	1.87
180	7.00	2.20	3.18	0.50	2.49
142	8.50	3.00	2.83	0.45	2.52
164	8.40	3.20	2.63	0.42	2.62
176	5.10	2.30	2.22	0.35	2.50
020	8.50	3.20	2.66	0.42	1.70
173	8.00	3.70	2.16	0.33	2.70
096	7.80	5.70	1.37	0.14	2.63
170	7.80	3.80	2.05	0.31	2.71
089	7.10	5.30	1.34	0.13	2.57
005	3.90	2.20	1.77	0.25	0.94
154	8.90	6.30	1.41	0.15	2.88
159	14.80	9.30	1.59	0.20	3.06
023	9.50	3.10	3.06	0.49	1.75
102	7.30	5.00	1.46	0.16	2.60
179	6.40	2.20	2.91	0.46	2.49
013	102.00	2.70	37.78	1.58	1.44
161	7.80	2.60	3.00	0.48	2.52
340	4.70	1.20	3.92	0.59	2.51
159	8.70	5.30	1.64	0.22	2.82
153	14.20	8.70	1.63	0.21	3.02
009	3.30	1.60	2.06	0.31	1.05
144	8.70	3.40	2.56	0.41	2.58
140	8.10	2.80	2.89	0.46	2.49
170	5.70	2.90	1.97	0.29	2.59
163	8.00	3.00	2.67	0.43	2.58
299	21.00	3.70	5.68	0.75	2.94
022	8.50	3.80	2.24	0.35	1.82
175	8.50	3.80	2.24	0.35	2.72
099	7.40	5.50	1.35	0.13	2.63
024	9.80	3.40	2.88	0.46	1.81
169	8.20	4.00	2.05	0.31	2.73
164	4.90	1.60	3.06	0.49	2.31
090	7.80	5.20	1.50	0.18	2.57
126	32.00	17.50	1.83	0.26	3.24
156	8.60	6.00	1.43	0.16	2.87
156	14.50	9.00	1.61	0.21	3.04
007	3.60	1.90	1.89	0.28	1.02
174	9.00	5.60	1.61	0.21	2.88
175	5.00	1.60	3.13	0.49	2.34
173	5.40	2.60	2.08	0.32	2.55
026	8.60	4.30	2.00	0.30	1.94
180	7.50	2.30	3.26	0.51	2.51
177	8.80	4.10	2.15	0.33	2.76
167	8.50	4.30	1.98	0.30	2.75
091	7.90	5.70	1.39	0.14	2.61

sum	17.19	114.02
sum/N	0.36	2.38
average	2.28	237.42
wlog	1.45	37.65
N	48	48
S.D.	0.23	0.53
max	1.58	3.24
min	0.13	0.94

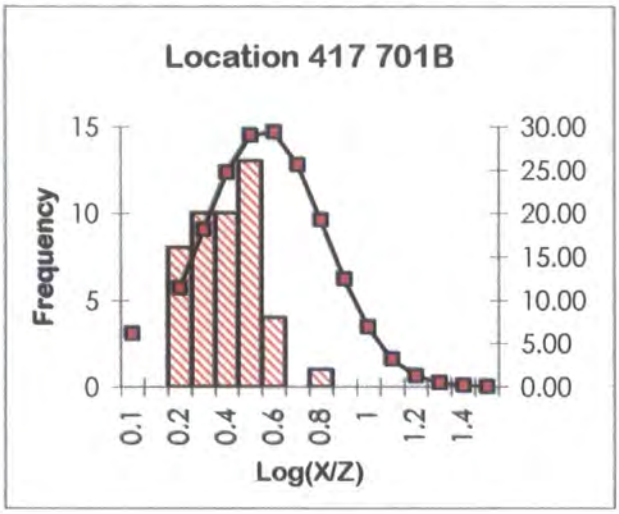

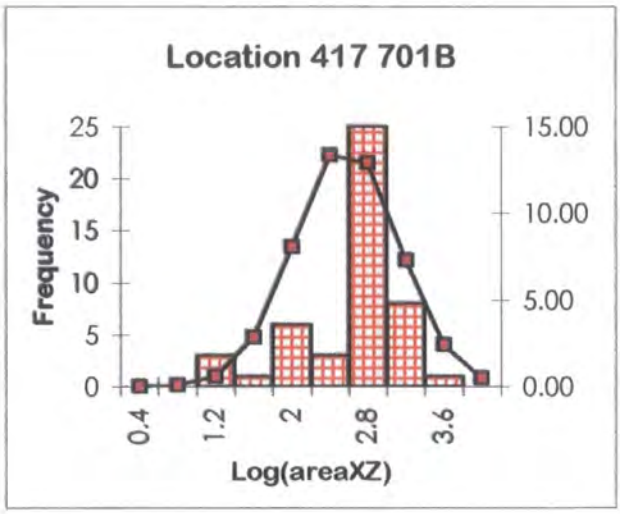

Strath Ossian Complex: Uisge Labhair
Intrusive Phase : The Sgòr Choinnich facies (G2)

Location [419 701]A

X Orientation	X	Z	X/Z	log(x/z)	log (X×Zπ/4)
107	9.00	4.30	2.09	0.32	2.56
068	8.00	3.20	2.50	0.40	2.23
102	13.40	8.00	1.68	0.22	2.81
C. R. Xenolith 094	16.00	3.10	5.16	0.71	2.36
024	8.00	3.00	2.67	0.43	1.75
127	6.00	2.00	3.00	0.48	2.30
124	27.00	13.00	2.08	0.32	3.10
128	12.40	3.20	3.88	0.59	2.51
080	6.80	3.60	1.89	0.28	2.35
095	10.70	7.40	1.45	0.16	2.74
084	5.00	2.00	2.50	0.40	2.12
043	7.30	5.00	1.46	0.16	2.23
140	5.90	4.60	1.28	0.11	2.70
111	8.70	4.80	1.81	0.26	2.62
095	12.60	5.80	2.17	0.34	2.64
175	7.20	5.10	1.41	0.15	2.85
105	9.00	3.70	2.43	0.39	2.48
104	13.40	8.60	1.56	0.19	2.85
069	8.30	3.50	2.37	0.38	2.28
109	9.20	4.80	1.92	0.28	2.61
127	11.40	3.00	3.80	0.58	2.48
114	8.10	4.20	1.93	0.29	2.58
048	11.80	5.40	2.19	0.34	2.31
085	4.60	1.80	2.56	0.41	2.08
128	5.40	2.00	2.70	0.43	2.30
023	7.70	2.70	2.85	0.46	1.69
098	13.20	7.50	1.76	0.25	2.76
066	7.50	3.10	2.42	0.38	2.21
128	12.00	3.00	4.00	0.60	2.48
080	6.20	3.60	1.72	0.24	2.35
096	10.30	7.20	1.43	0.16	2.73
140	5.40	4.50	1.20	0.08	2.69
070	24.00	13.00	1.85	0.27	2.85
112	8.40	4.50	1.87	0.27	2.60
054	12.00	5.80	2.07	0.32	2.39
173	7.00	4.70	1.49	0.17	2.81
168	4.00	1.50	2.67	0.43	2.30
045	7.70	5.20	1.48	0.17	2.26
085	5.00	2.60	1.92	0.28	2.24
126	6.10	2.50	2.44	0.39	2.39
027	8.20	3.40	2.41	0.38	1.86
082	6.10	3.10	1.97	0.29	2.30
099	9.80	7.10	1.38	0.14	2.74
140	5.40	3.90	1.38	0.14	2.63
171	6.70	4.40	1.52	0.18	2.77

sum	14.19	110.90
sum/N	0.32	2.46
average	2.07	291.39
wlog	0.63	5.08
N	45	45
S.D.	0.14	0.30
max	0.71	3.10
min	0.08	1.69

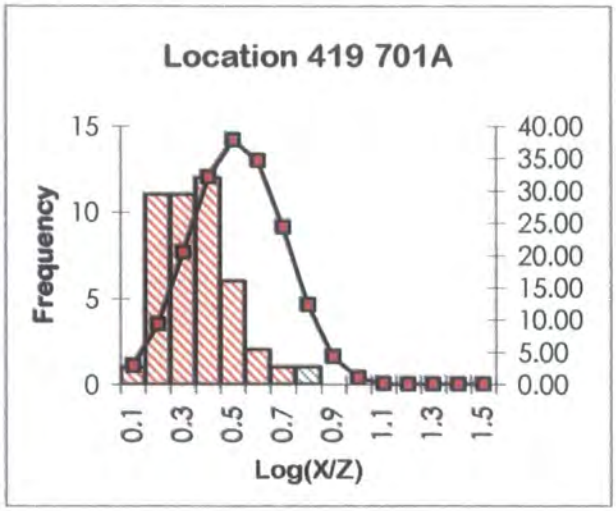

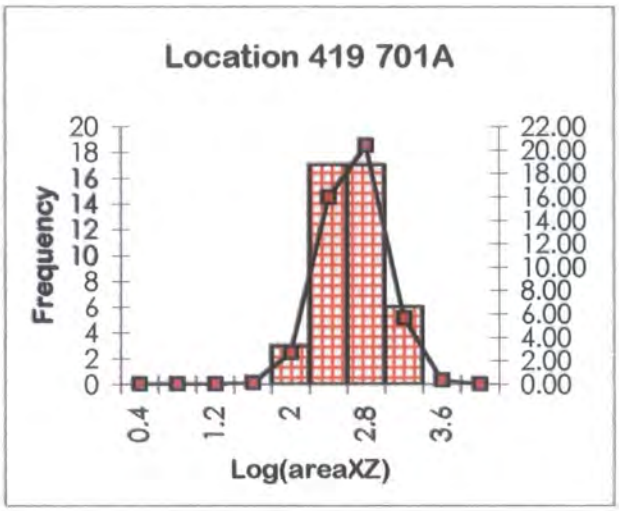

Strath Ossian Complex: Uisge Labhair
Intrusive Phase : The Sgòr Choinnich facies (G2)

Location [419 701]B

X Orientation	X	Z	X/Z	log(x/z)	log (X×Zπ/4)
096	9.9	3.3	3.00	0.48	1.41
065	7.7	3.7	2.08	0.32	1.35
076	6.9	4.1	1.68	0.23	1.35
057	13.4	6.3	2.13	0.33	1.82
066	10.7	3.5	3.06	0.49	1.47
044	15	7.7	1.95	0.29	1.96
068	11	2.8	3.93	0.59	1.38
067	9.5	3.5	2.71	0.43	1.42
065	6.3	4.5	1.40	0.15	1.35
065	7.5	2.3	3.26	0.51	1.13
047	10.3	4.5	2.29	0.36	1.56
072	8.4	4.6	1.83	0.26	1.48
069	7.6	5	1.52	0.18	1.47
063	14.5	6.8	2.13	0.33	1.89
064	11.4	3.2	3.56	0.55	1.46
048	14.6	7.3	2.00	0.30	1.92
061	7.9	5.1	1.55	0.19	1.50
061	10.7	2.3	4.65	0.67	1.29
074	13.2	8.3	1.59	0.20	1.93
063	11.8	4	2.95	0.47	1.57
095	9.8	4	2.45	0.39	1.49
051	6.8	4.8	1.42	0.15	1.41
070	8	2.6	3.08	0.49	1.21
068	11.2	3.8	2.95	0.47	1.52
050	14	6.5	2.15	0.33	1.85
098	7.3	4.7	1.55	0.19	1.43
065	8	4.22	1.90	0.28	1.42
062	7.5	3.5	2.14	0.33	1.31
052	9.8	3	3.27	0.51	1.36
066	7.8	3.2	2.44	0.39	1.29
072	6.8	5.2	1.31	0.12	1.44
071	10.2	4	2.55	0.41	1.51
065	9	2.8	3.21	0.51	1.30
069	11.6	3.4	3.41	0.53	1.49
069	14.5	7.2	2.01	0.30	1.91
068	10.2	2.4	4.25	0.63	1.28
066	15.8	8.1	1.95	0.29	2.00
064	14.3	7.2	1.99	0.30	1.91
065	9.7	3.6	2.69	0.43	1.44
063	6.6	4	1.65	0.22	1.32
048	6.5	2.1	3.10	0.49	1.03
064	6.8	2.2	3.09	0.49	1.07
067	5.8	4.2	1.38	0.14	1.28
068	9.3	2.9	3.21	0.51	1.33
063	10.9	4.3	2.53	0.40	1.57
065	8.7	4.7	1.85	0.27	1.51
067	11.6	4.6	2.52	0.40	1.62
066	10.7	3.1	3.45	0.54	1.42
066	13.6	5.7	2.39	0.38	1.78

063	5.6	4	1.40	0.15	1.25
072	10	4	2.50	0.40	1.50

sum	18.75	75.97
sum/N	0.37	1.49
average	2.33	30.87
wlog	0.55	4.54
N	51	51
S.D.	0.14	0.24
max	0.67	2.00
min	0.12	1.03

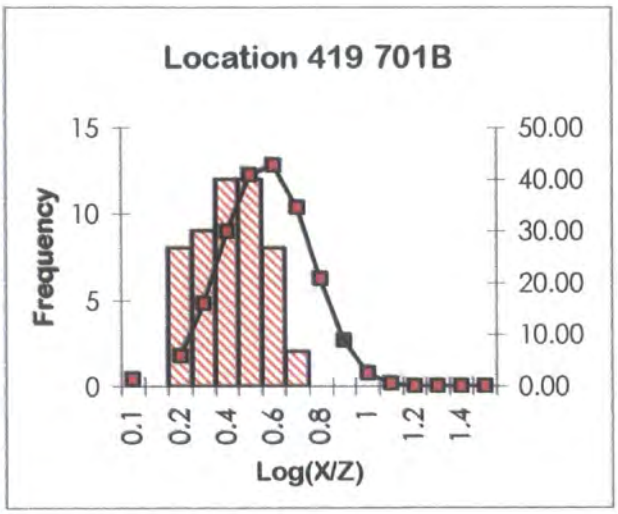

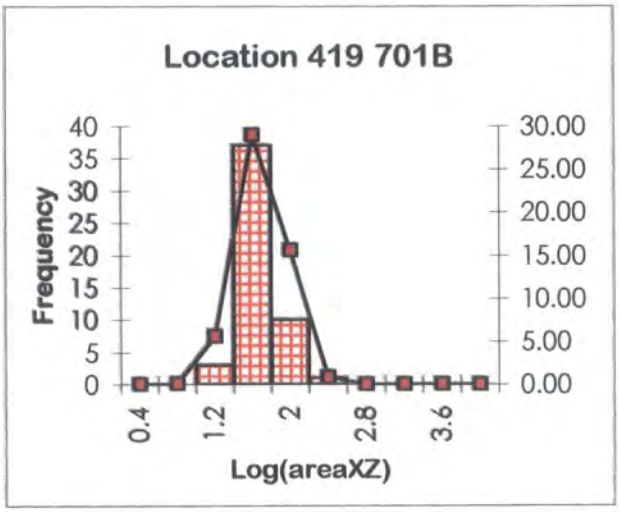

Strath Ossian Complex: Uisge Labhair
Intrusive Phase : The Sgòr Choinnich facies (G2)

Location [419 701]C

X Orientation	X	Z	X/Z	log(X/Z)	log (X×Zπ/4)
059	7.60	1.80	4.22	0.63	1.03
058	7.90	2.70	2.93	0.47	1.22
047	10.60	3.10	3.42	0.53	1.41
052	21.00	9.70	2.16	0.34	2.20
051	4.30	1.40	3.07	0.49	0.67
060	13.70	4.40	3.11	0.49	1.68
100	7.00	2.20	3.18	0.50	1.08
048	6.00	1.70	3.53	0.55	0.90
063	8.50	2.10	4.05	0.61	1.15
064	4.90	2.00	2.45	0.39	0.89
061	7.00	2.80	2.50	0.40	1.19
055	23.80	10.30	2.10	0.32	2.24
132	11.50	8.00	1.44	0.16	1.86
053	9.40	4.70	2.00	0.30	1.54
063	11.00	3.30	3.33	0.52	1.45
112	21.00	10.30	2.04	0.31	2.23
058	4.50	1.80	2.50	0.40	0.80
051	2.40	1.60	1.50	0.18	0.48
082	9.00	4.30	2.09	0.32	1.48
064	11.60	8.50	1.36	0.14	1.89
051	13.10	3.80	3.45	0.54	1.59
101	8.60	3.60	2.39	0.38	1.39
054	10.70	7.80	1.37	0.14	1.82
116	7.40	2.80	2.64	0.42	1.21
052	6.40	2.20	2.91	0.46	1.04
057	8.00	3.20	2.50	0.40	1.30
057	11.30	7.60	1.49	0.17	1.83
052	6.20	2.10	2.95	0.47	1.01
050	8.00	2.00	4.00	0.60	1.10
051	11.10	3.50	3.17	0.50	1.48
064	8.40	3.40	2.47	0.39	1.35
049	5.80	1.30	4.46	0.65	0.77
058	8.50	4.20	2.02	0.31	1.45
132	13.50	4.00	3.38	0.53	1.63
054	8.60	2.40	3.58	0.55	1.21

sum	14.54	47.59
sum/N	0.42	1.36
average	2.60	22.90
wlog	0.51	1.76
N	35	35
S.D.	0.14	0.44
max	0.65	2.24
min	0.14	0.48

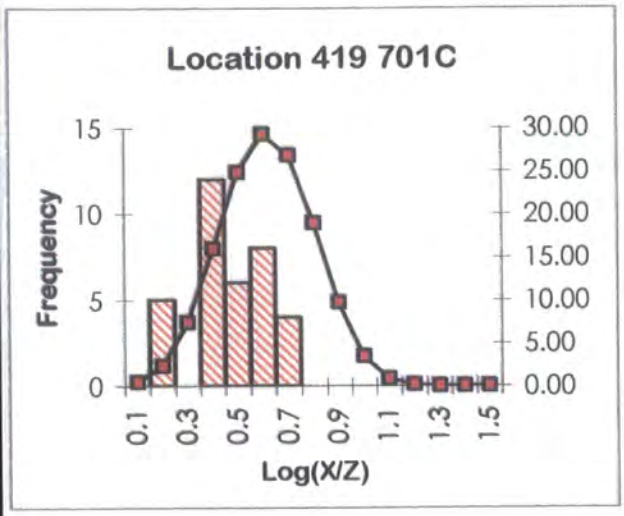
Location 419 701C
Frequency
15
10
5
0
30.00
25.00
20.00
15.00
10.00
5.00
0.00
0.1
0.3
0.5
0.7
0.9
1.1
1.3
1.5
Log(X/Z)

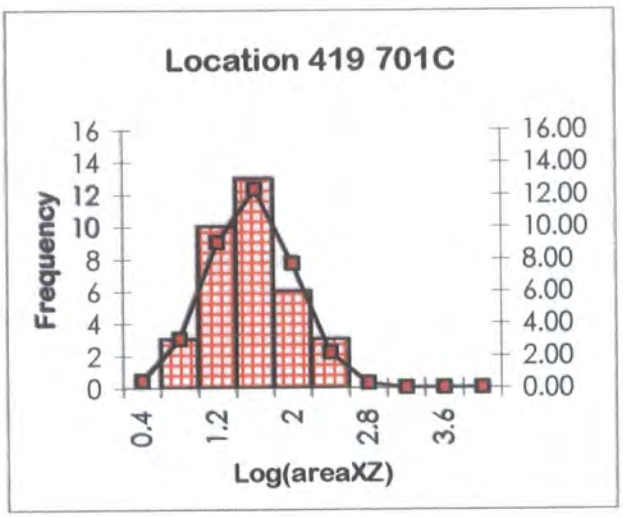
Location 419 701C
Frequency
16
14
12
10
8
6
4
2
0
16.00
14.00
12.00
10.00
8.00
6.00
4.00
2.00
0.00
0.4
1.2
2
2.8
3.6
Log(areaXZ)

Strath Ossian Complex: Uisge Labhair
Intrusive Phase : The Sgòr Choinnich facies (G2)

Location [420 701]A

X Orientation	X	Z	X/Z	log(X/Z)	log (X×Zπ/4)
072	17.00	11.80	1.44	0.16	2.20
160	14.00	6.00	2.33	0.37	1.82
050	17.00	8.90	1.91	0.28	2.07
077	7.40	4.10	1.80	0.26	1.38
058	11.50	3.50	3.29	0.52	1.50
058	9.30	4.20	2.21	0.35	1.49
040	13.50	4.20	3.21	0.51	1.65
068	16.50	7.40	2.23	0.35	1.98
064	10.50	5.50	1.91	0.28	1.66
158	8.20	4.10	2.00	0.30	1.42
110	20.80	9.00	2.31	0.36	2.17
057	12.00	3.20	3.75	0.57	1.48
057	6.80	2.70	2.52	0.40	1.16
050	6.60	4.30	1.53	0.19	1.35
052	7.00	4.50	1.56	0.19	1.39
058	7.00	3.10	2.26	0.35	1.23
056	12.40	3.40	3.65	0.56	1.52
157	8.20	4.70	1.74	0.24	1.48
065	11.10	5.50	2.02	0.30	1.68
068	16.70	7.80	2.14	0.33	2.01
042	13.90	4.40	3.16	0.50	1.68
060	9.80	4.30	2.28	0.36	1.52
064	11.60	4.00	2.90	0.46	1.56
072	7.60	4.50	1.69	0.23	1.43
048	17.40	9.10	1.91	0.28	2.09
158	14.10	6.50	2.17	0.34	1.86
074	17.50	11.90	1.47	0.17	2.21
045	13.30	3.80	3.50	0.54	1.60
070	16.10	7.20	2.24	0.35	1.96
067	10.40	5.00	2.08	0.32	1.61
152	7.70	4.00	1.93	0.28	1.38
055	11.80	2.80	4.21	0.62	1.41
056	6.40	2.50	2.56	0.41	1.10
053	6.30	4.00	1.58	0.20	1.30
075	16.90	11.30	1.50	0.17	2.18
159	13.50	5.90	2.29	0.36	1.80
048	16.80	8.50	1.98	0.30	2.05
076	7.00	3.90	1.79	0.25	1.33
065	11.50	2.90	3.97	0.60	1.42
058	8.70	4.20	2.07	0.32	1.46

sum	13.93	65.58
sum/N	0.35	1.64
average	2.23	43.61
wlog	0.47	1.11
N	40.00	40.00
S.D.	0.13	0.31
max	0.62	2.21
min	0.16	1.10

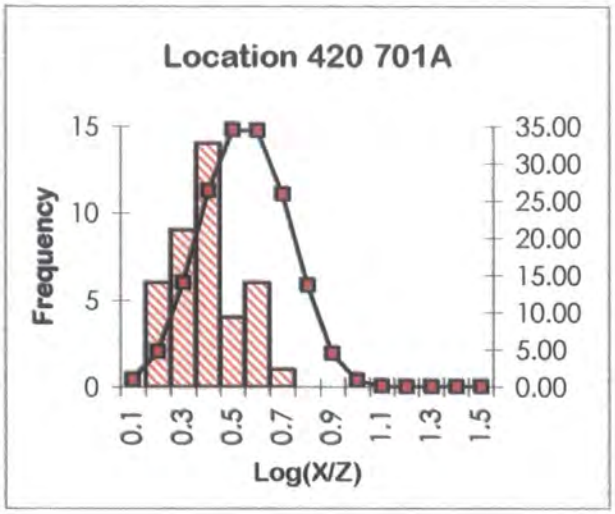

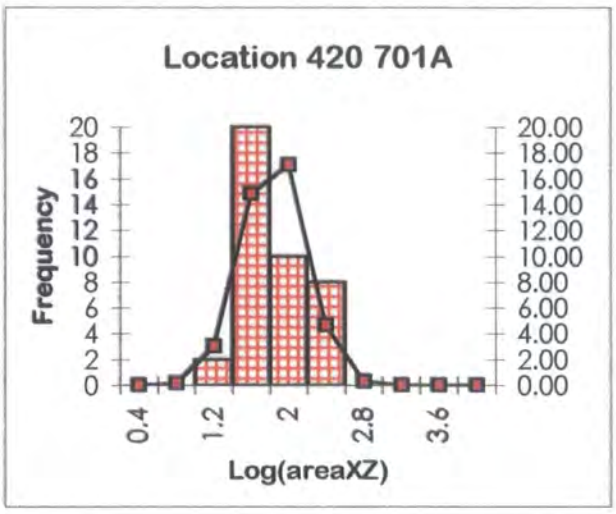

Strath Ossian Complex: Uisge Labhair
Intrusive Phase : The Sgòr Choinnich facies (G2)

Location [420 701]B

X	Z	X/Z	log(x/z)	log (X×Zπ/4)
25.00	12.20	2.05	0.31	2.38
7.00	2.60	2.69	0.43	1.16
6.00	2.10	2.86	0.46	1.00
7.00	2.50	2.80	0.45	1.14
8.00	2.50	3.20	0.51	1.20
48.00	30.00	1.60	0.20	3.05
22.50	6.80	3.16	0.50	2.06
9.00	2.30	3.91	0.59	1.21
7.00	2.70	2.59	0.41	1.17
21.00	9.00	2.33	0.37	2.17
5.20	2.90	1.79	0.25	1.07
7.00	3.50	2.00	0.30	1.28
6.50	4.00	1.63	0.21	1.31
20.60	9.40	2.19	0.34	2.18
8.80	2.50	3.52	0.55	1.24
7.40	3.10	2.39	0.38	1.26
5.70	2.40	2.38	0.38	1.03
24.60	12.60	1.95	0.29	2.39
6.40	3.20	2.00	0.30	1.21
6.30	3.20	1.97	0.29	1.20
21.10	7.20	2.93	0.47	2.08
6.20	3.50	1.77	0.25	1.23

X	Z	X/Z	log(x/z)	log (X×Zπ/4)
4.60	3.50	1.31	0.12	1.10
7.60	2.90	2.62	0.42	1.24
5.80	2.30	2.52	0.40	1.02
21.40	8.60	2.49	0.40	2.16
7.50	2.20	3.41	0.53	1.11
9.50	1.80	5.28	0.72	1.13
21.80	6.50	3.35	0.53	2.05
8.70	1.80	4.83	0.68	1.09
7.40	2.10	3.52	0.55	1.09
6.60	1.50	4.40	0.64	0.89
7.40	2.30	3.22	0.51	1.13
25.70	11.60	2.22	0.35	2.37

sum	14.08	50.38
sum/N	0.41	1.48
average	2.59	30.32
wlog	0.60	2.93
N	34.00	34.00
S.D.	0.14	0.56
max	0.72	3.05
min	0.12	0.89

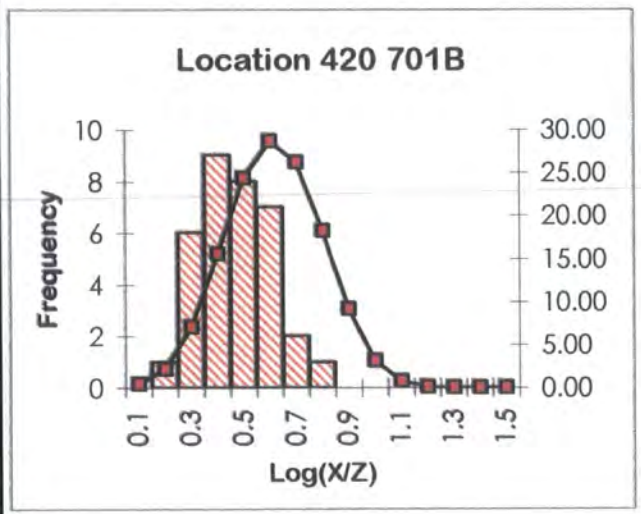

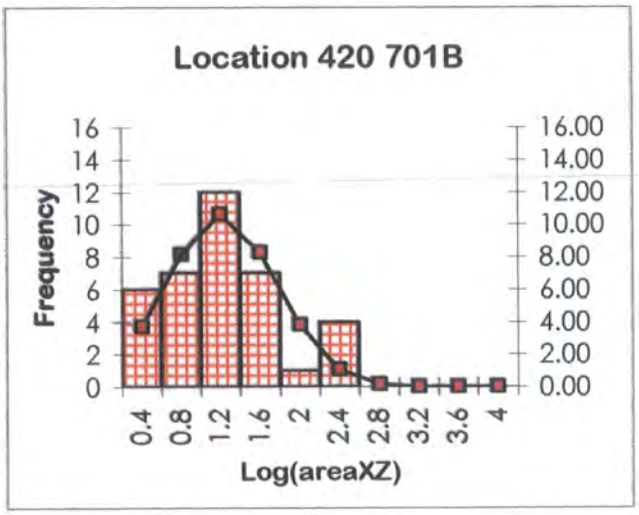

Strath Ossian Complex: Uisge Labhair
Intrusive Phase : The Sgòr Choinnich facies (G2)

Location [421 701]

X	Z	X/Z	log(x/z)	log (X×Zπ/4)
27.10	8.30	3.27	0.51	2.25
29.30	8.60	3.41	0.53	2.30
26.70	10.50	2.54	0.41	2.34
17.10	6.50	2.63	0.42	1.94
20.00	5.70	3.51	0.55	1.95
19.20	6.60	2.91	0.46	2.00
28.60	11.20	2.55	0.41	2.40
66.40	13.70	4.85	0.69	2.85
32.70	9.40	3.48	0.54	2.38
70.90	17.70	4.01	0.60	2.99
24.70	4.80	5.15	0.71	1.97
20.20	6.50	3.11	0.49	2.01
33.50	12.20	2.75	0.44	2.51
39.30	16.10	2.44	0.39	2.70
68.10	18.30	3.72	0.57	2.99
20.40	4.00	5.10	0.71	1.81
21.00	10.40	2.02	0.31	2.23
39.30	11.80	3.33	0.52	2.56
39.80	16.30	2.44	0.39	2.71
46.60	18.00	2.59	0.41	2.82
37.00	5.50	6.73	0.83	2.20
22.10	7.00	3.16	0.50	2.08
26.60	4.50	5.91	0.77	1.97
11.50	4.10	2.80	0.45	1.57
12.10	3.50	3.46	0.54	1.52
15.50	5.30	2.92	0.47	1.81
52.30	13.50	3.87	0.59	2.74
23.40	6.70	3.49	0.54	2.09
12.70	4.40	2.89	0.46	1.64
39.50	10.50	3.76	0.58	2.51
29.50	5.50	5.36	0.73	2.11
40.10	8.90	4.51	0.65	2.45
8.90	3.10	2.87	0.46	1.34
27.30	3.80	7.18	0.86	1.91
28.10	7.30	3.85	0.59	2.21
14.20	6.60	2.15	0.33	1.87
28.60	4.20	6.81	0.83	1.97
11.80	2.70	4.37	0.64	1.40
16.70	3.10	5.39	0.73	1.61

X	Z	X/Z	log(x/z)	log (X×Zπ/4)
39.10	10.50	3.72	0.57	2.51
23.40	7.10	3.30	0.52	2.12
14.20	3.70	3.84	0.58	1.62
28.70	6.50	4.42	0.64	2.17
12.40	3.10	4.00	0.60	1.48
20.50	2.60	7.88	0.90	1.62
17.00	7.10	2.39	0.38	1.98
20.20	5.50	3.67	0.56	1.94
33.50	15.20	2.20	0.34	2.60
19.50	5.50	3.55	0.55	1.93
25.50	4.50	5.67	0.75	1.95
25.30	4.60	5.50	0.74	1.96
47.60	5.30	8.98	0.95	2.30
59.60	17.00	3.51	0.54	2.90
10.00	3.60	2.78	0.44	1.45
30.20	9.10	3.32	0.52	2.33
21.10	5.80	3.64	0.56	1.98
35.80	5.10	7.02	0.85	2.16
12.10	3.10	3.90	0.59	1.47
21.10	4.10	5.15	0.71	1.83
32.50	9.10	3.57	0.55	2.37
14.60	3.50	4.17	0.62	1.60
11.50	2.50	4.60	0.66	1.35
13.50	3.70	3.65	0.56	1.59
9.00	2.50	3.60	0.56	1.25
11.50	2.70	4.26	0.63	1.39
22.00	9.80	2.24	0.35	2.23
21.00	10.00	2.10	0.32	2.22
27.60	8.50	3.25	0.51	2.27

sum	38.68	141.27
sum/N	0.57	2.08
average	3.71	119.56
wlog	0.65	2.69
N	68.00	68.00
S.D.	0.15	0.44
max	0.95	2.99
min	0.31	1.25

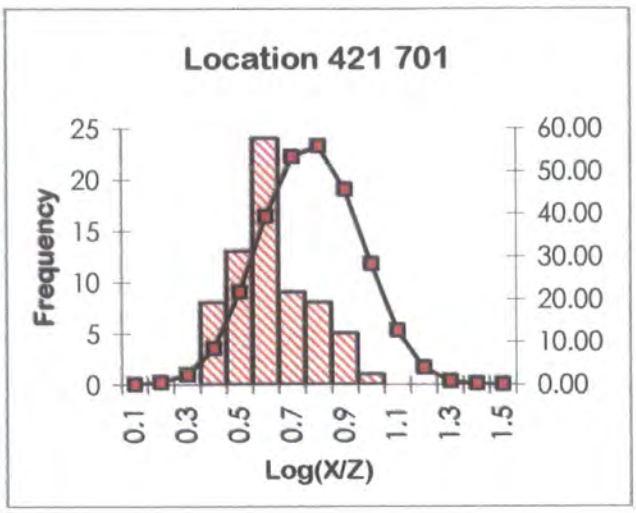
Location 421 701
Frequency
25
20
15
10
5
0
60.00
50.00
40.00
30.00
20.00
10.00
0.00
0.1
0.3
0.5
0.7
0.9
1.1
1.3
1.5
Log(X/Z)

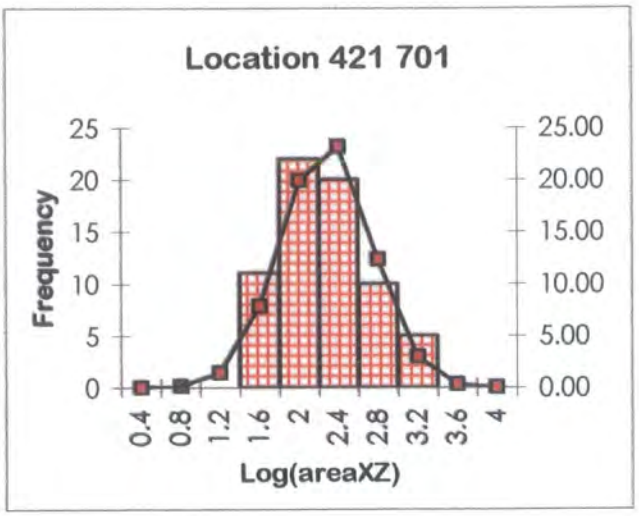
Location 421 701
Frequency
25
20
15
10
5
0
25.00
20.00
15.00
10.00
5.00
0.00
0.4
0.8
1.2
1.6
2
2.4
2.8
3.2
3.6
4
Log(areaXZ)

REFERENCES

AFTALION, M., VAN BREEMAN, O. & BOWES, D. R. 1984. Age constraints on basement of the Midland Valley Scotland. *Transactions of the Royal Geological Society of Edinburgh: Earth Sciences,* **75**, 53-64.

ALLAN, W. 1970. The Morven-Cabrach basic intrusion. *Scottish Journal of Geology,* **6**, 53-72.

ANDERSON, E. M. 1951. *The dynamics of faulting and dyke formation with applications to Britain.* Oliver and Boyd, Edinburgh.

ANDERSON, J. G. C. 1935. The marginal intrusions of Ben Nevis, the Coille Lianachain complex and the Ben Nevis dyke swarm. *Transactions of the Geological Society of Glasgow,* **19**, 225-269.

ANDERSON, J. G. C. 1937. The Etive Granite Complex. *Quarterly Journal of the Geological Society of London,* **93**, 487-533.

ANDERSON, J. G. C. 1956. The Moinian and Dalradian rocks between Glen Roy and the Monadliath Mountains, Inverness-shire. *Transactions of the Geological Society of Glasgow,* **63**, 15-36.

ANDERTON, R. 1976. Tidal-shelf sedimentation: an example from the Scottish Dalradian. *Sedimentology,* **23**, 429-458.

ANDERTON, R. 1977. A field guide to the Dalradian rocks of Jura, Argyll. *Scottish Journal of Geology,* **13**, 135-142.

ANDERTON, R. 1985. Sedimentation and tectonics in the Scottish Dalradian. *Scottish Journal of Geology,* **21**, 407-436.

ANDREWS, I. J. 1985. The deep structure of the Moine Thrust, southwest of Shetland. *Scottish Journal of Geology,* **21**, 213-217.

ARZI, A. A. 1978. Critical phenomena in the rheology of partially melted rocks. *Tectonophysics,* **44**, 173-184.

ASHCROFT, W. A., KNELLER, B. C., LESLIE, A. G & MUNRO, M. 1984. Major shear zones and autochtonous Dalradian in the north-east Scottish Caledonides. *Nature,* **310**, 760-762.

ASHWORTH, J. R. 1975. The sillimanite zones of the Huntly-Portsoy area in the north-east Dalradian, Scotland. *Geological Magazine,* **112**, 113-136.

ATTFIELD, P. 1987. The structural history of the Canisp Shear Zone. *In:* PARK, R. G. & TARNEY, J. (eds) *Evolution of the Lewisian and comparable Precambrian high grade terrains.* Geological Society, London, Special Publication, **27**, 165-173.

BAILEY, E. B. 1934. West Highland tectonics: Loch Leven to Glenn Roy. *Quarterly Journal of the Geological Society , London,* **90**, 462-523.

BAILEY, E. B. 1960. *Geology of Ben Nevis and Glencoe (Sheet 53).* Memoirs of the Geological Survey, U.K. (2nd Edition).

BAILEY, E. B. & MAUFE, A. B. 1916. *The Geology of Ben Nevis and Glencoe,* Memoirs of the Geological Survey of Great Britain, Sheet 53.

BAILEY, E. B., CLOUGH, C. T., WRIGHT, W. B., RICHEY, J. E. & WILSON, G. V. 1924. *Tertiary and post-Tertiary geology of Mull, Loch Aline and Oban.* Memoirs of the Geological Survey of Great Britain, Sheet 53.

BAILEY, E. B. & McCALLIEN, W. J. 1937. Perthshire tectonics: Schiehallion to Glen Lyon. *Transactions of the Royal Society of Edinburgh,* **54**, 79-118.

BAKER, A. J. 1987. Models for the tectonothermal evolution of the eastern Dalradian of Scotland. *Journal of Metamorphic Geology,* **5**, 101-118.

BALK, R. 1937. Structural behaviour of igneous rocks. *Memoir of the Geological Society of America,* **5**, 177pp.

BAMFORD, D. 1979. Seismic constraints on the deep geology of the Caledonides of northern Britain. *In:* HARRIS, A. L., HOLLAND, C. H. & LEAKE, B. E. (eds) *The Caledonides of the British Isles - reviewed.* Geological Society, London, Special Publication, **8,** 93-100.

BAMFORD, D., NUNN, K., PRODEHL, C. & JACOB, B. 1978. LISPB-IV. Crustal structure of northern Britain. *Geophysical Journal of the Royal Astronomical Society,* **54**, 43-60.

BARD, J. P. 1986. *Microtextures of igneous and metamorphic rocks.* Dordtecht D. Reidel, 264pp.

BARR, D., ROBERTS, A. M., HIGHTON, A. J., PARSON, L. M. & HARRIS, A. L. 1985. Structural setting and geochronological significance of the West Highland Granitic Gneiss, a deformed early granite within Proterozoic, Moine rocks of NW Scotland. *Journal of the Geological Society , London,* **142**, 663-75.

BARR, D., HOLDSWORTH, R. E. & ROBERTS, A. M. 1986. Caledonian ductile thrusting in a Precambrian metamorphic complex: The Moine of northwestern Scotland. *Geological Society of America Bulletin,* **97**, 754-764.

BARRITT, S. D. 1983. *The controls of radioelement distribution in the Etive and Cairngorm granites: implications for heat production.* PhD thesis, Open University.

BARROW, G. 1912. On the geology of lower Deeside and the southern Highland Border. *Proceedings of the Geological Association,* **23**, 268-273.

BATCHELOR, R, A. 1984. *Geochemistry of the Etive Granitoid Complex, Argyll, Scotland.* University of St. Andrews, Ph.D. thesis (unpublished).

BATCHELOR, R. A. 1987. Geochemical and petrological characteristics of the Etive granitoid complex, Argyll. *Scottish Journal of Geology,* **23**, 227-249.

BATEMAN, R. 1984. On the role of diapirism in the segregation, ascent and final emplacement of granitoids. *Tectonophysics,* **110**, 211-231.

BATEMAN, R. 1985. Aureole deformation by flattening around a diapir during in situ ballooning; the Cannibal Creek Granite. *Journal of Geology,* **93, 3**, 293-310.

BAXTER, A. N. & MITCHELL, J. G. 1984. Camptonite-monchiquite dyke swarms of Northern Scotland; age relationships and their implications. *Scottish Journal of Geology,* **20**, 297-308.

BEACH, A. 1975. The geometry of en-echelon vein array. *Tectonophysics,* **28**, 245-263.

BEACH, A., COWARD, M. P. & GRAHAM, R. H. 1974. An interpretation of the structural evolution of the Laxford front. *Scottish Journal of Geology,* **9**, 294-308.

BEACH, A. & TARNEY, J. 1978. Major and trace element patterns established during retrogressive metamorphism of granulite facies gneisses, NW Scotland. *Precambrian Research,* **7**, 325-348.

BEDDOE-STEPHENS, B. 1990. Pressures and temperatures of Dalradian metamorphism and the andalusite-kyanite transformation in the northeast Grampians. *Scottish Journal of Geology,* **26**, 3-14.

BEHRMANN, J. H. 1987. A precautionary note on shear bands as kinematic indicators. *Journal of Structural Geology*, **9**, 659-666.

BELL, T. H. 1981. Foliation development - the contribution, geometry and significance of progressive, bolk, inhomogeneous shortening. *Tectonophysics*, **75**, 273-296.

BELL, T. H. 1985. Deformation partitioing and porphyroblast rotation in metamorphic rocks: a radical reinterpretation; *Journal of Metamorphic Geology*, **3**, 109-118.

BELL, T. H. & HAMMOND, R. L. 1984. On the internal geometry of mylonite zones; *Journal of Geology*, **92**, 667-686.

BERGANTZ, G. W. 1989. Underplating and partial melting: Implications for melt generation and extraction. *Science,* **245**, 1093-1095.

BERGER, A. R. 1971. Dynamic analysis using dykes with oblique internal foliations; *Geological Society of America Bulletin*, **82**, 781-786.

BERGER, A. R. & PITCHER, W. S. 1970. Structures in granitic rocks. A commentary and a critique on granite tectonics. *Proceedings of the Geological Association of London,* **81**, 441-461.

BERGER, P. & JOHNSON, A. W. 1980. First order analysis of deformation on a thrust sheet moving over a ramp. *Tectonophysics,* **70**, T9-T24.

BERGMAN, S. C. 1987. Lamproites and other potassium-rich igneous rocks: a review of their occurrences, mineralogy and geochemisrty. *In:* FITTON, J. G. & UPTON, B. G. J. (eds), *Alkaline Igneous Rocks.* Geological Society, London, Special Publication, **30**, 103-190.

BERNER, H., RAMBERG, H. & STEPHANSSON, O. 1972. Diapirism in theory and experiment. *Tectonophysics*, **15**, 197-218.

BERTHE, D., CHOUKROUNE, P., & JEGOUZO, P. 1979a. Orthogneiss, mylonite and non-coaxial deformation of granites: the example of the South Armoricain shear zone; *Journal of Structural Geology*, **1**, 31-42.

BERTHE, D., CHOUKROUNE, P., & GAPAIS, D. 1979b. Orientations préfèrentielles du quartz et orthogneissification progressive en régime cisaillant: l'example du cisaillement sud-armoricain; *Bulletin de Minéralogie*, **102**, 265-272.

BEUTNER, E. C. & DIEGEL, F. A. 1985. Determination of fold kinematics from syntectonic fibres in pressure shadows, Martinsburg Slate, New Jersey*; American Journal of Science*, **285**, 16-50.

BIRD, P. 1979. Continental delamination and the Colorado Plateau. Journal of *Geophysics,* **84**, 7561-71.

BLANCHARD, J. P., BOYER, P. & GAGNY, C. 1979. Un nouveau critère de sens de mise en place dans une caisse filonienne: le "pincement" des minéreaux aux Epontes. *Tectonophysics,* **53**, 1-25.

BLAXLAND, A. B., AFTALION, M. & VAN BREEMAN, O. 1979. Pb isotopic composition of feldspars from Scottish Caledonian granites and the nature of the underlying crust. *Scottish Journal of Geology,* **15**, 139-151.

BLUMENFELD, P. 1983. Le "fuilage des mégacristaux", un critere d'écoulement rotationnel pour les flu roches magmatiques: aplication au granite de Barbey-Séroux (Vosages, France). *Bull. Soc. Geol.*, 309-18.
BLUMENFELD, P. & BOUCHEZ, J-L. 1988. Shear criteria in granite and migmatite deformed in the magmatic and solid states. *Journal of Structural Geology,* **10**, 361-372.

BLYTH, F. G. H. 1949. The sheared porphyrite dykes of South Galloway. *Journal of the Geological Society, London,* **105**, 393-421.

BLYTH, F. G. H. 1954. The southern margin of the Cairnsmore of Fleet granite at the Clints of Dromore, Galloway. *Proceedings of the Geological Association,* **65**, 224-250.

BOHLEN, S. R. 1991. On the formation of granulites. *Journal of Metamorphic Geology,* **9**, 223-229.

BOHLEN, S. R. & MEZGER, K. 1989. Origin of granulite terranes and the formation of the lowermost continental crust. *Science,* **224**, 326-329.

BOTT, M. H. P., HOLLAND, J. G. STONY, P. G. & WATTS, A. B. 1972. Geophysical evidence concerning the structure of the Lewisian of Sutherland, N.W. Scotland. *Journal of the Geological Society, London,* **128**, 559-612.

BOTTINGA, Y. & WEILL, D. F. 1972. The viscosity of magmatic silicate liquids: a model for calculation. *American Journal of Science,* **272**, 438-475.

BOWES, D. R. & WRIGHT, A. E. 1967. The explosion-breccia pipes near Kentallen, Scotland, and their geological setting. *Transactions of the Royal Society of Edinburgh: Earth Sciences,* **67**, 109-143.
BOYER, S. & ELLIOTT, D. 1982. Thrust systems. *Bull. Am. Assoc. Pet. Geol.*, **66**, 1196-1230.

BRANNEY, M. J. & KOKELARR, B. P. 1994. Volcanotectonic faulting, soft-state deformation, and rheomorphism of tuffs during the development of a piecemeal caldera, English Lake District. *Geological Society of America Bulletin,* **106**, 507-530.

BREWER, J. A., MATTHEWS, D. H., WARNER, M. R., HALL, J., SMYTHE, D. K. & WHITTINGTON, R. J. 1983. BIRPS deep seismic reflection studies of the British Caledonides. *Nature,* **305**, 206-210.

BREWER, J. A. & SMYTHE, D. 1984. MOIST and the continuity of crustal reflector geometry along the Caledonian-Appalachian orogen. *Journal of the Geological Society, London,* **141**, 105-120.

BREWER, M. S., BROOK, M. POWELL, D. 1979. Dating of the tectonometamorphic history of the SE Moine, Scotland. *In:* HARRIS, A. L., HOLLAND, C. H. & LEAKE, B. E. (eds) *The Caledonides of the British Isles - reviewed.* Geological Society, London, Special Publication, **8**, 129-137.

BRIDEN, J. C., TURNELL, H. B., WATTS, D. R., McCLELLAND-BROWN, E. & EVERETT, S. 1982. Palaeomagnetism of the Scottish Highlands and the question of magnitude of displacement on the Great Glen Fault. *Abstracts of European Geophysical Society meeting, Leeds,* **74**.

BROOK, M., POWELL, D. & BREWER, M. S. 1976. Grenville age for rocks in the Moine of north-western Scotland. *Nature,* **260**, 515-7.

BROOK, M., POWELL, D. & BREWER, M. S. 1977. Grenville events in the Moine rocks of the northern Highlands, Scotland. *Journal of the Geological Society, London,* **133**, 489-96.

BROWN, G. C., CASSIDY, J., LOCKE, C. A., PLANT, J. A. & SIMPSON, P. R. 1981. Caledonian plutonism in Britain: A summary. *Journal of Geophysical Reserch,* **86**, B11, 10502-10514.

BROWN, J. F. 1875. Rb-Sr studies and related geochemistry on the Caledonian calc-alkaline igneous rocks of N.W. Argyllshire. *University of Oxford, Ph.D thesis (unpublished).*

BROWN, M. 1992. The generation, segregation, ascent and emplacement of granite magma: the migmatite-to-crustally-derived granite connection in thickened orogens. *Earth-Science Reviews,* **36**, 83-130.

BROWN, M. 1994. The generation, segregation, ascent and emplacement of granite magma: The migmatite-to-crustally-derived granite connection in thickened orogens. *Earth-Science Reviews,* **36**, 83-130.

BROWN, P. E., MILLER, J. E. & GRASTY, R. L. 1968. Isotopic ages of late Caledonian granitic intrusions in the British Isles. *Proceedings of the Yorkshire Geological Society,* **36**, 251-276.

BRUNEL, M. 1980. Quartz fabrics in shear-zone mylonite: evidence for a major imprint due to late strain increments. *Tectonophysics*, **64**, T33-T44.
BRUNEL, M. 1986. Ductile thrusting in the Himalayas: shear sense criteria and stretching lineations; *Tectonophysics*, **5**, 247-265.

BRUN, J. P. & PONS, J. 1981. Strain patterns of pluton emplacement in a crust undergoing non-coaxial deformation, Sierra Morena, Southern Spain. *Journal of Structural Geology,* **3,** 219-230.

BRUN, J. P, GAPAIS, D., COGNE, J. P., LEDRU, P. & VIGNERESSE, J. L. 1990. The Flamanville granite (northwestern France): An unequivocal example of a syntectonically expanding pluton. *Geological Journal,* **25**, 271-286.

BUDDINGTON, A. F. 1959. Granite emplacement with special reference to North America. *Geological Society of America Bulletin,* **70**, 671-747.
BUSSEL, M. A. 1979. Structures of the south-west margin of the Glencoe fault intrusion on An-t-Sron. *Scottish Journal of Geology,* **15**, 279-287.

BUTLER, R. W. H. 1986. Structural evolution in the Moine of NW Scotland: A Caledonian linked thrust system? *Geological Magazine,* **123**, 1-11.

BUTLER, R. W. H. & COWARD, M. P. 1984. Geological constraints, structural evolution, and deep geology of the northwest Scottish Caledonides. *Tectonics,* **3**, 347-365.

CASTRO, A. 1986. Sructural pattern and ascent model in the Central Extramadura batholith, Hercynian belt, Spain. *Journal of Structural Geology,* **8,** 633-645.

CHAPMAN,H. J. 1979. 2390 Myr Rb-Sr whole rock age for the Scourie dykes of north-west Scotland. *Nature,* **277**, 642-643.

CHAPMAN, H. J. & MOORBATH, S. 1977. Lead isotope measurements from the oldest recognised Lewisian gneisses of north-west Scotland. *Nature,* **268**, 41-42.

CHAPPELL, B. W. & WHITE, A. J. R. 1974. Two contrasting granite types. *Pacific Geology,* **8**, 173-174.

CHEADLE, M., McGEARY, S., WARNER, M. R. & MATTHEWS, D. H. 1987. Extensional structures on the U.K. continental shelf: a review of evidence from deep seimic profiling. *In:* COWARD, M. P., DEWEY, J. F. & HANCOCK, L. (eds) *Continental Extension tectonics* Geological Society, London, Special Publication, **28,** 445-465.

CHOUKROUNE, P. 1971. Contribution à l'étude des mécanismes de la déformation avec schistosité grace aux cristallisations syncinématiques dans les "zones abritées" ("pressure shadows"; *Bulletin de la Societé géologique de France*, **13**, 257-271.

CHOUKROUNE, P. & LAGARDE, J. L. 1977. Plans de schistosité et déformation rotationelle: l'exemple du gneiss de Champtoceaux (Massif Armoricain); *Compte Rendue de l'Academie des Sciences de Paris*, **284**, 2331-2334.

CHOUKROUNE, P. & SEQURET, M. 1968. Exemple de relations entre joints de cisaillement, fentes de tension, plis et schistosité (autochthone de la nappe de Gavarnie - Pyrenées Centrales; *Revue de Géographie physique et de Géologie dynamique*, **10**, 239-247.
CLAYBURN, J. A. P. 1981. *Age and petrogenetic studies of some magmatic and metamorphic rocks in the Grampian Highlands*. Oxford University, thesis (unpublished).

CLAYBURN, J. A. P., HARMON, R. S., PANKHURST, R. J. & BROWN, J. F. 1983. Sr, O and Pb isotopic evidence for the origin and evolution of the Etive complex, Scotland. *Nature*, **303**, 492-497.

CLEMENS, J. D. & MAWER, C. K. 1992. Granitic magma transport by fracture propagation. *Tectonophysics*, **204**, 339-360.
CLIFFORD, T. N. 1957. The stratigraphy and structure of part of the Kintail district of southern Ross-shire; its relation to the Northern Highlands. *Quarterly Journal of the Geological Society of London*, **113**, 57-92.

CLOUGH, C. T. 1910. *The Geology of East Lothian (Sheet 33)*. Memoirs of the Geological Survey, U.K.

CLOUGH, C. T., MAUFE, H. B. & BAILEY, E. B. 1909. The cauldron subsidence of Glen Coe and associated igneous phenomena. *Quarterly Journal of the Geological Society of London*, **65**, 611-676.

COBBING, E. J., PITCHER, W. S., WILSON, J. J., BALDOCK, J. W., TAYLOR, W. P., McCOURT, W. J. & SNELLING, N. J. 1981. The geology of the western Cordillera of northern Peru. *Institute of Geological Sciences (London). Overseas Memoir*, **5**, 143pp.

COBBOLD, P. R. 1977. Description and origin of banded deformation structures. 1: Regional strain, local perturbations and deformation bands. *Canadian Journal of Earth Sciences*, **14**, 1721-1731.

COBBOLD, P. R., MEANS, W. D. & BAYLY, M. B. 1984. Jumps in deformation gradients and particle velocities across propagating coherent boundaries. *Tectonophysics*, **108**, 283-298.

COOK, J. & GORDON, J. E. 1964. A mechanism for the control of crack propagation in all-brittle systems. *Royal Society of London Proceedings*, **282**, 508-520.

COURRIOUX, G. 1987. Oblique diapirism: the Criffel granodiorite/granite zoned pluton (southwest Scotland). *Journal of Structural Geology*, **9**, 313-350.

COWARD, M. P. 1982. Surge zones in the Moine Thrust Zone of NW Scotland. *Journal of Structural Geology*, **4**, 247-256.

COWARD, M. P. 1983. The thrust and shear zones of the Moine Thrust Zone and the NW Scottish Caledonides. *Journal of the Geological Society of London*, **140**, 795-811.

COWARD, M. P. & KIM, J. H. 1981. Strain within thrust sheets. *In* McCLAY, K. R. & PRICE, N. J. (eds) *Thrust and Nappe Tectonics*. Geological Society, London, Special Publication, **9**, 275-292.

COWARD, M. P. & POTTS, G. J. 1983. Complex strain patterns developed at the frontal and latteral tips to shear zones and thrust zones. *Journal of Structural Geology*, **5**, 383-399.

COWARD, M. P. & PARK, R. G. 1987. The role of mid-crustal shear zones in the Early Proterozoic evolution of the Lewisian. *In:* PARK, R. G. & TARNEY, J. (eds) *Evolution of the Lewisian and comparable Precambrian high grade terrains*. Geological Society, London, Special Publication, **27**, 127-138.

CRAIG, G. Y. 1991. *Geology of Scotland*. Geological Society of London (3rd Edition).

CRUDEN, A. R. 1988. Deformation around a rising diapir modelled by creeping flow past a sphere. *Tectonics*, **7**, 1091-1101.

CRUDEN, A. R. 1990. Flow and fabric development during the diapiric rise of magma. *Journal of Geology,* **98**, 681-90.

DALZIEL, I. W. D. 1963. Zircons from the granitic gneiss of western Ardgour, Argyll: their bearing on its origin. *Transactions of the Geological Society, Edinburgh,* **19**, 349-362.

DALZIEL, I. W. D. 1966. A structural study of the granitic gneiss of western Ardgour, Argyll & Inverness-shire. *Scottish Journal of Geology,* **2**, 125-152.

DAVIES, G. H., GARDULSKI, A. F. & LISTER, G. S. 1987. Shear zone origin of quartzite mylonite and mylonitic pegmatite in the Coyotte Mountains metamorphic core complex, Arizona. *Journal of Structural Geology*, **9**, 289-297.

DAVIS, G. L. 1978. Zircons from the upper mantle. *Carnegie Institute of Washington Yearb.*, **77**, 895-7.

DEN TEX, E. 1969. Origin of ultramafic rocks, their tectonic setting and history. *Tectonophysics,* **7**, 457-462.

DE SOUZA, H. A. F. 1979. *The geochronology of Scottish Carboniferous volcanism.* University of Edinburgh, Ph.D. thesis (unpublished).

DE WIT, M. J. 1976. Metamorphic textures and deformation: a new mechanism for the development of syntectonic porphyroblasts and its implications for interpreting timing relationships in metamorphic rocks. *Geological Journal*, **11**, 71-100.

DE YOREO, J. J., LUX, D. R. & GUIDOTTI, C. V. 1989. The role of crustal anatexis and magma migration in the thermal evolution of regions of thickened continental crust. *In:* DALY, J. S., CLIFF, R. A. & YARDLEY, B. W. D. (eds) *Evolution of Metamorphic Belts.* Geological Society, London, Special Publication, **27**, 27-44.

DIXON, J. M. 1975. Finite strain and progressive deformation in models if dipiric structures. *Tectonophysics,* **28**, 89-124.

D'LEMOS, R. S., BROWN, M. & STRACHAN, R. A. 1992. Granite magma generation, ascent and emplacement within a transpressional orogen. *Journal of the Geological Society, London,* **149**, 487-490.

DONOVAN, R. N., ARCHER, R., TURNER, P. & TARLING, D. H. 1976. Devonian palaeogeography of the Orcadian Basin and the Great Glen Fault. *Nature,* **259**, 550-551.

DROOP, G. T. R. & TRELOAR, P. J. 1981. Pressures of metamorphism in the thermal aureole of the Etive Granite Complex. *Scottish Journal of Geology,* **17**, 85-102.

DURNEY, D. W. & RAMSAY, J. G. 1973. Incremental strains measured by syntectonic crystal growths; *In:* Gravity and Tectonics; (ed.) K. A. DE JONG & R. SCHOLTEN, Wiley, N. Y., 502.

ELLIOTT, D. 1981. The strength of rocks in thrust sheets (abstract). *Eos. Trans. AGU,* **62**, 397.

ELLIOTT, D. & JOHNSTON, M. R. 1980. Structural evolution of the northern part of the Moine thrust belt, NW Scotland. *Transactions of the Royal Society of Edinburgh,* **71**, 69-96.

ELLIS, D. J. 1992. Precambrian tectonics and the physiochemical evolution of the continental crust. II. Lithosphere delamination and ensialic orogeny. *Precambrian Research*, **55**, 507-524.

EMERMAN, S. H. & MARRETT, R. 1990. Why dikes? *Geology,* **18**: 231-233.

ENGLAND, P. C. & THOMPSON, A. B. 1984. Pressure-temperature-time paths of regional metamorphism. I. Heat transfer during the evolution of regions of thickened continental crust. *Journal of Petrology,* **25**, 894-928.

ENGLAND, P. C. & THOMPSON, A. B. 1986. Some thermal and tectonic models for crustal melting in continental collision belts. *In:* COWARD, M. P. & REIS, A. C. (eds) *Collision Tectonics.* Geological Society, London, Special Publication, **19**, 83-94.

ENGLAND, R. W. 1990. The identification of granitic diapirs. *Journal of the Geological Society, London,* **147**, 931-933.

ESKOLA, P. 1932. *Mineralogie und Petrologie Mitteilungen*, **42**, 455-481.

ETCHECOPAR, A. & MALAVIELLE, J. 1987. Computer models of pressure shadows: a method for strain measurement and shear-sense determination; *Journal of Structural Geology*, **9**, 667-677.

EVANS, C. R. 1965. Geochronology of the Lewisian basement near Lochinver, Sutherland. *Nature,* **207**, 54-56.

FABER, S. & BAMFORD, D. 1979. Lithospheric structural contrasts across the Caledonides of northern Britain. *Tectonophysics,* **56**, 17-30.

FABER, S. & BAMFORD, D. 1981. Moho-offset beneath northern Scotland. *Geophysical Journal of the Royal Astronomical Society,* **67**, 661-672.

FAIRBURN, H. W. 1950. Pressure shadows and relative movements in a shear zone; *Transactions of the American Geophysical Union*, **31**, 914-916.

FERNANDEZ, A. 1987. Preferred orientation developed by rigid markers in two-dimensional simple shear: theoretical and experimental study. *Ibid.,* **136**, 151-158.

FERNANDEZ, A. 1988. Strain analysis from shape preferred orientation in magmatic rocks. *In:* Geological Kinematic Dynamics, *Bulletin of the Geological Institute, University of Uppsala,* **14**, 61-66.

FERNANDEZ, A., FEYBESSE, J. L. & MELURE, J. F. 1983. Theoretical and experimental study of fabrics developed by different shaped markers in two-dimensional simple shear. *Bulletin of the Geological Society of France,* **25**, 319-326.

FERNANDEZ, A. & LAPORTE, D. 1991. Significance of low symmetry fabrics in magmatic rocks. *Journal of structural Geology,* **13**, 337-347.

FETTES, D. J. 1970. The structural and metamorphic state of the Dalradian rocks and their bearing on age of emplacement of the basic sheet. *Scottish Journal of Geology*, **6**, 108-118.

FETTES, D. J., GRAHAM, C. M., HARTE, B. & PLANT, J. A. 1986. Lineaments and basement domains: an alternative view of Dalradian evolution. *Journal of the Geological Society, London,* **143**, 453-464.

FETTES, D. J. & MENDUM, J. R. 1987. The evolution of the Lewisian complex in the Outer Hebrides. *In:* PARK, R. G. & TARNEY, J. (eds) *Evolution of the Lewisian and comparable Precambrian high grade terrains.* Geological Society, London, Special Publication, **27**, 27-44.

FETTES, D. J., LESLIE, A. G., STEPHENSON, D. & KIMBELL, S. F. 1991. Disruption of Dalradian stratigraphy along the Portsoy Lineament from new geological and magnetic surveys. *Scottish Journal of Geology*, **27**, 57-73.

FETTES, D. J., MENDUM, J. R., SMITH, D. I. & WATSON, J. 1991. *The geology of the Outer Hebrides.* Memoirs of the Geological Survey, U.K.

FITCH, F. J. & MILLER, J. A. 1967. The age of the Whin Sill. *Geological Journal,* **5**, 233-250.

FLINN, D. 1965. On the symmentry princple and the deformation ellipsoid. *Geological Magazine,* **102**, 36-45.

FORREST, M. D. & KEY, R. M. 1989. The Strath Ossian Lineament: geological and geochemical evidence. *Terra Abstracts,* **1**, 12.

FOUNTAIN, J. C., HODGE, D. S. & SHAW, R. P. 1989. Melt segregation in anatectic granulites: a thermo-mechanical model. *Journal of Volcanology and Geothermal Research,* **39**, 279-296.

FRANCE, D. S. 1971. *Structure and metamorphism of the Moine and Dalradian rocks in the Grampians of Scotland near Tyndrum and Moor of Rannoch.* University of Liverpool, Ph.D. thesis (unpublished).

FRANCIS, E. H. 1978. The Midland Valley as a rift, seen in comparison with the late Palaeozoic European rift system. *In:* RAMBERG, I. B. & NEUMANN, E. R. (eds) *Tectonics and Geophysics of Continental Rifts.* Leidal, Holland, 133-147

FRENCH, W. J. 1966. Appinitic intrusions clustered around the Ardara pluton, County Donegal. *Proceedings of the Royal Irish Academy,* **64B,** 303-322.

FROST, C. D. & O'NIONS, R. K. 1985. Caledonian magma genesis and crustal recycling. *Journal of Petrology,* **26**, 515-544.

GAMMOND, J. F. 1983. Displacement features associated with fault zones: a comparison between observed examples and experimental models. *Journal of Structural Geology*, **5**, 33-46.

GARNHAM, J. A. 1988. *Ring-faulting and associated intrusions, Glencoe, Scotland.* University of London, Ph.D. thesis (unpublished).

GHOSH, S. K. & RAMBERG, H. 1976. Reorientations of inclusions by combination of pure shear and simple shear. *Tectonophysics*, **34**, 1-70.

GILL, J. 1981. *Orogenic andesites and plate tectonics.* Springer-Verlag, 97-161.

GLOVER, B. W. 1995. A Neoproterozoic multi-phase rift sequence: The Grampian and Appin groups of the southern Monadhliath Mountains, Scotland. *Journal of the Geological Society, London,* **152**.

GOODMAN, S. 1994. The Portsoy-Duchray Lineament: a review of the evidence. *Geological Magazine,* **130**, 407-415.

GOWER, P. J. 1977. Dalradian rocks of the west coast of the Tayvallich Peninsula. *Scottish Journal of Geology*, **13**, 125-134.

GRAHAM, C. M. 1976. Petrochemistry and tectonic significance of Dalradian metabasaltic rocks of the SW Scotttish Highlands. *Journal of the Geological Society, London,* **132**, 61-84.

GRAHAM, C. M. 1986. The role of the Cruachan lineament during Dalradian evolution. *Scottish Journal of Geology*, **22**, 257-270.

GRAHAM, C. M. & BORRODAILE, G. J. 1984. The petrology and structure of Dalradian metabasaltic dykes of Jura: implications for early Dalradian evolution. *Scottish Journal of Geology*, **20**, 257-270.

GRAHAM, C. M. & BRADBURY, H. J. 1981. Cambrian and Late Cambrian basaltic activity in the Scottish Dalradian: a review. *Geological Magazine,* **118**, 27-39.

GROOME, D. R. & HALL, A. 1974. The geochemistry of the Devonian lavas of the Northern Lorne Plateau, Scotland. *Mineralogical Magazine,* **39**, 621-640.

GROUT, F. F. 1945. Scale models of structures related to batholiths. *American Journal of Science,* **243A**, 260.

GUGLIELMO, G., Jr. 1993. Interference between pluton expansion and coaxial tectonic deformation: three-dimensional computer model and field implications. *Journal of Structural Geology,* **15,** 593-608.

GUGLIELMO, G., Jr. 1994. Interference between pluton expansion and coaxial tectonic deformation: three-dimensional computer model and field implications. *Journal of Structural Geology,* **16,** 237-252.

GUINEBERTEAU, B., BOUCHEZ, J. L. & VIGNERESSE, J. L. 1987. The Mortagne granite pluton (France) emplaced by pull apart along a shear zone: stuctural and gravimetric arguements and regional implication. *Geological Society of America Bulletin,* **99,** 763-770.

HALL, A. 1967. The chemistry of appinitic rocks associated with the Ardara Pluton, Donegal, Ireland. *Contributions to Mineralogy and Petrology,* **16**, 156-171.

HALL, J. 1985. Geophysical constraints on crustal structure in the Dalradian region of Scotland. *Journal of the Geological Society, London,* **142**, 149-155.

HALL, J. 1986. Geophysical lineaments and deep continental structure. *Philosophical Transactions of the Royal Society of London,* **317**, 33-44.

HALL, J. 1986. Nature of the lower continental crust: Evidence from BIRPS work on the Caledonides, *In:* BARAZANGI, M. & BROWN, L., (eds) *Reflection Seismology: The Continental Crust,*. Geodyn.Ser., **14**, 223-232.

HALL, J., BREWER, J. A., MATTHEWS, D. H. & WARNER, M. R. 1984. Crustal structure across the Caledonides from the 'WINCH' seismic reflection profile: influences on the evolution of the Midland Valley of Scotland. *Transactions of the Royal Society of Edinburgh,* **75**, 97-109.

HALLIDAY, A. N. 1984. Coupled Sm-Nd and U-Pb (zircon) systematics in the late Caledonian granites and the nature of the basement under northern Britain. *Nature,* **307**, 229-33.

HALLIDAY, A. N. & STEPHENS, W. E. 1984. Crustal controls on the genesis of the 400 Ma old Caledonian granites. *Physics of the Earth and Planetary Interiors,* **35,** 89-104.

HAMIDULLAH, S. & BOWES, D. R. 1987. Petrogenesis of the appinite suite, Appin district, western Scotland. *Acta Universitatis Carolinae Geologica,* **4,** 296-396.

HANMER, S. 1981. Tectonic significance of the northeastern Gander Zone, Newfoundland: an Acadian ductile shear zone. *Canadian Journal of Earth Sciences*, **18**, 120-135.

HANMER, S. 1984a. The potential use of planar and elliptical structures as indicators of strain regime and kinematics of tectonic flow. *Geological Survey of Canada*, Paper **84-1B**, 133-142.

HANMER, S. 1988a. Great Slave Lake Shear Zone, Canadian Shield: reconstructed vertical profile of a crustal-scale fault zone. *Tectonophysics*, **149**, 245-264.

HANMER, S. 1990. Natural rotated inclusions in non-ideal shear. *Tectonophysics*, **176**, 245-255.

HANMER, S. & PASSCHIER, C. 1991. Shear sense indicators: A review. *Geological Survey of Canada,* Paper **90-17**.

HARMON, R. S. & HALLIDAY, A. N. 1980. Oxygen and strontium isotope relationships in the British late Caledonian granites. *Nature,* **283**, 21-25.

HARMON, R. S., HALLIDAY, A. N., CLAYBURN, J. A. P. & STEPHENS, W. E. 1984. Chemical and isotope systematics of the Caledonian intrusions of Scotland and Northern England: a guide to magma source region and magma-crust interaction. *Philosophical Transactions of the Royal Society of London Ser. A.*, **310**, 709-742.

HARDIE, W. G. 1963. Explosion breccias near Stob Mhic Mhartuin, Glencoe, Argyll, and their bearing on the origin of the nearby flinty crush-rock. *Transactions of the Royal Society of Edinburgh: Earth Sciences,* **19**, 426-438.

HARRIS, L. B. & PITCHER, W. S. 1975. The Dalradian Supergroup. *In:* HARRIS, L. B., SHACKELTON, R. M., WATSON, J., DOWNIE, C., HARLAND, W. B. & MOORBATH, S. (eds) *A correlation of Precambrian rocks in the British Isles.* Geological Society, London, Special Publication, **6**, 52-75.

HARRIS, L. B. & COBBOLD, P. R. 1985. Development of conjugate shear bands during bulk simple shearing. *Journal of Structural Geology*, **7**, 37-44.

HARRIS, L. B., BRADBURY, H. J. & McGONIGAL, M. H. 1976. The evolution and transport of the Tay nappe. *Scottish Journal of Geology,* **12**,103-113

HARRIS, L. B., BALDWIN, C. T., BRADBURY, H. J., JOHNSON, H. G. & SMITH, R. A. 1978. Ensialic basin sedimentation: The Dalradian Supergroup. *In:* BOWES, D. R. & LEAKE, B. E. (eds) *Crustal evolution in northwestern Britain and adjacent regions.* Geological Journal Special Issue, **10**, 115-138.

HARRIS, L. B., HOLLAND, C. H. & LEAKE, B. E. 1979. *The Caledonoids of the British Isles - Reviewed.* Geological Society, London, Special Publication, **8**.

HARRISON, T. N. 1986. The mode of employment of the Cairngorm granite. *Scottish Journal of Geology,* **22**, 303-314.

HARRY, W. T. 1954. The composite granitic gneiss of Western Ardgour. *Quarterly Journal of the Geological Society, London,* **109**, 285-309.

HARRY, W. T. 1958b. A re-examination of Barrow's older granites in Glen Clova, Angus. *Transactions of the Royal Society of Edinburgh: Earth Sciences,* **63**, 393-412.

HARTE, B. 1979. The Tarfside succession and its bearing on the structure and stratigraphy of the Eastern Scottish Dalradian. *In:* HARRIS, A. L., HOLLAND, C. H. & LEAKE, B. E. (eds) *The Caledonides of the British Isles - reviewed.* Geological Society, London, Special Publication, **8**, 699-70.

HARTE, B., BOOTH, J. E., DEMPSTER, T. J., FETTES, D. J., MENDUM, J. R. & WATTS, D. 1984. Aspects of the post depositional of Dalradian and Highland Boundary rocks of the Southern Highlands of Scotland. *Transactions of the Royal Society of Edinburgh: Earth Sciences,* **75**, 151-163.

HASLAM, H. W. 1968. The crystallization of intermediate and acid magmas at Ben Nevis, Scotland. *Journal of Petrology,* **9**, 84-104.

HENDERSON, P. 1982. *Inorganic geochemistry.* Pergamom Press.

HIBBARD, M. J. & WATTERS, R. J. 1988. Fracturing and diking in incompletely crystallized granitic plutons. *Lithos.* **18**, 1-12.

HICKMAN, A. H. 1978. Recumbent folds between Glenn Roy and Lismore. *Scottish Journal of Geology,* **14**, 191-212.

HIGHTON, A. J. 1994. A re-evaluation of 'metasedimentary xenoliths' in the West Highland Granitic Gneiss of Inverness-shire. *Scottish Journal of Geology,* **30,** 39-49.

HINXMAN, L. W., CARRUTHERS, R. G. & MACGREGOR, M. A. 1923. *The Geology of Corrour and the Moor of Rannoch (sheet 54).* Memoirs of the Geological Survey, G.B.

HIPKIN, R. G. & HUSSAIN, A. 1983. Regional gravity anomalies: Northern Britain. *Rep. Inst. geol. Sci. London,* **82**/10.

HOBBS, B. E., MEANS, W. D. & WILLIAMS, P. F. 1976. *An outline of structural geology.* Wiley and Sons, 571.

HODGE, D. S., ABBEY, D. A., HARBIN, M. A., PATTERSON, J. L., RING, M. J., & SWEENEY, J. F. 1982. Gravity studies of subsurface distributions of granitic rocks in Maine and New Hampshire. *American Journal of Science,* **282**, 1289-1324.

HOLDER, M. T. 1979. An emplacement mechanism for post-tectonic granites and its implications for their geochemical features. *In:* ATHERTON, M. P. & TARNEY, O. O. (eds) *Origin of Granite batholiths: geochemical evidence,* 116-128. Nantwich: Shiva.

HOLDSWORTH, R. E. 1989. Late brittle deformation in a Caledonian ductile thrust wedge: new evidence for gravitational collapse in the Moine Thrust sheet, Sutherland, Scotland. *Tectonophysics,* **170**, 17-28.

HOLDSWORTH, R. E., HARRIS, A. L. & ROBERTS, A. M. 1987. The stratigraphy, structure and regional significance of the Moine rocks of Mull, Argyllshire, W. Scotland. *Geological Journal,* **22**, 83-107.

HOLDSWORTH, R. E. & STRACHAN, R. A. 1991. Interlinked system of ductile strike slip and thrusting formed by Caledonian sinistral transpression in northeastern Greenland. *Geology,* **19**, 510-513.

HOLLAND, J. E. & LAMBERT, R. St. J. 1975. The chemistry and origin of the Lewisian gneisses of the Scottish mainland: the Scourie and Inver assemblages and sub-crustal accretion. *Precambrian Research,* **2**, 161-188.

HOPSON, C. A. & DELLINGER, D. A. 1987. Evolution of four-dimensional compositional zoning, illustrated by the diapiric Duncan Hill pluton, North Cascades, Washington. *Geol. Soc. Am. Abs. W. Prog.*, **19**, 707.

HORNE, R. R. 1974. Transverse fault control of base metal mineralisation in Ireland and Britain. *Economic Geology*, **69**, No. 7, 1181.

HORNE, R. R. 1975. Strike slip terranes and a model for the evolution of the British and Irish Caledonides. *Irish Naturalists Journal*, **18**, No. 5, 140-144.

HUMPHRIES, F. J. & CLIFF, R. A. 1982. Sm-Nd dating and cooling history of Scourian granulites, Sutherland. *Nature,* **295**, 515-517.

HUNTER, R. H. & ROCK, N. M. S. 1987. Late Caledonian dyke-swarms of northen Britain: spatial and temporal intimacy between lamprophyric and granitic magmatism around the Ross of Mull pluton, Inner Hebrides. *Geologische Rundschau,* **76**, 805-826.

HUSSAIN, A. & HIPKIN, R. G. 1981. Bouger anomaly map of the British Isles, northern sheet. *University of Edinburgh, Edinburgh.*

HUTTON, D. H. W. 1982. A tectonic model for the emplacement of the Main Donegal granite, NW Ireland. *Journal of the Geological Society, London,* **139**, 615-631.

HUTTON, D. H. W. 1987. Strike slip terranes and a model for the evolution of the British and Irish Caledonides. *Geological Magazine,* **124**, 405-425.

HUTTON, D. H. W. 1988a. Granite emplacement mechanisms and tectonic controls: inferences from deformation studies. *Transactions of the Royal Society of Edinburgh: Earth Sciences,* **79**, 245-255.

HUTTON, D. H. W. 1988b. Igneous emplacement in a shear zone termination: The biotite granite at Strontian, Scotland. *Geological Society of the American Bulletin,* **100**: 1392-1399.

HUTTON, D. H. W. 1992. Granite sheeted complexes: evidence for the dyking ascent mechanism. *Transactions of the Royal Society of Edinburgh: Earth Sciences,* **83**, 377-382.

HUTTON, D. H. W. & INGRAM, G. M. 1992. The Great Tonalite Sill of South East Alaska and British Columbia: emplacement into an active contractional high angle reverse shear zone. *Transactions of the Royal Society of Edinburgh: Earth Sciences,* **83**, 383-386.

HUTTON, D. H. W. & MCERLEAN, M. 1990. Silurian and Early Devonian sinistral deformation of the Ratagain granite, Scotland: constraints on the age of Caledonian movements on the great Glen Fault System. *Journal of the Geological Society, London,* **148**, 1-4.

HUTTON, D.H.W. & REAVY, R. J. 1992. Strike-slip tectonics and granite petrogenesis. *Tectonics,* **11**, 960-967.

HUTTON, D. H. W. & ALSOP, G. I. (*in press*). The Caledonian strike swing and associated lineaments; evidence from NW Ireland and adjacent areas.

HUTTON, J. 1794. "Observations on Granite" *TRSE* 3(2): 77-85. Read 4 January 1790 and 1 August 1791.

ILDEFONSE, B. 1987. *Les linéations et la déformation: aspects naturels, théoriques et expérimentaux des orientation préférentielles de forme.* Université de Lyon, thèse doctorat.

ILDEFONSE, B. & FERNANDEZ, A. 1988. Influence on the concentration of rigid markers in a viscous medium on the production of preferred orientations. An experimental contribution, 1. Non coaxial strain. *In: Geological Kinematics and Dynamics.* Bulletin of the Geological Institute, University of Uppsala, **1**, 55-60.

ILDEFONSE, B., LAUNEAU, P., BOUCHEZ, J-L. & FERNANDEZ, A. 1992. Effect of mechanical interactions on the development of shape preferred orientations: a two-dimensional experimental approach. *Journal of Structural Geology,* **14**, 73-84.

INGRAM, G. M. 1992. *Deformation, emplacement and tectonic inferences: the Great Tonalite Sill, southeast Alaska, USA.* University of Durham, Ph.D. thesis (unpublished).

INGRAM, G. M. & HUTTON, D. H. W. 1994. The Great Tonalite Sill: Emplacement into a contractional shear zone and implications for Late Cretaceous to early Eocene tectonics in southeastern Alaska and British Columbia. *Geological Society of America Bulletin,* **106**, 715-728.

JACKSON, M. P. A. & TALBOT, C. 1989. Anatomy of mushroom shaped diapirs. *Journal of Structural Geology,* **11**, 211-230.

JACQUES, J. M. & REAVY, R. J. 1994. Caledonian plutonism and major lineaments in the SW Scottish Highlands. *Journal of the Geological Society, London,* **151**, 955-969.

JACQUES, J. M. & REAVY, R. J. 1995. Interaction of tectonic-related strain fields during pluton construction; Argyll Suite, SW Grampian Highlands, Scotland. (In preparation).

JACQUES, J. M. 1995. Mechanisms of space creation during pluton construction; Argyll Suite, SW Grampian Highlands, Scotland. (In preparation).

JAMIESON, R. A. & VERNON, R. H. 1987. Timing of porphyroblast growth in the Fleur de Lys Supergroup, Newfoundland. *Journal of Metamorphic Geology,* **5**, 273-288.

JEFFERY, G. B. 1923. The motion of ellipsoidal particles immersed in a viscous fluid. *Proceedings of the Geological Society, London,* **102A**, 161-179.

JOHNSTONE, G. S., SMITH, D. I. & HARRIS, A. L. 1969. The Moinian Assemblage of Scotland. *In:* KAY, M. (ed.) *North Atlantic geology and continental drift.* Am. Assoc. Petrol. Geol., **12**, 159-180.

KELLEY, S. P. & POWELL, D. 1985. Relationships between marginal thrusting and movement on major internal shear zones in the northern Highland Caledonides, Scotland. *Journal of Structural Geology,* **7**, 161-174.

KENNEDY, W. Q. 1946. The Great Glen fault. *Quarterly Journal of the Geological Society, London,* **102**, 41-76.

KERRICH, R., ALLISON, I., BARNETT, R. L., MOSS, S. & STARKEY, J. 1980. Microstructural and chemical transformations accompanying deformation of for stress corrosion cracking and superpastic flow. *Contributions to Minerology and Petrology,* **73**, 221-242.

KEY, R. M. 1989. Progress report on the mapping in the southern part of sheet 63W. *British Geological Survey, Technical Report.* RMK/1989/1.

KEY, R. M., PHILLIPS, E. R. & CHACKSFIELD, B. C. 1993. Emplacemnt and thermal metamorphism associated with the post-orogenic Strath Ossian pluton, Grampian Highlands, Scotland. *Geological Magazine,* **130,** 379-390.

KLEMPERER, S. L. & THE BIRPS GROUP 1987. *Geophysical Journal of the Royal Astronomical Society,* **89,** 217-222.

KNAPP, R. B. & KNIGHT, J. E. 1977. Differential thermal expansion of pore fluids: Fracture propagation and microearthquake production in hot pluton environments. *Journal of Geophysical Research,* **82**, 2515-2522.

KNELLER, B. C. & LESLIE, A. G. 1984. Amphibolite facies metamorphism in shear zones in the Buchan area of NE Scotland. *Journal of Metamorphic Geology,* **2**, 83-94.

KNELLER, B. & AFTALION, M. 1987. The isotopic and structural age of the Aberdeen granite. *Journal of the Geological Society, London,* **144**, 717-722.

KNILL, J. L. 1963. A sedimentary history of the Dalradian series. *In:* JOHNSON, M. R. W. & STEWART, F. H. (eds) *The British Caledonides.* Oliver & Boyd, London and Edinburgh.

KNIPE, R. J. & LAW, R. D. 1987. The influence of crystallographic orientation and grain boundary migration on microstructural and textural evolution in an S-C mylonite. *Tectonophysics,* **135**, 155-169.

KOKELAAR, B. P. 1992. Ordovician marine volcanic and sedimentary record of rifting and volcotectonism: Snowdon, Wales, UK. *Geological Society of America Bulletin,* **104**, 1433-1455.

KOYI, H. 1991. Mushroom diapirs penetrating overburdens with high effective viscosities. *Geology,* **19**, 1229-1232.

KUSZNIR, N. & PARK, R. 1987. The extensional strength of the continental lithosphere: Its dependence on geothermal gradient, and crustal composition and thickness. *Geological Society, London, Special Publication,* **28,** 35-52.

KYNASTON, H. & HILL, J. B. 1908. *The geology of Oban and Dalmally (Sheet 45).* Memoirs of the Geological Survey, U.K.

LAMBERT, R, St, J., WINCHESTER, J. A. & HOLLAND, J. G. 1979. Time, space and intensity relationships of the Precambrian and lower Palaeozoic metamorphisms of the Scottish Highlands. *In:* HARRIS, L. B., HOLLAND, C. H. & LEAKE, B. E. 1979. *The Caledonoids of the British Isles - Reviewed.* Geological Society, London, Special Publication, **8**.

LAW, R. D., CASEY, M., & KNIPE, R. J. 1986. Kinematic and tectonic significance of microstructures and crystallographic fabrics within quartz mylonites from the Assynt and Eriboll regions of the Moine Thrust zone, NW Scotland. *Philosophical Transactions of the Royal Society of Scotland*, **77**, 99-125.

LAW, R. D., KNIPE, R. J., & DAYAN, H. 1984. Strain partitioning within thrust sheets: microstructural and petrofabric evidence from the Moine Thrust zone at Loch Eriboll, north-west Scotland. *Journal of Structural Geology*, **6**, 477-497.

LEAKE, B. E. 1978. Granite emplacement: the granites of Ireland and their origin. *In:* BOWES, D. R. & LEAKE, B. E. (eds) *Crustal evolution in northwestern Britain and adjacent regions.* Geological Society, London, Special Publication, **10**, 221-248.
LEAKE, B. E. 1990. Granite magmas: their sources, initiation and consequences of emplacement. *Journal of the Geological Society, London,* **147**, 579-589.

LEAKE, B. E. & COBBING, J. 1993. Transient and long-term correspondence of erosion level and the tops of granite plutons. *Scottish Journal of Geology,* **29**, 177-182.

LEEDAL, G. M. 1952. The Cuanie igneous intrusion, Inverness-shire and Ross-shire. *Quarterly Journal of the Geological Society, London,* **108**, 311-39.

LEIGHTON, P. S. 1985. *A petrological and geochemical reconnaissance of the Moor of Rannoch pluton, S.W. Highlands, Scotland.* MSc thesis, University of St. Andrews.

LEI SHIHE & PARK, R. G. 1993. Reversals of movement sense in Lewisian brittle-ductile shear zones at Gairloch, NW Scotland, in context of Laxfordian kinematic history. *Scottish Journal of Geology,* **29**, 9-19.

LINDSAY, N. G. 1988. *Contrasts in Caledonian tectonics of the Northern and Central Highlands of Scotland.* University of Liverpool, Ph.D. thesis (unpublished).

LINDSAY, N. G., HASELOCK, P. J. & HARRIS, A. L. 1989. Short Paper: The extent of Grampian orogenic activity in the Scottish Highlands. *Journal of the Geological Society, London,* **146**, 733-735.

LIPMAN, P. W. 1976. Caldera collapse breccias in the San Juan Mountains, Colorado. *Geological Society of America Bulletin,* **87**, 1397-1410.

LIPMAN, P. W. 1984. Roots of ash-flow calderas in western North America: windows into the tops of granite batholiths. *Journal of Geophysical Research,* **89**, no. B10, 8801-8841.

LISTER, J. R. & SNOKE, A. W. 1984. S-C mylonites. *Journal of Structural Geology*, **6**, 617-638.

LISTER, J. R. & KERR, R. C. 1991. Fluid-mechanical models of crack propagation and their application to magma transport in dykes. *Journal of Geophysical Research,* **96**,10 049-10 077.

LITHERLAND, M. 1980. The stratigraphy of the Dalradian rocks around Loch Creran, Argyll. *Scottish Journal of Geology,* **16**, 105-124.

LITHERLAND, M. 1982. The structure of the Loch Creran Dalradian and a new model for the SW Highlands. *Scottish Journal of Geology,* **18**, 205-225.

LOOSVELD, R. & ETHERIDGE, M. A. 1990. A model for low-pressure facies metamorphism during crustal thickening. *Journal of Metamorphic Geology,* **8**, 257-267.

MACULLOCH, J. 1817. Observations on the mountain Cruachan in Argyllshire, with some remarks on the surrounding country. *Transactions of the Geology of Scotland,* **4**, 117-138.

MAHON, K. I., HARRISON, T. M. & DREW, D. A. 1988. Ascent of a granitoid diapir a temperature varying medium. *Journal of Geophysical Research,* **93**, 1174-1188.

MALAVEILLE, J. & COBB, F. 1986. Cinmatique des déformations ductiles dans trois massifs métamorphiques de l'Ouest des Etas-Unis: Albion (Idaho), Raft River et Gouse Creek (Utah). *Bulletin de la Société géologique de France*, **2**, 885-898.

MANDAL, N. & BANERJEE, S. 1987. Rotation rate versus growth of syntectonic porphyroblasts: the controlling parameter of the shape of the inclusion trail. *Tectonophysics*, **136**, 165-169.

MANDELBROT, B. B. 1982. *Fractal Geometry in Nature.* W. H. FREEMAN, New York. N.Y., 468pp.

MARCANTONIO, F., DICKIN, A. P., McNUTT, R. H. & HEAMAN, L. M. 1988. A 1,800-million-year-old Proterozoic gneiss terrane in Islay with implications for the crustal structure and evolution in Britain. *Nature,* **335**, 62-64.

MARSH, B. D. 1982. On the mechanics of igneous diapirism, stoping, and zone melting. *American Journal of Science,* **282**, 808-855.

MARSTON, R. J. 1971. The Foyers granite complex, Inverness-shire, Scotland. *Quarterly Journal of the Geological Society, London,* **126**, 331-368.

MATHEWS, D. H. & HIRN, A. 1984. Crustal thickening in Himalayas and Caledonides. *Nature,* **308**, 497-498.

MATTHEWS, D. & THE BIRPS GROUP 1987. Seismic reflections from the lower crust around Britain. *Geological Society, London, Special Publication*, **24**, 11-21.

MAUFE, H. B. 1910. *The geological structure of Ben Nevis.* Memoirs of the Geological Survey of the United Kingdom, Summary of progress (for 1909), 80-89.

McBRIDE, J. H. & ENGLAND, R. W. 1994. Deep seismic reflection structure of the Caledonian orogenic front west of Shetland. *Journal of the Geological Society, London,* **151**, 9-16.

McBIRNEY, A. R. & MURASE, T. 1984. Rheological properties of magmas. *Annual Review, Earth and Planetary Science,* **12**, 337-357.

McCAFFREY, K. J. W. 1989. *The emplacement and deformation of granitic rocks in a transpressional shear zone: The Ox Mountains Igneous Complex.* University of Durham, Ph.D. thesis (unpublished).

McCAFFREY, K. J. W. 1992. Igneous emplacement in a transpressive shear zone: Ox Mountains Igneous Complex. *Journal of the Geological Society, London,* **149**, 221-235.

McERLEAN, M. A. 1992. A new criteria for rocks deformed in the magmatic state: examples from the Thorr Granite, Co. Donegal. *Transactions of the Royal Society of Edinburgh: Earth Sciences,* **83**, 494.

MEANS, W. D. 1976. *Stress and Strain: basic concepts in continuum mechanics for geologists.* Springer Verlag, 339.

MEANS, W. D. 1981. The concept of steady-state foliation; *Tectonophysics*, **78**, 179-199.

MEISSNER, R., WENER,T. & BITTNER, R. 1987. Results of DEKORP 2-S and other reflection profiles through the Variscides. *Geophysical Journal of the Royal Astronomical Society,* **89**, 319-324.

MEISSNER, R. & KUSZNIR, N. 1987. Crustal viscosity and the reflectivity of the lower crust. *Annual of Geophysics,* **5B**, 365-373.

MENDUM, J. R. & FETTES, D. J. 1984. The Tay Nappe and associated folding in the Ben Ledi-Loch Lomond area. *Scottish Journal of Geology,* **21**, 41-56.

MENUGE, J. F. & DALY, J. S. 1991. Proterozoic evolution of the Erris Complex, N.W. Mayo, Ireland: neodymium isotope evidence. *In:* GOWER, C., RIVERS, T. & RYAN, B. (eds) *Mid-Proterozoic geology of the southern margin of Laurentia-Baltica.* Geological Association of Canada, Special Paper, **38**.

MERCY, E. L. P. 1963. The geochemistry of some Caledonian granitic and meta-sedimentary rocks. *In:* JOHNSON, M. R. W. & STEWART, F. J. (eds) *The British Caledonides,* 229-267, Oliver & Boyd, Edinburgh.

MILLER, C. F., WATSON, E. B. & HARRISON, T. M. 1988. Perspectives on the source, segregation and transport of granitoid magmas. *Transactions of the Royal Society of Edinburgh,* **79**, 135-156.

MOORE, H. E. & SIBSON, R. H. 1978. Experimental thermal fragmentation in relation to seismic faulting. *Tectonophysics,* **49**, T9-T17.

MORRIS, G. A. & HUTTON, D. H. W. 1993. Evidence for sinistral shear associated with the emplacement of the Early Devonian Etive Dyke Swarm. *Scottish Journal of Geology,* **29**, 69-72.

MUEHLBERGER, W. R. 1986. Different slip senses of major faults during different orogenies: The rule? pp76-81. *In:* ALDRICH, M. J. & LAUGLIN, A. W. (eds) *Proceedings of the Sixth International Conference on Basement Tectonics (Santa Fe, New Mexico, 1985).* International Basement Tectonics Association, Salt Lake City, Utah, USA., p208.

MUNRO, M. 1965. Some structural features of the Caledonian granitic complex at Strontian, Argyllshire. *Scottish Journal of Geology,* **1**, 152-175.

MUNRO, M. & GALLAGHER, J. W. 1984. Disruption of the 'Younger Basic' masses in the Huntly-Portsoy area, Grampian region. *Scottish Journal of Geology,* **20**, 361-382.

MURASE, T. & McBIRNEY, A. R. 1973. Properties of some common igneous rocks and their melts at high temperature. *Bulletin of the Geological Society of America,* **84**, 3563-92.

MURPHY, D. C. 1987. Suprastructure/infrastructure transition, east-central Cariboo Mountains, British Columbia: geometry, kinematics and tectonic implications. *Journal of Structural Geology,* **9**, 13-29.

MURPHY, T. 1981. Geophysical Evidence. *In:* HOLLAND, C. H. (ed.) *A Geology of Ireland.* Scottish Academic Press, Edinburgh, 225-229.

NEILSON, D. L., CLARK, R. G., LYONS, J. B., ENGLUND, E. J. & BORNS, D. J. 1976. Gravity models and modes of emplacement of the New Hampshire plutonic series. *Geological Society of American Memoirs,* **146**, 301-318.

NICHOLLS, G. D. 1951. The Glenelg-Ratagain igneous complex. *Quarterly Journal of the Geological Society, London,* **106**, 309-344.

NICOLAS, A. 1992. Kinematics in Magmatic rocks with Special Reference to Gabbros. *Journal of Petrology,* **33**, 891-915.

NICOLAS, A. & POIRIER, J. P. 1976. *Crystalline plasticity and solid state flow in metamorphic rocks.* Wiley, New York, 444.

OERTEL, G. 1955. Devonian pluton Von Loch Doon in Sudschottland. *Geotckt. Forsch.*, **11**, 1-83.

OTTINO, J. M., LEONG, C. W., RISING, H. & SWANSON, P. D. 1988. Morphological structures produced by mixing in chaotic flows. *Nature*, **333**, 419-425.

PANKHURST, R. J. 1979. Isotopic and trace element evidence for the origin and evolution of Caledonian granites in the Scottish Highlands. *In:* ATHERTON, M. P. & TARNEY, J. (eds) *Origin of Granite batholiths: geochemical evidence.* Shiva Publishing Cheshire, 18-33.

PARK, R. G. 1989. *Foundations of Structural Geology.* Blackie, Glasgow and London (2nd Edition).

PARK, R. G. & TARNEY, J. 1987. The Lewisian complex: a typical Precambrian high-grade terrain? *In* Park, R.G. and Tarney, J. (eds.), *Evolution of the Lewisian and comparable Precambrian high-grade terrains* Geological Society of London Special Publication **27**, 139-151.

PARK, R. G., CRANE, A. & NIAMATULLAH, M. 1987. Early Proterozoic structure and kinematic evolution of the southern mainland Lewisian and comparable Precambrian high grade terrains. *Geological Society, London, Special Publication,* **27**, 139-151.

PARSLOW, G. R. 1968. The physical and structural features of the Cairnsmore of Fleet granite and its aureole. *Scottish Journal of Geology*, **4** (2), 91-108.

PARSLOW, G. R. 1971. Variations in mineralogy and major elements in the Cairnsmore of Fleet Granite, SW Scotland. *Lithos*, **4**, 43-55.

PASSCHIER, C. W. & SIMPSON, C. 1986. Porphyroclast systems as kinematic indicators. *Journal of Structural Geology*, **8**, 831-844.

PATERSON, S. R. 1989. Are tectonic granites truely syn-tectonic? *Eos.* August 8, 1989.

PATERSON, S. R. & FOWLER, T. K. Jnr. 1993a. Re-examining pluton emplacement processes. *Journal of Structural Geology*, **15**, 191-206.

PATERSON, S. R., VERNON, R. H., & FOWLER, T. K. Jnr. 1991a. Aureole tectonics. *In*: KERRICK, D. M. (eds) *Contact Metamorphism.* Miner. Soc. Rev. Miner. **26**, 673-722.

PATTISON, D. R. M. & HARTE, B. 1988. Evolution of structurally contrasting anatectic migmatites in the 3-Kbar Ballachulish aureole, Scotland. *Journal of Metamorphic Geology,* **6**, 475-494.

PEACH, B. N., HORNE, J., GUNN, W., CLOUGH, C. T., HINXMAN, L. W. & TEALL, J. J. H. 1907. *The geological structure of the Northwest Highlands of Scotland.* Memoirs of the British Geological Survey.

PEARCE, J. A., HARRIS, N. B. W. & TINDLE, A. G. 1984. Trace element discrimination diagrams for the tectonic interpretation of granitic rocks. *Journal of Petrology,* **25**, 956-983.

PERKINS, S. G. 1986. *The southern part of the Cruachan Granitoid, Etive complex, Argyllshire.* Kingston Polytechnic, Ph.D. thesis (unpublished).

PETFORD, N. & ATHERTON, M. P. 1992. Granitoid emplacement and deformation along a major crustal lineament: The Cordillera Blanca, Peru. *Tectonophysics,* **205**, 171-185.

PETFORD, N., KERR, R. C. & LISTER, J. R. 1993. Dike transport of granitoid magmas. *Geology,* **21**, 845-848.

PHILLIPS. E. R. 1991. *Mineralogy, petrology and metamorphic history of the Grampian and Appin Groups, southern part of Sheet 63W.* British Geological Survey Technical Report, WG / 91 / 14.

PHILLIPS, W. E. A., STILLMAN, C. J. & MURPHY, T. 1976. A Caledonian plate tectonic model. *Journal of the Geological Society, London,* **132**, 579-609.

PHILLIPS, E. R., KEY, R. M., CLARK, G. C., MAY, F., GLOVER, B. W. & CHACKSFIELD, B. C. 1994. Tectonothermal evolution of the Neoproterozoic Grampian and Appin groups, southwestern Monadliath Mountains, Scotland. *Journal of the Geological Society, London,* **151**, 971-986.

PIASECKI, M. A. J. 1975. Tectonic and metamorphic history of the Upper Findhorn, Inverness-shire, Scotland. *Scottish Journal of Geology,* **11**, 87-115.

PIASECKI, M. A. J. 1980. New light on the Moine rocks of the Central Highlands of Scotland. *Journal of the Geological Society, London,* **137**, 41-59.

PIASECKI, M. A. J. & VAN BREEMAN, O. 1979. The Central Highland Granulites: cover-basement tectonics in the Moine. *In:* HARRIS, A. L., HOLLAND, C. H. & LEAKE, B. E. (eds) *The Caledonides of the British Isles - reviewed.* Geological Society, London, Special Publication, 8, 139-144.

PIASECKI, M. A. J., VAN BREEMAN, O. & WRIGHT, A. E. 1981. The Late Precambrian Geology of Scotland, England and Wales. *In:* KERR, J. W. & FERGUSSON, A. J. (eds) *Geology of the North Atlantic Borderlands.* Mem. Can. Soc. Petrol. Geol., 7, 57-94.

PIASECKI, M. A. J. & VAN BREEMAN, O. 1983. Field and isotopic evidence for c. 750 Ma tectonothermal event in the Moine rocks in the Central Highland region of the Scottish Caledonides. *Transactions of the Royal Society of Edinburgh,* 73, 114-134.

PIASECKI, M. A. J. & TEMPERLEY, S. 1988. The northern sector of the Central Highlands. *In:* ALLISON, I., MAY, F. & STRACHAN, R. A. (eds) *An excursion guide to the Moine geology of the Scottish Highlands.* Scottish Academic Press, Edinburgh, 51-79.

PIDGEON, R. T. & BOWES, D. R. 1972. Zircon U-Pb ages of granulites from the central region of the Lewisian of north-western Scotland. *Geological Magazine,* **109**, 247-258.

PIDGEON, R. T. & AFTALION, M. 1978. Cognetic and inherited zircon U-Pb systems in granites: Proterozoic granites of Scotland and England. *In: Crustal evolution in north-west Britain and adjacent regions.* Geological Journal Special Issue, **10**, 183-220.

PITCHER, W. S. 1978. The anatomy of a batholith. *Journal of the Geological Society, London,* **135**, 157-182.

PITCHER, W. S. 1979. The nature, ascent and emplacement of granite magmas. *Journal of the Geological Society, London,* **136**, 627-662.

PITCHER, W. S. 1982. Granite type and tectonic environment. *In:* HSU, K. (ed) *Mountain Building Processes.* London and New York: Academic Press, 19-40.

PITCHER, W. S. 1983. Granite typology, geological environment and melting relationships. *In:* ATHERTON, M. P. & GRIBBLE, C. D. (eds) *Migmatites, melting and metamorphism.* Shiva Publishing.

PITCHER, W. S. & BERGER, A. R. 1972. *The Geology of Donegal: a study of granite emplacement and unroofing.* London: Wiley Interscience.

PITCHER, W. S. & READ, H. H. 1959. The Main Donegal Granite. *Quarterly Journal of the Geological Society of London,* **114** (for 1958), 259-305.

PLANT, J., BROWN, G. C., SIMPSON, P. R. & SMITH, R. T. 1980. Signatures of metalliferous granites in the Scottish Caledonides. *Transactions of the Institute of Mining and Metallurgy B,* 198-210.

PLATT, J. P. 1984. Secondary cleavges in ductile shear zones. *Journal of Structural Geology*, **6**, 439-442.

PLATT, J. P. 1986. Dynamics of orogenic wedges and the uplift of high-pressure metamorphic rocks. *Geological Society of America Bulletin,* **97**, 1037-1053.

PLATT, J. P, & VISSERS, R. L. 1980. Extensional structures in anisotropic rocks. *Journal of Structural Geology*, **2**, 397-410.

POIRIER, J. P. & GUILLOPÊ, M. 1979. Deformation induced rcrystallisation of minerals. *Bulletin de Minéralogie*, **102**, 67-74.

POLLARD, D. D. 1977. Derivation and evaluation of a mechanical model for sheet intrusions. *Tectonophysics,* **19**, 233-269.

POLLARD, D. D. & HOLZHAUSEN, G. 1979. On the mechanical interaction between a fluid-filled fracture and the earth's surface. *Tectonophysics*, **53**, 27-57.
PONCE DE LEON, M. I. & CHOUKROUNE, P. 1980. Shear zones in the Iberian Arc. *In:* CARRERAS,J., COBBOLD, P. R., RAMSAY, J. G. & WHITE, S. H. (eds) *Shear zones in rocks.* Journal of Structural Geology, **2**, 63-68.

POWELL, D. W. 1970. Magnetised rocks within the Lewisian of western Scotland and under the Southern Uplands. *Scottish Journal of Geology,* **6**, 353-369.

POWELL, D. W. 1974. Stratigraphy and structure of the western Moine and the problem of Moine orogenesis. *Journal of the Geological Society , London*, **130**, 575-593.

POWELL, D., BROOK, M. & BAIRD, A. W. 1983. Structural dating of a Precambrian pegmatite in Moine rocks of northern Scotland and its bearing on the status of the "Morarian Orogeny". *Journal of the Geological Society , London*, **140**, 813-128.

POWELL, D. & PHILLIPS, W. E. A. 1985. Time and deformation in the Caledonian orogen of Britain and Ireland. *In:* HARRIS, A. L. (ed.) *The nature and timing of orogenic activity in the Caledonian rocks of the British Isles.* Memoirs of the Geological Society, London, **9**, 17-39.

PRUCHA, J. J. 1989. Zones of weakness concept: A review and evaluation. *International Basement Tectonics Association,* **8**, 83-92.

RAMBERG, H. 1967. *Folding and Fracturing of Rocks.* McCraw Hill, New York, 568.

RAMBERG, H. 1970. Model studies in relation to intrusion of plutonic bodies. In: Mechanisms of Igneous Intrusion. *Geological Journal,* **2**, 261-286.

RAMBERG, H. 1972. Theoretical models of density stratification and diapirism in the Earth. *Journal of Geophysical Research,* 77, 877-889.

RAMBERG, H. 1981. *Gravity, Deformation and the Earth's Crust.* Academic Press, London.

RAMSAY, J. G. 1958. Moine-Lewisian relations at Glenelg, Inverness-shire. *Quarterly Journal of the Geological Society , London*, **113**, 487-523.

RAMSAY, J. G. 1967. Folding and fracturing of rocks.

RAMSAY, J. G. 1980a. Shear zone geometry: a review. *Journal of Structural Geology*, **2**, 83-99.

RAMSAY, J. G. 1989. Emplacement kinematics of a granite diapir: the Chindamora batholith, Zimbabwe. *Journal of Structural Geology, Volume 1: Strain Analysis:* London, Academic Press, 307pp.

RAMSAY, J. G. & GRAHAM, R. H. 1970. Strain variation in shear belts. *Canadian Journal of Earth Sciences*, 7, 786-813.

RAMSAY, J. G. & HUBER, M. I. 1983. *The techniques of modern structural geology, Volume 1: Strain Analysis*; Academic Press, London, 307pp.

RAMSAY, J. G. & HUBER, M. I. 1987. *The techniques of modern structural geology, Volume 2: Folds and Fractures* ; Academic Press, London, 391pp.

RAMSAY, J. G., CASEY, M. & KLIGFIELD, R. 1983. Role of shear in development of the Helvetic fold-thrust belt of Switzerland. *Geology*, **11**, 439-442.

RAST, N. 1963. Structure and metamorphism of the Dalradian rocks of Scotland. *In:* JOHNSON, M. R. W. & STEWART, F. H. (eds) *The British Caledonides.* Oliver & Boyd, Edinburgh and London.

RATHBONE, P. A. & HARRIS, A. L. 1979. Basement-cover relationships at Lewisian inliers. *In:* HARRIS, A. L., HOLLAND, C. H. & LEAKE, B. E. (eds) *The Caledonides of the British Isles - reviewed.* Geological Society, London, Special Publication, **8**, 101-107.

RATHBONE, P. A., COWARD, M. P. & HARRIS, A. L. 1983. Cover and basement: a contrast in style and fabrics. *In* HARRIS, L. D. & WILLIAMS, H. (eds) *Tectonics and Geophysics of Mountain Chains. Memoir of the Geological Society of America,* **158**, 213-23.

READ, H. H. 1919. The two magmas of Strathbogie and Lower Banffshire. *Geological Magazine,* **56**, 364-371.

READ, H. H. 1949. A contemplation of time in plutonism. *Quarterly Journal of the Geological Society , London,* **105**, 101-156.

READ, H. H. 1957. *The Granite Controversy.* London: Thomas Murby and Co.

READ, H. H. 1961. Aspects of Caledonian magmatism in Britain. *Liverpool and Manchester Geological Journal,* **2,** 653-683.

READ, H. H. & PHEMISTER, J. 1925. *The geology of the country around Golspie, Sutherlandshire.* Memoirs of the Geological Survey of Scotland.

READ, H. H., PHEMISTER, J. & ROSS, G. 1926. *The geology of Strath Oykell and Lower Loch Shin.* Memoirs of the Geological Survey of Scotland.

REAVY, R. J. 1989. Structural controls on metamorphism and syn-tectonic magmatism: the Portuguese Hercynian collision belt. *Journal of the Geological Society, London,* **146**, 649-657.

RESTON, T. J. 1988. Evidence for shear zones in the lower crust offshore Britain. *Tectonics,* **7**, 929-945.

REYNOLDS, D. L. 1954. Fluidisation as a geological process, and its bearing on the problem of intrusive granites. *American Journal of Science,* **252**, 577-614.

REYNOLDS, D. L. 1956. Calderas and ring complexes. *Nederlander Geol. Mijnb. Gen. Ver. Geol. Series,* **16**, 355-379.

RICHEY, J. E. 1932. Tertairy and ring structures in Britain. *Transactions of the Geological Society, Glasgow,* **19**, 42-410.

RICHEY, J. E. 1939. The dykes of Scotland. *Transactions of the Geological Society, Edinburgh,* **13**, 393-435.

ROBERTS, A. M. 1984. *Stratigraphy and structure in the Moine rocks along the Loch Quoich Line, Inverness-shire, Scotland.* University of Liverpool Ph.D. thesis (unpublished).

ROBERTS, A. M. & HARRIS, A. L. 1983. The Loch Quoich Line - a limit of early Palaeozoic crustal reworking in the Moine of the Northern Highlands of Scotland. *Journal of the Geological Society, London,* **140**, 883-892.

ROBERTS, A. M., SMITH, D. I. & HARRIS, A. L. 1984. The structural setting and tectonic significance of the Glen Dessary Syenite, Inverness-shire. *Journal of the Geological Society, London,* **141**, 1033-42.

ROBERTS, A. M., STRACHAN, R. A., HARRIS, A. L., BARR, D. & HOLDSWORTH, R. E. 1987. The Sgurr Beag nappe: a reassessment of the stratigraphy and structure of the northern Highland Moine. *Geological Society of America Bulletin,* **98**, 497-506.

ROBERTS, J. L. 1963. Source of Glencoe ignimbrites. *Nature,* **199**, 90.

ROBERTS, J. L. 1966a. Ignimbrite eruptions in the volcanic history of the Glencoe cauldron subsidence. *Geological Journal,* **5**, 173-184.

ROBERTS, J. L. 1966b. The emplacement of the Main Glencoe Fault-Intrusion at Stob Mhic Mhartuin. *Geological Magazine,* **103**, 299-316.

ROBERTS, J. L. 1974. The evolution of the Glencoe cauldron. *Scottish Journal of Geology,* **10**, 269-282.

ROBERTS, J. L. 1974. The structure of the Dalradian rocks in the SW Highlands of Scotland. *Journal of the Geological Society, London,* **130**, 93-123.

ROBERTS, J. L. & TREAGUS, J. E. 1977. Polyphase generation of nappe structures in the Dalradian rocks of the Southwest Highlands of Scotland. *Scottish Journal of Geology,* **13**, 237-254.

ROBERTSON, S. 1994. Timing of Barrovian metamorphism and 'Older Granite' emplacement in relation to Dalradian deformation. *Journal of the Geological Society, London,* **151**, 1-8.

ROBIN, P-Y. F. & CRUDEN, A. R. 1994. Strain and vorticity patterns in ideally ductile transpression zones. *Journal of Structural Geology,* **16**, 447-466.

ROCK, N. M. S., MACDONALD, R., WALKER, B. H., MAY, F., PEACOCK, J. D. & SCOTT, P. 1985. Intrusive metabasite belts within the Moine assemblage, west of Loch Ness, Scotland: evidence for metabasite modification by country rock interactions. *Journal of the Geological Society, London,* **142**, 643-61.

ROCK, N. M. S., COOPER, C. & GASKARTH, J. W. 1986. Late Caledonian subvolcanic vents and associated dykes in the Kirkcudbright area, Galloway, south-west Scotland. *Yorkshire Geological Society,* **46**, 29-37.

ROGERS, G., DEMPSTER, T. J., BLUCK, B. J. & TANNER, P. W. G. 1989. A high precision U/Th age for the Beinn Vuirich granite: implications for the evolution of the Scottish Dalradian. *Journal of the Geological Society, London,* **146**, 789-798.

ROGERS, G. & DUNNING, G. R. 1991. Geochronology of appinitic and related granitic magmatism in the W. Highlands of Scotland: constraints on the timing of transcurrent fault movement. *Journal of the Geological Society, London,* **148**, 17-27.

ROGERS, G. & PANKHURST, R. J. 1993. Unravelling dates through ages: geochronology of the Scottish metamorphic complexes. *Journal of the Geological Society, London,* **150**, 447-464.

ROSCOE, R. 1952. The viscosity of suspensions of rigid spheres. *British Journal of Applied Physics,* **3**, 267-269.

ROSENFELD, J. L. 1968. Garnet rotations due to major Paleozoic deformations in Southeast Vermont. *In:* ZEN, E. A. (ed)*Studies of Appalachian Geology.* Wiley. N. Y., 185-202.

ROSENFELD, J. L. 1970. Rotated garnets in metamorphic rocks. *Geological Society of America, Special Paper*, **129**, 105.

SABINE, P. A. 1963. The Strontian granite complex, Argyllshire. *Bulletin of the Geological Survey, G. B.,* **20**, 6-41.

SALTZER, S. D. & HODGES, K. V. 1988. The Middle Mountain shear zone, southern Idaho: Kinematic analysis of an early Tertiary high-temperature detatchment. *Geological Society of America Bulletin*, **100**, 96-103.

SANDERS, I. S. 1991. Exhumed lower crust in NW Ireland, and a model for crustal conductivity. *Journal of the Geological Society, London,* **148,** 131-135.

SANDERSON, D. J. & MARCHINI, W. R. D. 1984. Transpression. *Journal of Structural Geology,* **6,** 44-58.

SANDIFORD, M. & POWELL, R. 1991. Some remarks on high-temperature-low-pressure metamorphism in convergent orogens. *Journal of Metamorphic Geology,* **9**, 333-340.

SCHEWERDTNER, W. M. 1990. Structural tests of diapir hypotheses in Archean crust of Ontario. *Canadian Journal of Earth Science,* **27**, 387-402.

SCHEWERDTNER, W. M. & TROENG, B. 1978. Strain distribution in arcuate diapiric ridges of silicone putty. *Tectonophysics,* **50**, 13-28.

SCHMELING, H., CRUDEN, A. R. & MARQUART, G. 1988. Finite deformation in and around a fluid sphere moving through a viscous medium: Implications for diapiric ascent. *Tectonophysics,* **149**, 17-34.

SCHMIDT, C. J., SMEEDS, H. W. & O'NEILL, J. M. 1990. Syncompressional emplacement of the Boulder and Tabacco Root batholiths (Montana, USA) by pull apart along old fault zones. *Geological Journal,* **25**, 305-318.

SHAW, H. R. 1965. Comments on viscosity, crystal settling and convection in granite magmas. *American Journal of Earth Science,* **263**, 120-152.

SHAW, H. R. 1969. Rheology of basalt in the melting range. *Journal of Petrology,* **10**, 510-535.

SHAW, H. R., WRIGHT, T. L., PECK, D. L. & OKAMURA, R. 1968. The viscosity of basaltic magma: an analysis of field measurements in Makaopuhi Lava Lake, Hawaii. *American Journal of Science,* **266**, 225-264.

SHEPHERD, J. 1973. The structure and structural dating of the Carn Chinneag intrusion, Ross-shire. *Scottish Journal of Geology*, **9**, 63-88.

SIMPSON, C. 1985. Deformation of granitic rocks across the brittl-ductile transition. *Journal of Structural Geology*, **7**, 503-511.

SIMPSON, C. 1986. Determination of movement sense in mylonites. *Journal of Geological Education*, **34**, 246-261.

SIMPSON, C. & SCHMID, S. M. 1983. An evaluation of criteria to deduce the sense of movement in sheared rocks. *Geological Society of America Bulletin*, **94**, 1281-1288.

SIMPSON, C. & WINTSCH, R. P. 1989. Evidence for deformation induced K-feldspar replacement by myrmekite. *Journal of Metamorphic Geology*, 7, 261-275.

SIMPSON, P. R., BROWN, G. C., PLANT, J. & OSTLE, D. 1979. Uranium mineralisation and granite magmatism in the British Isles. *Philosophical Transactions of the Royal Society of London*, **291**, 385-412.

SIRIEYS, P. 1984. Déformation homogénéissée des roches par glissements hétérogénes continus et discontinus. *Bulletin de la Société géologique de France*, **26**, 185-192.

SMITH, D. I. 1979. Caledonian minor intrusions of the Northern Highlands of Scotland. *In:* HARRIS, A. L., HOLLAND, C. H. & LEAKE, B. E. (eds) *The Caledonides of the British Isles - reviewed.* Geological Society, London, Special Publication, **8**, 683-697.

SMITH, R. L. & BAILEY, E. B. 1968. Resurgent cauldrons. *In*: Studies in volcanology. *Geological Society of American Memoirs*, **116**, 613-662.

SMYTHE, D. K., RUSSELL, M. J. & SKUCE, A. G. 1995. Intra-continental rifting inferred from the major late Carboniferous quartz-dolerite dyke swarm of NW Europe. *Scottish Journal of Geology*, **31** (II), 151-162.

SNYDER, D. B. & FLACK, C. A. 1990. A Caledonian age for reflectors within the mantle lithosphere North and West of Scotland. *Tectonics*, **9**, 903-922.

SOPER, N. J. 1963. The structure of the Rogart igneous complex, Sutherland, Scotland. *Quarterly Journal of the Geological Society, London*, **119**, 445-478.

SOPER, N. J. 1986. Geometry of transecting, anastomosing solution cleavage in transpression zones. *Journal of Structural Geology*, **8**, 937-940.

SOPER, N. J., WEBB, B. C. & WOODCOCK, N. H. 1987. Late Caledonian (Acadian) transpression in northeast England: timing, geometry and geotectonic significance. *Proceedings of the Yorkshire Geological Society*, **46**, 175-192.

SOPER, N. J. 1994. Was Scotland a Vendian RRR junction? *Journal of the Geological Society, London*, **151**, 579-582.

SOPER, N. J. & BARBER, A. J. 1982. A model for the deep structure of the Moine Thrust Zone. *Journal of the Geological Society, London*, **139**, 127-238.

SOPER, N. J. & HUTTON, D. H. W. 1984. Late Caledonian sinistral displacements in Britain: implications for a three plate collision model. *Tectonics*, **3**, 781-794.

SPARKS, R. S. J., PINKERTON, H. & McDONALD, R. 1977. The transport of xenoliths in magmas. *Earth and Planetary Science Letters*, **35**, 234-238.

SPEER, J. A., HARRY, Y., McSWEEN, Jr. & GATES, A. E. 1994. Generation, segregation, ascent and emplacement of Alleghanian plutons in the Southern Appalachians. *Journal of Structural Geology*, **102**, 249-267.

SPRY, A. 1969. Metamorphic Textures; Pergamon Press, Oxford, 350.

STEPHENS, W. E. 1992. Spatial, compositional and rheological constraints on the origin of zoning in the Criffel pluton, Scotland. *Transactions of the Royal Society of Edinburgh: Earth Sciences*, **83**, 191-199.

STEPHENS, W. E. & HALLIDAY, A. N. 1984. Geochemical contrasts between late Caledonian granitoid plutons of northern, central and southern Scotland. *Transactions of the Royal Society of Edinburgh: Earth Sciences,* **75**, 259-273.

STOKER, M. S. 1983. The stratigraphy and structure of the Moine rocks of eastern Ardgour. *Scottish Journal of Geology,* **19**, 369-385.

STORETVEDT, K. M. 1974. A possible large scale sinistral displacement along the Great Glen Fault in Scotland. *Geological Magazine,* **111**, 23-30.

STRACHAN, R. A. 1985. The stratigraphy and structure of the Moine rocks of the Loch Eil area, West Inverness-shire. *Scottish Journal of Geology,* **21**, 9-22.

STRACHAN, R. A. & HOLDSWORTH, R. E. 1988. Basement-cover relationships within Moine rocks of Central and southeast Sutherland. *Journal of the Geological Society, London,* **145**, 23-36.

STRACHAN, R. A., TRELOAR, P. J. & SANDERS, I. S. 1985. A Grenville Sm / Nd age for the Glenelg eclogite; discussion and reply. *Nature,* **314**, 754-755.

SUTHERLAND, D. S. 1982. Igneous rocks of the British Isles. *Wiley, London.* p. 645.

SUTTON, J. & WATSON, J. V. 1951. The pre-Torridonian metamorphic history of the Loch Torridon and Scourie areas in the North-West Highlands and its bearing on the chronological classification of the Lewisian. *Quarterly Journal of the Geological Society, London,* **106**, 241-196.

SWEENEY, J. F. 1975. Diapiric granite batholiths in south-central Maine. *American Journal of Science,* **275**, 1183-1191.

SWEENEY, J. F. 1976. Subsurface distribution of granitic rocks, south-central Maine. *Geological Society of America Bulletin,* **87**, 241-249.

TAKADA, A. 1990. Experimental study on propagation of liquid-filled crack in gelatin: Shape and velocity in hydrostatic stress condition. *Journal of Geomorphology Research,* **B95**, 8471-8481.

TALBOT, C. J. 1974. Fold nappes as asymmetric mantled gneiss domes and ensialic orogeny. *Tectonophysics,* **24**, 259-276.

TALBOT, C. J. 1977. Inclined and asymmetric upward-moving gravity structures. *Tectonophysics,* **42**, 159-181.

TALBOT, C. J. 1982. Obliquely foliated dykes as deformed incompetent single layers. *Geological Society of America Bulletin,* **93**, 450-460.

TARNEY, J. 1963. Assynt dykes and their metamorphism. *Nature,* **199**, 672-674.

TAUBENECK, M. F. 1967. Notes on the Glen Coe cauldron subsidence, Argyllshire, Scotland. *Geological Society of America Bulletin,* **78**, 1295-1316.

THIRLWALL, M. F. 1981. Implications for Caledonian plate tectonic models of chemical data from volcanic rocks of the British Old Red Sandstone. *Journal of the Geological Society, London,* **138**, 123-138.

THIRLWALL, M. F. 1982. Systematic variation in chemistry and Nd-Sr isotopes across a Caledonian calc-alkaline volcanic arc: implications for source materials. *Earth Planet Sci. Lett.,* **58**, 27-50.

THIRLWALL, M. F. 1986. Lead isotope evidence for the nature of the mantle beneath Caledonian Scotland. *Earth and Planetary Science Letters,* **80**, 55-60.

THIRLWALL, M. F. 1988. Geochronolgy of late Caledonian magmatism in northern Britain. *Journal of the Geological Society, London,* **145**, 951-968.

THOMAS, P. R. 1979. New evidence for a Central Highland Root Zone. In: HARRIS, A. L., HOLLAND, C. H. & LEAKE, B. E. (eds) *The Caledonides of the British Isles - reviewed.* Geological Society, London, Special Publication, **8**.

THOMAS,P. R. 1980. The stratigraphy and structure of the Moine rocks N of the Schiehallion complex, Scotland. *Journal of the Geological Society, London,* **137**, 469-482.

TURCOTTE, D. L. 1983. Mechanisms of crustal deformation. *Journal of the Geological Society, London,* **140**, 701-724.

TYLER, I. M. & ASHWORTH, J. R. 1983. The metamorphic environments of the Foyers granitic complex. *Scottish Journal of Geology,* **19**, 271-285.

UPTON, B. G.J., ASPEN, P. & HUNTER, R. H. 1984. Xenoliths and their implications for the deep geology of the Midland Valley of Scotland and adjacent regions. *Transactions of the Royal Geological Society of Edinburgh: Earth Sciences,* **75**, 65-70.

URAI, J., MEANS, W. D. & LISTER, G. S. 1986. Dynamic recrystallization of minerals. *American Geophysical Union Monograph*, **36**, 161-200.

VAN BREEMAN, O., AFTALION, M., PANKHURST, R. J. & RICHARDSON, S. W. 1979. Age of the Glen Dessary Syenite, Inverness-shire: diachronous Palaeozoic metamorphism across the Great Glen. *Scottish Journal of Geology,* **15**, 49-62.

VAN BREEMAN, O. & PIASECKI, M. A. J. 1983. The Glen Kyllachy granite and its bearing on the nature of the Caledonian orogeny in Scotland. *Journal of the Geological Society, London,* **140**, 47-62.

VAN DER MOLEN, I. & PATERSON, M. S. 1979. Experimental deformation of partially melted granite. *Contributions to Mineral Petrology,* **70**, 299-318.

VAN DER VOO, R. & SCOTESE, C. 1982. Palaeomagnetic evidence for a large (c. 2000 km) sinistral offset along the Great Glen Fault during Carboniferous times. *Geology,* **9**, 583-589.

VERNON, R. H., WILLIAMS, V. A. & D'ARCY, W. F. 1983. Grain-size reduction and foliation development in a deformed granitoid batholith. *Tectonophysics*, **92**, 123-145.

VIALON, P. 1979. Les déformations continues-discontinues des roches anisotropes. *Eclogae Geologicae Helveticae*, **72**, 531-549.

VIGNERESSE, J. L. 1988a. Formes et volumes des plutons granitiques. *Bull. Soc. Géol. Fr,* **8**, 897-906.

VIGNERESSE, J. L. 1988b. Heat flow, heat production and crustal structure in peri-atlantic regions. *Earth and Planetary Science Letters,* **87**, 303-312.

VIGNERESSE, J. L. 1990a. Use and misuse of geophysical data to determine the shape at depth of granitic intrusions. *Journal of Geology,* **25**, 249-260.

VIGNERESSE, J. L. 1990b. Forme en profondeur du massif granitique de Flamanvile (Cotentin). *C.R. Acad. Sci. Paris*, **311**, 2, 87-93.

WALTON, M. S. 1955. The emplacement of "granite". *American Journal of Science*, **253**, 1-18.

WATSON, J. V. 1984. The ending of the Caledonian orogeny in Scotland. *Journal of the Geological Society, London,* **141**, 193-214.

WATTERSON, J. 1975. Mechanism for the persistence of tectonic lineaments. *Nature,* **253**, 520-521.

WEERTMAN, J. 1971. Theory of water-filled crevasses in glaciers applied to magma transport beneath oceanic ridges. *Journal of Geophysical Research,* **76**, 1171-1189.

WEGMANN, C. E. 1935. *Geologisches Rundschau*, **26**, 307-350.

WEISS, S. & TROLL, G. 1989. The Ballachulish Igneous Complex, Scotland: Petrography, Mineral Chemistry and Order of Crystallisation in the Monzodiorite-Quartz Diorite Suite and in the Granite. *Journal of Petrology,* **30**, 1069-1115.

WESTBROOK, G. K. & BORRODAILE, G. J. 1978. The geological significance of the magnetic anomalies in the region of Islay. *Scottish Journal of Geology,* **14**, 213-244.

WHITE, S. H. 1976. The effects of strain on microstructures, fabrics and deformation mechanisms in quartzites; *Philosophical Transactions of the Royal Society of London*, **A283**, 69-86.

WHITE, S. 1979. Grain and sub-grain size variations across a Mylonite zone. *Contributions to Mineral Petrology,* **70**, 193-202.

WHITE, S. H. & CHAPPELL, B. W. 1988. Some supracrustal (S-type) granites of the Lachan Fold Belt. *Transactions of the Royal Society of Edinburgh: Earth Sciences,* **79**, 169-181.

WHITE, S. H. & WILSON, C. J. L. 1978. Microstructure of some quartz pressure fringes. *Neues Jahrbuch fur Mineralogie, Abhandlungen,* **134**, 33-51.

WHITE, S. H., BURROWS, S. E., CARRERAS, J., SHAW, N. D. & HUMPHREYS, F. J. 1980. On mylonites in ductile shear zones. *Journal of Structural Geology*, **2**, 175-187.

WHITE HEAD, J. A. & LUTHER, D. S. 1975. Dynamics of laboratory diapir and plume models. *Journal of Geophysical Research,* **80**, 705-711.

WICKHAM, S. M. 1987. The segregation and emplacement of granitic magmas. *Journal of the Geological Society, London,* **144**, 281-297.

WILSON, D. & SHEPHERD, J. 1979. The Carn Chuinneag granite and its aureole. *In:* HARRIS, A. L., HOLLAND, C. H. & LEAKE, B. E. (eds) *The Caledonides of the British Isles - reviewed.* Geological Society, London, Special Publication, **8**, 699-675.

WILSON, R. W. 1971. On syntectonic porphyroblast growth. *Tectonophysics*, **11**, 239-260.

WINCHESTER, J. A. 1976. Different Moinian amphibolite suites in the northern Ross-shire. *Scottish Journal of Geology,* **12**, 187-204.

WINCHESTER, J. A. 1988. Later Proterozoic environments and tectonic evolution in the northern Atlantic borderlands. *In:* WINCHESTER, J. A. (ed) *Later Proterozoic stratigraphy of the Northern Atlantic Regions.* Blackie, Glasgow and London, 253-270.

WOIDT, W. D. 1978. Finite elements calculations applied to salt dome analysis. *Tectonophysics,* **50**, 339-356.

WOOLETT, R. W. 1988. *Digital image processing and isostatic studies of the regional gravity field of Great Britain and adjacent marine regions.* University of Durham, Ph. D. thesis (unpublished).

WRIGHT, A. E. & BOWES, D. R. 1979. Geochemistry of the appinite suite. *In:* HARRIS, A. L., HOLLAND, C. H. & LEAKE, B. E. (eds) *The Caledonides of the British Isles - reviewed.* Geological Society, London, Special Publication, **8**, 699-70.

ZHOU, J. X. 1987. An occurrence of shoshonites near Kilmelford in the Scottish Caledonides and its tectonic implications. *Journal of the Geological Society, London,* **144**, 699-706.

ZWART, H. J. & OELE, J. A. 1966. Rotated magnetite crystals from the Rocroi Massif (Ardennes). *Geologie en Mijaboaw*, **45**, 70-74.